ЖУРНАЛ
ЭКСПЕРИМЕНТАЛЬНОЙ И ТЕОРЕТИЧЕСКОЙ
ФИЗИКИ
АКАДЕМИЯ НАУК СССР

SOVIET PHYSICS

JETP

VOLUME 6 NUMBER 1

A Translation
of the
Journal of Experimental and Theoretical Physics
of the
Academy of Sciences of the USSR

Volume 33

JANUARY, 1958

Published by the
AMERICAN INSTITUTE OF PHYSICS
INCORPORATED

SOVIET PHYSICS
JETP

A translation of the Journal of Experimental and Theoretical Physics of the USSR.

A publication of the

AMERICAN INSTITUTE OF PHYSICS

Governing Board

FREDERICK SEITZ, *Chairman*
Members:
WALTER S. BAIRD
JESSE W. BEAMS
RAYMOND T. BIRGE
R. H. BOLT
J. W. BUCHTA
J. H. DILLON
VERNET E. EATON
HERBERT A. ERF
IRVINE C. GARDNER
S. A. GOUDSMIT
C. KITTEL
WINSTON E. KOCK
R. BRUCE LINDSAY
WALTER C. MICHELS
G. E. PAKE
R. RONALD PALMER
JOSEPH B. PLATT
RALPH A. SAWYER
H. D. SMYTH
JOHN STRONG
GEORGE E. UHLENBECK

Administrative Staff

ELMER HUTCHISSON
Director
HENRY A. BARTON
Associate Director
WALLACE WATERFALL
Secretary and Treasurer
THEODORE VORBURGER
Advertising Manager
RUTH F. BRYANS
Publication Manager
ALICE MASTRO
Circulation Manager
KATHRYN SETZE
Assistant Treasurer
EUGENE H. KONE
Director of Public Relations

American Institute of Physics Advisory Board on Russian Translations

ROBERT T. BEYER, *Chairman*
FREEMAN J. DYSON, DWIGHT GRAY, DAVID HARKER,
MORTON HAMERMESH, VLADIMIR ROJANSKY

Editor of SOVIET PHYSICS—JETP

J. GEORGE ADASHKO, DEPARTMENT OF ELECTRICAL ENGINEERING,
THE CITY COLLEGE, CONVENT AVENUE AND 139TH STREET
NEW YORK 31, NEW YORK.

SOVIET PHYSICS is a monthly journal published by the American Institute of Physics for the purpose of making available in English reports of current Soviet research in physics as contained in the Journal of Experimental and Theoretical Physics of the Academy of Sciences of the USSR. The page size of SOVIET PHYSICS will be 8½" x 11", the same as other Institute journals.

Transliteration of the names of Russian authors follows the system employed by the Library of Congress.

This translating and publishing project was undertaken by the Institute in the conviction that dissemination of the results of researches everywhere in the world is invaluable to the advancement of science. The National Science Foundation of the United States encouraged the project initially and is supporting it in large part by a grant.

The American Institute of Physics and its translators propose to translate faithfully all the material in the Journal of EXPERIMENTAL AND THEORETICAL PHYSICS OF THE USSR appearing after January 1, 1955. The views expressed in the translated material, therefore, are intended to be those expressed by the original authors, and not those of the translators nor of the American Institute of Physics.

Two volumes are published annually, each of six issues. Each volume contains the translation of one volume of the Journal of EXPERIMENTAL AND THEORETICAL PHYSICS OF THE USSR.

Subscription Prices:

Per year (12 issues)	
United States and Canada	$75.00
Elsewhere	79.00
Back Numbers	
Single copies	$ 8.00

Subscriptions should be addressed to the American Institute of Physics, 335 East 45th Street, New York 17, New York.

Copyright by American Institute of Physics 1958

SOVIET PHYSICS

JETP

A translation of the Journal of Experimental and Theoretical Physics of the USSR.

SOVIET PHYSICS – JETP VOL. 6, NO. 1, pp. 1-244 January, 1958

ELECTRODYNAMIC ACCELERATION OF PLASMA BUNCHES

L. A. ARTSIMOVICH, S. IU. LUK'IANOV, I. M. PODGORNYI, S. A. CHUVATIN

Institute of Atomic Energy

Submitted to JETP editor March 16, 1957

J. Exptl. Theoret. Phys. (U.S.S.R.) 33, 3-8 (July 1957)

An electrodynamic method of accelerating plasma bunches is proposed. The results of preliminary experiments are described. The data obtained are in qualitative agreement with the elementary theory of the phenomenon.

THE flow of an electric current is always accompanied by the formation of electrodynamic forces tending to deform the individual circuit elements. If one of the elements of a current circuit can be displaced freely, it acquires kinetic energy from the electromagnetic field energy. The force F acting on a mobile element is defined by the expression

$$F = \partial U/\partial x = {}^1/_2 J^2 dL/dx.$$

The acceleration of an electrically neutral substance has a number of advantages over the usual method of obtaining high-speed charged particles. The acceleration of a quasi-neutral gas discharge plasma (or of metal formations) affords the possibility of bypassing the difficulties relating to beam defocusing under the action of the space-charge force and permits, in principle, a gigantic number of accelerated particles per pulse to be obtained. The method proposed is especially suitable for production of heavy high-energy particles since the energy of the guided motion of each of the atoms is proportional to its atomic weight if a circuit element of fixed mass is to be accelerated.

This article explains the principle of electrodynamic acceleration, analyzes the elementary theory, and describes the results of preliminary experiments.

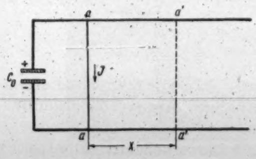

FIG. 1. Circuit diagram

1. THEORY

Let us consider a circuit (Fig. 1) consisting of a capacitor bank and two parallel rigid conductors along which a piece of metal wire (a – a), serving as the mobile circuit element, can be freely displaced without friction. Understandably, such a simplified circuit cannot be the design of a new kind of accelerator. For simplicity, however, we shall consider in this section the idealized problem of the motion of a mobile wire.

The process of accelerating a mobile circuit element is described completely by the system of equations

$$mx'' = {}^1/_2 c^{-2} J^2 dL/dx, \tag{1}$$

$$J = -C_0 dV/dt, \tag{2}$$

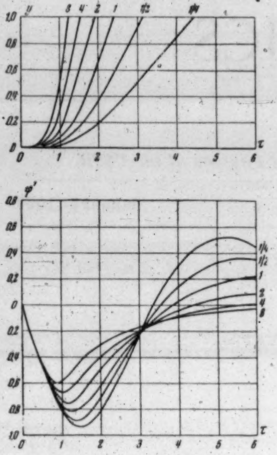

FIG. 2. Results of the numerical solution of the equations of motion for various values of the parameter q. The upper graph shows the time dependence of the distance traversed by the wire. Shown below is the time dependence of the discharge current. The quantities are plotted in nondimensional units.

$$V = c^{-2} d(LJ)/dt, \tag{3}$$

$$L = L_0 + bx, \tag{4}$$

where m is the mass of the wire to be accelerated, J the current in the circuit, C_0 the capacitance of the capacitor bank, V the capacitor voltage, L_0 the initial circuit inductance, and b the increment in the system inductance as the wire moves 1 cm.

The initial conditions at t = 0 are:

$$V = V_0, \quad x = 0, \quad J = 0, \quad x' = 0.$$

Let us introduce the nondimensional variables

$$y = bx / L_0, \quad \varphi = V / V_0, \quad \tau = \omega_0 t,$$

where $\omega_0 = (L_0C_0)^{-1/2}$. After substituting L and J into (1) and (3), we obtain:

$$y'' = q\varphi'^2, \tag{5}$$

$$\varphi = -(d/d\tau)\,[(1+y)\,\varphi'] \tag{6}$$

The initial conditions become

$$y(0) = 0 \text{ and } y'(0) = 0; \quad \varphi(0) = 1 \text{ and } \varphi'(0) = 0.$$

The part of the dimensionless parameter is played in these equations by

$$q = b^2C_0^2V_0^2 / 2\,mc^2L_0.$$

Without solving the equation in general form, let us analyze two limiting cases.

1. Initial stage of the process ($y \ll 1$; $\tau \ll 1$)

$$\varphi = -d\varphi' / d\tau. \tag{7}$$

Integrating (7) and substituting the result in (5), it is easy to see that

$$y = {}^1\!/_4\, q\,[\tau^2 - {}^1\!/_2\,(1 - \cos 2\tau)], \tag{8}$$

from which, because $\tau \ll 1$

$$y = q\tau^4 / 12.$$

2. The following asymptotic equation is obtained in the other limiting case ($\tau \to \infty$):

$$\varphi = B\tau^{-1/4} \cos\left((8/q)^{1/4}\sqrt{\tau} + \alpha\right). \tag{9}$$

It follows from this expression that as the wire is accelerated the amplitude of the voltage oscillations gradually attenuates but the period of the oscillations is increased. However, such a variation of the period and amplitude could be predicted on the basis of simple qualitative reasoning (it is explained by the growth in circuit inductance as the wire moves).

A numerical solution of (5) and (6) was obtained by G. A. Mikhailov and G. A. Bykov using the TsEM-1 electronic computer. The solutions obtained for various values of the parameter q are plotted in Fig. 2.

2. APPARATUS

A gas discharge plasma generated by the electric explosion of a fine metal wire was the mobile circuit element in all the experiments to be discussed. The electric circuit consisted of a 75 μF capacitor bank connected through a spherical discharge gap to massive copper electrodes ("rails"). These latter were placed in a continuously evacuated glass cylindrical chamber. Figure 3 shows schematically the arrangement of the fundamental elements of the apparatus.

An elementary analysis shows that in order to obtain high-speed plasma bunches the operation should be carried out with small values of the initial inductance. Hence, the capacitor-bank wiring described by Komel'kov and Aretov[1] was used.

The vacuum in the discharge chamber at the moment preceding the explosion of the wire was $1 - 2 \times 10^{-6}$ mm Hg.

High-speed photography was used to measure the speed of the plasma and the variation in the magnetic field intensity along the path of the plasma was recorded. The magnetic field was measured by using small coils in which an electromotive force proportional to $\frac{\partial H}{\partial t}$ was induced. The turns of the magnetic pick-off were oriented so that they recorded only the magnetic field intensity component parallel to the rails. This magnetic field intensity component should not change sign when the plasma bunch (current filament) passes the pick-off. The pulses from the magnetic pick-offs K_1 and K_2 are integrated by an RC network and fed to a two-beam pulse oscillograph OK-17M. The second beam of the oscillograph recorded the current in the circuit or the pulse from another magnetic pick-off placed at a definite distance from the first. The loop locations are shown in Fig. 3.

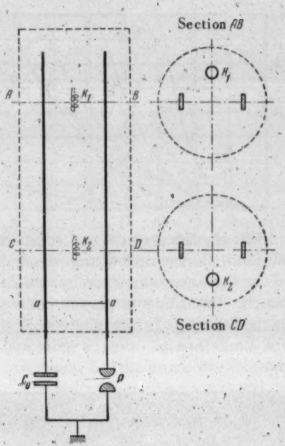

FIG. 3. Schematic diagram of the elements of the apparatus and the locations of the magnetic pick-offs K_1 and K_2.

3. MEASUREMENT RESULTS

High-speed photographs of the glow of the gas discharge plasma which occurs in the explosion of a wire moving along rails are given on Fig. 4. The film speed was 2×10^6 frames per second with a 0.2 μsec frame exposure. The capacitor bank was discharged in these experiments through copper wires of varying diameters. The initial capacitor voltage was 30 kv. By determining the position of the luminous front on each frame, the displacement of the plasma along the rails could be plotted as a function of time. Figure 5 shows a family of curves plotted by the method indicated (see the dashed curves).

The oscillographs of the pulses from the magnetic loops are shown in Fig. 6. The upward swing

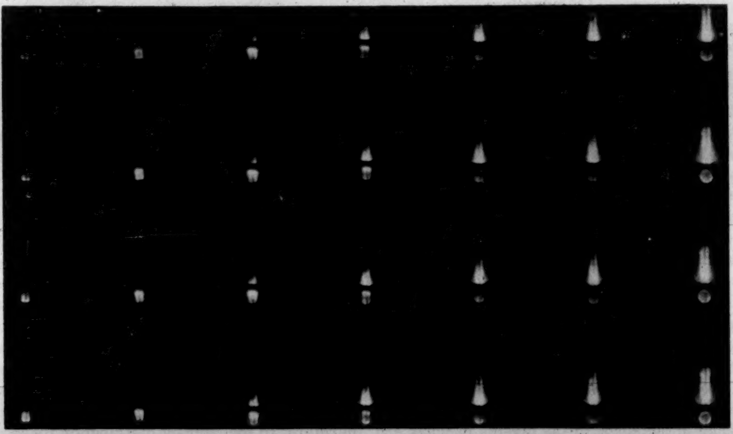

FIG. 4. High-speed photography frames. Lower part of the discharge chamber is metallic, consequently, part of the rails near the original position of the wire is not seen on the photographs. Frames are obtained during burning of 0.02 mm copper wire ($C_0 = 75$ μF, $V_0 = 30$ kv). Rails enclosed between vitreous plates.

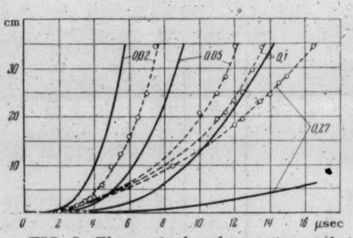

FIG. 5. Theoretical and experimental (dashed) curves of the time-dependence of the distance traversed by the plasma bunch. The different curves correspond to the burning of copper wires of different diameters (diameters indicated in mm).

corresponds to that direction of the magnetic field component which must occur when a hypothetical current filament passes the pick-off. In reality, as is seen from the figure, the magnetic field intensity is seen to change sign during the first current half period. The reason for this change is analyzed below. The speed of the plasma along different sections of the path was determined by the relative time shift between the pulses from two pick-offs located in a suitable manner. The value of the velocity obtained by processing sufficiently clear photographs is in satisfactory agreement with the results obtained from magnetic measurements. Thus, for example, at 30 kv the maximum value of the velocity in experiments with a copper wire of 0.02 mm diameter at a 30 cm distance from the initial position of the wire is 1.1×10^7 cm/sec by magnetic measurements and 1.2×10^7 cm/sec by photographic measurements.

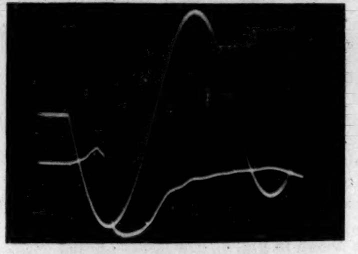

FIG. 6. Oscillogram of a pulse from the magnetic pick-off in phase with the discharge current.

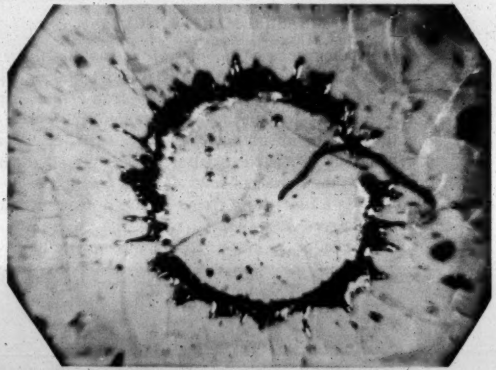

FIG. 7. Microphotograph of the deposit on a vitreous target obtained during the explosion of an 0.07 mm iron wire. Amplification 130×.

The set of experimental results obtained indicates the obvious inadequacy of the elementary theory given in Sec. 1 in at least two respects.

First, it is assumed in the theory that the mass m in the equation is the same as the mass of the evaporating wire. In reality, not all the material of the wire can be transformed into a cloud of ionized gas during an electric explosion. On the other hand, the plasma bunch interacts with the surface of the rails and with the inner chamber walls as it moves. This interaction can lead to an increase in the number of ionized particles participating in the acceleration process. Hence, the real mass of the substance to be accelerated can be either greater or smaller than m. The second inadequacy of the theory developed is the assumption that the shape of the plasma formation is invariant during the acceleration.

It follows from an analysis of the experimental results, that both assumptions of the theory do not correspond to reality. Actually, as is seen from Fig. 5, the experimental values of the transit time appears to be larger than the theoretical for fine wires while the reverse picture holds for thicker wires. The slower motion of the plasma bunches than results from the theoretical formulas is apparently due to the change in the shape of the plasma bunches and, therefore, to the current distribution therein during acceleration. Analyzing the individual frames of Fig. 4, it is easy to be convinced that what moves along the rails is not a sharply delimited luminous cloud but a rapid increase in the longitudinal size of the luminous region. If it is assumed that the distribution of the current density is in agreement with the distribution of plasma luminescence then the electrodynamic forces accelerating the leading edge of the plasma will be less than computed, resulting in slower motion. Photographs obtained by burning thicker wires show that the broadening of the plasma bunch is retained when the wire diameter changes. However, the influence of another factor seems to be more essential in the explosion of a wire of relatively large diameter, namely the incomplete evaporation and the incomplete ionization of the wire material. A direct proof, confirming the validity of this assumption, has been obtained by a microscopic investigation of the metallic deposit on vitreous targets situated at the end of the path of the plasma motion. The electric explosion of the wire is accompanied by the appearance of metallic formations, occasionally of very startling shape (Fig. 7), on the surface of the vitreous targets, such formations could not result from condensation of the vaporized material on the cold target.

Measurements of the magnetic field distribution during the plasma acceleration along the rails completely confirm the abovementioned assumption of the absence of any clear localization of the discharge current. At the very instant when the magnetic pick-off located at the end of the rails starts to indicate passage of current, the pick-off located at the beginning of the rails still continues to indicate a current flow in that region.

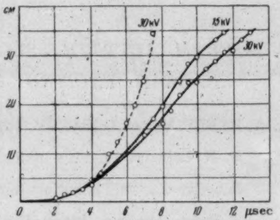

FIG. 8. Time-dependence of the distance traversed by the plasma bunch along the rails. Solid curves are obtained by processing photographs with accessory glass. Dashed curve is obtained for the same parameters but without the accessory glass and is given for comparison purposes.

The results obtained with magnetic pick-offs indicate also a lateral broadening of the region occupied by the discharge current. Actually, as has already been said, the direction of the magnetic field recorded by the magnetic pick-offs changes sign while the discharge current direction remains invariant. A natural explanation of the character of the oscillograms obtained would be the assumption that the discharge current flows around the measuring coil (hence, the sign of the magnetic field at the coil location must become reversed). The similar character of the oscillograms of the pulses from the magnetic pick-offs located relative to the rails as shown in Fig. 3 indicates that an approximately symmetrical broadening of the region occupied by the dishcarge current occurs in a number of cases as the plasma bunch accelerates. In reality, as numerous investigations of the electric explosion of a wire in a vacuum indicate,[2] the propagation velocity of the explosion products can reach $10^5 - 10^6$ cm/sec and, therefore, the plasma bunch broadens in all directions in addition to having its center of inertia accelerate along the rails. The electromagnetic contraction appears to be inadequate to prevent broadening of the plasma ($\frac{H^2}{8\pi} < nkT$). Moreover, it should be kept in mind that the presence of the pick-off can itself cause additional distortion of the shape of the plasma bunch.

In order to confirm the assumption made about the lateral broadening of the bunch, the rails were enclosed between glass plates so that the discharge current could not flow around the magnetic pick-offs. An oscillographic investigation of the impulses of the magnetic field along the path traced by the plasma indeed disclosed that no negative excursions in this case. However, the plasma acceleration process appears to be a complicated, new, troublesome phenomenon. The discharge current is not a thin current filament moving along the rails but it occupies a sufficiently extended section of the rails. Consequently, the plasma reacts violently with the vitreous surface and heats it, which leads to a continuous growth in the mass of the moving substance. Such a continuous increase in the mass of the gas is equivalent to friction in certain respects and it must lead to a decrease in the plasma velocity, as is observed in experiments both during oscillographic measurements and during processing of the given high-speed photographs (Fig. 8).

Hence, on the basis of the preliminary experiments conducted, the conclusion can be made that the electrodynamic acceleration of a plasma is really observed, but that the acceleration process is characterized by considerably more complex laws than could be assumed a priori.

---

[1] V. S. Komel'kov and G. N. Aretov, Dokl. Akad. Nauk SSSR 110, 559 (1956).

[2] W. Conn, ZS. angew. Physik 7, 539 (1955); I. F. Kartskhava, V. V. Bondarenko, et al., J. Exptl. Theoret. Phys. (U.S.S.R.) 31, 737, 745 (1956), Soviet Phys. JETP 4, 623, 637 (1957).

Translated by M. D. Friedman

SOVIET PHYSICS JETP VOLUME 6, NUMBER 1 JANUARY, 1958

MEASUREMENTS WITH A SLOWING-DOWN-TIME NEUTRON SPECTROMETER EMPLOYING LEAD. EXCITED LEVEL OF THE He^4 NUCLEUS

A. A. BERGMAN, A. I. ISAKOV, IU. P. POPOV, and F. L. SHAPIRO

P. N. Lebedev Physics Institute, Academy of Sciences, U.S.S.R.

Submitted to JETP editor January 22, 1957

J. Exptl. Theoret. Phys. (U.S.S.R.) 33, 9-16 (July, 1957)

Results of measurement of the energy dependence of the cross sections are presented for the following reactions: (n, γ) in Fe, Pb and Cl; (n, p) in He^3, N^{14} and Cl; (n, α) in Li^6 and B^{10}. Neutron energies up to 30 kev were employed. It is shown that the cross section for the B^{10} (n, α) reaction lies below the 1/v law, the deviation being smaller than 5 — 10%. The deviation of the Li^6 (n, α) cross section from the 1/v law is even less. It is concluded that the B^{11} nucleus has an excited level with an angular momentum $J = 5/2^+$ or $7/2^+$, a neutron resonance energy $E_r \sim 250$ kev, and widths $\Gamma_\alpha \sim 400$ and $\Gamma_n \sim 200$ kev. An appreciable deviation of the He^3 (n, p) cross section from the 1/v law has been detected which may indicate the existence in the He^4 nucleus of an excited level with one of the two sets of parameters: 1) $J = 1^+$, $-E_r \sim 200$ kev, proton width for an excitation energy equal to the neutron binding energy $\Gamma_{p0} \sim 200$ kev and 2) $J = 0^+$, $-E_r \sim 500$ kev, $\Gamma_{p0} \sim 1200$ kev.

I. Measurements with the slowing-down-time-in-lead neutron spectrometer[1,2] were extended in the neutron energy region up to ~ 30 kev. To determine the resolving power and the dependence of the average neutron energy E on the slowing down time t, of the energy dependence of the capture cross section was measured for a number of elements with widely spaced levels. A scintillation counter with a stilbene crystal of small size was used to register γ-rays from neutron capture in the samples. The duration of the neutron burst and the width of the channel of the time-of-flight analyzer were 0.5 μ sec each. The results of the measurements are presented in Figs. 1 and 2. For E < 1000 ev the effective flight path[2] of the spectrometer is constant to within ± 1.5% and is

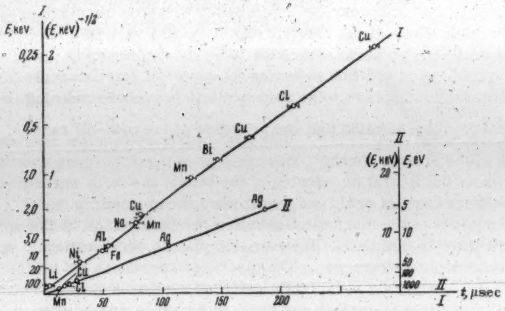

FIG. 1. Curve of $E^{-1/2} = f(t)$, where t is the slowing-down time corresponding to the maximum of the resonance peak and E is the energy corresponding to the resonant state. I — energy region E > 0.2 kev. II — E > 5 ev. Data on the energies of the levels are taken from Ref. 4 for Cl, Ref. 5 for Al, and Ref. 3 for the other elements. Note added in proof: The points for Al and Fe must be raised somewhat in accordance with the latest published data.[18] As a result the change in slope of curve I disappears and all points lie on one straight line given by $E^{-1/2} = 0.074\ (t + 0.3)$.

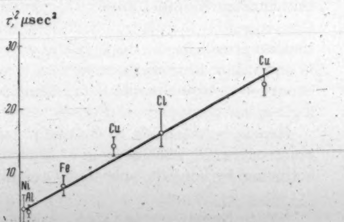

FIG. 2

L = 600 cm. For E > 1 kev, L keeps the same value within 3–5%, which shows that the average scattering cross section of neutrons in lead is constant within these limits.

The half-widths of the resonance peaks satisfy the relation $\tau^2 = at^2 + b$, where the coefficient a is 40 – 50% larger than the theoretical value for pure Pb: $a = (16 \ln 2)(3M)^{-1}$, where M = 207, the atomic weight of lead.[2] The constant term b is a characteristic of the experimental spread and of the spread connected with the width of the original neutron spectrum. From the measurements of the half-widths of the resonance peaks it follows that the spread of the neutron energies around the average value for the assigned analyzer channel is $(\overline{\Delta E^2})^{1/2}/\overline{E} \cong 15\%$ for E < 1 kev and $(\overline{\Delta E^2})^{1/2}/\overline{E} \cong 35\%$ for E = 10 kev. Such a spectrum width, while not favorable for the resolution of resonance peaks, permits nevertheless a sufficiently precise measurement of cross sections that vary smoothly on energy. In this work we investigated principally light nuclei, where the smooth variation of the cross section in the interval E < 30 kev is connected with the large distances between levels. The second possible field of application of the slowing-down-time spectrometer is the measurement of the cross sections of (n, γ) reactions in heavy nuclei in the energy region greater than several hundred electron volts, where because of the large number of levels the averaging of the cross sections over the resonances is of interest.

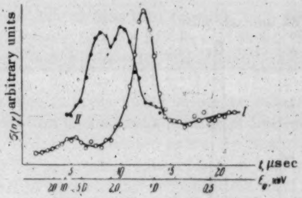

FIG. 3. Energy dependence of the cross sections of the (n, γ) reactions in iron and lead. I – specimen of A iron (99.7% Fe) 4 mm thick; II – background in the absence of a specimen. The curves are represented in different scales; in the Fe peak at 1.2 kev, the ratio of the effect to the background is ~ 3 : 1.

Together with the known levels, used for calibration, three new levels were found in the course of the measurements (Fig. 3). In measurements with iron a level appeared at an energy $E_r = 1200 \pm 100$ ev. The absence in this region of any peak in the total cross section curves for iron[3] indicates that this level is either narrow or belongs to one of the rare isotopes of iron. In measurements on lead (γ-background of the spectrometer*) levels with energies $E_r = 1700 \pm 150$ and $E_r = 2800 \pm 200$ ev appeared.

2. With the help of proportional counters, filled with N_2 and CCl_4 vapors, measurements were carried out on the energy dependence of the ratios of the cross sections of the $N^{14}(n, p)$ and $Cl^{35}(n, p)$ reactions to the $Li^6(n, \alpha)$ reaction cross section. For nitrogen the ratio of the cross sections is constant to within 3% up to an energy of ~ 5 kev, beyond which it increases. The rise reaches a magnitude of the order of 10% for E = 25 kev. In the measurements with chlorine, which will be continued, the level at 405 ev[4] appeared both in the (n, p) and in the (n, γ) reactions (the latter was detected by the yield of γ-rays measured with a scintillation counter). In the region below this resonance and down to E = 40 ev the $\sigma(n, p)/\sigma(n, \gamma)$ cross-section ratio decreases with decreasing neutron energy. This indicates that the odd-parity chlorine level,[4] principally responsible for the (n, γ) cross section at low energies, has a substantially smaller proton width than the 405-ev level.

3. Measurements of the ratios of the cross sections of the reactions $Li^6(n, \alpha)$ and $B^{10}(n, \alpha)$ were continued (Fig. 4). For E > 25 kev the known resonance maximum of Li^6 at $E_r = 250$ kev appeared in the measurements. The area of the peak in Fig. 3 corresponds to the known parameters of the 250-kev level[3] if one assumes that in the spectrum, formed as the results of multiple inelastic scattering of the primary neutrons (E = 14 Mev) with lead nuclei, ~ 30% of the neutrons have an energy less than 250 kev.

In the region E < 25 kev the ratio σ_{Li}/σ_B changes very little, varying by not more than 3% from its value for thermal neutrons. The constancy of the cross section ratio indicates the small magnitude of the deviation from the 1/v law in the course of the cross sections of both reactions. Indeed, if one were to assume appreciably larger deviations from the 1/v law, these must be almost precisely the same for the $Li^6(n, \alpha)$ and $B^{10}(n, \alpha)$ reactions [and also for $N^{14}(n, p)$ – see above]. But the Li^7, B^{11} and N^{15} nuclei differ sharply in the location and character of their excited states. Because of this any constancy in the deviations from the 1/v law for the above reactions is unlikely.

4. Since the reactions $B^{10}(n, \alpha)$ and $Li^6(n, \alpha)$ are often used in measurements of the flux of neutrons of low and intermediate energies, it is essential to obtain a quantitative estimate of the deviation of the

---

*Control experiments have shown that in the 1 – 5 kev region the background is connected with the ground state neutron capture in lead (grade SO, 99.99% Pb), and the contribution from capture in the materials of the amplifier and assembly is negligible.

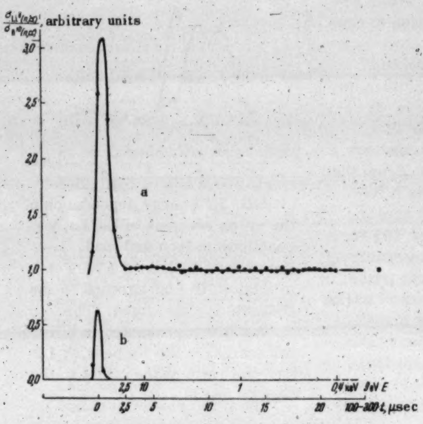

FIG. 4. a — ratio of the cross sections of the reactions $Li^6(n, \alpha)$ and $B^{10}(n, \alpha)$ vs. the slowing-down-time t or of the neutron energy E; b — the shape of the primary neutron burst (in arbitrary units).

cross sections of these reactions from the 1/v law. With this goal we shall analyze the course of the cross sections of these reactions using the known facts[6] on the excited states of Li^7 and B^{11}. In these nuclei, at excitation energies on the order of the neutron binding energy, the distances between neighboring levels of the same momentum and parity is large compared with the widths of the levels. Since for $E \to 0$ the cross section of a reaction is inversely proportional to the square of the energy of the level, one can assume that for low energies the cross section is determined to a large extent by a single level (or by two levels with different momenta). In that case the course of the cross section will be described by the Breit-Wigner formula for a single level. From this formula it is not difficult to obtain the following expression for the course of the cross section of the (n, x) reaction with s-neutrons for $E \ll E_r$, where E_r is the energy of the resonance state, and E is the neutron energy (in the laboratory system of coordinates):

$$(\sigma E^{1/2})_0/\sigma E^{1/2} = 1 + \alpha\sqrt{E} + \beta E, \tag{1}$$

where

$$\alpha = \frac{m}{\pi\hbar^2}\left(\frac{A}{A+1}\right)^2 \frac{(\sigma E^{1/2})_0}{g}, \tag{2}$$

$$\beta = -\frac{2 - \alpha E_1^{1/2}}{E_r} - (1 - \alpha E_1^{1/2})\left(\frac{d \ln \Gamma_x}{dE}\right)_0 + \frac{\alpha}{2E_1^{1/2}}, \tag{3}$$

m is the neutron mass, A is the mass number of the target nucleus, $g = (2J + 1)/2(2i + 1)$, i and J are respectively the momenta of the target nucleus and of the compound nucleus, Γ_x and Γ_n are respectively the widths for emission of particles x and of a neutron by the compound nucleus, and E_1 is the neutron energy at which the neutron width Γ_n, proportional to $E^{1/2}$, becomes equal to the width Γ_{x0}. The index 0 always indicates the value of the term at zero neutron energy.

The term $\alpha\sqrt{E}$ in (1) is connected with the energy dependence of the neutron width which appears in the denominator of the Breit-Wigner formula. The values of the coefficients α, presented in Table I for several nuclei, are computed from formula (2) using the values of $(\sigma E^{1/2})_0$ from Ref. 3. In several non-interfering levels introduce a contribution in the cross section of the reactions for low neutron energies, then the values of α will be less than those shown in Table I. For levels excited by p-neutrons for $E \ll E_r$ we get $\sigma E^{1/2} \sim E$, i.e., such levels influence the value of the coefficient β in (1).

TABLE I.

$\alpha \cdot 10^2$, $keV^{-1/2}$

Target Nucleus	Momentum of the compound nucleus	
	$J=i+1/2$	$J=i-1/2$
He^3	1.55	4.65
Li^6	0.40	0.80
B^{10}	2.22	2.96

The energy dependence of the ratio of the cross sections of the two reactions is also described by expression (1), but with coefficients α and β equal to the difference between the corresponding coefficients for the two reactions.

5. Combining by the method of least squares the ratio σ_{Li}/σ_B obtained in our measurements with the relation (1) gives the following values for the coefficients:

$$\alpha_B - \alpha_{Li} = (1.5 \pm 0.7) \cdot 10^{-2}\ \text{kev}^{-1/2},$$
$$\beta_B - \beta_{Li} = (-2 \pm 1) \cdot 10^{-3}\ \text{kev}^{-1}.$$

Since $\alpha_{Li} \leq 0.8 \times 10^{-2}\,\text{kev}^{-1/2}$, it follows from the results of the measurements it follows that $\alpha_B \leq (2.3 \pm 0.7) \times 10^{-2}\,\text{kev}^{-1/2}$ which is in agreement with the theoretical estimate (Table I).

In estimating the constant β it is necessary to use information on the location and character of the levels of Li^7 and B^{11} closest to the binding energies.[6] The large cross section of lithium for thermal neutrons may be due to the wide level at $E_r = -750$ kev. In that case, taking also into account the level with $E_r = 250$ kev, excited by p-neutrons, the calculated value becomes $\beta_{Li} \approx 0.6\times10^{-3}$ kev^{-1}. If distant levels contribute appreciably to the thermal cross section of lithium, then $\beta_{Li} \approx -1.7\times10^{-3}$ kev^{-1}. With the help of these estimates we find, from the experimental value of $\beta_B - \beta_{Li}$ that $(-1.4 \pm 1)\times10^{-3} \geq \beta_B > (-3.7 \pm 1)\times10^{-3}$ kev^{-1}. The $B^{10}(n, \alpha)$ cross section for $E > 400$ kev is appreciably below the values extrapolated from the 1/v law.[7] This indicates that the main contribution to the cross section at low energies is due to levels with $E_r < 400$ kev. On the other hand, the levels of B^{11} located below the binding energy cannot lead to a negative value for β_B. The course of the $B^{10}(n, \alpha)$ cross section for $E < 1$ Mev (in particular the non-linear decrease of the cross section for $E > 400$ kev) and the course of the total cross section of B^{10} in the same energy interval[8] can be satisfactorily explained by the existence in B^{11} of a wide level with momentum $5/2^+$ or $7/2^+$, with $E_r \sim 250$ kev, with alpha width $\Gamma_\alpha \sim 400$ kev, and with neutron width $\Gamma_n \sim 200$ kev. Such a level leads to a value $\beta_B \sim -5\times10^{-3}$ kev^{-1}. This value can be brought into agreement with the estimate, which follows from our measurements, if some contribution (of the order of 30%) to the thermal cross section of B^{10} is introduced by odd-parity levels of B^{11}.

The wide level of B^{11} which we discussed above may coincide with the level at $E_r \sim 370$ kev noticed in the study of the $N^{14}(n, \alpha)$ reaction[9] and with the possible level at $E_r \sim 200$ kev being discussed in the literature.[5] The downward deviation of the $B^{10}(n, \alpha)$ cross section from the 1/v law, connected with the $\alpha\sqrt{E}$ term, is compensated to an appreciable extent by the βE term to the extent that for boron $\beta < 0$. As follows from the estimates of α_B and β_B introduced earlier, the $B^{10}(n, \alpha)$ cross section in the interval $E < 25$ kev goes below the 1/v law with a deviation not exceeding 5 – 10%. For the $Li^6(n, \alpha)$ reaction the deviation from the 1/v law in the same energy interval is even less.

6. The slowing-down-time-in-lead neutron spectrometer was also used to measure the energy dependence of the ratio of the effective cross sections of the $He^3(n, p)$ reaction and the $Li^6(n, \alpha)$ and $B^{10}(n, \alpha)$ reactions. Proportional counters filled with a mixture of He^3 + Ar + methylal or Co_2, and proportional counters or ionization chambers with a thin layer of boron of Li^6F were used to detect the corresponding reactions.

It turned out that the ratios $\sigma_{He^3}/\sigma_{Li}$ or σ_{He^3}/σ_B decrease with increasing energy, with the decrease exceeding 15% for $E = 27$ kev (Fig. 5). It was shown above that the cross sections of boron and lithium in this energy region are somewhat lower than given by 1/v. Therefore, the cross section of the $He^3(n, p)$ reaction decreases with energy appreciably faster than by the 1/v law. This result is confirmed by the measurements carried out at Harwell[3] at $E \geq 120$ kev (Fig. 5).

One can attempt to attribute the large cross section of the $He^3(n, p)$ reaction ($\sigma = 5400 \pm 300$ bn for thermal neutrons[3]) and the energy dependence of the cross section to the existence in the He^4 nucleus of an excited state with momentum 0^+ or 1^+ located not far from the binding energy of a neutron in He^4. The values of the coefficient α in formula (1) expected in this case are indicated in Table I. Combining by the method of least squares the results of the measurements with expression (1) gives the following value of the coefficient of the term $\sqrt{E}$:

$$\alpha_{He} - \alpha_{Li} = (1.9 \pm 0.6)\cdot10^{-2} \text{ kev}^{-1/2};$$

$$\alpha_{He} - \alpha_B = (0.4 \pm 0.6)\cdot10^{-2} \text{ kev}^{-1/2}.$$

The errors shown are root-mean-square statistical errors; the true uncertainty in the result is greater because of the possible systematic errors. To the extent that $\alpha_{Li} \leq 0.8\times10^{-2}$ kev$^{-1/2}$ and $\alpha_B \leq 2.3\times10^{-2}$ kev$^{-1/2}$, the experimental results are not in disagreement (taking into account the experimental error) with the value $\alpha_{He} = 1.55\times10^{-2}$ kev$^{-1/2}$ and agree less well with the value $\alpha_{He} = 4.65\times10^{-2}$ kev$^{-1/2}$.

The β_{He} coefficient related to the level energy was determined from measurements of σ_{Li}/σ_{He}; β_{Li} was taken equal to 0.6×10^{-3} kev^{-1}, $\alpha_{He} - \alpha_{Li} = 0.95\times10^{-2}$ kev$^{-1/2}$ for J = 1 and $\alpha_{He} - \alpha_{Li} = 4.05\times10^{-2}$ kev$^{-1/2}$ for J = 0. β_{He} was found equal to 7.6×10^{-3} kev^{-1} if J = 1 and equal to 1×10^{-3} kev^{-1} if J = 0. Assuming that the introduced proton and neutron widths of the He^4 level are equal to each other, we obtain the estimate $E_1 = 630$ kev. With the help of (3), introducing a small correction for the contribution of p-neutrons in the $He^3(n, p)$ cross section (see below), we obtain for the level energy the value presented in Table II. Values of Γ_{p0}, the proton width at an excitation energy equal to the binding energy of a neutron in He^4, are also given in Table II. Γ_{p0} is determined from relation (4) which is derived from the Breit-Wigner formula:

$$\Gamma_{p0}/|E_r| = [2\alpha E_1^{1/2}/(2 - \alpha E_1^{1/2})]^{1/2}. \qquad (4)$$

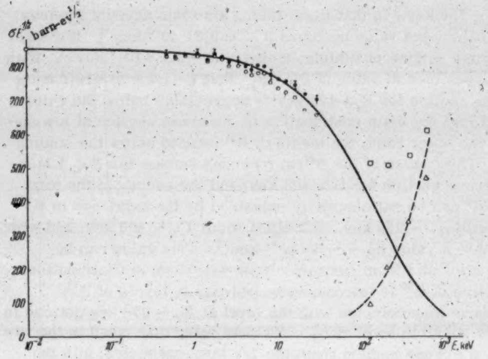

FIG. 5. Energy dependence of the cross-section of the $He^3(n, p)$ reaction. ● — values of σ_{He}/σ_{Li} obtained with the slowing-down-time spectrometer (normalized to $(\sigma_{He}E^{1/2})_0$). ⊙ — values of $\sigma_{He}E^{1/2}$ calculated from ●, assuming that the variation of the cross section of the $Li^6(n, \alpha)$ reaction in this region is due only to the level with $E_r = -750$ kev. □ — values of $\sigma_{He}E^{1/2}$ from the Harwell[3] measurements. Δ — differences between points □ and the solid curve. The solid curve represents the values of $\sigma_{He}E^{1/2}$ calculated for levels with parameters J = 1, E = − 250 kev, Γ_{p0} = 250 kev (contribution of s-neutrons). The dashed curve represents the dependence of const × E (which can be interpreted as the contribution of p-neutrons).

The negative sign of E_r shows that the level is located below the binding energy of a neutron in He^4.

The solid curve of Fig. 5 represents $\sigma E^{1/2} = f(E)$ calculated for a level with parameters $J = 1^+$, $E_r = -250$ kev, $\Gamma_{p0} = 250$ kev. For $E \geq 120$ kev the experimental points lie above this curve while the difference $(\sigma_{exp.} - \sigma_{calc.}) E^{1/2}$ is approximately equal to E which would be expected if the reaction were cause by p-neutrons.

7. The investigated level of He^4 must manifest itself in the scattering of protons by tritium, at a proton resonance energy of $E_r \sim 800$ kev if J = 1 and $E_r \sim 500$ kev if J = 0. In the only work in this energy region,[10] measurements carried out at E = 700, 990, 1100 kev (etc) showed a sharp rise in the scattering cross section from the point at 990 kev to that at 700 kev. In light of the arguments presented above, we consider this result as the manifestation of resonance scattering although the authors of Ref. 10 adhere to another explanation. Frank and Gammel[11] have carried out a phase analysis of the data on the $p - H^3$ scattering in the energy region of 1 to 3.5 Mev and obtained an indication of the existence of a 0^+ level with a proton resonance energy $E_r \sim 800$ kev and a width of a few Mev. To explain the magnitude of the $He^3(np)$ cross section for slow neutrons, the reduced neutron width of such a level must be several times less than the reduced proton width, which is difficult to reconcile with the charge independence of nuclear forces.

A 1^+ level, unlike a 0^+ level, could appear in principle in the $H^3(p, \gamma)$ reaction. The experiment discussed in Ref. 12 gives no indications of a resonance in the yield of γ-rays. However, this fact cannot be used as evidence for $J = 0^+$ since, as follows from the angular distribution of the γ-rays, s-protons generally do not make any appreciably noticeable contribution to the $H^3(p, \gamma)$ reaction.[12] References 13 and 14 report on a study of the energy spectrum of protons scattered from He^4 and Ref. 15 reports on the spectrum of the products of the $He^3(d, p)He^4$ reaction. No excited state of He^4 with excitation energy less than 28 Mev was observed and an upper limit of 0.1 − 1 mb/sterad was established for the cross sections for scattering or for the excitation to such an excited state. This result indicates that the 1^+ (0^+) level of He^4 considered in that work either does not exist or for some reason the transition probability to it is extremely small (the same situation is also true of the 2^- state of He^4, evidence for which is contained in the work of Refs. 16 and 17).

TABLE II. Parameters of the He^4 level derived from the course of the cross section of the $He^3(n, p)$ reaction.

Momentum and parity	Resonance energy E_r, in kev	Excitation energy of the He^4 nucleus in Mev	Proton width Γ_{p0} in kev
1^+	−200	20.3	200
0^+	−500	20	1200

To clarify this question, and to get more accurate data on the behavior of the $He^3(n, p)$ cross section, it is proposed to carry out in the first place a detailed measurement of $p—H^3$ scattering in the proton energy region $E < 1$ Mev.

This work was carried out with the participation of A. N. Volkov, A. M. Klabukov, and I. V. Shtranikh who developed and adjusted the electronic equipment of the slowing-down-time spectrometer. A description of this equipment will published elsewhere.

The authors thank I. M. Frank for his interest in this work and L. M. Gorbunov and G. A. Sokolin for preparing the counters and for participating in the measurements with nitrogen and chlorine.

Note added in proof (June 26, 1957). The measurements of the ratio of the cross sections for $Li^6(n, \alpha)$ and $He^3(n, p)$ were repeated with better statistics and under conditions which made systematic errors less likely. The results are in agreement, within the limits of errors, with the data presented in Fig. 5; the more accurate values of the parameters α and β are the same: $\alpha_{He} - \alpha_{Li} = \left(3.5 \begin{matrix} +0.8 \\ -0.5 \end{matrix}\right) \times 10^{-2}$ kev$^{-1/2}$, $\beta_{He} - \beta_{Li} = \left(2.8 \begin{matrix} +1.5 \\ -1 \end{matrix}\right) \times 10^{-3}$ kev^{-1}. These limits shown include the root mean square statistical error and an estimate of the limits of systematic errors. The course of the cross section is described satisfactorily by the Breit-Wigner formula with the following parameters for the resonant state: the contribution of a $J = 0^+$ state in the $He^3(n, p)$ cross section for thermal neutrons is $x = (94 \pm 6)\%$; if x is taken to be 94% then $-E_r \approx 250$ kev, while for $x = 100\%$, $-E_r = 500 - 1000$ kev; $\Gamma_{p0} | E_r | \sim 2.1$.

---

[1] Lazareva, Feinberg, and Shapiro, J. Exptl. Theoret. Phys. (U.S.S.R.) 29, 381 (1955), Soviet Phys. 2, 351 (1956).

[2] Bergman, Isakov, Murin, Shapiro, Shtranikh, and Kazarnovskii, Paper P-642 at the Geneva International Conference on the Peaceful Ultilization of Atomic Energy, 1955.

[3] D. J. Hughes and J. A. Harvey, Neutron Cross Sections, BNL 325 (1955).

[4] Brugger, Evans, Joki, and Shankland, Bull. Amer. Phys. Soc. 1, 176 (1956).

[5] Rohrer, Newson, Gibbons, and Cap, Phys. Rev. 95, 302 (1954).

[6] F. Ajzenberg and T. Lauritsen, Revs. Mod. Phys. 27, 77 (1955).

[7] Petree, Johnson, and Miller, Phys. Rev. 83, 1148 (1951).

[8] Bockelman, Miller, Adair, and Barschall, Phys. Rev. 84, 69 (1951).

[9] A. B. Lillie, Phys. Rev. 87, 716 (1952).

[10] Hemmendinger, Jarvis, and Taschek, Phys. Rev. 76, 1137 (1949).

[11] R. M. Frank and J. L. Gammel, Phys. Rev. 99, 1406 (1955).

[12] J. E. Perry, Jr. and S. J. Bame, Jr., Phys. Rev. 99, 1368 (1955).

[13] J. Benveniste and B. Cork, Phys. Rev. 89, 422 (1953).

[14] R. M. Eisberg, Phys. Rev. 102, 1104 (1956).

[15] J. C. Allred, Phys. Rev. 84, 694 (1951).

[16] A. I. Baz' and Ia. A. Smorodinskii, J. Exptl. Theoret. Phys. (U.S.S.R.) 27, 382 (1954).

[17] Vlasov, Kalinin, Oglobin, Samoilov, Sidorov, and Chuev, J. Exptl. Theoret. Phys. (U.S.S.R.) 28, 639 (1955), Soviet Phys. JETP 1, 500 (1955).

[18] D. J. Hughes and R. B. Schwartz, BNL 325, Supplement 1 (1957).

Translated by Fay Ajzenberg Selove
2

SOVIET PHYSICS JETP VOLUME 6, NUMBER 1 JANUARY, 1958

ON THE PRODUCTION OF THE ELECTRON-PHOTON COMPONENT IN THE INTERACTION OF COSMIC-RAY PARTICLES OF ENERGIES GREATER THAN 10^{11} EV WITH BERYLLIUM NUCLEI

L. T. BARADZEI, V. I. RUBTSOV, IU. A. SMORODIN, M. V. SOLOV'EV, B. V. TOLKACHEV, and Z. I. TULINOVA

P. N. Lebedev Physics Institute, Academy of Sciences, U.S.S.R.

Submitted to JETP editor February 6, 1957

J. Exptl. Theoret. Phys. (U.S.S.R.) 33, 17-20 (July, 1957)

Four events of electron-nuclear showers produced by cosmic-ray particles of energy exceeding 10^{11} ev interacting with beryllium nuclei in a cloud chamber are discussed. The energy transferred to π^0-mesons in the interactions is determined. Large fluctuations in the π^0-meson energy were observed. One of the photographs is an example of an interaction in which π^0-mesons are apparently not generated.

RESULTS of experiments carried out with a Wilson cloud chamber in a magnetic field[1] are described in this article. The chamber operated for 52 hours at an altitude of 9000 m. A block of beryllium of thickness 26.5 g/cm^2 was placed above the chamber. Inside was a lead plate of thickness 17.5 g/cm^2 (3.3 radiation lengths). Photographs were taken upon generation of electron-nuclear showers in the absorbers.

In all, 1490 photographs were obtained. On 86 of these electron-nuclear showers from the beryllium block were registered. Among these, 5 cases were found of electron-nuclear showers in which the observed number of particles was greater than 10. The plate shows photographs of four interactions, in which the position in the chamber made it possible to draw definite conclusions about the character of the interaction.

Row		Number of shower			
		8550	1403	3183	3402
1.	Number of particles above the lead plate	12	15	16	17
2.	Number of electrons among them	1	1	0	2
3.	Number of penetrating particles in the shower	9—11	10—18	15—16	7—15
4.	Range of the secondary particles in g/cm^2 in matter above the chamber	11	2	3	13
5.	Magnitude of the angle $\theta_{1/2}$	3.5°	4°	4.5°	6°
6.	Energy of the primary particles, in nucleon masses	450±120	340±70	300±60	230±50
7.	Total energy of the secondary particles in Bev	>30	>52	>29	>25
8.	Number of electrons of energy greater than 6 Mev	62—68	21	13	68—74
9.	Number of electrons of energy greater than 30 Mev	30	15	3	35
10.	Energy definitely belonging to electrons, in Bev	>7	3.8	0.3	>7
11.	Energy of the electron-photon component, in Bev	14—40	7.6—15	0.7—1	14—50
12.	Ratio of the energy of the electron-photon component to the energy of the incident particle, in %	4.4—12	2—6	0.2—0.5	5—29
13.	Number of secondary interactions in the lead block	1	1—2	0—1	2

The main data characterizing the showers considered are given in the table. Row 1 of the table gives the number of particles observed above the lead plate. The position of the particle tracks in the chamber was such that the proportion of ionizing particles not registered on the photographs constituted several per cent. A certain number of electrons coming from conversion in beryllium of photons from π^0-decays could have been among particles observed above the plate. In row 2 the number of particles identified as electrons is given.

In row 3 the first number indicates the number of particles going through the lead plate without cascade multiplication and which are therefore not electrons. Part of the tracks could not, because of their unfavorable position, be observed under the lead plate, and the question as to whether these tracks belonged to penetrating particles could not be directly answered. The second number in row 3, does include the tracks not traced, and gives therefore the maximum number of penetrating particles in the interaction. However, if among the tracks not traced the proportion of electrons is the same as among those traced, the main part of the tracks not seen should belong to penetrating particles. Thus, the true number of penetrating particles should be close to the maximum, given in row 3. The place at which the shower has been produced is indicated in row 4.

The angular distribution of the secondary particles can be characterized by the value of the angle $\theta_{1/2}$, inside of which half the particles are emitted. The magnitude of the angle $\theta_{1/2}$, given in row 5, was determined for both the particles known to be penetrating and for the maximum number of penetrating particles, given in row 3. In all cases the difference did not exceed 0.5°.

The angles of the emitted particles were measured from the axis of the shower, the direction of which was determined such that in two mutually perpendicular projections there were the same number of particles on both sides of the axis. The error in the determination of the axis constituted, on the average, 1°. However, because the angular distribution of the penetrating particles was strongly peaked forward, the error in the determination of $\theta_{1/2}$ connected with the inaccuracy in the determination of the axis of the shower was about 0.5°.

Assuming that the observed interactions are nucleon-nucleon ones, the energy of the incident nucleon can be determined by the angular distribution of particles in the shower. In row 6 values are given for γ_0, calculated according to the formula of Dilworth et al.[2]

$$N_s/2\Gamma^2 = \sum_{i=1}^{N_s} 1/(\Gamma^2 + \cot \theta_i),$$

where $\Gamma^2 = (\gamma_0 + 1)/2$. The errors given take into account a possible asymmetry in the emission of the particles in the center-of-mass system by the technique, proposed in the same article, for the upper limit of the number of particles in the shower.

The assumption that the incident nucleon interacts with several nucleons leads to an increase in the value of the energy of the incident particle. The detection of four showers in the conditions of the experiment described corresponds to a current of shower-producing particles $(1.7 \pm 0.8) \times 10^{-5}$ particles per cm^2 per sec per sterad, if the interaction cross section in beryllium is geometrical. Assuming, according to the data of Refs. 3 and 4, that the absorption of particles in the atmosphere takes place with a range of 120 g-cm^{-2}, one obtains a value of the current at the limit of the atmosphere equal to $(2 \pm 1) \times 10^{-4}$ particles per cm^2 per sec per sterad. According to the data given in the review of Fradkin,[5] this quantity corresponds to a beam of particles with energy in excess of 250 Bev.

The presence of a magnetic field in the chamber makes it possible to evaluate the energy of the shower particles. Because more than half the shower particles have momenta larger than that measurable, which is 3 Bev/c, the quantity given in row 7 is the lower limit of the total energy of the penetrating particles.

The number of electrons below the lead plate with energies in excess of 6 and 30 Mev are given, respectively, in rows 8 and 9. Row 10 gives the total electron energy obtained by measuring the electron momenta under the plate. In showers 8550 and 3402, these measurements gave the lower limit of the total electron energy because, the electron momenta could not be measured if they did not exceed 500 Mev/c, owing to the high electron density. The quantities given made it possible to determine the energy of the electron-photon component generated in the interaction (row 11). The lower limit of the energy of the electron-photon component was obtained from the data in row 10 on the assumption that the photon component of the shower has the same energy as the electron component. An upper limit on the energy can be obtained from the number of electrons under the lead plate on the assumption that they are produced in one cascade shower caused by the photon. The calculation was carred out with the formula of cascade theory in approximation A of Ref. 6 for the number of electrons with energy greater than 30 Mev.

The ratio of the energy of the electron-photon component to the energy of the incident particle is given in row 12. The two quantities in the row give, respectively, the minimum possible proportion of the energy in the electron-photon component, calculated as the ratio of the minimum possible value of the energy of the electron-photon component to the maximum value of the energy of the incident particle, and the maximum value obtained under the opposite assumptions. The data given indicate the existence of large fluctuations in the proportion of the energy transferred to the electron-photon component in the interaction.

Shower No. 3183, where the proportion of energy in the electron-photon component does not exceed several tenths of a percent, is of particular interest. In this case the existence of processes other than the decay of π^0-mesons leading to production of an electron-photon component should be considered, such as δ-electrons, bremsstrahlung of mesons in the lead plate, and radiation of photons in the accleration of charges in the nuclear interaction process. Besides these, low-energy π^0-mesons can be generated in secondary interactions in the beryllium block.

Estimates show that the contribution of the first two processes does not exceed 10% of the measured energy. The radiation of photons in the acceleration of charges in nuclear interactions, according to an estimate from formulae given by Feinberg[7] and Schiff,[8] gives a contribution of several hundred Mev to the energy of the electron-photon component if the generating particles are π-mesons. If, together with π-mesons, mesons of spin 1 are generated, then the photon energy increases.

If a Poisson law is taken for the fluctuations in the number of particles, the mean value of the ratio $N_{\pi 0}/N_{\pi^\pm}$ is 0.5, and the energy distribution of the π^0-mesons is taken to coincide with the energy distribution of charged π-mesons, then the probability of production of one π^0-meson of energy less than 10^8 ev is 7×10^{-4}. The production of more π^0-mesons is still less probable. Consequently, it is improbable that the electron-photon component observed in this shower was brought about by π^0-mesons.

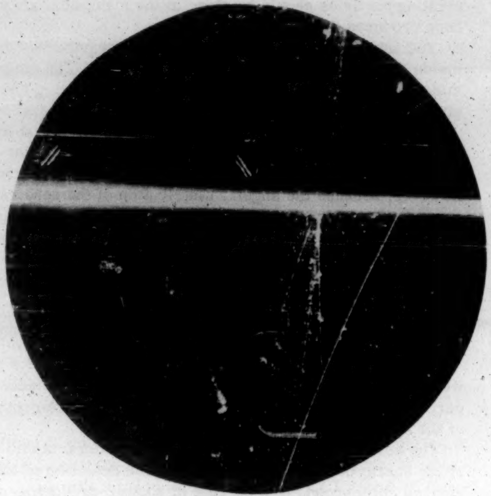

1403

In shower No. 1403 one cascade pencil of electrons was observed, which means that the number of generating π^0-mesons was small. At the same time, the number of electron pencils in shower No. 8550 was not less than 4, and in shower No. 3402 it was not less than 10.

It should be noted that penetrating particles generated in the showers interact with lead nuclei with a cross section equal to the geometrical one. Row 13 of the table indicates the number of secondary interactions observed in the lead plate. Their total number is 4 — 6, which coincides with the expected number of secondary interactions if the interaction cross section in lead is geometrical.

Thus, the data given indicate that in the interaction of charged cosmic-ray particles of energy $10^{11} - 10^{12}$ ev with light nuclei, the proportion of energy transferred to the electron-photon component is subject to considerable fluctuations and can drop to several tenths of a per cent. Shower No. 3183 is, apparently, an example of such interactions in which π^0-mesons are not generated, whereas the number of charged particles generated in the shower is about 15.

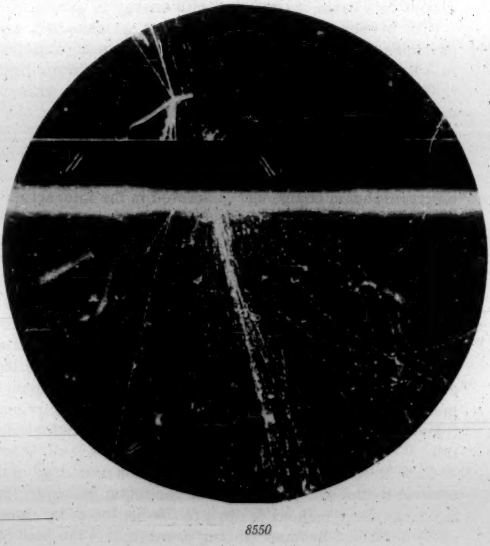

8550

In conclusion, the authors use this opportunity to express deep gratitude to Professor

S. N. Vernov for discussion of the results given here.

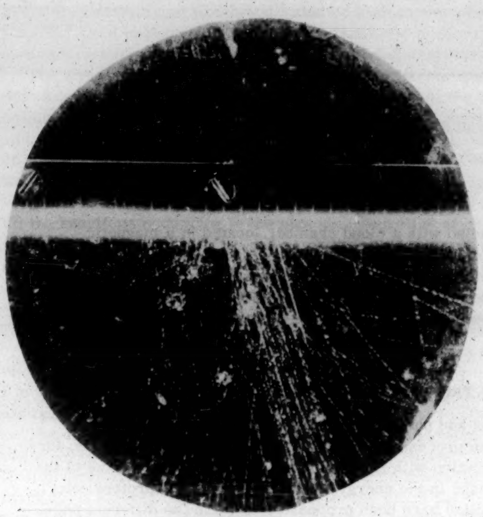

3402

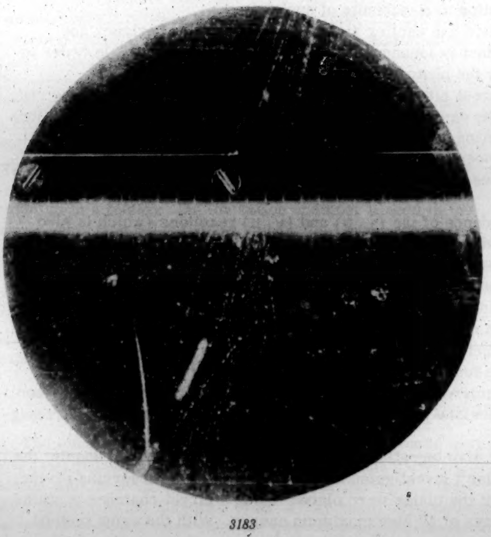

3183

Photographs of electron-nuclear showers, produced by 10^{11}-ev cosmic-ray protons interacting with beryllium. The shower number is printed below the photograph

---

[1] Baradzei, Rubtsov, Smorodin, Solov'ev, Tolkachev, and Tulinova, Dokl. Akad. Nauk SSSR 115, 685 (1957).

[2] Dilworth, Goldsack, Hoang, and Scarsi, Nuovo cimento 10, 1261 (1953).

[3] K. P. Ryzhkova and L. I. Sarycheva, J. Exptl. Theoret. Phys. (U.S.S.R.) 28, 618 (1955), Soviet Phys. JETP 1, 572 (1955).

[4] Kaplan, Klose, Ritson, and Walker, Phys. Rev. 91, 1573 (1953).

[5] M. I. Fradkin, Usp. Fiz. Nauk 53, 304 (1954).

[6] B. Rossi and K. Greizen, The Interaction of Cosmic Rays with Matter (Moscow) 1948 (Russian translation).

[7] E. L. Feinberg, J. Exptl. Theoret. Phys. (U.S.S.R.) 19, 1098 (1949).

[8] L. I. Schiff, Phys. Rev. 76, 89 (1949).

Translated by G. E. Brown
3

SOVIET PHYSICS JETP VOLUME 6, NUMBER 1 JANUARY, 1958

PHOTODISINTEGRATION OF HELIUM, I.

A. N. GORBUNOV and V. M. SPIRIDONOV

P. N. Lebedev Physics Institute, Academy of Sciences, U.S.S.R.

Submitted to JETP editor February 11, 1957

J. Exptl. Theoret. Phys. (U.S.S.R.) 33, 21-32 (July, 1957)

The photodisintegration of helium was studied with a cloud chamber located in a magnetic field and synchronized with a 170 Mev bremsstrahlung beam. The yields of the different photonuclear reactions on helium were determined. The energy dependence of the cross section and the angular distributions of the protons and the tritons were measured for the reaction $He^4(\gamma, p)H^3$. The results are compared with data obtained in other investigations and with theoretical predictions.

1. INTRODUCTION

THE investigations of high energy photoprotons and photoneutrons emitted from different nuclei[1-7] have demonstrated many characteristics of these processes (asymmetry of angular distributions, forward shift of the maximum in the angular distribution with increasing photon energy, large size of the isotropic component, the presence of distinct peaks in the energy spectrum of the photoprotons, etc.). Many different models of photon-nucleon interaction have been proposed to explain the different phenomena. In particular, for photon energies > 100 Mev the experiments are satisfactorily described by the pseudo-deuteron model.[8,9] At lower energies the angular distributions of protons according to Yoshida[10] are better in agreement with absorption in α-subunits of nuclei.

The α-particle model of nuclear γ-absorption has earlier also been suggested by Levinger and Bethe[11] to explain the characteristics of the giant resonance of the photonuclear reactions. In order to develop this model further it is useful to study the photodisintegration of free α-particles.

The photodisintegration of helium is of interest also from other considerations. Contrary to the case of more complicated nuclei, it is possible in the case of helium to analyze fully the angular distributions and consequently to draw conclusions on the character of the photon absorption. This is due to the fact that the final state in the (γ, p) and (γ, n) processes (the fundamental photonuclear reactions in He) is a two-body system [$p + H^3$ in the (γ, p) process and $n + He^3$ in the (γ, n) process], and both H^3 and He^3 do not have excited states.

Furthermore, by studying the energy dependence of the (γ, p) and (γ, n) reactions (which is also considerably simplified by the above mentioned circumstances) one can obtain the energy dependence of the photon absorption cross section. This allows one then to determine the integrated cross section as well as the mean and the harmonic mean energy of photon absorption. Comparing these with the theoretical expressions derived in several papers by use of the sum rule [11-13] one can estimate the contribution of exchange forces to the integrated absorption cross section. By comparing the experimental curves of the cross sections of the (γ, p) and (γ, n) reactions with theoretical predictions found for example in Ref. 14 one can obtain information on the wave functions of the α-particle, H^3, and He^3.

Finally, $He^4(\gamma, p)H^3$ and $He^4(\gamma, n)He^3$ are mirror reactions in iso-space. Therefore a comparison of these reactions will allow one to draw conclusions on the interaction operator between the electromagnetic field and the nucleus.

Up to now only very few experiments on the disintegration of helium have been performed despite the considerable importance of this reaction. Fuller[15] investigated the (γ, p) reaction by observing proton tracks in nuclear emulsions. In his experiment the plates were placed inside a target chamber containing helium gass which was irradiated with x-rays of 40 Mev maximum energy. With the same method De Saussure and Osborne[16] sutided the (γ, n) reaction observing the He^3 recoils; their maximum photon energy was 150 Mev. Gaerttner and Yeater[17] studied the photodisintegration of helium with a cloud chamber (without a magnetic field) with a bremsstrahlung spectrum of $E_{\gamma\,max} = 100$ Mev. At an energy of

300 Mev, Benedict and Woodward[18] studied high energy photoprotons with scintillation counters while Kikuchi[19] used nuclear emulsions under similar conditions. Goldwasser and Nicolai[20] published a short communication on an experiment of the photodisintegration of helium above the meson threshold.

The above experiments were performed at different energies and in different experimental arrangements, and usually in a way which allowed only one of the reactions occurring in the photodisintegration of helium to be observed. Their results on the angular distributions and energy dependence of the (γ, p) and (γ, n) reactions cannot therefore be reliably compared. Furthermore, they do not give information on the other possible reactions. We therefore undertook the investigation of the photodisintegration of helium with a cloud chamber in a magnetic field. The x-ray spectrum had a maximum energy of 170 Mev. We chose a cloud chamber since this was the only method available allowing simultaneous observation of all the reactions occurring in the photodisintegration of helium. In the present paper we shall give the results of the (γ, p) reaction and some results concerning the other reactions. Detailed results on the reactions $He^4(\gamma, pn)H^2$ and $He^4(\gamma, n)He^3$ will be presented later.

2. EXPERIMENTAL ARRANGEMENT

The special considerations connected with the use of a cloud chamber in an x-ray beam from a synchrotron and the apparatus connected with such a work were discussed earlier.[21,22] We shall therefore limit ourselves to a short description of the experimental arrangement (see Fig. 1).

The collimated bremsstrahlung beam of the synchrotron of the Physics Institute of the Academy of Sciences was first cleaned from electron contamination with a sweeping magnet. It entered the sensitive region of the cloud chamber through a thin window made of cellulose triacetate. The cloud chamber had a diameter of 30 cm and a depth of 8 cm. In order to decrease the electron background the beam travelled between the sweeping magnet and the cloud chamber through an evacuated pipe. The expansion of the cloud chamber was synchronized with the yield pulse of the synchrotron in an appropriate way. Pictures were taken at 55 sec intervals. The applied magnetic field had a strength of 5500 gauss. The inhomogeneity of the field did not exceed 2% over the sensitive region of the cloud chamber.

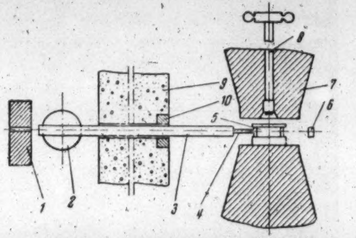

FIG. 1. Diagram of the experimental setup. 1 — lead collimator, 2 — sweeping magnet, 3 — evacuated tube, 4 — beam entrance arrangement into the cloud chamber, 5 — cloud chamber, 6 — pulsed ionization chamber, 7 — magnet, 8 — stereoscopic camera, 9 — concrete wall, 10 — lead absorber.

To monitor the yield of only those x-ray bursts which resulted in a picture, the ionization chamber placed in the x-ray beam was pulsed at the appropriate burst. The chamber was calibrated in terms of intensity in an absolute way utilizing the β^+ activity induced in a carbon sample by the reaction $C^{12}(\gamma, n)C^{11}$; the absolute value of this cross section was taken from Ref. 23. The procedure of calibration of an ionization chamber has been described in Ref. 22. The calibration of our chamber was performed twice during the experiments and the results of the calibration agreed within the experimental accuracy of 2%.

3. ANALYSIS OF THE PICTURES

The obtained cloud chamber pictures where treated in the following sequence: (a) the pictures were scanned; (b) all nuclear reactions due to γ-quanta were identified; (c) the events to be analyzed were selected and the lengths of the projection of the tracks, the radius of curvature, and the angle of emission with respect to the direction of the x-ray beam were determined. All films were scanned twice. Ordinary stereoscopes were used for this purpose. Furthermore, all unclear or spoiled events were scrutinized on a 30× microscope (type UIM-21). This scanning procedure practically eliminated the possibility that any reaction has been overlooked.

One can classify all near reactions observed in a gas cloud chamber according to the number of emitted visible tracks, i. e., according to the number of charged particles in the final state. Since the maximum energy of the x-rays used in this experiment (170 Mev) was insufficient to create a charged meson in addition to disintegrating helium, all reactions with three or more tracks had to be due to the oxygen and carbon impurities.

The following reactions lead to two charged particles:

$$He^4 + \gamma \rightarrow p + H^3, \quad (1)$$

$$He^4 + \gamma \rightarrow d + d, \quad (2)$$

$$He^4 + \gamma \rightarrow p + n + d, \quad (3)$$

$$He^4 + \gamma \rightarrow p + p + n + n, \quad (4)$$

$$I + \gamma \rightarrow p + \text{recoil nucleus} \quad (5)$$

$$I + \gamma \rightarrow p + n + \text{recoil nucleus} \quad (6)$$

Here I stands for an impurity nucleus present in the chamber other than helium (C or O).

In the reactions (1), (2) and (5) the final state is a two body state. Therefore the particles in the center of mass system go in opposite directions, and the tracks are complanar with the incoming photons. In the laboratory system the angle between the tracks is not smaller than 160°. With these characteristics one can distinguish between the reactions (1), (2), (5) on the one hand and (3), (4), (6) on the other. The (γ, p) (see Fig. 2) and the $(\gamma, 2d)$ reactions give tracks with different relative ionization density. In reaction (1) the ionization due to the H^3 is considerably greater than that due to the proton (5 — 9 times depending on the angle of emission), while the ionization density of both tracks is roughly the same for reaction (2). The reactions of the $I(\gamma, p)$ type are distinguished by the very great difference between the ionization density of the two tracks (see Figs. 2 and 3); the track of the recoil nucleus always ends inside the chamber. This way it is possible uniquely to distinguish between (γ, p) reactions in helium and in the impurity nuclei. In the reactions (3), (4) and (6) (see Fig. 3) the outgoing particles may leave with arbitrary angles with respect to each other and the direction of the incoming x-rays. The reaction $I(\gamma, np)$ can be distinguished from the reaction $He^4(\gamma, pn)H^2$ in the same way as $I(\gamma, p)$ from $He^4(\gamma, p)H^3$.

One charged particle is emitted in the following reaction:

$$He^4 + \gamma \rightarrow n + He^3, \quad (7)$$

$$I + \gamma \rightarrow n + \text{recoil nucleus} \quad (8)$$

Furthermore, the elastic production of π^0-mesons, $He^4(\gamma, \pi^0)He^4$, is energetically possible. However, one can neglect contributions from this reaction, in accordance with the estimated small probability of this event.

The yields from the reaction $I(\gamma, p)$, $I(\gamma, pn)$ and $I(\gamma, n)$ were determined under similar operating conditions with a filling of the cloud chamber with hydrogen instead of helium. The following ratio for the yields was obtained: $I(\gamma, n)/[I(\gamma, p) + I(\gamma, pn)] = 0.57$. When the chamber is filled with helium one can obtain from the number of the observed reactions $I(\gamma, p)$ and $I(\gamma, pn)$ the number of the reactions $I(\gamma, n)$. Subtracting this number from the total number of observed reactions with one charged particle one obtains the number of (γ, n) reactions in helium.

To obtain the angular distributions and the energy dependences one has to know the momenta of the particles and the angles of emission with respect to the direction of the incoming γ-quantum. For the determination of these quantities tracks were used whose projection on the bottom of the cloud chamber had a length ≥ 53 mm. It was not possible to measure with sufficient accuracy the radius of curvature for shorter tracks. When restricting oneself to still longer tracks some accuracy is gained, on the one hand, in the determination of the curvature, but on the other hand the statistical accuracy is then reduced and a low γ-ray energy region in the yield curves is cut off.

The projections of the angles between the tracks and the incoming γ-rays were determined with a microscope of the UIM-21 type. The error in this determination was less than 0.5°. The actual angles were obtained from the projected angles by the relation

$$\theta = \arccos \{\cos \alpha / \sqrt{1 + (h/l)^2}\},$$

where θ is the angle of emission of the particle, α its projection on the plane of the camera, 2h the height of the illuminated region, and ℓ the length of the projection of the track. Under the conditions of the present experiment the difference between θ and α is significant only for small angles with the beam direction and for small ℓ.

The radii of curvature were determined by comparing the tracks with standard circles. This method is very fast and sufficiently accurate up to radii of curvature of 200 — 300 cm. The radii of curvature were independently determined twice. The average deviations of the measurements were 3 — 5%. In the final results a correction was added to take into account the momentum parallel to the magnetic field.

Since in the reaction $He^4(\gamma, p)H^3$ the final state has only two particles it is possible to determine the energy of the γ-quantum from the emission angle and momentum for only one of the outgoing particles. By measuring both tracks one can therefore check the correctness of the measurement. The calculations were performed by means of nomograms, one for protons and one for tritons. For known momentum and emission angle in the laboratory system they gave the energy of the photon and the angle of emission in the center-of-mass system. The construction of such nomograms is straightforward. For a given photon energy E_γ one finds the momentum of the particle due to the c.m.s. momentum p_0, and the momentum p_c in the c.m.s. Then the momentum in the laboratory system is $p_{lab} = p_0 + p_c$. p_c depends only on E_γ and not on the kind of particle, while p_0 depends both on E_γ and on the mass of the particle. Such nomograms are shown in Fig. 4. Each half circle corresponds to a given photon energy, and the radial curves correspond to given angles in the c.m.s.

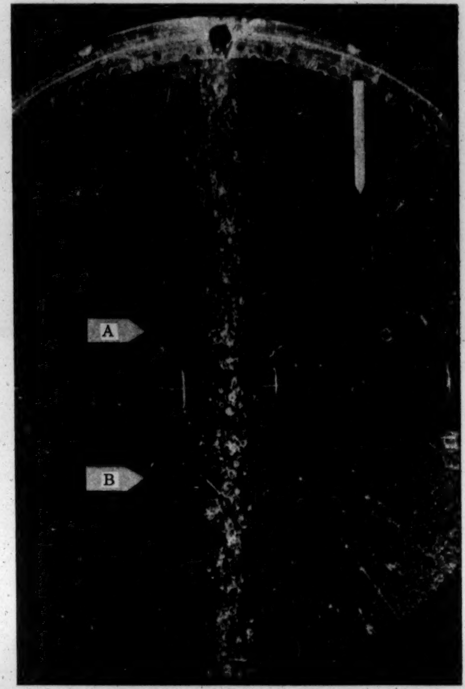

FIG. 2. A — reaction $He^4(\gamma, p)H^3$. The proton travels forward, the triton backward (the direction of the incoming photon beam is indicated by the arrow). B — (γ, p) reaction with impurity nucleus; the heavy short track belongs to the recoil nucleus.

The above method was used to measure 742 proton tracks and 709 triton tracks. All these data were entered on nomograms, protons and tritons separately, to obtain the angular and energy distributions in the c.m.s. The number of points falling into each interval are given in Fig. 4. Since only tracks with length ≥ 5.3 cm were measured there are no points in the nomograms for $E_\gamma < 21$ Mev for protons and $E_\gamma < 30$ Mev for tritons. The nomogram is drawn only for $E_\gamma \leq 70$ Mev.

Owing to the limited height of the illuminated region, only a certain fraction of the particles emitted at an angle θ with respect to the direction of the γ-quantum beam have been measured. This fraction depends on θ. To obtain the actual number of particles emitted at an angle θ from the number of tracks having projections ≥ 5.3 cm it is therefore necessary to apply the correction factor

$$k(\theta) = \frac{\pi}{2 \arcsin(\sin\theta_0 / \sin\theta)},$$

where $\tan\theta_0 = (h/5.3)$ and 2h is the height of the illuminated region. The coefficients $k(\theta)$ vary almost linearly with θ in different θ intervals even for large changes in h. Therefore a change of the illuminated region will have a very small influence on the angular distributions and an even smaller influence on the energy distributions. To obtain the angular distributions the measured quantities have to be related to

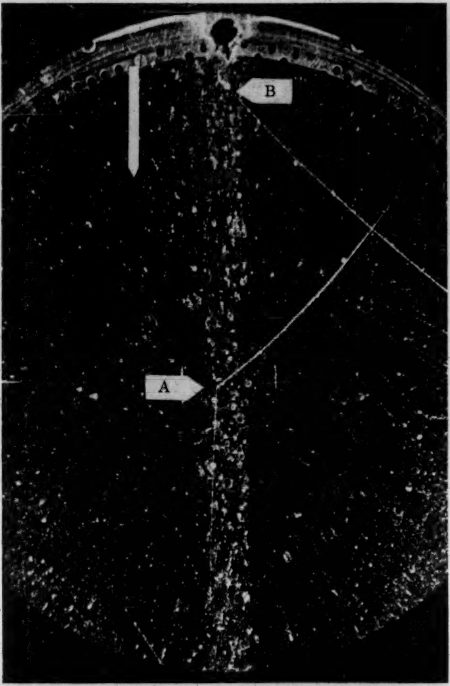

FIG. 3. A— reaction $He^4(\gamma, pn)H^2$. The proton travels forward, the deuteron backward (the direction of the incoming photon beam is indicated by the arrow). B— (γ, p) reaction with impurity nucleus; the heavy short track belongs to the recoil nucleus.

unit solid angle. The experimental numbers therefore were multiplied by $\kappa(\theta) = k(\theta)/\Omega(\theta)$.

To check the correctness of the assumed depth of the illuminated region and consequently the correctness of $k(\theta)$ and $\kappa(\theta)$ the total number of observed (γ, p) events was compared with the total number of protons, determined from the nomogram and corrected with $k(\theta)$. Further, in this comparison it had to be taken into account that the events due to photons of energy between the reaction threshold (19.8 Mev) and 21 Mev were not included in the nomogram.

4. RESULTS OF THE MEASUREMENTS

The total numbers of photonuclear reactions on helium are given in Table I. They were obtained from 9000 cloud chamber pictures.

The analyzed events due to (γ, p) reactions and falling within the indicated ranges of photon energy and center-of-mass emission angles are shown in the nomogram, Fig. 4. Only tracks whose projection of the track lengths was ≥ 5.3 cm were utilized. This was done both for protons and for tritons. These numbers together with the known number of helium nuclei per unit volume in the cloud chamber and the known integrated photon flux through the chamber, along with the correction factors $k(\theta)$ and $\kappa(\theta)$ respectively, yield the energy dependence of the (γ, p) cross section (Fig, 5) and the angular distributions for photon energies 21 — 30 Mev and 30 — 170 Mev (Fig. 6). These two energy ranges for the angular distribution were chosen using the ratios $N_p(0-90°)/N_p(90-180°)$, given in Table II. Here $N_p(0-90°)$ and $N_p(90-180°)$ are the number of protons emitted in the c.m.s. in the forward and the backward hemispheres respectively.

TABLE I

Reaction	Number of observed curves	Yield relative to the (γ, p) reaction
$He^4(\gamma p)H^3$	2835	1
$He^4(\gamma n)He^3$	2685	0.95 ± 0.04
$He^4(\gamma pn)d +$ $+ He^4(\gamma 2p2n)$	547	0.19 ± 0.01
$He^4(\gamma 2d)$	$\leqslant 59$	$\leqslant 0.02$

As can be seen from Table II, a sharp change occurs in the angular distributions of the protons at a photon energy 30 — 35 Mev. The angular distributions obtained independently from proton and from triton tracks are plotted separately. They agree within the statistical accuracy. This indicates the correctness of the measurements.

5. ERRORS OF MEASUREMENT

(a) The error in the true spatial angle is due to the inaccuracy with which the correction for the dip angle has been performed, and due to the neglect of the fact that the photographic picture is the result of a conical projection and not a parallel projection. One can show that the rms errors introduced this way

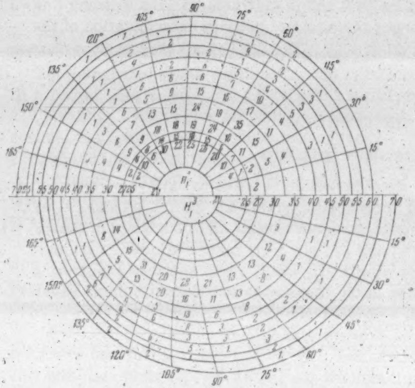

FIG. 4. Nomogram for the determination of the energy and angular dependence of the $He^4(\gamma, p)H^3$ cross section: from proton tracks (upper half) and from H^3 tracks (lower half).

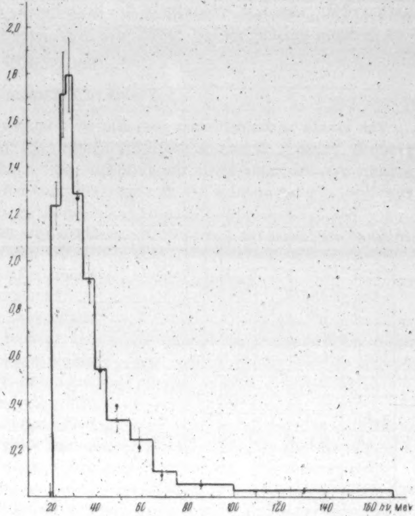

FIG. 5. Energy dependence of the cross section for the reaction $He^4(\gamma, p)H^3$ as determined from proton tracks. Only the statistical uncertainties are indicated. The threshold (19.8 Mev) is indicated by the arrow. The cross sections obtained from triton tracks are indicated by the full circles.

do not exceed ±3.5° for each track. Since this error is statistical in character it practically does not show up in the numbers of tracks falling into a particular angular interval (each interval was chosen to be 15°).

(b) The error in the determination of the energy of the photon responsible for a (γ, p) reaction is compounded of the following parts: errors in the determination of the magnetic field strength, errors due to the nonuniformity of the magnetic field and due to the fluctuations in the magnetizing current, and, finally, errors in the curvatures of the emerging particles and in the angles with respect to the beam and to a plane perpendicular to the magnetic field. The magnetic field was measured with a fluxmeter which was calibrated at two field values in a standard field determined by nuclear magnetic resonance. The total error in the field measurements was ± 0.5%.

The rms error associated with the measurement of curvatures and angles was determined by obtaining the energy of the photon from the two emitted tracks separately. The magnitude of these errors changes between 2.5 and 4% depending on the energy of the photon (this error obviously includes the influence of the inhomogeneity of the magnetic field).

(c) The error in the absolute value for the intensity of the radiation is compounded of the following parts: (1) errors in the calibration of the ionization chamber in terms of the activity of the carbon sample and errors due to apparative instabilities; (2) errors in the determination of the absolute activity of the carbon sample, and (3) errors in the quantity $\int \sigma_{\gamma n}(W)\, \eta(W)\, dW$ where $\eta(W)$ is the bremsstrahlung spectrum. Error (1) was determined by performing the

TABLE II

Ratio $N_p(0-90°)/N_p(90-180°)$ for protons

Photon energy Mev	From proton tracks	From triton tracks
21—25	1.10	—
25—27	0.93	—
27—30	1.21	—
30—35	1.96	2.04
35—40	2.34	1.89
40—170	2.48	2.70
Below 30	1.09±0.13	—
Above 30	2.23±0.26	2.23±0.30

calibration twice. It was found to be ± 2.0%. Error (2) does not exceed 5% according to Ref. 24. Our measurement of the yields of the (γ, n) and (γ, p) reactions in C and O which entered the working mixture of our cloud chamber confirmed in a qualitative manner the absolute activity determination of the carbon sample. According to Ref. 23 error (3) has a magnitude ± 2%. The total rms error in the determination of the absolute intensity of the radiation is 6%.

6. DISCUSSION OF THE RESULTS

Yields of Photonuclear Reactions in Helium

The yields of the different possible photonuclear reactions in helium relative to the (γ, p) reaction are given in Table I. It can be seen that within experimental accuracy the yields for the (γ, p) and (γ, n) reactions are the same while the yield for the $(\gamma, 2d)$ reaction does not exceed 2% of the yield of the (γ, p) reaction. These results are as expected since both (γ, n) and (γ, p) reactions are allowed in a dipole transition and have practically equal cross sections (neglecting the slight difference in the thresholds and in the Coulomb barrier). On the other hand, a dipole transition is forbidded for the $(\gamma, 2d)$ reaction because of isotopic spin selection rules.

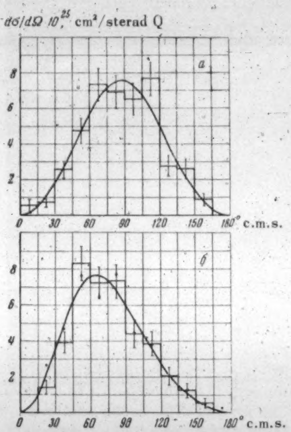

FIG. 6. Angular distributions of the protons from the reaction $He^4(\gamma, p)H^3$ in the c.m.s. (a) proton energy 21 — 30 Mev; (b) 30 — 170 Mev. In (b) the full circles indicate the proton angular distribution inferred from the measurements on triton tracks. The full curves represent Eq. (9).

The experiments in Refs. 17, 20 were also performed with cloud chambers. They yielded for the $(\gamma, n)/(\gamma, p)$ yield ratio the values 1.3 and 1.8 respectively. (In Ref. 17 this ratio is based on 59 single tracks which were assumed to belong to the (γ, n) reaction, and on 45 tracks from the (γ, p) reaction; in Ref. 20 the number of events was not given.) This large $(\gamma, n)/(\gamma, p)$ ratio, besides being based on a small statistical sample, could possibly be connected with operation of the cloud chamber at lower sensitivity in order to decrease the electron background. As a result of this there may have been lost some proton tracks from the (γ, p) reaction which then would be counted as a (γ, n) reaction.

The yield of the (γ, pnd) reaction comprises about 9% of the reaction leading to two particles in the final state, for photon energies 20 to 170 Mev. From the preliminary results of this experiment it seems that this reaction has the character of the pseudodeuteron effect.

Energy Dependence of the (γ, p) Cross Section

As can be seen from Fig. 7, the cross section for the (γ, p) reaction in helium has a resonance-like shape with a maximum cross section ~ 1.8×10^{-27} cm² at a photon energy 27 — 28 Mev. The halfwidth is around 15 Mev. For a photon energy $E_\gamma \geq 35$ Mev the energy dependence of the cross section is well represented by a function of the form $E_\gamma/(E_\gamma - \epsilon)^{2.5}$. On Fig. 7 there are also shown the cross sections for the (γ, p) reaction obtained by Fuller[15] with a photon spectrum of maximum energy of 40 Mev. In this experiment there had to be made large corrections due to the fact that triton and He³ tracks could sometimes not be distinguished from proton tracks. The results for photon energies between threshold and 26 Mev therefore are not too reliable. Fuller's cross section shows a maximum at the energy 26 Mev and has there a magnitude in agreement with the present experiment. However, his halfwidth is ~ 10 Mev, i. e., somewhat smaller than our halfwidth.

In Fig. 7 there further are given points obtained from the cross section of the inverse reaction $H^3(p, \gamma)He^4$ from Ref. 25. This experiment covers proton energies up to 6.5 Mev. These points are in good agreement with the present experiment. The dashed curve of Fig. 7 is a theoretical curve for the absorption cross section for dipole radiation given by Gunn and Irving.[14] In this paper the nuclei He⁴ and H³ were described by exponential wave functions with the parameters $1/\mu_\alpha = 1.7 \times 10^{-13}$ cm and $1/\mu_T = 2.5 \times 10^{-13}$ cm. They were determined to give the correct binding energy for He⁴ and the correct Coulomb energy for He^3. The motion of the proton and triton in the final state were described by plane waves. In this calculation noncentral forces were not taken into account.

One sees from Fig. 7 that the experimental cross sections decrease with increasing energy much faster than the theoretical cross section of Gunn and Irving.

The integrated cross sections for the reaction $He^4(\gamma, p)H^3$ obtained from our curve are given in Table III together with those found by the other workers. One sees from this Table that the energy interval 40 – 170 Mev (i.e., the region far removed from the resonance) contributes a considerable fraction (~ 34%) to the integrated cross section.

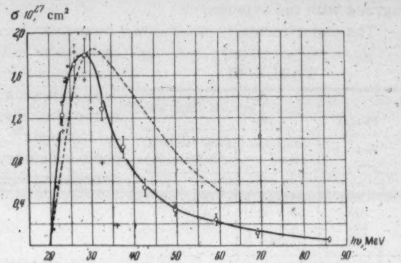

FIG. 7. Comparison of the cross section of the reaction $He^4(\gamma, p)H^3$ with the data of other investigations. Open circles and solid curve drawn through these — results of the present work; crosses — Fuller's[15] points; full circles — inferred from the inverse reaction $H^3(p, \gamma)He^4$ as per Perry and Bame;[25] dotted curve — theoretical curve for the cross section calculated by Gunn and Irving[14] employing an exponential wave function for He^4 and H^3 with $1/\mu_\alpha = 1.7 \times 10^{-13}$ cm and $1/\mu_T = 2.5 \times 10^{-13}$ cm.

Taking into account that the yield and also the position of the maximum for the reaction $He^4(\gamma, n)He^3$ are approximately the same as in the (γ, p) reaction one can expect* that the integrated cross section for the (γ, n) reaction will be close to that of the (γ, p) reaction. For the integrated cross section of the reaction $He^4(\gamma, pn)H^2$ we have obtained the value 10.0 ± 1.4 Mev. mb. With these data one can make a preliminary discussion of the integrated photon absorption cross section of the helium nucleus.

$$\sigma_{\text{int}} = \int_0^{170} \sigma(W)\,dW = 2\sigma_{\text{int}}(\gamma p) + \sigma_{\text{int}}(\gamma pnd) + \\ + \sigma_{\text{int}}(\gamma 2p2n) + \sigma_{\text{int}}(\gamma 2d) = 88 \pm 7 \text{ Mev. mb}$$

This value can be compared with the sum rule calculation of Levinger and Bethe[11] of the integrated electric dipole absorption cross section which included the effects of exchange forces:

$$\int \sigma(W)\,dW = 0.015 \cdot A\,(1 + 0.8x) \text{ Mev. bn}$$

where x is the fractional strength of the exchange forces. This expression yields for helium with $x = 0.5$ the value $\int \sigma(W)\,dW = 84$ Mev. mb which agrees well with the experimental value 88 ± 7 Mev. mb.

In a similar way one can evaluate a different moment of the photodisintegration cross section of helium

$$\sigma_b = \int \frac{\sigma(W)}{W}\,dW,$$

For this quantity we obtain from our experiment the value $\sigma_b = 2.40 \pm 0.15$ mb. This quantity is connected with the rms radius of the nucleus. It was shown in Ref. 26 that for electric dipole transitions holds

$$\int \frac{\sigma_{E_1}(W)}{W}\,dW = \frac{4\pi^2}{3}\left(\frac{e^2}{\hbar c}\right)\frac{NZ}{A-1}\,(1-\Lambda)\int \rho(r)\,r^2 d\tau,$$

where r is the distance from the center of mass of the nucleus, and $\rho(r)$ is the charge density of the nucleus normalized to $\int \rho(r)\,d\tau = 1$. The value of Λ takes the inequality of the nucleons into account. This inequality can be due only to the Coulomb energy or the Pauli principle. In He^4 the Coulomb forces are small and there are no restrictions from the Pauli principle. Therefore for He^4 we have $\Lambda = 0$. If $\rho(r)$ is constant we have

$$\int \rho(r)\,r^2 d\tau = \frac{3}{5}R^2,$$

where $R = r_0 A^{1/3}$. This yields for helium

---

*Our results on the $(\gamma; n)$ reaction are being at present analyzed. The results will be reported at a later date.

$$\int \frac{\sigma_{E_1}(W)}{W} dW = \frac{4\pi^2}{5}\left(\frac{e^2}{\hbar c}\right) \cdot \frac{4}{3} R^2.$$

With the experimentally obtained value $\sigma_b = 2.4 \pm 0.15$ mb we have $r_0 = (1.12 \pm 0.04) \times 10^{-13}$ cm. This agrees with the value $(1.01 \pm 0.06) \times 10^{-13}$ cm obtained from high energy electron scattering experiments on helium[27] and with $r_0 = (1.1 \pm 0.1) \times 10^{-13}$ cm obtained similarly for heavier elements.[28] As shown by Khokhlov[29] and Levinger,[13] taking $r_0 = 1.1$ to 1.2×10^{-13} cm also gives for heavy nuclei a value of σ_b that agrees with the experiments.

The experimentally determined moments of the photodisintegration cross section thus agree well with theoretical values calculated for electric dipole transitions by means of phenomenological sum rules including the effect of exchange forces. This indicates that electric quadrupole absorption plays a minor role in the photodisintegration of helium.

Levinger[30] and Khokhlov[31] also have calculated σ_{int} and σ_b for the photodisintegration of deuterium and found good agreement with the experimental values.

TABLE III

Photon energy Mev	$\sigma_{\text{int}} = \int_{19.8}^{E_\gamma} \sigma(W)\,dW$ (Mev. mb)	
	From our data	From the data of other authors
40	25.0±1.8	16±5 [15]
100	35.8±2.6	34 [17]
135	—	15 [20]
170	37.8±2.8	—

Angular Distributions

The angular distributions of protons from the reaction $He^4(\gamma, p)H^3$ have been derived by Daragan (private communication) for different multipolarities of photon absorption. In accordance with his results we tried to fit our angular distributions to the expression

$$A\,[\sin^2\theta + \beta \sin^2\theta \cos\theta + \gamma \sin^2\theta \cos^2\theta], \tag{9}$$

where the term with $\sin^2\theta$ corresponds to E_1 absorption (no spin change of the system), the term with $\sin^2\theta \cos^2\theta$ corresponds to E_2 absorption, and the term with $\sin^2\theta \cos\theta$ is due to E_1, E_2 interference.

The coefficients A, β, γ obtained by least squares fitting are given in Table IV.

One sees from Table IV that for photon energies below 30 Mev the (γ, p) reaction goes almost completely via electric dipole transitions. The absence of an isotropic component indicates that the particles leave with antiparallel spins. As mentioned earlier there occurs a sharp change in the angular distributions at $E_\gamma = 30 - 35$ Mev. For $E_\gamma = 30 - 170$ Mev the maximum of the angular distribution has moved forward to an angle 65 – 70°. An isotropic component is absent also in this energy range. This change in the angular distribution shows that from $E_\gamma \sim 30$ Mev on electric quadrupole absorption sets in and produces the interference term $\sin^2\theta \cos\theta$. The analysis of the angular distribution indicates that the contribution of electric quadrupole absorption to the (γ, p) cross section in the energy interval 30 – 170 Mev is around 10%. Assuming that the electric quadrupole absorption contributes with the same strength to the other processes one finds that the contribution of electric quadrupole absorption to the integrated cross section does not exceed 6%. This agrees with the above findings on the smallness of the contributions of electric quadrupole absorption obtained from the agreement of the experimental and theoretical moments of the absorption cross section.

TABLE IV

E_γ, Mev	$A\left(10^{29}\frac{\text{cm}^2}{\text{sterad}\ Q}\right)$	β	γ
21—30	7.6±0.7	0.11±0.13	−0.2±0.3
30—170	6.1±0.6	1.05±0.16	0.53±0.25

It is of interest to compare the angular distributions of the protons from the (γ, p) reaction on helium with those obtained in a (γ, p) reaction from deuterium (see Refs. 32, 33) and also from the light nuclei.[6,7] The angular distributions for deuterium are already unsymmetrical at photon energy 20 Mev. They also contain an isotropic component the magnitude of which increases with increasing photon energy.

As has been shown by Shevchenko[7] the angular distributions of fast photoprotons from light nuclei also consist of a large anisotropic and a strong isotropic component. The analysis carried out by Shevchenko shows that they agree well with the angular distributions of photoprotons from deuterium (at the equivalent proton energies). This has been interpreted as a confirmation of the pseudodeuteron effect. The absence of an isotropic component in the angular distribution of the process $He^4(\gamma, p)H^3$, perhaps, is an indication that in helium in (γ, p) and (γ, n) processes the pseudodeuteron effect is unimportant even for high photon energies.

In conclusion, the authors wish to express their gratitude to Professor P. A. Cerenkov for his continuing interest in this work, to Iu. K. Khokhlov and V. Daragan for the communication of their results, to S.

I. Shornikov, A. G. Gerasimov, V. S. Silaeva, N. N. Novikova, and K. V. Chekhova who participated in taking and processing the pictures, and to the synchrotron crew.

---

[1] D. Walker, Phys. Rev. 81, 634 (1951).

[2] C. Levinthal and A. Silverman, Phys. Rev. 82, 822 (1951).

[3] J. S. Keck, Phys. Rev. 85, 410 (1952).

[4] J. W. Rosengreen and J. M. Dudley, Phys. Rev. 89, 603 (1953).

[5] J. W. Weil and B. D. McDaniel, Phys. Rev. 92, 391 (1953).

[6] S. A. E. Johansson, Phys. Rev. 97, 434 (1955).

[7] I. V. Chivilo and V. Shevchenko, J. Exptl. Theoret. Phys. (U.S.S.R.) 32, 1335 (1957), Soviet Phys. JETP 5, 1090 (1957).

[8] J. S. Levinger, Phys. Rev. 84, 43 (1951).

[9] Iu. K. Khokhlov, J. Exptl. Theoret. Phys. (U.S.S.R.) 23, 241 (1952).

[10] S. Yoshida, Progr. Theoret. Phys. 6, 1032 (1951).

[11] J. S. Levinger and H. A. Bethe, Phys. Rev. 78, 115 (1950).

[12] A. B. Migdal, J. Exptl. Theoret. Phys. (U.S.S.R.) 15, 81 (1945).

[13] J. S. Levinger, Phys. Rev. 97, 122 (1955).

[14] J. C. Gunn and J. Irving, Phil. Mag. 42, 1353 (1951).

[15] E. G. Fuller, Phys. Rev. 96, 106 (1954).

[16] G. De Saussure and L. S. Osborne, Phys. Rev. 99, 843 (1955).

[17] E. R. Gaerttner and M. L. Yeater, Phys. Rev. 83, 146 (1951).

[18] T. S. Benedict and W. M. Woodward, Phys. Rev. 83, 1269 (1951).

[19] S. Kikuchi, Phys. Rev. 86, 126 (1952).

[20] V. O. Nicolai and E. L. Goldwasser, Bull. Am. Phys. Soc. 29, 18 (1954); Phys. Rev. 94, 755 (1954).

[21] Gorbunov, Spiridonov, and Cerenkov, Приборы и техника эксперимента (Instr. and Exptl. Tech.) 2, 29 (1957).

[22] Gerasimov, Gorobunov, Ivanov, Kutsenko, V. M. Spiridonov Приборы и техника эксперимента (Instr. and Exptl. Tech.) 3, 10 (1957).

[23] Barber, George, and Reagan, Phys. Rev. 98, 73 (1955).

[24] Roganov, Baranov, and Gol'danskii, J. Exptl. Theoret. Phys. (U.S.S.R.) 33, 1123 (1957), Soviet Phys. JETP (in press) (1958).

[25] J. E. Perry and S. Bame, Phys. Rev. 99, 1368 (1955).

[26] Iu. K. Khokhlov, J. Exptl. Theoret. Phys. (U.S.S.R.) 32, 124 (1957), Soviet Phys. JETP 5, 88 (1957).

[27] R. W. McAllister and R. Hofstadter, Phys. Rev. 102, 851 (1956).

[28] Hofstadter, Hahn, Kundsen, and McIntyre, Phys. Rev. 95, 512 (1954).

[29] Iu. K. Khokhlov, Dokl. Akad, Nauk SSSR 97, 239 (1954).

[30] J. S. Levinger, Phys. Rev. 97, 970 (1955).

[31] Iu. K. Khokhlov, Thesis, Physics Institute, Academy of Sciences, U.S.S.R. (1957).

[32] L. Allen, Phys. Rev. 98, 705 (1955).

[33] Aleksandrov, Delone, Slovokhotov, Sokolov, and Shtarkov, J. Exptl. Theoret. Phys. (U.S.S.R.) 33, 614 (1957), Soviet Phys. JETP (in press) (1958).

Translated by M. Danos
4

SOVIET PHYSICS JETP VOLUME 6, NUMBER 1 JANUARY, 1958

CHANGE IN THE ELASTICITY CONSTANTS OF SODIUM NITRATE DURING A PHASE TRANSITION OF THE SECOND KIND

M. I. KORNFEL'D and A. A. CHUBINOV

Institute of Semiconductors, Academy of Sciences, U.S.S.R. and Molotov State University

Submitted to JETP editor February 23, 1957

J. Exptl. Theoret. Phys. (U.S.S.R.) 33, 33-36 (July, 1957)

The temperature dependence of the elasticity coefficient of $NaNO_3$ crystals has been investigated in the temperature interval from 20 to 300° C. The change in these coefficients at 275.5° C, the point of a second-kind phase transition, has been noted.

In theory of second-kind phase transitions usually only the change in the scalar quantities at the transition point is considered.[1] Yet in studying effects in crystals, tensor quantities are actually of the greatest interest. The purpose of the present investigation was to stimulate the development of theory in this direction.

For the specific subject of our investigation we chose crystals of $NaNO_3$, which according to Kracek[2] undergoes a transition of the second kind at 275.5° C and the quantity investigated was the set of elastic coefficients.

Sodium nitrate crystals belong to the rhombohedral system and six coefficients are necessary for a complete description of its elastic properties. These coefficients are commonly referred to a cartesian system of coordinates oriented in the crystal so that the z axis coincides with the third order symmetry axis, while the x axis is aligned with the second-order symmetry axis. The x and z axes together with the third coordinate axis (y) form a right-handed coordinate system in which the elasticity of the crystal is characterized by the coefficients s_{11}, s_{33}, s_{44}, s_{12}, s_{13}, and s_{14}.

As is known, application of a torque to a cylindrical single crystal specimen produces torsion in addition to bending, while the application of a tensile force produces shear in addition to elongation. These effects are absent only in specimens oriented along the crystallographic symmetry axes, i.e., in our case along the x and z axes. Having measured the speed of sound in such specimens with longitudinal and torsional oscillations one can directly find the four elasticity coefficients

$$s_{11} = 1/\rho c_x^2;\ s_{33} = 1/\rho c_z^2;\ s_{44} = 1/\rho c_z'^2;\quad s_{12} = {}^1/_2 s_{44} + s_{11} - 1/\rho c_x'^2,$$

where c_x and c_z are the velocities of sound in longitudinal oscillations, c_x' and c_z' are the velocities of sound in torsional oscillations, and ρ is the density.*

To find the other coefficients one must work with samples whose axes do not coincide with the symmetry axes. In this case, in view of the above-mentioned effects, calculations become very complicated and the accuracy of determination is greatly impaired.[4] Hence we decided to forego determination of the coefficients s_{13} and s_{14} for the time being.

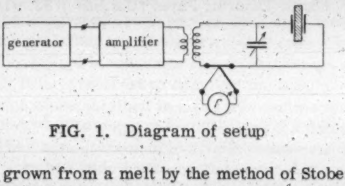

FIG. 1. Diagram of setup

The samples were prepared in the following manner. Rectangular bars of the requisite length and orientation were cut from large single crystals of chemically pure sodium nitrate grown from a melt by the method of Stober. The bars were ground down to a diameter of 5 mm (tolerance 0.01 – 0.04 mm) while held in a parabolic-section groove. The final determination of the orientation was made on a goniometer by measuring the angles between the axis of the rod and the cleavage planes. Only samples whose axes deviated less than 3° from the requisite crystallographic direction were accepted for further experimentation; the ends of these rods were ground off in a special holder.

---

*The density of sodium nitrate at 20° C is 2.261.[3] The variation of the density with temperature can be found with the data given by Kraček.[2]

The speed of sound was measured by the "composite rod" method[5] following the procedure developed by one of the present writers.[6] The method consists of measuring the natural frequency of oscillation of a composite rod consisting of a cylindrical quartz piezocrystal and a sample of the same diameter cemented to its end. The velocity of sound in the sample (both with longitudinal and with torsional oscillations) is calculated by means of the formula $C = 2\pi f\ell/z$, where z is a root of the equation

$$\frac{\tan z}{z} = \frac{P}{p}\,\frac{\tan((n+1)\pi f/f_0)}{(n+1)\pi f/f_0}.$$

Here. P is the weight of the quartz crystal, p the weight of the sample, ℓ the length of the sample, f_0 the natural frequency of oscillation of the quartz rod, f the natural frequency of the composite rod, and n the order of the harmonic.

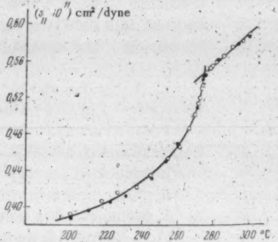

FIG. 2

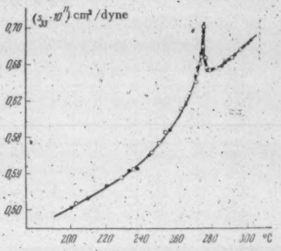

FIG. 3

We used cylindrical quartz rods 16 and 19 mm in length and 5.00 mm in diameter cut along the electric axis. The contact electrodes were applied chemically. Location of the electrodes was varied according to the mode it was required to excite. The samples were cemented to the quartz by means of an adhesive of water glass and talcum. The cement was allowed to set for a period of 2 hours at a temperature of 180° C and a pressure of 0.5 kg on the ends.

A holder of special design (located in a thermostatic chamber) clamped the quartz rod at the node and at the same time served to apply the voltage to the electrodes. The leads from the quartz-rod holder were connected to an oscillating tank circuit. The last was inductively coupled with a coil which was fed through an amplifier from a GSS-6 type standard signal generator. The current in the tank circuit was measured by a sensitive vacuum-thermocouple galvanometer connected between the capacitance and the inductance (Fig. 1).

The frequency of the tank circuit could be matched to the natural frequency of the composite rod by appropriate adjustment of the variable capacitor. Then as the frequency of oscillation of the generator is gradually changed the resonance curve of the circuit current exhibits a deep dip due to the sharp decrease in the impedance of the quartz rod at resonance. Measuring the frequency corresponding to the center of the dip with an accurate wavemeter, we obtain the natural frequency of the composite rod. The natural frequency of the quartz rod alone is determined in an analogous manner.

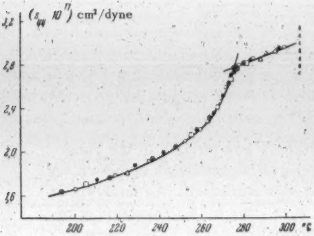

FIG. 4

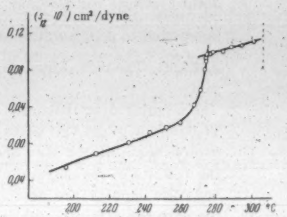

FIG. 5

Preliminary tests showed that the absorption of sound in the sodium nitrate is very small for the entire range of investigated temperatures, which makes it possible to use specimens having a length of about half the wavelength of sound (or close to the full wavelength). This does away with the necessity of taking into account the mass of the electrodes and of the layer of cement; there is also no need to allow for the effect of transverse compression of the sample incident to longitudinal oscillations. The corresponding corrections proved to be smaller than the random experimental errors. Moreover, the fact that the absorption is very small indicates the absence of any noticeable dispersion of sound. Hence one can disregard the fact that the frequency of the longitudinal oscillations (~ 170 cps) differed somewhat from the frequency of the torsional oscillations (~ 120 cps).

The final results of the measurements are shown in the accompanying table and Figs. 2 through 5. The table lists the values of the elasticity coefficients obtained by smoothing and interpolation of the experimental curves in the temperature interval from 20 to 300° C. The figures show the variation of the coefficients in the temperature interval from 200 to 300° C, i.e., the vicinity of the phase transition point.

As can be seen from the figures the elasticity coefficients of an $NaNO_3$ crystal change in different manners at the phase transition point: the constant s_{33} exhibits a jump, while in the case of the coefficients s_{11}, s_{44}, and s_{12} only the derivatives with respect to the temperature show a true jump. As Dzialoshinskii and Lifshitz[7] showed, this fact is in agreement with the theory of one phase transition of the second kind.

°C	$(s \cdot 10^{11})$ cm²/dyne			
	s_{11}	s_{33}	s_{44}	s_{12}
20	0.32	0.42	1.18	−0.05
100	0.34	0.45	1.34	−0.04
150	0.36	0.47	1.45	-0.03_5
200	0.39	0.50	1.65	−0.02
230	0.41_5	0.54	1.86	0.00
250	0.44_5	0.57	2.07	$+0.01_5$
260	0.46_5	0.60	2.20	$+0.02_5$
270	0.50	0.64	2.48	+0.05
275.5	0.54_5	0.70	2.78	$+0.09_5$
280	0.55_5	0.65_5	2.82	+0.10
290	0.57	0.66_5	2.88	$+0.10_5$
300	0.59	0.68_5	2.95	+0.11

---

[1] L. D. Landau and E. M. Lifshitz, Статистическая физика (Statistical Physics) Moscow, 1951.

[2] F. C. Kracek, J. Amer. Chem. Soc. 53, 2609 (1931); Kracek, Posnjak, and Hendricks, J. Amer. Chem. Soc. 53, 3339 (1931).

[3] Handbook of Chemistry and Physics, 34 ed., 1952-1953.

[4] R. F. S. Hearmon, Revs. Mod. Phys. 18, 409 (1946).

[5] J. Stefan, Wiener Berichte 57, 697 (1868).

[6] M. I. Kornfel'd, J. Exptl. Theoret. Phys. (U.S.S.R.) 13, 116 (1943); M. I. Kornfel'd and E. M. Zhurkhovitskii, J. Tech. Phys. (U.S.S.R.) 25, 1998 (1955).

[7] I. E. Dzialoshinskii and E. M. Lifshitz, this issue, 233.

Translated by E. J. Rosen

5

SOVIET PHYSICS JETP VOLUME 6, NUMBER 1 JANUARY, 1958

POLARIZATION IN (p—p) SCATTERING AT 635 MEV

M. G. MESCHERIAKOV, S. B. NURUSHEV, and G. D. STOLETOV

Joint Institute for Nuclear Research

Submitted to JETP editor April 16, 1957

J. Exptl. Theoret. Phys. (U.S.S.R.) 33, 37-45 (July, 1957)

The angular distribution of polarization arising in (p—p) scattering was studied in the range $11.6 \leq \theta \leq 90.3°$ (cms) by means of single and paired telescopes of scintillation counters. A proton beam of 635 Mev energy and polarization of 0.58 ± 0.03 was employed. An analysis of the results of measurement of the differential cross-sections $\sigma_0(\theta)$ for elastic scattering of 657 Mev unpolarized protons, was performed on basis of the optical model of (p—p) scattering with the aim of establishing the nature of interference between the Coulomb and nuclear scattering amplitudes. The polarization data can be satisfactorily approximated by a function of the form (9). The presence of the term $\sin\theta\cos\theta\, P_4(\cos\theta)$ in this formula indicates that triplet F-states play an important role in the scattering. It is found that at 635 Mev the polarization in quasi-elastic (p—p)-scattering by beryllium comprises about 85% of the polarization of protons scattered by hydrogen.

I. INTRODUCTION

It is well known that the empirical facts examined by nuclear shell theory as well as the observations on the polarization of fast nucleons resulting from elastic scattering by nuclei are in general agreement with predictions based on the assumption that nuclear forces have a non-central character connected in some way with a spin-orbit interaction. The source of such interactions between nuclei, in the final analysis, must be a tensor force between pairs of nucleons. As a result of such forces, nucleon-nucleon interaction in the triplet state gives rise to a polarization of the secondary nucleons. This was first observed by Oxley et al.[1]

The use of high energy polarized nucleons in nucleon-nucleon scattering experiments gives information on the two-nucleon interaction in various spin states. The number of independent experiments needed to analyze uniquely the data from these experiments depends, in the last analysis, on the structure of the scattering matrix. According to Wolfenstein[2] the general form of this matrix in (p—p) scattering is:

$$M = BS + C(\sigma_1 + \sigma_2)\mathbf{n} + {}^1/_2 G[(\sigma_1\mathbf{k})(\sigma_2\mathbf{k}) + (\sigma_1\mathbf{p})(\sigma_2\mathbf{p})]T + {}^1/_2 H[(\sigma_1\mathbf{k})(\sigma_2\mathbf{k}) - (\sigma_1\mathbf{p})(\sigma_2\mathbf{p})]T + N(\sigma_1\mathbf{n})(\sigma_2\mathbf{n})T, \quad (1)$$

where σ_1 and σ_2 are the Pauli spin operators for the incoming and struck protons, S and T are the singlet and triplet projection operators, n, k, and p are unit vectors directed along $k_i \times k_f$, $k_f - k_i$ and $k_i + k_f$, respectively; here k_i and k_f are the initial and final momenta in the center of mass system (c.m.s.). Thus the scattering of protons by protons is described by five complex amplitudes, B, C, G, H, and N, which depend on the energy and on the angle of scattering θ. Of these, B, $C/\sin\theta$, and H are even functions and G and N are odd functions of $\cos\theta$.

Independent experiments on single, double, and triple scattering of protons are needed to establish the amplitudes of the scattering matrix [Eq. (1)].[2,3] The first step in this direction is the measurement of the differential cross-section of scattering for an unpolarized beam impinging on an unpolarized hydrogen target, $\sigma_0(\theta)$; the next step is a measurement of the polarization $P(\theta)$ in the scattering of an initially polarized beam by an unpolarized hydrogen target. Triple scattering in one plane and triple scattering under conditions where the planes of the successive scatterings are perpendicular to each other determine the magnitude of the parameters $D(\theta)$ and $R(\theta)$. These represent the changes in magnitude and direction of the polarization vector upon second scattering. $\sigma_0(\theta)$, $P(\theta)$, $D(\theta)$, and $R(\theta)$ can be expressed as functions of the amplitudes of the scattering matrix in the following way:

$$\sigma_0(\theta) = {}^1/_4|B|^2 + 2|C|^2 + {}^1/_4|G-N|^2 + {}^1/_2|N|^2 + {}^1/_2|H|^2, \quad (2)$$

$$\sigma_0(\theta)\cdot P(\theta) = 2\,\mathrm{Re}(C^*N), \quad (2a)$$

$$\sigma_0(\theta)[1 - D(\theta)] = {}^1/_4|G - N - B|^2 + |H|^2 \quad (2b)$$

which become in the non-relativistic approximation

$$\sigma_0(\theta)R(\theta) = {}^1/_2\,\mathrm{Re}[(G-N)^*(N+H) + B^*(N-H)]\cos\frac{\theta}{2} + \mathrm{Im}[C^*(G-N+B)]\sin\frac{\theta}{2}. \quad (2c)$$

Further experiments can be directed either toward the observation of triple scattering under conditions where a magnetic field is introduced between the first and second scattering perpendicular to the momentum of the singly scattered proton and the vector n, as was done by Segre's group,[3] or toward measurement of the components of the correlation tensor of polarization P_{ik}.[4-6]

In principle, the execution of five of the described experiments determines uniquely the scattering matrix at energies less than or close to the threshold of π-meson production.[6] However, at higher energies, where inelastic processes begin to play a significant role, the determination of the elements of the scattering matrix and the unique determination of the phases from experimental data becomes very difficult. The study of polarization effects in inelastic collisions can give significant additional evidence on the character of the (p—p) interaction.[7]

The work described below, a part of the program of studying elastic and inelastic (p—p) collisions on the six meter synchrocyclotron of the Joint Institute for Nuclear Research, was undertaken with the purpose of getting evidence on the angular distribution of the polarization in (p—p) scattering at 635 Mev. The results of measurements of the differential scattering cross-section of unpolarized protons by protons in the same energy region have been reported earlier.[8-10]

2. EXPERIMENTAL PROCEDURE

The object of the experiment was the measurement of the asymmetry of the scattering of a polarized proton beam by protons. This asymmetry is defined by the relationship $\epsilon = \frac{L - R}{L + R}$, where L and R are the normalized counts of protons scattered to the left and to the right (seen by an observer looking along the beam) at the same angle relative to the beam and in the plane of the original scattering producing the polarization. The technique of obtaining a polarized proton beam at the six meter synchrocyclotron and the determination of the energy of the protons in such beams has been described in our previous paper.[11] In this work we used the beam B (in the nomenclature indicated in Fig. 1 of Ref. 11) containing polarized protons with an energy of 635 ± 15 Mev. This beam had an intensity of about 10^5 protons/cm^2 sec at the position of the second scatterer. The beam intensity was monitored by an ionization chamber filled with argon using an integrating dc amplifier. The degree of polarization of the beam was 0.58 ± 0.03, as determined by experiments involving double scattering of the protons by beryllium.

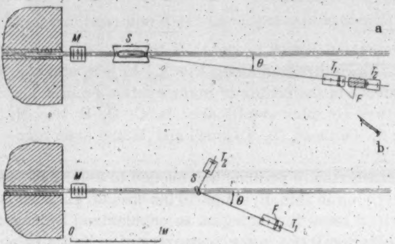

FIG. 1. Experimental setup. M — Monitor, S — Scatterer, T_1, T_2 — telescopes, F — copper absorber.

In the measurements of the asymmetry in the angular region 5° ≤ Θ ≤ 12° in the laboratory system, the scatterer consisted of a thin metallic container filled with liquid hydrogen and placed in vacuum. This is shown in Fig. 1a. The thickness of the hydrogen was 2.1 g/cm^2. The measurements were carried out with the chamber first filled with liquid hydrogen and then empty. The protons came through a 2 cm diameter opening in the shield. The scattered protons were detected by two telescopes T_1 and T_2 standing in back of each other, connected in coincidence, and consisting of scintillation counters which could be locked into the coincidence circuit separately in various combinations. This detector subtended a solid angle of 1.3×10^{-4} sterad for the scattered protons. Since in this angular region the range of the protons from elastic p—p scattering is greater than the range of the π-mesons from the reactions $p + p \rightarrow d + \pi^+$, the elastically scattered protons could be separated from the π-mesons by a 21 cm copper absorber placed between the counters. Taking into account the increased path in the copper due to multiple scattering the threshold for registering the protons was about 560 Mev. One of the deficiencies of this method of distinguishing scattered protons from π-mesons is the large loss in counting rate due to nuclear absorption and scattering of the protons in the absorber.

In the angular region 12° ≤ Θ ≤ 41°, the elastic p—p scattering was measured, as is shown in Fig. 1b, by using a pair of telescopes placed in positions corresponding to the kinematics of the elastic p—p scattering to the right and to the left of the beam. In this case a 3 cm diameter opening in the shield was used. The solid angles subtended by telescopes T_1 and T_2 were 1×10^{-3} and 4.3×10^{-2} sterad respectively. The yield of protons from the elastic p—p scattering was determined by the difference in counting rates of polyethylene and graphite scatterers. These contained the same number of carbon atoms per unit surface area. A control experiment, in which the counting rate was measured when the telescopes were placed in positions not corresponding to the kinematics of the elastic p—p scattering, showed that the contribution of inelastic p—p scatterings was less than 1% of the counting rate.

The same scintillation counters and electronics were used as in our previous work.[11] The number of accidental events was determined, for all angles at which ϵ was measured, by introducing delays for the signals from the counters; ordinarily these accidental events contributed not more than 1% to the counting rate. Before the start of each series of measurements it was established that the counters were operating on the plateaus of the photomultiplier voltages.

The position of the central trajectory of the beam was determined photographically and also by measuring the counting rates of telescopes placed at angles small enough to detect the protons that had suffered multiple scattering. The center of the beam was used to center the scintillators, the angle-measuring circle, and the zero point of the scale on this circle. Special attention was paid to balancing the apparatus in the measurements at small angles. Several checks showed that the shift in the zero point of the angle-measuring device relative to the central trajectory to the beam was less than 0.03°. The error in the asymmetry as influenced by the errors in the measurements of angles and inaccuracies in defining the center of the beam could amount to 5% at Θ = 5° but fell to 0.5% at Θ = 41°. The angular resolution, ± Δθ, was established from the corresponding geometrical factors, the beam size, and the multiple scattering of the protons in the scatterers.

The averaged final results of four series of measurements of the asymmetry, together with the standard measurement errors as well as data on the angular resolution, are presented in Table I. It should be mentioned that the main source of errors in these measurements was the statistical error of the measurements; the errors in the determination of the angles, the errors connected with the measurement of the beam intensity over the profile of the beam, and the errors arising from the shape of the scatterers and dimensions of the scintillators were relatively less important.

TABLE I. Values of the Asymmetry and Polarization in (p—p) Scattering at 635 Mev

$\Theta°$	$\theta°$	$\pm\Delta\theta°$	$\varepsilon \pm \Delta\varepsilon$%	$P_H \pm \Delta P_H$ %	Nature of the Second Scatterer
5	11.6	1.1	-1.3 ± 5.6	-2.2 ± 9.5	H_2
7	16.2	1.2	11.4 ± 2.6	19.7 ± 4.6	»
9	20.8	1.4	16.0 ± 2.1	27.6 ± 3.9	»
12	27.6	1.6	22.3 ± 2.6	38.4 ± 4.9	»
12	27.6	1.6	23.3 ± 1.5	40.2 ± 3.3	CH_2-C
15	34.4	1.6	23.2 ± 1.3	40.0 ± 3.0	»
18	41.2	2.5	24.6 ± 1.1	42.4 ± 2.9	»
21	47.9	2.5	21.9 ± 1.1	37.8 ± 2.7	»
24	54.5	2.5	20.7 ± 0.8	35.7 ± 2.3	»
27	64.0	2.5	17.8 ± 0.8	30.7 ± 2.1	»
30	67.5	2.6	16.2 ± 1.3	27.9 ± 2.7	»
33	73.8	2.6	11.3 ± 1.5	19.5 ± 2.8	»
36	80.1	2.6	9.7 ± 1.4	16.7 ± 2.6	»
39	86.3	2.6	4.9 ± 2.3	8.4 ± 4.0	»
41	90.3	2.6	-0.9 ± 1.4	-1.6 ± 2.5	»

3. ANGULAR DISTRIBUTION OF THE POLARIZATION IN (p—p) SCATTERING

The polarization arising from the p—p scattering in our experiment was calculated from the relation $\epsilon = P P_H$, where P is the polarization of the beam being used, taken as equal to 0.58 ± 0.03. The values of P_H obtained are presented, together with the standard errors, in Table I and in Fig. 2 as a function of the scattering angle in the c.m.s.

The angular distribution of the polarization, P_H has the following features:

(a) The polarization goes through zero at a scattering angle of 90° as it should in view of the identity of the of the colliding particles;

(b) The maximum value of the polarization is 0.42 ± 0.03 at $\theta = 41°$;

(c) At smaller angles the polarization falls rapidly and reaches -0.02 ± 0.09 at $\theta = 11.6°$. In view of the possibility of systematic errors and the large errors associated with the measurements at small angles, one cannot vouch for the validity of this change in sign of the polarization.

Earlier studies of the angular distribution of the polarization in p—p scattering have been carried out in the energy regions 130 — 439 Mev.[12 — 17]* Figure 2 shows, for comparison, the results obtained at 170, 315, and 415 Mev. It is seen that increasing the energy from 415 to 635 Mev does not lead to any further increase in polarization outside of experimental errors.

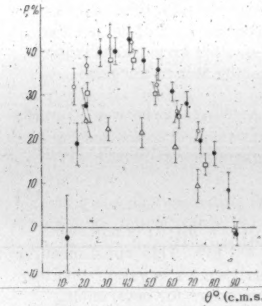

FIG. 2. Dependence of the polarization $P_H(\theta)$ in elastic p—p scattering on the angle of scattering: ● — present work, ○ — 415 Mev,[15] □ — 315 Mev,[12] Δ — 170 Mev.[16]

The fact that the angular distribution of the polarization in p—p scattering does not change significantly as the energy is increased by 200 Mev appears to be a very significant point concerning the p—p interaction, especially if it is kept in mind that in the same energy interval the angular distribution of the p—p scattering changes from an isotropic one to a distribution concentrated at small angles.

4. ELASTIC SCATTERING OF UNPOLARIZED PROTONS BY PROTONS AT 657 MEV

The differential cross-section $\sigma_0(\theta)$ of the elastic p—p scattering consists of three terms

$$\sigma_0(\theta) = \sigma_N(\theta) + \sigma_C\;) + \sigma_{\text{int}}(\theta), \tag{3}$$

corresponding to the cross-section for nuclear scattering, for Coulomb scattering, and for interference between the two, respectively. In the same way one can write for $\sigma_0(\theta)\,P(\theta)$:

$$\sigma_0(\theta)\,P(\theta) = \sigma_N P_N + \sigma_C P_C + (\sigma P)_{\text{int}}. \tag{4}$$

In order to examine the question of the angular dependence of $\sigma_0(\theta)\,P(\theta)$, it is necessary to know the lower limit of the angular range in which only nuclear processes play an important role. In the present study, use was made of data on the differential cross-section of scattering of unpolarized protons by protons obtained in our laboratory at 657 Mev. These data are presented in Table II and Fig. 3, together with their statistical errors. The total elastic p—p scattering cross-section at 657 Mev is $(24.7 \pm 1.0) \times 10^{-27}$ cm^2.[10]

---

*We are indebted to Prof. A. Roberts (Univ. of Rochester) for sending to our laboratory a manuscript in which are described results of experiments on polarization in p—p scattering at 130, 170, and 210 Mev.

In the case of isotropic nuclear (p—p) scattering in the c.m.s., evidence concerning the character of the interference of the amplitudes of the Coulomb and nuclear scattering is obtained from a comparison of observations at small angles of p—p scattering with the sum of the Coulomb and isotropic nuclear scattering. In this way it has been established that at 170 and 260 Mev,[18] and likewise at 330 Mev,[19] the interference between Coulomb and nuclear scattering has a destructive character. For protons having an energy of 330 Mev, Coulomb scattering produces effects at angles of scattering less than 20°.

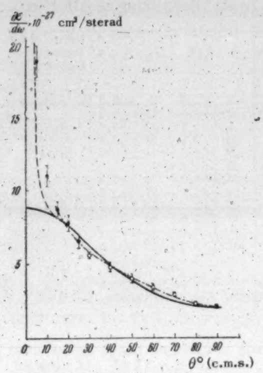

FIG. 3. Dependence of the cross-section for elastic p—p scattering at 657 Mev on the angle of scattering from the following sources: ● — Ref. 10, ○ — Ref. 8, ■ — average of results from (8) and (9); the solid curve corresponds to formula (5); the dashed curve gives the sum $\sigma_N(\theta) + \sigma_C(\theta)$; the dot-dashed curve has been drawn through the points visually.

In view of the strong anisotropy of the p—p scattering at 657 Mev, we had to extrapolate the measurements of $\sigma_N(\theta)$ to sufficiently small angles in the forward direction in order to evaluate the Coulomb effects. This extrapolation was made using the optical model of p—p scattering,[20—22] according to which:

$$\sigma_N(\theta) \sim |J_1(kR\sin\theta)/kR\sin\theta|^2, \tag{5}$$

where J_1 is the Bessel function of the first order, $R = (\sigma_t/2\pi)^{1/2}$, $k = (ME/2\hbar^2)^{1/2}$, and M and E are the mass of the proton and its energy in the laboratory system. At 657 Mev the total cross-section σ_t is about 41×10^{27} cm^2,[23] so that $kR = 2.28$. The determination of the proportionality constant in Eq. (5) was carried out by a least squares fit to the experimental data in the range $20 \leq \theta \leq 90°$. The solid curve of Fig. 3 shows the angular distribution given by Eq. (5). The extent to which the calculated curve represents the experimental data in the angular region considered is shown by the fact that the Gaussian mean square relative deviation of the calculated points from the experimental ones comes out to be ~ 0.05. The dashed curve in Fig. 3 gives the sum of the nuclear scattering, given by Eq. (5), and the cross-section for purely Coulomb scattering, $\sigma_C(\theta)$. The latter was calculated by Mott's formula:

$$\sigma_C(\theta) = \left(\frac{\eta}{2k}\right)^2 \left[\sin^{-4}\frac{\theta}{2} + \cos^{-4}\frac{\theta}{2} - \sin^{-2}\frac{\theta}{2}\cos^{-2}\frac{\theta}{2}\cos\left(2\eta\ln\tan\frac{\theta}{2}\right)\right], \tag{6}$$

where, following Breit,[24]

$$\eta = \left(\frac{e^2}{\hbar c}\right)\left(1 + \frac{E}{Mc^2}\right)\left[\frac{E}{Mc^2}\left(2 + \frac{E}{Mc^2}\right)\right]^{-1/2}. \tag{7}$$

From Fig. 3 it is seen that the total cross-section obtained in this way $\sigma_N(\theta) + \sigma_C(\theta)$ is somewhat less than the corresponding experimental values, $\sigma_0(\theta)$, in the interval $5 \leq \theta \leq 15°$. This would mean, if the method used to determine the nuclear p—p scattering in the region of small angles is valid,* that the interference term in Eq. (3) is positive at 657 Mev. The accuracy of this procedure for determining $\sigma_{\text{int}}(\theta)$ is not large, and for this reasion it is impossible to exclude the possibility that $\sigma_{\text{int}}(\theta) = 0$. To the extent that the real part of the amplitude of the Coulomb scattering is repulsive and significantly greater than the imaginary part, then if $\sigma_{\text{int}}(\theta) > 0$, the real part of the amplitude of the nuclear scattering in the forward direction must also be repulsive. The imaginary part of the amplitude of the forward nuclear scattering must be positive and equal to $k\sigma_t/4\pi$.

5. ANGULAR DEPENDENCE OF $\sigma_0(\theta)P(\theta)$

From the analysis of the angular dependence of the asymmetric part of the p—p scattering cross-section, $\sigma_0(\theta)P(\theta)$, it is possible to get some evidence concerning the highest orbital angular momentum contributing to the scattering. We start from the statement of Wolfenstein[26] that if the scattering is determined by interactions in states of angular momentum up to L_{max}, then

---

*Recently Rarita[25] has brought forth arguments against the use of the optical model of p—p scattering at an energy of about one Bev.

$$\sigma_0(\theta)P(\theta)=\sin\theta\cos\theta\sum_{n=0}^{N}a_{2n}\cos^{2n}\theta, \qquad (8)$$

where $N = L_{max} - 1$ for odd L, and $N = L_{max} - 2$ for even L. In the calculation of $\sigma_0(\theta)P(\theta)$, the values of $\sigma_0(\theta)$ for angles for which the measurements of had been carried out were taken from a smooth curve drawn visually through the experimental points taking account the probable errors and the angular resoltuion (see Fig. 3). On the assumption that the angular distribution of polarization in p—p scattering does not change if the energy is raised from 635 to 657 Mev, the values of $\sigma_0(\theta)P(\theta)$ obtained in this work can be ascribed to an energy of 657 Mev.

TABLE II. Summary of Data on the Differential p—p Scattering Cross-Section at 657 Mev

Angle of Scattering (c.m.s.)	$\sigma_0(\theta)\times 10^{27}$ cm²/sterad	Literature Source
5°	18.9±1.1	[10]
10°	11.0±0.7	»
15°	8.67±0.53	»
20°	7.75±0.48	»
25°	6.56±0.40	»
30°	5.58±0.15	[8]
40°	4.78±0.26	»
50°	3.99±0.20	»
60°	3.41±0.13	»
70°	2.94±0.12	»
80°	2.20±0.05	»
90°	2.10±0.07	»
90°	2.05±0.07	[9]

Figure 4 shows the dependence of $\sigma_0(\theta)P(\theta)/\sin\theta\cos\theta$ on $\cos^2\theta$ in the interval $16.2° \leq \theta \leq 80.5°$. Shown also are the limits of error which have been calculated taking into account all the errors contributing to the measurements of $\sigma_0(\theta)$ and $P(\theta)$. The data show that the angular distribution of $\sigma_0(\theta)P(\theta)$ definitely differs from $\sin\theta\cos\theta$. This latter is the form expected if the polarization arose from the interference only of triplet P-states.

A least squares fit was made to the values of $\sigma_0(\theta)P(\theta)/\sin\theta\cos\theta$ using even Legendre polynomials. After several attempts with various numbers of polynomials it was found possible to approximate the experimental data by the function:

$$\sigma_0(\theta)P(\theta)=\sin\theta\cos\theta\{(3.20\pm0{,}08)P_0(\cos\theta)+(3.13\pm0.29)P_2(\cos\theta)$$
$$+(1.20\pm0.32)P_4(\cos\theta)-(0.12\pm0.37)P_6(\cos\theta)\}\cdot10^{-27}\ \text{cm}^2/\text{sterad}. \qquad (9)$$

This expression gives a sufficiently good fit to the experimental data as is evidenced by the magnitude of the value of the sum of the least squares

$$M=\sum_{i=1}^{11}\{\delta[\sigma_0(\theta)P(\theta)]_i/\Delta[\sigma_0(\theta)P(\theta)]_i\}^2$$

(where $\delta[\sigma_0(\theta)P(\theta)]$ is the difference, at an angle θ_i, of the calculated value of $\sigma_0(\theta)P(\theta)$ from the experimental value, and $\Delta[\sigma_0(\theta)P(\theta)]$, is the probable error in the determination of $\sigma_0(\theta)P(\theta)$ from the experimental data for this angle). The value of M is equal to 1.6; the expected value of M, equal to the difference between the number of experimental points and the number of independent parameters in the approximating function, should equal 7. The distribution calculated from Eq. (9) is shown in Fig. 4 as a solid curve.

That the approximating function contains a term $\sin\theta\cos\theta P_4(\cos\theta)$, with a coefficient whose value is several times the probable error, appears to be definitely established. Thus the results of the present measurements indicate the presence of non-vanishing terms up to and including $\sin\theta\cos^5\theta$ in the expansion of $\sigma_0(\theta)P(\theta)$. This means that at the energies in question triplet P- and F-states play a significant role in p—p scattering. The calculations of Breit et al.,[27] carried out taking into account orbital momenta $L < 4$, indicate that a term of the form $\sin\theta\cos^5\theta$ can appear in the expansion of $\sigma_0(\theta)P(\theta)$ only if interactions occur in the $^3F_4$-state.

The fact that partial waves with angular momenta $L = 3$ contributed strongly to a scattering associated with a large polarization is, by itself, evidence that the p—p interaction in the triplet F-states is noncentral to a considerable extent.

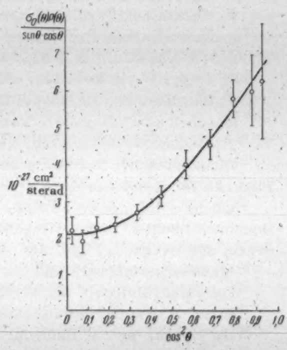

FIG. 4. Dependence of $\sigma_0(\theta)P(\theta)/\sin\theta\cos\theta$ on $\cos^2\theta$. The solid curve shows the function (9).

6. CONCERNING POLARIZATION IN QUASI-ELASTIC p—p SCATTERING

It has been noted earlier[11] that the polarization of the protons undergoing quasi-elastic scattering from Be at an angle $\theta = 40°$ is only a little less than the polarization in free p—p scattering. The results of the present experiments indicate that a similar situation exists in a large angular region of scattering. A comparison of the data given in Table I and Fig. 7 of Ref. 11 indicates that, in the angular region $27 \leq \theta \leq 90°$, the polarization in the quasi-elastic scattering from beryllium is about 85% of the polarization of protons scattered in hydrogen. This is in contrast to the situation in the energy region of ~ 300 Mev, where, according to Donaldson and Bradner,[28] the quasi-elastic p—p scattering leads to a polarization lower by almost a factor of two than does elastic scattering.

These results indicate definitely that raising the energy from 300 to 600 Mev washes out, to a large extent, the difference between scattering by free protons and by protons bound in nuclei.

7. CONCLUSIONS

Experiments determining the asymmetry in the scattering of polarized protons by hydrogen at 635 Mev have established a polarization, which does not differ significantly in either amount or angular distribution from the polarization p—p scattering in the region 300 — 400 Mev.

If an analysis of the experimental data on p—p scattering at 657 Mev is carried out on the basis of the optical model, it is found that the interference between Coulomb and nuclear scattering is not large, the small amount leading to a raising of the differential p—p scattering cross-section in the regions $5 \leq \theta \leq 15°$.

The angular distribution of the asymmetric part of the p—p scattering cross-section contains the term $\sin\theta\cos^5\theta$ which means that triplet F-states contribute significantly to the scattering in the investigated energy region.

No significant difference in the angular distribution or in the amount of polarization is observed at 635 Mev between quasi-elastic p—p scattering in beryllium and elastic p—p scattering.

The authors express their thanks to R. M. Ryndin and L. M. Soroko for participating in discussions of the results of the present work; to A. S. Kuznetsov for help in the construction of the electronic apparatus; and to L. A. Kuliukin for carrying out a series of calculations.

---

[1] C. Oxley, W. Cartwright, J. Rouvina, Phys. Rev. **93**, 806 (1954).

[2] L. Wolfenstein, Phys. Rev. **96**, 1654 (1954).

[3] E. Segre, Physica **22**, 1079 (1956). J. Simmons, Phys. Rev. 104, 416 (1956).

[4] H. Stapp, Bull. Am. Phys. Soc. **29**, 8, 19 (1954).

[5] V. Vladimirskii and Ia. Smorodinskii, Dokl. Akad. Nauk SSSR **104**, 713 (1955).

[6] J. Smorodinskii, Proc. CERN Symposium, **2**, 148 (1956); Puzikov, Ryndin, and Smorodinskii, J. Exptl. Theoret. Phys. (U.S.S.R.) **32**, 592 (1957), Soviet Phys. JETP **5**, 489 (1957).

[7] R. Tripp, Phys. Rev. **102**, 862 (1956).

[8] N. Bogachev and I. Vzorov, Dokl. Akad. Nauk SSSR **99**, 931 (1954).

[9] Mescheriakov, Neganov, Soroko, and Vzorov, Dokl. Akad. Nauk SSSR **99**, 959 (1954).

[10] N. Bogachev, Dokl. Akad. Nauk SSSR **108**, 806 (1956), Soviet Phys. "Doklady" **1**, 361 (1956).

[11] Mescheriakov, Nurushev, and Stoletov, J. Exptl. Theoret. Phys. (U.S.S.R.) **31**, 361 (1956), Soviet Phys. JETP **4**, 337 (1957).

[12] Chamberlain, Segre, Tripp, Wiegand, and Ypsilantis, Phys. Rev. **93**, 1430 (1954); Chamberlain, Donaldson, Segre, Tripp, Wiegand, and Ypsilantis, Phys. Rev. **95**, 850 (1954); Chamberlain, Pettengill, Segre, and Wiegand, Phys. Rev. **95**, 1348 (1954).

[13] Marshall, Marshall, and Carvalho, Phys. Rev. **93**, 1431 (1954).

[14] Carvalho, Heiberg, Marshall, and Marshall, Phys. Rev. **94**, 1796 (1954).

[15] Kane, Stallwood, Sutton, Fields, and Fox, Phys. Rev. **95**, 1694 (1954).

[16] D. Fischer and J. Baldwin, Phys. Rev. **100**, 1445 (1955).

[17] Baskir, Hafner, Roberts, and Tinlot. Polarization in proton-proton scattering at 130, 170 and 210 Mev, NYO-7818 (1956).

[18] O. Chamberlain and J. Garrison, Phys. Rev. **95**, 1349 (1954).

[19] D. Fischer and G. Goldhaber, Phys. Rev. **95**, 1350 (1954).

[20] Ia. Smorodinskii, Проблемы современной физики, (Problems of Contemporary Physics) **7**, No. 7 (1954).

[21] R. Serber and W. Rarita, Phys. Rev. **99**, 629 (1955).
[22] A. Batson, L. Riddiford, Proc. Roy. Soc. A**237**, 175 (1956).
[23] Dzhelepov, Moskalev, and Medved, Dokl. Akad. Nauk SSSR **104**, 380 (1955).
[24] G. Breit, Phys. Rev. **99**, 1581 (1955).
[25] W. Rarita, Phys. Rev. **104**, 221 (1956).
[26] L. Wolfenstein, Phys. Rev. **75**, 1664 (1949).
[27] Breit, Ehrman, Saperstein, and Hull, Phys. Rev. **96**, 807 (1954).
[28] R. Donaldson and H. Bradner, Phys. Rev. **99**, 892 (1955).

Translated by A Turkevich
6

SOVIET PHYSICS JETP VOLUME 6, NUMBER 1 JANUARY, 1958

COUPLING BETWEEN INTERMOLECULAR AND INTRAMOLECULAR VIBRATIONS IN A CRYSTAL

N. N. PORFIR'EVA

Leningrad Shipbuilding Institute

Submitted to JETP editor July 23, 1956

J. Exptl. Theoret. Phys. (U.S.S.R.) 33, 47-52 (July, 1957)

A model of a molecular cyrstal with "semi-rigid" molecules is examined. The conditions for separation of intermolecular and intramolecular vibrations are investigated. By way of example a two-dimensional lattice with C_{4v} symmetry is examined.

BORN'S theory of crystal lattices gives the most general solution of the problem of propagation of elastic waves in a crystal. In the case of complex molecular crystals, however, direct application of the theory leads merely to several very general deductions; hence it is natural to seek approximate models that would make it possible to move forward in utilizing the Born theory of crystal lattices. One such model for molecular cyrstals consists of separating the molecules as a whole from the lattice; in the first approximation the molecules are considered as solids with six degrees of freedom.[1] Solution of the problem formulated in this way made it possible to investigate the propagation of orientational-translational waves in the crystal and to determine the conditions for separation of the translational and orientational oscillations. In the following approximation the molecules are regarded as "semi-rigid" systems, that is, systems for which the magnitude of the intramolecular interactions is much greater than that of the intermolecular ones. In this case the interaction between molecules can be treated as a perturbation.

The solution should result in free-molecule vibrations that are modulated by lattice vibrations. A problem of this kind has been examined by Davydov,[2] but was solved only in the general form and primarily from the standpoint of energy transfer from the intramolecular vibrations to the lattice vibrations, a transfer leading to attenuation of the vibrations and broadening of the absorption bands.

A more detailed solution of this problem permits an investigation of the interaction between intermolecular and intramolecular vibrations.

The present study is devoted to an examination of the coupling between intermolecular and intramolecular vibrations and the conditions for their separation. We solve only the classical problem through the application of group theory.

1. Let us examine a three-dimensional crystal containing N molecules of S atoms each. The unit cell contains ν molecules; n is the ordinal number of the cell and n_ν is the index of the molecule. The

potential energy of the interaction of the atoms in the crystal are given by

$$U=\frac{1}{2}\sum_{n_\nu,\,n'_\nu,\,\alpha,\,\alpha'}\lambda^{\alpha\alpha'}_{n_\nu n'_\nu}(\mathbf{r}^{\alpha}_{n_\nu}-\mathbf{r}^{\alpha'}_{n'_\nu})^2\cos^2\gamma^{\alpha\alpha'}_{n_\nu n'_\nu}+\sum_{n_\nu,\,\alpha,\,\beta}k^{\alpha\beta}_{n_\nu}(\mathbf{r}^{\alpha}_{n_\nu}-\mathbf{r}^{\beta}_{n_\nu})^2\cos^2\gamma^{\alpha\beta}_{n_\nu}, \tag{1}$$

where $\mathbf{r}^{\alpha}_{n_\nu}$ is the displacement vector of the αth atom of the n_νth molecule, $k^{\alpha\beta}_{n_\nu}$ and $\lambda^{\alpha\alpha'}_{n_\nu n'_\nu}$ are the coefficients of elastic interaction of two atoms belonging and not belonging to one and the same molecule, respectively, and $\gamma^{\alpha\alpha'}_{n_\nu n'_\nu}$ is the angle between the vector $\mathbf{r}^{\alpha}_{n_\nu}-\mathbf{r}^{\alpha'}_{n'_\nu}$ and the line connecting the centers of gravity of both atoms in the equilibrium position. This line has an invariable orientation in space; we denote its direction cosines relative to the coordinate axes through a, b and c with appropriate indices.

Let us separate the displacements of the molecule as a whole; to this end we write

$$\mathbf{r}^{\alpha}_{n_\nu}=\mathbf{r}_{n_\nu}+\mathbf{l}^{\alpha}_{n_\nu}\times\theta_{n_\nu}+\sum_{\beta}\boldsymbol{\eta}^{\alpha\beta}_{n_\nu}, \tag{2}$$

where $\mathbf{r}_{n_\nu}$ is displacement of the center of gravity of the nth molecule, θ_{n_ν} is the angle of rotation of the n_νth molecule about its instantaneous axis, $\mathbf{l}^{\alpha}_{n_\nu}$ is the distance of the α atom from the instantaneous axis, $\eta^{\alpha\beta}_{n_\nu}$ is the relative displacement of atoms α and β in the molecule, satisfying the condition

$$m_{n_\nu\alpha}\boldsymbol{\eta}^{\alpha\beta}_{n_\nu}+m_{n_\nu\beta}\boldsymbol{\eta}^{\beta\alpha}_{n_\nu}=0$$

and expressed in the system rigidly connected with the principal axes of the ellipsoid of inertia of the molecule. Here $m_{n_\nu\alpha}$ and $m_{n_\nu\beta}$ are the masses of the α and β atoms in the nth molecule.

For small angular oscillations

$$\theta_{n_\nu}=\vartheta_{n_\nu}+\varphi_{n_\nu}+\psi_{n_\nu},$$

where ϑ_{n_ν}, φ_{n_ν} and ψ_{n_ν} are the angles of rotation about the principal axes of the inertia ellipsoid.

In the new coordinates the total energy of the crystal is given by

$$\begin{aligned}U=\frac{1}{2}\sum_{n_\nu n'_\nu\alpha\alpha'}\lambda^{\alpha\alpha'}_{n_\nu n'_\nu}\Big\{&(\mathbf{r}_{n_\nu}-\mathbf{r}_{n'_\nu})+\mathbf{l}^{\alpha}_{n_\nu}\times(\vartheta_{n_\nu}+\varphi_{n_\nu}+\psi_{n_\nu})\\&-\mathbf{l}^{\alpha'}_{n'_\nu}\times(\vartheta_{n'_\nu}+\varphi_{n'_\nu}+\psi_{n'_\nu})+\sum_{\beta}^{s}\boldsymbol{\eta}^{\alpha\beta}_{n_\nu}-\sum_{\beta'}^{s}\eta^{\alpha'\beta'}_{n'_\nu}\Big\}^2\cos^2\gamma^{\alpha\alpha'}_{n_\nu n'_\nu}+\sum_{n_\nu\alpha\beta}^{sN}k^{\alpha\beta}_{n_\nu}(\boldsymbol{\eta}^{\alpha\beta}_{n_\nu x})^2,\\T=\frac{1}{2}\sum_{n_\nu}^{N}\Big\{&M_{n_\nu}\dot{\mathbf{r}}^2_{n_\nu}+J_{n_\nu\vartheta}\dot{\vartheta}^2_{n_\nu}+J_{n_\nu\varphi}\dot{\varphi}^2_{n_\nu}+J_{n_\nu\psi}\dot{\psi}^2_{n_\nu}+\sum_{\alpha,\beta}\mu^{\alpha\beta}_{n_\nu}(\dot{\boldsymbol{\eta}}^{\alpha\beta}_{n_\nu})^2\Big\},\end{aligned} \tag{3}$$

where M_{n_ν} is the mass of the molecule and $\mu^{\alpha\beta}_{n_\nu}$ is the reduced mass of the α and β atoms of the nth molecule.

Writing the Lagrangian and seeking the solution in the form of plane waves

$$x_{n_\nu}=X_\nu\exp\{i(\omega t-a_x n\tau)\},\qquad \vartheta_{n_\nu x}=\Theta_{\nu x}\exp\{i(\omega t-a_{\vartheta x}n\tau)\},\quad \eta^{\alpha\beta}_{n\nu x}=H^{\alpha\beta}_{\nu x}\exp\{i(\omega t-a_x n\tau)\}, \tag{4}$$

where a is the distance between molecules belonging to one simple lattice, we obtain the determinant:

$$\left|\begin{array}{c|c}-M_{n_\nu}\omega^2+A\;.\;.\;R_1\;.\;.\;.\;K\;.\;.\;. & P\;.\;.\;.\\ .\;.\;R_2\;.\;.\;.\;.\;.\;.\;.\;.\;.\;. & .\;.\;.\;.\;.\\ .\;.\;.\;.\;.\;.\;.\;.\;.\;.\;.\;.\;.\;. & .\;.\;.\;.\;.\\ .\;.\;K\;.\;.\;-J_{n_\nu\vartheta}\omega^2+B\;.\;.\;.\;N\;.\;. & M\;.\;.\;.\\ .\;.\;.\;.\;.\;.\;.\;.\;.\;.\;.\;.\;.\;. & .\;.\;.\;.\;.\\ \hline .\;.\;P\;.\;.\;.\;M\;.\;.\;.\;.\;.\;. & -\mu\omega^2+C\;.\;.\;.\\ .\;.\;.\;.\;.\;.\;.\;.\;.\;.\;.\;.\;.\;. & .\;.\;.\;.\;.\\ .\;.\;.\;.\;.\;.\;.\;.\;.\;.\;.\;.\;.\;. & L\;.\;.\;.\end{array}\right|$$

where

$$\begin{gathered}
A=\sum_{\alpha\alpha'n'}\lambda^{\alpha\alpha'}_{n_\nu n'_\nu}(a^{\alpha\alpha'}_{n_\nu n'_\nu})^2,\quad R_1=\sum_{\alpha\alpha'}\lambda^{\alpha\alpha'}_{n_\nu n'_\nu}a^{\alpha\alpha'}_{n_\nu n'_\nu}b^{\alpha\alpha'}_{n_\nu n'_\nu}e^{i(na_x-n'a_y)\tau},\quad R_2=\sum_{\alpha\alpha'}\lambda^{\alpha\alpha'}_{n_\nu n'_\nu}(a^{\alpha\alpha'}_{n_\nu n'_\nu})^2e^{i(n-n')a_x\tau},\\
K=\sum_{\alpha\alpha'}\lambda^{\alpha\alpha'}_{n_\nu n'_\nu}a^{\alpha\alpha'}_{n_\nu n'_\nu}(c^{\alpha\alpha'}_{n_\nu n'_\nu}l^{\alpha}_{n'_\nu y}-b^{\alpha\alpha'}_{n_\nu n'_\nu}l^{\alpha'}_{n'_\nu z})e^{i(n-n')a_x\tau},\quad B=\sum_{\alpha\alpha'n'}{}'\lambda^{\alpha\alpha'}_{n_\nu n'_\nu}[(b^{\alpha\alpha'}_{n_\nu n'_\nu}l^{\alpha}_{n_\nu z})^2-(c^{\alpha\alpha'}_{n_\nu n'_\nu}l_{n_\nu y})^2],\\
N=-\sum_{\alpha\alpha'}\lambda^{\alpha\alpha'}_{n_\nu n'_\nu}[(b^{\alpha\alpha'}_{n_\nu n'_\nu})^2l^{\alpha}_{n_\nu z}l^{\alpha'}_{n'_\nu z}+(c^{\alpha\alpha'}_{n_\nu n'_\nu})^2l^{\alpha}_{n_\nu y}l^{\alpha'}_{n'_\nu y}]e^{i(n-n')a_x\tau},\quad P=\sum_{\alpha}{}'\lambda^{\alpha\alpha'}_{n_\nu n'_\nu}(a^{\alpha\alpha'}_{n_\nu n'_\nu})^2e^{i(n-n')a_x\tau},\\
M=\sum_{\alpha}{}'\lambda^{\alpha\alpha'}_{n_\nu n'_\nu}(b^{\alpha\alpha'}_{n_\nu n'_\nu}l^{\alpha}_{n_\nu z}-c^{\alpha\alpha'}_{n_\nu n'_\nu}l^{\alpha}_{n_\nu y})a^{\alpha\alpha'}_{n_\nu n'_\nu}e^{i(n-n')a_x\tau},\quad C=k^{\alpha\beta}_{n_\nu}+\sum_{n'\alpha'}\lambda^{\alpha\alpha'}_{n_\nu n'_\nu}(a^{\alpha\alpha'}_{n_\nu n'_\nu})^2,\quad L=\lambda^{\alpha\alpha'}_{n_\nu n'_\nu}e^{i(n-n')a_x\tau}.
\end{gathered}\tag{5}$$

From expressions (3) and (5) we see that the variables do not separate along the dispersion curve; consequently, all types of vibrations are coupled with each other.

The motion of absolutely rigid molecules is determined by the condition

$$\eta^{\alpha\alpha'}_{n_\nu n'_\nu}=0,$$

i.e., is described by the determinant in the upper left-hand corner (this case was examined earlier in Ref. 3).

The movement of atoms inside a fixed molecule, obtained when the motion of the molecule as a whole is eliminated is described by the determinant in the lower right hand corner. We see that the intramolecular frequencies in the crystal are displaced by an amount on the order of the natural frequencies of the crystal. Each frequency of the isolated molecule splits and gives rise to ν dispersion modes.

In both intermolecular and intramolecular vibrations there is obtained a determinant of the $3s\nu$th order in which the nondiagonal terms between the blocks contain linear functions of the coefficients λ, i.e., quantities of the next lower order compared with terms pertaining to the intramolecular oscillations. Solution of the determinant in general form is impossible. However, the presence of different orders of the coefficients indicates than an approximate solution is possible in principle.

The most direct, although cumbersome, method consists of reducing the secular equation to a polynomial form, for example, by the method of A. N. Krylov, and then finding the roots by Newton's method of successive approximations.

The presence of symmetry in the crystal makes it possible to utilize the method of group theory to quasi-linearize the determinant that corresponds to the limiting frequencies by introducing geometrically symmetrical coordinates. The blocks in the determinant thus obtained correspond to the coordinates of the non-separating oscillations. The frequencies associated with the determinant blocks can also be found by Newton's method.

Separation of the lattice and intermolecular vibrations is possible only for the limiting frequencies in special cases of symmetry. It will be seen from the expression for the potential energy that the intramolecular displacement vectors $\boldsymbol{\eta}^{\alpha\beta}_{n_\nu}$ enter into the vector $\mathbf{r}^{\alpha}_{n_\nu}$ with different signs relative to the coordinates of the displacement of the center of gravity of the molecules for each atomic pair α and β. The same thing applies to the rotation vectors $\mathbf{l}_n \times \boldsymbol{\theta}_n$. This means that these vectors are characterized by identical symmetry relative to the coordinates of displacement of the center of gravity and that therefore the separation of the translational and intermolecular oscillations for the limiting frequencies occurs for the same types of symmetry as the separation of the translational and orientational oscillations. The conditions for separation of the last have been analyzed in Refs. 1 and 3.

2. By way of illustrative example let us examine a two-dimensional square lattice containing two diatomic molecules per unit cell (see figure). For it to be possible to determine the limiting frequencies corresponding not only to the wave vector $\tau = 0$ but also to the vector $\tau = \pi/a$, let us double the number of molecules in the cell.

According to expression (2), the coordinates of the atoms will be

$$\begin{gathered}
x^{\alpha}_{2k-1}=x_{2k-1}+{}^1/_2(-1)^{\alpha}\,l\vartheta_{2k-1};\quad x^{\alpha}_{2k}=x_{2k}+{}^1/_2(-1)^{\alpha}\,\eta_{2k};\\
y^{\alpha}_{2k-1}=y_{2k-1}+{}^1/_2(-1)^{\alpha}\,\eta_{2k-1};\quad y^{\alpha}_{2k}=y_{2k}-{}^1/_2(-1)^{\alpha}\,l\vartheta_{2k}
\end{gathered}\tag{6}$$

($\alpha = 1, 2$ and $k = 1, 2$). We shall neglect second-order quantities in the projections of the displacements.

Let us agree to limit our examination to interaction with nearest neighbors: then each molecule will interact only with 8 neighbors and consequently each atom with 14 neighboring atoms. Accordingly, the total energy of the unit cell, corresponding to the limiting frequencies, can be written in the form

$$U = f[(y_1 - y_2) - (x_1 - x_2)]^2 + f[(y_2 - y_3) - (x_2 - x_3)]^2 + f[(y_3 - y_4) + (x_3 - x_4)]^2 + f[(y_4 - y_1) - (x_4 - x_1)]^2$$
$$+ {}^1/_4 f[(\eta_1 + \eta_2)^2 + (\eta_2 + \eta_3)^2 + (\eta_3 + \eta_4)^2 + (\eta_4 + \eta_1)^2] + w[(x_4 - x_2)^2 + (y_3 - y_1)^2 + {}^1/_4(\eta_4 + \eta_2)^2 + {}^1/_4(\eta_3 + \eta_1)^2]$$
$$+ \overline{w}[(x_1 - x_3)^2 + (\eta_4 - \eta_2)^2] + {}^1/_2 k(\eta_1^2 + \eta_2^2 + \eta_3^2 + \eta_4^2) + A(\vartheta_1^2 + \vartheta_2^2 + \vartheta_3^2 + \vartheta_4^2) + \gamma(\vartheta_1\vartheta_3 + \vartheta_4\vartheta_2)$$
$$+ c(\vartheta_1\vartheta_2 + \vartheta_2\vartheta_3 + \vartheta_3\vartheta_4 + \vartheta_4\vartheta_1) + d[(\vartheta_1 - \vartheta_2)(\eta_1 + \eta_2) + (\vartheta_2 - \vartheta_3)(\eta_2 + \eta_3) + (\vartheta_3 - \vartheta_4)(\eta_3 + \eta_4) + (\vartheta_4 - \vartheta_1)(\eta_4 + \eta_1)$$
$$+ d^*[(\vartheta_1 + \vartheta_2)(\eta_1 + \eta_2) + (\vartheta_2 + \vartheta_3)(\eta_2 + \eta_3) + (\vartheta_3 + \vartheta_4)(\eta_3 + \eta_4) + (\vartheta_4 + \vartheta_1)(\eta_4 + \eta_1)]; \qquad (7)$$

$$A = {}^1/_2 l^2(\lambda + \overline{\lambda} + 2\lambda' + \lambda^* + \lambda^{**}), \quad \gamma = 2(\lambda^{**} - \lambda^*)l^2, \quad \overline{w} = \lambda_x = \lambda_y, \quad \overline{w} = 2(\lambda^* + \lambda^{**}),$$
$$f = (\lambda + \overline{\lambda} + 2\lambda'), \quad c = 2l^2\lambda'',$$

where f and c are elastic coefficients characterizing, respectively, the translational and orientational interaction of the molecule in the x = y direction, $\overline{w}$ and w are the translational interactions of the molecule in the directions x and y, respectively, with sequential and parallel arrange of the molecule, γ is the orientational interaction of the molecules arranged parallel, A is the orientational interaction of a molecule oscillating in the field of the neighboring fixed molecules, k is the elastic coefficient characterizing the intramolecular interaction, and $d(\lambda + \overline{\lambda})l/2$ and $d^* = \lambda' l$ are elastic coefficients characterizing the coupling between the intramolecular and intermolecular vibrations.

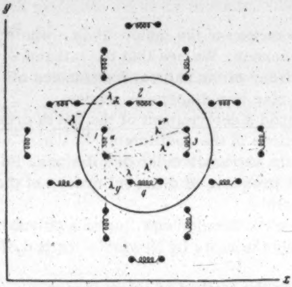

Introducing the small parameter $\chi = h\nu_\lambda / h\nu_k = \lambda x^2 / k\eta^2$, we see that the energy (7) contains both first order terms $\lambda x^2/2 \sim \chi$ and terms of order one and a half, $d\vartheta\eta \sim \chi^{3/2}$.

In the given case, in view of the symmetry of the lattice there is no coupling between the translational and orientational oscillations for the limiting frequencies and, consequently, no coupling between the translational and intramolecular vibrations.

The analytic form of the frequencies and the selection rules have been determined by the aid of group theory. The given lattice pertains to the symmetry group C_{4v}. The unit cell comprises 16 degrees of freedom. The normal vibrations of the lattice are characterized by 16 frequencies, belonging to 5 types of oscillation; 8 frequencies are degenerate in pairs.

The frequencies corresponding to the limiting oscillations of equivalent molecules with phases 0 and π and the geometrically symmetrical coordinates corresponding thereto are given by

$$\omega_1(0) = 2(k + w + 2f)/m, \quad s_1 = \eta_1 + \eta_2 + \eta_3 + \eta_4; \qquad \omega_2(0) = 2(k + w)/m, \quad s_2 = (\eta_4 + \eta_2) - (\eta_3 - \eta_1);$$
$$\omega_3(0) = (2A + \gamma + 2C)/J, \quad s_3 = \vartheta_1 + \vartheta_2 + \vartheta_3 + \vartheta_4; \qquad \omega_4(0) = (2A + \gamma - 2C)/J, \quad s_4 = (\vartheta_3 - \vartheta_2) + (\vartheta_1 - \vartheta_4);$$
$$\omega_{5,6}(0) = 4f/J, \quad s_5 = (x_3 + x_1) - (x_4 + x_2), \quad s_6 = (y_2 + y_4) - (y_3 + y_1); \quad \omega_{7,8}(0) = 0, \quad s_7 = x_1 + x_2 + x_3 + x_4,$$
$$s_8 = y_1 + y_2 + y_3 + y_4; \ y_3 + y_4; \quad \omega_{9,10}(\pi) = \frac{2(k + f)}{m} - \frac{32(d - d^*/2)}{(I + k)J - (2A - \gamma)m/2}, \quad \left.\begin{matrix} s_9 = \eta_2 - \eta_1 \\ s_{10} = \eta_3 - \eta_4 \end{matrix}\right\};$$
$$\omega_{11,12}(\pi) = \frac{2A}{J} - \frac{32(d - d^*/2)}{(I + k)J - (2A - \gamma)m/2}, \quad \left.\begin{matrix} s_{11} = \vartheta_3 - \vartheta_1 \\ s_{12} = \vartheta_2 - \vartheta_4 \end{matrix}\right\};$$
$$\omega_{13}(\pi) = (3f + 2w)/m, \quad s_{13} = (y_3 - y_1) - (x_4 - x_2); \quad \omega_{14}(\pi) = (3f + 2\overline{w})/m, \quad s_{14} = (y_2 - y_4) + (x_3 - x_1);$$
$$\omega_{15}(\pi) = (2f + 2w)/m; \quad s_{15} = (y_3 - y_1) + (x_4 - x_2); \quad \omega_{16}(\pi) = (f + 2w)/m, \quad s_{16} = (y_4 - y_2) + (x_3 - x_1).$$

The frequencies 1, 2, 4, 13, 14, 15 and 16 are active in the Raman spectrum; frequencies 5, 6, 9, 10, 11 and 12 are active in the infrared spectrum. Coupling of the intramolecular vibrations with the orientational ones is realized in the oscillations corresponding to the frequencies 9 & 10 and 11 & 12. Thus we see that our examination of a two-dimensional lattice has fully confirmed the deductions made in our analysis of the general case. We plan to carry out the calculation of a three-dimensional lattice for a real crystal.

In conclusion the writer desires to express her sincere thanks to Prof. A. I. Ansel'm for useful discussions and constant interest in the work.

---

[1] A. I. Ansel'm and N. I. Porfir'eva, J. Exptl. Theoret. Phys. (U.S.S.R.) 19, 438 (1949).

[2] A. S. Davydov, Теория поглощения света в молекулярных кристаллах, (Theory of Light Absorption in Molecular Crystals), Kiev, 1951.

[3] N. N. Porfir'eva, J. Exptl. Theoret. Phys. (U.S.S.R.) 19, 692 (1949).

Translated by E. J. Rosen
7

SOVIET PHYSICS JETP VOLUME 6, NUMBER 1 JANUARY, 1958

ANGULAR DISTRIBUTIONS OF PHOTOFISSION FRAGMENTS FROM URANIUM

B. P. BANNIK, N. M. KULIKOVA, L. E. LAZAREVA, and V. A. IAKOVLEV

P. N. Lebedev Physics Institute, Academy of Sciences, U.S.S.R.

Submitted to JETP editor February 7, 1957

J. Exptl. Theoret. Phys. (U.S.S.R.) 33, 53-55 (July, 1957)

The angular distributions of photofission fragments from uranium at x-ray energies of 9.4, 12 and 26.5 Mev were determined using a 30 Mev synchrotron. The anisotropy was found to increase sharply with decreasing x-ray energy. The ratios of the anisotropic to the isotropic fission yields at the above energies 0.55 ± 0.09, 0.13 ± 0.05, and 0.05 ± 0.04 respectively.

THE angular distributions of photofission fragments from uranium were determined with nuclear emulsions. The source of the x-rays was the 30 Mev synchrotron of the Physics Institute of the Academy of Sciences.

Ilford D-1 plates of 100 and 200μ thickness were impregnated with a saturated solution of uranyl acetate and were placed in the x-ray beam at a distance of 1 m from the synchrotron target. The method of Belovitskii and Romanova[1] of impregnation and final development of the emulsions was utilized. By a careful timing of the different steps in the processing of the emulsions we succeeded in obtaining clearly legible tracks of the fission fragments while the α-tracks were scarcely noticeable. The plates were irradiated at the following three synchrotron energies: 9.4, 12, and 26.5 Mev.

The scanning was performed with MBI-2 microscopes with a 60× objective and 5× ocular. In scanning, all tracks with dip angles greater than 15° were rejected. For the retained tracks the angles between the direction of motion of the fragments and the x-ray beam were measured. Since the origin of the tracks could not be determined the angles ϑ and $\pi - \vartheta$ were indistinguishable and the obtained angular distribution is actually $[I(\vartheta) + I(\pi - \vartheta)]$.

TABLE I. Angular distribution of photofission fragments from U^{238}

Maximum x-ray energy, E_{max} Mev	Number of tracks	Distribution of tracks (per steradian)		
		0–30° 180–150°	30–60° 150–120°	60–90° 120–90°
9.4	3901	1 ∓ 0.03	1.35 ∓ 0.04	1.36 ∓ 0.04
12	2053	1 ∓ 0.04	1.09 ∓ 0.04	1.16 ∓ 0.04
26.5	2507	1 ∓ 0.04	1.10 ∓ 0.04	1.06 ∓ 0.04

In order to determine the fraction of fissions due to background neutrons some of the uranium-impregnated plates were placed at the time of the irradiation outside of the x-ray beam. The fissions in these plates could be due to the background neutrons which are approximately uniformly distributed around the synchrotron, and to scattered γ-rays. The scanning of these plates revealed that for all x-ray energies the number of fissions due to neutrons was less than 2 – 3%. A similar result (less than 1%) was obtained when placing a plate in the beam behind a large lead block at an energy $E_{max} = 12$ Mev.

The results obtained for $E_{max} = 9.4$, 12, and 26.5 Mev are given in Table I. The relative yields per steradian are given for the indicated angular ranges. In natural uranium the isotope U^{238} has an abundance of 99.28%. Since the cross sections for photofission of the different isotopes of uranium differ only by a factor 2 – 3 (Ref. 2) the given data reflect the properties of U^{238}. As can be seen from the table the maximum of the angular distribution occurs at an angle of 90° to the x-ray beam. The anisotropy decreases sharply with increasing x-ray energy.

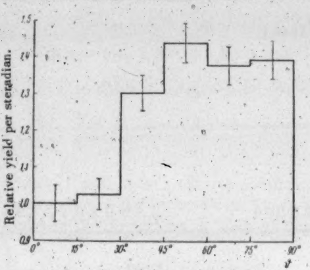

Angular distribution of fission fragments from irradiation with x-rays of maximum energy E_{max} = 9.4 Mev

In general the angular distribution from photonuclear reaction has the form

$$I(\vartheta) = a + b(\sin\vartheta + p\sin\vartheta\cdot\cos\vartheta)^2.$$

The term with forward-backward asymmetry is due to electric dipole–electric quadrupole interference in photon absorption. When adding the contributions for ϑ and $(\pi - \vartheta)$ the interference term disappears. In the present work the following distribution was determined:

$$I(\vartheta) + I(\pi - \vartheta) = a + b\cdot\sin^2\vartheta + c\sin^2\vartheta\cdot\cos^2\vartheta.$$

The coefficient a describes the isotropic part in the angular distribution and coefficients b and c are connected with dipole and quadrupole γ-absorption respectively. The ratio of the anisotropic to the isotropic part for all fission fragments is given by $\frac{2}{3}\frac{b}{a} + \frac{2}{15}\frac{c}{a}$.

The angular distributions obtained with $E_{max} = 12$ and 26.5 Mev can be represented within errors by $a + b\sin^2\vartheta$. The ratios b/a equal 0.20 ± 0.07 and 0.07 ± 0.06 respectively.

The angular distribution for $E_{max} = 9.4$ Mev is shown in the figure. It indicates both dipole and quadrupole abosrption. A least squares fit yields the following form for the distribution

$$1 + 0.55\sin^2\vartheta + 1.38\sin^2\vartheta\cos^2\vartheta \quad (b/a = 0.55 \mp 0.09;\ c/a = 1.38 \mp 0.41).$$

The following relation holds for the coefficients: $c/b = 5\sigma_{fq}/\sigma_{fd}$ where σ_{fq} and σ_{fd} are the cross sections for fission from absorption of electric quadrupole and dipole radiation respectively. The angular distribution for $E_{max} = 9.4$ Mev yields $c/5b = 0.50 \mp 0.14$. A large contribution from quadrupole absorption at energies below 10 Mev is to be expected due to the suppression of dipole transitions in this energy region as pointed out by Migdal.[3]

TABLE II. Anisotropy coefficients for U^{238} photofission

E_{max} Mev	b/a	Ratio of anisotropic and isotropic fission yields $\left(\frac{2}{3}\frac{b}{a} + \frac{2}{15}\frac{c}{a}\right)$
9.4	0.55∓0.09	0.55∓0.09
12	0,20∓0.07	0.13∓0,05
26.5	0,07∓0.06	0.05∓0.04

The coefficients of the angular distributions for the three x-ray energies are collected in Table II.

Angular distributions of photofission fragments have also been obtained by Winhold and Halpern.[4] This work has been performed with a linear accelerator counting the β-activities of the fission fragments. They measured the ratio of the yield of fission fragments emitted parallel and normal to the x-ray beam at several electron energies between 6.5 and 14 Mev. Assuming that the angular distribution has the form $a + b\sin^2\vartheta$, one can obtain ratios a/b that agree within errors with the values of Table II of the present paper.

The scanning of the plates explored at $E_{max} = 26.5$ Mev was performed by the Scanning Group of the International Joint Institute for Nuclear Research under the direction of M. I. Podgoretskii. The authors express their deep gratitude to the scanning group and to M. I. Podgoretskii.

---

[1] G. E. Belovitskii and T. A. Romanova, Report, Phys. Inst. Acad. Sci. U.S.S.R. (1951).

[2] I. V. Chivilo, Thesis, Phys. Inst. Acad. Sci. U.S.S.R. (1951).

[3] A. B. Migdal, J. Exptl. Theoret. Phys. (U.S.S.R.) 15, 81 (1945).

[4] E. J. Winhold and I. Halpern, Phys. Rev 103, 990 (1956).

Translated by M. Danos

INCONSISTENCY BETWEEN THE THEORETICAL AND EXPERIMENTAL DELTA-SHOWER FREQUENCIES AT HIGH ENERGIES

P. S. CHIKIN

Moscow State University

Submitted to JETP editor September 10, 1956; resubmitted January 3, 1957

J. Exptl. Theoret. Phys. (U.S.S.R.) 33, 56-58 (July, 1957)

Experimental data on the frequency of high-energy δ-electron production are tabulated. Calculation of the frequency of small underground ionization bursts is carried out. All the data point to a contradiction between theory and experiment at energies $\geq 5 \times 10^8$ ev.

A hypothesis that the finite dimensions of the structure of the electric charge may manifest themselves in electromagnetic interactions at very high energies has been proposed and substantiated in a series of articles.[1] In connection with this, we have studied the currently available experimental data on δ-electron production by cosmic-ray μ-mesons in order to find out whether a systematic inconsistency exists between the experiment and the predictions of the present-day theory which assumes an elementary electric point charge.

The results of interest to us, obtained in experiments in which the energy of δ-electrons was directly measured, are given in Table I. The theoretically expected number of δ-electrons is given in the second column, the experimentally obtained number and the purely statistical error of the measurement in the third. In addition, the probability P_i of deviation of the experimental result from the theory (estimated by means of the error integral) is given in the fourth column of the table.

TABLE I. Summary of experimental data

Energy of secondary particles (Mev)	N_{theor}	N_{exp}	P_i
Walker[2] δ-process			
Series A: $E_\delta \geqslant 100$	25	39 ± 6.3	0.04
$E_\delta \geqslant 200$	10.3	17 ± 4.1	0.10
Series B: $E_\delta \geqslant 100$	22.3	27 ± 5.2	0.35
$E_\delta \geqslant 200$	9.7	14 ± 3.8	0.25
Kannagara et al[3] δ-process			
$E_\delta \geqslant 100$	22.5*	27.5 ± 5.2	0.35
$E_\delta \geqslant 200$	10*	14 ± 3.8	0.28
Pair production: $E_{2\gamma} \geqslant 100$	16	23 ± 4.8	0.23
$E_{2\gamma} \geqslant 200$	8.5	18.5 ± 4.3	0.03
Trident production: $E_3 \geqslant 140$	10	16.2 ± 4.0	0.13

* Theoretical curve renormalized to the number of δ-electrons with energies between 100 and 300 Mev.

It can be seen that deviations of ~ 50 percent (towards higher values) exist both in the work of Walker[2] carried out at sea level with a cloud chamber and in that of Kannagara et al.,[3] who used photographic emulsions at the depth of 60 meters water equivalent (m.w.e.). If we also take into the account that the same situation exists for the processes of pair and trident production[3] we can maintain that either a systematic discrepancy exists between the theoretical and experimental results or that a highly improbable chance coherence of the results of several experiments has occurred.

A numerical-graphical computation of the frequency of ionization chamber bursts at the depth of 60 m.w.e. in the conditions of the experiment of George and Trent[4] was carried out by us in view of the conclusion reached by the authors about an agreement of theory and experiment, contradicting the data of Table I. The computation was carried out following formula (31.2) of Belen'kii's book.[5] The transition effect for electron-photon cascades developing in lead before attaining their maximum and then passing through the 12 mm thick aluminum walls of the ionization chamber, which decreases the number of particles in a shower by a factor of 2.5, was taken into account.

The vertical differential spectrum of μ-mesons at the depth of 60 m.w.e. was taken, following Refs. 3, 4, and 6, in the form

$$S(W)\,dW = 2 \cdot 10^{17}\,(W + 1.3 \cdot 10^{10})^{-3}\,dW \text{ particles/cm}^2\cdot\text{sec}\cdot\text{sterad}\cdot\text{ev}.$$

Normalization of the spectrum was carried out according to the data of Owen and Wilson[7] at the point

W = 10^{10} ev accounting for ionization losses (from sea level to the given depth) amounting to 1.4×10^{10} ev. Angular distribution of μ-mesons was assumed as $\sim \cos^2\theta$.[6,8] The assumed normalization and angular distribution yield a total flux of μ-mesons smaller by ~ 15% than the value accepted in Refs. 3 and 9. Only the processes of production of δ-electrons and radiative photons were taken into the account in the calculation, and the cross-sections for these processes, following Rossi,[10] were taken for μ-mesons with mass M = 209 and spin $^1/_2$. The process of direct electron pair production by μ-mesons was disregarded; its contribution was found to be negligible (cf. Ref. 11). The intermediate result of the calcuations, in the form of δ-electron and radiative-photon spectra, is given in Table II.

The final theoretical result for the frequency of ionization bursts produced by showers with the number of particles in a burst $n \geq 20$, in the conditions of Ref. 4, is B = 0.14 bursts/hour, while the experiment yields the value B = 0.54 bursts/hour. The calculation shows that δ-electrons and radiative photons yield similar contributions to the frequency of bursts, the energy of these primaries being $\geq 4.5 \times 10^9$ ev. The contribution of nuclear disintegrations induced by μ-mesons is not greater than 0.01 bursts/hour, according to George and Trent's[4] and our estimates. The discrepancy between our theoretical result and that of Ref. 4 is mainly due to our accounting for the transition effect: since this effect decreases the number of particles in a shower by a factor of 2.5 and since the slope of the experimental curve of ionization-burst frequency vs. the number of particles in a burst has a power exponent 1.6 ± 0.2, the results will differ by $(2.5)^{1.6} \approx 4.3$

If we calculate, according to formula (29.21) and Table XVII of Belen'kii's book and with normalization of the μ-meson spectrum following Owen and Wilson,[7] the frequency of ionization bursts with number of particles $n \geq 25$ ($E_\delta \geq 2 \times 10^9$ ev) in the conditions of Ref. 12 where the frequency of bursts was measured at sea level in a spherical chamber shielded with lead, we shall obtain an analogous discrepancy between the theory and experiment: $B_{theor} = 17$ bursts/hour, $B_{exp} = 4-5$ bursts/hour. Further theoretical and experimental investigations are necessary to disclose the causes of this systematic inconsistency between the theoretical frequency of δ-showers and the experimental results at $E_\delta \gtrsim 10^9$ ev.

TABLE II. Calculated vertical differential spectrum of δ-electrons and radiative photons produced by μ-mesons in lead at the depth of 60 m.w.e. (57° N) (particles/cm^2·sec·sterad·ev)

E_δ, E_γ (eV)	N_γ	N_δ
10^8	$2.8\cdot10^{-16}$	$1.50\cdot10^{-14}$
$5\cdot10^8$	$4.0\cdot10^{-17}$	$4.4\cdot10^{-16}$
10^9	$1.6\cdot10^{-17}$	$8.60\cdot10^{-17}$
$4\cdot10^9$	$2.1\cdot10^{-18}$	$2.57\cdot10^{-18}$
10^{10}	$4.5\cdot10^{-19}$	$2.2\cdot10^{-19}$
$3\cdot10^{10}$	$4.5\cdot10^{-20}$	$8.0\cdot10^{-21}$
$6\cdot10^{11}$	$8.5\cdot10^{-21}$	$7.9\cdot10^{-22}$
10^{11}	$2.4\cdot10^{-21}$	$1.3\cdot10^{-22}$

It is interesting to note the following: δ-electrons of ~ 1 Bev are efficiently produced by μ-mesons of ~ 10 Bev. The estimate of the minimum impact parameter r between an electron and a μ-meson of ~ 10 Bev in a head-on collision yields

$$e^2/r = \sqrt{2m_ec^2E_{\mu^-}}, \quad r \approx 1.4\cdot10^{-15} \text{ cm.}$$

It follows that the cross-section for the production of δ-electrons of ~ 1 Bev is roughly $\pi r^2 \approx 6 \times 10^{-30}$ cm^2. At energies ≥ 4.5 Bev the experiment yields a cross-section a few times larger (see above) than that predicted by theory and does not contradict the assumption that the value of the cross-section remains constant above ~ 1 Bev. The μ-meson—nucleon interaction cross section is of the same value (cf. Ref. 9) which, as it was shown by Fowler,[13] is also larger than the theoretical. It is possible that the finite structure of the electric charge, of dimension ~ 10^{-15} cm, manifests itself in the numerical equality of both cross-sections and their common discrepancy with the theoretical values, the cross-sections reaching in both cases their minimal "geometrical" value[13] determined by the new forces of such a structure.

---

[1] Landau, Abrikosov, and Khalatnikov, Dokl. Akad. Nauk SSSR **95**, 497, 773, 1177 (1954); L. D. Landau and I. Ia. Pomeranchuk, Dokl. Akad. Nauk SSSR **102**, 489 (1955).

[2] W. D. Walker, Phys. Rev. 90, 234 (1953).

[3] M. L. T. Kannagara and M. Zivkovic, Phil. Mag. 44, 797 (1953).

[4] E. P. George and P. T. Trent, Proc. Phys. Soc. A64, 733 (1951).

[5] S. Z. Belen'kii, Лавинные процессы в космических лучах, (Cascade Processes in Cosmic Rays), Moscow-Leningrad 1948.

[6] E. P. George, Nuclear Physics 1, 54 (1956).

[7] B. G. Owen and J. G. Wilson, Proc. Phys. Soc. A68, 409 (1955).

[8] J. G. Wilson, editor, Progress in Cosmic Ray Physics, 1954.

[9] E. P. George and J. Evans, Proc. Phys. Soc. A68, 829 (1955).

[10] B. Rossi, High Energy Particles, New York, 1952 (Russ. Transl.).
[11] Hirokawa, Komori, and Gawa, Nuovo cimento 4, 736 (1956).
[12] H. Carmichael and J. F. Steljes, Phys. Rev. 99, 1542 (1955).
[13] G. N. Fowler, Proc. Phys. Soc. A68, 482 (1955).

Translated by H. Kasha
9

SOVIET PHYSICS JETP VOLUME 6, NUMBER 1 JANUARY, 1958

NONLINEAR MESON FIELD EQUATIONS

A. A. BORGARDT

Dnepropetrovsk State University

Submitted to JETP editor October 27, 1956

J. Exptl. Theoret. Phys. (U.S.S.R.) 33, 60-66 (July, 1957)

All possible variants of pseudoscalar mesodynamics with third-order self-action are considered. Asymptotic expressions are obtained for the nonrelativistic potentials of point nucleons. Studies are also made of the solutions of the resulting nonlinear equations that correspond to plane waves, and of the question of the definite character of the energy density.

THE introduction of nonrenormalizable nonlinear equations into the quantum field theory seems to be the only promising way of overcoming a number of difficulties in the present mesodynamics and meson theory of nuclear forces. The different values of the coupling constant $g^2/\hbar c$ obtained from various experiments on the interaction of nucleons give a quite definite indication that the interaction of nucleons is a nonlinear one, and that the value of the coupling constant is always an effective value depending on the nature of the experiment. Also it is hardly possible to give a convincing explanation of the fact of the saturation of nuclear forces outside the framework of a nonlinear theory.

In the present paper we consider nonlinearities in the equations of the meson field in the form of terms of third order with respect to φ. Out of all possible forms of such self-action, that of the type $\lambda\varphi^3$, and the associated Schiff equation[1-3]

$$(\Box^2 - k_0^2 - \lambda\varphi^2)\varphi = 0.$$

have been studied in more or less detail.

Here consideration is given to all possible variants of pseudoscalar mesodynamics with third-order self-action. Asymptotic expressions are obtained for the nonrelativistic potentials of point nucleons for the various types of self-action. They all show the presence of movable singularities for a definite sign of λ. The conditions for saturation are examined in connection with the sign of λ. Studies are also made of the wave solutions of the nonlinear equations that correspond to plane waves, and of the question of the definiteness of the energy density.

1. GENERAL RELATIONS

The initial assumptions adopted are as follows:

(1) General covariance of all equations in the four-dimensional space; (2) conservation of energy and momentum in the free field; (3) the possibility of the passage to the limit $k_0 \to 0$ for arbitrary nonlinearities without the appearance of additional divergences.

The first-order[4] Lagrangian most convenient for our purposes is taken in the form

$$L^{(1)} = \alpha\left(\psi^{+}(\beta_\lambda \partial/\partial x_\lambda + k_0)\psi + (\Lambda/2)\,\psi^{+}\beta'\psi\cdot\psi^{+}\beta''\psi\right), \tag{1.1}$$

where

$$\beta_\mu\beta_\nu\beta_\rho + \beta_\rho\beta_\nu\beta_\mu - \delta_{\mu\nu}\beta_\rho - \delta_{\rho\nu}\beta_\mu = 0, \tag{1.2}$$

$$\psi^{+} = \psi^{*}R_4, \quad R_\mu = 2\beta_\mu^2 - I. \tag{1.3}$$

The matrix ψ is either a complete (in the case of a separable mixture of fields) or a contracted (in the case of a pure field) undor of the second rank.[5]

From postulate (1) it follows obviously that $\psi^{+}\beta'\psi \times \psi^{+}\beta''\psi$ is an invariant contraction of the operators β' and β'' belonging to the complete Kemmer group G_{126}, and also that these two matrices can differ only by diagonal factors belonging to the commutative subgroup of G_{126}. These latter, again from the requirement of covariance, must be expressible in terms of the restricted basis I, R_5 ($R_5 = \prod_{\mu=1}^{4} R_\mu$)[6]

$$\beta' = R'\beta, \quad \beta'' = R''\beta, \tag{1.4}$$

$$R' = a'I + b'R_5, \quad R'' = a''I + b''R_5. \tag{1.5}$$

The variation in $L^{(1)}$ to obtain the field equations is carried out independently with respect to the potentials and the intensities,

$$\psi^{(I)} = (1/2k_0)(I - R_5)\psi, \quad \psi^{(II)} = (1/2)(I + R_5)\psi, \tag{1.6}$$

and therefore requires precise specification of the commutative properties of β with respect to the separation operators. The possible cases are

$$\text{(A)}\ (I \pm R_5)\beta(I \mp R_5) = 0, \quad \text{(B)}\ (I \pm R_5)\beta(I \pm R_5) = 0.$$

In case (A) the operator β is diagonal in the space $\psi^{(I)}\psi^{(II)}$, but not so in case (B).

It is now easy to obtain the field equations for the cases (A) and (B) from the Lagrangian (1.1).

2. ON THE METHOD OF MERGING THE FIELDS

The problem of merging two spinor fields with nonlinear self-action is very elementary, so that we confine ourselves to some brief remarks.

The order of the self-action is lowered by the merging. If the order of the self-action in the spinor equations is n, then the order of the self-action in the boson equations obtained by merging them in pairs is simply (n + 1)/2.

The merging of Dirac fields with third-order self-action gives the general result

$$\beta_\lambda \partial\psi/\partial x_\lambda + k_0\psi + \Lambda_1 S\psi^{+}R'\psi + \Lambda_2 S\beta_\mu\psi^{+}R''\beta_\mu\psi + \Lambda_3 S[\beta_\mu\beta_\nu]\,\psi^{+}R'''\,[\beta_\mu\beta_\nu]\,\psi + (\widetilde{NL}) = 0, \tag{2.1}$$

where $(\widetilde{NL})$ denotes nonlinear terms formed from those stated by a Larmor transformation, and

$$S = (1/2)^4 \prod_{\mu=1}^{4}(I + R_\mu)$$

is a scalar projection operator. The total number of constants Λ is fixed by the choice of the original nonlinearity.

An essential point is that in a pure pseudoscalar field a quadratic self-action is impossible, and the ps-field obtained by the merging of Dirac fields with self-action of the type $\lambda\varphi^3$ is linear. A paper by Heisenberg[7] has proposed for the universal description of quantum fields the nonlinear spinor equation

$$\gamma_\lambda \partial\psi/\partial x_\lambda + \lambda\psi\psi^{+}\psi = 0. \tag{2.2}$$

In addition to the serious criticism of this theory, given by Kita,[8] it must be remarked that the merging of such fields does not give the needed result for meson fields for the following reasons:

1) There is no term in k_0, and the connection between the intensities and the potentials in the meson equations depends on λ; also the field intensity diverges for $\lambda \to 0$. Thus the entire scheme does not conform to the correspondence principle.

2) The second-order self-action obtained by the merging gives nonlinear corrections in static fields with central symmetry only for the practically uninteresting case of scalar fields.

3. PSEUDOSCALAR FIELDS

The pseudoscalar theory is obviously of the greatest interest for practical purposes, both because of the pseudoscalar nature of π-mesons and because for this type the linear approximation gives the least bad results.

Let us consider the different operators β in the nonlinear terms of the wave equations of a ps field with self-action of the third order. For such fields the densities with $\beta = [\beta_\mu \beta_\nu]$ and $\beta = \beta_5 \beta_\mu$ are in general equal to zero.

The self-action with $\beta = \{\beta_\mu \beta_\nu\}$ refers to a type of weak gravitational self-actions, and we shall not consider it. There remain the cases

$$\text{(A)}\ \beta = I,\ R_5, \tag{3.1}$$

$$\text{(B)}\ \beta = \beta_\mu,\quad R_5\beta_\mu. \tag{3.2}$$

For the R-operators we confine ourselves to the simplest types (the other possibilities are equivalent to pairwise combinations of the nonlinearities obtained below, with the introduction of two constants λ_1 and λ_2):

$$1.\quad R' = R'' = I, \tag{3.3}$$

$$2.\quad R' = R'' = (1/2)(I + R_5), \tag{3.4}$$

$$3.\quad R' = R'' = (1/2)(I - R_5), \tag{3.5}$$

$$4.\quad R' = (1/2)(I \pm R_5),\quad R'' = (1/2)(I \mp R_5). \tag{3.6}$$

Cases A_1 and A_2 lead to extremely complicated equations; in the static approximation they are equivalent and give oscillating potentials with movable singularities. These equations will not be considered in what follows. The remaining cases give the following equations for real fields (besides the wave equations we give the expressions for the corresponding energy-momentum tensors, which are needed in what follows; the question of the derivation of these equations will not be considered owing to lack of space):

$$\text{I.}\qquad (\Box^2 - k_0^2)\varphi - \lambda\varphi^3 = 0 \qquad (A_3) \tag{3.7}$$

$$T^{(NL)}_{\mu\nu} = T^{(L)}_{\mu\nu(0)} + (k_0^2/2)\,\delta_{\mu\nu}\varphi^2(1 + \lambda\varphi^2/2). \tag{3.8}$$

$$\text{II.}\qquad (\Box^2 - k_0^2)\varphi - \lambda\varphi(\partial\varphi/\partial x_\lambda)^2 = 0 \qquad (B_3) \tag{3.9}$$

$$T^{(NL)}_{\mu\nu} = (T^{(L)}_{\mu\nu(0)} + (k_0^2/2)\,\delta_{\mu\nu}(\exp(\lambda\varphi^2) - 1))\exp(-\lambda\varphi^2). \tag{3.10}$$

$$\text{III.}\quad (\Box^2 - k_0^2(1 + \lambda\varphi^2))\varphi - \lambda\varphi(\partial\varphi/\partial x_\lambda)^2/(1 + \lambda\varphi^2) = 0 \quad (A_4, B_1, B_2) \tag{3.11}$$

$$T^{(NL)}_{\mu\nu} = (T^{(L)}_{\mu\nu(0)} - (k_0^2/2\lambda)\,\delta_{\mu\nu}(1 - \lambda^2\varphi^4))/(1 + \lambda\varphi^2). \tag{3.12}$$

$$\text{IV.}\quad (\Box^2 - k_0^2(1 + \lambda\varphi^2))\varphi - 2\lambda\varphi(\partial\varphi/\partial x_\lambda)^2/(1 + \lambda\varphi^2) = 0 \quad (B), \tag{3.13}$$

$$T^{(NL)}_{\mu\nu} = (T^{(L)}_{\mu\nu(0)} + (k_0^2/2\lambda)\,\delta_{\mu\nu}(1 + \lambda\varphi^2)^2\ln(1 + \lambda\varphi^2))/(1 + \lambda\varphi^2)^2. \tag{3.14}$$

Here

$$T^{(L)}_{\mu\nu(0)} = -(\partial\varphi/\partial x_\mu)(\partial\varphi/\partial x_\nu) + {}^1/_2\delta_{\mu\nu}(\partial\varphi/\partial x_\lambda)^2, \tag{3.15}$$

$$\varphi = (1/2)(I - R_5)\psi,\quad \psi^+ = \psi R_4. \tag{3.16}$$

4. STATIC SOLUTIONS[9]

For $\lambda > 0$ Schiff's equation has the asymptotic solution[10]

$$\varphi(\mathbf{x}) \approx g/x \ln(x/x_0), \tag{4.1}$$

where

$$x_0 = g\lambda^{1/2}. \tag{4.2}$$

In the limit $k_0 \to 0$, corresponding to $|\mathbf{x}| \to 0$ (more precisely, $|\mathbf{x}| \ll k_0^{-1}$), Eqs. II to IV take the form

$$\ddot{\varphi} - \lambda\dot{\varphi}^2 F(\varphi) = 0, \quad \dot{\varphi} = d\varphi/d\varphi_L, \tag{4.3}$$

where

$$\nabla^2 \varphi_L(\mathbf{x}) = 0.$$

Generally speaking, one must take a dipole solution

$$\varphi_L(\mathbf{x} - \mathbf{x}_0) = f(\boldsymbol{\sigma}, \mathbf{x} - \mathbf{x}_0)/|\mathbf{x} - \mathbf{x}_0|^3,$$

providing directional and noncentral forces between the singularities of the field.

Integration of Eq. (4.3) (under the condition $\varphi(\mathbf{x}) \to 0$ for $|\mathbf{x}| \to \infty$) leads to a general solution of the form:

$$\int_0^{\varphi(\mathbf{x})} d\xi \exp\left(-\lambda \int_0^{\xi} F(\xi')\, d\xi'\right) = \varphi_L(\mathbf{x}). \tag{4.4}$$

This solution can be applied with regard to $\varphi(\mathbf{x})$ only in cases III and IV:

$$\int_0^{\varphi(\mathbf{x})} d\xi \exp(-\lambda\xi^2/2) = \varphi_L(\mathbf{x}) \qquad \text{(II)}, \tag{4.5}$$

$$\varphi(\mathbf{x}) = \lambda^{-1/2} \sin(\lambda^{1/2}\varphi_L) \qquad \text{(III)}, \tag{4.6}$$

$$\varphi(\mathbf{x}) = \lambda^{-1/2} \tan(\lambda^{1/2}\varphi_L) \qquad \text{(IV)}, \tag{4.7}$$

When the sign of λ is changed, hyperbolic functions appear in Eqs. (4.6) and (4.7). All three of these solutions are extremely interesting because of the presence of the movable singular point $|\mathbf{x}| = x_0 \sim \lambda^{1/2}$ for $\lambda > 0$. In case II the potential diverges for $|\mathbf{x}| \to x_0$ and is simply nonexistent for $|\mathbf{x}| < x_0$. In case III the potential is everywhere finite and for $|\mathbf{x}| < x_0$ oscillates between the values $\pm \lambda^{-1/2}$; the frequency of the oscillations becomes infinite for $|\mathbf{x}| \to 0$. Analagous oscillations, but of a discontinuous nature, occur in case IV. For $\lambda < 0$ the potentials (4.5) and (4.6) diverge monotonically and relatively weakly at the origin, and the potential (4.7) is finite at the origin and equal to $\lambda^{-1/2}$.

Saturation in heavy nuclei is provided by those potentials for which

$$\varphi(n\varphi_L) < n\varphi(\varphi_L), \tag{4.8}$$

this condition being satisfied by the various cases as follows:

$$\text{I} - \text{for } \lambda > 0, \quad \text{II} - \text{for } \lambda < 0, \quad \text{III} - \text{for } \lambda > 0, \quad \text{IV} - \text{for } \lambda < 0.$$

It must be noted that the existence of the potential of a charge in a nonlinear theory does not make it possible to obtain from it the potential of a dipole by differentiating; this approach is based on the principle of superposition and is not admissible in a nonlinear theory. Cap[11] obtained erroneous results just for this reason.

5. WAVE SOLUTIONS

Let us study the solutions of the wave equations I–IV that depend on a phase $\varphi = \varphi(\theta)$ with a constant wave vector k_μ

$$\theta(\mathbf{x}, t) = k_\lambda x_\lambda = -\omega t + \mathbf{k}\mathbf{x}, \tag{5.1}$$

$$k_\lambda^2 = -k_0^2. \tag{5.2}$$

For $\lambda \to 0$ such solutions go over into ordinary linear plane waves. For convenience in the discussion we introduce the amplitude φ_0 explicitly and go over everywhere to dimensionless quantities $\xi = \varphi/\varphi_0$ and, according to circumstances, $\overline{\lambda} = \lambda(\varphi_0/k_0)^2$ or $\lambda_0 = \lambda\varphi_0^2$. We shall carry out the study in the phase plane (η, ξ), where $\eta = d\xi/d\theta$.

Then the following results are obtained.

I. For this case the equation of the phase contours is

$$\eta^2 + \xi^2(1+\lambda\xi^2/2) = C. \tag{5.3}$$

a) $\lambda > 0$. There is one singular point of the type of a center, at $\eta = \xi = 0$; to it there corresponds the value $C_0 = 0$. The process is always periodic. The solution reduces to the elliptic integral

$$(1+\bar{\lambda})^{-1/2} F(\Phi, k) = -\theta(x) + C', \tag{5.4}$$

where

$$\Phi = \arccos(\varphi/\varphi_0),\ k^2 = \bar{\lambda}/2(1+\bar{\lambda}). \tag{5.5}$$

b) $\lambda < 0$. There are three singular points, $\eta = \xi = 0$ and $\eta = 0$, $\xi_0 = \pm\bar{\lambda}^{-1/2}$ — a center and two saddle-points. The equation of the separatrix passing through the saddle-points (cf. Fig. 1, A) is

$$\eta^2 - ({}^1/_2)(1-\bar{\lambda}\xi^2) = 0. \tag{5.6}$$

Wave processes are possible only for

$$1/2\bar{\lambda} > C > 0. \tag{5.7}$$

The solution is again obtained in the form of an elliptic integral

$$(1-\bar{\lambda}/2)^{-1/2} F(\Phi, k) = \theta(x) + C', \tag{5.8}$$

where

$$\Phi = \arcsin(\varphi/\varphi_0),\quad k^2 = \bar{\lambda}/2(1-\bar{\lambda}/2). \tag{5.9}$$

The process is periodic only under the condition $\bar{\lambda} \leq 1$ or $\varphi_0 \leq k_0/\lambda^{1/2}$. The energy density $\mathcal{E}$ is not positive definite; $\mathcal{E} < 0$ in the region of aperiodic motions for large ξ.

II. The equation of the phase contours is

$$\eta^2 - C\exp(\lambda_0\xi^2) = \lambda_0^{-1}. \tag{5.10}$$

a) $\lambda > 0$. There is a singular point of the center type, $\eta = \xi = 0$ ($C_0 = -\lambda_0^{-1}$), and a separatrix at $C_{\text{lim}} = 0$, with the equation $\eta^2 = \lambda_0^{-1}$. Beyond the separatrix $C > 0$ and the motions are aperiodic (cf. Fig. 1, B).

The general form of the solution (for arbitrary λ) is

$$\int_0^{\varphi/\varphi_0} d\xi\,(C\exp(\lambda_0\xi^2) + \lambda_0^{-1})^{-1/2} = \theta(x) + C'. \tag{5.11}$$

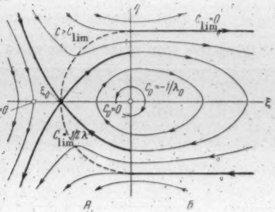

FIG. 1

To the separatrix there corresponds a solution of the form

$$\varphi(x) = \pm\lambda^{-1/2}\theta(x) + C'. \tag{5.12}$$

The asymptotic solutions for $\lambda > 0$ and $C \gg 0$ reduce to Kramp functions.

b) $\lambda < 0$. The center remains and the separatrix disappears. All motions are periodic. For any sign of λ the energy density remains positive definite in the entire phase plane (η, ξ) [cf. Eq. (3.10)].

III. The equation of the phase contours is

$$\eta^2 - (C-\xi^2)(1+\lambda_0\xi^2) = 0. \tag{5.13}$$

a) $\lambda > 0$. There is a center at $\eta = \xi = 0$. All the phase contours are closed. The general solution is

$$(1+\lambda_0)^{-1/2} F(\Phi, k) = -\theta(x) + C', \tag{5.14}$$

where

$$\Phi = \arccos(\varphi/\varphi_0),\quad k^2 = \lambda_0/(1+\lambda_0).$$

The energy density is positive definite inside a finite region which contracts to the center for $c|\mathbf{k}|/\omega \to \infty$.

b) $\lambda < 0$. Two new singular points appear at $\eta = 0$, $\xi_0 = \pm\lambda_0^{-1/2}$, through which there passes a separatrix ($C_{\text{lim}} = -1/\lambda_0$) (cf. Fig 2, A)

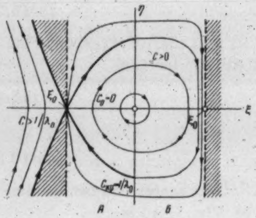

FIG. 2

$$\eta^2 - (1/\lambda_0)(1 - \lambda_0\xi^2)^2 = 0. \qquad (5.15)$$

The energy-density is always positive definite in the region of the oscillatory processes.

IV. The equation of the phase contours is

$$\eta^2 - (C - (1/\lambda_0)\ln(1 + \lambda_0\xi^2))(1 + \lambda_0\xi^2)^2 = 0. \qquad (5.16)$$

a) $\lambda > 0$. There is a center at $\eta = \xi = 0$ ($C_0 = 0$). All the phase curves are closed. $\mathcal{E} > 0$ everywhere.

b) $\lambda < 0$. In this case no points with $|\xi| \gtrsim 1/\lambda_0$ exist in the plane (η, ξ). Inside the allowed region (cf. Fig 2, B) all the curves are closed and $\mathcal{E} > 0$.

APPENDIX

1. The conversion of the original matrix wave equation into an ordinary second-order differential equation requires the use of projection operators constructed from the reflection matrices of the Kemmer algebra.[12,13] The well known contractions are given by the following method. Let us consider the wave solutions of the nonlinear equation

$$\beta_\lambda \partial\psi/\partial x_\lambda + k_0\psi + \lambda R'\beta_{\mu,\ldots,\nu}\psi \cdot \psi^+ R''\beta_{\mu,\ldots,\nu}\psi = 0, \qquad (A.1)$$

$$\psi = \psi(\theta), \quad \theta(x) = k_\lambda x_\lambda. \qquad (A.2)$$

The wave function can be put in this case in the form

$$\psi(x) = k_0(\psi_1(\theta) + (\beta_\lambda k_\lambda/k_0)\psi_2(\theta))a, \qquad (A.3)$$

$$\psi^+(x) = k_0 a^* R_4(\psi_1(\theta) - (\beta_\lambda k_\lambda/k_0)\psi_2(\theta)). \qquad (A.4)$$

In the case of the s or ps field the constant undor a is simply given by

$$a = (1/2)(I - R_5)E, \qquad (A.5)$$

and in the case of a vector or pseudovector field it is

$$a = (1/16)(I - R_5)S_\mu(I + R_5/R_\mu)(2 + M_1)E, \qquad (A.6)$$

where E is the unit undor, $M_1 = \sum_{\mu=1}^{4} R_\mu$, and S_μ is an operator specifying the spin state of the wave. Using this, we find that

$$\psi^+ R''\beta_{\mu,\ldots,\nu}\psi = k_0^2(A_{\mu,\ldots,\nu}\psi_1^2 - (k_\lambda/k_0)A_{\mu,\ldots,\nu\lambda}\psi_1\psi_2 - (k_\lambda k_\sigma/k_0^2)A_{\mu,\ldots,\nu\lambda\sigma}\psi_2^2), \qquad (A.7)$$

where

$$A_{\mu,\ldots,\nu} = a^* R_4 R''\beta_{\mu,\ldots,\nu}a, \qquad (A.8)$$

$$A_{\mu,\ldots,\nu\lambda} = a^* R_4 R''\beta_{\mu,\ldots,\nu}\beta_\lambda a, \qquad (A.9)$$

$$A_{\mu,\ldots,\nu\lambda\sigma} = a^* R_4 R''\beta_{\mu,\ldots,\nu}\beta_\lambda\beta_\sigma a \qquad (A.10)$$

are constant tensors.

The simplest example is that of a pseudoscalar wave in a field with $\beta_{\mu,\ldots,\nu} = I$ and $R' = R'' = (\frac{1}{2}k_0)(I - R_5)$; here, setting the diagonal and off-diagonal parts of Eq. (A.1) separately equal to zero, we get the system (with $\dot{\psi} = d\psi/d\theta$)

$$\dot{\psi}_2 + \psi_1 + \lambda A\psi_1^3 = 0, \qquad (A.11)$$

$$\dot{\psi}_1 - \psi_2 = 0, \qquad (A.12)$$

equivalent to Schiff's equation.[1]

To obtain static solutions possessing spherical symmetry, we apply the substitution

$$\psi(\mathbf{x}) = (k_0\psi_1(x) - (\beta, \mathbf{x}^0)\psi_2(x))a, \qquad (A.13)$$

$$\psi^{+}(\mathbf{x}) = a^{*}R_4(k_0\psi_1(x) + (\beta, \mathbf{x}^0)\psi_2(x)). \tag{A.14}$$

The quantity a is taken in the form (A.5), or, in the case of a v or pv field, in the form (A.6) with $S = 0$, $S_4 = 1$, and so on.

The complete picutre of the interaction of nonlinear meson waves with a singularity in the meson field — a nucleon — is extremely complicated and requires special investigation. We therefore confine ourselves to a remark regarding the specifically nonlinear scattering of a meson by a nucleon. Let the solution of the nonlinear equation

$$\beta_\lambda \partial\psi/\partial x_\lambda + k_0\psi + \lambda R'\beta\psi\cdot\psi^{+}R''\beta\psi = 0 \tag{A.15}$$

be a sum of the following form [we refrain as a matter of principle from the introduction of any sort of interaction terms into the nonlinear theory; both the nucleon itself and the wave incident on it are already contained in Eq. (A.15)]

$$\psi(x) = \psi_0(\mathbf{x}) + \psi'(\mathbf{x})\exp(-i\omega t), \tag{A.16}$$

where $\psi_0(\mathbf{x})$ is a solution of the static equation

$$\beta, \nabla\psi_0 + k_0\psi_0 + \lambda R'\beta\psi_0\psi_0^{+}R''\beta\psi_0 = 0. \tag{A.17}$$

Assuming $\psi' \ll \psi_0$, we get for the determination of ψ' in the first approximation the linear equation

$$\beta, \nabla\psi' + (k_0 - \beta_4\omega/c)\psi' + \lambda R'\beta\psi'\cdot\psi_0^{+}R''\beta\psi_0 + \lambda R'\beta\psi_0(\psi_0^{+}R''\beta\psi' + \psi^{+\prime}R''\beta\psi_0) = 0. \tag{A.18}$$

Proceeding further to choose ψ' in the form

$$\psi'(\mathbf{x}) = a\exp(i\mathbf{k}\mathbf{x}) + \psi''(\mathbf{x}) \tag{A.19}$$

and solving the resulting equation for ψ', one can convince oneself that ψ'' is spherically symmetric at large distances, and the nonlinear scattering is almost always isotropic.

The second-order equation for a weak meson wave colliding with a nucleon at rest can in many cases be reduced to the form

$$(\nabla^2 - k_0^2)\psi - (n^2(\mathbf{x})/c^2)\,\partial^2\psi/\partial t^2 = 0, \tag{A.20}$$

where $n \to 1$ for $\lambda \to 0$.

This equation contains a curious effect of the nonlinear capture of rays falling on the source with impact parameter smaller than a certain value l_{cr}. In this process the rays wind up spirally around the singularity of the field.

---

[1] L. Schiff, Phys. Rev. 84, 1 (1951).
[2] B. Malenka, Phys. Rev. 85, 686 (1952).
[3] R. Fornaguera, Nuovo cimento 1, 132 (1955).
[4] F. Belinfante, Phys. Rev. 74, 779 (1948).
[5] F. Belinfante, Physica 6, 849 (1939).
[6] A. A. Borgardt, J. Exptl. Theoret. Phys. (U.S.S.R.) 24, 24 (1953).
[7] W. Heisenberg, Zeitschr. f. Naturforsch. 9A, 292 (1954).
[8] H. Kita, Prog. Theor. Phys. 15, 83 (1956).
[9] A. A. Borgardt, Dokl. Akad. Nauk SSSR 110, 42 (1956), Soviet Phys. "Doklady" 1, 524 (1957).
[10] V. Iaichnitsyn, J. Exptl. Theoret. Phys. (U.S.S.R.) 31, 1082 (1956), Soviet Phys. JETP 4, 925 (1957).
[11] F. Cap, Phys. Rev. 95, 287 (1954).
[12] A. A. Borgardt, J. Exptl. Theoret. Phys. (U.S.S.R.) 24, 284 (1953).
[13] I. Lujiwara, Prog. Theor. Phys. 10, 589 (1953).

Translated by W. H. Furry

SOVIET PHYSICS JETP VOLUME 6, NUMBER 1 JANUARY, 1958

INTERACTION BETWEEN GRAVITATIONAL-CAPILLARY AND MAGNETOHYDRODYNAMIC WAVES

M. F. SHIROKOV

Moscow Aviation Institute

Submitted to JETP editor November 13, 1956

J. Exptl. Theoret. Phys. (U.S.S.R.) 33, 67-71 (July, 1957)

The uniqueness theorem is proved for the solutions of the hydrodynamic equations for an incompressible strongly conducting ideal liquid. Walen's exact solution for the case in which gravitational and capillary forces act on the liquid is shown to be valid. Relations for the stability conditions, penetration depth etc. are derived for potential and vortex harmonic waves. In the case of potential motion of the liquid the current density in the surface layer is found to be exactly zero.

MAGNETOHYDRODYNAMIC waves are described by the system of equations

$$\rho d\mathbf{v}/dt = -\nabla(p+U) + \mathbf{j}\times\mathbf{B}/c; \quad \operatorname{curl}\mathbf{H} = 4\pi\mathbf{j}/c, \quad \partial\rho/\partial t + \operatorname{div}(\rho\mathbf{v}) = 0; \quad \operatorname{curl}\mathbf{E} = -\partial\mathbf{B}/c\,\partial t; \quad \mathbf{E} + \mathbf{v}\times\mathbf{B}/c = 0, \tag{1}$$

where U is the potential associated with the forces of non-electromagnetic origin, where

$$\mathbf{H} = \mathbf{H}_0 + \mathbf{h}. \tag{2}$$

It will be assumed that the field $\mathbf{H}_0$ is uniform and known and that the liquid is incompressible; these assumptions are justified under the conditions of the present problem. Using the system of equations given in (1) and taking

$$\boldsymbol{\sigma} = \frac{c}{4\pi}\mathbf{E}\times\mathbf{H}; \quad W = \frac{1}{8\pi}(\varepsilon\mathbf{E}^2 + \mu\mathbf{H}^2), \quad T_{ik} = \frac{1}{4\pi}\{(\varepsilon\mathbf{E}^2 + \mu\mathbf{H}^2)^2\delta_{ik} - \varepsilon E_i E_k - \mu H_i H_k\},$$

it is possible to find the non-relativistic equations for conservation of momentum and energy in a volume τ bounded by a surface S:

$$\frac{d}{dt}\left\{\int_\tau \left(\rho v_i + \frac{\sigma_i}{c^2}\right) d\tau\right\} = -\oint_S (\rho v_i v_k + p\delta_{ik} + T_{ik})\, n_k dS; \tag{3}$$

$$\frac{d}{dt}\left\{\int_\tau \left(\frac{1}{2}\rho v^2 + W\right) d\tau\right\} = -\oint_S \left\{\left(\frac{1}{2}\rho v^2 + p\right) v_i + \sigma_i\right\} n_i dS - \int_\tau \frac{j^2}{\sigma}\, d\tau. \tag{4}$$

If we are given the quantities:

$$v_n = v_i n_i, \; p, \; E_\tau \;(\text{or } H_t) \tag{5}$$

on the surface S and the velocity and directions of the fields are given as functions of the coordinates inside the volume τ at time t = 0:

$$\mathbf{v} = \mathbf{v}(x_k), \; \mathbf{E} = \mathbf{E}(x_k), \; \mathbf{H} = \mathbf{H}(x_k), \tag{6}$$

and if the condition of incompressibility is satisfied

$$\operatorname{div}\mathbf{v} = 0 \tag{7}$$

the system of equations in (1) has a unique solution which satisfies the initial conditions and the boundary conditions (5) and (6), provided μ, ϵ, and σ are independent of the coordinates and time. The proof, as in electrodynamics, is based on the fact that the differences of the solutions $\mathbf{v}'$, $\mathbf{E}'$, $\mathbf{H}'$ and $\mathbf{v}''$, $\mathbf{E}''$ and $\mathbf{H}''$, which satisfy Eqs. (5) and (6), are also solutions of the equations in (1), where the continuity equation is taken in the form given in Eq. (7), and the fact that the total energy cannot increase.

To calculate the effects of gravitational and capillary forces, acting on the surface of the liquid S, on the propogation of the magnetohydrodynamic waves, we can use as boundary conditions the equations which describe the discontinuities in the physical quantities at the interface between two media; these relations are derived from Maxwell's equations, the theory of capillary action and the conservation laws

$$[E_t] = 0;\ [H_t] = 0;\ [\varepsilon E_i n_i] = 0;\ [\mu H_i n_i] = 0; \tag{8}$$

$$[(\rho v_i v_k + p\delta_{ik} + T_{ik}) n_k] = -\pi; \quad [\{(^1/_2\rho \mathbf{v}^2 + p)\, v_i + \sigma_i\} n_i] = 0, \tag{9}$$

where the square brackets denote the differences in the values of the quantities associated with the second medium and first medium (the given liquid) and

$$\pi = \alpha\,(1/R_1 + 1/R_2) \tag{10}$$

is the Laplace pressure.

The surface which divides the two media will be assumed to be approximately the same as the surface

$$S_0(x_l) = 0, \tag{11}$$

which corresponds to the equilibrium configuration of the liquid. We assume that the quantities which appear in the boundary conditions (8) and (9) are given at this surface; because of Eq. (11) these are equivalent to the condition given in (5). Applying the initial conditions in the region which is filled by the liquid and bounded by the surface given by (11), we have a complete formulation of the problem, which has a unique solution.

As is well known, Walen[2] has given an exact solution for Eq. (1) in the case of an incompressible liquid:

$$\mathbf{v} = \pm \mathbf{h}\sqrt{\mu/4\pi\rho}; \quad \mathbf{E} = \pm\, \mathbf{h} \times \mathbf{H}_0 \sqrt{\mu/4\pi\rho}; \tag{12}$$

$$p + \rho u + \frac{\mu}{8\pi}(\mathbf{H}_0 + \mathbf{h})^2 + \psi(t) = 0, \tag{13}$$

where the vector $\mathbf{h}$ satisfies the equation

$$(\mathbf{H}_0 \nabla)\,\mathbf{h} = (4\pi\rho/\mu)^{1/2}\,\partial\mathbf{h}/\partial t, \tag{14}$$

and $\psi(t)$ is an arbitrary function of time.

We now show that there are exact Walen solutions which satisfy the boundary conditions in (8) and (9) thus constituting a solution of the problem stated above. The only quantity assumed given is the pressure p'' in medium 2, which is assumed to be a rarefied gas or even a vacuum. In this case it is sufficient to use only one of the relations in (9); this relation assumes the form:

$$\left[p + \rho \mathbf{v}^2 + \frac{1}{8\pi}(\varepsilon \mathbf{E}^2 + \mu H^2)\right] = -\pi.$$

To make the problem somewhat more concrete we also assume that both media are in a fixed gravitational field

$$U = \rho g z, \tag{15}$$

where the medium fills the half space along the negative z-axis. Then, in view of Eq. (12), assuming that

$$\varepsilon'' = \mu'' = 1, \quad \varepsilon' = \varepsilon, \quad \mu' = \mu, \quad \rho'' v''^2 = 0,$$

the preceding relation can be rewritten in the form

$$p' - p'' + \frac{\mu}{4\pi}(\mathbf{H}' - \mathbf{H}_0)^2 + \frac{1}{8\pi}\{(\varepsilon - 1)\,[E_x'^2 + E_y'^2 - \varepsilon E_z'^2] + (\mu - 1)\,[H_x'^2 + H_y'^2 - \mu H_z'^2]\} = -\alpha\,(\partial^2 z/\partial x^2 + \partial^2 z/\partial y^2). \tag{16}$$

At $z = 0$ this equation must be compatible with Eq. (1). Hence the boundary condition for the solution in the form given in (12) – (14) can be obtained by differentiating (16) and (13) with respect to time and eliminating dp'/dt (dp''/dt is taken as zero). We find

$$\frac{\partial}{\partial t}\left\{\frac{\mu}{4\pi}(\mathbf{H}' - \mathbf{H}_0)^2 + \frac{1}{8\pi}\left\{(\varepsilon - 1)\,[\mathbf{E}'^2 - (\varepsilon + 1)\,E_z'^2] + (\mu - 1)\,[\mathbf{H}'^2 - (\mu + 1)\,H_z'^2] - \frac{\mu}{8\pi}\mathbf{H}'^2\right\}\right\} \mp g\sqrt{\frac{\mu\rho}{4\pi}}\,h_z'$$
$$\pm\, \alpha\sqrt{\frac{\mu}{4\pi\rho}}\left(\frac{\partial^2 h_z'}{\partial x^2} + \frac{\partial^2 h_z'}{\partial y^2}\right) + \varphi(t) = 0, \tag{17}$$

where, as before, $\varphi(t)$ is an arbitrary function of t. The Walen solution for gravitational-capillary and magnetohydrodynamic waves which is of interest to us can be obtained in the following manner. We have the solution of Eq. (7) in the form:

$$\mathbf{v} = \operatorname{curl} \mathbf{a}, \tag{18}$$

or

$$\mathbf{v} = \operatorname{grad} \varphi. \tag{19}$$

Then h, being determined by the first of the equations in (12), automatically satisfies (14). Furthermore, h, and thus v, must be chosen to satisfy the boundary condition in (17) in the plane z = 0. The solution in (18) and the h which corresponds to it satisfy (7) and (14) with the choice of any three functions of the coordinates and time a_i; for the condition in (17), however, we require any two functions of the three a_i.

The solution for v and h in the form (19) reduces to the search for h (or v) from the Laplace equations

$$\Delta \chi = 0, \tag{20}$$

which satisfy the boundary condition in (17) when the following substitution is made:

$$\mathbf{h} = \operatorname{grad} \chi. \tag{21}$$

In all cases — for vortex and potential gravitational-capillary and magnetohydrodynamic waves — the velocity in the direction of the fixed external magnetic field $\mathbf{H}_0$ has the usual value

$$u = \pm \mathbf{H}_0 \sqrt{\mu/4\pi\rho}. \tag{22}$$

It should be noted, however, that in potential waves, as defined by (19) and (21), up to and including the dividing surface between the two media we have

$$\mathbf{j} = 0, \tag{23}$$

this result contradicts the conclusions reached in Ref. 3, in which the boundary conditions $\mathbf{j} \neq 0$ and even $\mathbf{j} = \infty$ have been assumed without justification.

We now consider some simple cases: these correspond to the linear approximation and to fields which are perpendicular and parallel to the surface of the liquid:

$$H_z^0 = H_0 \neq 0; \quad H_x^0 = H_y^0 = 0; \tag{I}$$

$$H_x^0 = H_0 \neq 0; \quad H_y^0 = H_z^0 = 0. \tag{II}$$

Furthermore, for simplicity we assume

$$\varepsilon - 1 = 0, \quad \mu - 1 = 0. \tag{24}$$

First, we consider the potential waves (19) and (21). We have

$$\frac{\partial}{\partial x_i}\left(H_{0k} \frac{\partial}{\partial x_k}\right) \chi = H_{0k} \frac{\partial^2 \chi}{\partial x_i \partial x_k}.$$

On the other hand,

$$\left(H_{0k} \frac{\partial}{\partial x_k}\right) \frac{\partial \chi}{\partial x_i} = H_{0k} \frac{\partial^2 \chi}{\partial x_i \partial x_k},$$

thus, $(\mathbf{H}_0 \nabla)\mathbf{h} = \nabla(\mathbf{H}_0 \mathbf{h})$. In accordance with these relations and (14), Eq. (13) can be transformed as follows:

$$\frac{\partial \varphi}{\partial t} + gz + \frac{1}{\rho}\left(p + \frac{1}{2}\rho v^2\right) + f(t) = 0, \tag{25}$$

where f(t) is an arbitrary function of the time which may be taken equal to zero. In the linear approximation, using Eqs. (16) and (25), differentiating with respect to time and eliminating $\partial p'/\partial t$, we have in the plane z = 0

$$\frac{\partial^2 \varphi'}{\partial t^2} + g \frac{\partial \varphi'}{\partial z} - \frac{\alpha}{\rho} \frac{\partial}{\partial z}\left(\frac{\partial^2 \varphi'}{\partial x^2} + \frac{\partial^2 \varphi'}{\partial y^2}\right) = 0. \tag{26}$$

This boundary condition is in complete agreement with the boundary condition for gravitational-capillary waves.

We consider the solution of (7) in the form

$$\varphi = \varphi_0 e^{i(\omega t - \mathbf{kr})}. \tag{27}$$

Substituting this expression for φ in (7) and (26) we find

$$k_x^2 + k_y^2 + k_z^2 = 0, \tag{28}$$

$$\omega^2 = -ik_z[g + (\alpha/\rho)(k_x^2 + k_y^2)], \tag{29}$$

from which it is apparent that k_z must be an imaginary number, with

$$ik_z = -k = -\sqrt{k_x^2 + k_y^2}, \tag{30}$$

where k is a real positive number and k_x and k_y are also real.

From Eqs. (14) and (29), we have in cases (I) and (II):

$$\omega = -k_z u = -iku, \tag{31.I}$$

$$\omega = -k_z u. \tag{31.II}$$

Thus, in case I a stable wave of the form given in (27) cannot exist. In case II such a wave is possible. It is localized in a layer of thickness $d = 1/k$ and has the velocity of the usual magnetohydrodynamic wave, given by (22), in the direction of the z-axis, which is perpendicular to the surface of the liquid.

From Eqs. (29), (30) and (31.II) we obtain the equation for the damping factor

$$k_x^2 u^2 = k(g + \alpha k^2/\rho). \tag{32}$$

If $k_x = k$,

$$k = (\rho u^2/2\alpha)(1 \pm \sqrt{1 - 4\alpha g/u^4\rho}). \tag{33}$$

Whence, from Eq. (22) it is also obvious that the stability condition for waves of this type is:

$$H_0^4 \geqslant 64\pi^2\alpha g\rho. \tag{34}$$

In mercury, for example, the smallest magnetic field for which this type of magnetohydrodynamic potential wave is possible is $H_{0m} = 246.2$ gauss. When $H_0 \gg H_{0m}$ the thickness of the surface layer is given by the formula

$$d = \alpha/\rho u^2. \tag{35}$$

In the long-wave case

$$d = u^2/g. \tag{36}$$

In mercury with $H_0 = 10^4$ gauss, i.e., with a field approximately 100 times larger than the minimum value H_{0m}, we have $d \sim 10^{-2}$ cm from Eq. (35) and $d \approx 10^3$ cm from Eq. (36).

Thus, the strongest effect on the concentration of the potential magnetohydrodynamic waves in the surface layer is that due to the capillary forces. However, when these forces are present the thickness of the surface-wave layer, in general, is smaller than for the skin effect; moreover, the current density is exactly zero for the potential surface waves, in contrast to the skin effect and in contradiction with the statements of Ref. 3. In the case of vortex waves (18), in the linear approximation using (I), (II), and (24) the boundary condition in (17) assumes the form

$$\frac{\partial h_z'}{\partial t} + \frac{g}{u} h_z' - \frac{\alpha}{\rho u}\left(\frac{\partial^2 h_z'}{\partial x^2} + \frac{\partial^2 h_z'}{\partial y^2}\right), \tag{17.I}$$

$$\frac{\partial h_x'}{\partial t} + \frac{g}{u} h_z' - \frac{\alpha}{\rho u}\left(\frac{\partial^2 h_z'}{\partial x^2} + \frac{\partial^2 h_z'}{\partial y^2}\right). \tag{17.II}$$

We consider a solution in the form

$$\mathbf{v} = \pm\frac{1}{\sqrt{4\pi\rho}}\operatorname{curl}\mathbf{a} = \pm\frac{h}{\sqrt{4\pi\rho}}, \quad \mathbf{a} = \mathbf{a}_0 e^{i(\omega t - kr)}, \tag{37}$$

which is known to satisfy Eq. (1) and the condition given in (7). In cases (I) and (II) we have

$$\omega = i\left[\left(\frac{g}{u} + \frac{\alpha}{\rho u}\right)(k_x^2 + k_y^2)\right] = -uk_z, \tag{38.I}$$

$$k_y = 0;\ k_x = ik_z = k \leqslant 0, \qquad \omega = \frac{1}{u}\left(g + \frac{\alpha}{\rho}k^2\right) = -uk_x. \tag{38.II}$$

In case I we do not obtain stable waves of the form given in (37). In case II we obtain a wave which decays in the z-direction and which is characterized by a penetration depth

$$d = -1/k = (\rho u^2/2\alpha)(1 \pm \sqrt{1 - 4\alpha g/\rho u^4}). \tag{39}$$

Thus, the vortex magnetohydrodynamic surface waves have the same propogation and decay relations as the potential waves with the one exception that the current density is not zero; these waves are similar to the skin effect in this respect.

---

[1] H. Alfven, Cosmical Electrodynamics, (Russ. Transl.), IIL, Moscow, 1952.

[2] C. Walen, Ark. f. Mat., astr., o. fysik, 30A, 15; 31B, 3 (1944).

[3] A. Kislovskii, Theory of Surface Waves in Magnetohydrodynamics, Moscow State University, 1956 (Author's abstract of dissertation).

Translated by H. Lashinsky
11

SOVIET PHYSICS JETP VOLUME 6, NUMBER 1 JANUARY, 1958

7

ON THE DYNAMICS OF A BOUNDED PLASMA IN AN EXTERNAL FIELD

L. M. KOVRIZHNYKH

P. N. Lebedev Physics Institute, Academy of Sciences, U.S.S.R.

Submitted to JETP editor November 16, 1956

J. Exptl. Theoret. Phys. (U.S.S.R.) 33, 72-76 (July, 1957)

Some problems relating to the dynamics of a quasi-neutral plasma formation situated in the field of a plane electromagnetic wave are considered. The method of successive approximations is employed. It is shown that within the limits of the assumptions underlying the analysis a plasma bunch tends to spread out.

IN connection with the proposal of a radiation method of accelerating particles[1] the question has arisen of the behavior of a quasi-neutral plasma condensation situated in the field of an electromagnetic wave and, in particular, the question of the stability of such a condensation. A more or less rigorous solution of this problem encounters formidable mathematical difficulties. Therefore it is not without interest to consider a simplified problem which would nevertheless allow one to obtain approximate estimates of the magnitude and the nature of the forces acting on the condensation. The present paper is devoted to the examination of one of these simplest cases.

We consider a system of electrons and ions subjected to an incident plane electromagnetic wave with a propagation vector k parallel to the z axis. By using the hydrodynamic description of plasma,* which is apparently quite permissible in order to obtain results of an exploratory nature, we shall describe the system by specifying the densities ρ_i, ρ and the velocities $\mathbf{v}_i$ and $\mathbf{v}$ of the ions and the electrons respectively, and we shall assume that the total number of electrons is equal to the total number of ions, i.e.,

---

* We shall not consider here questions concerning the permissibility of applying the hydrodynamic approximation.

$$\int \rho_i(\mathbf{r})\,d\mathbf{r} = \int \rho(\mathbf{r})\,d\mathbf{r}.$$

Since the mass of the ion is much larger than the mass of the electron, then in the first approximation we may consider the ions to be at rest, i.e., $\mathbf{v}_i = 0$, and to have a time-independent density distribution $\rho_i = \rho_0(\mathbf{r})$. If the variable external field is described by means of the vector-potential $\mathbf{A}_{ext} = \{A_0, 0, 0\} \times e^{ikz - i\omega t}$ while the self-field is described by means of the potentials $\mathbf{A}(\mathbf{r}, t)$ and $\varphi(\mathbf{r}, t)$ then the equations which determine ρ, $\mathbf{v}$, φ and $\mathbf{A}$ will have the form:

$$\partial\rho/\partial t = -\nabla(\rho\mathbf{v}); \tag{1}$$

$$\rho\left[\frac{\partial\mathbf{v}}{\partial t} + (\mathbf{v}\nabla)\mathbf{v}\right] = -\frac{e}{m}\rho\left\{\nabla\varphi + \frac{1}{c}\frac{\partial\mathbf{A}}{\partial t} + \frac{1}{c}\frac{\partial\mathbf{A}_{ext}}{\partial t} - \frac{1}{c}[\mathbf{v}[\nabla\mathbf{A}]] - \frac{1}{c}[\mathbf{v}[\nabla\mathbf{A}_{ext}]]\right\} - v_T^2\nabla\rho; \tag{2}$$

$$\Box\mathbf{A} = -(4\pi e/c)\rho\mathbf{v}; \quad \Box\varphi = -4\pi e(\rho_0 - \rho). \tag{3}$$

Here v_T plays the role of the speed of sound in the plasma. Equations (1) – (3) represent a system of non-linear differential equations. By utilizing the formalism of Green's functions we shall write the system of equations (2), (3) in the form of a single (non-linear) integro-differential equation. We then obtain:

$$\partial\rho/\partial t = -\nabla(\rho\mathbf{v}); \tag{4}$$

$$\frac{\partial\mathbf{v}}{\partial t} + (\mathbf{v}\nabla)\mathbf{v} = \frac{e}{m}\left\{\mathbf{E}_{ext} + \mathbf{E}(\rho\mathbf{v}) + \frac{1}{c}[\mathbf{v}\mathbf{H}_{ext}] + \frac{1}{c}[\mathbf{v}\mathbf{H}(\rho\mathbf{v})]\right\} - v_T^2\frac{\nabla\rho}{\rho}; \tag{5}$$

where

$$\mathbf{E}_{ext} = -\frac{1}{c}\frac{\partial\mathbf{A}_{ext}}{\partial t}, \quad \mathbf{H}_{ext} = \operatorname{curl}\mathbf{A}_{ext},$$

$$\mathbf{E}(\rho\mathbf{v}) = -\frac{e}{c^2}\frac{\partial}{\partial t}\iint G(\mathbf{r}\mathbf{r}'tt')\,\mathbf{v}(\mathbf{r}'t')\,\rho(\mathbf{r}'t')\,d\mathbf{r}'dt' + e\operatorname{grad}\operatorname{div}\iint G(\mathbf{r}\mathbf{r}'tt')\,d\mathbf{r}'dt'\int\mathbf{v}(\mathbf{r}'t'')\,\rho(\mathbf{r}'t'')\,dt''; \tag{6}$$

$$\mathbf{H}(\rho\mathbf{v}) = \frac{e}{c}\operatorname{curl}\iint G(\mathbf{r}\mathbf{r}'tt')\,\mathbf{v}(\mathbf{r}'t')\,\rho(\mathbf{r}'t')\,d\mathbf{r}'dt'; \tag{7}$$

$$G(\mathbf{r}\mathbf{r}'tt') = \delta(t' - t + |\mathbf{r} - \mathbf{r}'|/c)/|\mathbf{r} - \mathbf{r}'$$

is the Green function satisfying the equation:

$$\Box G(\mathbf{r}\mathbf{r}'tt') = -4\pi\delta(\mathbf{r} - \mathbf{r}')\,\delta(t - t').$$

The exact solution of Eqs. (4), (5) is difficult;* however, under certain assumptions it is possible to obtain an approximate estimate of the magnitude of the forces and apparently to reach some conclusions with respect to the nature of the possible deformations. In particular, we shall tackle the problem on the assumption of small non-linearity and of weak self-fields. Thus, we assume: (1) that the particle density is not too high, i.e., $E_{ext} \gg E$, (2) that the external field and the wavelength are such that† $v/c \ll 1$, and we shall solve the system of equations (4), (5) by the method of successive approximations taking for our small parameter λ the ratios E/E_{ext} and v/c. Moreover, we shall assume that $\rho_0(\mathbf{r})$ satisfies the following conditions: (1) $\rho_0(\mathbf{r})$ is a function of the radius only, (2) $\rho_0(\mathbf{r})$ varies slowly for $r < a$, and falls off sufficiently rapidly for $r > a$ where a is a characteristic dimension of the system (for example, like $\exp\{-(r/a)^n\}$ where $n \geq 2$).

Now by representing ρ and $\mathbf{v}$ in the form

---

* In general, the exact solution of (4), (5) does not appear to be required since it will not be able to give us a sufficiently detailed answer to the questions of interest to us because of the assumption made above that the ions are at rest; however, the consideration of the case of high densities is of some interest even within the limitations imposed on the problem considered above.

†The criterion for the fulfillment of the above conditions will be obtained below.

$$\rho = \rho_0(r) + \sum \lambda^n \rho_n(\mathbf{r}), \quad \mathbf{v} = \mathbf{v}_0(\mathbf{r}) + \sum \lambda^n \mathbf{v}_n(\mathbf{r}) \tag{8}$$

and substituting into (4) and (5) we shall obtain after restricting ourselves to terms up to the second order (in λ) inclusively:

$$\frac{\partial \mathbf{v}_0}{\partial t} = \frac{e}{m}\mathbf{E}_{\text{ext}}, \quad \frac{\partial \mathbf{v}_2}{\partial t} = \frac{e}{m}\Big[\mathbf{E}(\rho_0 \mathbf{v}_1) + \mathbf{E}(\rho_1 \mathbf{v}_0) + \frac{1}{c}[\mathbf{v}_1 \mathbf{H}_{\text{ext}}]\Big] - (\mathbf{v}_0 \nabla)\mathbf{v}_0, \quad \frac{\partial \mathbf{v}_1}{\partial t} = \frac{e}{m}\Big[\mathbf{E}(\rho_0 \mathbf{v}_0) + \frac{1}{c}[\mathbf{v}_0 \mathbf{H}_{\text{ext}}]\Big] - (\mathbf{v}_0 \nabla)\mathbf{v}_0,$$

$$+ \frac{1}{c}[\mathbf{v}_0 \mathbf{H}(\rho_0 \mathbf{v}_0)]\Big] - (\mathbf{v}_0 \nabla)\mathbf{v}_1 - (\mathbf{v}_1 \nabla)\mathbf{v}_0 - v_T^2 \frac{\nabla \rho_0}{\rho_0} \tag{9}$$

so that consequently the force acting on the electrons of the condensation is given by

$$\mathbf{F} = e\Big\{\mathbf{E}_{\text{ext}} + \mathbf{E}(\rho_0 \mathbf{v}_0) + \mathbf{E}(\rho_1 \mathbf{v}_0) + \mathbf{E}(\rho_0 \mathbf{v}_1) + \frac{1}{c}[\mathbf{v}_0 \mathbf{H}_{\text{ext}}] + \frac{1}{c}[\mathbf{v}_1 \mathbf{H}_{\text{ext}}] + \frac{1}{c}[\mathbf{v}_0 \mathbf{H}(\rho_0 \mathbf{v}_0)]\Big\}$$

$$- m\Big[(\mathbf{v}_0 \nabla)\mathbf{v}_0 + (\mathbf{v}_0 \nabla)\mathbf{v}_1 + (\mathbf{v}_1 \nabla)\mathbf{v}_0 - v_T^2 \frac{\nabla \rho_0}{\rho_0}\Big], \tag{10}$$

where $\mathbf{v}_0$, $\mathbf{v}_1$, ρ are determined by (9). We note that if we start to calculate the next approximations we shall obtain secular terms, and that consequently the series for ρ and $\mathbf{v}$ diverge. However, for sufficiently small times $t < \tau \approx c\omega/v\omega_0^2$ the expressions for ρ, $\mathbf{v}$ and consequently for $\mathbf{F}$, remain valid, and since for the reasons given above (see second footnote) we are not interested in an exact solution of our problem, the result obtained above appears to be satisfactory. Moreover, we regarded the term $v_T^2 \nabla \rho_0/\rho_0$ as being of second order; in the opposite case (i.e., at sufficiently high temperatures) instability apparently occurs.

Since we are interested either in constant forces, or in forces varying slowly in time (in comparison with the frequency of the external field) the expression for $\mathbf{F}$ may be averaged over a time of the order of several periods $T = 2\pi/\omega$, and it may be easily shown that in the course of this averaging a number of terms drops out and we obtain:

$$\overline{\mathbf{F}} = \frac{e}{c}\overline{\{[\tilde{\mathbf{v}}_1 \mathbf{H}_{\text{ext}}] + [\tilde{\mathbf{v}}_0 \mathbf{H}(\rho_0 \tilde{\mathbf{v}}_0)]\} - m[(\tilde{\mathbf{v}}_1 \nabla)\tilde{\mathbf{v}}_0 + (\tilde{\mathbf{v}}_0 \nabla)\tilde{\mathbf{v}}_1]} - m v_T^2 \frac{\nabla \rho_0}{\rho_0}, \tag{11}$$

where $\tilde{\mathbf{v}}_0$ and $\tilde{\mathbf{v}}_1$ are determined by

$$\partial \tilde{\mathbf{v}}_0/\partial t = \frac{e}{m}\mathbf{E}_{\text{ext}}, \quad \partial \tilde{\mathbf{v}}_1/\partial t = (e/m)\mathbf{E}(\tilde{\rho}_0 \tilde{\mathbf{v}}_0), \tag{12}$$

while the bar indicates averaging in time.

The physical nature of the first two terms in the expression for the force is clear: they take into account the interaction of the particles with the external and the self magnetic field; the term $\overline{\mathbf{v} \cdot \nabla \mathbf{v}}$ has a form analogous to the force acting on a dipole in an inhomogeneous field. Indeed, since $\partial \mathbf{v}/\partial t \sim \mathbf{E}$ and $\mathbf{v} \sim \partial \mathbf{P}/\partial t$, then

$$(\mathbf{P}\nabla)\mathbf{E} \sim \Big(\int \mathbf{v}\,dt \nabla\Big)\partial \mathbf{v}/\partial t,$$

and since

$$\overline{\frac{\partial}{\partial t}\Big(\int \mathbf{v}\,dt \nabla\Big)\mathbf{v}} = 0,$$

then it follows from this that $\overline{\mathbf{v} \cdot \nabla \mathbf{v}} \sim \overline{\mathbf{P} \cdot \nabla \mathbf{E}}$ (here $\mathbf{P}$ denotes the dipole moment).

Thus the problem has been reduced to finding $\mathbf{E}(\rho_0 \mathbf{v}_0)$ and $\mathbf{H}(\rho_0 \mathbf{v}_0)$, or by virtue of the relations

$$\mathbf{E} = -\nabla\varphi - \frac{1}{c}\frac{\partial \mathbf{A}}{\partial t}, \quad \mathbf{H} = [\nabla \mathbf{A}], \quad (\nabla \mathbf{A}) + \frac{1}{c}\frac{\partial \varphi}{\partial t} = 0$$

to finding the vector potential

$$\mathbf{A}(\mathbf{r}t) = \frac{e}{c}\iiiint G(\mathbf{r}\mathbf{r}'tt')\rho_0(r')\tilde{\mathbf{v}}_0(\mathbf{r}'t')\,d\mathbf{r}'dt'. \tag{13}$$

Substituting $\tilde{\mathbf{v}}_0$ from (12) (the solution of which is elementary) into (13) and integrating we obtain:

$$\mathbf{A} = \{A, 0, 0\},$$

$$A = -4\pi k A_0 \frac{e^2}{mc^2} \sum_{n=0}^{\infty} i^{n+1} (2n+1) I_n(kr) P_n(\cos\theta) e^{-i\omega t}, \qquad I_n(kr) = h_n^{(1)}(kr) \int_0^r \rho_0(r') j_n^2(kr') r'^2 dr'$$
$$+ j_n(kr) \int_r^{\infty} \rho_0(r') j_n(kr') h_n^{(1)}(kr') r'^2 dr'. \qquad (14)$$

Here r is the radius drawn from the center of the condensation to the given point, θ is the angle between the z axis and r, $j_n(kr)$ and $h_n^{(1)}(kr)$ are the spherical Bessel and Hankel functions, P_n are the Legendre polynomials.

Now by determining E and H from (14) and $\widetilde{v}_1$ from (12) and substituting into (11) we obtain (after averaging) the desired expression for the force. We can specify the conditions under which we can use the expressions obtained in this way by taking into account the conditions under which the method of successive approximations may be used:

$$\omega_0^2/\omega^2 \ll 1, \; eA_0/mc^2(ka)^{\alpha} \ll 1, \qquad \text{where } \alpha = \begin{cases} 1 & \text{for } ka \ll 1 \\ 0 & \text{for } ka > 1, \end{cases} \quad \omega_0^2 = \frac{4\pi e^2}{m} \rho_0(0). \qquad (15)$$

Thus the problem has been solved. However, the expression for the average force obtained in the form of an infinite series is extremely complicated, and this does not permit us to draw any direct conclusions with respect to the nature of the deformations obtained. Therefore we shall take as an example a particular case in which the characteristic dimensions of the system and the wavelength are such that ka ≪ 1. In this case by expanding the expressions obtained above in powers of ka and by limiting ourselves to terms of order ka we shall obtain for r ≤ a:

$$\begin{aligned}
\overline{F}_x &= -kx \frac{9\sigma_T N\overline{W}}{2(ka)^3} \left\{ \frac{24}{105} + \frac{\Delta}{(kr)^2} \left[5\frac{x^2}{r^2} - 3 \right] - \frac{\Delta'}{kr} \frac{x^2}{r^2} \right\} - \frac{mv_T^2}{\rho_0} \frac{\partial \rho_0}{\partial x}, \\
\overline{F}_y &= -ky \frac{9\sigma_T N\overline{W}}{2(ka)^3} \left\{ \frac{32}{105} + \frac{\Delta}{(kr)^2} \left[5\frac{x^2}{r^3} - 1 \right] - \frac{\Delta'}{kr} \frac{x^2}{r^2} \right\} - \frac{mv_T^2}{\rho_0} \frac{\partial \rho_0}{\partial y}, \\
\overline{F}_z &= -kz \frac{9\sigma_T N\overline{W}}{2(ka)^3} \left\{ \frac{24}{105} + \frac{\Delta}{(kr)^2} \left[5\frac{x^2}{r^2} - 1 \right] - \frac{\Delta'}{kr} \frac{x^2}{r^2} \right\} - \frac{mv_T^2}{\rho_0} \frac{\partial \rho_0}{\partial z},
\end{aligned} \qquad (16)$$

and for r ≥ a:

$$\begin{aligned}
\overline{F}_x &= -kx \frac{9\sigma_T N\overline{W}}{2(ka)^3} \left\{ \frac{24}{105} \frac{a^3}{r^3} + \frac{\widetilde{\Delta}}{(kr)^2} \left[5\frac{x^2}{r^2} - 3 \right] - \frac{\Delta'}{kr} \frac{x^2}{r^2} - \Phi_x \right\} - \frac{mv_T^2}{\rho_0} \frac{\partial \rho_0}{\partial x}, \\
\overline{F}_y &= -ky \frac{9\sigma_T N\overline{W}}{2(ka)^3} \left\{ \frac{32}{105} \frac{a^3}{r^3} + \frac{\widetilde{\Delta}}{(kr)^2} \left[5\frac{x^2}{r^2} - 1 \right] - \frac{\Delta'}{kr} \frac{x^2}{r^2} - \Phi_y \right\} - \frac{mv_T^2}{\rho_0} \frac{\partial \rho_0}{\partial y}, \\
\overline{F}_z &= -kz \frac{9\sigma_T N\overline{W}}{2(ka)^3} \left\{ \frac{24}{105} \frac{a^3}{r^3} + \frac{\widetilde{\Delta}}{(kr)^2} \left[5\frac{x^2}{r^2} - 1 \right] - \frac{\Delta'}{kr} \frac{x^2}{r^2} - \Phi_z \right\} - \frac{mv_T^2}{\rho_0} \frac{\partial \rho_0}{\partial z},
\end{aligned} \qquad (17)$$

where

$$\begin{aligned}
\Phi_x &= \frac{a^3}{r^3}\left(1 - \frac{a^2}{r^2}\right) \left\{ \frac{3}{70}\left(9 - 5\frac{a^2}{r^2}\right) - \frac{3z^2 + x^2}{2r^2}\left(1 - \frac{a^2}{r^2}\right) + \frac{x^2 z^2}{2r^4}\left(5 - 9\frac{a^2}{r^2}\right) \right\}; \\
\Phi_y &= \frac{a^3}{r^3}\left(1 - \frac{a^2}{r^2}\right) \left\{ \frac{1}{70}\left(9 - 5\frac{a^2}{r^2}\right) - \frac{x^2 + z^2}{2r^2}\left(1 - \frac{a^2}{r^2}\right) + \frac{x^2 z^2}{2r^4}\left(5 - 9\frac{a^2}{r^2}\right) \right\}; \\
\Phi_z &= \frac{a^3}{r^3}\left(1 - \frac{a^2}{r^2}\right) \left\{ \frac{3}{70}\left(9 - 5\frac{a^2}{r^2}\right) - \frac{3x^2 + z^2}{2r^2}\left(1 - \frac{a^2}{r^2}\right) + \frac{x^2 z^2}{2r^4}\left(5 - 9\frac{a^2}{r^2}\right) \right\}; \\
\sigma_T &= \frac{8\pi}{3}\left(\frac{e^2}{mc^2}\right)^2, \; \overline{W} = \frac{(kA_0)^2}{8\pi}, \; \Delta = 1 - \frac{\rho_0(r)}{\rho_0(0)}, \; \widetilde{\Delta} = \frac{a^3}{r^3} - \frac{\rho_0(r)}{\rho_0(0)}, \; \Delta' = \frac{\partial \Delta}{\partial kr},
\end{aligned} \qquad (18)$$

N is the total number of electrons in the condensation.

Since we are mainly interested in questions of stability it is easier to deal not with the Cartesian components, but only with the radial component of the force. For r ≤ a it has the form:

$$F_r = -\frac{3\sigma_T N\overline{W}}{2(ka)^3} \left\{ \frac{8}{35}\left[3 + \frac{y^2}{r^2}\right] kr + \frac{3\,[1 - \rho_0(r)/\rho_0(0)]}{kr} \left[3\frac{x^2}{r^2} - 1\right] + \frac{3}{\rho_0(0)} \frac{x^2}{r^2} \frac{\partial \rho_0(r)}{\partial kr} \right\} - \frac{v_T^2 m}{\rho_0(r)} \frac{\partial \rho_0(r)}{\partial r}; \qquad (19)$$

and for r ≥ a:

$$F_r = -\frac{3\sigma_T N\overline{W}}{2(ka)^3} \left\{ \frac{8}{35}\left[3 + \frac{y^2}{r^2}\right] \frac{a^3}{r^3} kr + \frac{3}{kr}\left[\left(\frac{a}{r}\right)^3 - \frac{\rho_0(r)}{\rho_0(0)}\right]\left[3\frac{x^2}{r^2} - 1\right] + \Phi_r(r) + 3\frac{1}{\rho_0(0)} \frac{x^2}{r^2} \frac{\partial \rho_0(r)}{\partial kr} \right\} - \frac{mv_T^2}{\rho_0(r)} \frac{\partial \rho_0(r)}{\partial r}, \qquad (20)$$

where

$$\Phi_r = -3\frac{a^3}{r^3}\left(1-\frac{a^2}{r^2}\right)\left\{\frac{1}{70}\left(9-5\frac{a^2}{r^2}\right)\left(3-2\frac{y^2}{r^2}\right)kr - \frac{x^2+z^2}{2r^2}\left(1-\frac{a^2}{r^2}\right)kr + \frac{x^2z^2}{2r^4}\left(1-5\frac{a^2}{r^2}\right)kr\right\}. \tag{21}$$

Let us examine these expressions. First of all we emphasize once again that the results obtained above are only valid for a final time $t < \tau$ and consequently become invalid when the deformation of the condensation becomes appreciable. Therefore the present calculation does not pretend to give a more or less complete solution of the problem of stability, but is in the nature of only an approximate estimate, which, nevertheless, enables us to establish at least in general outline the tendency of the condensation to become deformed, and the nature of such a deformation.

Since we have assumed that $(ka) \ll 1$ the second and the third terms in the curly brackets will, generally speaking, be larger than the first one by a factor $1/(kr)^2$ and, consequently, in the region where Δ and Δ' differ from zero they will play a determining role. The first term is alway positive and consequently gives rise to a force directed towards the center of the condensation; on the other hand, the third term is always negative and gives the largest contribution at points of the most rapid rate of falling off of the function $\rho_0(r)$, i.e., at the "boundary" of the condensation. With respect to the second term we see that, depending on the value of x, it can be either positive or negative, i.e., it can give rise to a force directed either inwards or outwards with respect to the condensation, and that at sufficiently large distances (at points where $\rho_0 \to 0$ and $\partial\rho_0/\partial r \to 0$) it plays the decisive role.

We thus see that near the center of the condensation the force acting on the electrons (and, in particular, its sign) is completely determined by the behavior near zero of the function $\rho_0(r)$ and of its first derivative; while at values of r such that $\rho_0 \to 0$ and $\partial\rho_0/\partial\rho \to 0$ forces appear which are directed away from the center and which lead to the spreading of the peripheral particles of the condensation in the yz plane.

Thus, summarizing, we can say that the results obtained above show that the plasma condensation has a tendency to spread, at least for $ka \ll 1$. With respect to the case $ka \geq 1$ we have not succeeded in drawing any definite conclusions in view of the extremely complicated nature of the expressions obtained for **v**, **E**, **H** and **F**.

We note in conclusion that calculations made taking into account a constant magnetic field along the z axis have shown that in broad outline the picture remains the same with the only difference that the spreading in the yz plane is now replaced by spreading along the z axis.

---

[1] V. I. Veksler, Proceedings CERN Symposium on High Energy Accelerators and Pion Physics, Geneva, June 1956, Vol. 1, p. 80.

Translated by G. Volkoff
12

SOVIET PHYSICS JETP VOLUME 6, NUMBER 1 JANUARY, 1958

MAGNETORESISTIVE PHENOMENA IN n-Ge TYPE SEMICONDUCTORS IN STRONG MAGNETIC FIELDS

M. I. KLINGER and P. I. VORONIUK

Chernovtsy State University; Semiconductor Institute, Academy of Sciences, U.S.S.R.

Submitted to JETP editor November 19, 1956

J. Exptl. Theoret. Phys. (U.S.S.R.) 33, 77-87 (July, 1957)

The equilibrium electron concentration, Hall constant, and electrical resistance of n-Ge type semiconductors in a strong magnetic field are considered. The dependence of these quantities on the field strength is determined. It is found that the quantities under consideration are anisotropic, the nature of this anisotropy being determined by the anisotropy of the electron mass and by the number and mutual arrangement of the constant-energy ellipsoids.

IN the past, a number of papers[1,2] have appeared in which the electric resistivity in a magnetic field ρ_H and the Hall constant R in n-Ge type semiconductors have been considered. It is necessary to take into account here the anisotropy of the electron mass the the presence of several constant-energy ellipsoids in the Brillouin zone (six for Si and eight for Ge). However, the analysis was made by the usual kinetic-equation method without taking into account quantization of the electron energy by the field H, a procedure valid only for sufficiently small H.

In this connection, it is of interest to calculate ρ_H and R of n-Ge type semiconductors taking the electron mass anisotropy in strong magnetic fields into account. For this purpose it is necessary to take into account the above-mentioned electron energy quantization by the field H. The present paper is devoted to this.

1. CALCULATION OF THE CURRENTS

Let us assume that the electric field E is directed along the X axis and the magnetic field H perpendicular thereto is along the Z axis. To calculate ρ_H and R taking the energy quantization by the field H into account, we use the stationary states method.[3,4] Following this method, let us calculate the components of the electric current j in the presence of the crossed fields E and H. Inasmuch as several ellipsoids correspond to a given electron energy in the first Brillouin zone of n-Ge type crystals, the current j^i should be evaluated for each i-th ellipsoid and these currents should then be summed over all ellipsoids, taking their relative arrangement in the Brillouin zone into account. This is valid if the interellipsoid transitions caused by electron scattering are neglected, as can probably be done at low temperatures.

The energy spectrum of an electron with an anisotropic mass in the crossed fields E and H and its wave function (for the electron of the i-th ellipsoid) must be found in order to calculate the currents j^i. To do this, let us write the appropriate Hamiltonian in the system of the principal axes X_i, Y_i, Z_i of the i-th ellipsoid

$$\mathcal{H} = \frac{1}{2m_1}\left[\left(p_{x_i} - \frac{e}{c}A_{x_i}\right)^2 + \left(p_{y_i} - \frac{e}{c}A_{y_i}\right)^2\right] + \frac{1}{2m_2}\left(p_{z_i} - \frac{e}{c}A_{z_i}\right)^2 + e(\mathbf{E}\mathbf{r}_i), \tag{1}$$

where A is a vector-potential, m_1 is the electron transverse mass, m_2 is its longitudinal mass (it is assumed that the constant-energy ellipsoids are ellipsoids of revolution, as in n-Ge). By transforming coordinates

$$x'_i = x_i,\ y'_i = y_i,\ z_i = z'_i/\sqrt{s},\ s = m_2/m_1$$

and introducing correspondingly the new quantities

$$A'_{xi} = A_{xi},\ A'_{yi} = A_{yi},\ A'_{zi} = A_{zi}/\sqrt{s};\quad E'_{xi} = E_{xi},\ E'_{yi} = E_{yi},\ E'_{zi} = E_{zi}/\sqrt{s} \tag{2}$$

the operator (1) can be reduced to the following form:

$$\mathscr{H} = \frac{1}{2m_1}\left(\mathbf{p}_i' - \frac{e}{c}\mathbf{A}_i'\right)^2 + e\mathbf{E}_i'\mathbf{r}_i'. \tag{3}$$

Here, it should be noted that the transformations (2) also lead to the introduction of the field $\mathbf{H}' = \operatorname{curl}\mathbf{A}'$:

$$H_{xi} = H_{xi}'\sqrt{s}, \quad H_{yi} = H_{yi}'\sqrt{s}, \quad H_{zi} = H_{zi}'. \tag{4}$$

It is not difficult to verify that $\mathbf{E}_i'\mathbf{H}_i' = \mathbf{EH} = 0$, i.e., $\mathbf{E}_i' \perp \mathbf{H}_i'$. Hence, the original problem (1) is reduced to finding the energy spectrum and wave function of particles of isotropic mass m_1 in the presence of the crossed fields $\mathbf{E}_i'$ and $\mathbf{H}_i'$. To solve this problem, it is expedient to transform by rotation to a coordinate system X_i', Y_i', Z_i' in which $\mathbf{E}_i' \parallel OX_i'$ and $\mathbf{H}_i' \parallel OZ_i'$.

The electron wave function ψ_Q in this coordinate system is[3,4]

$$\Psi_{Qi} = \exp\left[\frac{1}{\hbar}(p_{yi}'y_i' + p_{zi}'z_i')\right]e^{-\xi_i^2/2}\mathscr{H}_n(\xi_i), \quad \xi_i = (x_i' - x_{0i}')\sqrt{m_1\omega_{0i}'/\hbar}, \quad \omega_{0i}' = eH_i'/m_1c, \tag{5}$$

where $x_{0i}' = -eE_i'/m_1\omega_{0i}'^2 - p_{yi}'/m_1\omega_{0i}'$ and $\mathscr{H}_n(\xi)$ is the normalized Chebyshev-Hermite polynomial. The electron energy spectrum is known to be:

$$\mathscr{E}_{Qi} = \hbar\omega_{0i}'\left(n + \frac{1}{2}\right) + eE_i'x_{0i}' + p_{zi}'^2/2m_1. \tag{6}$$

Since we must calculate the components of the total current along the X, Y, Z axes in (5) and (6), a transformation should be made from the X_i', Y_i', Z_i' system to the X, Y, Z system. This transformation yields the following result:

$$\begin{gathered}
\mathscr{E}_{Qi} = \hbar\omega_{0i}'\left(n + \frac{1}{2}\right) + eEx_{0i} + p_{zi}^2/2m_1\beta_i, \quad x_{0i} = -\frac{p_{yi}}{m_1\omega_0} - \frac{\beta_i^{-1}}{m_1\omega_0}p_{zi}(1-s)\sin\vartheta_i\cos\vartheta_i\cos\varphi_i - \frac{eE}{m_1\omega_0^2}\frac{(1-s)\sin^2\vartheta_i\sin^2\varphi_i}{s+(1-s)\sin^2\vartheta_i\sin^2\varphi_i}, \\
\Psi_{Qi} = \exp\left\{\frac{i}{\hbar}\left[p_{yi}y_i + p_{zi}z_i + x_i(\sin\vartheta_i\cos\varphi_i p_{yi} + \cos\vartheta_i p_{zi})\frac{(s-1)\sin\vartheta_i\sin\varphi_i}{s+(1-s)\sin^2\vartheta_i\sin^2\varphi_i}\right]\right\} \\
\exp\left[-\frac{(x_i - x_{0i})^2}{2\hbar}\frac{m_1\omega_{0i}'s}{s+(1-s)\sin^2\vartheta_i\sin^2\varphi_i}\right]\mathscr{H}_n\left[\sqrt{\frac{m_1\omega_{0i}'}{\hbar}}(x_i - x_{0i})\frac{\sqrt{s}}{(s+(1-s)\sin^2\vartheta_i\sin^2\varphi_i)^{1/2}}\right], \\
Q = (n,\ p_{yi},\ p_{zi}), \ \omega_0 = eH/m_1c; \ \omega_0' = \omega_0\sqrt{\beta_i/s}, \ \beta_i = \sin^2\vartheta_i + s\cos^2\vartheta_i.
\end{gathered} \tag{7}$$

Here φ_i and ϑ_i are the first two Eulerian angles of the X, Y, Z system with respect to the principal axes of the i-th ellipsoid.

Let us turn to the computation of the currents $\mathbf{j}^i$. In order to calculate the y and z components, the average quantum-mechanical values of the corresponding carrier velocity components must be calculated and the quantities obtained must then be averaged over the electron equilibrium distribution:[3]

$$\overline{v_y^i} = \overline{\partial\mathscr{E}_{Qi}/\partial p_{yi}} = -cE/H, \quad \overline{v_z^i} = \overline{\partial\mathscr{E}_{Qi}/\partial p_{zi}} = -(cE/H)\alpha_i, \quad \alpha_i = \beta^{-1}(1-s)\sin\vartheta_i\cos\vartheta_i\cos\varphi_i, \tag{8}$$

where the bar denotes the statistical average. The currents are correspondingly determined by the following expressions

$$j_y^i = -eN^icE/H, \quad j_z^i = -eN^ic(E/H)\alpha_i, \tag{9}$$

where N^i is the density of the number of electrons in the i-th ellipsoid. The currents (9) are not ohmic – they are not related to the electron scattering and are independent of the scattering mechanism; the current j_z^i appears exclusively because of the anisotropy of the electron mass.

The current j_z^i is purely ohmic, i.e., it is determined essentially by electron scattering. In reality, $\overline{v_z^i} = 0$; consequently, the current is determined as the flow of charge through a unit area of the $x = 0$ plane,[4,5] caused by scattering:

$$j_x^i = -e\sum_{QQ'}\sum_{\alpha=\pm1}(W_{QQ'}^i\chi_{Q'\alpha}^i - W_{Q'Q}^i\chi_{Q\alpha}^i), \quad x_{0i}' = x_{0i}(Q') > 0, \quad x_{0i} = x_{0i}(Q) > 0, \tag{10}$$

where $W_{QQ'}^i$ is the probability of a quantum transition of the current carrier from the Q state into the Q′ state under the influence of a scattering factor (within the i-th ellipsoid);* $\chi_{Q\alpha}^i$ is the electron equilibrium distribution function. Since we are limited to the case of such fields E for which $j_x^1 \sim E$ (Ohm's law) and since a non-degenerate electron gas is assumed in the semiconductor,* we have (taking spin into account):

---

* We neglect the probability of interellipsoid transitions because they occur through the agency of phonons with large f, which are few in number at the low temperatures under consideration (f is the wave vector of the phonon).

$$\chi^{i}_{Q\alpha} = \exp\left\{\frac{1}{kT}\left[\mu - \alpha\mu_{B}H - \frac{\hbar\omega_0}{\sqrt{s}}\sqrt{\beta_i}\left(n + \frac{1}{2}\right) - \frac{\beta_i^{-1}}{2m_1}p_z^2\right]\right\}, \tag{11}$$

where $\alpha = \pm 1$, μ is the chemical potential, and $\mu_B = e\hbar/2mc$ is the Bohr magneton.

Let us consider the interaction between electrons and long-wave longitudinal acoustic phonons (deformation potential)[6] as the electron scattering mechanism and let us disregard scattering by impurity ions for the following reasons. We are interested in how energy-level quantization by the field H affects the dependence of magnetoresistive phenomena in n-Ge type semiconductors on the direction of the field H and on H/T. Hence, it appears that a significant exponential anisotropy of ρ_H and R, dependent on the anisotropy of the equilibrium electron concentration N, occurs. It will be shown by further computations that precisely this large anisotropy determines essentially the dependence of ρ_H and R on the direction of H; the scattering factor (the interaction with phonons in our case) makes only an insignificant contribution to the anisotropy of ρ_H, i.e., the anisotropy of the effective mobility $u_0 = (Ne\rho_H)^{-1}$ is not very substantial. On the other hand, allowance for the scattering by impurity ions, within the framework of our method of calculating ρ_H, leads to an additional current δj_x (j_y and j_z are not determined by the scattering) and, therefore, to an additional resistance $\delta\rho \simeq E\delta j_x/j_y^2$ ($j_z = 0$, as will be shown). Hence, it can be shown that the exponential anisotropy of N(H) is fundamental, as before; while the dependence of u_0 is determined by the same functions φ_i and ϑ_i as in the case of scattering by phonons (by the functions α_i, β_i) and, as before, is not essential.

It is understood that $\delta\rho$ can be substantial in magnitude for a sufficient impurity concentration or in the case of compensated impurities. But we are interested not in the absolute value of ρ_H but in the ratio $\rho_H(H)/\rho_{H_0}$, where ρ_{H_0} is the resistance for a certain direction of H and E ($E \perp H$). This dependence is determined basically by the anisotropy of N(H). It must also be said that if the impurity concentration is small enough ($n_1 \lesssim 10^{15} - 10^{16}$) and if the impurity compensation can be neglected, then the energy gap between the impurity level and the bottom of the band will be large in comparison with kT at the low temperatures under consideration, so that only a very small portion of the impurities is ionized, the scattering by the impurity ions is insignificant and its influence on the resistance ρ_H can be neglected. Actually, an essential condition for the appearance of a sudden anisotropy in ρ_H and R is the absence of degeneracy (see Appendix). In connection with the above, we should like to emphasize that both the sharp dependence of ρ_H and R on the field strength H and the strong dependence of these quantities on its direction (exponential anisotropy) depend basically on the character of the change in the equilibrium conduction-electron concentration for $\hbar\omega_0 \gg kT$ in the absence of electron-gas degeneracy, and not on the character of the scattering mechanism.[5]

Consequently, we disregard scattering by the impurity ions and assume that the perturbation operator V that causes the scattering is the deformation potential:[6]

$$V = D\,\mathrm{div}\,\mathbf{R}(\mathbf{r}).$$

where R(r) is the displacement of the lattice at point r.

Using (7) in the usual manner to determine the matrix elements of V, which are then substituted into

$$W^{i}_{QQ'} = \frac{2\pi}{\hbar}\sum_{(f)}|V^{if}_{QQ'}|^2\delta(\mathcal{E}^{l}_{Q} - \mathcal{E}^{i}_{Q'} \pm \hbar v f)$$

and into (10), we obtain the following expression for the current:

$$j^{i}_{x} = \frac{\pi e D^2 L^3}{Mv\,\hbar^4(2\pi)^6}\sum_{\alpha=\pm 1}\sum_{n,n'=0}^{\infty}\sum_{f_y,\,f_z}\int_{-f_0}^{f_0} df_x \iint_{(x'_{0i}>0} dp_{zi}\,dp'_{zi}\iint_{x_{0i}<0)} dp_{yi}\,dp'_{yi}\,f\overline{W}^{i}_{QQ'}\{[\chi^{i}_{Q\alpha}N_f - \chi^{i}_{Q'\alpha}(N_f+1)]$$

$$\times\Delta(p_{yi} - p'_{yi} + \hbar f_y)\Delta(p_{zi} - p'_{zi} + \hbar f_z)\delta(\mathcal{E}^{i}_{Q} - \mathcal{E}^{i}_{Q'} + \hbar v f) + [\chi^{i}_{Q\alpha}(N_f+1) - \chi_{Q'\alpha}N_f]\Delta(p_{yi} - p'_{yi} - \hbar f_y)$$

$$\times\Delta(p_{zi} - p'_{zi} - \hbar f_z)\delta(\mathcal{E}^{l}_{Q} - \mathcal{E}^{i}_{Q'} - \hbar v f)\}, \tag{12}$$

---

* Conditions under which there is no degeneracy in the conduction band are analyzed in the Appendix.

where L is the linear dimension of the base region of the crystal, M is its mass, $\Delta(\eta) = 0$ for $\eta \neq 0$ and 1 for $\eta = 0$, v is the velocity of sound, and N_f is the number of phonons with the wave vector f:

$$N_f \to \overline{N}_f = [\exp(\hbar v f / kT) - 1]^{-1}, \qquad \overline{W}^i_{QQ'} = \left| \int_{-\infty}^{\infty} dx\, \varphi^*_Q(x - x_{0i})\, \varphi_{Q'}(x - x'_{0i})\, e^{ixf_x} \right|^2,$$

$$\varphi_Q(x - x_{0i}) = \Psi_Q(x - x_{0i}) \exp\left\{ -\frac{i}{\hbar}(y_i p_{yi} + z_i p_{zi}) \right\}.$$

Using the properties of the symbol $\Delta(\eta)$ and of the δ-function, transforming to the variables

$$x'_{0i} - x_{0i} = r, \quad x'_{0i} + x_{0i} = t, \quad p_{zi} - p'_{zi} = w, \quad p_{zi} + p'_{zi} = u,$$

$$r_{\max} \geqslant r \geqslant 0, \quad -r \geqslant t \geqslant r; \quad -\hbar f_0 \leqslant w \leqslant \hbar f_0, \quad -\hbar f_0 \leqslant u \leqslant \hbar f_0$$

and integrating over u and t, we reduce j^i_x to the following:

$$j^i_x = \frac{\pi e D^2 m_1 (m_1\omega_0)^3 \beta_i}{8 v \hbar^4 (2\pi)^5} e^{\mu/kT} \cosh\left(\frac{\mu_B H}{kT}\right) \sum_{n,n'=0}^{\infty} \int_{-f_0}^{f_0} df_x \int_{-\hbar f_0}^{\hbar f_0} dw \int_0^{r_{\max}} dr \frac{r f \sinh(eEr/2kT)}{|w| \sinh(\hbar v f/2kT)} \overline{W}^i_{QQ'} \exp\left(-\frac{w^2}{8 m_1 kT}\beta_i^{-1}\right)$$
$$\times \{\exp(-X^+_{0i} - X^+_{1i}) + \exp(-X^-_{0i} - X^-_{1i})\}, \tag{13}$$

where

$$X^{\pm}_{0i} = \frac{1}{kT}\left\{\frac{\hbar\omega_{0i}}{2}(n + n' + 1) + \frac{m_1\beta_i}{2w^2}[\hbar\omega'_{0i}(n - n') \pm \hbar v f]^2\right\},$$

$\delta = M/L^3$; f_0 is the maximum wave vector of the phonon; $-f_0 \leq f_x, f_y, f_z \leq f_0$; $X^{\pm}_{1i} \sim E$ and, consequently, we obtain in the region where Ohm's law holds

$$X^{\pm}_{1i} = 0, \quad \sinh(eEr/2kT) \approx eEr/2kT.$$

Let us introduce the symbol

$$P = \sum_{n,n'=0}^{\infty} \overline{W}^i_{QQ'} [\exp(-X^+_{0i}) + \exp(-X^-_{0i})].$$

Let us also make the change of variable

$$w = \hbar f_z, \quad r^2 = (\hbar/m_1\omega_0)^2 (f_y + \alpha_i f_z)^2,$$

then

$$j^i_x = c\frac{E}{H} \frac{\pi e D^2 m_1 \beta_i}{8 v \hbar\, kT (2\pi)^5} e^{\mu/kT} \cosh\left(\frac{\mu_B H}{kT}\right) \iint_{-f_0}^{f_0} df_x df_z \int_{-\alpha_i f_z}^{f_0} df_y \frac{f(f_y + \alpha_i f_z)^2}{|f_z| \sinh(\hbar v f/2kT)} \exp\left(-\frac{\hbar^2 f_z^2}{8 m_1 kT}\beta_i^{-1}\right) P. \tag{14}$$

Analysis of (14) for arbitrary $\hbar\omega_0$ leads to very awkward and immense formulas so that the explanation of the dependence of j^i_x on $\hbar\omega_{0i}/kT$ requires in general numerical integration. We shall consider only the case $\hbar\omega_0 \gg kT$ (in fact, it is sufficient that $\hbar\omega_0 \gtrsim 3kT$), since it is the only one of interest to us.

It is easy to show[5,7] that for $\hbar\omega_0 \gg kT$:

$$P_i \approx 2\exp\left\{-\frac{\hbar\omega_{0i}}{2kT} - \frac{m_1 v^2}{2kT}\frac{f^2}{f_z^2}\beta_i\right\}. \tag{15}$$

Substituting (15) into (14), we obtain

$$j^i_x = c\frac{E}{H}\frac{\pi e D^2 m_1 \beta_i}{8\hbar v kT (2\pi)^5} \exp\left[\frac{1}{kT}\left(\mu - \frac{\hbar\omega'_{0i}}{2}\right)\right] \cosh\frac{\mu_B H}{kT} I_i, \tag{16}$$

where I_i becomes after some manipulation and the introduction of spherical coordinates in the f-space:

$$I_i = \frac{\pi}{2}\int_0^{f_0} df \int_0^{\pi/2} d\theta\, [\tan\theta + (2\alpha_i^2 - 1)\sin\theta\cos\theta] \frac{f^4}{\sinh(\hbar v f/2kT)} \exp\left\{-\frac{\hbar^2 f^2 \cos^2\theta}{8 m_1 \beta_i kT} - \frac{\beta_i m_1 v^2}{\cos^2\theta\, 2kT}\right\}.$$

Introducing new variables

$$\lambda = \cos\theta, \quad \hbar v f/kT = \zeta, \quad 0 \leqslant \zeta \leqslant \hbar v f_0/kT = T_D/T,$$

and using the notation $\epsilon = m_1v^2/\alpha kT \ll 1$, we obtain for $T \ll T_D$:

$$I_l = \frac{\pi}{2}\left(\frac{kT}{\hbar v}\right)^5 \int_0^\infty d\zeta \int_0^1 d\lambda \left[\frac{1}{\lambda}(2\alpha_i^2 - 1)\lambda\right] \frac{\zeta^4}{\sinh\zeta/2} \exp\left\{-\frac{\zeta^2\lambda^2}{16\epsilon\beta_i} - \frac{\epsilon\beta_i}{\lambda^2}\right\} . \tag{17}$$

This integral can be evaluated approximately for $\epsilon \ll 1$:

$$I_l \approx 64\pi\,(kT/\hbar v)^5\,(1 + 2\alpha_i^2 c_1), \quad c_1 = \text{const} \approx 1.$$

Substituting it in (16), we obtain finally

$$j_x^i = E\,\frac{2e^2D^2\,(kT)^4}{8\pi^3\,\hbar^6 v^6\,\omega_0} \exp\left(-\frac{\hbar\omega_{0i}'}{2kT}\right)\cosh\frac{\mu_B H}{kT}\,\beta_i\,(1 + 2\alpha_i^2 c_1)\,e^{\mu/kT}. \tag{18}$$

It was already indicated that to obtain the components of the total current the appropriate components of the partial single-ellipsoid currents must be summed over all the constant-energy ellipsoids. Hence, the relative arrangement of the ellipsoids in the Brillouin zone must be taken into account. As regards the y component of the total current,

$$j_y = \sum_i j_y^i = -ec\,\frac{E}{H}\sum_i N^i = -ec\,\frac{E}{H}\,N, \tag{19}$$

where N is the total density of the number of electrons in the conduction band

To calculate j_x and j_z, it is expedient to express the angles φ_i and ϑ_i by means of angles which the electric field E and the magnetic field H, as well as the Y axis, make with the cubic axes in the Brillouin zone (we denote the cosines of these angles by $\overline{m}_1\overline{m}_2\overline{m}_3$, $\ell_1\ell_2\ell_3$, and $n_1n_2n_3$ respectively).

A different number of ellipsoids, mutually arranged in a different way, can correspond to any one value of the energy in the Brillouin zone. We shall confine the analysis to two cases: (1) 8 ellipsoids arranged in the [111] directions in the reciprocal cell lattice, and (2) 6 ellipsoids arranged in the [100] directions. It is not difficult to confirm that $j_z = 0$ in both cases, as it should be for cubical symmetry of the reciprocal lattice.

In the first case, (n-Ge), after a number of simple transformations, we obtain:

$$j_x = \frac{2D^2em_1\,(kT)^4}{8\pi^3\hbar^6v^6}\,c\,\frac{E}{H}\cosh\left(\frac{\mu_B H}{kT}\right)e^{\mu/kT}A_{\mathrm{Ge}}, \tag{20}$$

$$A_{\mathrm{Ge}} = \sum_{\alpha_1,\alpha_2,\alpha_3=\pm 1} \exp\left\{-\frac{\hbar\omega_0}{2\sqrt{s}\,kT}\left[1 + \frac{s-1}{3}(\alpha_1l_1 + \alpha_2l_2 + \alpha_3l_3)^2\right]^{1/2}\right\}\left\{1 + \frac{s-1}{3}(\alpha_1l_1+\alpha_2l_2+\alpha_3l_3)^2\right.$$

$$\left. +2c_1(1-s)^2(\alpha_1l_1+\alpha_2l_2+\alpha_3l_3)(\alpha_1n_1+\alpha_2n_2+\alpha_3n_3)\left[1 + \frac{s-1}{3}(\alpha_1l_1 + \alpha_2l_2 + \alpha_3l_3)^2\right]^{-1}\right\}. \tag{21}$$

In the second case, (n-Si), the expression for j_x remains the same as (20) but

$$A_{\mathrm{Si}} = 2\sum_{t=1}^{3}\exp\left\{-\frac{\hbar\omega_0}{2\sqrt{s}\,kT}(1 + (s-1)\,l_t^2)^{1/2}\right\}\{1 + (s-1)\,l_t^2 + 2c_1\,(1-s)^2\,l_t^2n_t^2\,(1 + (s-1)\,l_t^2)^{-1}\}.$$

2. EXPONENTIAL ANISOTROPY OF THE CURRENT CARRIER CONCENTRATION

To determine completely the dependence of j_x and j_y on H and T, both $\mu(H, T)$ and $N(H, T)$ should be evaluated. Taking (7) into account, we obtain the following formula for the i-th ellipsoid, assuming no degeneracy (see Appendix)

$$N^i(H, T) = Z_0\,\frac{\hbar\omega_{0i}'}{2kT}\exp\left\{-\frac{\hbar\omega_{0i}'}{2kT} + \frac{\mu}{kT}\right\}2\cosh\frac{\mu_B H}{kT}, \tag{22}$$

in which we assume that $\hbar\omega_{0i}' \gg kT$; $Z_0 = 2(2\pi m_1kT/h^2)^{3/2}$. Introducing again the quantities $\ell_1\ell_2\ell_3$ and $n_1n_2n_3$, we obtain

$$N = \sum_i N^i = Z_0\,\frac{\hbar\omega_0}{\sqrt{s}\,kT}\cosh\left(\frac{\mu_B H}{kT}\right)e^{\mu/kT}B; \tag{23}$$

$$B_{\mathrm{Ge}} = \sum_{\alpha_1\alpha_2\alpha_3=\pm 1}\exp\left\{-\frac{\hbar\omega_0}{2\sqrt{s}\,kT}\left(1 + (\alpha_1l_1 + \alpha_2l_2 + \alpha_3l_3)^2\,\frac{s-1}{3}\right)^{1/2}\right\}\left[1 + \frac{s-1}{3}(\alpha_1l_1 + \alpha_2l_2 + \alpha_3l_3)^2\right], \tag{24}$$

$$B_{Si} = 2\sum_{t=1}^{3}\exp\left\{-\frac{\hbar\omega_0}{2\sqrt{s}\,kT}\left(1+(s-1)\,l_t^2\right)^{1/2}\right\}[1+(s-1)\,l_t^2]. \tag{25}$$

To determine the chemical potential μ we use the neutrality equation and consider a Wilson type impurity semiconductor. In this case, the neutrality equation for any $\mu_B H$ is the following (see Appendix):

$$n_1\left[1+2\exp\left(\frac{\Delta E+\mu}{kT}\right)\cosh\frac{\mu_B H}{kT}\right]^{-1} = Z_0\frac{\hbar\omega_0}{\sqrt{s}\,kT}\cosh\frac{\mu_B H}{kT}\,e^{\mu/kT}B, \tag{26}$$

where n_1 is the concentration of monovalent donor impurities, ΔE is the gap between the impurity level and the bottom of the conduction band. Since $\Delta E \gg kT$ for low temperatures, then

$$e^{\mu/kT} \approx \frac{1}{2\cosh\frac{\mu_B H}{kT}}\left(\frac{n_1\sqrt{s}\,kT}{Z_0\hbar\omega_0}\right)^{1/2} e^{-\Delta E/2kT}B^{-1/2}. \tag{27}$$

Substituting (27) into (23), we obtain

$$N = {}^1\!/_2\,(n_1 Z_0\hbar\omega_0/\sqrt{s}\,kT)^{1/2}e^{-\Delta E/2kT}B^{1/2}; \tag{28}$$

It follows from (28) that, first, the number N decreases exponentially as $\hbar\omega_0/kT$ increases;[5] and second, that this number depends essentially on the direction of H. This second fact is very important; it is manifested in the significant "exponential" anisotropy of N. This anisotropy increases with the anisotropy of the electron mass and its character depends on the number and mutual arrangement of the ellipsoids in the Brillouin zone (B_{Si}, B_{Ge} depend differently on ℓ_t). This anisotropy is caused by the fact that in strong fields H the different ellipsoids contain different numbers of electrons which depend on the direction of E.

3. ELECTRIC RESISTIVITY AND HALL CONSTANT IN A STRONG MAGNETIC FIELD

Substituting (19), (20), and (23) into the known formulas of the stationary-states method[3] and keeping in mind that $j_x^2 \ll j_y^2$ in our case, we obtain the following expressions

$$R \approx -(2/ec)\,(kT\sqrt{s}/n_1 Z_0\hbar\omega_0)^{1/2}e^{\Delta E/2kT}B^{-1/2}; \tag{29}$$

$$\rho_H \approx AB^{-3/2}e^{\Delta E/2kT}D^2 m_1^{5/4}m_2^{5/4}(kT)^{11/2}/8\pi^3\hbar^6 v^6(\hbar Z_0)^{3/2}e^2\sqrt{n_1\omega_0}. \tag{30}$$

Hence, it follows that as $\hbar\omega_0/kT$ increases both R and ρ_H increase rapidly, basically as $\exp(\hbar\omega_0/4kT)$, in conformance with the behavior of N(H, T). Both R and ρ_H have considerable anisotropy, i.e., depend on the direction of H; ρ_H depends also on the direction of E.

The anisotropy of ρ_H is determined by the factor $AB^{-3/2}$, and $R \sim B^{-1/2}$. The mobility u_0 contained in $\rho_H = 1/Neu_0$ is also anisotropic; its anisotropy is determined by the factor B/A and is considerably less pronounced than the anisotropy of N(H, T). Consequently, the anisotropies of ρ_H and R increase with the anisotropy of the mass and depend on the number and mutual arrangement of the ellipsoids in the Brillouin zone (see Figs. 1 and 2).

Let us note, by the way, that if H is directed along one of the cubic axes all the above-mentioned quantities are isotropic (independent of the direction of E).

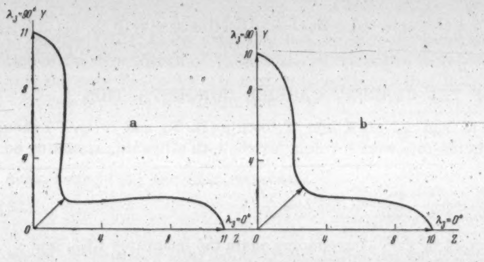

FIG. 1. Curve a: $A_{Ge}/B_{Ge}^{3/2}$ is the quantity defining the anisotropy of ρ_H for Ge. Curve b: $B_{Ge}^{-1/2}$ is the quantity defining the anisotropy of R for Ge. E is parallel to X and H in the YZ plane; $\ell_1 = 0$; $\ell_3 = \cos\lambda_3$; $s = m_2/m_1 = 19$.

In conclusion, let us point out that it seems to us that an experimental investigation of ρ_H and R in semiconductors in strong magnetic fields at low temperatures affords the possibility of obtaining additional information on the carrier mass anisotropy and on the number, relative arrangement, and character of the constant-energy surfaces in the Brillouin zone near the energy extrema. In reality, if the dependences of $\rho_H(\ell_1\ell_2\ell_3;\ n_1n_2n_3)$ and $R(\ell_1\ell_2\ell_3)$ are established experimentally for a semiconductor in a strong field H, then, for a given number and arrangement of the constant-energy ellipsoids in the Brillouin zone, the exponential anisotropy of ρ_H and R would permit the quantities $\omega_0 = eH/m_1c$ and $s = m_2/m_1$, i.e., m_1 and m_2, to be determined by a comparison of experimental and theoretical results. The character of the dependences of $\rho_H(\ell_1\ell_2\ell_3;\ n_1n_2n_3)$ and $R(\ell_1\ell_2\ell_3)$ is determined by the arrangement of the constant-energy ellipsoids and by their number, which again affords a possibility of obtaining answers to this question by a comparison with experiment.

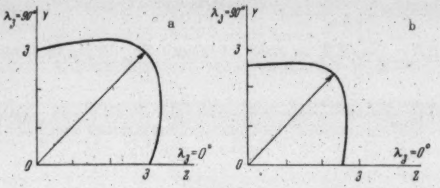

FIG. 2. Curve a: $A_{Si}/B_{Si}^{3/2}$. Curve b: $B_{Si}^{-1/2}$. E' is parallel to X and H in the YZ plane; $\ell_1 = 0$; $\ell_3 = \cos\lambda_3$; $s = m_2/m_1 = 5$.

It should be noted that the magnetic susceptibility of the conduction electrons, as is easy to see, is determined by the expression

$$\chi = \frac{\mu_B^2}{kT}\left(\frac{m^2}{m_1m_2}\right)^{1/2} B^{-1}\frac{\partial B}{\partial H} N(H, T),$$

and, therefore, depends on the direction of **H**; hence, the anisotropy of χ is again determined essentially by the dependence of N on the angles, i.e., on $\ell_1\ell_2\ell_3$. It can be assumed that other kinetic coefficients have a significant anisotropy for Ge type semiconductors in the presence of a strong field H.

All the results obtained above are valid for unipolar impurity semiconductors in the absence of electron gas degeneracy.

The case of large impurity concentration, when degeneracy of the conduction electrons, scattering by impurity ions, and impurity bands can play a substantial role, must be investigated especially as is being done at present.

We take the opportunity to express our gratitude to Prof. A. G. Samoilovich for very fruitful discussions.

APPENDIX

Let us determine the conditions under which the electron gas in the conduction band can be considered non-degenerate. To do this, let us write the neutrality equation for a Wilson type semiconductor:

$$n_1 - n = N, \tag{I}$$

where n is the density of the number of electrons in the impurity levels and N is the density of the number of electrons in the conduction band. As shown in Ref. 9, taking into account the Coulomb repulsion of electrons in the impurity level (monovalent impurity), we get

$$n = 2n_1 \exp\left(\frac{\mu + \Delta E}{kT}\right)\cosh\frac{\mu_B H}{kT}\left(1 + 2\exp\left(\frac{\mu + \Delta E}{kT}\right)\cosh\frac{\mu_B H}{kT}\right)^{-1}. \tag{II}$$

On the other hand, under the same conditions

$$N = \sum_i N^i = \sum_i \sum_{n=0}^{\infty} \int_{-\infty}^{\infty} dp_z \frac{eH}{\hbar^2 c}\left\{\left[\exp\left(\frac{\hbar\omega'_{0i}}{2kT}(2n+1) + \frac{\beta_i^{-1}p_z^2}{2m_1kT} + \frac{\mu_B H - \mu}{kT}\right) + 1\right]^{-1}\right.$$
$$\left. + \left[\exp\left(\frac{\hbar\omega'_{0i}}{2kT}(2n+1) + \frac{\beta_i^{-1}p_z^2}{2m_1kT} - \frac{\mu_B H + \mu}{kT}\right) + 1\right]^{-1}\right\}, \tag{III}$$

where

$$\omega'_{0i} = \omega_0 s^{-1/2}(\sin^2\vartheta_i + s\cos^2\vartheta_i)^{1/2}, \quad \beta_i = \sin^2\vartheta_i + s\cos^2\vartheta_i.$$

It is seen from (III) that the Boltzmann distribution can be used in this case if $\mu \ll \frac{1}{2}\hbar\omega'_{0i} - \mu_B H$, or, in order of magnitude

$$\mu \ll {}^1\!/_2 h\omega_0(\beta_i/s)^{1/2} - \mu_B H = \varepsilon_{\min}.$$

(The quantity $\hbar\omega'_{0i}/2 - \mu_B H$ determines the bottom of the zone for the i-th ellipsoid.) Let us assume that this condition is satisfied and let us explain what the parameters n_1, ΔE, m_1, and m_2 must be here.

Equation (I) becomes (for $\hbar\omega_0/2 \gg kT$)

$$\left[1 + 2e^{\tilde{\mu}/kT}\cosh\frac{\mu_B H}{kT}\right]^{-1} = \frac{Z_0}{n_1}\frac{\hbar\omega_0}{\sqrt{s}\,kT}e^{-\Delta E/kT}\cosh\left(\frac{\mu_B H}{kT}\right)Be^{\tilde{\mu}/kT}, \qquad \text{(IV)}$$

where $\tilde{\mu} = \mu + \Delta E$. It is easy to find from (IV) that $\Delta E \gg kT$ for $\hbar\omega_0/2kT \gg 1$.

$$\frac{\mu}{kT} \approx -\frac{\Delta E}{2kT} - \frac{\ln B}{2} + \frac{1}{2}\ln\frac{n_1\sqrt{s}\,kT}{Z_0\hbar\omega_0} - \ln\left(2\cosh\frac{\mu_B H}{kT}\right). \qquad \text{(V)}$$

It is not difficult to see from (24) and (25) that $\ln B \approx -\hbar\omega_0/2kT$ in order of magnitude. Using this, we reduce (V) to

$$\mu \approx \varepsilon_{\min} - \frac{\Delta E}{2} - \frac{\hbar\omega_0}{4} + \frac{kT}{2}\ln\frac{n_1\sqrt{s}\,kT}{Z_0\hbar\omega_0} + kT\left[\frac{\mu_B H}{kT} - \ln\left(2\cosh\frac{\mu_B H}{kT}\right)\right]. \qquad \text{(VI)}$$

It is seen from (VI) that $\mu \ll \epsilon_{\min}$ if

$$\frac{\Delta E}{2} + \frac{\hbar\omega_0}{4} \gg \frac{kT}{2}\ln\frac{n_1\sqrt{s}\,kT}{Z_0\hbar\omega_0} + kT\left[\frac{\mu_B H}{kT} - \ln\left(2\cosh\frac{\mu_B H}{kT}\right)\right].$$

This inequality is satisfied for the values of ΔE and s frequently encountered at low T and not too large n_1. For example, if $\Delta E \approx 0.01$ ev, $T \sim 10°$ K, $s \sim 10$, $\hbar\omega_0/kT \sim 3$, then $\mu/kT \approx -4 + \ln(2n_1 \times 10^{-16})$; if $n_1 < 10^{20}$, μ is not only less than $\epsilon_{\min}$ ($\epsilon_{\min} \approx 3/2$ in this case) but $\mu < 0$. Even if it is assumed that a certain overestimate of $|\mu/kT|$ (which is not large, as shown in Ref. 6) is made by replacing (III) by the right side of (IV), the assumed non-degeneracy of the electron gas is justified.

Hence, the electron gas in the conduction band can apparently be assumed to be non-degenerate at the low T and high H under consideration for not too large n_1 and s and for large enough ΔE.

The above conclusion is in agreement with results of Refs. 9 and 10, where a detailed investigation of the conditions of electron gas degeneracy is made for $H = 0$. However, large H contribute to the absence of degeneracy because the field quantization of the energy level leads to a large increase, in comparison with kT, in the energy gap between the impurity level and the bottom of the band: $\hbar\omega_0/2 \gg kT$.

Let us take the opportunity to note that the expression for n in Ref. 5 is not completely exact, but let us emphasize that the results of Ref. 5 are true not only for $\mu_B H \gg kT$ but for any $\mu_B H$ if $\exp(\mu_B H/kT)$ in the formulas of Ref. 5 are everywhere replaced by $\cosh(\mu_B H/kT)$.

---

[1] M. Shibuya, Phys. Rev. 95, 1385, (1954).
[2] B. Abeles and S. Meiboom, Phys. Rev. 95, 31, (1954).
[3] M. I. Klinger, J. Exptl. Theoret. Phys. (U.S.S.R.) 26, 212 (1954).
[4] S. Titeica, Ann. Phys. 22, 129 (1935).
[5] M. Klinger, J. Exptl. Theoret. Phys. (U.S.S.R.) 31, 1055 (1956), Soviet Phys. JETP 4, 831 (1957).
[6] W. Shockley, Theory of Electron Semiconductors, GTTI, 1954 (Russ. Transl.).
[7] Iu. B. Rumer, J. Exptl. Theoret. Phys. (U.S.S.R.) 22, 214 (1952).
[8] A. G. Samoilovich, Doklady, Acad. Sci. Ukrainian S.S.R., 1954, p. 174.
[9] A. G. Samoilovich, Doklady, Acad. Sci. Ukrainian S.S.R., 1954, p. 259.
[10] G. Busch and H. Labhart, Helv. Phys. Acta 19, 463 (1946).

Translated by M. D. Friedman
13

SOVIET PHYSICS JETP VOLUME 6, NUMBER 1 JANUARY, 1958

ON THE THEORY OF THE SHUBNIKOV-DE HAAS EFFECT

I. M. LIFSHITZ and L. M. KOSEVICH

Physico-Technical Institute, Academy of Sciences, Ukrainian S.S.R.

Submitted to JETP editor November 22, 1957

J. Exptl. Theoret. Phys. (U.S.S.R.) 33, 88-100 (July, 1957)

Quantum oscillations of the electrical conductivity $\sigma^{\alpha\beta}$ and specific resistance $\rho^{\alpha\beta}$ tensors are investigated on the basis of some general formulae presented in Ref. 1. It is shown that the oscillations of $\sigma^{\alpha\beta}$ and $\rho^{\alpha\beta}$ may be expressed in terms of the magnetic moment oscillations in the de Haas-van Alphen effect and in terms of the classical values of the mobility tensor. The asymptotic values of the oscillation amplitudes in strong magnetic fields are investigated and some simple cases are considered for which calculation of the oscillation amplitudes may be completely carried out.

In Ref. 1 I. M. Lifshitz developed a consistent quantum theory of the conductivity of metals in magnetic fields. The relation between the quantum kinetic equation and its classical analog derived there permits one to determine quantum corrections to the classical value of the electrical conductivity, and, in particular, to determine those corrections which account for the quantum oscillations of the conductivity. The present communication is devoted to a detailed study of these oscillations (Shubnikov-de Haas effect[2]).

It was shown in Ref. 1, that the simple (classical) part of the electrical conductivity tensor can be written in the form

$$\sigma^{\alpha\beta}_{\text{cl}} = -2\iint \frac{\partial f_0}{\partial \varepsilon} \chi^{\alpha\beta} m^* d\varepsilon\, dp_z \quad (\alpha, \beta \neq z, z), \qquad \sigma^{zz}_{\text{cl}} = -2\iint \frac{\partial f_0}{\partial \varepsilon} (\chi^{zz} + \chi_0^{zz}) m^* d\varepsilon\, dp_z, \tag{A}$$

where $\chi(\epsilon, p_z)$ is constructed in a specific way from Green's function for the classical kinetic equation [see Eq. (59) in Ref. 1], and $f_0(\epsilon)$ is the Fermi distribution function.

Quantum oscillations of the conductivity tensor occur when $\chi(\epsilon, p_z)$ has the values determined by the following equations:[1]

$$\Delta\sigma^{\alpha\beta} = \sum_{k=1}^{\infty} I_k^{\alpha\beta} \quad (\alpha, \beta \neq z, z), \qquad \Delta\sigma^{zz} = \sum_{k=1}^{\infty} (I_k^{zz} - L_k^{zz}), \qquad I_k^{\alpha\beta} = 2\iint f_0 \frac{\partial(\chi^{\alpha\beta} m^*)}{\partial \varepsilon} \hbar\omega^* e^{2\pi i k n}\, dn\, dp_z,$$
$$L_k^{zz} = 2\iint \frac{\partial f_0}{\partial \varepsilon} \chi_0^{zz} m^* \hbar\omega^* e^{2\pi i k n}\, dn\, dp_z, \tag{B}$$

where $\omega^* = (eH/m^*c)$, $m^* = (1/2\pi)(\partial S/\partial\epsilon)$, and $S = S(\epsilon, p_z)$ is the area of intersection of the constant-energy surface for the electron having an arbitrary dispersion law $\epsilon = \epsilon(p)$ with the plane $p_z =$ const., perpendicular to the magnetic field.

The structure entering into the integrals in Eq. (B) permits one to determine easily from them the oscillatory factor in which we are interested and to determine in this way the oscillation of $\Delta\sigma^{\alpha\beta}$ from the oscillation of the magnetic moment and of the magnitude of the classical conductivity tensor.

1. CONDUCTIVITY OSCILLATIONS

Let us determine the oscillatory part of the expressions I_k and L_k in (B). To do this we shall use the concepts introduced in Ref. 3, and the same method, slightly modified and simplified.

First let us consider the contribution to the oscillatory part of the electrical conductivity of a single group of electrons with a given dispersion law.

In the integrals of I_k and L_k, let us transform from the variables n, p_z to n, ϵ changing the order and the limits of integration, and also using the relation

$$\hbar\omega^* \frac{D(n, p_z)}{D(n, \varepsilon)} = \left(\frac{\partial n}{\partial p_z}\right)_\varepsilon^{-1},$$

which results from the quasi-classical expression for the energy levels of an electron in a magnetic field:

$$S(\varepsilon, p_z) = (n + \gamma)\, ehH/c \quad (0 < \gamma < 1), \quad n \gg 1.$$

This gives for I_k

$$I_k = 2\int f_0(\varepsilon) \sum \left\{ \int_{n_{\min}}^{n_{\max}} \frac{\partial(\chi^* m)}{\partial \varepsilon} \left| \frac{\partial n}{\partial p_z} \right|_\varepsilon^{-1} e^{2\pi i k n}\, dn \right\} d\varepsilon, \tag{1}$$

where the summation sign refers to summation over uniform intervals of change of $n(\epsilon, p_z)$ for a fixed value of ϵ.

The idea of the calculations which follow is based on the observation, that, with the exception of $f_0(\epsilon)$ and $e^{2\pi iKn}$, all the quantities entering the integrals for I_k and L_k change very slowly as functions of ϵ and n (in comparison with the range of variation of ϵ and n). Therefore, by virtue of the condition $n \gg 1$ the basic contribution to the internal integral (1) is made by integrating in the vicinity of the extreme points $n_m(\epsilon)$. Near these points

$$n - n_m = {}^1\!/_2\, (p_z - p_z^m)^2 (\partial^2 n / \partial p_z^2)_m,$$

where $n = n(\epsilon, p_z)$ and $n_m = n(\epsilon, p_z^m)$ and consequently

$$|\partial n / \partial p_z| = \sqrt{2 (\partial^2 n / \partial p_z^2)_m (n - n_m)}.$$

This last relation permits one to determine the contribution to the inner integral of (1) very simply by evaluating the integral in the vicinity of the extreme points:

$$\int^{n_m} \frac{\partial(\chi m^*)}{\partial \varepsilon} \left| \frac{\partial n}{\partial p_z} \right|^{-1} e^{2\pi i k n}\, dn = \left| 2 \frac{\partial^2 n}{\partial p_z^2} \right|_m^{-1/2} \int^{n_m} \frac{\partial(\chi m^*)}{\partial \varepsilon} \frac{e^{2\pi i k n}}{\sqrt{|n - n_m|}}\, dn$$

$$\approx w_m(\varepsilon)\, e^{2\pi i k n_m} \int_{+\infty}^{0} e^{2\pi i k x} |x|^{-1/2}\, dx = w_m(\varepsilon)\, e^{2\pi i k n_m} e^{\pm i\pi/4} / \sqrt{2k},$$

where

$$w_m(\varepsilon) = \frac{\partial(\chi m^*)}{\partial \varepsilon} \left| 2 \frac{\partial^2 n}{\partial p_z^2} \right|_{p_z = p_z^m}^{-1/2}$$

The plus sign in the expression $e^{\pm i\pi/4}$ refers to $n_{\min}$, while the minus sign refers to $n_{\max}$. The term corresponding to $n_{\min} = 0$ does not contribute to the oscillatory part of I_k and may be omitted. All the remaining extremal points are repeated twice (for adjacent uniform intervals of change of $n(\epsilon, p_z)$ for a fixed value of ϵ), so that we may transform (1) into the form:

$$I_k \approx 2\sqrt{\frac{2}{k}} \sum_m e^{\pm i\pi/4} \int f_0(\varepsilon)\, w_m(\varepsilon)\, e^{2\pi i k n_m(\varepsilon)}\, d\varepsilon, \tag{2}$$

where the summation is made over all extremal points. In what follows we shall omit the summation sign for summing over extremal points.

Considering the behavior of $f_0(\epsilon)$ in the vicinity $\epsilon = \zeta$ and assuming that $(\partial n_m / \partial \epsilon)_{\epsilon = \zeta} \neq 0$, we find from (2)

$$I_k \approx 2\sqrt{\frac{2}{k}}\, w_m(\zeta) \exp\left\{2\pi i k n_m(\zeta) \pm i\frac{\pi}{4}\right\} \int_0^\infty f_0(\varepsilon) \exp\left\{2\pi i k \frac{dn_m}{d\zeta}(\varepsilon - \zeta)\right\} d\varepsilon = \frac{\sqrt{2}}{\pi k^{3/2}} \frac{w_m(\zeta)}{(dn_m / d\zeta)} \frac{k\lambda}{\operatorname{sh} k\lambda}$$

$$\times \exp\left\{2\pi i k n_m(\zeta) - i\frac{\pi}{2} \pm i\frac{\pi}{4}\right\}, \tag{3}$$

where $\lambda = 2\pi^2\theta / \hbar\omega^*$, and ζ is the chemical potential.

Thus, the oscillatory part of $\sigma^{\alpha\beta}$ $(\alpha, \beta \neq z, z)$ is given by the expression

$$\Delta\sigma^{\alpha\beta} = \sum_{k=1}^{\infty} \frac{\sqrt{2}}{\pi k^{3/2}} \frac{w_m^{\alpha\beta}(\zeta)}{(dn_m / d\zeta)} \left(\frac{k\lambda}{\operatorname{sh} k\lambda}\right) \exp\left\{2\pi i k n_m(\zeta) - i\left(\frac{\pi}{2} \mp \frac{\pi}{4}\right)\right\}. \tag{4}$$

Equation (4) for $\Delta\sigma^{\alpha\beta}$ can be rewritten in a much more compact form, if we introduce the quantity

$$F_k = 2\iint f_0 e^{2\pi ikn} 2\pi m^* d\varepsilon\, dp_z. \tag{5}$$

It can be easily shown by calculation, analogous to that performed above, that integration in the vicinity of the extremal points (excluding the trivial case $n_{\min} = 0$) makes the following contribution to F_k:

$$F_k = A_k(\zeta)\exp\left\{2\pi ikn_m(\zeta) - i\left(\frac{\pi}{2} \mp \frac{\pi}{4}\right)\right\},$$
$$A_k(\zeta) = \frac{2m^*(\zeta, p_z^m)(k\lambda/\operatorname{sh} k\lambda)}{k^{3/2}(dn_m/d\zeta)\left|\partial^2 n/\partial p_z^2\right|^{1/2}_{m,\zeta}} = 2\left(\frac{ehH}{kc}\right)^{3/2}\frac{m^*(\zeta, p_z^m)(k\lambda/\operatorname{sh} k\lambda)}{(dS_m/d\zeta)\left|\partial^2 S(\zeta, p_z)/\partial p_z^2\right|^{1/2}_m}. \tag{6}$$

From this last equation we can see the relation between the quantum numbers $n(\epsilon, p_z)$, and the area $S(\epsilon, p_z)$. As has been shown, all the quantities, which enter into Eqs. (4) and (6), are to be evaluated at the points $\epsilon = \zeta$ and $p_z = p_z^m$ which correspond to extremal areas of cross sections of the boundary Fermi surface. (This problem is examined in greater detail in Ref. 3 and integrals similar to I_k and F_k are evaluated there.)

From Eqs. (3) and (4), it can be seen that

$$I_k = \frac{1}{2\pi m^*}\left(\frac{\partial}{\partial\varepsilon}\chi^{\alpha\beta}m^*\right)_{\zeta,\, p_z^m}\cdot F_k. \tag{7}$$

Finally, Eq. (4) can be written thus:

$$\Delta\sigma^{\alpha\beta} = \frac{1}{2\pi m^*}\left(\frac{\partial}{\partial\varepsilon}\chi^{\alpha\beta}m^*\right)_{\zeta,\, p_z^m}\cdot F,\; F = \sum_k F_k. \tag{8}$$

Note, that the oscillatory part of the magnetic moment of the electron gas in the de Haas-van Alphen effect can also be written in terms of the quantity F:

$$\Delta M^z = -h^{-3}\sum_k\iint f_0\frac{\partial\varepsilon}{\partial H}e^{2\pi ikn}2\pi m^*\, d\varepsilon p_z \approx -\frac{S_m(\zeta)F}{h^3 H(dS_m/d\zeta)}.$$

Hence, we find that

$$F = -h^3 H(d\ln S_m/d\zeta)\Delta M^z. \tag{9}$$

Substitution of (9) into (8), permits one to express the oscillatory part of $\Delta\sigma^{\alpha\beta}$ in terms of the oscillatory part of the magnetic moment ΔM^z, thus;

$$\Delta\sigma^{\alpha\beta} = -\frac{h^3 H}{(dS_m/d\zeta)}\frac{\partial}{\partial\zeta}(\chi^{\alpha\beta}m^*)_m\frac{d\ln S_m}{d\zeta}\Delta M^z. \tag{10}$$

Let us introduce the "classical mobility tensor" $q^{\alpha\beta}$, which is related to the classical conductivity tensor in the following manner:

$$\sigma_{\text{кл}}^{\alpha\beta} = 2h^{-3}\iint f_0 q^{\alpha\beta}2\pi m^* d\varepsilon\, dp_z = N_0\overline{q^{\alpha\beta}}, \tag{11}$$

where N_0 is the number of electrons in the conduction band, and $\bar{q}$ is the mean value of the mobility, weighted by f_0.

Since, on the other hand, the classical Eq. (A) can be transformed into

$$\sigma_{\text{кл}}^{\alpha\beta} = 2\iint f_0\left(\frac{\partial}{\partial\varepsilon}\chi^{\alpha\beta}m^*\right)d\varepsilon\, dp_z \quad (\alpha, \beta \neq z, z),$$

one obtains the following expression for $q^{\alpha\beta}$:

$$q^{\alpha\beta} = \frac{h^3}{2\pi m^*}\frac{\partial}{\partial\varepsilon}(\chi^{\alpha\beta}m^*) \quad (\alpha, \beta \neq z, z). \tag{12}$$

Substituting (12) into (10), one finds the following expression for the oscillatory part of $\Delta\sigma^{\alpha\beta}$ (for $\alpha, \beta \neq z, z$) in terms of the independent variables H, ζ:

$$(\Delta\sigma^{\alpha\beta})_{H,\zeta} = -q_m^{\alpha\beta}H(d\ln S_m/d\zeta)\Delta M^z. \tag{13}$$

If there are several groups of electrons which determine the electrical conductivity of the metal, i.e., if there are several overlapping, partially filled energy bands, then every group of electrons makes its own contribution to $\Delta\sigma^{\alpha\beta}$, so that $\Delta\sigma^{\alpha\beta}$ assumes the form of a summation of terms like Eq. (13).

In a similar way one finds the expression for the oscillatory part of $\Delta\sigma^{zz}$. Integrating L_k^{zz} in the way described above one finds

$$L_k^{zz} = \frac{2}{\sqrt{k}} \left(\chi_0^{zz} m^* \left| \partial^2 n / \partial p_z^2 \right|^{-1/2} \right)_{\zeta,\, p_z^m} \left(\frac{k\lambda}{\operatorname{sh} k\lambda} \right) \exp\left\{ 2\pi i k n_m(\zeta) + i\left(\pi \pm \frac{\pi}{4} \right) \right\},$$

which can be written in terms of F_k:

$$L_k^{zz} = -ik\chi_{0m}^{zz}(\zeta)\,(dn_m/d\zeta)\,F_k. \tag{14}$$

Because of the additional coefficient of $\partial n_m/\partial\zeta$, the integral L_k^{zz} [Eq. (14)] is considerably greater than I_k^{zz} (in the ratio $\zeta/\mu^* H$ where $\mu^* H \equiv \hbar\omega^*$). Therefore, the fundamental contribution to $\Delta\sigma^{zz}$ from those extremal sections, (of the boundary Fermi surface) on which χ_0^{zz} does not vanish, is made by such terms, namely:

$$\Delta\sigma^{zz} = i\chi_{0m}^{zz}(\zeta) \frac{dn_m}{d\zeta} \sum_k kF_k.$$

Using the relation between F and ΔM^z, it is easy to show for this case to this degree of approximation

$$(\Delta\sigma^{zz})_{H,\,\zeta} = \frac{h^3}{2\pi} H^2 \chi_{0m}^{zz}(\zeta) \left(\frac{d \ln S_m}{d\zeta} \right)^2 \frac{\partial \Delta M^z}{\partial H}. \tag{15}$$

If χ_0^{zz} vanishes on the extremal cross-section (of the boundary Fermi surface) [in particular, as is evident from the form of the general Eq. (59) of Ref. 1 for χ_0^{zz}, and from symmetry considerations, χ_0^{zz} vanishes on central cross-sections of the Fermi surface], one must take account in the integrals

$$Q_k(\varepsilon) = \int^{n_m} \chi_0^{zz} m^* \left| \frac{\partial n}{\partial p_z} \right|^{-1} e^{2\pi i k n}\, dn$$

of the subsequent (non-vanishing) terms of the expansion of χ_0^{zz} in powers of $(p_z - p_z^m)$.

Assume that near the extremal points

$${}_s\chi_0^{zz} = (p_z - p_z^m)^s \frac{1}{s!} \frac{\partial^s}{\partial p_z^s} \chi_0^{zz}. \tag{16}$$

Then

$$Q_k(\varepsilon) \approx (\pm 1)^s \frac{2^{(s-1)/2}}{s!} \frac{\partial^s \chi_0^{zz}}{\partial p_z^s} m^* \left| \frac{\partial^2 n}{\partial p_z^2} \right|_m^{-(s+1)/2} \int^{n_m} |n - n_m|^{(s-1)/2} e^{2\pi i k n}\, dn, \tag{17}$$

where as before the plus sign goes with n_{min} and the minus sign with n_{max}.

In evaluating the integral in Eq. (17), one can make use of the asymptotic equation for integrals of this form, which is given in Ref. 3.

Note that if $\chi(\epsilon, p_z)$ is an even function of p_z, then from the equality $\chi_0(\epsilon, p_z) = \chi_0(\epsilon, -p_z)$ it follows that $\partial\chi_0/\partial p_z = 0$ for $p_z = 0$, and consequently for central cross-sections, the expansion in Eq. (16) commences with a quadratic term. This means that for central cross-sections

$$Q_k(\varepsilon) = \frac{m^*}{8\pi k^{3/2}} \frac{\partial^2 \chi_0^{zz}}{\partial p_z^2} \left| \frac{\partial^2 n}{\partial p_z^2} \right|_0^{-3/2} \exp\left\{ 2\pi i k n_m \pm i \frac{3}{4}\pi \right\},$$

and the basic contribution to the oscillatory part is given by

$$\Delta\sigma^{zz} = \frac{1}{2\pi} \left\{ \frac{1}{m^*} \frac{\partial(\chi^{zz} m^*)}{\partial\varepsilon} \mp \frac{1}{2} \frac{dS_m/d\zeta}{|\partial^2 S/\partial p_z^2|} \frac{\partial^2 \chi_0^{zz}}{\partial p_z^2} \right\}_{\zeta,\, p_z=0} \cdot F. \tag{18}$$

By introducing the component q^{zz} of the "classical conductivity tensor" into this equation by analogy with Eq. (11), viz:

$$q^{zz} = \left(\frac{h^3}{2\pi m^*} \right) \frac{\partial}{\partial\varepsilon} (\chi^{zz} + \chi_0^{zz})\, m^* - \frac{h^3}{m^*} \frac{\partial}{\partial p_z} \left(\frac{\chi_0^{zz} m^{*2}}{\partial S/\partial p_z} \right), \tag{19}$$

it is easy to verify that for central cross-sections

$$q_m^{zz} = \frac{h^3}{2\pi} \left\{ \frac{1}{m^*} \frac{\partial(\chi^{zz} m^*)}{\partial\varepsilon} \mp \frac{dS_m/d\varepsilon}{2\,|\partial^2 S/\partial p_z^2|} \frac{\partial^2 \chi_0^{zz}}{\partial p_z^2} \right\}_{p_z = 0},$$

and therefore, Eq. (18) can be written in the form

$$(\Delta\sigma^{zz})_{H,\zeta} = -q_m^{zz} H\left(\frac{d\ln S_m}{d\zeta}\right)\Delta M^z. \tag{20}$$

If the boundary Fermi surface is convex, there is a unique extremal cross-section, i.e., the central one, and consequently the oscillatory part of the electrical conductivity of the given group of electrons is determined from Eqs. (13) and (20). Thus all the components of $\Delta\sigma^{\alpha\beta}$ have one single order of magnitude of oscillation. If there are other extremal cross-sections in addition to a central cross-section, $\Delta\sigma^{zz}$ is determined from Eq. (15), and the amplitude of oscillation of $\Delta\sigma^{zz}$ will be considerably greater than the amplitude of oscillation of $\Delta\sigma^{\alpha\beta}$ $(\alpha,\beta \neq z,z)$ for these groups of electrons.

Eqs. (13), (15) and (20) for the oscillatory part of $\Delta\sigma^{\alpha\beta}$ derived above are given in terms of the independent variables ζ and H. It was shown in Ref. 1 that for a concrete application of these equations and for comparison with experiment it is necessary to examine the oscillation of the chemical potential $\zeta = \zeta(H)$, resulting from the constancy of the number of electrons in all bands:

$$2h^{-3}\sum_j\sum_n\int f_0 2\pi m_j\, dp_z \Delta\varepsilon_n \equiv \sum_j N_j = N = \mathrm{const}$$

(summation over j is extended over all bands).

In this case, in contrast to the de Haas-van Alphen effect, in which they can be neglected, these oscillations play a fundamental role, because of the larger magnitude of $\sigma^{\alpha\beta}$.

If we symbolize by $N_0(\zeta)$ the classical relation between the electron concentration and the chemical potential, namely

$$N^0(\zeta) = 2h^{-3}\sum_j\iint f_0 2\pi m_j^*\, dp_z d\varepsilon = 2h^{-3}\sum_j\int f_0 (d\,\mathbf{p}),$$

we have, using Poisson's equation and considering Eq. (5),

$$N(\zeta) = N^0(\zeta) + h^{-3}\sum_j\sum_{k=1}^{\infty} F_k^j = N^0(\zeta) + h^{-3}\sum_j F^j(\zeta). \tag{21}$$

Next, putting $\zeta = \zeta_0 + \Delta\zeta$, where ζ_0 is the chemical potential for $H = 0$, we can write

$$N^0(\zeta) = N^0(\zeta_0) + \sum_j (\partial N_j^0/\partial\zeta)\Delta\zeta,$$

and then it follows from Eq. (21) that

$$\Delta\zeta h^3\sum_j(\partial N_j^0/\partial\zeta) = -\sum_j F^j(\zeta_0). \tag{22}$$

Taking into consideration that the oscillatory pertubation on $\sigma^{\alpha\beta}$, as a function of the relation $\zeta = \zeta(H)$, has the form

$$\Delta\sigma_1^{\alpha\beta} = (\partial\sigma^{\alpha\beta}/\partial\zeta_0)\Delta\zeta, \tag{23}$$

we can substitute into Eq. (23) the expression for $\Delta\zeta$ from Eq. (22):

$$\Delta\sigma_1^{\alpha\beta} = -(\partial\sigma^{\alpha\beta}/\partial\zeta_0)\sum_j F^j(\zeta_0) \Big/ h^3\sum_j(\partial N_j^0/\partial\zeta_0).$$

If we now use (9), the $\Delta\sigma_1^{\alpha\beta}$ are expressed in terms of:

$$\Delta\sigma_1^{\alpha\beta} = H\frac{\partial\sigma^{\alpha\beta}}{\partial\zeta_0}\sum_j\frac{d\ln S_{mj}}{d\zeta_0}\Delta M_j^z \Big/ \sum_k\frac{\partial N_k^0}{\partial\zeta_0}. \tag{24}$$

Finally in Eq. (24), one can express $\sigma^{\alpha\beta}$ in terms of the mean value of the "classical mobility tensor",

$$\Delta\sigma_1^{\alpha\beta} = H\sum_k\frac{\partial}{\partial\zeta_0}(N_k^0\overline{q_k^{\alpha\beta}})\sum_j\frac{d\ln S_{mj}}{d\zeta}\Delta M_j^z \Big/ \sum_k\frac{\partial N_k^0}{\partial\zeta_0}. \tag{25}$$

The experimentally observed oscillations of the conductivity as a function of the magnetic field are described by the sum $\Delta\sigma^{\alpha\beta} + \Delta_1\sigma^{\alpha\beta}$ so that in Eqs. (13), (15), and (20) (or in equations corresponding to them) one should substitute $\zeta = \zeta_0$.

For $\alpha, \beta \neq z, z$ this sum becomes

$$\Delta\sigma^{\alpha\beta} + \Delta\sigma_1^{\alpha\beta} = H \sum_j \left[\sum_k \frac{\partial}{\partial\zeta_0} (N_k^0 \overline{q_k^{\alpha\beta}}) \Big/ \sum_k \frac{\partial N_k^0}{\partial\zeta_0} - q_{mj}^{\alpha\beta}(\zeta_0) \right] \frac{d \ln S_{mj}}{d\zeta_0} \Delta M_j^z . \tag{26}$$

If all the Fermi surfaces are convex, then $\Delta\sigma^{zz} + \Delta\sigma_1^{zz}$ are determined by the analogous expression:

$$\Delta\sigma^{zz} + \Delta\sigma_1^{zz} = H \sum_j \left[\sum_k \frac{\partial}{\partial\zeta_0} (N_k^0 \overline{q_k^{zz}}) \Big/ \sum \frac{\partial N_k^0}{\partial\zeta_0} - q_{mj}^{zz}(\zeta_0) \right] \frac{d \ln S_{mj}}{d\zeta_0} \Delta M_j^z . \tag{27}$$

If there are Fermi surfaces with non-central extremal cross-sections, then

$$\Delta\sigma^{zz} + \Delta\sigma_1^{zz} = \frac{\hbar^3}{2\pi} H^2 \sum_i \chi_{0mi}^{zz}(\zeta_0) \left(\frac{d \ln S_{mi}}{d\zeta_0} \right)^2 \frac{\partial \Delta M_i^z}{\partial H} , \tag{28}$$

where the summation extends over all Fermi surfaces with non-central cross-sections.

From the formulae for the oscillatory part of the conductivity $\Delta\sigma^{\alpha\beta}$ [in what follows $\Delta\sigma^{\alpha\beta}$ will be used to symbolize all the terms of $\sigma^{\alpha\beta}$ which oscillate as the magnetic field changes, i.e., sums of the form of Eqs. (26) and (27)] it is evident that each group of electrons makes its own contribution to $\Delta\sigma^{\alpha\beta}$. It turns out, that the contribution of each band is related to ΔM^z only for similar groups of electrons. Therefore, the period of oscillation of $\Delta\sigma^{\alpha\beta}$ is always determined by the same coefficient as the period of oscillation of ΔM^z, and, of course, it coincides with that of the de Haas-van Alphen effect.[3]

$$\Delta(1/H) = e\hbar/cS_m(\zeta_0).$$

Principal emphasis in what follows will be on the amplitude of the oscillations of $\Delta\sigma^{\alpha\beta}$. First, in contrast to the oscillations of ΔM^z, the amplitude of the summands in $\Delta\sigma^{\alpha\beta}$ corresponding to given "anomalously narrow" bands are determined by all the "normal" groups of electrons. Secondly, the undetermined quantities $\chi(\epsilon, p_z)$ enter into a calculation of the amplitude. These quantities are also involved in the classical expression for the conductivity.

In certain concrete cases, which are introduced in Sec. 4, the quantities $\chi(\epsilon, p_z)$ can be obtained from the solution of the corresponding kinetic equations, and the magnitudes of the oscillations can be calculated exactly.

2. ASYMPTOTIC VALUES OF THE CONDUCTIVITY OSCILLATIONS IN STRONG MAGNETIC FIELDS

Let us now examine the behavior of the amplitude of oscillation of $\Delta\sigma^{\alpha\beta}$ in strong magnetic fields, when $\gamma_0 \ll 1$, where, in accordance with Ref. 4, we denote by γ_0 the relation $\gamma_0 = 1/(\epsilon H t_0/m_0 c)$ where m_0 and t_0 are the characteristic mass and relaxation time, respectively. In this case we can make an asymptotic expansion of the amplitude in powers of γ_0 making use of the asymptotic value of $\sigma_0^{\alpha\beta} \equiv \sigma_{KL}^{\alpha}$ obtained in Refs. 1 and 4. If the boundary Fermi surface is split into several closed surfaces, the asymptotes, $\sigma_0^{\alpha\beta}$, have the form

$$\sigma_0^{\alpha\beta}(H) = \begin{pmatrix} \gamma_0^2 a_{n} & \gamma_0 a_{12} + \gamma_0^2 a_{12}' & \gamma_0 a_{13} \\ \gamma_0 a_{21} + \gamma_0^2 a_{21}' & \gamma_0^2 a_{22} & \gamma_0 a_{23} \\ \gamma_0 a_{31} & \gamma_0 a_{32} & a_{33} \end{pmatrix} . \tag{29}$$

Here $a_{\alpha\beta}(\zeta_0)$ is a matrix whose elements can be expanded in powers of γ_0 beginning with a zero order term, such that

$$\gamma_0 a_{12} = \frac{ec}{H} \left(\sum_k N_k^+ - \sum_i N_i^- \right), \tag{30}$$

where N^+ is the electron density, and N^- is the hole density for corresponding groups.

Since for every group of electrons $\sigma^{\alpha\beta} = N_0 \overline{q^{\alpha\beta}}$ the asymptotic expansion of the elements of $\overline{q^{\alpha\beta}}$ begins with terms of the same order in γ_0, as $\sigma_0^{\alpha\beta}$, namely

$$\overline{q^{\alpha\beta}} = \begin{pmatrix} \gamma_0^2 \overline{u_{11}} & ec/H + \gamma_0^2 \overline{u_{12}} & \gamma_0 \overline{u_{13}} \\ -ec/H + \gamma_0^2 \overline{u_{21}} & \gamma_0^2 \overline{u_{22}} & \gamma_0 \overline{u_{23}} \\ \gamma_0 \overline{u_{31}} & \gamma_0 \overline{u_{32}} & \overline{u_{33}} \end{pmatrix} . \tag{31}$$

The expansion of the elements of the matrix $\overline{u_{\alpha\beta}}$ in powers of γ_0 begins, generally speaking, with a zero order term (in some cases, the expansion of $a_{\alpha\beta}$ is the same as $\overline{u_{\alpha\beta}}$, cf. Ref. 4). All the elements of $\overline{u^{\alpha\beta}}$ depend on the form of the collision integral, and generally speaking, they turn out to be functions of ζ_0.

Since $q_m^{\alpha\beta}$ is generally of the same order of magnitude as $q^{\alpha\beta}$, the asymptotes of $q_m^{\alpha\beta}$, in strong magnetic fields, should have the form of Eq. (31). In this case it is interesting to examine the possibility of an exact calculation of the first term in the asymptotic expansion of q_m^{xy} as follows.

For perpendicular magnetic field H (applied along the axis OZ) and electric field E (along the axis OY) the electron finds itself in a steady state with a constant velocity (depending on its state) whose mean value differs from zero. This velocity is directed along the axis OX and it is given by cE/H.[*] Note that the indicated velocity does not depend on the dispersion law for the electrons nor on the state of the electrons, i.e., it does not change because of collisions experienced by the electron. The steady state mobility of the electron $q_0^{xy} = ec/H$ is related to this velocity.

In strong magnetic fields when the mean time between collisions of the electrons is much greater than the time required for one revolution of the electron around its classical orbit, q_0^{xy} makes the principal contribution to the elements q^{xy} of the mobility tensor, and consequently

$$q_m^{xy} = ec/H + \gamma_0^2 u_m^{12}, \tag{32}$$

where $\gamma_0^2 u_m^{12}$ is the mobility, which is a function of the collision integrals. Thus it is seen by equating (32) and (31), that the first terms in the expansion of $\overline{q^{xy}}$ and $\overline{q_m^{xy}}$ in powers of γ_0 are identical.

From Eqs. (26) and (27), and also from Eqs. (31) and (32), it follows that the amplitudes of all the elements of $\Delta\sigma^{\alpha\beta}$, with the exception of $\Delta\sigma^{xy}$, have the same order of magnitude in terms of γ_0, as do the corresponding elements of $\sigma_0^{\alpha\beta}$. As for $\Delta\sigma^{xy}$, its ratio to γ_0 has a higher order of magnitude than that of σ_0^{xy}, if $\sum_k N_k^+ \neq \sum_i N_i^-$. One can write for the relative magnitude of the oscillations in the case of convex Fermi surfaces and for $\sum_k N_k^+ \neq \sum_i N_i^-$

$$\Delta\sigma^{\alpha\beta}/\sigma_0^{\alpha\beta} = H \sum_j \Psi_j^{\alpha\beta} \frac{d \ln S_m}{d\zeta_0} \Delta M_j^z, \tag{33}$$

where

$$\Psi^{\alpha\beta} = \begin{pmatrix} \psi_{11} & \gamma_0\psi_{12} & \psi_{13} \\ \gamma_0\psi_{21} & \psi_{22} & \psi_{23} \\ \psi_{31} & \psi_{32} & \psi_{33} \end{pmatrix}, \tag{34}$$

and the matrix $\psi_{\alpha\beta}$

$$\psi_{\alpha\beta}^j = \frac{\partial \ln a_{\alpha\beta}}{\partial\zeta_0} \Big/ \sum_k \frac{\partial N_k^0}{\partial\zeta_0} - u_{mj}^{\alpha\beta} \Big/ a_{\alpha\beta}, \quad (\alpha, \beta \neq x, y),$$

$$\psi_{xy}^j = \frac{\partial a_{12}'}{\partial\zeta_0} \Big/ a_{12} \sum_k \frac{\partial N_k^0}{\partial\zeta_0} - u_{mj}^{12} \Big/ a_{12},$$

and, consequently, the expansion of the terms of the $\psi_{\alpha\beta}$ matrix begins, generally speaking, with a zero order term in γ_0.

It is characteristic that the relative order of magnitude of the oscillations of σ^{xy} (in terms of γ_0) is less than the relative magnitude of oscillation of the remaining elements of the tensor $\sigma^{\alpha\beta}$.[†] There is a simple physical reason for this conclusion, namely that the asymptotic value σ_0^{xy} in strong fields for

---

[*] It is easier to verify that this is so by noting that in a steady state the mean value of the Lorentz force acting on the electron is zero. Since the expression for the Lorentz force does not depend on the form of the dispersion law, the steady-state velocity acquired by the electron in crossed magnetic and electric fields is independent of the dispersion law.

[†] In some concrete cases, in particular for an isotropic dispersion law, the expansion of Ψ^{xy} can begin with a term of the order γ_0^2 (for $\sum_k N_k^+ \neq \sum_i N_i^-$)

$\sum_k N_k^+ \neq \sum_i N_i^-$ in Eq. (30) has a fixed value for a given metal, and it does not experience any quantum oscillations.

If $\sum_k N_k^+ = \sum_i N_i^-$ the expansion of σ_0^{xy} begins with γ_0^2 and therefore the expansion of Ψ^{xy} begins with a a zero order term $\Psi^{xy} = \psi'_{12}$ where

$$\psi'_{12} = \frac{\partial \ln a'_{12}}{\partial \zeta_0} \bigg/ \sum_k \frac{\partial N_k^0}{\partial \zeta_0} - u_m^{12} \bigg/ a'_{12}.$$

The expansion of the remaining elements in $\Psi^{\alpha\beta}$ results as before in equations of the form of Eq. (34).

3. OSCILLATIONS OF THE RESISTIVITY

In experiments one usually measures not the electrical conductivity tensor $\delta^{\alpha\beta}$ but rather the specific resistivity tensor $\rho^{\alpha\beta} = \sigma_{\alpha\beta}^{-1}$. Consequently it is necessary to determine the oscillatory part of $\rho^{\alpha\beta}$.

The relation between the elements of the tensor $\rho^{\alpha\beta}$ and those of $\sigma^{\alpha\beta}$ is defined by the well known expression

$$\rho^{\alpha\beta} = D_{\beta\alpha} / \| \sigma \|, \quad \| \sigma \| = \det | \sigma^{\alpha\beta} |, \tag{35}$$

where $D_{\alpha\beta}$ are the algebraic complement of the elements of $\sigma^{\alpha\beta}$ in the determinant $\| \sigma \|$.

Let us write $\sigma^{\alpha\beta} = \sigma_0^{\alpha\beta} + \Delta\sigma^{\alpha\beta}$ designating by $\Delta\sigma^{\alpha\beta}$ the oscillatory part of $\sigma^{\alpha\beta}$, which, as is known, represents a small quantum perturbation to $\sigma^{\alpha\beta}$. Then, leaving only linear terms in $\Delta\sigma^{\alpha\beta}$, it can be easily shown.

$$\| \sigma \| = \| \sigma_0 \| + D^0_{\alpha\beta} \Delta\sigma^{\alpha\beta} = \| \sigma_0 \| (1 + \rho_0^{\alpha\beta} \Delta\sigma^{\alpha\beta}) \tag{36}$$

(we omit the sign for summation over indices which are to be taken in pairs from 1 to 3).

Similarly we find to the same degree of approximation

$$D_{\alpha\beta} = D^0_{\alpha\beta} + \varepsilon_{\alpha kl} \varepsilon_{\beta pq} \sigma_0^{kp} \Delta\sigma^{lq}, \tag{37}$$

where ϵ_{ikl} is an antisymmetric unit tensor of the third rank.

By using Eqs. (36) and (37), there follows from Eq. (35)

$$\Delta\rho^{\alpha\beta} = (\| \rho_0 \| \varepsilon_{\beta kl} \varepsilon_{\alpha pq} \sigma_0^{kp} - \rho_0^{\alpha\beta} \rho_0^{lq}) \Delta\sigma^{lq}, \quad \Delta\rho^{\alpha\beta}(\mathbf{H}) = \Delta\rho^{\beta\alpha}(-\mathbf{H}), \tag{38}$$

where

$$\| \rho_0 \| = \det | \rho_0^{\alpha\beta} | = \| \sigma_0 \|^{-1}.$$

It is evident from Eq. (38), that the equation for the oscillatory part of the electrical resistivity tensor in the general case has an exceedingly cumbersome form. The expression for $\Delta\rho^{\alpha\beta}$ retains the classical value and the oscillatory parts, generally speaking, of all the components of $\sigma^{\alpha\beta}$. Even in the simplest cases $\Delta\rho^{\alpha\beta}$ retains some terms, which can have a single order of magnitude of amplitude and various periods of oscillation. Simplification of Eq. (38) occurs only for certain special cases.

In particular, if there are boundary Fermi surfaces with non central cross-sections (it is obvious that these always occur in even numbers, so that the cross-section which are placed symmetrically around $p_z = 0$ make equal contributions to the oscillation $\Delta\sigma^{\alpha\beta}$), on which $\chi_0^{zz} \neq 0$, then, in magnetic fields that satisfy the relation $\gamma_0 \sim 1$, one need retain in Eq. (38) only those terms which contain $\Delta\sigma^{zz}$.

The components of $\Delta\rho^{\alpha\beta}$ in this case have the form

$$\Delta\rho^{xx} = (\| \rho_0 \| \sigma_0^{yy} - \rho_0^{xx} \rho_0^{zz}) \Delta\sigma^{zz}, \Delta\rho^{yy} = (\| \rho_0 \| \sigma_0^{xx} - \rho_0^{yy} \rho_0^{zz}) \Delta\sigma^{zz},$$
$$\Delta\rho^{xy} = -(\| \rho_0 \| \sigma_0^{xy} + \rho_0^{xy} \rho_0^{zz}) \Delta\sigma^{zz}, \quad \Delta\rho^{\alpha z} = -\rho_0^{\alpha z} \rho_0^{zz} \Delta\sigma^{zz} \quad (\alpha = x, y, z),$$

where $\Delta\sigma^{zz}$ is determined by Eq. (28).

If the Fermi surfaces are all convex, one can calculate the asymptotic values of $\Delta\rho^{\alpha\beta}$ in strong magnetic fields ($\gamma_0 \ll 1$). To do this, just as was done in Sec. 2, one uses the asymptotes of the tensors $\sigma_0^{\alpha\beta}$

[Eq. (29)] and $\rho^{\alpha\beta}$ (Ref. 4), which allow one to express the relative value of the oscillations of the specific resistance tensor in the following way:

$$\Delta\rho^{\alpha\beta}/\rho_0^{\alpha\beta} = H\sum_j \Phi_j^{\alpha\beta}\frac{d\ln S_{mj}}{d\zeta_0}\Delta M_j^z. \tag{39}$$

If $\sum\limits_k N_k^+ \neq \sum\limits_i N_i^-$, the matrix $\Phi^{\alpha\beta}$ has the form:

$$\Phi^{\alpha\beta} = \begin{pmatrix} \varphi_{11} & \gamma_0\varphi_{12} & \varphi_{13} \\ \gamma_0\varphi_{21} & \varphi_{22} & \varphi_{13} \\ \varphi_{31} & \varphi_{32} & \varphi_{33} \end{pmatrix}. \tag{40}$$

Expansion of the elements of the $\phi_{\alpha\beta}$ matrix in powers of γ_0 begins with zero order terms.

It can be shown, just as in the oscillations of the conductivity, that the relative magnitudes of the oscillations of the elements, ρ^{xy} is smaller by orders of magnitude (in terms of γ_0) than the relative magnitude of the oscillation of the remaining elements in the $\rho^{\alpha\beta}$ tensor.

If $\sum\limits_k N_k^+ = \sum\limits_i N_i^-$, the expansion of the element ϕ^{xy} again begins with a zero order term in γ_0, and the expansions of the other terms in the $\Phi^{\alpha\beta}$ matrix have the form shown in Eq. (40).

4. CALCULATION OF THE OSCILLATIONS IN SOME CONCRETE CASES.

In this section we will examine a series of simple cases, which permit simplification of the general formulae for the oscillatory parts of the tensors $\sigma^{\alpha\beta}$ and $\rho^{\alpha\beta}$.

The relations for $\Delta\sigma^{\alpha\beta}$ are greatly simplified in the presence of a single conduction band with convex Fermi surfaces. In fact, in Eqs. (26) and (27), we retain only one term and find

$$\Delta\sigma^{\alpha\beta} = H\left\{\overline{q^{\alpha\beta}} - q_m^{\alpha\beta}(\zeta_0) + \frac{\overline{\partial q^{\alpha\beta}}}{\partial\zeta_0}\Big/\frac{\partial\ln N^0}{\partial\zeta_0}\right\}\frac{d\ln S_m}{d\zeta_0}\Delta M^z. \tag{41}$$

It is interesting to note that if $q^{\alpha\beta}$ does not depend on ϵ and p_z the sum in Eq. (41) vanishes. This means, that the oscillations of $\sigma^{\alpha\beta}$ and $\rho^{\alpha\beta}$ for the case of a single conduction band with convex Fermi surfaces depend on the functional relation between the mobility and ϵ and p_z.

To calculate the amplitude of the oscillations of $\Delta\sigma^{\alpha\beta}$ and $\Delta\rho^{\alpha\beta}$, whether there exist one or several groups of electrons, it is necessary to know the functions $\chi(\epsilon, p_z)$, which can be determined only on the basis of certain assumptions concerning the collision integrals.

If the collision integrals in the kinetic equation can be replaced by a "relaxation time" t_0, which generally depends on ϵ and p_z, then

$$\chi^{\alpha\beta} = 2\pi e^2 t_0 h^{-3} 2\,\mathrm{Re}\sum_k \frac{\gamma}{\gamma + ik} v_{-k}^{\alpha} v_k^{\beta}, \quad \chi_0^{zz} = 2\pi e^2 t_0 h^{-3}(v_0^z)^2, \ \gamma = 1/t_0\omega^* = m^* c/e t_0 H; \tag{42}$$

where $\mathbf{v}_k$ are the Fourier components of the velocity of the electron.

In the isotropic case Eq. (42) becomes even simpler. Noting that for any isotropic dispersion law $\epsilon = \epsilon(p)$ the relations $\mathbf{p} = m^*\mathbf{v}$ and $\mathbf{v} = \nabla_p \epsilon^*$ are satisfied we have

$$\begin{gathered} \chi^{xx} = \chi^{yy} = \frac{e^2 t_0}{h^3}\frac{\gamma^2}{1+\gamma^2}\frac{S(\varepsilon, p_z)}{m^{*2}}, \qquad \chi^{xy} = \frac{e^2 t_0}{h^3}\frac{\gamma}{1+\gamma^2}\frac{S(\varepsilon, p_z)}{m^{*2}}, \\ \chi^{\alpha z} = 0(\alpha = x, y, z), \quad \chi_0^{zz} = 2\pi\frac{e^2 t_0}{h^3}\frac{p_z^2}{m^{*2}}, \ S(\varepsilon, p_z) = \pi(p^2(\varepsilon) - p_z^2), \end{gathered} \tag{43}$$

where $p = p(\epsilon)$ is an inverse function of $\epsilon = \chi(p)$.

From Eq. (43) and from the definition of the mean value of the "classical mobility tensor [Eq. (11)], with the assumption that $f_0'(\epsilon)$ can be approximated by a δ-function, it follows that:

$$\overline{q^{xx}} = \overline{q^{yy}} = q_0/(1 + \omega^{*2} t_0^2), \ \overline{q^{xy}} = \omega^* t_0 q_0/(1 + \omega^{*2} t_0^2), \quad \overline{q^{zz}} = q_0 e^2 t_0/m^*, \ \overline{q^{xz}} = \overline{q^{yz}} = 0, \ t_0 = t_0(\zeta_0), \tag{44}$$

---

*In the isotropic case $\mathbf{v} = (\partial\epsilon/\partial p)p/p$ and from the expression $S(\epsilon, p_z) = \pi(p^2(\epsilon) - p_z^2)$ it follows that $m^* = p(\partial p/\partial\epsilon) = p(\partial\epsilon/\partial p)$ so that $\mathbf{p} = m^*\mathbf{v}$.

where, as above, $\omega^* = eH/m^*c$.

Furthermore, from Eqs. (12) and (19), using Eq. (43), we find that

$$q_m^{\alpha\beta}(\zeta_0) = \overline{q^{\alpha\beta}} + \frac{p^2(\zeta_0)}{2m^*}\,\overline{\frac{\partial q^{\alpha\beta}}{\partial\zeta_0}} \quad (\alpha,\beta \neq z,z);\ q_m^{zz} = \overline{q^{zz}}. \tag{45}$$

We will now apply Eqs. (44) and (45) to an examination of two models.

(1) One Conduction Band

If there is only one conduction band, when

$$\partial \ln N^0/\partial\zeta_0 = 3m^*/p^2(\zeta_0),$$

the oscillating terms of $\Delta\sigma^{\alpha\beta}$ have the form

$$\Delta\sigma^{\alpha\beta} = -\frac{1}{3}H\,\overline{\frac{\partial q^{\alpha\beta}}{\partial\zeta_0}}\,\Delta M^z \quad (\alpha,\beta \neq z,z);\ \Delta\sigma^{zz} = \frac{2}{3}H\,\overline{\frac{\partial q^{zz}}{\partial\zeta_0}}\,\Delta M^z, \tag{46}$$

where $\overline{q^{\alpha\beta}}$ is determined from Eq. (44).

In strong magnetic fields ($\gamma \ll 1$) all the elements of $\overline{q^{\alpha\beta}}$ and their derivatives can be readily expressed in terms of q_0, and we find*

$$\frac{\Delta\sigma^{xx}}{\sigma_0^{xx}} = \frac{\Delta\sigma^{yy}}{\sigma_0^{yy}} = \frac{1}{3}H\frac{\partial \ln q_0}{\partial\zeta_0}\frac{\Delta M^z}{N_0},\quad \frac{\Delta\sigma^{xy}}{\sigma_0^{xy}} = -\frac{2}{3}\gamma^2 H\frac{\partial \ln q_0}{\partial\zeta_0}\frac{\Delta M^z}{N_0},\quad \frac{\Delta\sigma^{zz}}{\sigma_0^{zz}} = \frac{2}{3}H\frac{\partial \ln q_0}{\partial\zeta_0}\frac{\Delta M^z}{N_0}. \tag{47}$$

The expression for the oscillatory parts of the magnetic moment ΔM^Z in the case of an isotropic dispersion law can be found from the general equations,[3] in which one should substitute

$$S_m(\zeta_0) = \pi p^2(\zeta_0),\quad dS_m/d\zeta_0 = 2\pi m^*,\quad |\partial^2 S/\partial p_z^2| = 2\pi.$$

Using $\sigma_0^{\alpha\beta} = N_0\overline{q^{\alpha\beta}}$, and also Eqs. (38) and (46), we can calculate the oscillations of the specific resistivity tensor

$$\Delta\rho^{xx} = \Delta\rho^{yy} = \frac{H}{3\sigma_0^2}\left\{(1-\omega^{*2}t_0^2)\,\overline{\frac{\partial q^{xx}}{\partial\zeta_0}} - 2\omega^* t_0\,\overline{\frac{dq^{xy}}{\partial\zeta_0}}\right\}\Delta M^z,\quad \Delta\rho^{xy} = \frac{H}{3\sigma_1^2}\left\{(1+3\omega^{*2}t_0^2)\,\overline{\frac{\partial q^{xy}}{\partial\zeta_0}} - 2\omega^* t_0\,\overline{\frac{\partial q^{xx}}{\partial\zeta_0}}\right\}\Delta M^z,$$
$$\Delta\rho^{zz} = -\frac{2H}{3\sigma_0^2}\left\{2\omega^* t_0\,\overline{\frac{\partial q^{xy}}{\partial\zeta_0}} + \overline{\frac{\partial q^{zz}}{\partial\zeta_0}}\right\}\Delta M^z, \tag{48}$$

where $\sigma_0 = N_0 e^2 t_0/m^*$ is the conductivity of the metal in the absence of a magnetic field.

In strong magnetic fields one can substitute $\omega^* t_0 \gg 1$, which transforms Eq. (48) into

$$\frac{\Delta\rho^{xx}}{\rho_0^{xx}} = \frac{\Delta\rho^{yy}}{\rho_0^{yy}} = \frac{1}{3}H\frac{\partial \ln q_0}{\partial\zeta_0}\frac{\Delta M^z}{N_0},\quad \frac{\Delta\rho^{xy}}{\rho_0^{xy}} = -\frac{8}{3}\gamma^2 H\frac{\partial \ln q_0}{\partial\zeta_0}\frac{\Delta M^z}{N_0},\quad \frac{\Delta\rho^{zz}}{\rho_0^{zz}} = -\frac{2}{3}\frac{\partial \ln q_0}{\partial\zeta_0}\frac{\Delta M^z}{N_0}. \tag{49}$$

It should be observed that the relative magnitudes of the oscillations of $\Delta\sigma^{xy}/\sigma_0{}^{xy}$, and also of $\Delta\rho^{xy}/\rho_0{}^{xy}$ in strong magnetic fields in our case are smaller by two orders of magnitude of γ_0 than the relative magnitudes of the oscillations of the remaining terms in the $\sigma^{\alpha\beta}$ and $\rho^{\alpha\beta}$ tensors.

(2) Two Bands with $N^+ = N^-$

Let us assume, that there are two groups of electrons having a quadratic dispersion law, for one of which $(1/2\pi)\,dS_{m1}/d\zeta_0 = m_1 > 0$ (electrons), and for the other $(1/2\pi)\,dS_{m2}/d\zeta_0 = -m_2 < 0$ (holes), and that $N^+ = N^-$.

Symbolizing by q_1 the mobility of the electrons, and by q_2 that of the holes, it can be easily shown from the general Eqs. (26) and (27)

---

* If $m^* = m = \text{const}$, then $\partial \ln q_0/\partial\zeta = \partial \ln t_0/\partial\zeta_0$ and the expression for $\Delta\sigma^{xy}/\sigma_0^{xy}$ in Eq. (47) coincides with that given elsewhere,[5] where, however, there is a misprint in the numerical coefficient.

$$\Delta\sigma^{\alpha\beta} = -\frac{H}{(1+\mu)\zeta_0}\left\{\left[\mu\,(\overline{q_1^{\alpha\beta}} - \overline{q_2^{\alpha\beta}}) + \left(\mu + \frac{1}{3}\right)\zeta_0\,\overline{\frac{\partial q_1^{\alpha\beta}}{\partial\zeta_0}} + \frac{2}{3}\,\zeta_0\,\overline{\frac{\partial q_2^{\beta\alpha}}{\partial\zeta_0}}\right]\Delta M_1^z\right.$$

$$\left.+\left[\mu\,(\overline{q_1^{\alpha\beta}} - \overline{q_2^{\alpha\beta}}) + \frac{2}{3}\,\mu\zeta_0\,\overline{\frac{\partial q_1^{\alpha\beta}}{\partial\zeta_0}} - \left(\frac{5}{3}\,\mu + 1\right)\zeta_0\,\overline{\frac{\partial q_2^{\alpha\beta}}{\partial\zeta_0}}\right]\Delta M_2^z\right\}, \quad (50)$$

for $\alpha, \beta \neq z,z$ and

$$\Delta\sigma^{zz} = -\frac{H}{(1+\mu)\zeta_0}\left\{\left[\mu\,(\overline{q_1^{zz}} - \overline{q_2^{zz}}) - \frac{2}{3}\,\zeta_0\left(\overline{\frac{\partial q_1^{zz}}{\partial\zeta_0}} - \overline{\frac{\partial q_2^{zz}}{\partial\zeta_0}}\right)\right]\Delta M_1^z + \left[\mu\,(\overline{q_1^{zz}} - \overline{q_2^{z}}) + \frac{2}{3}\,\mu\zeta_0\left(\overline{\frac{\partial q_1^{zz}}{\partial\zeta_0}} - \overline{\frac{\partial q_2^{zz}}{\partial\zeta_0}}\right)\right]\Delta M_2^z\right\}, \quad (51)$$

where $\mu = m_2/m_1$, and the mobilities are determined from Eqs. (44) in which one substitutes in the case of the electrons $m^* = m_1$, and for the holes, $m^* = -m_2$.

For the extreme cases $\mu \gg 1$ or $\mu \ll 1$, one can leave out some of the terms in Eqs. (50) and (51); however, the general character of the expressions does not change.

Eqs. (50) and (51) show that the assumption $N^+ = N^-$ does not introduce any fundamental simplification of the general expressions for $\Delta\sigma^{\alpha\beta}$.

---

[1] I. Lifshitz, J. Exptl. Theoret. Phys. (U.S.S.R.) 32, 1509 (1957), Soviet Phys. JETP 5, 1227 (1957).

[2] L. Schubnikow and W. de Haas, Proc. Amsterdam Acad. 33, 418 (1930), W. de Haas and L. Schubnikow, Leid Comm. 207, 210 (1930).

[3] I. Lifshitz and A. Kosevich, J. Exptl. Theoret. Phys. (U.S.S.R.) 29, 730 (1956), Soviet Phys. JETP 2, 636 (1956).

[4] I. Lifshitz, M. Azbel' and M. Kaganov, J. Exptl. Theoret. Phys. (U.S.S.R.) 31, 64 (1956), Soviet Phys. JETP 4, 41 (1957).

[5] I. Lifshitz, J. Exptl. Theoret. Phys. (U.S.S.R.) 30, 814 (1956); Soviet Phys. JETP 3, 774 (1956).

Translated by J. J. Loferski
14

SOVIET PHYSICS JETP VOLUME 6, NUMBER 1 JANUARY, 1958

ON THE BRIGHTNESS OF STRONG SHOCK WAVES IN AIR

IU. P. RAIZER

Academy of Sciences, (U.S.S.R.)

Submitted to JETP editor November 29, 1956

J. Exptl. Theoret. Phys. (U.S.S.R.) 33, 101 (1957)

The emission and absorption of light at high temperatures in a shock wave front in air are considered. The dependence of the brightness of the shock wave front on its amplitude is derived.

IN our preceding article[1]* we considered in a general form the problem of the internal structure of the front of strong shock waves in gases, taking account of radiation. We operated throughout with integral characteristics of the radiation — the total energy flux and density. Also, passing from the geometrical coordinate to the optical thickness, we excluded from consideration the actual distribution of quantities in space, which is determined by the coefficient of absorption of light in the gas. This approach is inadequate when we are interested in the flux of visible radiation passing from the wave front to infinity (brightness of the wave front), the measurement of which is one of the important experimental methods for the study of shock waves and the determination of their amplitudes.

---

*Hereafter referred to as I.

The brightness depends in an essential way on the coefficient of absorption of visible light at various points of the wave front, and on the distribution of the light sources, i.e., the temperature distribution in the wave.

In I, temperature profiles were obtained as a function of the mean over the spectrum of the optical thickness. Therefore, to calculate the brightness it is necessary to find the relation between the coefficient of absorption of visible light and the mean over the spectrum. The latter is determined by the character of the radiation spectrum involved in the transfer of energy in the wave, which in turn depends on the coefficients of absorption of the various frequencies at different temperatures.

These questions are considered in the present article as applied to air. The results will allow us to draw conclusions regarding the general character of the relation between the brightness or effective wave temperature and the temperature behind the shock wave front.

Let us recall that by effective (visible) temperature we mean the temperature that a black body would have to have in order to give exactly the same flux of visible light as passes from the shock wave front to infinity.

1. COEFFICIENT OF ABSORPTION OF LIGHT BY AIR

We begin with low temperatures. Cold air, as is well known, is transparent to visible light. Strong molecular absorption begins in the ultraviolet region; the absorption coefficient reaches the value $\kappa_\nu \approx 100\ \mathrm{cm}^{-1}$ for $h\nu \approx 8$ev * at normal density.[2]

Quanta with energy greater than the ionization potentials of oxygen and nitrogen molecules, $I_{O_2} = 12.5$ ev, $I_{N_2} = 15.5$ ev (for atoms, $I_O = 13.5$ ev, $I_N = 14.5$ ev), undergo strong photoelectric absorption. The effective absorption crossections from ground levels depend only slightly on frequency in the interval $I \approx h\nu$ to $h\nu = 25$ ev, and are $\sigma_O = 3 \times 10^{-18}\ \mathrm{cm}^2$, $\sigma_N = 5 + 10^{-18}\ \mathrm{cm}^2$ per atom,[3] which gives $\kappa_\nu = 120$ cm. As the frequency increases, the absorption coefficient goes through jumps corresponding to the successive inclusion in the absorption of various electrons filling the L-shells of oxygen and nitrogen atoms. The L-shell levels do not differ too strongly from one another, so that the jumps apparently lie in the frequency region from $h\nu = 13$ up to $h\nu \approx 30$ ev. At higher frequencies the absorption decreases monotonically up to quanta with energy $h\nu = 410$ ev, equal to the binding energy of K-electrons in nitrogen (530 ev in oxygen). Experimental data on the absorption of intermediate frequencies between the far ultraviolet and soft x-rays is extremely scanty. Combining the various data, we may set up Table I as an approximate representation of the absorption coefficient in this region.

TABLE I

$h\nu$ (ev)	κ_ν (cm^{-1})	Ref.
8	100	2
13-25	120	3
182	12	4
280	5.3	5
410	1.6	6
415	35	7

At not too high temperatures, lower than $\approx 30{,}000°$, when the degree of ionization is not great, quanta with energies less than the ionization potentials are absorbed principally by photoeffect with excited levels of neutral atoms (and molecules) of oxygen and nitrogen. For an estimate of this absorption we may, as is commonly done in astrophysics, use Kramer's formula, derived for hydrogenlike atoms and ions. The formula for κ_ν, integrated over the levels taking account of their degree of excitation, has the form:[8]

$$\varkappa_\nu = \frac{16\pi^2}{3\sqrt{3}} \frac{e^6}{hc} \frac{kT}{(h\nu)^3} e^{h\nu/kT} \sum_i Z_i^2 n_i e^{-I_i/kT}. \tag{1}$$

The summation is carried out over all the types of atoms and molecules (n_i is the number of these particles per cubic centimeter). Z_i is the effective charge of the atomic residue, which according to Ref. 8 should be set equal to $Z_i = 2.5$.†

The temperature dependence is apparently represented correctly by the Boltzmann exponential factor. Taking account of the equilibrium composition of air at the various temperatures, we may use this formula to calculate the absorption coefficient for red light, $h\nu = 1.91$ ev ($\lambda = 6500$ A), which is com-

---

*It will be convenient in what follows to express the frequency in electron volts.

†Model''s data[9] are in satisfactory agreement with this value.

monly used to photograph shock waves (see Table II; concerning the last two values in this table, see below). κ_ν depends extremely sharply on temperature because of the high ionization potentials.

TABLE II

$10^{-3}\cdot T$	11	12	15	17	20	30	50	100
$\varkappa_\nu$	0.09	0.31	4.1	13.5	60	290	350	2000

The absorption coefficient (1) considered as a function of frequency at a given temperature has a minimum at $h\nu = 3kT$. Eq. (1) may be used only for values of $h\nu$ sufficiently small with respect to unity, when the absorption occurs in highly excited levels which may to some extent be considered "hydrogenlike." Both Kramer's formula and the replacement of summation over levels by integration become inapplicable at $h\nu \approx I$.

A rough estimate of the absorption at $h\nu = I$ may be obtained from Kramer's fromula for the absorption in the ground level of a hydrogenlike atom,[8] which for air gives

$$\varkappa_\nu = 430Z^{-2}(I/h\nu)^3 \text{ cm}^{-1}. \tag{2}$$

At $h\nu = I$, Eq. (2) gives the correct order of magnitude ($\kappa_\nu \approx 100 \text{ cm}^{-1}$) with $Z = 2$. The absorption coefficient has a maximum at $h\nu = I$.

Absorption at high frequencies, $h\nu \gg I$, and not too high temperatures, when air consists principally of neutral atoms, takes place in the same way as in cold air, i.e., according to Table I.

At high temperatures the atoms are strongly ionized, and as a rule, at every temperature air consists principally of ions of two multiplicities: at T = 50,000° singly and doubly ionized, at T = 100,000° doubly and triply ionized, etc. The absorption of quanta with energies less than the lowest ionization potential of the ions present in sufficient quantity* may be estimated by a formula of type (1). The last three numbers in Table II were obtained in this way.

The maximum absorption, corresponding to $h\nu = I_{\min}$, may be estimated by Eq. (2), setting Z equal to the charge of the ion. The magnitude of the maximum decreases with Z, i.e., with increased temperature, and is of the order $\kappa_\nu \sim 100$ to 10 cm^{-1}. Then, with further increase of frequency, there are successive maxima corresponding to the inclusion in the absorption of different ions (more exactly, different levels of different ions), and at sufficiently high frequencies, κ_ν decreases monotonically with increasing frequency up to the K-jump.

This is the general picture of the absorption of light in air. The state of theory in connection with this question is such that it is very difficult to go further than crude estimates of order of magnitude and the establishment of qualitative relations, which naturally shows in the character of the conclusions regarding the spectrun and effective temperature. The qualitative dependence of the absorption coefficient on frequency at a given temperature is illustrated by Fig. 1.

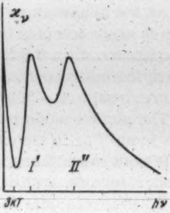

FIG. 1

2. THE CHARACTER OF THE RADIATION SPECTRUM IN THE HEATING ZONE AND THE ABSORPTION COEFFICIENT AVERAGED OVER THE SPECTRUM

The radiation emanating from the surface of the discontinuity of a strong shock wave is absorbed in the gas layers lying in front of it and heats them.

In I, temperature profiles were found in the heating zone, assuming constant heat capacity. In air as well as in other gases, the heat capacity at high temperatures depends on temperature because of ionization processes. In this regard, all the relations in I concerning the heating zone must be generalized somewhat. Thus, the condition that the flux of radiant energy and the hydrodynamic flux are equal (Eq. 12 in I) is now written in the form:

$$S = D\rho_0\varepsilon(T). \tag{3}$$

Keeping in mind that the compression in the heating zone is small, and that the specific internal energy depends only weakly on density, we may take $\epsilon(T)$ at normal air density in this equation.

The temperature profile in the diffusion approximation is determined by the formula

---

*At $T < 30{,}000°$: $I_{\min} = I_0 \sim 13$ ev, At $T \sim 50{,}000°$: $I_{\min} = I_1 \sim 30$ ev,
At $T \sim 100{,}000°$: $I_{\min} = I_2 \sim 50$ ev, At $T \sim 150{,}000°$: $I_{\min} = I_3 \sim 75$ ev.

$$\varepsilon(T) = \varepsilon(T_-)\exp(-\sqrt{3}\tau) \quad \tau > 0, \tag{4}$$

similar to Eq. (15) in I.

The greatest heating temperature T_- in front of the shock discontinuity is found from the equation

$$\sigma T_1^4 = D\rho_0\varepsilon(T_-), \tag{5}$$

in which it is necessary to substitute the actual function $D(T_1)$ for air. Values of T_- as a function of T_1, the temperature behind the front, were calculated with this formula and are given in Table III.

TABLE III

$10^{-3}T_1^\circ$	$D\left(\frac{\text{km}}{\text{sec}}\right)$	$\varepsilon(T_-)\left(\frac{\text{ev}}{\text{molec.}}\right)$	$10^{-3}T_-^\circ$
285	88.1	1020	285
275	86.2	910	240
250	81.6	635	175
150	56.5	122	60
100	40.6	32.7	25
75	32.1	13.1	12
65	28.5	8.4	9
50	23.3	3.7	4

We used Selivanov's[10] data with regard to the calculation of thermodynamic functions and the shock adiabatic of air, taking account of ionization.* It is clear from the table that the temperature behind the front at which the quantities T_- and T_1 are comparable, and which is the characteristic temperature for the problem of the structure of a shock wave front, is of the order $T_k \approx 285{,}000^\circ$ in air.

We will now estimate the mean over the spectrum of κ, the absorption coefficient of light in the heating zone.

Our problem is the calculation of the effective temperature of the wave front. It will be shown in the next section that at a temperature $T_1 < 90{,}000^\circ$ behind the front, the effective temperature is practically equal to the temperature behind the front; therefore, we will consider only stronger waves.

It follows from Sec. 1 that the absorption coefficient for the various frequencies at the various temperatures lies, as a rule, between 100 and 10 cm^{-1}. The exceptions consist only of sufficiently low frequencies having insignificant energy.

Consequently, the mean coefficient also has the same order of magnitude. For example, at $T_1 = 100{,}000^\circ$ the maximum of the Planck spectrum (as a function of frequency) occurs at $h\nu = 24$ ev. Here, the greatest heating temperature is $T_- = 25{,}000^\circ$. At temperatures less than $25{,}000^\circ$, quanta greater than 13 ev are absorbed in the same way as in cold air. Quanta lower than 13 ev carry little energy. Thus, 85% of the total spectral energy is included in the interval from 13 to 150 ev.

Quanta with lower energy are absorbed more strongly. Therefore, as we go away from the surface of the discontinuity, the spectrum becomes harder and harder and the mean absorption coefficient decreases, varying within the limits from 100 to 10 cm^{-1}.

As the temperature behind the front is raised, the picture does not change in general; it only becomes more complex because the temperature in the heating zone becomes high, and the "leading" frequencies, i.e., the frequencies which carry the principal energy (so to say, "lead" the heating) and to which the mean coefficient κ corresponds, lie in the region of absorption jumps. The order of κ remains as previously: $\kappa \sim 100$ to 10 cm^{-1}.

The picture again becomes clear at sufficiently high temperatures behind the front $T_1 > T_k$ ("isothermal jump") or in the case of a thermal wave.

In both cases there is a region in the wave in which radiation is in local equilibrium with matter. The temperature separating the equilibrium and nonequilibrium regions is $T_k \approx 285{,}000^\circ$.

We shall consider in detail the case of very strong waves, because it is a limiting case with respect to the effective temperature.

At temperatures above $\approx 285{,}000^\circ$ the radiation is in equilibrium with matter; therefore, we may approximately consider that a Planck spectrum of temperature T_k leaves the surface where $T = T_k$, no matter how high the temperature is behind this surface. As we go away from the point at which $T = T_k$ in the direction of lower temperatures, the radiation density exceeds equilibrium at the given temperature to a greater and greater extent. Using Eqs. (12), (16), and (32) of I, and the proportionality ϵ we $\sim T^{1.4}$, we obtain

$$U(T)/U_r(T) = U_r(T_k)\varepsilon(T)/U_r(T)\varepsilon(T_k) = (T_k/T)^{2.6}. \tag{6}$$

The general tendency of absorption is such that κ decreases with increasing frequency. At $T = 285{,}000^\circ$ the Planck maximum corresponds to $h\nu = 70$ ev, and the principal energy of the primary spectrum lies in a region in which κ decreases more or less monotonically with ν. In order to estimate the "leading" frequency ν_m at each point of the wave, we may schematize the spectrum as follows: we will assume that frequencies $\nu < \nu_m$ which are absorbed more strongly than ν_m are in local equilibrium, and that frequencies $\nu > \nu_m$ are distributed in the same way as in the initial spectrum, i.e., arrive at the point x without having undergone absorption along the way from the point at which $T = T_k$. This becomes all the more valid as with increasing x the leading role moves to higher frequencies, so that for a given frequency ν, the ratio $\nu/\nu_m(x)$ increases with decreasing x.

---

*Let us note that in the temperature interval from $10{,}000^\circ$ to $300{,}000^\circ$, $\epsilon(T)$ may be approximated by the power law $\epsilon \sim T^{1.4}$.

At not too high temperatures, according to Eq. (6), the equilibrium part of the spectrum carries negligible energy. Therefore, we may set

$$U_\nu(x) = \begin{cases} 0 & \nu < \nu_m \\ U_{\nu r}(T_k) & \nu > \nu_m. \end{cases} \tag{7}$$

The "leading" frequency is determined by the formula

$$U(x) = \int\limits_{\nu_m}^{\infty} U_{\nu r}(T_k)\,d\nu = U_r(T_k)\frac{\varepsilon(T)}{\varepsilon(T_k)}. \tag{8}$$

Some calculated values of $\nu_m(T)$ are given in the second column of Table IV. They lie in the sufficiently far Wien region where the spectrum drops rapidly; therefore, the average absorption coefficient corresponds simply to ν_m.

Keeping in mind that at temperatures lower than ≈30,000° energetic quanta are absorbed in the same way as in cold air, we may use the data of Table I to associate a mean absorption coefficient with each temperature at the lower boundary of the wave (third column of Table IV).

3. THE EFFECTIVE TEMPERATURE OF A STRONG SHOCK WAVE AND OF THERMAL WAVES

According to the general formula (26) in I, the flux of visible light passing from the shock wave front to infinity is

$$S_\nu = \frac{c}{2}\int\limits_{-\infty}^{\tau_\nu} U_{\nu r}\,E_2(\tau_\nu - \tau_\nu')\,d\tau_\nu', \tag{9}$$

where τ_ν is the total optical thickness of the heated layer for the frequency ν, corresponding to $x = +\infty$. In distinction from the mean optical thickness τ, equal to $+\infty$ at $x = +\infty$, τ_ν for visible light is finite, thanks to the condition $S = 0$, because the absorption coefficient for visible light drops extremely rapidly with decreasing temperature. Since the mean coefficient κ depends only weakly on temperature, the temperature T^* at which

$$\kappa_\nu(T^*) = \kappa(T^*), \tag{10}$$

may be called the boundary of transparency of air in the shock wave front in the sense that for $T < T^*$, air is practically transparent to visible light. A simple calculation shows that the optical thickness of the heated layer from $x = +\infty$ to the point $x = x^*$ at which $T = T^*$ (when $T_- \geq T^*$) is very small; $\Delta\tau_{\nu\max} \approx 0.1$. Therefore, the total optical thickness τ_ν is practically equal to the optical thickness of the layer $0 < x < x^*$. When $T_- < T^*$, the optical thickness of the entire heated layer $\Delta\tau_\nu \ll \Delta\tau_{\nu\max}$.

It is clear from Table II that $T^* \approx 20{,}000$–$17{,}000°$ when $\kappa \sim 100$ to $10\ \mathrm{cm}^{-1}$. When the temperature behind the shock wave front is lower than $T_1^* \approx 90{,}000°$, the maximum heating temperature $T_- < T^*$ as follows from Table III, and the heated layer is transparent to visible radiation. Since under these conditions black body radiation near the temperature T_1 leaves the surface of the discontinuity, the effective temperature T_{eff} of the visible radiation will almost coincide with T_1, the temperature behind the front.

As the shock wave amplitude is raised, for $T_1 > T_1^*$, the greatest temperature T_- in front of the discontinuity becomes higher than the transparency temperature, and an absorbing layer $0 < x < x^*$ with temperatures $T_- > T > T^*$ appears in the heating zone, which strongly screens the visible radiation leaving the surface of the discontinuity.

Let $B_\nu(T)$ denote the flux of Planck radiation of frequency ν leaving the surface of a black body at the temperature T:

$$B_\nu(T) = (2\pi h/c^2)(e^{h\nu/kT} - 1)^{-1}. \tag{11}$$

Than the effective temperature is determined by the expression*

$$B_\nu(T_{\text{eff}}) = 2\int_{-\infty}^{\tau_\nu} B_\nu(T)\,E_2(\tau_\nu - \tau_\nu')\,d\tau_\nu'. \tag{12}$$

We will separate the integral into two parts. The first of them, from $-\infty$ to 0, corresponds to the part of the flux going toward infinity which came from the surface of the discontinuity and was partially screened by the heated layer. The second part, from 0 to τ_ν, corresponds to the visible light generated in the heated layer itself. Using the well known properties of integral exponents, and also the fact that the temperature behind the discontinuity is very close to T_1, we find that the first part is approximately

$$2\int_{-\infty}^{0} B_\nu(T)\,E_2(\tau_\nu - \tau_\nu')\,d\tau_\nu' \approx B_\nu(T_1)\cdot 2E_3(\tau_\nu). \tag{13}$$

To calculate the second integral over the heating zone we note that the radiating capacity which is proportional to the Planck function $B_\nu(T)$, does not depend very strongly on the coordinate, while the screening factor E_2 decreases rapidly as its argument increases. As we advance through the heating zone in the direction of increasing temperature, beginning at the point x^*, the absorption coefficient of visible light increases rapidly, but the mean over the spectrum changes only slightly. Therefore, the radiating layer, i.e., the layer which is the principal contributor to the integral and has a thickness with respect to τ_ν of the order of several units, has a comparatively small optical thickness averaged over the spectrum.

Consequently, the temperature therein varies only slightly [see Eq. (4)], and we may simply set $T \approx \text{const} = T^*$ in the integral. Then

$$2\int_{0}^{\tau_\nu} B_\nu(T)\,E_2(\tau_\nu - \tau_\nu')\,d\tau_\nu' \approx B_\nu(T^*)\,[1 - 2E_3(\tau_\nu)]; \tag{14}$$

$$B_\nu(T_{\text{eff}}) = B_\nu(T_1)\cdot 2E_3(\tau_\nu) + B_\nu(T^*)\,[1 - 2E_3(\tau_\nu)]. \tag{15}$$

A rough estimate of the total optical thickness of the heating zone for visible radiation may be obtained by assuming that the absorption coefficient κ_ν depends on temperature through Boltzmann's law $\kappa_\nu \sim \exp(-1/kT)$, but that κ does not generally depend on temeperature. Taking Eq. (10) into account and changing from x to a new independent variable, the temperature in the integral for τ_ν, we find using Eq. (4) and the proportionality $\epsilon \sim T^{1.4}$,

$$\tau_\nu = \int_0^\infty \varkappa_\nu\,dx \approx \int_0^{x^*} \varkappa_\nu\,dx = \int_{T^*}^{T_-} \exp\left(-\frac{1}{kT} + \frac{1}{kT^*}\right)\frac{1{,}4}{\sqrt{3}}\,\frac{dT}{T} \approx \frac{1{,}4}{\sqrt{3}}\,\frac{kT_-}{I}\left[\exp\left(\frac{I}{kT^*} - \frac{I}{kT_-}\right) - 1\right]. \tag{16}$$

Now, using Eq. (15), it is easy to see how the effective temperature varies as the amplitude of the wave increases. For $T_1 < T_1^* \approx 90{,}000°$, $\tau_\nu \approx 0$ and $2E_3(\tau_\nu) \approx 1$, i.e., $T_{\text{eff}} = T_1$. When $T_1 > T_1^*$, τ_ν increases very rapidly with increasing T_1 and the first term in Eq. (15) tends rapidly toward zero because of the screening, in spite of the increase of the flux $B_\nu(T_1)$. Even at $T_1 \approx 110{,}000°$, $T_- = 30{,}000°$: $\tau_\nu = 2.2$ and the first term is less than the second. Since under these circumstances the coefficient is practically equal to unity for $B_\nu(T^*)$, the effective temperature simply coincides with the transparancy temperature T^*. Continuing, $T_{\text{eff}} \approx T^*$ as the shock wave amplitude increases without limit, as well as in the case of a thermal wave. Since the mean absorption coefficient decreases somewhat as the wave amplitude increases, T^* drops slightly from $\approx 20{,}000°$ to $\approx 17{,}000°$.

In the limit of a sufficiently strong wave, $\kappa \approx 10\ \text{cm}^{-1}$ according to Table IV, and the effective tem-

---

*Its meaning becomes clear when we remember that

$$2\int_0^\infty E_2(z)\,dz = 1.$$

TABLE IV

$10^{-3}\cdot T^\circ$	$h\nu_m$ (ev)	κ (cm^{-1})
50	140	
20	200	10.5
15	212	9.8
10	225	8.6

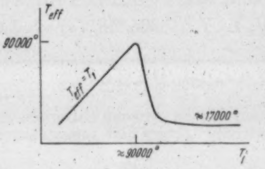

FIG. 2

perature, equal to the transparency temperature, is $\approx 17{,}000^\circ$. It should be noted that in spite of our extremely poor knowledge regarding the absolute magnitudes of $\kappa_\nu(T)$ and κ, the above value of the effective temperature is fairly accurate because of the sharp dependence of κ_ν on temperature.

A curve of $T_{eff}(T_1)$ is given in Fig. (2).

I wish to express profound thanks to Ia. B. Zel'dovich for his interest in this work, and for valuable discussions and remarks.

APPENDIX

THE ROLE OF ELECTRONIC HEAT CONDUCTIVITY IN THE ESTABLISHMENT OF THE TEMPERATURE PROFILE IN THE HEATING ZONE

At high temperatures, air is strongly ionized, and we should estimate whether the flux of electronic thermal conductivity is comparable to the energy flux transferred by radiation, which generally speaking may lead to some spreading of the temperature profile in the shock wave as compared with the profile accounting for radiant heat exchange alone.

Electrons in a plasma undergo elastic collisions with electrons, ions and neutral atoms. Sufficiently energetic electrons may excite and ionize atoms (and ions). The mean free path for elastic Coulomb scattering of electrons in a plasma may be estimated by Landau's formula,[11] which for air may be written in the form

$$l_e \approx \frac{2\cdot 10^{-7}}{Z(T)}\left(\frac{T^\circ}{10^4}\right)^2 \text{cm}, \tag{17}$$

where Z(T) is the mean number of free electrons per atom. The coefficient of electronic thermal conduction is then

$$\chi_e = \frac{4{,}5}{Z(T)}\left(\frac{T^\circ}{10^4}\right)^{5/2} \frac{\text{cm}^2}{\text{sec}}, \tag{18}$$

where l_e is essentially the distance required to establish a Maxwellian distribution in the electron gas. It is very small: at $T = 10^{5\circ}$, $l_e \approx 10^{-5}$ cm.

The elastic mean free path of very fast electrons, which are formed as a result of photoelectric absorption of energetic quanta, may be estimated by Eq. (17), if we replace the temperature therein by the electron energy. Thus, for $E \sim 100$ ev, we obtain $l \sim 2 \times 10^{-3}$ cm.

However, such energetic electrons quickly lose energy by ionization and excitation of atoms (the cross section is $\sim 10^{-16}$ to 10^{-17} cm^2, the free path is $l_{\text{inelas.}} \sim 2 \times 10^{-4}$ to 2×10^{-3} cm). The inelastic free path is comparable with the elastic free path at $E \sim 70$ ev.

At low temperatures, where ionization is small, the electrons do not have the ability to ionize ($E > 13$ ev), and lose energy through elastic collisions with atoms; $\sigma \sim 10^{-16}$ cm^2, $l \sim 2 \times 10^{-4}$ cm. In order to become thermalized, they must undergo $N \sim 3 \times 10^4$ collisions, i.e., the thermalization length is $\sim \sqrt{l^2 N} \sim 4 \times 10^{-2}$ cm. All of these free paths are less than the free path for the absorption of radiation, which, as was shown in Secs. 1 and 2, is of the order of 10^{-2} to 10^{-1} cm. Therefore, we may assume that the energy of absorbed quanta is transformed into heat at the point of absorption. This energy is transmitted directly to electrons, which then exchange it with ions considerably more slowly than the time required to establish Maxwellian distributions in the ion and electron gases. The exchange time may be estimated by Landau's formula.[11] The characteristic exchange length (the time multiplied by the velocity of the front) is

$$l_{\text{exch}} \sim 10^{-3}\,(10^{-4}\,T_e^\circ)^{3/2}\ \text{cm}.$$

In the heating zone, the difference between the electronic and the ionic temperatures is not great.

It is easy to estimate the flux of electronic thermal conductivity assuming approximately that the electronic and ionic temperatures coincide,

$$S_e = -\chi_e \rho_0 d\varepsilon / dx.$$

Let us compare this with the flux of radiant energy, Eq. (3), using Eq. (4) to obtain the gradient of the internal energy. We obtain

$$S_e / S_{\mathrm{rad}} = (l_e / l_{\mathrm{rad}}) v_e / D,$$

where v_e is the thermal velocity of the electrons.

Calculation shows that the fluxes are comparable only at very high temperatures ~300,000°. At lower temperatures: $S_e \ll S_{\mathrm{rad}}$.

The difference between the electronic and the ionic temperature has an essential effect only on the structure of the temperature peak behind the discontinuity, but this in no way influences the behavior of the effective temperature of the wave.

---

[1] Iu. P. Raizer, J. Exptl. Theoret. Phys. (U.S.S.R.) 32, 1518 (1957), Soviet Phys. JETP 5, 1242 (1957).

[2] E. G. Schneider, J. Opt. Soc. Am. 30, 128 (1940).

[3] V. A. Ambartsumian et al., Теоретическая астрофизика (Theoretical Astrophysics), GITTL, M., 1952, page 66.

[4] R. H. Messner, Z. Physik. 85, 727 (1933).

[5] E. Dershem, Phys. Rev. 37, 1696 (1931).

[6] K. K. Aglinstev, Дозиметрия ионизирующих излучений, (Dosimetry of Ionizing Radiation), GITTL, M.-L., 1950, page 46.

[7] Landolt-Bornstein, "Tables", sixth ed. (1950) Vol. 1, Chap. 1, page 316.

[8] A. Unsöld, Physics of Stellar Atmospheres (Russian Transl.), IIL, 1949.

[9] I. Sh. Model', J. Exptl. Theoret. Phys. (U.S.S.R.) 32, 714 (1957), Soviet Phys. JETP 5, 589 (1957).

[10] V. V. Selivanov, J. Phys. Chem. (U.S.S.R.) in press.

[11] L. D. Landau, J. Exptl. Theoret. Phys. (U.S.S.R.) 7, 203 (1937).

Translated by D. Lieberman
15

SOVIET PHYSICS JETP VOLUME 6, NUMBER 1 JANUARY, 1958

DISPERSION OF SOUND IN A FERMI LIQUID

I. M. KHALATNIKOV and A. A. ABRIKOSOV

Institute of Physical Problems, Academy of Sciences, U.S.S.R.

Submitted to JETP editor December 11, 1956

J. Exptl. Theoret. Phys. (U.S.S.R.) 33, 110-115 (July, 1957).

On the basis of the theory proposed by Landau for a Fermi liquid the attenuation and dispersion of sound oscillations in such a liquid are investigated. Specific calculations are performed for the case of liquid He^3.

THE characteristics of sound in a Fermi liquid are determined by the kinetic equation for the excitations, which, according to Landau,[1] has the form

$$\frac{\partial n}{\partial t} + \frac{\partial n}{\partial \mathbf{r}} \frac{\partial \varepsilon}{\partial \mathbf{p}} - \frac{\partial n}{\partial \mathbf{p}} \frac{\partial \varepsilon}{\partial \mathbf{r}} = I(n). \qquad (1)$$

Here ϵ is the energy of a single excitation, a function of the excitation density n. For small deviations of the distribution function n from the equilibrium Fermi distribution at T = 0 (n_0), the function ϵ can be represented in the form

$$\varepsilon = \varepsilon_0 + \int f(\mathbf{p},\mathbf{p}')\, n_1(\mathbf{p}')\, d\tau_{p'} \quad (n_1 = n - n_0). \tag{2}$$

Let oscillations in the excitation density n take place within the liquid with small amplitude ν_1 and frequency ω. n_1 can now be written in the form

$$n_1 = \nu_1 e^{i(\mathbf{kr} - \omega t)}. \tag{3}$$

We substitute (3) in Eq. (1), confining ourselves to terms linear in n_1

$$-i\omega n_1 + i n_1 \mathbf{k}\frac{\partial\varepsilon}{\partial\mathbf{p}} - i\mathbf{k}\frac{\partial n_0}{\partial\mathbf{p}}\int f(\mathbf{p},\mathbf{p}')\, n_1(\mathbf{p}')\, d\tau_{p'} = I(n_1). \tag{4}$$

We now recall that the derivative $\partial n_0/\partial\epsilon$ has the form of a δ-function, and introduce the notation

$$\nu_1 = \nu\partial n_0/\partial\varepsilon; \quad f(\partial\tau/\partial\varepsilon)_{\varepsilon=\varepsilon_0} = F. \tag{5}$$

We now rewrite Eq. (4) in the form

$$\left\{(\mathbf{kv} - \omega)\nu + \mathbf{kv}\int F\nu'\frac{do'}{4\pi}\right\}\frac{\partial n_0}{\partial\varepsilon} = I \quad \left(\mathbf{v} = \frac{\partial\varepsilon}{\partial\mathbf{p}}\right). \tag{6}$$

The function F evidently depends only upon the angle ϑ between the momenta p and p', since in the approximation under consideration these vectors are equal in absolute value to p_0. In the general case F is a complicated function of the angle ϑ. Therefore the function ν is likewise a complicated function of the angle between the vectors k and p.

Landau has shown[2] that at absolute zero, where the collision integral I is equal to zero, Eq. (4) leads to the occurrence of undamped oscillations (zero sound). The velocity of propagation of these oscillations is determined by a transcendental equation (cf. Appendix) involving in a fundamental way the function F(ϑ). We do not know the form of this function; knowing the effective mass of the excitation and its compressibility, however, we can determine $\overline{F}$ and $\overline{F\cos\vartheta}$ from the formulas (cf. Ref. 1)

$$1/m = (1/m^*)(1 + \overline{F\cos\vartheta}), \tag{7}$$

$$c^2 = (p_0^2/3m^2)(1 + \overline{F})/(1 + \overline{F\cos\vartheta}) \tag{8}$$

Specific calculations for He^3 can therefore be carried out, taking the function in the form of a binomial

$$F = F_0 + F_1\cos\vartheta. \tag{9}$$

At temperatures different from zero ordinary sound will be propagated in the Fermi liquid. For low frequencies ω the attenuation of the sound is determined by the usual expression[3]

$$\gamma = \frac{\omega^2}{2\rho c^3}\left\{\left(\frac{4}{3}\eta + \zeta\right) + \frac{\varkappa}{c_p}\left(\frac{c_p}{c_v} - 1\right)\right\}; \tag{10}$$

here γ is the sound attenuation coefficient, η is the coefficient of first viscosity, ζ is the coefficient of second viscosity, κ is the thermal conductivity coefficient, and c is the specific heat. In the case of the ideal gas model, for which the Fermi boundary surface has the form of a sphere, the second viscosity coefficient is very small.[4] The first viscosity coefficient varies with the temperature as $1/T^2$. The ratio κ/c_p, equal in order of magnitude to η, also varies as $1/T^2$ ($\kappa \sim 1/T$, $c_p \sim T$). The term involving κ/c_p, however, is multiplied by the factor $(c_p - c_v)/c_v$. This ratio, as can readily be seen from the well-known relation

$$\frac{c_p}{c_v} - 1 = -\frac{T}{c_v}\left(\frac{\partial p}{\partial T}\right)_v^2 \Big/ \left(\frac{\partial p}{\partial V}\right)_T,$$

varies with the temperature as T^2 ($\partial p/\partial T \sim \partial S/\partial V \sim T$). At low temperatures this factor is extremely small. Therefore at low temperatures the attenuation of sound is determined entirely by the viscosity.

Eq. (10) is valid for the case in which the frequency of the sound is low and the inequality $\omega\tau \ll 1$ is fulfilled; τ is the time between collisions of the excitations. The time τ is inversely proportional to the square of the temperature.[4,5] The above inequality will be violated both at sufficiently low temperatures and at sufficiently high frequencies. If the frequency of the sound is sufficiently high that the reverse inequality $\omega\tau \gg 1$ applies, this signifies that collisions between the excitations play no part, and that the collision integral may be neglected. In this case, however, the oscillations investigated by Landau[2] (zero sound) can be propagated in the Fermi liquid. It is of interest to follow the process by which the transition from ordinary sound to zero sound takes place as the frequency ω is increased. For this it is necessary to solve the kinetic equation (4). We shall not solve this difficult problem for the general case, particularly in view of the fact that the interaction law for the excitations is unknown.

It would be possible to simplify the problem by introducing a certain effective time τ and substituting for the integral I in (4) the expression n_1/τ. With such a substitution, however, the conservation laws for number of excitations, momentum, and energy will not come out of the kinetic equation, making the transformation to hydrodynamics impossible. Since the thermal conductivity and the second viscosity are negligibly small in the present case, the terms in the collision integral which involve the zero and first spherical harmonics are absent. We shall therefore replace the collision integral by the following expression:*

$$I(n) \rightarrow -\tau^{-1}\left(n_1 - \bar{n}_1 - 3\overline{n_1\cos\vartheta}\cos\vartheta\right) \tag{11}$$

It can readily be seen that when integrated over $d\tau_p$ this expression reduces to zero. It also reduces to zero when multiplied by $p\cos\theta$ and integrated over $d\tau_p$.† Thus the conservation equations for the number of particles and for the momentum are automatically fulfilled. Thus, from (4) and (11), the final kinetic equation has the following form

$$(kv\cos\vartheta - \omega)\nu + kv\cos\vartheta\int F\nu'\,\frac{do'}{4\pi} = -\frac{1}{i\tau}\left(\nu - \bar{\nu} - \overline{3\nu\cos\vartheta}\cos\vartheta\right). \tag{12}$$

Bearing in mind the applicability of these results to He^3 we write the function F in the binomial form of Eq. (9), in order not to complicate the problem.

We introduce the notation

$$\bar{\nu} = \nu_0, \quad 3\overline{\nu\cos\vartheta} = \nu_1, \quad \sigma = i\tau kv, \quad \xi = (i\omega\tau - 1)/i\tau kv, \tag{13}$$

following which we readily obtain, from (12)

$$(\cos\vartheta - \xi)\nu + \cos\vartheta\left(F_0\nu_0 + \frac{1}{3}F_1\nu_1\cos\vartheta\right) = \frac{1}{\sigma}(\nu_0 + \nu_1\cos\vartheta). \tag{14}$$

We next solve this equation for ν and compute $\bar{\nu} = \nu_0$ and $\overline{\nu\cos\vartheta} = \nu_1/3$. We thus obtain for the two quantities ν_0 and ν_1 the two equations

$$\nu_0 = F_0\nu_0 w + \frac{1}{3}wF_1\nu_1 - \frac{1}{\sigma}\frac{w+1}{\xi}\nu_0 - \frac{\nu_1}{\sigma}w, \tag{15}$$

$$\frac{1}{3}\nu_1 = F_0\nu_0\xi w - \frac{1}{3}\left(\frac{1}{3} - \xi^2 w\right)F_1\nu_1 - \frac{w}{\sigma}\nu_0 - \frac{\xi w}{\sigma}\nu_1, \tag{16}$$

where

$$w = \frac{1}{2}\ln\frac{\xi+1}{\xi-1} - 1.$$

Solving Eqs. (15) and (16) simultaneously we obtain an equation which determines the complex sound velocity

$$\left(1 + \frac{1}{\xi\sigma}\right)\left(1 + \frac{F_1}{3}\right) - w\left\{\left(1 + \frac{F_1}{3}\right)\left(F_0 - \frac{1}{\xi\sigma}\right) + \xi^2\left(F_1 - \frac{3}{\xi\sigma}\right)\left(1 + \frac{1}{\xi\sigma}\right)\right\} = 0. \tag{17}$$

This is the desired equation expressing the dependence of the velocity of sound upon the frequency, or, in other words, describing the dispersion of sound in a Fermi liquid. Let us first consider the two limiting cases.

a) Low frequencies: $\omega\tau \ll 1$. In consequence, $\sigma \rightarrow 0$, $\xi\sigma \rightarrow -1$, $\xi \rightarrow \infty$. Expansion of the function w in powers of $1/\xi$ yields

---

*Here and below we indicate by a superscribed line a quantity averaged over angle.

†In this integration only the range of values for the momentum near p_0 are of importance, since in accordance with (5) the function n_1 includes a δ-function at $p = p_0$.

$$w = 1/3\xi^2 + 1/5\xi^4$$

and, after some simplification, Eq. (17) takes the form

$$\left(1 + \frac{1}{\xi\sigma}\right)^2 = \frac{1}{3\xi^2}\left(1 + \frac{F_1}{3}\right)\left(F_0 - \frac{1}{\xi\sigma}\right) + \frac{1}{5\xi^2}\left(1 + \frac{1}{\xi\sigma}\right)\left(F_1 - \frac{3}{\xi\sigma}\right). \tag{18}$$

From the relations (13) we have

$$\left(\frac{1 + \xi\sigma}{\sigma}\right)^2 = \left(\frac{\omega}{kv}\right)^2.$$

From (18) and (13) we find, to the first order in $i\omega\tau$

$$\left(\frac{\omega}{kv}\right)^2 = \frac{1}{3}(1 + F_0)\left(1 + \frac{F_1}{3}\right) - \frac{4}{15} i\omega\tau\left(1 + \frac{F_1}{3}\right). \tag{19}$$

The first term corresponds to the velocity of ordinary sound in a Fermi liquid. The attenuation of sound in the region $\omega\tau \ll 1$ is obtained in an elementary fashion from (19), as the imaginary component of the wave vector:

$$\gamma = \operatorname{Im} k = (2\omega^2\tau v^2 / 15c^3)(1 + F_1/3). \tag{20}$$

Comparing expressions (20) and (10) we set up the relation

$$\eta = {}^1/_5\, \rho\tau v^2 (1 + {}^1/_3 F_1), \tag{20′}$$

which eneables us to find the time τ from experimental values of the viscosity. At the present time data is lacking on the viscosity of He^3 at temperatures below the degeneracy temperature. There are available only preliminary data (by K. Zinov'eva) in the temperature region near the degeneracy temperature. From these data we obtain the very rough value

$$\tau \approx 0.4 \cdot 10^{-12}\, T^{-2} \text{ sec.}$$

With this we obtain for the attenuation coefficient

$$\gamma \sim 1 \cdot 10^{-18} (\omega/T)^2 \text{ cm}^{-1}.$$

b) We now consider the second limiting case of high frequencies and low temperatures: $\omega\tau \gg 1$. In this case

$$\sigma \to \infty, \quad \xi\sigma \to \infty, \quad \xi = s + i\xi', \quad |\xi'| \ll s,$$

Eq. (17) assumes the form

$$(1 + F_1/3) + w(s)\{(1 + F_1/3)F_0 + s^2 F_1\} = 0. \tag{21}$$

This equation agrees completely with the equation determing the velocity of zero sound [cf. Appendix, Eq. (A8)] $u_0 = sv$.

As regards the attenuation of zero sound, in order to calculate this it is necessary to find the imaginary component of the sound velocity ξ'. From (19) we obtain the equation

$$\xi'\left\{\frac{1}{w(s)}\left(1 + \frac{F_1}{3}\right)\left(\frac{s}{s^2 - 1} - \frac{w(s) + 1}{s}\right) - 2sw(s)F_1\right\} - \frac{1}{\omega\tau}\left\{\left(1 + \frac{F_1}{3}\right)(1 + w(s)) + w(s)s^2(3 - F_1)\right\} = 0. \tag{22}$$

With the aid of Eq. (13) we find the attentuation coefficient

$$\gamma = \operatorname{Im} k = 1/s\tau v - \omega\xi'/s^2 v. \tag{23}$$

If we substitute in this the values of the parameters for He^3 ($s = 1.84$, $v = 1.13 \times 10^4$ cm/sec) we obtain

$$\xi' = 1.5/\omega\tau, \quad \gamma = 2.2 \cdot 10^7 T^2 \text{ cm}^{-1}. \tag{24}$$

The attenuation of zero sound is thus independent of frequency and increases with increasing temperature as $1/\tau$; i.e., proportionately to T^2.

In conclusion, we shall comment upon the attenuation of sound in a Fermi liquid at extremely low temperatures, for which the inequality $\hbar\omega \gg kT$ holds. It is evident that in this region the classical treatment is inapplicable. The attenuation process must here be treated quantum-mechanically.

Detailed calculations performed by Landau[2] yield for the attenuation of sound in this limiting case the following results:

$$\gamma = \gamma_{cl}\,(1 + (\hbar\omega/2\pi kT)^2), \tag{25}$$

γ_{cl} is determined from Eq. (23). Since τT^2 = const., we have in the limit $\hbar\omega \gg kT$

$$\gamma \sim 10^{-15}\omega^2\ \mathrm{cm}^{-1}.$$

In the quantum region the attenuation of zero sound is independent of temperature and is proportional to the square of the frequency.

APPENDIX

The integral equation for the velocity of zero sound derived by Landau[2] has the following form:

$$(v\cos\theta - u)\,\nu(\theta, \varphi) + v\cos\theta \int F(\vartheta)\,\nu(\theta', \varphi')\,\frac{do'}{4\pi} = 0, \tag{A1}$$

$\vartheta = (\theta'\varphi', \theta\varphi)$. In Ref. 2 the solution of this equation is given for the case in which the function $F(\vartheta)$ is independent of the angle ϑ. We shall derive here the solution of Eq. (4) at $T = 0$ for an arbitrary function $F(\vartheta)$.

In the general case $F(\vartheta)$ can be represented as a sum of spherical harmonics

$$F(\vartheta) = \sum F_n P_n(\vartheta), \tag{A2}$$

Here the F_n are the coefficients in the expansion of $F(\vartheta)$ in Legendre polynomials. We substitute (A2) in (A1), using the addition theorem for Legendre polynomials

$$P_n(\vartheta) = \sum_{m=-n}^{n} P_n^m(\theta)\,P_n^m(\theta')\,e^{im(\varphi-\varphi')}\,(n-|m|)!\,/\,(n+|m|)!,$$

where $P_n^m = P_n^{-m}$ are the associated Legendre polynomials. After making the substitutions indicated above we obtain

$$(v\cos\theta - u)\,\nu + v\cos\theta \sum \frac{(n-|m|)!}{(n+|m|)!}\,P_n^m(\theta)\,F_n e^{im\varphi} \int P_n^m(\theta')\,\nu(\theta', \varphi')\,e^{-im\varphi'}\,\frac{do'}{4\pi} = 0. \tag{A3}$$

We introduce the notation

$$F_n \frac{(n-|m|)!}{(n+|m|)!} \int P_n^m(\theta')\,\nu(\theta', \varphi')\,e^{-im\varphi'}\,\frac{do'}{4\pi} = \Phi_{nm} \tag{A4}$$

and solve (A3) for ν $(s = u/v)$;

$$\nu = -\frac{\cos\theta}{\cos\theta - s} \sum \Phi_{nm}\,P_n^m(\theta)\,e^{im\varphi} \tag{A5}$$

Setting this expression into the relation (A4) and carrying out the integration over φ', we obtain

$$F_n \frac{(n-|m|)!}{(n+|m|)!} \int \sum_k P_n^m(\theta')\,\frac{\cos\theta'}{\cos\theta' - s}\,P_k^m(\theta')\,\frac{do'}{4\pi}\,\Phi_{km} = \sum_k \Phi_{km}\delta_{kn}. \tag{A6}$$

We have thus obtained a system of homogeneous equations determining the quantity Φ_{km}. This system is separated into independent subsystems corresponding to various values of m. It follows from Eq. (A6) that in a Fermi liquid at absolute zero there can be propagated oscillations of various types, distinguished basically by a differing dependence of amplitude upon the angle φ. To the value $m = 0$ there correspond oscillations for which ν is isotropic in the plane perpendicular to **k**. For $m \neq 0$ the oscillations are polarized in a definite manner in this plane. The number of types of oscillations is determined by the number of possible values of m $(|m| \leq n)$. The propagation velocity for the oscillations is determined from the condition that the determinant of the corresponding system be equal to zero:

$$|\delta_{kn} + F_n\Omega_{kn}^m(s)| = 0 \quad (N \geqslant n,\ k \geqslant |m|), \quad \Omega_{kn}^m(s) = \frac{(n-|m|)!}{(n+|m|)!} \int P_k^m(\theta')\,\frac{\cos\theta'}{\cos\theta' - s}\,P_n^m(\theta')\,\frac{do'}{4\pi}. \tag{A7}$$

In view of the fact that $P_n^m = P_n^{-m}$ the coefficients Ω_{kn}^m are independent of the sign of m, so that oscillations differing in the sign of m are propagated with the same velocity.

From (A7) it is evident that the equations for the velocity are transcendental. In the general case they do not always posses real roots. Cases are possible, however, in which there are some real roots. These correspond to certain types of oscillations having identical polarization in the plane perpendicular to **k**.

We shall consider as an example the case for which the function F (ϑ) includes only the zero and first harmonic [Eq. (9)]. Here the coefficients Ω_{kn}^m are

$$\Omega_{00}^0 = \frac{1}{2}\int_{-1}^{1} \frac{x\,dx}{x-s} = 1 - \frac{s}{2}\ln\frac{s+1}{s-1} = -w; \quad \Omega_{10}^0 = \Omega_{01}^0 = \frac{1}{2}\int_{-1}^{1}\frac{x^2dx}{x-s} = -sw,$$

$$\Omega_{11}^0 = \frac{1}{2}\int_{-1}^{1}\frac{x^3dx}{x-s} = \frac{1}{3} - s^2w, \quad \Omega_{11}^1 = \frac{1}{4}\int_{-1}^{1}\frac{(1-x^2)\,x\,dx}{x-s} = \frac{1}{2}\left[(s^2-1)\,w - \frac{1}{3}\right].$$

For the velocity of propagation of oscillations of the type m = 0 we obtain, after substitution into the determinant (A7), the equation

$$w = \frac{1+F_1/3}{F_0 + F_0F_1/3 + F_1s^2}. \tag{A8}$$

For the case m = 1 we obtain the equation

$$w = (F_1 - 6)/3F_1(s^2 - 1). \tag{A9}$$

This equation has one real root for $F_1 > 6$.

We shall now conclude with the application of these formulas to the case of liquid He^3. We do not possess any extensive information concerning the function F (ϑ); knowing the effective mass and the compressibility, however, we can determine $\overline{F}$ and $\overline{F\cos\vartheta}$ from Eqs. (7) and (8) of the text. It is therefore reasonable to confine ourselves to the approximation (9) for F. It follows from the temperature dependence of the entropy, in accordance with Ref. 6, that

$$m^* = 1.43m\,(\mathrm{He}^3).$$

Data on the compressibility yield c = 195 m/sec. From this we find $F_0 = 5.2$ and $F_1 = 1.3$. Using these values it follows that to the oscillations of the type m = 0 there corresponds the single velocity (the root of Eq. (A8))

$$s = u/v = 1.84, \quad u = 206 \text{ m/sec}.$$

Oscillations of the type m = 1 are absent (as are all those for m > 1). It is of course possible that this result is due to the crudity of the approximation we have chosen for F (ϑ), but we see no reason to draw such a conclusion.

From Eqs. (A8) and (8) we can obtain for the velocity of sound c the following approximation relation characterizing the width of the region of dispersion:

$$(u-c)/c \approx 2/5\,(F_0+1).$$

For the case of He^3 the width of this region is on the order of 10 m/sec for a velocity c ~ 200 m/sec.

In conclusion the authors wish to express their gratitude to L. D. Landau for numerous discussions.

---

[1] L. D. Landau, J. Exptl. Theoret. Phys. (U.S.S.R.) 30, 1058 (1956), Soviet Phys. JETP 3, 920 (1957).

[2] L. D. Landau, J. Exptl. Theoret. Phys. (U.S.S.R.) 32, 59 (1957), Soviet Phys. JETP 5, 101 (1957).

[3] L. D. Landau and E. M. Lifshitz, Mechanics of Continuous Media; GTTI, 1953.

[4] A. Abrikosov and I. Khalatnikov, J. Exptl. Theoret. Phys. (U.S.S.R.) 32, 1083 (1957); Soviet Phys. JETP 5, 887 (1957).

[5] I. Ia Pomeranchuk, J. Exptl. Theoret. Phys. (U.S.S.R.) 20, 919 (1950).

[6] Abraham, Osborne, and Weinstock, Phys. Rev. 98, 551 (1955).

[7] G. K. Walters and W. M. Fairbank, Phys. Rev. 103, 263 (1956).

Translated by S. D. Elliott

SOVIET PHYSICS JETP VOLUME 6, NUMBER 1 JANUARY, 1958

FLOW INSTABILITY OF A SUPERFLUID FILM

R. G. ARKHIPOV

Institute for Physical Problems, Academy of Sciences, U.S.S.R.

Submitted to JETP editor December 12, 1956

J. Exptl. Theoret. Phys. (U.S.S.R.) 33, 116-123 (July, 1957)

Instability of flow of a superfluid film with respect to the appearance of wave motion on its surface is shown to be theoretically possible. The value obtained for the critical velocity is appreciably greater than the experimental value. The problem of the shape of a He II film moving in a gravitational field has been solved by taking into consideration hydrodynamic forces, surface tension and Van der Waals forces.

THE phenomenon of superfluidity, discovered by Kapitza[1] in 1938, received its interpretation in the subsequent development by Landau[2] of a two fluid model of the quantum liquid. Landau derived the hydrodynamic equations of He II by starting out from the conservation laws. Later, Khalatnikov[3] obtained them from the Boltzmann equation for the excitation. It was established experimentally that the superfluidity is destroyed at sufficiently small velocities of flow. This should be connected with the instability of flow of the liquid with respect to the appearance of a different type of excitation. Unfortunately, it is not possible to investigate the appearance of instability in the general case and we must consider each specific type of excitation separately. Thus, it is necessary that the flow velocity exceed the sound velocity for the appearance of an individual phonon, while for the appearance of a roton it need exceed the quantity Δ/p_0 ~ 60 m/sec. These values are appreciably larger than the real critical velocities. Actually, it is evident that the destruction of superfluidity is connected with the appearance in the liquid of vortex filaments of the Onsager type, as was shown by Feynman.[4] However, a quantitative criterion for the loss of stability can be obtained only for the case of the rotation of a cylinder in the superfluid.*

---

* Consider the following simple calculations. A single vortex creates a velocity distribution $v_s = \hbar/mr$ in the superfluid component. The corresponding kinetic energy per unit length is

$$\int \rho_s \frac{v_s^2}{2} 2\pi r dr = \pi\rho_s \frac{\hbar^2}{m^2} \ln \frac{R}{a_0}$$

and the momentum per unit length

$$\int \rho_s v_s r \cdot 2\pi r\, dr = \pi\rho_s \frac{\hbar}{m} R^2$$

(m is the atomic mass of helium, R the radius of the vessel, and a_0 the distance between atoms). The part of the free energy per unit length of a column of fluid depending on Ω is

$$F = \frac{1}{4}\rho_n \pi R^4 \Omega^2 + \frac{I\Omega^2}{2} + \pi\rho_s \frac{\hbar^2}{m^2} \ln \frac{R}{a_0},$$

while its momentum is

$$M = \frac{1}{2}\rho_n \pi R^4 \Omega + I\Omega + \pi\rho_s \frac{\hbar}{m} R^2$$

(I is the moment of inertia of the vessel). In the state of thermodynamic equilibrium, the following quantity must have a minimum:

$$F - M\Omega = -\frac{1}{4}\rho_n \pi R^4 \Omega^2 - \frac{I\Omega^2}{2} + \pi\rho_s \frac{\hbar}{m}\left(\frac{\hbar}{m} \ln \frac{R}{a_0} - \Omega R^2\right).$$

Formation of the first vortex is favorable when the last term becomes negative, whence

$$R^2\Omega_{\text{cr}} = \frac{\hbar}{m} \ln \frac{R}{a_0}.$$

Extension of the formula for the rotation of a cylinder to an estimate of the critical velocity in the case of a slit of a film gives excellent order-of-magnitude agreement with experiment. In the present paper we consider one additional mechanism: the loss of stability in superfluid flow in a film, brought about by the appearance of an unusual vibration, and the transition of the flow to the wave regime reminiscent of the studies of Kapitza.[5] The phenomenon is analogous to the instability of a tangential disturbance.[6,6a] It reduces to the dissipation of energy in the normal component and to the appearance of a damping force. Although the values of the critical velocity computed in this way considerably exceed the experimental, consideration of the problem presents methodological interest. Moreover, there is the hope of isolating the mechanism experimentally, about which more will be said below.

We consider an incompressible superfluid which forms a layer of thickness h on the surface of a solid wall. As the unperturbed motion, we take $v_s^0 = U = \text{const}$, $v_n^0 = 0$ and look for a first approximation in the form of a traveling wave $e^{ikz - i\omega t}$. We draw the x axis perpendicular to the surface and consider $x = -h$ the bounding coordinate between solid and liquid. For the incompressible fluid, as is well known,[2] we can write the equations for the normal and superfluid components separately; for the normal component it suffices to use a linearized equation. The system of equations for superfluid hydrodynamics can be written in the following form:

$$\mathbf{v}_s = \nabla\varphi, \Delta\varphi = 0, \quad \partial \mathbf{v}_n / \partial t = \nu \Delta \mathbf{v}_n - (1/\rho_n) \nabla p_n, \ \operatorname{div} \mathbf{v}_n = 0. \tag{1}$$

Here $p = p_n + p_s$ is the total pressure, $p_s = -\rho_s \partial\varphi/\partial t - \rho_s v_s^2/2$, $\eta = \rho_n \nu$ is the viscosity of He II.

The solutions satisfying the boundary conditions

$$v_{nx} = v_{nz} = 0, \ v_{sx} = \partial\varphi/\partial x = 0 \ \text{for} \ x = -h,$$

have the form

$$\begin{aligned} &\varphi = a e^{i(kz - \omega t)} \cosh k(x+h) + yU_y + zU_z, \\ &v_{nz} = e^{i(kz-\omega t)} \left\{ A \left[\sinh k(x+h) - \frac{m}{k} \sinh m(x+h)\right] + B\left[\cosh k(x+h) - \cosh m(x+h)\right] \right\}, \\ &v_{nx} = e^{i(kz-\omega t)} \left\{ -iA\left[\cosh k(x+h) - \cosh m(x+h)\right] - iB\left[\sinh k(x+h) - \frac{k}{m}\sinh m(x+h)\right] \right\}, \\ &p_n = \rho_n \frac{\omega}{k} e^{i(kz-\omega t)} \left[A \sinh k(x+h) + A \cosh k(x+h)\right]; \quad m^2 = k^2 - \frac{i\omega}{\nu}. \end{aligned} \tag{2}$$

We now introduce the quantity

$$\xi = b e^{i(kz - \omega t)}, \tag{3}$$

which describes the vibration of the boundary, and write down a set of boundary conditions at the free surface (for $x = 0$). For simplicity, we shall not consider the effect of the vapor.

The rate of change of the x coordinate of the surface is equal to the velocity v_{nx} of the normal component:

$$\partial\xi / \partial t = v_{nx} \tag{4}$$

and, on the other hand, can be expressed by means of the velocity of the superfluid component

$$\frac{\partial\xi}{\partial t} = \frac{\partial\varphi}{\partial x} - U_z \frac{\partial\xi}{\partial z} - U_y \frac{\partial\xi}{\partial y} = \frac{\partial\varphi}{\partial x} - U_z \frac{\partial\xi}{\partial z}, \quad \text{since} \ \frac{\partial\xi}{\partial y} = 0. \tag{5}$$

Moreover, the component σ_{xz} of the momentum flux tensor should be equal to zero on the surface, whence

$$\eta\,(\partial v_{nz} / \partial x + \partial v_{nx} / \partial z) = 0. \tag{6}$$

Finally, the latter condition expresses the equality σ_{xx} with the total force acting on the liquid. After linearization, we have

$$\rho_s \frac{\partial\varphi}{\partial t} + \rho_s U_z \left(\frac{\partial\varphi}{\partial z} - U_z\right) - p_n + \rho\gamma\xi - \alpha \frac{\partial^2\xi}{\partial z^2} + 2\rho_n \nu \frac{\partial v_{nx}}{\partial x} = 0. \tag{7}$$

Here α is the surface tension, the first two terms correspond to the pressure of the superfluid, while the term $\rho\gamma\xi$ corresponds to the force which is connected with the Van der Waals interaction of the film with the substratum.* We note that only the U_z component of the velocity is involved, and will therefore put everywhere $U = U_z$.

Upon substitution of the solutions (2) (3) in the four conditions (4) to (7), we get a system of four homogeneous linear equations, which can be solved if their determinant vanishes. After evaluation of the determinant and rather lengthy transformations, we get an equation for ω:

$$\omega^2 - 2\frac{\rho_s}{\rho}Uk\omega - k^2\left[\left(\frac{\gamma}{k}+\frac{\alpha k}{\rho}\right)\tanh kh - \frac{\rho_s}{\rho}U^2\right] = -\frac{\rho_n}{\rho}\omega^2\left[\frac{k}{m}\frac{\tanh mh}{\sinh kh\cosh kh} + 4i\frac{\nu k^2}{\omega}\left(1-2\frac{k}{m}\tanh kh\tanh mh - \frac{1}{\cosh kh\cosh mh}\right)\right.$$
$$\left.-8\frac{\nu^2k^4}{\omega^2}\left(1-\frac{k}{m}\tanh kh\tanh mh - \frac{1}{\cosh kh\cosh mh}\right)\right]\Big/\left[1-(k/m)\coth kh\tanh mh\right]. \tag{8}$$

Even if only one of the roots ω of this equation has a positive imaginary part, the motion will be unstable. For the investigation of Eq. (8) we call attention to the fact that when the square bracket on the left side is equal to zero, then the equation certainly has the root $\omega = 0$. In order to establish this fact, we expand the numerator and replace the right hand side by $m^2 - k^2 = i\omega/\nu$. Neglecting terms $\sim \omega^2$, we get

$$2\frac{\rho_s}{\rho}Uk\omega + k^2\left[\left(\frac{\gamma}{k}+\frac{\alpha k}{\rho}\right)\tanh kh - \frac{\rho_s}{\rho}U^2\right] = -2i\frac{\rho_n}{\rho}\nu k^2\omega\,\frac{1+k^2h^2/\cosh^2 kh}{1-2kh/\sinh 2kh},$$

$$\omega = k^2\,\frac{\frac{\rho}{\rho_s}\left(\frac{\gamma}{k}+\frac{\alpha k}{\rho}\right)\tanh kh - U^2}{2i\frac{\rho_n}{\rho_s}\nu k^2\left(1+\frac{k^2h^2}{\cosh^2 kh}\right)\Big/\left(1-\frac{2kh}{\sinh 2kh}\right) - 2Uk}. \tag{9}$$

It is evident from the last equation, in particular, that if

$$U^2 \geqslant \min\frac{\rho}{\rho_s}\left(\frac{\gamma}{k}+\frac{\alpha k}{\rho}\right)\tanh kh, \tag{10}$$

then there always exists a region k where $\operatorname{Im}\omega > 0$ and, consequently, the motion is unstable. Investigation of the expansion of the right side of Eq. (8) under the limiting conditions $\nu k^2/\omega \ll 1$ and $\nu k^2/\omega \gg 1$ shows that the inequality (10) is not only a sufficient but is evidently a necessary condition of instability.

We can put the condition (10) in parametric form in terms of k, which corresponds to the minimum $U^2(k)$. Replacing the velocity by the volume flow $Q = \rho_S Uh/\rho$, and expressing γ in terms of a and h, we get the following expression for the transfer rate

$$Q^2 = \frac{\rho_s}{\rho}\left(\frac{3a}{kh^2}+\frac{\alpha kh^2}{\rho}\right)\tanh kh, \tag{11}$$

where k is determined from the condition

$$\frac{\sinh 2kh}{2kh} = \left(1+\frac{\alpha k^2h^4}{3a\rho}\right)\Big/\left(1-\frac{\alpha k^2h^4}{3a\rho}\right), \tag{12}$$

which expresses $\partial U^2/\partial k = 0$. Expanding Eq. (12) in a series, we can see that for $h > (a\rho/\alpha)^{1/2}$, Eq. (12) has only $k = 0$ as a root.

In this case the transfer rate is expressed by the formula

$$Q = (3a\rho_s/h\rho)^{1/2}.$$

For $h = (a\rho/\alpha)^{1/2}$, a root $k = 0$ appears, which quickly increases with increasing h. For sufficiently small h, $kh \gg 1$, and we can determine k by letting the denominator of the right side of Eq. (12) vanish; this yields:

$$kh^2 = (3a\rho/\alpha)^{1/2}.$$

In this case the discharge tends to the h-independent value

$$Q = (\rho_s/\rho)^{1/2}(12a\alpha/\rho)^{1/4}.$$

---

* The thickness-dependent part of the chemical potential of the film is known from Ref. 7 to be $-am/h^3$ while the pressure is $(3am/h^4)(\rho/m)\xi$, where $\xi = \delta h$. Thus $\gamma = 3a/h^4$ ($a \sim 10^{-15}$ is connected with the thickness of the static film by the relation $gz = a/h^3$).

A plot of Q^2 vs. h is shown in Fig. 1.

For a complete solution of the problem we must solve simultaneously the equations (11) and (12) for the transfer rate and the equation for shape of the film in a gravitational field with account of the Van der Waals forces, the forces of surface tension, and the hydrodynamic pressure acting on it. In the case of stationary flow of the superfluid, we have, from the equation of Ref. 2

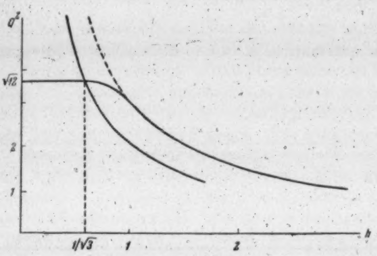

FIG. 1. Broken line shows the dependence of Q^2 [in units of $(\rho_s/\rho)(a\alpha/\rho)^{1/2}$] on h [in units of $(a\rho/\alpha)^{1/2}$]. The point of intersection of this curve with the curve of (19) determines the critical thickness and transfer rate in the film.

$$\partial v_s/\partial t + \nabla(\mu + v_s^2/2) = 0$$

the relation $\mu + u_s^2/2 = \text{const}$ on the free surface. Eliminating the velocity dependence from the chemical potential μ, the gravitational forces, Van der Waals forces[7] and the surface tension, we get an equation which determines the form of the film:

$$\frac{\rho_s}{\rho}\frac{v_s^2}{2} + gz - \frac{a}{h^3} - \frac{\alpha}{\rho}\frac{d^2h}{dz^2}\left[1 + \left(\frac{dh}{dz}\right)^2\right]^{-3/2} = 0. \tag{13}$$

The constant here is so chosen that, upon neglect of the Van der Waals forces and the hydrodynamical term, we get an equation for the capillary meniscus, wherein measurement of the height is taken from the horizontal surface of the liquid. In a region located at a sufficient distance from the "bounding" meniscus,

$$z_0 = (2\alpha/\rho g)^{1/2},$$

and the form of the film is described by the equation of the capillary meniscus[6b]

$$h = \left(\frac{\alpha}{\rho g}\right)^{1/2}\left[\left(\cosh^{-1}\left(\frac{2}{z}\left(\frac{\alpha}{\rho g}\right)^{1/2}\right) - \cosh^{-1}\sqrt{2}\right) - 2\left(\sqrt{1 - \frac{z^2\rho g}{4\alpha}} - \frac{1}{\sqrt{2}}\right)\right] \tag{14}$$

At heights much greater than z_0 we can neglect the effect of the surface tension; moreover, taking it into account that dh/dz is very small in this region, we can express v_s on the surface in terms of the discharge $Q = \rho_s v_s h/\rho$. We then obtain an equation describing the shape of the film in this region:

$$z = g^{-1}(a/h^3 - \rho Q^2/2\rho_s h^2). \tag{15}$$

We can see from the shape that the thickness of the film decreases upon increase in the discharge. This result was obtained by Kontorovich.[8]

At points close to the boundary of the static meniscus, $|z - z_0| \ll z_0$, we can consider approximately that $gz = gz_0$ in Eq. (13). Moreover, the value of the derivative dh/dz is sufficiently small that we can neglect it in the term with the surface tension, and express v_s in terms of the discharge. As a result, we get the following equation for the solution of the combination of Eqs. (14) and (15):

$$\frac{\alpha}{\rho}\frac{d^2h}{dz^2} = \left(\frac{2\alpha g}{\rho}\right)^{1/2} - \frac{a}{h^3} + \frac{\rho Q^2}{2\rho_s h^2}, \tag{16}$$

which does not contain z and which can therefore be integrated by successive quadratures. The result

$$z + C_2 = -\int^{h} dh\left\{2h\left(\frac{2\rho g}{\alpha}\right)^{1/2} + \frac{\rho}{\alpha}\frac{a}{h^2} - \frac{\rho^2Q^2}{\rho_s\alpha h} + C_1\right\}^{-1/2} \tag{17}$$

depends on two constants of integration, by the choice of which we can join the upper and lower solutions. Here we have a large parameter $A \sim 10^4$, which has the meaning of the ratio of the capillary constant z_0 to the thickness of the film at the height of the boundary of the capillary meniscus $H_0 = (a/gz_0)^{1/2}$. Consideration of conditions of continuity of z and dh/dz (written in non-dimensional form) at the point h_0 of the junction of the solution of (17) with the solution of (15) shows that for arbitrarily large A, the following conditions must be satisfied:

$$2h_0(2\rho g/\alpha)^{1/2} + \rho a/\alpha h_0^2 - \rho^2Q^2/\rho_s\alpha h_0 + C_1 = 0, \tag{18}$$

$$(2\rho g/\alpha)^{1/2} - \rho a/\alpha h_0^3 + \rho^2Q^2/2\rho_s\alpha h_0^2 = 0. \tag{19}$$

In these conditions there appears the parameter h_0, which is determined by the discharge Q [from Eq. (19)] and which is a multiple root of the expression found under the radical in the integral in (17). In the case of a multiple root, the integral is written in terms of elementary functions, which gives

$$z = z_0 - \sqrt{z_0 h + \frac{a}{2gh_0^2} + h_0^2}\left(\frac{a\rho}{\alpha} + \frac{4h_0^3}{z_0}\right)^{-1/2} \cos^{-1} \frac{h + h_0 + a/gz_0h_0^2}{h - h_0} \qquad (20)$$

Joining of the solution in the region of the meniscus is done automatically; this is demonstrated by expanding Eq. (14) near z_0, giving the formula

$$h = (z - z_0)^2/z_0,$$

which coincides with that in (20) for $z_0 \gg h \gg h_0$ and $h_0 \gg (a\rho/\alpha)^{1/2}$. A graph of the function (2), which describes the shape of the surface, is given in Fig. 2.

The condition for stability can now be written in the form

$$f(h) - Q^2 > 0,$$

where f(h) is determined by Eqs. (11) and (12). Increase in the flow Q brings about a change in the function at the left side, for the condition of stability, by an amount

$$\left[\frac{df}{dh}\left(\frac{\partial h}{dQ^2}\right)_z - 1\right]\delta Q^2;$$

df/dh is always negative, since f is a monotonically decreasing function of h: $(\partial h/\partial Q^2)_z$ is also always negative, inasmuch as the thickness of the film decreases with increase in its velocity. As calculations with Eqs. (15) and (20) show, the minimum value of $(df/dh)(\partial h/\partial Q^2)_z$ is assumed at h_0, where the first condition of stability for growth of the discharge is disturbed. Simultaneous solution of the equation for h_0 (19) and the discharge [Eqs. (11) and (12)] gives, with considerable accuracy,

$$h_0 = (a\rho/3\alpha)^{1/2}, \qquad (21)$$

$$Q^2 = (\rho_s/\rho)(12a\alpha/\rho)^{1/2}; \qquad (22)$$

here $kh \sim 3$ and the error in Eqs. (21) and (22) is of the order $e^{-6} \sim 1/400$. For the value of $h_0 = (a\rho/3\alpha)^{1/2}$ that is obtained, the solution (20) is already unsuitable, for in this case the derivative

$$\frac{dh}{dz} = -\frac{h - h_0}{h}\sqrt{\frac{4h}{z_0} + \frac{a\rho}{\alpha h_0}}$$

is of the order of unity in a very small region $h \sim h_0$. This comes about as a result of the strong hydrodynamic compression of the film at large discharges Q. As a result, the meniscus disappears and the film should have a constant thickness h_0 along almost the entire height. An exact determination of the shape of the film under these conditions is extremely difficult, since, in addition to calculation of dh/dz in the capillary term of Eq. (13), we would also be obliged to solve it simultaneously with the equation for the potential flow of the superfluid component, in view of the fact that the velocity v_s on the free surface is no longer expressed in simple form in terms of the discharge. However, we can consider that this difficulty does not lessen the value of Eq. (22) for the transfer rate. Let us estimate the damping forces which arise in the presence of a developed wave regime. We shall consider that for $U \sim 2U_{cr}$, the amplitude of the waves on the surface is of the order of the thickness of the layer. Assuming that in order of magnitude $h\,dp/dz \sim \sigma_{xz}$; $\sigma_{yz} \sim \eta v_m/h$; $v_n \sim \omega h$, we get $h\,dp/dz \sim \rho_n \nu \omega$; we can estimate ω from Eq. (9):

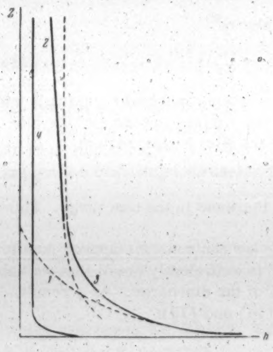

FIG. 2. Curve 1 corresponds to the shape of the capillary meniscus [Eq. (14)]. Curve 2 corresponds to Eq. (15). Curve 3 is the joined solution (20) (Q = 0). Curve 4 corresponds to the shape of the film for large discharges (22), when the meniscus disappears.

$$\omega \sim (U_{cr}^2 - U^2)/(\rho_n/\rho_s)\nu.$$

As a result we obtain

$$\frac{dp}{dz} \sim \frac{\rho_s U^2}{h} \approx \rho \frac{\rho}{\rho_s} \frac{Q^2}{h^3} \approx \rho \frac{(a\alpha/\rho)^{1/2}}{(a\rho/\alpha)^{1/2}} = \frac{\rho}{a}\left(\frac{\alpha}{\rho}\right)^2.$$

The ratio of this quantity to the actual hydrostatic pressure is of the order

$$(\alpha/\rho)^2/ag \sim 10^{12},$$

i.e., loss of stability carries an extraordinary rigid character, and the value of the critical discharge is very close to Eq. (22).

Many measurements of the phenomenon of helium transfer along a film are described in the literature.[9,10] These give approximately the same temperature dependence of the volume discharge Q. They show that this dependence can be represented, within the limits of error, as ρ_s/ρ or $(\rho_s/\rho)^{1/2}$, wherein the first formula describes the experimental data somewhat better.

Equation (22) gives the temperature dependence of the discharge proportional to $(\rho_s/\rho)^{1/2}$, which does not contradict the experimental data. However, if we calculate a by the formula $gz = a/h^3$, considering that at $z = 1$ cm the thickness of the film $h \sim 2.0 \times 10^{-6}$ cm[11], we obtain $a \sim 8 \times 10^{15}$ and when the value $\alpha = 0.35$, measured along the rise in the capillary,[12] and $\rho = 0.145$ are substituted in the formula, we get for the discharge $Q \cong 6.9 \times 10^{-4}$ cm^2/sec, which is considerably larger than the experimentally observed value 1.7×10^{-4} cm^2/sec. The corresponding critical thickness of the film is of the order of atomic dimensions: $h \sim 3.4 \times 10^{-8}$ cm, and is extraordinarily small. The thickness of the film was measured simultaneously with the flow only in a single work,[13] in which $Q = 1.68 \times 10^{-4}$ cm^2/sec, and $h = 1.66 \times 10^{-6}$ cm for $T = 1.5°$.

The value of the thickness differs sharply from what has been expected; this points evidently to the action of a mechansim of destruction of the superfluidity, different from the described formation of a vortex. However, the effect of flow on the thickness of the film should be carefully noted, since the film ought to experience considerable hydrodynamic compression. An increase in the thickness of the flowing film of about 20% has already been observed by Burge and Jackson.[14]

In conclusion, we note that there is reason for assuming that if the formation of vortices is due to the destruction of superfluidity, then we can expect that this process requires an appreciable time (in the experiments of Hall and Vinen[15] vortices were formed within a time on the order of a minute).

In this case the mechanism just described takes place, yielding a much higher value of the discharge. According to our calculations, the capillary meniscus ought to disappear during the time of action of this mechanism. Also, during this time vortices evolve in the film and the discharge is established. The shape of the film will be described by Eqs. (15), (20), and (14) at all regions of height.

I regard it as my pleasant duty to express my deep gratitude to L. D. Landau and I. M. Khalatinkov for constant discussions on the work and for valuable advice.

---

[1] P. L. Kapitza, Dokl. Akad. Nauk SSSR 18, 21 (1938).

[2] L. D. Landau, J. Exptl. Theoret. Phys. (U.S.S.R.) 11, 592 (1941); J. Phys. (U.S.S.R.) 8, 1 (1944).

[3] I. M. Khalatnikov, J. Exptl. Theoret. Phys. (U.S.S.R.) 23, 8 (1952).

[4] R. P. Feynman, Progress in Low Temperature Physics 1, p. 17 (Amsterdam, 1955); L. Onsager, Nuovo cimento, 6 Suppl. 2, 279 (1949).

[5] P. L. Kapitza, J. Exptl. Theoret. Phys. (U.S.S.R.) 18, 3 (1948).

[6] L. D. Landau and I. M. Lifshitz, Механика сплошных сред, (Mechanics of Continuous Media), (2nd ed., Moscow, 1954); (a) Problem 3 in Sec. 61; (b) Problem 2 in Sec. 60.

[7] L. D. Landau and I. M. Lifshitz, Статистическая физика (Statistical Physics), (2nd ed., Moscow, 1951), p. 467.

[8] V. M. Kontorovich, J. Exptl. Theoret. Phys. (U.S.S.R.) 30, 805 (1956); Soviet Phys. JETP 3, 770 (1956).

[9] D. G. Daunt and R. F. Smith, Revs. Mod. Phys. 26, 172 (1954).

[10] V. Smith and H. A. Boorse, Phys. Rev. 99, 367 (1955); R. K. Waring, Jr., Phys. Rev. 99, 1704 (1955).

[11] L. C. Jackson and E. J. Burge, Nature 164, 660 (1949).

[12] Y. F. Allen and A. D. Misener, Proc. Camb. Phil. Soc. 34, 299 (1938).

[13] L. C. Jackson and D. G. Heshaw, Phil. Mag. 41, 1081 (1950).

[14] E. U. Burge and L. C. Jackson, Proc. Roy. Soc. (London) A 205, 270 (1951).
[15] H. E. Hall and W. F. Viven, Conference de Physique des basses temperatures, (Paris, 1955), p. 22.

Translated by R. T. Beyer
17

SOVIET PHYSICS JETP VOLUME 6, NUMBER 1 JANUARY, 1958

MANY-PHONON PROCESSES IN CRYSTALS

V. F. TURCHIN

Submitted to JETP editor December 12, 1956

J. Exptl. Theoret. Phys. (U.S.S.R.) 33, 124-131 (July, 1957)

We have calculated the differential cross section for the inelastic scattering of a neutron by a crystal with either emission or absorption of an arbitrary number of phonons. The first case is of interest when the temperature of the crystal is low, and the second when the neutron energy is very small and the crystal temperature sufficiently high. Formulae are obtained for crystals with an arbitrary spectrum of the normal vibrations. If we choose a specific spectrum, the calculations can be pursued to the end, leading to a simple final formula. We have also given the formula for the limiting case of the scattering of high energy neutrons by a free nucleus.

1. INTRODUCTION

To investigate the interaction of slow neutrons with crystalline substances, one uses the Debye model of a crystal. In that case the transfer of energy from the neutron to the crystal is treated as the excitation of one or several "phonons," that is, quanta of the thermal motion of the crystal. The transfer of energy from the crystal to the neutron corresponds to the absorption of phonons by the neutron. These processes have often been considered in the literature. Weinstock[1] derived formulae for the effective cross section for elastic and inelastic neutron scattering with the emission or absorption of one phonon (one-phonon process). The evaluation of processes involving simultaneously the emission and absorption of several phonons is in principle not difficult, but in practice very cumbersome.

Squires[2] in calculating the cross section for scattering of slow neutrons by Mg and Ni considered terms d_{mn} corresponding to processes where m phonons are emitted and n phonons absorbed. For $m + n \geq 2$ he did not take into account the interference between the waves scattered coherently from different atoms. Squires' calculations agree well with his own experiments. The neutron energy in those experiments was very small ($\lesssim 0.003$ ev), and it was therefore sufficient for the author to calculate several terms with the smallest values of m and n. In those cases where the number of phonons involved in the scattering can be large, the number of terms d_{mn} contributing to the cross section also becomes large; it becomes therefore impossible to evaluate the cross section by evaluating every term separately, as was done by Squires, and it is necessary to develop a method for summing the terms d_{mn}.

In the present paper we calculate the cross section for inelastic neutron scattering by evaluating only processes of identical character: either only emission, or only absorption of an aribrary number of phonons. In Squires' notation this corresponds to $\sum_{m=1}^{\infty} d_{m0}$ and $\sum_{n=1}^{\infty} d_{0n}$. Interference is not considered. The formulae obtained have practical value in two cases.

1. The case of low crystal temperatures and sufficiently large neutron energies. In this case absorp-

tion of phonons is unlikely, so that Σd_{m0} will give the total scattering cross section. (If the temperature of the crystal is not very low, one can evaluate from Weinstock's formula the cross section d_{01} for scattering involving the absorption of one phonon.) Furthermore, if the neutron energy is sufficiently large so that several Miller planes are involved in the inelastic scattering, interference can be neglected (we are dealing with polycrystalline matter). However, the formulae have an exact meaning, independent of the number of Miller planes involved; namely, if we take instead of $\overline{a^2}$ the amplitude of the incoherent scattering, $\overline{a^2} - (\overline{a})^2$, we obtain the incoherent part of the scattering of the neutron by the crystal. As the ratio E/Θ (Θ is the Debye temperature in energy units) tends to infinity, we find, as was to be expected, the formulae for the scattering of a neutron by a free nucleus.

2. The case of low neutron energies and sufficiently high crystal temperatures. In this case it is very unlikely that the neutron will lose energy; if the neutron wave length exceeds some critical value, the coherent part of elastic and inelastic scattering, involving loss of energy, will in general tend to zero, so that the sum Σd_{0n} will give the total inelastic scattering cross section. As regards interference, several Miller planes will be involved in the majority of substances even for zero neutron energy and the absorption of one phonon by the neutron.[3] The number of planes involved increases rapidly with increasing number of absorbed phonons and increasing neutron energy.* Interference is thus of no consequence for practically important cases.

2. DERIVATION OF THE GENERAL FORMULAE

Since the theory of the scattering of slow neutrons by a crystal is well known (see, for instance, Refs. 1, 4, 5) we shall not discuss in detail the basic principles, but only remind our readers of them, and also explain the notation.

The scattering is considered in Born approximation; for the interaction between the neutron and the crystal we take the potential

$$V = \sum_{\mathbf{R}} \alpha_{\mathbf{R}} \delta(\mathbf{r} - \mathbf{R}). \tag{1}$$

where $\mathbf{r}$ is the position of the neutron and $\mathbf{R}$ that of the nucleus,

$$\alpha_{\mathbf{R}} = (2\pi h^2 / m)(1 + m / M_{\mathbf{R}}) a_{\mathbf{R}}, \tag{2}$$

where m is the neutron mass, $M_{\mathbf{R}}$ the mass of the nucleus at the position $\mathbf{R}$, and $a_{\mathbf{R}}$ the scattering amplitude (depending in general on the nuclear spin). The sum is taken over all nuclei in the crystal.

As far as we are interested in the average cross section of scattering by one nucleus, assuming no interference to be present, we must leave in the sum (1) only one term corresponding to the interaction with the given nucleus $\mathbf{R} = \mathbf{R}_0$, and replace $\alpha_{\mathbf{R}}$ by α, defined by the equation $|\alpha|^2 = \overline{|\alpha_{\mathbf{R}}|^2}$, where the average is taken over the nuclei of the lattice and their spins,

$$V = \alpha\delta(\mathbf{r} - \mathbf{R}); \tag{1a}$$

Considering a crystal consisting of identical atoms of mass M and taking for M the average mass of the isotopes, one can easily obtain in Born approximation a formula for the differential cross section (with respect to angle and energy) for the scattering by one nucleus,

$$\frac{d^2\sigma}{d\Omega dE} = \frac{k}{k_0} (\overline{a^2}) \left(1 + \frac{m}{M}\right)^2 \sum_{\tau} |F_{\tau\tau_0}|^2 \delta(E_\tau + E - E_{\tau_0} - E_0), \tag{3}$$

where $\mathbf{k}_0$, E_0, $\mathbf{k}$, and E are the wave vectors and energies of the neutron before and after scattering, τ_0 and τ the initial and final state of the crystal, and E_{τ_0} and E_τ the corresponding energies; $F_{\tau\tau_0}$ is the matrix element of the operator

$$F \equiv \exp\{i(\mathbf{k}_0 - \mathbf{k})\cdot\mathbf{R}_0\}, \tag{4}$$

and $\overline{a^2}$ the square of the scattering amplitude averaged over the different isotopes and over the spins.

---

* For instance, for neutrons of wavelength 10.5 A and scattering, involving one phonon by magnesium this number is 106 (Ref. 2).

We shall consider a crystal with a simple lattice and neglect the difference in mass of the various isotopes. We shall go over to the normal coordinates of the crystal using the equations

$$\mathbf{R} - \boldsymbol{\rho} \equiv \mathbf{u}_\rho = \left(\frac{2}{N}\right)^{1/2} \sum_s \left\{ \sum_{j=1}^{3} \mathbf{e}_{sj} \xi_{sj} B_{s\rho} \right\}, \tag{5}$$

$$B_{s\rho} = \begin{cases} \sin \mathbf{q}_s \boldsymbol{\rho}, & \text{if} \quad \mathbf{q}_s \in P_+ \\ \cos \mathbf{q}_s \boldsymbol{\rho}, & \text{if} \quad \mathbf{q}_s \in P_-. \end{cases} \tag{6}$$

where ρ is the equilibrium position of the nucleus and $\mathbf{u}_\rho$ the deviation from it. The vectors ρ form a spatial crystal lattice of N lattice points. Equation (5) is the expansion of $\mathbf{u}_\rho$ in a Fourier series in the wave vectors $\mathbf{q}_s$ which form the so-called reciprocal lattice which has also N lattice points, in wave vector space. This space we divide into two half-spaces by an arbitrary plane through the origin. The notation $\mathbf{q}_s \in \mathbf{P}_+$ indicates that the end of the vector $\mathbf{q}_s$ lies in a point of that half-space which we arbitrarily call the upper one, while $\mathbf{q}_s \in \mathbf{P}_-$ indicates that $\mathbf{q}_s$ belongs to the other (lower) half-space. The vectors $\mathbf{e}_{sj}$ are three unit vectors corresponding to the polarization of the vibration; one of them is parallel and the other two are perpendicular to $\mathbf{q}_s$. N is the total number of nuclei in the crystal which tends to infinity. Finally, ξ_{sj} are the amplitudes of the expansion which also are the new (normal) coordinates of the crystal. The wave function of the crystal expressed in the new coordinates has the form

$$\Psi = \prod_{sj} \psi_{n_{sj}}(\xi_{sj}); \tag{7}$$

where ψ_n is the function of the linear oscillator in the n-th excited state. The operator F expressed in the new variables has the form

$$F = \exp\{i(\mathbf{k}_0 - \mathbf{k})(\rho_0 + \mathbf{u})\} = \exp\{i(\mathbf{k}_0 - \mathbf{k})\rho_0\} \prod_{sj} \exp\{i(\mathbf{k}_0 - \mathbf{k})\mathbf{e}_{sj}(2/N)^{1/2} B_{s\rho_0} \xi_{sj}\}. \tag{8}$$

If we put the origin in the point ρ_0 where the nucleus under consideration is situated and if we take into account that

$$B_{s0} = \begin{cases} 0, & \text{if} \quad \mathbf{q}_s \in P_+ \\ 1, & \text{if} \quad \mathbf{q}_s \in P_-' \end{cases}$$

we get

$$F = \prod_{sj}^{P_-} \exp\{i(\mathbf{k}_0 - \mathbf{k})\mathbf{e}_{sj}(2/N)^{1/2}\xi_{sj}\}, \tag{9}$$

where the symbol $\mathbf{P}_-$ above the $\prod$ indicates that only variables referring to the lower half-space enter into the product.

Thanks to the separation of variables in both the wave function and the operator the matrix element $F_{\tau\tau_0}$ can also be written as a product

$$F_{\tau\tau_0} = \prod_{sj}^{P_-} F^{(sj)}_{n'_{sj}, n_{sj}}, \tag{10}$$

where n_{sj} characterizes the initial state of the crystal and n'_{sj} its final state. It is easy to show[1] that as $N \to \infty$ the only final states that give a contribution different from zero are those for which n'_{sj} differs at most by unity from n_{sj} for each pair of indicies (sj), and that in the expansion of the corresponding matrix elements it is sufficient to take along only the dominant term for $N \to \infty$. These matrix elements have the form

$$F^{(sj)}_{n_{sj}, n_{sj}} = 1 - [(\mathbf{k}_0 - \mathbf{k})\mathbf{e}_{sj}]^2 h\left(n + \frac{1}{2}\right) / NM\omega_{sj} + \cdots, \tag{11}$$

$$F^{(sj)}_{n_{sj}+1, n_{sj}} = \frac{i}{\sqrt{2}}(\mathbf{k}_0 - \mathbf{k})\mathbf{e}_{sj}\left(\frac{2h}{NM\omega_{sj}}\right)^{1/2}(n_{sj} + 1)^{1/2} + \cdots, \tag{12}$$

$$F^{(sj)}_{n_{sj}-1, n_{sj}} = -\frac{i}{\sqrt{2}}(\mathbf{k}_0 - \mathbf{k})\mathbf{e}_{sj}\left(\frac{2h}{NM\omega_{sj}}\right)^{1/2}(n_{sj})^{1/2} + \cdots. \tag{13}$$

where ω_{sj} is the frequency corresponding to the oscillator ξ_{sj} of wave vector $\mathbf{q}_s$ and polarization $\mathbf{e}_{sj}$.

We consider the process of the emission of n phonons. This corresponds to such matrix elements $F_{\tau\tau_0}$ where of the 3N factors in Eq. (10) n have the form $F_{n+1,n}$ and the rest the form $F_{n,n}$. If we number those oscillators which are involved in the transition from 1 to n and write

$$(\mathbf{k}_0-\mathbf{k})\,\mathbf{e}_{sj}=|\mathbf{k}_0-\mathbf{k}|\cos\alpha_{sj},\quad r=h^2(\mathbf{k}_0-\mathbf{k})^2/2M\Theta, \tag{14}$$

where Θ is a unit of energy which can for the sake of convenience be chosen to be of the order of the magnitude of the Debye temperature of the crystal, we get

$$|F^{(n)}_{\tau\tau_0}|^2=e^{-2W}\left(\frac{2r}{N}\right)^n\sum_{i=1}^{n}\cos^2\alpha_i\,(n_i+1)\,\frac{\Theta}{h\omega_i}, \tag{15}$$

where e^{-2W}, the so-called thermal factor, is the product of all $|F_{n_{sj}n_{sj}}|^2$ with n finite and with $N\to\infty$.

We introduce now the spectrum of the normal vibrations of the crystal, $\varphi(h\omega)$, in such a way that $\varphi(h\omega)\,d(h\omega)$ is the number of oscillators (sj) with energy $h\omega$ within the interval $d(h\omega)$. The normalization condition is obviously

$$\int\limits_0^\infty \varphi(h\omega)\,d(h\omega)=3N. \tag{16}$$

Equation (15) must be multiplied by $\delta(E_\tau+E-E_{\tau_0}-E_0)$ and summed over τ. The summation over τ is equivalent to multiplication by*

$$\prod_{i=1}^{n}{}^1\!/_2\,\varphi(h\omega_i)\,d(h\omega_i)$$

and integration over all $d(h\omega)$ from 0 to ∞, replacing $\cos^2\alpha$ by its average value $1/3$ (this is always correct for polycrystalline substances and for a single crystal provided the lattice is cubic). The result obtained must be divided by n! since states for which the excitation of the oscillators differs only in the numbering are identical (in corpuscular language this is the fact that phonons are identical). If the temperature of the crystal is T (in energy units) we must replace n_i+1 by

$$\overline{n_i+1}=(1-e^{-h\omega_i/T})^{-1}.$$

Taking all this into account and introducing dimensionless quantities

$$x\equiv h\omega/\Theta;\quad \varepsilon\equiv(E-E_0)/\Theta;\quad \varphi_0(x)\equiv(\Theta/3N)\,\varphi(h\omega), \tag{17}$$

we get

$$\sum_\tau|F_{\tau\tau_0}|^2\,\delta(E_\tau+E-E_{\tau_0}-E_0)=\frac{e^{-2W}}{\Theta n!}\left(\frac{2r}{N}\right)^n\left(\frac{N}{2}\right)^n\int\limits_0^\infty\cdots\int\limits_0^\infty\delta\left(\sum_{i=1}^{n}x_i-\varepsilon\right)\prod_{i=1}^{n}\frac{\varphi_0(x_i)\,dx_i}{(1-\exp\{-x_i\Theta/T\})\,x_i}\equiv\frac{e^{-2W}}{\Theta}\,z_n, \tag{18}$$

$$z_n=\frac{1}{n!}\int\limits_0^\infty r\lambda(x_1)\,dx_1\ldots\int\limits_0^\infty r\lambda(x_n)\,dx_n\,\delta(x_1+\cdots+x_n-\varepsilon), \tag{19}$$

where

$$\lambda(x)=x^{-1}\varphi_0(x)\,(1-e^{-x\Theta/T})^{-1}. \tag{20}$$

A completely analogous expression can be obtained for the absorption of n phonons; only $\overline{n_i+1}$ must be replaced by $\overline{n_i}$ so that $\lambda(x)$ has the form

$$\lambda(x)=x^{-1}\varphi_0(x)\,(e^{x\Theta/T}-1)^{-1}. \tag{21}$$

We introduce the Laplace transform of z_n considered as a function of ϵ

$$\widetilde{z}_n(s)=\int\limits_0^\infty z_n(\varepsilon)\,e^{-\varepsilon s}\,d\varepsilon=\frac{r^n}{n!}\,[\widetilde{\lambda}(s)]^n, \tag{22}$$

where

---

* The factor $1/2$ arises because the summation is over a half-space.

$$\widetilde{\lambda}(s) = \int_0^\infty \lambda(x) e^{-sx} dx.$$

We sum over n,

$$\sum_{n=1}^\infty \widetilde{z}_n(s) = \sum_{n=1}^\infty [r\widetilde{\lambda}(s)]^n/n! = e^{r\widetilde{\lambda}(s)} - 1. \tag{23}$$

Transforming back we get

$$z(\varepsilon) = \sum_{n=1}^\infty z_n = \frac{1}{2\pi i} \int_{\sigma - i\infty}^{\sigma + i\infty} \{e^{r\widetilde{\lambda}(s)} - 1\} e^{s\varepsilon} ds. \tag{24}$$

Taking Eqs. (3) and (18) into account we find

$$\frac{d^2\sigma}{d\Omega dE} = \frac{k}{k_0} (\overline{a^2}) \left(1 + \frac{m}{M}\right)^2 e^{-2W} \frac{z(\varepsilon, r)}{\Theta}. \tag{25}$$

The thermal factor is calculated without any difficulty

$$W = r \int_0^\infty \frac{\varphi_0(x)}{x} \left(\frac{1}{e^{x\Theta/T} - 1} + \frac{1}{2}\right) dx. \tag{26}$$

3. EXAMPLES

We consider now two examples, choosing a definite form of the function $\varphi_0(x)$. The usual Debye spectrum has the form

$$\varphi_0(x) = \begin{cases} 3x^2 & \text{if} \quad x < 1 \\ 0 & \text{if} \quad x > 1 \end{cases} \tag{27}$$

and Θ is called the Debye temperature of the crystal. This function is very inconvenient for computations. We assume a different form for $\varphi_0(x)$, namely,

$$\varphi_0(x) = {}^1/_2 \beta^3 x^2 e^{-\beta x}. \tag{28}$$

This function satisfies the normalization condition (16), goes to zero as x^2 and contains a cutting-off factor $e^{-\beta x}$. The dimensionless quantity β which is of the order of unity can be varied.

In the two limiting cases, discussed above, we can easily pursue the calculations unto the end.

1. Scattering of slow neutrons by hot substances, $T \gg \Theta$. From Eq. (21) we get, accurate up to terms of the order $x\Theta/T$,

$$\lambda(x) \cong \frac{\varphi_0(x)}{x} \frac{T}{x\Theta} e^{-x\Theta/2T} = \frac{T\beta^3}{2\Theta} \exp\left\{-\left(\beta + \frac{\Theta}{2T}\right) x\right\}. \tag{29}$$

Its Laplace transform is

$$\widetilde{\lambda}(s) = T\beta^3/2\Theta(\beta + \Theta/2T + s).$$

Moreover, from Eq. (24) we get, omitting the intermediate calculations, the following result

$$z(\varepsilon, r) = \exp\left\{-\left(\beta + \frac{\Theta}{2T}\right)\varepsilon\right\} \left[\frac{T}{\Theta} \frac{\beta^3}{2} \frac{r}{\varepsilon}\right]^{1/2} I_1 \left[\left(\frac{T}{\Theta} 2\beta^3 r\varepsilon\right)^{1/2}\right], \tag{30}$$

where I_1 is the Bessel function of imaginary argument.

2. Scattering of neutrons by cold substances, $T \ll \Theta$. We have from Eq. (20) for the emission of an arbitrary number of phonons by the neutron,

$$\lambda(x) \approx \varphi_0(x)/x = {}^1/_2 \beta^3 x e^{-\beta x}. \tag{31}$$

Its Laplace transform is

$$\widetilde{\lambda}(s) = {}^1/_2 \beta^3 (\beta + s)^{-2}. \tag{32}$$

Again omitting the calculations we quote the result following from Eq. (24)

$$z(\varepsilon, r) = \frac{e^{-\beta\varepsilon}}{\varepsilon} f\left(\frac{\beta^3}{2} r\varepsilon^2\right), \tag{33}$$

where

$$f(x) \equiv \sum_{n=1}^{\infty} x^n/n!\,(2n-1)! \tag{34}$$

Since the expansion (34) is in powers of r, it is an expansion in the number of phonons involved in the scattering process. The condition that it is necessary to consider only one-phonon processes is, obviously, $x \ll 1$. Since $\frac{1}{2}\beta^3 \approx 1$ we get, if we take into account Eqs. (14) and (17)

$$\frac{(\mathbf{p}_0-\mathbf{p})^2}{2M}\frac{1}{\Theta}\frac{(E-E_0)^2}{\Theta^2} \ll 1. \tag{35}$$

Hence we get the following condition for the initial energy

$$(m/M)(E_0/\Theta)^3 \ll 1. \tag{36}$$

If inequality (35) is taken in the opposite sense, the main contribution comes from many-phonon processes. In Eq. (34) there are many terms which are important. Using the Stirling formula and differentiating with respect to n we find the value n_0 for which the expression under the $\sum$ sign is maximum

$$\ln x + \ln(1/n_0) - 2\ln(2n_0-1) + O(1/n_0) = 0, \quad n_0 \approx (x/4)^{1/3}. \tag{37}$$

In this way we find the most probable number of phonons which will be emitted for a given angle of scattering and energy loss (which determine r and ϵ),

$$n_0 = \tfrac{1}{2}\beta(r\varepsilon^2)^{1/3} \tag{38}$$

If Θ tends to zero we must obtain the scattering by a free nucleus. From Eqs. (14) and (17) it follows that as $\Theta \to 0$, $r \to \infty$, $\epsilon \to \infty$. For large values of x one can obtain the following asymptotic equation for $f(x)$

$$f(x) = (x/4)^{1/6}(3\pi)^{-1/2}\exp\{3(x/4)^{1/3}\}. \tag{39}$$

From Eqs. (26) and (28) we find

$$W = \beta r/4 \quad \text{for } T = 0. \tag{40}$$

If we perform successively the various limiting transitions we get

$$\frac{e^{-2W}}{\Theta} z(r, \varepsilon) \to \frac{1}{\Theta}\delta(r-\varepsilon) = \delta\left[\frac{(\mathbf{p}_0-\mathbf{p})^2}{2M} - \Delta E\right], \tag{41}$$

$$\frac{d^2\sigma}{d\Omega dE} = \frac{k}{k_0}\overline{a^2}\left(1+\frac{m}{M}\right)\delta\left[\frac{(\mathbf{p}_0-\mathbf{p})^2}{2M} - \Delta E\right]. \tag{42}$$

This is, as can easily be seen, the cross section for scattering by a free nucleus. Indeed, the δ-function in Eq. (42) assures the conservation of energy provided momentum is conserved (the momentum taken up by the nucleus is equal to $\mathbf{p}_0 - \mathbf{p}$). Integration over the angles gives

$$\frac{d\sigma}{dE} = \begin{cases} 4\pi(\overline{a^2})/\Delta E_{\max} & \text{for } 0 < E_0 - E < \Delta E_{\max} \\ 0 & \text{for } E_0 - E > \Delta E_{\max}, \quad \text{or} \quad E_0 - E < 0, \end{cases} \tag{43}$$

where

$$\Delta E_{\max} = E \cdot 4Mm/(M+m)^2. \tag{44}$$

Integration over the energy gives

$$\sigma = 4\pi(\overline{a^2}). \tag{45}$$

In the figure we have given as an illustration the cross section $d^2\sigma/d\Omega dE$ for a given angle of 90° as a function of the relative energy loss $\Delta E/E_0$ for $M/m = 9$. The value of β was taken to be 3. In this case the thermal factor (40) coincides with the thermal factor for the Debye spectrum. It can be seen from the figure how for increasing E_0/Θ the cross section tends to the δ-function (42) since for the scattering by a free nucleus the energy loss is simply by the angle of scattering from the laws of conservation of energy and momentum. For $E/\theta = 100$ the width of the curve is still fairly large. In a real crystal the approach to a δ-function will, apparently, occur fast owing to the possibility of knocking a nucleus out of the lattice, a process not considered in our paper.

The calculations, using Eq. (34), can be simplified by using the circumstances that for $x \lesssim 10$ the series (34) converges very rapidly, while for $x \gtrsim 10$ the asymptotic formula

$$\log f(x) = 0.8207 \cdot x^{1/3} + \frac{1}{6} \log x - 0.5875 - 0.1028\, x^{-1/3}. \tag{46}$$

is correct with a large degree of accuracy.

In conclusion the author expresses his gratitude to A. S. Davydov and V. M. Agranovich for valuable discussions and suggestions.

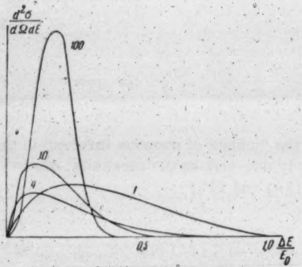

Energy distribution of neutrons scattered by a crystal over an angle of 90°. The numbers indicate the value of E/Θ. The scale of the curve for $E/\Theta = 1$ is increased 10 times with respect to the other curves

---

[1] R. Weinstock, Phys. Rev. 65, 1 (1944).

[2] G. L. Squires, Proc. Roy. Soc. A212, 192 (1952).

[3] G. Placzek and L. van Hove, Phys. Rev. 93, 1207 (1954).

[4] J. M. Cassels, Progr. Nucl. Phys. 1, 185 (1950).

[5] A. I. Akhiezer and I. Ia. Pomeranchuk, Некоторые вопросы теории ядра, (Some Problems in the Theory of Nuclei), Moscow-Leningrad, 1950.

Translated by D. ter Haar
18

SOVIET PHYSICS JETP VOLUME 6, NUMBER 1 JANUARY, 1958

QUANTUM KINETIC EQUATION FOR PLASMA WITH ACCOUNT OF CORRELATION

IU. L. KLIMONTOVICH and S. V. TEMKO

Moscow State University

Submitted to JETP editor December 13, 1956

J. Exptl. Theoret. Phys. (U.S.S.R.) 33, 132-134 (July, 1957)

A quantum kinetic equation has been obtained for a system of particles with Coulomb interaction. This equation differs from the known quantum kinetic equation by the fact that correlation of the mutual positions of charged particles has been taken into account.

A quantum kinetic equation for a set of interacting particles can be obtained by solution of the system of equations for the quantum distribution functions f_1 and f_2.[1,2] In this case the function f_3 which enters the equation for the distribution function f_2, is expressed approximately in terms of the functions f_1 and f_2. For a solution of this system of equations, quantum conditions for the vanishing of correlation at infinity are necessary. However, as was noted by N. N. Bogoliubov, the solution of the equation for the density matrix (or, correspondingly, for the quantum distribution function) can be reduced to a solution of the equation for the quantum function F_s with classical boundary conditions. Here $f_s = \gamma_s F_s$, γ_s is the symmetrization operator for s particles. In the case of systems with central interaction, the equations for F_1 and F_2 have the following form:

$$\frac{\partial F_1}{\partial t}+\frac{p}{m}\frac{\partial F_1}{\partial q}=\frac{ni}{(2\pi)^9\hbar}\int[\Phi(|q-q'-\frac{1}{2}\hbar(\tau-\tau')|)-\Phi(|q-q'+\frac{1}{2}\hbar(\tau-\tau')|)]\exp\{i\tau(\eta-p)$$

$$+i\tau'(\eta'-p')\}(1+P_{1,2})F_2(q,q',\eta,\eta';t)\,d\tau\,d\tau'\,d\eta\,d\eta'\,dq'\,dp'; \qquad (1)$$

$$\frac{\partial F_2}{\partial t}+\frac{p}{m}\frac{\partial F_2}{\partial q_1}+\frac{p_1}{m}\frac{\partial F_2}{\partial q_2}=\frac{i}{(2\pi)^6\hbar}\int\Big[\Phi\Big(|q_1-q_2-\frac{1}{2}\hbar(\tau_1-\tau_2)|\Big)-\Phi\Big(|q_1-q_2+\frac{1}{2}\hbar(\tau_1-\tau_2)|\Big)\Big]\exp\{i\tau_1(\eta_1-p_1)$$

$$+i\tau_2(\eta_2-p_2)\}F_2(q_1,q_2,\eta_1,\eta_2;t)\,d\tau_1\,d\tau_2\,d\eta_1\,d\eta_2+\frac{ni}{(2\pi)^6\hbar^4}\int\Big[\Phi\Big(|q_1-q'-\frac{1}{2}\hbar\tau_1|\Big)-\Phi\Big(|q_1-q'+\frac{1}{2}\hbar\tau_1|\Big)\Big]e^{i\tau_1(\eta_1-p_1)}$$

$$\times(1+P_{1,3}+P_{2,3})F_3(q_1,q_2,q',\eta_1,p_2,p';t)\,d\tau_1 d\eta_1 dq' dp'+\frac{ni}{(2\pi)^6\hbar^4}\int\Big[\Phi\Big(|q_2-q'-\frac{1}{2}\hbar\tau_2|\Big)$$

$$-\Phi\Big(|q_2-q'+\frac{1}{2}\hbar\tau_2|\Big)\Big]e^{i\tau_2(\eta_2-p_2)}(1+P_{1,3}+P_{2,3})F_3(q_1,q_2,q'_1,p_1,\eta_2,p';t)\,d\tau_2 d\eta_2 dq' dp'. \qquad (2)$$

Here Φ is the energy of interaction of a pair of particles, n is the number of particles per unit volume, and P_{ik} is the permutation operator for a pair of particles. Limiting ourselves to consideration of pair correlation, we can write

$$F_2(q_1,q_2,p_1,p_2;t)=F_1(q,p_1;t)F_1(q_2,p_2;t)+g(q_1,q_2,p_1,p_2;t) \qquad (3)$$

and a similar expression for F_3. The function g is small in comparison with the first term for weak interactions.

In the case of short range forces or for a region in which we can restrict ourselves to pair interaction, we obtain a kinetic equation for the quantum distribution function F_1 corresponding to the equation for the density matrix which was obtained by Bogoliubov and Gurov.[3] Here F_3 is expressed only in terms of the derivative of the function F_1.

We have considered Eqs. (1) and (2) for a system of particles with Coulomb interaction. If the interaction is weak and the correlation distance, determined by the exchange interaction r_{ex} is less than the correlation distance of the Coulomb interaction of the particles r_D, then for the region $r > r_{ex}$ the equations for F_1 and F_2 are simplified and in the similar case take the following form:

$$\frac{\partial F_1(p,t)}{\partial t}=\frac{ni}{(2\pi)^9\hbar^4}\int\Big[\Phi\Big(|q-\frac{1}{2}\hbar(\tau_1-\tau_2)|\Big)-\Phi\Big(|q+\frac{1}{2}\hbar(\tau_1-\tau_2)|\Big)\Big]\exp\{i\tau_1(\eta_1-p_1)$$

$$+i\tau_2(\eta_2-p_2)\}(1+P_{12})g(q,\eta_1,\eta_2;F_1)\,d\tau_1\,d\tau_2\,d\eta_1\,d\eta_2\,dq\,dp_2; \qquad (4)$$

$$g(q,p_1,p_2;F_1)=-\frac{im}{(2\pi)^6\hbar}\int\int\int_0^\infty\Big[\Phi\Big(|q-(p_1-p_2)\theta-\frac{1}{2}\hbar(\tau_1-\tau_2)|\Big)-\Phi\Big(|q-(p_1-p_2)\theta+\frac{1}{2}\hbar(\tau_1-\tau_2)|\Big)\Big]$$

$$\times\exp\{i\tau_1(\eta_1-p_1)+i\tau_2(\eta_2-p_2)\}F_1(\eta_1,t)F_2(\eta_2,t)\,d\tau_1\,d\tau_2\,d\eta_1\,d\eta_2\,d\theta\mp\frac{nim}{(2\pi)^6\hbar^4}\int\int\int_0^\infty\Big[\Phi\Big(|q-q'-(p_1-p_2)\theta-\frac{1}{2}\hbar\tau|\Big)$$

$$-\Phi\Big(|q-q'-(p_1-p_2)\theta+\frac{1}{2}\hbar\tau|\Big)\Big]\exp\{iq'(\pi'-\pi'')/\hbar)\}\Big(e^{i\tau(\eta-p_1)}\delta\Big(p_2-\frac{\pi'+\pi''}{2}\Big)F_1(\eta_1,t)F_1(\pi',t)F_1(\pi'',t)$$

$$-e^{i\tau(\eta-p_1)}\delta\Big(p_1-\frac{\pi'+\pi''}{2}\Big)F_1(\pi',t)F_1(\eta_1,t)F_1(\pi'',t)\Big)dp'\,d\theta\,dq'\,d\tau\,d\eta\,d\pi'\,d\pi''$$

$$-\frac{nim}{(2\pi)^6\hbar^4}\int\int\int_0^\infty\Big[\Phi\Big(|q-q'-(p_1-p_2)\theta-\frac{1}{2}\hbar\tau|\Big)-\Phi\Big(|q-q'-(p_1-p_2)\theta+\frac{1}{2}\hbar\tau|\Big)\Big]$$

$$\times(e^{i\tau(\eta_1-p_1)}F_1(\eta_1,t)g(-q',p_2,p';F_1)-e^{i\tau(\eta-p_1)}F_1(\eta_1,t)g(q',p_1,p';F_1))\,dp'\,d\theta\,dq'\,d\tau\,d\eta. \qquad (5)$$

The function depends on the time only through $F_1(p, t)$. Equations (4) and (5) transform as $\hbar \to 0$, into the corresponding equations of Sec. 11 of the well-known monograph of Bogoliubov.[4]

To obtain the kinetic equation we must express the function g in terms of F_1 and substitute in Eq. (4). However, Eq. (5), the equation for g, is very difficult to solve exactly for F_1; therefore, for the solution of this equation we have made use of the method of expansion in terms of a small parameter. Here we have considered the case in which the motion of the isolated particle does not disturb the statistical equilibrium of the totality of charged particles being considered. We then get the kinetic equation for the function $F_1(p; t)$ from Eqs. (4), (5) [as a result of transformation of the brackets]:

$$\frac{\partial w(t;p)}{\partial t}=\frac{2\pi v}{(2\pi\hbar)^6\hbar}\int\left\{\frac{\nu(|p'-p|/\hbar)\,\nu(|p-p'|/\hbar)}{1+B((p'-p)/\hbar;(p'+p)/2)}\pm\frac{\nu(|p-p_1'|/\hbar)\,\nu(|p'-p_1|/\hbar)}{1+B((p-p_1')/\hbar;(p+p_1')/2)}\right\}\delta(p+p_1-p'-p_1')\,\delta(E+E_1-E'-E_1')$$
$$\times[(1\pm w(p))(1\pm w(p_1))\,w(p')\,w(p_1')-(1\pm w(p'))(1\pm w(p_1'))\,w(p)\,w(p_1)]\,dp_1\,dp'\,dp_1'. \qquad (6)$$

Here

$$w(t;p)=(2\pi)^3 nF_1(t;p);\ \nu(|k|)=\int e^{ikq}\Phi(|q|)\,dq;\ E(p)=p^2/2m;$$

$$B(k,p)=\left|\mathrm{Re}\,\frac{im\nu(|k|)}{(2\pi)^3\hbar^4}\iint_0^\infty[e^{i\hbar k\tau/2}-e^{-i\hbar k\tau/2}]\exp\{i\theta k(p'-p)+i\tau(\eta-p')\}\,w(\eta)\,d\theta\,d\tau\,d\eta\,dp'\right|;v=1/n. \qquad (7)$$

An expression is omitted in Eq. (6) which corresponds to consideration of the effect of the particles of the system upon one another. Equation (6) (for B = 0) goes over into the quantum kinetic equation obtained by Bogoliubov and Gurov.[3] If it is assumed that all the functions w in Eq. (6) depend on the time, then this equation can be regarded as the quantum analogue of the well known kinetic equation for a classical system with Coulomb interaction, obtained by Landau,[5] in which, however, the divergence at large distances is automatically eliminated by account of correlation. If we consider that the motion of the individual particle with momentum p (or of an outside charged particle moving in a plasma) does not disrupt the thermal equilibrium of the particles of the system surrounding it, then Eq. (6) for $\hbar \to 0$ goes over into the Fokker-Planck equation for the plasma.[6] In the stationary case, the solution of Eq. (6) coincides with the Fermi or Bose distribution.[7] For B in the case of systems obeying Fermi statistics, for complete degeneracy, we find after expanding in a series:

$$B(k,p)=\frac{1}{r_D^2k^2}+\frac{1}{2r_D^2k^2}\left(\frac{kp}{kp_0}\right)\ln\left|\frac{1-kp/kp_0}{1+kp/kp_0}\right|. \qquad (8)$$

Here $r_D = (p_0^2/12\pi mne^2)^{1/2}$ is the Debye radius for the Fermi distribution, and p_0 is the limiting momentum.

We take this opportunity to thank Academician N. N. Bogoliubov for discussions on the present aspects of the problem and D. N. Zubarev who read through the manuscript of the work for the comments he made.

---

[1] J. E. Moyal, Proc. Camb. Phil. Soc. 45, 95 (1949).

[2] Iu. L. Klimontovich and V. P. Silin, J. Exptl. Theoret. Phys. (U.S.S.R.) 23, 151 (1952).

[3] N. N. Bogoliubov and K. P. Gurov, J. Exptl. Theoret. Phys. (U.S.S.R.) 17, 614 (1947).

[4] N. N. Bogoliubov, Проблемы динамической теории в статистической физике, (Problems of Dynamical Theory in Statistical Physics), (Gostekhizdat, Moscow, 1946).

[5] L. D. Landau, Phys. Z. Sowjetunion 10, 154 (1936).

[6] S. V. Temko, J. Exptl. Theoret. Phys. (U.S.S.R.) 31, 1021 (1956); Soviet Phys. JETP 4, 898 (1957).

[7] K. P. Gurov, Dissertation, Moscow State University (1946).

Translated by R. T. Beyer
19

SOVIET PHYSICS JETP VOLUME 6, NUMBER 1 JANUARY, 1958

ENERGY SPECTRUM OF CASCADE ELECTRONS IN LIGHT MATERIALS

I. P. IVANENKO

Moscow State University

Submitted to JETP editor December 15, 1956

J. Exptl. Theoret. Phys. (U.S.S.R.) **33**, 135-138 (July, 1957)

The energy spectrum of cascade electrons in showers produced by a primary electron or photon in light substances has been computed. A brief analysis of the numerical results is given.

BELOW we present the results of a calculation of the energy spectrum of cascade electrons in light materials in electron-photon showers, carried out by the method of moments.[1] Recursion formulas have been obtained which make it possible to obtain all moments of the distribution functions for electrons with energies higher than E in a shower produced by a primary electron or photon with energy E_0. Explicit analytical expressions have been derived for the first two moments of the functions and numerical values

TABLE I. The Function $\{N_p(E_0, t, E)\}^P$

t \ ε	0.6; 0	0.6; 0.03	0.6; 0.06	0.6; 0.1	0.6; 0.2	0.6; 0.4	1.4; 0	1.4; 0.06	1.4; 0.2	1.4; 0.4	1.4; 0.8
0.1	0.0303	0.0277	0.0240	0.0203	0.0133	0.0035	0.063	0.056	0.043	0.030	0.012
0.3	0.0747	0.0681	0.0591	0.0498	0.0326	0.0085	0.156	0.137	0.106	0.073	0.029
0.5	0.102	0.0927	0.0805	0.0679	0.0444	0.0115	0.214	0.188	0.144	0.100	0.039
0.7	0.117	0.106	0.0918	0.0775	0.0505	0.0131	0.246	0.215	0.165	0.114	0.045
0.9	0.122	0.110	0.0958	0.0808	0.0526	0.0137	0.260	0.226	0.173	0.120	0.046
1.2	0.119	0.107	0.0927	0.0783	0.0508	0.0132	0.256	0.221	0.169	0.116	0.045
1.4	0.112	0.0998	0.0869	0.0734	0.0475	0.0123	0.243	0.209	0.159	0.109	0.042
1.6	0.102	0.0911	0.0793	0.0670	0.0432	0.0112	0.225	0.192	0.146	0.100	0.038
2.0	0.0812	0.0713	0.0622	0.0526	0.0337	0.0087	0.183	0.154	0.116	0.079	0.030
2.3	0.0652	0.0566	0.0494	0.0418	0.0266	0.0069	0.151	0.125	0.094	0.064	0.024
2.6	0.0505	0.0431	0.0377	0.0319	0.0201	0.0052	0.121	0.099	0.073	0.049	0.018
3.0	0.0340	0.0280	0.0245	0.0208	0.0128	0.0033	0.086	0.068	0.049	0.033	0.012
3.5	0.0180	0.0138	0.0122	0.0104	0.0061	0.0015	0.052	0.038	0.027	0.017	0.006
4.0	0.0073	0.0044	0.0040	0.0035	0.0016	—	0.028	0.018	0.012	0.007	0.002

t \ ε	3; 0	3; 0.06	3; 0.2	3; 0.4	3; 08	3; 2	5; 0	5; 0.03	5; 0.1	5; 0.4	5; 0.8	5; 2
0.1	0.110	0.095	0.085	0.071	0.057	0.020	0.147	0.142	0.132	0.105	0.094	0.057
0.3	0.274	0.245	0.212	0.176	0.140	0.049	0.374	0.360	0.373	0.264	0.232	0.139
0.5	0.381	0.340	0.292	0.241	0.191	0.065	0.527	0.505	0.466	0.366	0.319	0.189
0.7	0.444	0.395	0.338	0.278	0.218	0.073	0.623	0.594	0.546	0.426	0.367	0.214
0.9	0.475	0.420	0.358	0.294	0.227	0.074	0.676	0.642	0.587	0.455	0.386	0.223
1.2	0.479	0.421	0.355	0.291	0.220	0.068	0.698	0.658	0.598	0.458	0.380	0.216
1.4	0.462	0.405	0.340	0.277	0.206	0.060	0.686	0.644	0.582	0.442	0.361	0.199
1.6	0.437	0.381	0.317	0.257	0.189	0.052	0.661	0.616	0.554	0.417	0.335	0.180
2.0	0.374	0.321	0.262	0.211	0.148	0.036	0.585	0.539	0.479	0.353	0.272	0.138
2.3	0.318	0.272	0.219	0.174	0.118	0.024	0.518	0.473	0.416	0.301	0.224	0.108
2.6	0.266	0.225	0.178	0.140	0.090	0.015	0.451	0.407	0.355	0.251	0.179	0.080
3.0	0.204	0.170	0.130	0.101	0.059	0.004	0.366	0.326	0.280	0.192	0.126	0.047
3.5	0.141	0.114	0.083	0.062	0.030		0.275	0.239	0.201	0.131	0.076	0.021
4.0	0.093	0.072	0.049	0.035	0.010		0.201	0.171	0.140	0.085	0.040	0.008
5.0	0.036	0.024	0.012				0.103	0.082	0.063	0.031	0.010	
6.0							0.050	0.038	0.027	0.009		
7.0							0.025	0.018	0.011			
8.0												

ε / t	10; 0	10; 0.03	10; 0.1	10; 0.4	10; 0.8	10; 2	15; 0.03	15; 0.1	15; 0.2	15; 0.4	15; 0.8	15; 2
0.1	0.207	0.197	0.182	0.154	0.142	0.108	0.206	0.202	0.193	0.18	0.179	0.145
0.3	0.537	0.510	0.469	0.396	0.563	0.275	0.551	0.535	0.506	0.490	0.457	0.363
0.5	0.742	0.703	0.644	0.557	0.502	0.371	0.785	0.761	0.695	0.681	0.620	0.487
0.7	0.939	0.887	0.811	0.664	0.590	0.429	1.023	0.970	0.908	0.815	0.771	0.588
0.9	1.046	0.984	0.897	0.726	0.637	0.454	1.171	1.103	1.022	0.910	0.842	0.629
1.2	1.123	1.051	0.955	0.759	0.653	0.451	1.310	1.216	1.116	0.982	0.878	0.635
1.4	1.134	1.059	0.958	0.753	0.638	0.430	1.358	1.250	1.140	0.995	0.870	0.614
1.6	1.123	1.044	0.951	0.731	0.610	0.401	1.378	1.258	1.140	0.987	0.844	0.580
2.0	1.054	0.973	0.872	0.659	0.533	0.331	1.356	1.218	1.092	0.929	0.759	0.494
2.3	0.977	0.897	0.800	0.593	0.466	0.276	1.301	1.155	1.027	0.864	0.681	0.424
2.6	0.892	0.814	0.722	0.524	0.400	0.224	1.225	1.077	0.949	0.789	0.601	0.356
3.0	0.774	0.701	0.616	0.435	0.317	0.164	1.106	0.960	0.837	0.685	0.498	0.274
3.5	0.633	0.568	0.494	0.336	0.231	0.104	0.946	0.809	0.698	0.560	0.384	0.191
4.0	0.508	0.451	0.388	0.254	0.163	0.061	0.790	0.667	0.583	0.448	0.289	0.128
5.0	0.315	0.274	0.229	0.138	0.075	0.014	0.521	0.431	0.360	0.274	0.158	0.051
6.0	0.189	0.161	0.130	0.072	0.031		0.326	0.266	0.217	0.160	0.084	0.018
7.0	0.111	0.093	0.073	0.037	0.012		0.195	0.158	0.127	0.091	0.045	0.006
8.0	0.065	0.053	0.040	0.019	0.004		0.114	0.091	0.072	0.050	0.024	0.003

TABLE II. The Function $\{N_p(E_0, t, E)\}^{\Gamma}$

ε / t	0.6; 0	0.6; 0.06	0.6; 0,1	0.6; 0.4	1.4; 0	1.4; 0,06	1.4; 02	1.4; 0.4	1.4; 0.8	3; 0	3; 0.06	3; 0.2	3; 0.4	3; 0.8	3; 2	5; 0	5; 0.03	5; 0.06
0.1	0.814	0.806	0.803	0.778	0.871	0.860	0.844	0.829	0.805	0.954	0.934	0.912	0.904	0.876	0.826	1.028	1.015	1.006
0.3	0.517	0.498	0.488	0.430	0.655	0.627	0.590	0.553	0.495	0.861	0.810	0.757	0.709	0.666	0.544	1.046	1.011	0.990
0.5	0.300	0.276	0.263	0.186	0.487	0.449	0.399	0.349	0.272	0.767	0.698	0.625	0.559	0.500	0.337	1.025	0.975	0.946
0.7	0.147	0.120	0.105	0.019	0.356	0.313	0.257	0.201	0.115	0.677	0.587	0.513	0.432	0.370	0.187	0.976	0.918	0.883
0.9	0.041	0.013			0.256	0.211	0.153	0.096	0.008	0.591	0.507	0.419	0.340	0.268	0.081	0.911	0.848	0.809
1.2					0.148	0.105	0.050			0.473	0.392	0.304	0.229	0.156		0.796	0.731	0.691
1.6					0.062	0.025				0.341	0.270	0.193	0.129	0.063		0.636	0.574	0.536
2.0					0.016					0.236	0.179	0.117	0.066	0.011		0.486	0.432	0.397
2.3										0.174	0.127	0.077	0.037			0.389	0.340	0.310
2.6										0.124	0.088	0.047	0.017			0.304	0.262	0.235
3.0										0.074	0.049	0.021	0.002			0.212	0.178	0.156
3.5										0.033	0.018	0.002				0.127	0.102	0.086
4.0										0.008	0.001					0.070	0.052	0.040

ε / t	5; 0.1	5; 0.2	5; 04	5; 08	5; 2	10; 0	10; 0.06	10; 0.2	10; 0.4	10; 0.8	10; 2	15; 0.03	15; 0.06	15; 0.2	15; 0.4	15; 08	15; 2
0.1	0.994	0.973	0.949	0.929	0.884	1.156	1.118	1.069	1.041	1.013	0.955	1.193	1.182	1.140	1.102	1.078	1.006
0.3	0.960	0.907	0.847	0.797	0.687	1.376	1.276	1.152	1.081	1.007	0.861	1.480	1.449	1.340	1.240	1.171	0.988
0.5	0.905	0.832	0.749	0.677	0.527	1.493	1.352	1.180	1.077	0.970	0.765	1.658	1.612	1.452	1.307	1.201	0.942
0.7	0.836	0.752	0.656	0.571	0.399	1.535	1.368	1.167	1.042	0.912	0.671	1.753	1.694	1.498	1.322	1.186	0.878
0.9	0.760	0.671	0.570	0.476	0.297	1.522	1.341	1.126	0.987	0.842	0.582	1.785	1.717	1.495	1.300	1.139	0.804
1.2	0.643	0.555	0.453	0.355	0.181	1.436	1.249	1.030	0.832	0.726	0.460	1.749	1.672	1.429	1.220	1.032	0.684
1.6	0.493	0.416	0.324	0.231	0.081	1.254	1.075	0.874	0.727	0.570	0.322	1.607	1.513	1.274	1.066	0.861	0.527
2.0	0.363	0.300	0.224	0.140	0.021	1.045	0.886	0.712	0.576	0.429	0.214	1.412	1.329	1.090	0.895	0.686	0.388
2.3	0.281	0.230	0.165	0.091		0.893	0.750	0.600	0.474	0.338	0.150	1.257	1.176	0.950	0.770	0.566	0.300
2.6	0.212	0.171	0.118	0.053		0.751	0.626	0.497	0.384	0.260	0.100	1.103	1.026	0.818	0.654	0.459	0.226
3.0	0.140	0.111	0.071	0.018		0.585	0.482	0.380	0.283	0.177	0.051	0.912	0.842	0.658	0.517	0.339	0.147
3.5	0.076	0.058	0.032			0.437	0.338	0.264	0.187	0.101	0.011	0.704	0.645	0.491	0.376	0.223	0.077
4.0	0.035	0.025				0.293	0.231	0.178	0.119	0.050		0.535	0.485	0.360	0.269	0.141	0.033
5.0						0.138	0.103	0.075	0.041			0.297	0.264	0.185	0.130	0.048	
6.0						0.064	0.043	0.029	0.011			0.159	0.140	0.112	0.061	0.012	
7.0						0.032	0.019	0.010				0.084	0.073	0.046	0.028		

have been obtained for primary-particle energies E_0 from 0.6 to 15 and values of E from 0.03 to 2.*

The distribution functions for electrons with energies higher than E in a shower, produced by a primary electron $\{N_p(E_0, t, E)\}^{P}$ or photon $\{N_p(E_0, t, E)\}^{\Gamma}$, as in Ref. 2, has been approximated by a sum of Laguerre polynomials L_n^0 and $L_n^1(x)$ respectively.

---

*The energy of shower particles in cascade theory is measured in units of $q\beta$ where β is the critical energy for the given material and q is a constant equal to 2.29.

The results of the calculations of these functions are shown in Tables I and II.* An investigation of the computed functions (cf. for example, Refs. 2 and 3, in which this type of analysis was first applied) shows that in the present case the error in the electron energy spectrum is approximately 10 percent. We may note that the method of moments is so far the only method which makes it possible to determine with reasonable accuracy the average behavior of an electron-photon shower in the energy region being considered. In calculating the moments, the photon absorption coefficient σ has been assumed constant and equal to its asymptotic value $\sigma = \sigma_0$. However, in computing the distribution functions the photon absorption coefficient has been assumed equal to $\sigma_{\min} = 0.65$. As follows from the results of Ref. 1, this method makes it possible to take account of the approximate dependence of $\sigma(E)$ on energy, leading to better agreement of theory and experiment. The value 0.65 corresponds to the value of $\sigma_{\min}$ in air; the computed curves, however, apply to the development of showers in materials with atomic number Z approximately up to 30 with good accuracy.[4] The numerical results which have been presented may be useful in the analysis of certain cosmic-ray experiments.

---

[1] I. P. Ivanenko, J. Exptl. Theoret. Phys. (U.S.S.R.) **31**, 86 (1956), Soviet Phys. JETP **4**, 115 (1957).

[2] I. P. Ivanenko and M. A. Malkov, J. Exptl. Theoret. Phys. (U.S.S.R.) **32**, 150 (1957), Soviet Phys. JETP **5**, 112 (1957).

[3] I. P. Ivanenko, J. Exptl. Theoret. Phys. (U.S.S.R.) **32**, 491 (1957), Soviet Phys. JETP **5**, 413 (1957).

[4] P. S. Isaev, J. Exptl. Theoret. Phys. (U.S.S.R.) **28**, 374 (1955), Soviet Phys. JETP **1**, 379 (1955).

Translated by H. Lashinsky
20

SOVIET PHYSICS JETP VOLUME 6, NUMBER 1 JANUARY, 1958

CONTRIBUTION TO THE THEORY OF SCATTERING OF LIGHT NEAR POINTS OF SECOND-ORDER PHASE TRANSITIONS

M. A. KRIVOGLAZ and S. A. RYBAK

Institute of Metal Physics, Academy of Sciences, Ukrainian S.S.R.

Submitted to JETP editor December 25, 1956

J. Exptl. Theoret. Phys. (U.S.S.R.) **33**, 139-150 (July, 1957)

The scattering of light by ferroelectric and ferromagnetic crystals in the vicinity of second-order transition points is considered. Calculations are performed both for single component crystals and for solid solutions. By way of illustration light scattering by $BaTiO_3$ type crystals as well as by Rochelle salt or KH_2PO_4 type crystals is examined. The effect of an external field on the scattering is investigated.

1. Ginzburg[1] has shown that at temperatures close to the temperature of a second-order transition there occurs additional scattering of light which is particularly intense near the critical point, that is, near the point where the curve for second-order transitions merges into the curve for transitions of the first order. This effect has been experimentally detected by Iakovlev, Mikheeva, and Velichkina[2] who investigated the dispersion of light in quartz near the point of the $\alpha \rightleftarrows \beta$-transformation. Herein we shall carry out a further theoretical investigation of the problem, primarily where ferroelectric materials are con-

---

* In the first line of each column of the tables the first number denotes the energy of the initial electron or photon and the second the energy of the secondary electron.

cerned. We shall explicitly take into account the anisotropy of the fluctuation of the dielectric constant ϵ^0 (for light), which obtains even in cubic (or almost cubic) crystals, and the depolarization of light associated therewith. We shall investigate the influence of the electric field on the intensity of scattering. In addition to the case considered by Ginzburg, when there are only square terms in the expansion of $\delta\epsilon^0$ in powers of the components of the polarization vector, we shall also examine the case which obtains in certain ferroelectrics (for example, in Rochelle salt), when this expansion also comprises linear terms. We shall also consider the scattering of light by solid solutions of ferroelectrics.

2. The additional scattering of light near the second-order transition points is associated with the inhomogeneities of the dielectric constant ϵ^0, caused by the fluctuation of the internal parameters that characterize the long range order in the less symmetric phase (in the case of ferroelectrics, such internal parameters are the components of the polarization vector). Near second-order transition points inhomogeneities of this type can always be regarded as static. For anisotropic crystals the question of scattering of light by inhomogeneities of the dielectric constant, caused by thermal vibrations of the lattice, has been examined by Motulevich.[3] Carrying out exactly the same examination for light scattering by the static distribution of the inhomogeneities of the dielectric constant tensor, we find that the intensity of the scattered light is

$$\frac{J_1}{J_0} = K_1 K_2 \frac{\omega^4 V^2}{16\pi^2 c^4 R^2} \frac{n_2}{n_1} \cos^{-2}\delta_1 \cdot \cos^{-2}\delta_2 \left| \sum_{\alpha,\beta=1}^{3} \varepsilon_{\alpha\beta q} e^1_\alpha e^2_\beta \right|^2. \tag{1}$$

Here J_1 is the intensity of the scattered wave, J_0 is the intensity of the wave incident on the crystal, V is the volume of the crystal, c is the speed of light, R is the distance from the point of observation to the scattering crystal (the size of which is assumed to be appreciably smaller than R), k_1 and k_2 are the wave vectors of the incident and scattered waves (in the crystal), e^1 and e^2 are the unit polarization vectors of these waves (having the components e^1_α and e^2_β, where the indices α and β designate the respective Cartesian coordinates), n_1 and n_2 are respectively the indices of refraction for the incident and scattered waves, and δ_1 and δ_2 are the angles between the electric field vectors and the induction vectors in the incident and scattered waves (in the crystal), respectively. The factors K_1 and K_2 take into account the decrease in the intensity of the incident and scattered rays in passing through the crystal-air interface and can be calculated by means of the familiar formulas of crystal optics.* Lastly, $\epsilon_{\alpha\beta q}$ denotes the q-th Fourier component of the deviation of the $\delta\epsilon^0_{\alpha\beta}$ component of the dielectric-constant tensor from the mean value

$$\varepsilon_{\alpha\beta q} = \frac{1}{V} \int_V \delta\varepsilon^0_{\alpha\beta} e^{iqr}\, d\tau, \tag{2}$$

where $q = k_2 - k_1$. In deducing expression (1) it was assumed that rotation of the plane of polarization in the crystal is absent or can be neglected. It was further assumed that light absorption in the specimen is negligible.

In the case of cubic crystals, in which the index of refraction is independent of the direction of the wave vector and of the polarization vector and the angles δ_1 and δ_2 are zero, the expression for the intensity of the scattered radiation is simplified to

$$\frac{J_1}{J_0} = K_1 K_2 \frac{\omega^4 V^2}{16\pi^2 c^4 R^2} \left| \sum_{\alpha,\beta=1}^{3} \varepsilon_{\alpha\beta q} e^1_\alpha e^2_\beta \right|^2. \tag{3}$$

The change in the dielectric constant connected with the fluctuation of polarization in this case is also a tensor (not a scalar) quantity.

The further examination will be carried out in terms pertaining specifically to ferroelectric crystals. In the vicinity of the temperature T_0 of the transition to the ferroelectric state we can retain only the first terms of the expansion of the components of the tensor $\epsilon^0_{\alpha\beta}$ in powers of the components of the polarization vector:

$$\varepsilon^0_{\alpha\beta} = \varepsilon^0_{\alpha\beta 0} + \lambda_{\alpha\beta,\gamma} P_\gamma + \lambda_{\alpha\beta,\gamma\delta} P_\gamma P_\delta, \tag{4}$$

---

* Repeated reflections from the other faces of the crystal, which greatly complicate the picture, can be eliminated by blackening these faces.

where the coefficients do not depend on the polarization. Here and below summation from 1 to 3 over all twice-repeating indices (in a given term) is implied. The polarization vector **P** can be regarded as consisting of a mean value $\overline{\mathbf{P}}$ and a fluctuating part $\Delta\mathbf{P}$. Replacing **P** in (4) by the sum $\mathbf{P} + \Delta\mathbf{P}$, we determine $\delta\epsilon^0_{\alpha\beta}$, retaining only the terms linear in ΔP_γ, and then, invoking (2), express the Fourier components of the dielectric constant tensor in terms of the Fourier components of the polarization vector $P_{\gamma q}$

$$\varepsilon_{\alpha\beta q} = \lambda_{\alpha\beta,\gamma} P_{\gamma q} + 2\lambda_{\alpha\beta,\gamma\delta} \overline{P}_\delta P_{\gamma q}. \tag{5}$$

Substituting (5) in (1), we obtain the following formula for the intensity of the scattered light, connected with the fluctuations of the polarization:

$$\frac{J_1}{J_0} = \frac{1}{2} F(1,\ 2)\, V \left[\lambda_{\alpha\beta,\gamma}\lambda_{\alpha'\beta',\gamma'} + 4\lambda_{\alpha\beta,\gamma}\lambda_{\alpha'\beta',\gamma'\delta'}\overline{P}_{\delta'} + 4\lambda_{\alpha\beta,\gamma\delta}\lambda_{\alpha'\beta',\gamma'\delta'}\overline{P}_\delta\overline{P}_{\delta'}\right] e^1_\alpha e^1_{\alpha'} e^2_\beta e^2_{\beta'} \left(\overline{P_{\gamma q}P^*_{\gamma' q}} + \overline{P^*_{\gamma q}P_{\gamma' q}}\right), \tag{6}$$

where the function

$$F(1,\ 2) = K_1 K_2 \frac{\omega^4 V}{16\pi^2 c^4 R^2} \frac{n_2}{n_1} \cos^{-2}\delta_1 \cdot \cos^{-2}\delta_2 \tag{7}$$

may be regarded as independent of the temperature.

The mean values of the squares and products of the Fourier terms constituting the fluctuation of the components of the polarization vector can be determined by means of the thermodynamic theory of fluctuations. The distribution of fluctuation probabilities, as is known, is given by the expression

$$w \sim \exp(-\Delta\Phi / kT), \tag{8}$$

where $\Delta\Phi$ is the change in the thermodynamic potential incident to the appearance of fluctuation. In the case when the polarization of the crystal undergoes fluctuational changes, $\Delta\Phi$ can be written in the form

$$\Delta\Phi = \frac{1}{2}\int\limits_V \left[\varphi_{\alpha\beta}\Delta P_\alpha \Delta P_\beta + A_{\alpha\beta\gamma\delta}\frac{\partial P_\alpha}{\partial x_\gamma}\frac{\partial P_\beta}{\partial x_\delta}\right] d\tau. \tag{9}$$

Here φ is the thermodynamic potential per unit volume,* $A_{\alpha\beta\gamma\delta}$ is a fourth rank tensor and x_γ and x_δ are Cartesian coordinates (γ and $\delta = 1, 2, 3$); the last term takes into account the changes in the thermodynamic potential incident to the appearance of inhomogeneities in the fluctuation distribution; terms with higher order derivatives can be disregarded, provided (as in the case of scattering of light) the predominant part is played by sufficiently smooth fluctuations.

The thermodynamic potential per unit volume of a ferroelectric in the presence of an external electric field **E** can be written as $\varphi = f(\mathbf{P}) - \mathbf{EP}$, where $f(\mathbf{P})$ is independent of **E**. Hence differentiating the equilibrium conditions $\varphi_\alpha = 0$ with respect to P_β, we obtain

$$\varphi_{\alpha\beta} \equiv \partial^2 f / \partial P_\alpha \partial P_\beta = \partial E_\alpha / \partial P_\beta. \tag{10}$$

Comparing Eq. (10) with the equation for the dielectric susceptibility tensor $\kappa_{\alpha\beta}: P_\alpha = \kappa_{\alpha\beta}E_\beta$, we find that the derivatives $\varphi_{\alpha\beta}$ are components of a tensor that is the reciprocal of the dielectric susceptibility tensor:

$$\varphi_{\alpha\beta} = \varkappa^{-1}_{\alpha\beta}. \tag{11}$$

Replacing the fluctuations ΔP_α by their Fourier expansions

$$\Delta P_\alpha = \sum_{\varkappa}{}' (P_{\alpha\varkappa} e^{i\varkappa r} + P^*_{\alpha\varkappa} e^{-i\varkappa r}), \tag{12}$$

from Eqs. (8), (9), and (11), we obtain

$$w \sim \exp\left\{-\frac{V}{2kT}\sum_{\varkappa}{}' (\varkappa^{-1}_{\alpha\beta} + A_{\alpha\beta\gamma\delta}\varkappa_\gamma \varkappa_\delta)(P_{\alpha\varkappa}P^*_{\beta\varkappa} + P^*_{\alpha\varkappa}P_{\beta\varkappa})\right\}. \tag{13}$$

---

* For simplicity of notation we shall designate the partial derivatives with respect to φ through indices: $\varphi_\alpha \equiv \partial\varphi/\partial P_\alpha$, $\varphi_c \equiv \partial\varphi/\partial c$, etc.

By means of the distribution of probabilities (13) we can express the mean value of the products of the Fourier components corresponding to any value of κ in terms of the elements of the matrix that is the reciprocal of the $\kappa_{\alpha\beta}^{-1} + A_{\alpha\beta\gamma\delta}\kappa_\gamma\kappa_\delta$. Substituting the values so obtained for the case of $\kappa = \mathbf{q}$ in place of $\overline{P_{\gamma\mathbf{q}}P^*_{\gamma'\mathbf{q}}} + \overline{P^*_{\gamma\mathbf{q}}P_{\gamma'\mathbf{q}}}$ in Eq. (6), we obtain

$$\frac{J_1}{J_0} = F(1.2)\,kT\,[\lambda_{\alpha\beta,\gamma}\lambda_{\alpha'\beta',\gamma'} + 4\lambda_{\alpha\beta,\gamma}\lambda_{\alpha'\beta',\gamma'\delta'}\overline{P}_{\delta'} + 4\lambda_{\alpha\beta,\gamma\delta}\lambda_{\alpha'\beta',\gamma'\delta'}\overline{P}_\delta\overline{P}_{\delta'}]\,e^1_\alpha e^1_{\alpha'} e^2_\beta e^2_{\beta'}(\varkappa^{-1}_{\gamma\gamma'} + A_{\gamma\gamma'\nu\nu'}q_\nu q_{\nu'})^{-1}. \qquad (14)$$

In the case of scattering of light, when the wavelength is much greater than the lattice constant, the second addend in the last factor in (14) — except for a narrow region near the temperature of the second-order phase transition, (where some components of the tensor $\kappa_{\alpha\beta}^{-1}$ vanish) — is appreciably smaller than the first term. In this case the expression for the intensity of the scattered light assumes the more simple form

$$\frac{J_1}{J_0} = F(1.2)\,kT\,[\lambda_{\alpha\beta,\gamma}\lambda_{\alpha'\beta',\gamma'} + 4\lambda_{\alpha\beta,\gamma}\lambda_{\alpha'\beta',\gamma'\delta'}\overline{P}_{\delta'} + 4\lambda_{\alpha\beta,\gamma\delta}\lambda_{\alpha'\beta',\gamma'\delta'}\overline{P}_\delta\overline{P}_{\delta'}]\,e^1_\alpha e^1_{\alpha'} e^2_\beta e^2_{\beta'}\varkappa_{\gamma\gamma'}. \qquad (15)$$

All the quantities in formula (15) can be determined from independent measurements. Thus $\lambda_{\alpha\beta,\gamma}$ and $\lambda_{\alpha\beta,\gamma\delta}$, according to (4), can be found, for example, by investigating the influence of an external electric field on the index of refraction, while the constants in expression (7) for F(1, 2) can be determined from ordinary optical measurements. Thus formula (15) enables us to calculate, in the general case of a ferroelectric with an arbitrary structure, the intensity and polarization of the part of the scattered light associated with the fluctuations of polarization. If the second addend in the last factor of Eq. (14) cannot be neglected, a more complicated formula must be used for evaluating J_1/J_0. Components of the tensor $A_{\alpha\beta,\gamma\delta}$ entering into (14), which are also important in determining the intensities of scattering of x-rays, thermal neutrons, and other types of waves at temperatures near the second-order transition temperature, can be determined from comparisons of theory with experiment. They can also be calculated with the aid of the statistical theory of ferroelectrics based on a specific atomic model.

In many crystals all the components of the tensor $\lambda_{\alpha\beta,\gamma}$ vanish identically, owing to the requirements imposed by symmetry of the crystal. In particular, this occurs in crystals with centers of symmetry in the nonferroelectric phase. (It was exactly this case that was examined in Ref. 1.) Temperature dependence of the intensity of the scattered light near the second-order phase transition temperature T_0 differs markedly for crystals in which $\lambda_{\alpha\beta,\gamma} = 0$ as compared with crystals in which $\lambda_{\alpha\beta,\gamma} \neq 0$. In the first case with $T \geq T_0$, when $\mathbf{P} = 0$, according to (14) the intensity of the scattered radiation associated with fluctuations of polarization becomes zero.* With $T < T_0$ the ratio J_1/J_0 increases very quickly, attains a maximum value and then falls off. When $\lambda_{\alpha\beta,\gamma} \neq 0$, the intensity of this scattering is not zero even with $T > T_0$. The ratio J_1/J_0 attains a maximum at $T = T_0$ and then decreases with further reduction of the temperature.

---

*It must be emphasized that in the present contribution we consider only scattering by fluctuations of polarization and do not take into account scattering by thermal oscillations or by fluctuations of the internal parameters characterizing the short-range order the orientation of the dipole moments of different cells. The presence of inhomogeneities associated with fluctuations of these internal parameters must lead to additional scattering, which must occur both above and below the temperature T_0. There is reason to think, however, that in the most ineresting cases in the vicinity of the critical point for crystals with $\lambda_{\alpha\beta,\gamma} = 0$ or near the usual transition point for crystals with $\lambda_{\alpha\beta,\gamma} \neq 0$, when the intensity of the scattering under examination here becomes anomalously great (see below), the scattering by fluctuations of the short-range order parameters plays a relatively insignificant part. It should also be noted that $\lambda_{\alpha\beta,\gamma}$ and $\lambda_{\alpha\beta,\gamma\delta}$ entering into the deduced expressions for the intensity (in which only fluctuations of polarization were taken into account) must be determined for constant values of the short-range order parameters, corresponding to thermodynamic equilibrium. Consequently, generally speaking, these quantities will differ somewhat from the corresponding quantities determined from the dependence of the equilibrium value of ϵ^0 on the intensity of the electric field, inasmuch as in the last case the short-range order parameters as well as $\mathbf{P}$ change.

For the purpose of a detailed investigation of the dependence of the intensity of scattering on the temperature and on the intensity of the electric field we shall examine below certain specific cases of ferroelectrics.

3. Let us start our examination with crystals of cubic symmetry (in the nonferroelectric state), having a center of symmetry, and in which the spontaneous polarization is directed along the cubic axis. In particular, barium titanate, one of the important ferroelectrics where practical engineering applications are concnerned, possesses such symmetry.[4,5] For simplicity let us assume that the electric field is directed along the ferroelectric axis which we shall choose as the OZ axis.

In crystals of this symmetry all the components of the tensor $\lambda_{\alpha\beta,\gamma}$ vanish identically, while the tensor $\lambda_{\alpha\beta,\gamma\delta}$ in the nonferroelectric state has only three nonzero components: $\lambda_{11,11}$, $\lambda_{12,12}$ and $\lambda_{11,12}$. In the ferroelectric state the crystal has tetragonal symmetry with which the nonzero components of the tensor $\lambda_{\alpha\beta,\gamma\delta}$ are those identified by the indices 11, 11; 33, 33; 11, 22; 11, 33; 33, 11; 12, 12; 13, 13; 11, 13; 13, 11. (If the crystal has a center of symmetry, $\lambda_{11,13} = \lambda_{13,11} = 0$.) Below the transition temperature the dielectric susceptibility tensor has two nonzero components: κ_{33} and $\kappa_{11} = \kappa_{22}$.

It follows from Eq. (5) that in the given case in the region where one can neglect the terms square in q the intensity of the scattered light is

$$J_1/J_0 = F(1,2)\,\overline{P}^2 kT\,\{4\lambda^2_{33,33}\varkappa_{33}(e_3^1)^2(e_3^2)^2 + 4\lambda^2_{11,33}\varkappa_{33}(e_1^1e_1^2 + e_2^1e_2^2)^2 + 8\lambda_{33,33}\lambda_{11,33}\varkappa_{33}e_3^1e_3^2(e_1^1e_1^2 + e_2^1e_2^2)$$
$$+ \lambda^2_{13,13}\varkappa_{11}[((e_1^1)^2 + (e_2^1)^2)(e_3^2)^2 + (e_3^1)^2((e_1^2)^2 + (e_2^2)^2) + 2(e_1^1e_1^2 + e_2^1e_2^2)e_3^1e_3^2]\}. \qquad (16)$$

Neglecting the relatively minor tetragonality in calculating the factor F(1, 2) we can set

$$F(1.2) = K_1K_2\omega^4V/16\pi^2c^4R^2. \qquad (17)$$

Equation (16) enables us to determine the dependence of the intensity of scattering on the orientation of the polarization vectors of the incident and scattered radiation relative to the crystal axes and to investigate the depolarization of the light. Thus, for example, if the vectors $\mathbf{e}^1$ and $\mathbf{e}^2$ lie in a plane perpendicular to the Z axis and are mutually perpendicular, the intensity of scattering according to (16) goes to zero. On the other hand, if these vectors have components parallel to the Z axis, then even if $\mathbf{e}^1$ is perpendicular to $\mathbf{e}^2$ the intensity of scattering is not zero. In the narrow temperature interval near T_0, where one cannot neglect the terms square in q, the dependence of the scattering intensity on the direction of the vectors $\mathbf{e}^1$ and $\mathbf{e}^2$ becomes appreciably more complicated. Above the temperature T_0, as has already been noted, the scattering associated with the fluctuations of polarization in the crystals of this type vanishes.

In order to find the spontaneous polarization and the dielectric susceptibility tensor, which, according to (16), determine the temperature dependence of the scattering intensity, let us make use of the expansion of the thermodynamic potential per unit volume φ in powers of P_α, introduced in other investigations[6–12] on the basis of the theory of phase transitions of the second order:[13]

$$\varphi = \varphi_0 + {}^1\!/_2 a(T - T_0)P^2 + {}^1\!/_4 B_1P^4 + {}^1\!/_2 B_2\sum_{\alpha,\alpha'=1}^{3} P_\alpha^2P_{\alpha'}^2 + {}^1\!/_6 C_1P^6 + {}^1\!/_2 C_2\sum_{\alpha,\alpha'=1}^{3} P_\alpha^4P_{\alpha'}^2 + C_3P_1^2P_2^2P_3^2 - \mathbf{EP}. \qquad (18)$$

The expansion has been carried out to terms containing P_α to the sixth power inclusive, in order to allow for a more detailed examination of the vicinity of the critical point where the intensity of scattering becomes particularly great.

The equilibrium value of the spontaneous polarization is determined from the condition $\varphi_\alpha = 0$ (α = 1, 2, 3). In the examined case (when $\mathbf{P} \parallel$ OZ), if $\mathbf{E} = 0$, the solution of this equation is of the form:

$$\overline{P}^2 = \overline{P}_3^2 = [-B_1 + \sqrt{B_1^2 + 4aC_1(T_0 - T)}]/2C_1^2. \qquad (19)$$

The dielectric susceptibility tensor can be found by substituting (18) in (11). Bearing in mind the equilibrium condition $\varphi_3 = 0$, we obtain that with $\mathbf{E} = 0$, the nonzero components of the tensor $\kappa_{\alpha\beta}$ are described by

$$1/\varkappa_{33} = a(T - T_0) + 3B_1\overline{P}^2 + 5C_1\overline{P}^4 = 4a(T_0 - T) + 2B_1\overline{P}^2 = 2B_1\overline{P}^2 + 4C_1\overline{P}^4 - 4a(T_0 - T)$$
$$- B_1^2/C_1 + \frac{B_1}{C_1}\sqrt{B_1^2 + 4aC_1(T_0 - T)}; \quad 1/\varkappa_{11} = 1/\varkappa_{22} = B_2\overline{P}^2 + C_2\overline{P}^4. \qquad (20)$$

Substituting (20) and (19) in Eq. (16), we obtain

$$\frac{J_1}{J_0} = F(1,2)\,kT\,\{[2\lambda_{33,33}^2 (e_3^1)^2 (e_3^2)^2 + 2\lambda_{11,33}^2 (e_1^1 e_1^2 + e_2^1 e_2^2)^2 + 4\lambda_{33,33}\lambda_{11,33} e_3^1 e_3^2 (e_1^1 e_1^2 + e_2^1 e_2^2)]\,(B_1^2 + 4aC_1(T_0 - T))^{-1/2}$$

$$+ \lambda_{13,13}^2 [((e_1^1)^2 + (e_2^1)^2)(e_3^2)^2 + (e_3^1)^2((e_1^2)^2 + (e_2^2)^2) + 2(e_1^1 e_1^2 + e_2^1 e_2^2) e_3^1 e_3^2] / (B_2 + C_2 P^2)\}. \qquad (21)$$

At the critical point where the second-order phase transition curve becomes the first-order transition curve, $B_1 = 0$. Consequently near this point, where the phase transition curve B_1 can be represented in the form of the expansion $b(p - p_c)$ (here p is the pressure and p_c is the critical pressure), the scattering intensity becomes particular great, as may be seen from (21). The greatest contribution near the critical point is made by the first three terms in expression (21) (provided, of course, the constant B_2 does not by chance also become small near the critical point). The temperature dependence of J_1/J_0 is determined primarily by the factor $[B_1^2 + 4aC_1(T_0 - T)]^{-1/2}$. If $B_1^2 \gg 4aC_1(T_0 - T)$, then

$$(B_1^2 + 4aC_1(T_0 - T))^{-1/2} \approx 1/b(p - p_c); \qquad (22)$$

that is, the intensity of scattering near the critical point must be strongly dependent on the pressure. In the vicinity of the critical point even a small decrease of temperature below the phase transition temperature results in the opposite condition: $B_1^2 \ll 4aC_1(T_0 - T)$. In this case, with some approximation,

$$J_1/J_0 \sim 1/\sqrt{(T_0 - T)}. \qquad (23)$$

If the transition corresponds to the critical point ($p = p_c$), the relationship (23) begins to hold on condition that the terms with $A_{\gamma\gamma',\nu\nu'}\,q_\nu q_{\nu'}$ can be neglected.

In a first-order transition at the transition point $aC_1(T - T_0) = 3B_1^2/16$, that is,

$$[B_1^2 + 4aC_1(T_0 - T)]^{-1/2} = 2/B_1$$

and J_1/J_0 is also approximately inversely proportional to the difference $(p - p_c)$.

In the presence of an electric field parallel to the Z axis the scattering intensity can be determined from Eq. (16), replacing $\overline{P}$ by the solution of the equation

$$a(T - T_0)P + B_1 P^3 + C_1 P^5 = E \qquad (24)$$

and determining κ_{33} by means of the first part of the equality (20) for $1/\kappa_{33}$. Specifically, in weak fields

$$\overline{P} = \overline{P}_0 + \varkappa_{033} E, \qquad (25)$$

where $\overline{P}_0$ and κ_{033} are, respectively, the values of spontaneous polarization and the dielectric susceptibility κ_{33} with no field. In this case application of the field will lead to replacement of the factor $[B_1^2 + 4aC_1(T_0 - T)]^{-1/2}$ in Eq. (21) by

$$[B_1^2 + 4aC_1(T_0 - T)]^{-1/2}\left[1 - \frac{(B_1 + 6C_1\overline{P}_0^2)\varkappa_{033} E}{(B_1 + 2C_1\overline{P}_0^2)\overline{P}_0}\right]. \qquad (26)$$

Changes in the factor $(B_2 + C_2\overline{P}^2)^{-1}$ can be neglected at temperatures close to the phase transition temperature, when $C_2\overline{P}^2 \ll B_2$. It will be seen from Eq. (26) that if the electric field is parallel to the spontaneous polarization, the scattering intensity decreases, while if the field is directed in the direction opposite to the polarization, the intensity of scattering increases. In view of the fact that in the vicinity of the phase transition point the dielectric susceptibility is very great while the spontaneous polarization is small, there should be observed in relatively weak fields a strong influence of the electric field on the scattering of light, i.e., a unique electro-optical effect. Thus, for example, assuming $\overline{P}_0 \sim 10^4$ cgs electrostatic units ($\sim 1/5$ the saturation polarization for $BaTiO_3$) and $\kappa_{033} \sim 500$, we obtain that the electric field substantially changes the intensity of light scattering when the field intensity is of the order of $10^3 - 10^4$ v/cm.

Proceeding in an analogous fashion one can readily obtain the expressions for the scattering of light by ferroelectrics in which the spontaneous polarization vector is not directed along the cubic axis at $T < T_0$.

4. Crystals such as Rochelle salt and KH_2PO_4 exhibit piezoelectric attributes not only in the ferroelectric but also in the nonferroelectric state.[14,7] Fluctuation of the polarization in such crystals even in the nonferroelectric region produces a proportional fluctuation of the deformation. Inasmuch as deformation

of the crystal in turn changes the dielectric constant (for light) by an amount proportional to this deformation, the components of the tensor $\lambda_{\alpha\beta,\gamma}$ in Eq. (4) for crystals of this type are nonzero. In these crystals there is a preferred ferroelectric axis (OZ) at temperatures above the transition temperature, while in the vicinity of this temperature only the fluctuation of the component P_3 of the polarization vector becomes abnormally great. As follows from the general formulas (14) and (15), in the nonferroelectric region the terms containing the components of the tensor $\lambda_{\alpha\beta,\gamma\delta}$ vanish. In the ferroelectric region these terms can be neglected near the transition temperature. As a result Eq. (14) in the given case assumes the form

$$J_1/J_0 = g(1,2)/(\varkappa_{33}^{-1} + B_{33\nu}q_\nu + A_{33\nu\nu'}q_\nu q_{\nu'}), \tag{27}$$

where the quantity

$$g(1,2) = F(1,2)\,kT\,(\lambda_{\alpha\beta,3}e^1_\alpha e^2_\beta)^2 \tag{28}$$

can be assumed to be temperature independent near the phase transition temperatre. This quantity depends on the direction of propagation of the incident and scattered waves and on their polarization relative to the crystal and can be determined through measurements of the index of refraction (for different values of **k** and **e**) and its dependence on the electric field intensity. If the values of $\lambda_{\alpha\beta,\gamma\delta}$ and P_{3H} (where P_{3H} is the saturation polarization) are much greater than $\lambda_{\alpha\beta,\gamma}$, then somewhat below the transition temperature it is necessary to take account of the terms containing $\lambda_{\alpha\beta,\gamma\delta}$. In this case $g(1, 2)$ will strongly depend on the temperature:

$$g(1,2) = F(1,2)\,kT\,[(\lambda_{\alpha\beta,3} + 2\lambda_{\alpha\beta,33}P_3)e^1_\alpha e^2_\beta]^2. \tag{29}$$

In order to determine the temperature dependence of the intensity of scattering let us make use of the expansion* of the thermodynamic potential per unit volume in powers of P_3.[7]

$$\varphi = \varphi_0 + {}^1/_2\,a(T - T_0)P_3^2 + \frac{B_1}{4}P_3^4 + \frac{C_1}{6}P_3^6 - E_3P_3. \tag{30}$$

It follows from Eqs. (11), (30), and (28) that in the nonferroelectric region above the second-order phase transition temperature $T_0\kappa_{33} = 1/a(T - T_0)$ and that the intensity of scattering is

$$J_1/J_0 = g(1,2)/[a(T - T_0) + B_{33\nu}q_\nu + A_{33\nu\nu'}q_\nu q_{\nu'}]. \tag{31}$$

Thus, in contrast to the case of $BaTiO_3$ crystals, scattering of light by fluctuations of the polarization occurs in the present case not only in the ferroelectric but also in the nonferroelectric region. Moreover the intensity of scattering becomes abnormally great not only in the vicinity of the critical point but also near the second-order phase transition point. (The sum $A_{33\nu\nu'}q_\nu q_{\nu'}$ becomes comparable with $a(T - T_0)$ only at very small values of $T - T_0$.)

Below the temperature T_0 the spontaneous polarization is determined by expression (19) and the scattering intensity, according to (27), (11), (30), and (19), equals (cf. Ref. 15):

$$J_1/J_0 = g(1,2)C_1/[4aC_1(T_0 - T) + B_1^2 - B_1\sqrt{B_1^2 + 4aC_1(T_0 - T)} + C_1B_{33\nu}q_\nu + C_1A_{33\nu\nu'}q_\nu q_{\nu'}]. \tag{32}$$

If $B_1^2 \gg 4aC_1(T_0 - T)$, then

$$J_1/J_0 = g(1,2)/[2a(T_0 - T)B_{33\nu}q_\nu + A_{33\nu\nu'}q_\nu q_{\nu'}] \tag{33}$$

The inequality $B_1^2 \gg 4aC_1(T_0 - T)$ always holds in the case of ordinary phase transitions of the second order as well as in second-order phase transitions close to the critical point if $T_0 - T$ is sufficiently small. In the case of transitions close to the critical point, however, the inequality $B_1^2 \ll 4aC_1(T_0 - T)$ begins to obtain at relatively small values of $T_0 - T$ and in this case

---

* In the expansion (30) it is assumed that the component of the strain tensor $u_{\alpha\beta}$ are already expressed through the polarization P_3 (proportional to them) and eliminated from the expression for the thermodynamic potential. Analogously, in the expansion of $\epsilon^0_{\alpha\beta}$ the tensor $u_{\alpha\beta}$ is also eliminated, i.e., the expansion (4) is carried out not for a constant deformation but for a constant pressure.

$$J_1/J_0 = g(1,2)/[4a(T_0 - T) + B_{33\nu}q_\nu + A_{33\nu\nu'}q_\nu q_{\nu'}]. \tag{34}$$

In the case of a first-order phase transition close to the second-order transition, utilizing the expressions[15] for the second derivatives of the thermodynamic potential, we find that above the transition temperature in the nonferroelectric phase

$$J_1/J_0 = g(1,2)\,C_1/[3B_1^2/16 + C_1B_{33\nu}q_\nu + C_1A_{33\nu\nu'}q_\nu q_{\nu'}], \tag{35}$$

while below the transition temperature in the ferroelectric phase

$$J_1/J_0 = g(1,2)\,C_1/[3B_1^2/4 + C_1B_{33\nu}q_\nu + C_1A_{33\nu\nu'}q_\nu q_{\nu'}]. \tag{36}$$

Thus, if $C_1A_{33\nu\nu'}q_\nu q_{\nu'} \ll B_1^2$, then in case of a phase transition the first order to the ferroelectric phase the intensity of scattering is reduced by a factor of four.

5. The above analyses pertained only to single-component crystals. In binary solid solutions, in addition to fluctuations of the polarization, there are also fluctuations of the concentration of one of the solution components. These fluctuations are not statistically independent (cf. Ref. 16), which can lead to the appearance of new effects.

When there are concentration fluctuations Δc (with constant polarization), the components of the tensor $\epsilon^0_{\alpha\beta}$ change by amounts $\lambda_{\alpha\beta,4}\Delta c$ proportional to Δc. Consequently in solid solutions, where there are fluctuations of both the polarization and composition, the Fourier component of the dielectric constant is defined by an expression which is a generalization of (5):

$$\varepsilon_{\alpha\beta,\mathbf{q}} = [\lambda_{\alpha\beta,\mathbf{q}} + 2\lambda_{\alpha\beta,\gamma\delta}\bar{P}_\delta]\,P_{\gamma\mathbf{q}} + \lambda_{\alpha\beta,4}\,c_{\mathbf{q}}, \tag{37}$$

where $c_{\mathbf{q}}$ is the Fourier component of the concentration while the quantities $\lambda_{\alpha\beta,4}$ can be regarded as independent of $\mathbf{P}$ near the transition temperature. These constants correspond to changes in $\epsilon^0_{\alpha\beta}$ with changes of c at constant values of P_α. They are connected with the constants $\lambda'_{\alpha\beta,4}$, corresponding to changes in $\epsilon^0_{\alpha\beta}$ with changes in c at equilibrium values of P_α (which vary with changes in the composition) by the simple relationship

$$\lambda_{\alpha\beta,4} = \lambda'_{\alpha\beta,4} - \frac{\partial\varepsilon_{\alpha\beta}}{\partial P_\gamma}\frac{dP_\gamma}{dc}.$$

Substituting Eq. (37) in (1) we find that the light scattering intensity is expressed through the mean values $\overline{P_{\gamma\mathbf{q}}P^*_{\gamma'\mathbf{q}}}$, $\overline{P_{\gamma\mathbf{q}}c^*_{\mathbf{q}}}$ and $\overline{|c_{\mathbf{q}}|^2}$. These mean values, as before, can readily be found by considering the terms proportional to $\Delta P_\alpha \Delta P_\beta$, $\Delta P_\alpha \Delta c$ and $(\Delta c)^2$ in the expansion of the thermodynamic potential. Carrying out the same calculations as for the single-component ferroelectric, we find that in ferroelectric solid solutions the scattering intensity associated with fluctuations of polarization and composition is given by the expression

$$J_1/J_0 = F(1,2)\,kT\,[\lambda_{\alpha\beta,i}\lambda_{\alpha'\beta',i'}K^{-1}_{ii'} + 4\lambda_{\alpha\beta,i}\lambda_{\alpha'\beta',\gamma'\delta'}\bar{P}_{\delta'}K^{-1}_{i\gamma'} + 4\lambda_{\alpha\beta,\gamma\delta}\bar{P}_\delta\bar{P}_{\delta'}K^{-1}_{\gamma\gamma'}]\,e^1_\alpha e^1_{\alpha'} e^2_\beta e^2_{\beta'}. \tag{38}$$

[instead of Eq. (15)].

Here i and i' go through 1, 2, 3, and 4 (while γ and γ' run through 1, 2, and 3), the quantities $K^{-1}_{ii'}$ are matrix elements of the matrix that is the reciprocal of the matrix $K_{ii'}$, while the matrix elements of the latter matrix are

$$K_{ii'} = \varphi_{ii'} = \varkappa^{-1}_{ii'} \quad \text{with } i = 1,\ 2,\ 3 \qquad K_{i4} = K_{4i} = \varphi_{ic} \quad \text{with } i = 1,\ 2,\ 3 \quad K_{44} = \frac{\partial^2\varphi}{\partial c^2}. \tag{39}$$

Since the equilibrium condition $\varphi_\alpha = 0$ is fulfilled at all concentrations, we have

$$d\varphi_\alpha/dc = \varphi_{\alpha\alpha'}\,dP_{\alpha'}/dc + \varphi_{\alpha c} = 0.$$

Therefore

$$\varphi_{\alpha c} = -\varphi_{\alpha\alpha'}\,dP_{\alpha'}/dc = -\varkappa^{-1}_{\alpha\alpha'}\,dP_{\alpha'}/dc. \tag{40}$$

In the nonferroelectric region the derivatives dP_α/dc equal zero and the fluctuations of the polarization and of the composition are statistically independent. In the ferroelectric region some of the derivatives

$\varphi_{\alpha c}$ are nonzero; consequently these fluctuations become statistically dependent. Further the derivative φ_{cc} near the second-order phase transition temperature can be written in the form

$$\varphi_{cc} = N\,(\partial\mu_A/\partial c - \partial\mu_B/\partial c), \tag{41}$$

where N is the number of molecules per unit volume and μ_A and μ_B are the chemical potentials of the first and second components of the solution in the nonferroelectric region.

Thus all the quantities entering into expression (38) for the intensity of scattering by solid solutions of ferroelectrics, just as in the case of single component ferroelectrics, can be determined by means of independent experiments. To find these quantities one must determine the index of refraction and its dependence on the electric field intensity and the concentration, the static dielectric susceptibility tensor, and the dependence of the spontaneous polarization and the chemical potentials of the components on the composition. In the immediate vicinity of the transition temperature the tensor $K_{ii'}$ should be replaced by

$$K_{ii'} + B_{ii'\nu}q_\nu + A_{ii'\nu\nu'}q_\nu q_{\nu'}\ (i, i' = 1, 2, 3, 4;\ \nu, \nu' = 1, 2, 3),$$

where $B_{ii'\nu}$ and $A_{ii'\nu\nu'}$ near T_0 can be regarded as temperature independent.

In the case of cubic ferroelectrics in which the spontaneous polarization is directed along the cubic axis and which have a center of symmetry, $\lambda_{\alpha\beta,i} = 0$ with $i = 1, 2,$ and 3, $\lambda_{\alpha\beta,4} = \lambda_4\delta_{\alpha\beta}$ and the only one of the derivatives $\varphi_{\alpha c}$ that is nonzero is φ_{3c}. In this case for $T < T_0$, we obtain the following expression for the intensity of scattering

$$\begin{aligned}\frac{J_1}{J_0} = F(1,2)\,kT\Big\{&\frac{4\overline{P}^2\varkappa_{33}}{1-(\varphi_{3c})^2\varkappa_{33}/\varphi_{cc}}[\lambda^2_{33,33}(e^1_3)^2(e^2_3)^2 + \lambda^2_{11,33}(e^1_1e^2_1 + e^1_2e^2_2)^2 + 2\lambda_{33,33}\lambda_{11,33}e^1_3e^2_3(e^1_1e^2_1 + e^1_2e^2_2)]\\ &+ \lambda^2_{13,13}\overline{P}^2\varkappa_{11}[((e^1_1)^2 + (e^1_2)^2)(e^2_3)^2 + (e^1_3)^2((e^2_1)^2 + (e^2_2)^2) + 2(e^1_1e^2_1 + e^1_2e^2_2)e^1_3e^2_3]\\ &+ \frac{4\lambda_4\overline{P}\varphi_{3c}\varkappa_{33}(\mathbf{e}^1\mathbf{e}^2)}{\varphi_{cc}[1-(\varphi_{3c})^2\varkappa_{33}/\varphi_{cc}]}[\lambda_{33,33}e^1_3e^2_3 + \lambda_{11,33}(e^1_1e^2_1 + e^1_2e^2_2)] + \frac{\lambda^2_4}{\varphi_{cc}-(\varphi_{3c})^2\varkappa_{33}}\Big\},\end{aligned} \tag{42}$$

where F (1, 2) is defined by Eq. (17). In the nonferroelectric region with $T > T_0$

$$\frac{J_1}{J_0} = F(1,2)\,kT\lambda^2_4/\varphi_{cc}. \tag{43}$$

In solid solutions there is thus scattering of light by fluctuations of the concentration with $T > T_0$ as well. The intensity of scattering increases in the ferroelectric region.

The intensity of scattering can also be expressed in terms of the constants entering into the expansion (18) of the thermodynamic potential in powers of P_α. Invoking Eqs. (19) and (20) and the expression $\varphi_{3c} = -a\overline{P}dT_0/dc$ which is valid near the transition temperature, we obtain

$$\begin{aligned}\frac{J_1}{J_0F_1(1,2)kT} = {}&[B^2_1 + 4aC_1(T_0-T)]^{-1/2}\left[1 - a^2\left(\frac{dT_0}{dc}\right)^2\left(2\varphi_{cc}\sqrt{B^2_1 + 4aC_1(T_0-T)}\right)^{-1}\right]\varphi^{-1}_{cc}\,\{2\varphi_{cc}[\lambda^2_{33,33}(e^1_3)^2(e^2_3)^2\\ &+ \lambda^2_{11,33}(e^1_1e^2_1 + e^1_2e^2_2)^2 + 2\lambda_{33,33}\lambda_{11,33}e^1_3e^2_3(e^1_1e^2_1 + e^1_2e^2_2)] - 2\lambda_4 a\frac{dT_0}{dc}(\mathbf{e}^1\mathbf{e}^2)[\lambda_{33,33}e^1_3e^2_3 + \lambda_{11,33}(e^1_1e^2_1 + e^1_2e^2_2)]\\ &+ \lambda^2_4\sqrt{B^2_1 + 4aC_1(T_0-T)} + \frac{\lambda^2_{13,13}}{B_2 + C_2\overline{P}^2}[((e^1_1)^2 + (e^1_2)^2)(e^2_3)^2 + (e^1_3)^2((e^2_1)^2 + (e^2_2)^2) + 2(e^1_1e^2_1 + e^1_2e^2_2)e^1_3e^2_3]\}.\end{aligned} \tag{44}$$

In solid solutions the critical point lies at the point where the second-order phase transition curve goes over into the decomposition curve.[17,13] According to Landau,[17] instead of the condition $B_1 = 0$, which is true for single component crystals, we have at this point the condition

$$\varphi_{cc}B_1 = {}^1\!/_2\,(adT_0/dc)^2.$$

It is evident from (44) that in solid solutions there should also be observed abnormally great scattering in the vicinity of the critical point. This scattering is associated both with fluctuations of the polarization and with fluctuations of the concentration. Even if the index of refraction is only weakly influenced by the polarization, i.e., if the values of $\lambda_{\alpha\beta,\gamma\delta}$ are small, extremely intense scattering of light (provided λ_4 is not small) due to fluctuation of the composition should be observed in solid solutions close to the critical point.

In solid solutions of ferroelectrics such as Rochelle salt or KH_2PO_4, where the components of the tensor $\lambda_{\alpha\beta,\gamma}$ ($\gamma = 1, 2, 3$) are nonzero, in ordinary second-order phase transitions (far from the critical point) fluctuations of the composition near the temperature T_0 play a relatively minor part in the scattering of light. Hence above the transition temperature, where $\varphi_{3c} = 0$, we can as before use expressions (27) or (31). Below the transition temperature in the ferroelectric region one should replace $1/\kappa_{33}$ by $(1/\kappa_{33})[1 - (\varphi_{3c})^2\kappa_{33}/\varphi_{cc}]$ in the denominator of (27). In terms of the thermodynamic theory of phase transitions of the second order this reduces to replacement of $2a(T_0 - T)$ in the denominator of Eq. (33) by

$$2a(T_0 - T)[1 - a^2(dT_0/dc)^2/2B_1\varphi_{cc}].$$

6. The results deduced above, after appropriate modification of the designations, can obviously be fully applied to transparent ferromagnetic crystals. The results obtained by means of the theory of phase transitions of the second order can also be applied to antiferroelectric and antiferromagnetic materials in the absence of an external electric field where the former are concerned or a magnetic field where the latter are concerned. In the presence of an external electric field the state of an antiferroelectric is characterized by two vector parameters and the formulas for the intensity of light scattering, just as in the cases discussed above, can be obtained on the basis of the thermodynamic theory of phase transitions.[18]

All the expressions given above pertain to the scattering of light by a single crystal having no domains. A single crystal of this type can be realized by placing the ferroelectric in a capacitor.[7] Our results can also be applied to the scattering of light by individual domains provided their dimensions are appreciably greater than the wavelength of the light. If, however, the dimensions of the domains are of the same order of magnitude or smaller than the wavelength, then in addition to the scattering examined above there must also be evinced an additional extremely intense scattering by the domain walls.

In addition to scattering of light by the fluctuations of the polarization and the composition, in crystals there is always also some scattering connected with lattice vibrations. The intensity of this part of the scattering can be calculated[3] if the elastic and elastic-optical constants of the crystals are known. Both types of scattering can often be partially separated experimentally inasmuch as they depend in different ways on the temperature and external fields.

It would be of great interest to carry out an experimental investigation of light scattering near the points of second-order phase transitions in different ferroelectric materials with simultaneous measurements of the static dielectric constant, the index of refraction and its dependence on the electric field and the composition.

CONCLUSIONS

1. We have deduced equations for determining intensity and polarization of light scattered both by single-component ferroelectrics (or ferromagnets) of arbitrary structure and by solid solutions. All the quantities entering into the expressions for the scattering associated with fluctuations of the polarization (magnetization) and of the composition can be found (or evaluated) by means of independent measurements of the index of refraction and its dependence on the external field and the composition, static dielectric constant and the concentration dependence of the spontaneous polarization and the chemical potentials (for solid solutions).

2. If the expansion of the dielectric constant (for light) in powers of the components of the polarization vector contains linear terms (the case, for example, in crystals such as Rochelle salt or KH_2PO_4), then both below and above the second-order phase transition temperature there must be observed anomalously great scattering. If there are no linear terms in this expansion (for example, in crystals such as $BaTiO_3$), then scattering of the type in question will occur only in the ferroelectric (ferromagnetic) region and will be absent (in single component crystals) above the transition temperature.

3. The temperature dependence of the intensity of light scattering by crystals of the $BaTiO_3$ and crystals of the type of Rochelle salt and KH_2PO_4 was evaluated by means of the thermodynamic theory of phase transitions of the second order. In crystals of the $BaTiO_3$ type (both in single component ferroelectrics and solid solutions) particularly intense scattering should occur near the critical point on the second-order phase transition curve.

4. There should be observed an appreciable change in the intensity of scattering by ferroelectrics in an external electric field; this should occur in relatively weak fields (for $BaTiO_3$ type crystals, in fields

of the order of $10^3 - 10^4$ v/cm). In the vicinity of the critical point the scattering should be strongly dependent on the pressure.

---

[1] L. Ginzburg, Dokl. Akad. Nauk SSSR **105**, 240, (1955).

[2] Iakovlev, Mikheeva, and Velichkina, Кристаллография (Crystallography) **1**, 123 (1956).

[3] G. P. Motulevich, Izv. Akad. Nauk SSSR, Ser. fiz. **11**, 390 (1947).

[4] B. M. Vul and I. M. Gol'dman, Dokl. Akad. Nauk SSSR **46**, 154 (1954); **49**, 179 (1945).

[5] A. V. Rzhanov, Usp. Fiz. Nauk (Advances in Phys. Sciences) **38**, 461 (1949).

[6] V. L. Ginzburg, J. Exptl. Theoret. Phys. (U.S.S.R.) **15**, 739 (1945); **19**, 36 (1949).

[7] V. L. Ginzburg, Usp. Fiz. Nauk **38**, 490 (1949).

[8] A. F. Devonshire, Phil. Mag. **40**, 1040 (1949); **42**, 1065 (1951).

[9] J. C. Slater, Phys. Rev. **78**, 748 (1950).

[10] M. Ia. Shirobokov and L. P. Kholodenko, J. Exptl. Theoret. Phys. (U.S.S.R.) **21**, 1239 (1951).

[11] S. Triebwasser, Phys. Rev. **101**, 993 (1956).

[12] L. P. Kholodenko, J. Exptl. Theoret. Phys. (U.S.S.R.) **31**, 244 (1956), Soviet Phys. JETP **4**, 188 (1957).

[13] L. Landau and E. Lifshitz, Статистическая физика, (Statistical Physics), Moscow, 1951.

[14] W. G. Cady, Piezoelectricity, (Russ. Transl.).

[15] M. A. Krivoglaz, Український фізичний журнал (Ukrainian Physics Journal) **2**, 3 (1957).

[16] M. A. Krivoglaz, J. Exptl. Theoret. Phys. (U.S.S.R.) **31**, 625 (1956), Soviet Phys. JETP **4**, 293 (1957).

[17] L. D. Landau, J. Exptl. Theoret. Phys. (U.S.S.R.) **7**, 19 (1937).

[18] C. Kittel, Phys. Rev. **82**, 729 (1951). A. F. Devonshire, Adv. in Phys. **3**, 85 (1954). L. E. Cross, Phil. Mag. **1**, 76 (1956).

Translated by E. J. Rosen
21

SOVIET PHYSICS JETP VOLUME 6, NUMBER 1 JANUARY, 1958

ON THE EFFECTIVE FIELD IN A PLASMA

B. B. KADOMTSEV

Submitted to JETP editor December 25, 1956

J. Exptl. Theoret. Phys. (U.S.S.R.) **33**, 151-157 (July, 1957)

The Bogoliubov equations for the "partial distribution functions" are used to compute the effective field acting on charged particles in a plasma. It is shown that the effective field differs from the mean field by a small quantity of the order $1/N$ where N is the number of particles within a sphere whose radius is equal to the Debye radius. This result also holds in the presence of a magnetic field.

As is well known, the electric field acting on an individual particle of a medium is not equal to the average field in the medium. For example, in a gas of free dipoles the effective field $\mathbf{E}_{\text{eff}}$ is given by the Lorentz formula $\mathbf{E}_{\text{eff}} = \mathbf{E} + 4\pi\mathbf{P}/3$ where $\mathbf{E}$ is the average field and $\mathbf{P}$ is the polarization of the medium. This formula is obtained on the assumption that the molecular dipoles are mutually impenetrable so that each dipole behaves as if it were placed inside a cavity in a polarized medium.

In the case of ionized plasma there is, of course, no basis for such an assumption. However, the effective field in a plasma should also, generally speaking, differ from the average field because there exists a certain correlation between the motions of individual particles. The question of the relation between E_{eff} and E in a plasma has been repeatedly discussed by different authors (see Ginzburg[1] and the literature cited there), and it has been shown that the effective field and the average field are the same. The most detailed proof of this assertion has been given by Ginzburg.[1] However, he used a method which did not allow him to obtain explicit expressions for the effective fields. As a result of this, in particular, there has remained the unsolved problem as to whether the effective and the mean fields remain the same in the presence of an external magnetic field.

In this paper Bogoliubov's method[2] is used to compute the effective field in a plasma. In the course of this computation the triple function is expressed approximately in terms of binary ones which corresponds to making an expansion with respect to the small parameter $1/nD^3$ where n is the density of particles and D is the Debye radius. By this method an analogous expansion is introduced in establishing the connection between the effective and the average fields and we restrict ourselves to the calculation of only the first order correction.

For the sake of simplicity we assume that the plasma in addition to electrons also contains only singly ionized ions of a single kind. We introduce the "microscopic density" of particles in phase space

$$F_e = \sum_k \delta(\mathbf{r} - \mathbf{r}_k(t))\,\delta(\mathbf{v} - \mathbf{v}_k(t))$$

for the electrons and

$$F_i = \sum_k \delta(\mathbf{r} - \mathbf{r}_k(t))\,\delta(\mathbf{v} - \mathbf{v}_k(t))$$

for the ions, where the summation is taken over all the electrons and ions respectively. It can be easily shown that in the absence of a magnetic field these functions satisfy the equations

$$\frac{\partial F_e}{\partial t} + (\mathbf{v}\nabla)F_e - \frac{e}{m}\mathbf{E}_m\frac{\partial F_e}{\partial \mathbf{v}} = 0, \tag{1}$$

$$\frac{\partial F_i}{\partial t} + (\mathbf{v}\nabla)F_i + \frac{e}{M}\mathbf{E}_m\frac{\partial F_e}{\partial \mathbf{v}} = 0, \tag{2}$$

which correspond to the system of Newton's equations of motion for all the electrons and ions. In (1) and (2) m is the mass of the electron, M the mass of the ion, and $\mathbf{E}_m$ the microscopic field, which can be obtained from the equation

$$\operatorname{div}\mathbf{E}_m = 4\pi e\int (F_i - F_e)\,d\mathbf{v}, \tag{3}$$

but in doing so one must omit in (1) and (2) the self-field of the electron or of the ion which is situated at the particular point in space.

Equations (1) and (2) can also be written

$$\frac{\partial F_e}{\partial t} + (\mathbf{v}\nabla)F_e - \frac{e}{m}\mathbf{E}_0\frac{\partial F_e}{\partial \mathbf{v}} - \frac{e^2}{m}\frac{\partial}{\partial \mathbf{v}}\int\frac{\mathbf{r}-\mathbf{r}'}{|\mathbf{r}-\mathbf{r}'|^3}F_e(\mathbf{r},\mathbf{v},t)\{F_i(\mathbf{r}',\mathbf{v}',t) - F_e(\mathbf{r}',\mathbf{v}',t)\}\,d\mathbf{r}'d\mathbf{v}' = 0, \tag{4}$$

$$\frac{\partial F_i}{\partial t} + (\mathbf{v}\nabla)F_i + \frac{e}{M}\mathbf{E}_0\frac{\partial F_i}{\partial \mathbf{v}} + \frac{e^2}{M}\frac{\partial}{\partial \mathbf{v}}\int\frac{\mathbf{r}-\mathbf{r}'}{|\mathbf{r}-\mathbf{r}'|^3}F_i(\mathbf{r},\mathbf{v},t)\{F_i(\mathbf{r}',\mathbf{v}',t) - F_e(\mathbf{r}',\mathbf{v}',t)\}\,d\mathbf{r}'d\mathbf{v}' = 0, \tag{5}$$

where in accordance with the stipulation made above the point $\mathbf{r}' = \mathbf{r}$ must be excluded in carrying out the integration over $\mathbf{r}'$. In Eqs. (4) and (5) $\mathbf{E}_0$ represents the external field; it satisfies the equation $\operatorname{div}\mathbf{E}_0 = 0$.

We shall go over from the exact microscopic equations (1) – (5) to a statistical treatment, and in order to do this we shall average all the quantities over a certain set of initial particle distributions. This means that we regard the exact densities F_e and F_i as random quantities. We shall denote the average values of F_e and F_i by f_e and f_i. The averaging of Eq. (3) yields

$$\operatorname{div}\mathbf{E} = 4\pi e\int\{f_i - f_e\}\,d\mathbf{v}, \tag{6}$$

where **E** denotes the average, i.e., the macroscopic field. On averaging (4) we obtain an equation which contains the binary distribution function:

$$\frac{\partial f_e}{\partial t} + (\mathbf{v}\nabla)f_e - \frac{e}{m}\mathbf{E}_0\frac{\partial f_e}{\partial \mathbf{v}} - \frac{e^2}{m}\frac{\partial}{\partial \mathbf{v}}\int\frac{\mathbf{r}-\mathbf{r}'}{|\mathbf{r}-\mathbf{r}'|^3}\{f_{ei}(\mathbf{r},\mathbf{v};\mathbf{r}',\mathbf{v}';t) - f_{ee}(\mathbf{r},\mathbf{v};\mathbf{r}',\mathbf{v}';t)\}\,d\mathbf{r}'d\mathbf{v}' = 0. \tag{7}$$

Here

$$f_{ei}(\mathbf{r},\mathbf{v};\mathbf{r}',\mathbf{v}';t)=\langle F_e(\mathbf{r},\mathbf{v},t)\,F_i(\mathbf{r}',\mathbf{v}',t)\rangle,$$

(the brackets denote averaging) is the binary distribution function for electrons and ions. With respect to the average value of F_eF_e' we can see that, strictly speaking, it is equal to

$$\langle F_e(\mathbf{r},\mathbf{v},t)\,F_e(\mathbf{r}',\mathbf{v}',t)\rangle=\langle\sum_j\delta(\mathbf{r}-\mathbf{r}_j)\,\delta(\mathbf{v}-\mathbf{v}_j)\,\delta(\mathbf{r}'-\mathbf{r}_j)\,\delta(\mathbf{v}'-\mathbf{v}_j)\rangle$$

$$+\langle\sum_{j\neq k}\delta(\mathbf{r}-\mathbf{r}_j)\,\delta(\mathbf{v}-\mathbf{v}_j)\,\delta(\mathbf{r}'-\mathbf{r}_k)\,\delta(\mathbf{v}'-\mathbf{v}_k)\rangle=\delta(\mathbf{r}-\mathbf{r}')\,\delta(\mathbf{v}-\mathbf{v}')\,f_e(\mathbf{r},\mathbf{v},t)+f_{ee}(\mathbf{r},\mathbf{v};\mathbf{r}',\mathbf{v}';t),$$

where the binary function f_{ee} is the "non-singular" part of the average value of F_eF_e'. However, since in the integration over $\mathbf{r}'$ we have excluded the point $\mathbf{r}'=\mathbf{r}$ the term with the δ-functions turns out to be unimportant in the present case.

We assume that the electrostatic interaction energy of the particles is much smaller than their kinetic energy, i.e., $e^2n^{1/3}\ll kT$, which is equivalent to the condition $nD^3\gg 1$. This condition is almost always fulfilled. It is evident that under this condition the correlation between the particles is very small, so that we may write $f(\mathbf{r},\mathbf{v};\mathbf{r}',\mathbf{v}',t)=f(\mathbf{r},\mathbf{v},t)f(\mathbf{r}',\mathbf{v}',t)+\varphi(\mathbf{r},\mathbf{v};\mathbf{r}',\mathbf{v}',t)$ where φ is a small quantity. In accordance with this, Eq. (7) and the analogous equation for f_i can be brought into the form

$$\frac{\partial f_e}{\partial t}+(\mathbf{v}\nabla)f_e-\frac{e}{m}\mathbf{E}\frac{\partial f_e}{\partial\mathbf{v}}-\frac{e^2}{m}\frac{\partial}{\partial\mathbf{v}}\int\frac{\mathbf{r}-\mathbf{r}'}{|\mathbf{r}'-\mathbf{r}'|^3}\{\varphi_{ei}(\mathbf{r},\mathbf{v};\mathbf{r}',\mathbf{v}';t)-\varphi_{ee}(\mathbf{r},\mathbf{v};\mathbf{r}',\mathbf{v}';t)\}\,d\mathbf{r}'d\mathbf{v}'=0, \qquad (8)$$

$$\frac{\partial f_i}{\partial t}+(\mathbf{v}\nabla)f_i+\frac{e}{M}\mathbf{E}\frac{\partial f_i}{\partial\mathbf{v}}+\frac{e^2}{M}\frac{\partial}{\partial\mathbf{v}}\int\frac{\mathbf{r}-\mathbf{r}'}{|\mathbf{r}-\mathbf{r}'|^3}\{\varphi_{ii}(\mathbf{r},\mathbf{v};\mathbf{r}',\mathbf{v}';t)-\varphi_{ie}(\mathbf{r},\mathbf{v};\mathbf{r}',\mathbf{v}';t)\}\,d\mathbf{r}'d\mathbf{v}'=0. \qquad (9)$$

Our problem consists of finding the functions $\varphi_{\alpha\beta}$. In order to do this we shall set up equations for the binary distribution functions. We shall here discuss in detail only the equation for f_{ei} — the discussion of the other equations can be carried out in a completely analogous fashion.

We multiply Eq. (4) by $F_i(\mathbf{r}',\mathbf{v}',t)$, replace in (5) $\mathbf{r},\mathbf{v}$ by $\mathbf{r}',\mathbf{v}'$ and after multiplying it by $F_e(\mathbf{r},\mathbf{v},t)$ we then add the results and take the average. Taking into account the fact that

$$\langle F_e(\mathbf{r},\mathbf{v},t)\,F_e(\mathbf{r}',\mathbf{v}',t)\,F_i(\mathbf{r}'',\mathbf{v}'',t)\rangle=f_{eei}(\mathbf{r},\mathbf{v};\mathbf{r}',\mathbf{v}';\mathbf{r}'',\mathbf{v}'';t)+\delta(\mathbf{r}-\mathbf{r}')\,\delta(\mathbf{v}-\mathbf{v}')\,f_{ei}(\mathbf{r},\mathbf{v};\mathbf{r}'',\mathbf{v}'';t)$$

etc., we obtain

$$\frac{\partial f_{ei}(\mathbf{r},\mathbf{v};\mathbf{r}'\,\mathbf{v}';t)}{\partial t}+(\mathbf{v}\nabla)f_{ei}+(\mathbf{v}'\nabla')f_{ei}-\frac{e}{m}\mathbf{E}_0\frac{\partial f_{ei}}{\partial\mathbf{v}}+\frac{e}{M}\mathbf{E}_0'\frac{\partial f_{ei}}{\partial\mathbf{v}'}-\frac{e^2(\mathbf{r}-\mathbf{r}')}{m|\mathbf{r}-\mathbf{r}'|^3}\frac{\partial f_{ei}}{\partial\mathbf{v}}+\frac{e^2(\mathbf{r}-\mathbf{r}')}{M|\mathbf{r}-\mathbf{r}'|^3}\frac{\partial f_{ei}}{\partial\mathbf{v}'}$$

$$-\frac{e^2}{m}\frac{\partial}{\partial\mathbf{v}}\int\frac{\mathbf{r}-\mathbf{r}''}{|\mathbf{r}-\mathbf{r}''|^3}\{f_{eii}(\mathbf{r},\mathbf{v};\mathbf{r}',\mathbf{v}';\mathbf{r}'',\mathbf{v}'';t)-f_{eie}(\mathbf{r},\mathbf{v};\mathbf{r}',\mathbf{v}';\mathbf{r}'',\mathbf{v}'';t)\}\,d\mathbf{r}''d\mathbf{v}''$$

$$+\frac{e^2}{M}\frac{\partial}{\partial\mathbf{v}'}\int\frac{\mathbf{r}'-\mathbf{r}''}{|\mathbf{r}'-\mathbf{r}''|^3}\{f_{eii}(\mathbf{r},\mathbf{v};\mathbf{r}',\mathbf{v}';\mathbf{r}'',\mathbf{v}'';t)-f_{eie}(\mathbf{r},\mathbf{v};\mathbf{r}',\mathbf{v}';\mathbf{r}'',\mathbf{v}'';t)\}\,d\mathbf{r}'',d\mathbf{v}''=0. \qquad (10)$$

In accordance with the assumption made earlier concerning the smallness of the correlation, we write

$$f(\mathbf{r},\mathbf{v};\mathbf{r}',\mathbf{v}';\mathbf{r}'',\mathbf{v}'';t)=f(\mathbf{r},\mathbf{v},t)\,f(\mathbf{r}',\mathbf{v}',t)\,f(\mathbf{r}'',\mathbf{v}'',t)+f(\mathbf{r},\mathbf{v},t)\,\varphi(\mathbf{r}',\mathbf{v}';\mathbf{r}'',\mathbf{v}'';t)$$

$$+f(\mathbf{r}',\mathbf{v}',t)\,\varphi(\mathbf{r},\mathbf{v};\mathbf{r}'',\mathbf{v}'';t)+f(\mathbf{r}'',\mathbf{v}'',t)\,\varphi(\mathbf{r},\mathbf{v};\mathbf{r}',\mathbf{v}';t)+\psi(\mathbf{r},\mathbf{v};\mathbf{r}',\mathbf{v}';\mathbf{r}'',\mathbf{v}'';t)$$

and neglect the last term on the right hand side. Then on taking (8) and (9) into account we obtain from (10)

$$\frac{\partial\varphi_{ei}(\mathbf{r},\mathbf{v};\mathbf{r}',\mathbf{v}';t)}{\partial t}+(\mathbf{v}\nabla)\varphi_{ei}+(\mathbf{v}'\nabla')\varphi_{ei}-\frac{e^2(\mathbf{r}-\mathbf{r}')}{m|\mathbf{r}-\mathbf{r}'|^3}\frac{\partial f_e}{\partial\mathbf{v}}f_i'-\frac{e^2(\mathbf{r}'-\mathbf{r})}{M|\mathbf{r}'-\mathbf{r}|^3}f_e\frac{\partial f_i'}{\partial\mathbf{v}'}-\frac{e}{m}\mathbf{E}\frac{\partial\varphi}{\partial\mathbf{v}}+\frac{e}{M}\mathbf{E}'\frac{\partial\varphi_{ei}}{\partial\mathbf{v}'}$$

$$=\frac{e^2(\mathbf{r}-\mathbf{r}')}{M|\mathbf{r}-\mathbf{r}'|^3}\frac{\partial\varphi_{ei}}{\partial\mathbf{v}}+\frac{e^2(\mathbf{r}'-\mathbf{r})}{M|\mathbf{r}'-\mathbf{r}|^3}\frac{\partial\varphi_{ei}}{\partial\mathbf{v}'}+\frac{e^2}{m}\frac{\partial f_e}{\partial\mathbf{v}}\int\frac{\mathbf{r}-\mathbf{r}''}{|\mathbf{r}-\mathbf{r}''|^3}\{\varphi_{ii}(\mathbf{r}',\mathbf{v}';\mathbf{r}'',\mathbf{v}'';t)-\varphi_{ie}(\mathbf{r}',\mathbf{v}';\mathbf{r}'',\mathbf{v}'';t)\}\,d\mathbf{r}''d\mathbf{v}''$$

$$+\frac{e^2}{M}\frac{\partial f_i'}{\partial\mathbf{v}'}\int\frac{\mathbf{r}'-\mathbf{r}''}{|\mathbf{r}'-\mathbf{r}''|^3}\{\varphi_{ee}(\mathbf{r},\mathbf{v};\mathbf{r}'',\mathbf{v}'';t)-\varphi_{ei}(\mathbf{r},\mathbf{v};\mathbf{r}'',\mathbf{v}'';t)\}\,d\mathbf{r}''d\mathbf{v}''. \qquad (11)$$

The quantities appearing on the right hand side of this equation are small, but they cannot be simply neglected since they turn out to be essential for large and for small values of $|\mathbf{r} - \mathbf{r}'|$. In contrast to the method adopted by Bogoliubov[2] of expanding in terms of a small parameter, we shall solve (11) in the following way. First we solve the stationary equation. We set

$$E = 0, \; f_e = n\left(\frac{m}{2\pi kT_e}\right)^{3/2}\exp\left(-\frac{mv^2}{2kT_e}\right), \; f_i = n\left(\frac{M}{2\pi kT_i}\right)^{3/2}\exp\left(-\frac{Mv^2}{2kT_i}\right), \; \varphi_{ee} = f_e f'_e \chi(|\mathbf{r} - \mathbf{r}'|)$$

etc., where n is the density of electrons (and ions), T_e the electron temperature, and T_i the ion temperature. We substitute this into (11) and in accordance with the assumption that $T_e \neq T_i$ we neglect the velocity of the ions in comparison with the velocity of the electrons. Since **v** is arbitrary we obtain

$$\nabla\chi_{ei}(r) + \frac{e^2\mathbf{r}}{kT_e r^3} = -\frac{e^2\mathbf{r}}{kT_e r^3}\chi_{ei}(r) - \frac{ne^2}{kT_e}\int\frac{\mathbf{r} - \mathbf{r}'}{|\mathbf{r} - \mathbf{r}'|^3}\{\chi_{ii}(r') - \chi_{ei}(r')\}\,d\mathbf{r}'. \tag{12}$$

For $r > e^2/kt$ we may neglect the first term on the right hand side and from this, taking it into account that $\chi \to 0$ as $r \to \infty$, we obtain:

$$\chi_{ei}(r) - \frac{ne^2}{kT_e}\int\frac{1}{|\mathbf{r} - \mathbf{r}'|}\{\chi_{ii}(r') - \chi_{ei}(r')\}\,d\mathbf{r}' = \frac{e^2}{rkT_e}. \tag{13}$$

In a similar fashion we can obtain equations for χ_{ee} and χ_{ii}

$$\chi_{ee}(r) - \frac{ne^2}{kT_e}\int\frac{1}{|\mathbf{r} - \mathbf{r}'|}\{\chi_{ei}(r') - \chi_{ee}(r')\}\,d\mathbf{r}' = -\frac{e^2}{rkT_e}, \tag{14}$$

$$\chi_{ii}(r) - \frac{ne^2}{kT_i}\int\frac{1}{|\mathbf{r} - \mathbf{r}'|}\{\chi_{ei}(r') - \chi_{ii}(r')\}\,d\mathbf{r}' = -\frac{1}{r}\,\frac{e^2}{kT_i}. \tag{15}$$

The solution of the system of equations (13) – (15) is

$$\chi_{ei}(r) = -\chi_{ee}(r) = (e^2/kT_e)\,e^{-r/D}/r, \quad \chi_{ii} = -(e^2/kT_i)\,e^{-r/D}/r, \tag{16}$$

where D is the Debye radius:

$$D = \{kT_e T_i/4\pi e^2 n(T_e + T_i)\}^{1/2}.$$

At distances smaller than e^2/kT Eq. (12) does not have a sensible solution. This is explained by the fact that the coincidence of particles of opposite sign, i.e., the formation of bound states, turns out to be statistically more favorable. Therefore, strictly speaking, a quantum mechanical treatment is required for the investigation of this region. However, one can make classical mechanics serve the purpose if one entirely excludes all elliptic orbits whose formation is not very probable as it requires triple collisions. In doing this it would be necessary to solve Eq. (11) without assuming a Maxwellian velocity distribution. Such a solution presents no difficulties but requires awkward calculations. Since the region of small $(\mathbf{r} - \mathbf{r}')$ occupies a small portion of the correlation region and makes only a small contribution to the final result, we shall not undertake this task. We shall simply neglect the first two terms in the right hand side of Eq. (11), which is equivalent to neglecting the bending of the particle trajectory as a result of collisions. In accordance with this we shall in future exclude collisions with impact parameters smaller than $\rho_0 = e^2/kT$.

We shall assume that the functions f_e and f_i do not differ appreciably from the Maxwellian ones. Then one can substitute the solutions $\varphi_{\alpha\beta} = f_\alpha f'_\beta \chi_{\alpha\beta}(|\mathbf{r} - \mathbf{r}'|)$ found above into the right hand side of Eq. (11), which is small in terms of $1/nD^3$. By limiting ourselves to the linear approximation for the field we substitute the stationary solution also into the last two terms in the left hand side of Eq. (11). From this, after setting for convenience $\varphi_{\alpha\beta} = \varphi'_{\alpha\beta} + \varphi''_{\alpha\beta}$, we obtain:

$$\frac{\partial\varphi'_{ei}}{\partial t} + (\mathbf{v}\nabla)\varphi'_{ei} + (\mathbf{v}'\nabla')\varphi'_{ei} = -\frac{e\mathbf{v}}{kT_e}\mathbf{E}(r, t)\,\chi_{ei}(|\mathbf{r} - \mathbf{r}'|)\,f_e(\mathbf{r}, \mathbf{v}, t)\,f_i(\mathbf{r}', \mathbf{v}', t)$$

$$+ \frac{e\mathbf{v}'}{kT_i}\mathbf{E}(\mathbf{r}', t)\,\chi_{ei}(|\mathbf{r} - \mathbf{r}'|)\,f_e(\mathbf{r}, \mathbf{v}, t)\,f_i(\mathbf{r}', \mathbf{v}', t); \tag{17}$$

$$\frac{\partial\varphi''_{ei}}{\partial t} + (\mathbf{v}\nabla)\varphi''_{ei} + (\mathbf{v}'\nabla')\varphi''_{ei} = \left\{\frac{1}{m}\,\frac{\partial f_e(\mathbf{r}, \mathbf{v}, t)}{\partial\mathbf{v}}\,f_i(\mathbf{r}', \mathbf{v}', t) - \frac{1}{M}\,f_e(\mathbf{r}, \mathbf{v}, t)\,\frac{\partial f_i(\mathbf{r}', \mathbf{v}', t)}{\partial\mathbf{v}'}\right\}\nabla U(|\mathbf{r} - \mathbf{r}'|), \tag{18}$$

where $U(r) = -e^2 e^{-r/D}/r$. Analogous equations may also be obtained for φ_{ee} and φ_{ii}.

If one substitutes the solutions of these equations into (8), (9) then terms of the form $\varphi''_{\alpha\beta}$ will give rise to the collision term (see Appendix), while $\varphi'_{\alpha\beta}$ will give the correction to the average field. We define the effective fields $\mathbf{E}^{e}_{\text{eff}}$ for the electrons and $\mathbf{E}^{i}_{\text{eff}}$ for the ions by means of the relation:

$$\mathbf{E}^{\alpha}_{\text{ef}} = \mathbf{E} + [f_\alpha(\mathbf{r},\mathbf{v},t)]^{-1}\int \frac{(\mathbf{r}-\mathbf{r}')}{|\mathbf{r}-\mathbf{r}'|^3}\{\varphi'_{\alpha i}(\mathbf{r},\mathbf{v};\mathbf{r}',\mathbf{v}';t) - \varphi_{\alpha e}(\mathbf{r},\mathbf{v};\mathbf{r}',\mathbf{v}';t)\}\,d\mathbf{r}'d\mathbf{v}'.$$

Then the kinetic equations can be written in the following form:

$$\frac{\partial f_e}{\partial t} + (\mathbf{v}\nabla) f_e - \frac{e}{m}\frac{\partial}{\partial \mathbf{v}}\mathbf{E}^{e}_{\text{ef}} f_e = \text{St}(f_e), \qquad \frac{\partial f_i}{\partial t} + (\mathbf{v}\nabla) f_i + \frac{e}{M}\frac{\partial}{\partial \mathbf{v}}\mathbf{E}^{i}_{\text{ef}} f_i = \text{St}(f_i),$$

where St denotes the collision term.

In order to find explicit expressions for the effective fields one must solve Eq. (17) and the analogous equations for φ'_{ee} and φ'_{ii}. In Eq. (17) we may neglect terms proportional to the ion velocity, and its solution is then given in the form:

$$\varphi'_{ei}(\mathbf{r},\mathbf{v};\mathbf{r}',\mathbf{v}';t) = -f_e(\mathbf{v}) f_i(\mathbf{v}') \int_{-\infty}^{t} \frac{e\mathbf{v}}{kT_{e_i}}\mathbf{E}(\mathbf{r}-\mathbf{v}(t-t'),t')\,\chi_{ei}(|\mathbf{r}-\mathbf{v}(t-t')-\mathbf{r}'|)\,dt', \tag{19}$$

where we have taken the functions f_e, f_i outside the integral having assumed that they do not change over a distance ~ D and during a time $\sim 1/\omega_0$ where $\omega_0 = \sqrt{4\pi e^2 n/m}$ is the plasma oscillation frequency.

Substituting (19) and the similar solutions for φ'_{ee} and φ'_{ii} into (8) and (9) we can easily obtain expressions for the effective fields. Since they depend on the velocity of the particle in a fairly complicated manner we shall average over this velocity. The terms with φ'_{ee} and φ'_{ii} evidently drop out as a result. We set $\mathbf{E} \sim e^{i\omega t}$ and we neglect in (19) the dependence of **E** on **r** by assuming that the wavelength $\lambda \gg D$. Then up to terms in $1/nD^3$ we obtain

$$\langle \mathbf{E}^{e}_{\text{eff}}\rangle_v = \langle \mathbf{E}^{i}_{\text{eff}}\rangle_v = \begin{cases} \mathbf{E}[1 - T_i^2/12\pi nD^3(T_i+T_e)^2] & \text{for } \omega \ll \omega_0, \\ \mathbf{E}[1 - (\omega_0/i\omega)\sqrt{2}\cdot T_i^{2}/12\pi^{3/2} nD^3(T_i+T_e)^2] \approx \mathbf{E} & \text{for } \omega \gg \omega_0. \end{cases} \tag{20}$$

We see that in a plasma the effective field coincides with the average field under the condition $nD^3 \gg 1$ which is usually fulfilled. For example, in the ionosphere, where according to Ginzburg[1] $n \sim 10^{16}$, $T \sim 300°$, we obtain $E_{\text{eff}} - E \sim 10^{-5}E$.

The difference between E_{eff} and E increases as the density increases and as the temperature decreases. However, even in an electric spark,[4] where $n \sim 10^{17}$, $T \sim (4 \times 10^4)°$, the difference is $E_{\text{eff}} - E \sim 10^{-3}E$, i.e., still negligibly small.

The calculation of the effective field can be easily generalized to the case when a constant magnetic field **H** is present. For this it is sufficient merely to add to (17) the Lorentz force term $-(e/c)\mathbf{v}\times\mathbf{H}$. For a field sufficiently weak so that $\Omega = eH/mc \ll \omega_0$ this leads to the same result as before, while in the opposite case when $\Omega \gg \omega_0$.

$$\langle \mathbf{E}^{e}_{\text{eff}}\rangle_v = \langle \mathbf{E}^{i}_{\text{eff}}\rangle_v = \begin{cases} \mathbf{E} - \dfrac{T_i^2}{4\pi nD^3(T_i+T_e)^2}\dfrac{\mathbf{H}(\mathbf{HE})}{H^2} & \text{for } \omega \ll \omega_0, \\ \approx \mathbf{E} & \text{for } \omega \gg \omega_0 \end{cases} \tag{21}$$

We see that the frequency $\omega = \Omega$ is not distinguished in any way. This can be easily understood since during the transit time of the electron through the correlation region which is of order $\sim 1/\omega_0$ no resonance effects have time to make themselves felt.

It is easy to see the physical reason for the difference between the effective field from the average field. In the equilibrium state a correlated electron "cloud" is formed near each ion. When an electric field is applied this "cloud" is displaced with respect to the ion, producing an additional field directed oppositely to the average field. In a strong magnetic field such a "polarization" occurs only along the magnetic field, which accounts for the form of formula (21).

APPENDIX

For the sake of completeness we shall briefly examine here the manner in which the collision term originates. We shall consider that the functions f_e and f_i vary sufficiently smoothly that they remain essentially constant over a distance D. Then it is possible in Eq. (18) first to neglect the time derivative and second to assume that $\varphi''_{ei} = \varphi_{ei}(\mathbf{r}-\mathbf{r}',\mathbf{v},\mathbf{v}')$. On introducing a cylindrical coordinate system with the z axis directed along $\mathbf{v} - \mathbf{v}'$, and on setting $\varphi''_{ei} = 0$ for $z = -\infty$ we obtain from (18):

$$\varphi''_{ei}(\rho, \varphi, z; \mathbf{v}, \mathbf{v}') = \left\{ \frac{1}{m} \frac{\partial f_e(\mathbf{v})}{\partial \mathbf{v}} f_i(\mathbf{v}') - \frac{1}{M} f_e(\mathbf{v}) \frac{\partial f_i(\mathbf{v}')}{\partial \mathbf{v}'} \right\} \nabla \int_{-\infty}^{z} \frac{U(\sqrt{\rho^2 + z^2})}{|\mathbf{v} - \mathbf{v}'|} dz'$$

and similarly for φ''_{ii} and φ''_{ee}.

Substituting this into (7) and carrying out some straightforward calculations we obtain the collision term in Landau's form:[3]

$$\mathrm{St}(f_\alpha) = \left(\frac{2\pi e^4}{m_\alpha}\right) \ln\left(\frac{D}{\rho_0}\right) \sum_\beta \sum_{k,j=1}^{3} \frac{\partial}{\partial v_k} \int \frac{u^2 \delta_{jk} - u_j u_k}{u^3} \left\{ \frac{1}{m_\alpha} \frac{\partial f_\alpha(\mathbf{v})}{\partial v_j} f_\beta(\mathbf{v}') - \frac{1}{m_\beta} f_\alpha(\mathbf{v}) \frac{\partial f_\beta(\mathbf{v}')}{\partial v'_j} \right\} d\mathbf{v}'.$$

Here $\alpha, \beta = e, i$, $u_k = v_k - v'_k$ is the k-th component of the relative velocity, and ρ_0 is the minimum impact parameter.

We note that in such a derivation the cut-off at the maximum impact parameter is taken into account automatically, while if Eq. (11) had been solved more accurately, the cut-off at the lower limit would also have come out automatically.

I express my sincere thanks to Academician M. A. Leontovich for discussions of this work.

---

[1] V. L. Ginzburg, Теория распространения радиоволн в ионосфере (Theory of the Propagation of Radio Waves in the Ionosphere), GITTL, 1949.

[2] N. N. Bogoliubov, Проблемы динамической теории в статистической физике (Problems of Dynamical Theory in Statistical Physics), GITTL, 1946.

[3] L. D. Landau, J. Exptl. Theoret. Phys. (U.S.S.R.) 7, 203 (1937).

[4] S. L. Mandel'shtam and N. K. Sukhodrev, J. Exptl. Theoret. Phys. (U.S.S.R.) 24, 701 (1953).

Translated by G. Volkoff
22

SOVIET PHYSICS JETP VOLUME 6, NUMBER 1 JANUARY, 1958

DECAY LAW FOR THE CONCENTRATION OF NON-EQUILIBRIUM CHARGE CARRIERS IN SEMICONDUCTORS

G. M. GOUREAU

P. N. Lebedev Physical Institute, Academy of Sciences, U.S.S.R.

Submitted to JETP editor December 25, 1956

J. Exptl. Theoret. Phys. (U.S.S.R.) 33, 158-165 (July, 1957)

Decay processes are considered for non-equilibrium carriers generated uniformly throughout the volume of a semiconductor. The decay law is found for the concentration of non-equilibrium carriers in a semiconductor containing a small concentration of recombination centers (traps), for arbitrary departures from thermal equilibrium. Approximate expressions for this law are obtained for various ranges of variation of the concentration of the non-equilibrium carriers. These expressions correspond to various kinetic patterns of recombination. It is shown that alongside such well known patterns as the monomolecular and the bimolecular, there is also a type of recombination at a steady rate corresponding to a lifetime proportional to the concentration of the non-equilibrium carriers. This occurs at low temperatures in semiconductors in which the recombination cross-section for the minority carriers is much larger than that for the majority carriers.

A paper by Adirovich and the writer[1] examined the problem of the existence of characteristic times of stationary and nonstationary electronic processes in semiconductors. In this connection a law was obtained for the decay of non-equilibrium carriers in the case of low generation level and arbitrary concentration of traps (recombination centers).

When the concentration of traps is sufficiently large, the characteristic times turn out to be different from the characteristic times of the stationary processes, as found by Shockley and Read.[2] In the present paper a study is made of the kinetics of the nonstationary process of decay of non-equilibrium carriers for the case of small concentration of traps and arbitrary level of generation, and the laws of the process under these conditions are found.

1. STATEMENT AND SOLUTION OF THE PROBLEM

During the process of decay the kinetics of the electronic processes, for uniform generation, are described by the equations*

$$dn/dt = -A_e n p_t + B_e n_t, \quad n_t + p_t = N_t, \quad dp/dt = -A_t p n_t + B_t p_t, \quad p - n - n_t = N_a - N_d - \delta. \tag{1}$$

The separation of the concentrations into equilibrium and non-equilibrium parts ($n = n_0 + n'$, and so on) leads to the following way of writing this system:

$$dn'/dt = -A_e p_{t0} n' + A_e (n_0 + n_1) n'_t - A_e n' p'_t, \quad dp'/dt = -A_h n_{t0} p' + A_h (p_0 + p_1) p'_t - A_h p' n'_t,$$

$$p' = n' + n'_t, \quad p'_t = -n'_t, \tag{2}$$

and linearization of the system with respect to the excess concentrations is possible only in the special case of small levels of generation. We shall carry out the calculation of the decay law in the general nonlinear case by the method used by Adirovich to obtain the decay law for crystalline phosphors.[3]

We assume that the concentrations of electrons and holes localized in the traps (recombination centers) are small in comparison with the corresponding concentrations in the zones. In this case

$$n' \approx p', \tag{3}$$

$$dn'/dt \approx dp'/dt. \tag{4}$$

---

* In the present paper we adopt the notation of Refs. 1 and 2.

Equating the expressions for dn′/dt and dp′/dt from the system (2) and replacing p′ by n′, we arrive at the following expression for the concentration of non-equilibrium electrons localized in the traps

$$n_t' = \frac{(A_e p_{t0} - A_h n_{t0})\, n'}{A_h (n_0 + n_1) + A_h (p_0 + p_1) + (A_e + A_h)\, n'}. \tag{5}$$

Introducing the lifetimes τ_0, τ_{p0}, τ_{n0},[2]

$$\tau_0 = \tau_0 \frac{n_0 + n_1}{n_0 + p_0} + \tau_{p0} \frac{p_0 + p_1}{n_0 + p_0}; \quad \tau_{n0} = \frac{1}{A_e N_t}; \quad \tau_{p0} = \frac{1}{A_h N_t}, \tag{6}$$

we put the relation (5) in the form:

$$n_t' = (\tau_{p0} p_{t0} - \tau_{n0} n_{t0})\, n' / [(n_0 + p_0)\, \tau_0 + (\tau_{p0} + \tau_{n0})\, n']. \tag{7}$$

Substituting n_t' from Eq. (7) into the first equation of the system (2), we get the differential equation

$$-\frac{dn'}{dt} = \frac{(n_0 + p_0)\, n' + (n')^2}{(n_0 + p_0)\, \tau_0 + n' (\tau_{p0} + \tau_{n0})},$$

and integration of this under the initial condition n′ = Δn at t = 0 gives the desired decay law

$$\exp\left(-\frac{t}{\tau_{p0} + \tau_{n0}}\right) = \frac{n'}{\Delta n} \left(\frac{1 + (n_0 + p_0)/n'}{1 + (n_0 + p_0)/\Delta n}\right)^{1 - \tau_0/(\tau_{p0} + \tau_{n0})} \tag{8}$$

Let us now determine the physical conditions corresponding to the assumptions (3) and (4), on which the decay law (8) is based. Since $p' = n' + n_t'$, the assumption (3) and (4) are equivalent to the inequalities

$$n_t' \ll n', \quad |dn_t'/dt| \ll |dn'/dt|.$$

From expression (5) it follows that

$$\left|\frac{n_t'}{n'}\right| = \frac{|A_e p_{t0} - A_h n_{t0}|}{|A_e (n_0 + n_1) + A_h (p_0 + p_1) + n' (A_h + A_e)} < \frac{A_e p_{t0} + A_h n_{t0}}{A_e (n_0 + n_1) + A_h (p_0 + p_1)} < \frac{N_t}{a (n_0 + n_1 + p_0 + p_1)},$$

where, a is the smaller of the ratios τ_{p0}/τ_{n0} and τ_{n0}/τ_{p0} [see Eq. (6)].

An analogous estimate can also be obtained for the ratio of derivatives $|dn_t'/dt|/|dn'/dt|$. Consequently, at small concentrations of traps[1] $N_t \ll a (n_0 + n_1 + p_0 + p_1)$, Eq. (8) gives the decay law for the concentration of non-equilibrium carriers at arbitrary levels of generation.

This discussion shows that at small concentrations of traps the non-equilibrium concentrations of electrons and holes in the zones are practically the same: $n' = p' + p_t' \approx p'$, not only for $n' \gg N_t$, which is trivial (or $p_t' \leq N_t$), but also at moderate and small levels of generation, and also at any stage of the decay process. Therefore the processes in question can be characterized by a single lifetime of a non-equilibrium electron-hole pair,[4] given by the expressions:

$$\tau = -\frac{n'}{dn'/dt} \approx -\frac{p'}{dp'/dt}. \tag{9}$$

The complicated form of the decay law (8) is due to the fact that τ depends on the level of generation. According to the Shockley-Read formula[2] τ_0 can be larger or smaller than $\tau_{p0} + \tau_{n0}$. Let us consider separately the two cases

$$\tau_0 \gg \tau_{p0} + \tau_{n0}, \tag{10}$$

$$\tau_0 \leqslant \tau_{p0} + \tau_{n0}. \tag{11}$$

In the first case one can distinguish three ranges of variation of the concentrations in which the decay law is approximated by simpler expressions, corresponding to the monomolecular and bimolecular patterns of recombination. In fact, for large generation levels,

$$n' \gg n_0 + p_0, \tag{12}$$

the decay law (8) can be written in the form:*

$$\left(1 - \frac{\tau_0}{\tau_{p0} + \tau_{n0}}\right) \frac{n_0 + p_0}{\Delta n} - \frac{t}{\tau_{p0} + \tau_{n0}} \approx \ln \frac{n'}{\Delta n} + \frac{n_0 + p_0}{n'} \left(1 - \frac{\tau_0}{\tau_{p0} + \tau_{n0}}\right),$$

---

* By transforming Eq. (8) by means of the limit relation $(1 + \alpha)^{1/\alpha} \approx e$ for $\alpha \to 0$ and taking logarithms, we get the expression given in the text.

or, using Eq. (10), we get:

$$\frac{n_0+p_0}{n'}+\frac{\tau_{p0}+\tau_{n0}}{\tau_0}\ln\frac{n_0+p_0}{n'}-\frac{n_0+p_0}{\Delta n}-\frac{\tau_{p0}+\tau_{n0}}{\tau_0}\ln\frac{n_0+p_0}{\Delta n}\approx\frac{t}{\tau_0}. \tag{13}$$

Then for

$$\frac{n_0+p_0}{n'}\Big/\left|\ln\frac{n_0+p_0}{n'}\right|\ll\frac{\tau_{p0}+\tau_{n0}}{\tau_0} \tag{14}$$

the decay law is exponential

$$n'\approx\Delta n\exp\{-t/(\tau_{p0}+\tau_{n0})\}, \tag{15}$$

and for

$$\frac{n_0+p_0}{n'}\Big/\left|\ln\frac{n_0+p_0}{n'}\right|\gg\frac{\tau_{p0}+\tau_{n0}}{\tau_0}, \tag{16}$$

it is hyperbolic

$$1/n'\approx t/(n_0+p_0)\tau_0+\text{const}. \tag{17}$$

In virtue of the condition (10) both the inequalities (14) and (16) are compatible with the condition (12) of a high generation level. The monomolecular law (15) corresponds to larger values of the ratio $n'(n_0+p_0)$ than the bimolecular law (17).

For small levels of generation

$$n'\ll n_0+p_0 \tag{18}$$

by steps analogous to those in Eq. (13), Eq. (8) takes the form:

$$\text{const}-\frac{t}{\tau_0}\approx\ln\frac{n'}{\Delta n}+\frac{\tau_{p0}+\tau_{n0}}{\tau_0}\left(1-\frac{\tau_0}{\tau_{p0}+\tau_{n0}}\right)\frac{n'}{n_0+p_0}. \tag{19}$$

Using the relation (10), we get

$$\frac{n'}{n_0+p_0}-\ln\frac{n'}{n_0+p_0}\approx\frac{t}{\tau_0}+\text{const}. \tag{20}$$

But by inequality (18) one always has

$$\frac{n'}{n_0+p_0}\ll\left|\ln\frac{n'}{n_0+p_0}\right|.$$

Consequently, at small concentrations of the non-equilibrium carriers the decay law is given by the exponential

$$n'\approx ce^{-t/\tau_0}, \tag{21}$$

For the opposite relationship between the lifetimes, given by the inequality (11), the conditions (12) and (16) are incompatible, and therefore the bimolecular decay law does not appear. In this case the approximating expressions are exponentials: Eq. (21) for small values of n' and Eq. (15) for large values.

In the case of exact equality

$$\tau_0=\tau_{p0}+\tau_{n0} \tag{22}$$

these two exponentials are the same, and it can be seen from Eq. (8) that the decay law is described by a single exponential

$$n'=\Delta ne^{-t/\tau},\ \tau=\tau_0=\tau_{p0}+\tau_{n0} \tag{23}$$

throughout its entire course.

Let us consider in particular the case

$$\tau_0\ll\tau_{p0}+\tau_{n0}. \tag{24}$$

In this case, for small values of n', a region of linear decay can be distinguished before the exponential region.

In fact, referring to Eq. (19) and using condition (24), we get the relation

$$\frac{n'}{n_0+p_0}+\frac{\tau_0}{\tau_{p0}+\tau_{n0}}\ln\frac{n'}{n_0+p_0}+\text{const}\approx-\frac{t}{\tau_{p0}+\tau_{n0}}, \tag{25}$$

in which it is possible to satisfy the inequality [cf. Eq. (17)]

$$\frac{n'}{n_0+p_0}\Big/\left|\ln\frac{n'}{n_0+p_0}\right|\gg\frac{\tau_0}{\tau_{p0}+\tau_{n0}}. \tag{26}$$

Consequently, in the range of values satisfying the inequalities (18) and (26), the decay law in the case (24) is of the form:

$$n'\approx\text{const}-t\,(n_0+p_0)/(\tau_{p0}+\tau_{n0}). \tag{27}$$

We note that when (24) is satisfied the exponential decay law holds for

$$\frac{n'}{n_0+p_0}\Big/\left|\ln\frac{n'}{n_0+p_0}\right|\ll\frac{\tau_0}{\tau_{p0}+\tau_{n0}}. \tag{28}$$

2. DISCUSSION OF RESULTS

According to Ref. 4* the inequality (10) is equivalent to

$$n_1\gg n_0\gg p_0\gg p_1 \text{ and } p_{t0}\gg n_{t0}, \tag{29a}$$

if the trapping level and the level of the dominant impurity are located in the same half of the forbidden zone, and

$$p_1\gg n_0\gg p_0\gg p_1,\quad n_{t0}\gg p_{t0}, \tag{29b}$$

if they are in different halves.

Similarly, (11) is equivalent to either

$$n_0\gg n_1\gg p_1\gg p_0, \tag{30a}$$

or

$$n_0\gg p_1\gg n_1\gg p_0. \tag{30b}$$

We note that n_1 and p_1 give the amount of thermal ejection of electrons and holes captured in the traps.† Consequently, the inequality (10) corresponds to a greater value of the thermal ejection, and on the other hand when (11) is satisfied thermal ejection does not play any important part.

The exponential decay law corresponds to a monomolecular kinetics of recombination, i.e., to constant lifetime (τ independent of n'). This is realized for small levels of generation [$\tau=\tau_0$, Eq. (21)] and for very large levels [$\tau=\tau_{p0}+\tau_{n0}$, Eq. (5)]. In the former case the equilibrium degree of filling of the traps is conserved; in the latter case the limiting degree of filling of the traps by electrons and holes is determined by the non-equilibrium carriers themselves and depends only on the effective capture cross-sections.††

---

* From Eq. (6.2) of Ref. 4 we get for an electron semiconductor $\frac{(1+\alpha_t/y)(1+\gamma/\alpha_t y)}{1+y^{-2}}\gg 1+\gamma$, which gives the relation

$$\left[\exp\left(\frac{E_t-F}{kT}\right)-\gamma\right]\left[1-\exp\left(-\frac{E_t+F}{kT}\right)\right]\gg 0,$$

which leads to the relations (29a) and (29b). In the treatment of a hole semiconductor one must replace F by $-F$ and γ by $1/\gamma$ ($\gamma=A_h/A_e$).

† Indeed, the constants B_e and B_h for thermal ejection of electrons and holes are determined by the system of equations (1) and the conditions of thermodynamic equilibrium:

$$B_e=A_en_0P_{t0}/n_{t0}=A_en_1 \quad\text{and}\quad B_h=A_hp_0n_{t0}/p_{t0}=A_hp_1.$$

†† Of course, small values of n' can be obtained not only for small generation levels, but also in the late stages of decay for large Δn. Therefore it is more correct to speak of small and large disturbances of thermal equilibrium.

The equality $\tau_0 = \tau_{p0} + \tau_{n0}$ (to which the exponential law (23) corresponds over the whole range of variation of the concentration of the non-equilibrium carriers) holds in two cases:

(a) If the equilibrium filling of the traps coincides with the limiting value corresponding to large generation levels, i.e., for

$$n_{t0}/p_{t0} = n_{t\infty}/p_{t\infty} = \tau_{f0}/\tau_{n0} = A_e/A_h, \tag{31}$$

$$n_{t0} = n_{t\infty} = \tau_{f0}N_t/(\tau_{p0} + \tau_{n0}), \ p_{t0} = p_{t\infty} = \tau_{n0}N_t/(\tau_{p0} + \tau_{n0}). \tag{32}$$

(b) If the equalities

$$n_0 = p_1, \ p_0 = n_1. \tag{32a}$$

hold. In case a the filling of the traps does not depend on n', and therefore the process of recombination occurs by the monomolecular pattern. Case b occurs for location of the trap levels and those of the dominant impurity in different halves of the forbidden zone. Then for small generation levels[4] the recombination is determined not by the equilibrium degree of filling (p_{t0}, n_{t0}) but by the existence of a "thermal barrier." The equalities (32a) also lead at low generation levels to the relations

$$A_e n_0/B_h = \tau_{f0}/\tau_{n0} = r_{n\infty}/p_{t\infty}, \tag{33a}$$

if the lifetime is determined by the recombination of non-equilibrium empty traps with equilibrium electrons (electron semiconductor), and

$$B_e/A_h p_0 = \tau_{f0}/\tau_{n0} = n_{t\infty}/p_{t\infty}, \tag{33b}$$

if the lifetime is determined by the recombination of non-equilibrium filled traps with equilibrium holes (hole semiconductor).

Thus if at small generation levels the ratio of the thermal ejection and recombination of the carriers captured by the traps, expressed by the relations (33a) and (33b), turns out equal to the limiting degree of filling at large generation levels, then also there is monomolecular recombination during the entire course of the process of decay of the non-equilibrium carriers.

According to Eqs. (29a), (29b), and (12) the bimolecular recombination described by the hyperbola (17) occurs for appreciable values of the thermal ejection and for large concentrations of non-equilibrium carriers. The existence of the thermal ejection brings it about that even at large generation levels the filling of the traps is still far from its limiting value given by Eq. (31).

In fact, using Eqs. (7), (10), and (12), we get:

$$p_t = p_{t0} + p'_t = p_{t0} + \frac{\tau_{n0} n_{t0} - \tau_{p0} p_{t0}}{(n_0 + p_0)\tau_0} p', \tag{34a}$$

$$\overline{n}_t = n_{t0} + n'_t = n_{t0} + \frac{\tau_{p0} p_{t0} - \tau_{n0} n_{t0}}{(n_0 + p_0)\tau_0} n'. \tag{34b}$$

But, unlike the case of small disturbance of thermodynamic equilibrium, for which one can assume that the filling of the traps is still that characteristic of equilibrium, we have here

$$p_{t0} \gg |n'_t| \gg n_{t0}, \tag{35a}$$

if (29a) holds, and

$$n_{t0} \gg |p'_t| \gg p_{t0}, \tag{35b}$$

for the case of (29b).

Consequently in this case the recombination given by the system of equations (2) is determined by terms that are quadratic in the non-equilibrium concentrations. Indeed, according to Ref. 4, if the lifetime is determined by the recombination of the minority carriers, then, using Eqs. (3), (12), and (35a), we get:

$$-\frac{dp'}{dt} \approx A_h p' n'_t \approx \frac{A_h N_t \tau_{p0}}{(n_0 + p_0)\tau_0} n'p' = \frac{(n')^2}{(n_0 + p_0)\tau_0}. \tag{36a}$$

In this case the traps are emptied by thermal ejection, and everything is determined by the recombination of the non-equilibrium holes ($p' \gg n_0 + p_0$) with non-equilibrium filled traps ($n'_t \gg n_{t0}$). But if the determining role is played by the recombination of the majority carriers, then, taking into account the relations (3), (12), (29b), and (35b), we get:

$$-\frac{dn'}{dt} \approx A_e n' p_t' \approx \frac{A_e N_t \tau_{n0}}{(n_0 + p_0)\tau_0} p'n' \approx \frac{(n')^2}{(n_0 + p_0)\tau_0}. \tag{36b}$$

Here, owing to the location of the trap levels and the dominant impurity levels in different halves of the forbidden zone, the traps are filled up, and everything is determined by the recombination of non-equilibrium electrons ($n' \gg n_0 + p_0$) with non-equilibrium empty traps ($p_t' \gg p_{t0}$). Thus we indeed arrive at Eqs. (36a) and (36b), which give the hyperbola (17).

From the relations (7), (12), and (16) one can obtain the inequality

$$a(n_0 + n_1 + p_0 + p_1) \Big/ \left| \ln \frac{n_0 + p_0}{n'} \right| \gg n' \gg n_0 + p_0,$$

where a is the smaller of the ratios A_e/A_h and A_h/A_e. Consequently, the best conditions for the bimolecular recombination (the widest range of variation of n') correspond to large values of the thermal ejection (the quantities n_1 and p_1). In fact, the thermal ejection of carriers back into the zones is the main effect hindering the establishment of the limiting degree of filling of the traps. Therefore the greater the thermal ejection, the wider the range of variation of n' in which the filling of the traps is still far from its limiting value even at large levels of generation. The conditions for the greatest thermal ejection are realized at temperatures corresponding to the maximum in the curve of τ_0 as function of the reciprocal temperature $1/T$, in semiconductors having narrow trap levels.

Of particular interest is the region of the linear decay law, corresponding to increase of the lifetime with increase of the generation level. The necessary condition for the realization of such a process is the inequality (24), which can be fulfilled only if τ_{p0} and τ_{n0} are quantities of different orders of magnitude, namely: for an electron semiconductor, if

$$\tau_{n0} \gg \tau_{p0}, \tag{37a}$$

and for a hole semiconductor, if

$$\tau_{p0} \gg \tau_{n0}. \tag{37b}$$

In this case, at low generation levels, according to Eq. (27), a region of variation of n' can be distinguished in which the rate of recombination is constant. Because of the smallness of the thermal ejection of carriers into the zones the limiting degree of filling of the traps is established for small disturbances of thermodynamic equilibrium (i.e., p_t' and n_t' are constants). In this case the system (2) (for an electron semiconductor) takes the form

$$dn'/dt = -A_e(n_0 + n_1)p_t' \approx -A_e n_0 p_t', \quad dp'/dt = -A_h n_{t0} p' + A_h(p_0 + p_1)p_t' - A_h p' n_t',$$
$$p' \approx n'; \quad p_t' = -n_t'. \tag{38}$$

Substituting into the first equation of the system (38) the value of p_t' given by the relations (32), we get

$$-dn'/dt \approx A_e N_t \tau_{n0} n_0 / (\tau_{p0} + \tau_{n0}) = n_0 / (\tau_{p0} + \tau_{n0}), \tag{39}$$

which for the case considered of an electron semiconductor ($n_0 \gg p_0$) indeed gives the linear decay law (27). Indeed, in this case, because of the smallness of the thermal ejection ($n_0 \gg n_1$) the traps in the equilibrium state are almost completely filled with electrons and everything is determined by the recombination of non-equilibrium empty traps ($p_t' \gg p_{t0}$) with equilibrium electrons ($n = n_0 + n' \approx n_0$, $n' \ll n_0$). But owing to the limited number of traps and the smallness of the recombination cross-section for an electron in comparison with the corresponding cross-section for holes, the traps are at once filled up with non-equilibrium holes ($p_t' \approx N_t$) and remain in this state for all $n' \gg N_t$. Therefore in the range of variation $n_0 + p_0 \gg n' \gg N_t$ the rate of recombination will be constant, as is indeed expressed by Eq. (39).

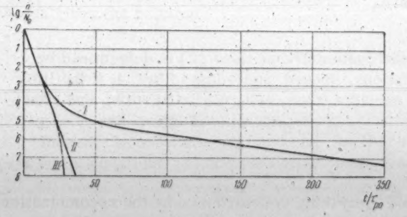

$I-T\ \ T_0=300$° K, $II-T=T_{cr}=220$° K, $III-T=150$° K

We note that the lifetime given by such a scheme of recombination will be proportional to the concentration of non-equilibrium carriers. In fact, by Eqs. (9) and (39), we have:

$$\tau \approx An'.$$

The case (24) is realized at low temperatures in semiconductors in which the recombination cross-section of the minority carriers is much larger than that of the majority carriers.

The diagram shows decay curves of non-equilibrium carriers for a semiconductor with the composition $N_d = 2.5 \times 10^{14}\ \mathrm{cm}^{-3}$, $N_a = 2.5 \times 10^{13}\ \mathrm{cm}^{-3}$, $E_1 - E_t = 0.2$ ev, and $A_e = A_h$, for various temperatures.*

CONCLUSIONS

1. The kinetics of the decay of non-equilibrium carriers in semiconductors containing a small concentration of traps is complicated. In some ranges of variation of the concentration of non-equilibrium carriers a dominant part is played by simple recombination schemes, which makes the decay law approximately exponential, hyperbolic, or linear form.

2. Besides the thoroughly studied monomolecular (τ = const) and bimolecular ($\tau = A/n'$) types of recombination kinetics, in a semiconductor there can also occur a situation of constant rate of recombination, which corresponds to a lifetime proportional to the concentration of non-equilibrium carriers, $\tau = An'$. Recombination occurs in this way at low temperatures in semiconductors in which the recombination cross-section of the minority carriers is much larger than that of the majority carriers.

3. Under definite conditions as to the composition and temperature, expressed by the equality $\tau_0 = \tau_{p0} + \tau_{n0}$, the decay of the non-equilibrium carriers follows the monomolecular pattern throughout its entire course.

In conclusion the writer expresses his gratitude to Professor E. I. Adirovich for valuable advice and his constant interest in this work.

---

[1] E. I. Adirovich and G. M. Goureau, Dokl. Akad. Nauk SSSR **108**, 417 (1956), Soviet Phys. "Doklady" **1**, 306 (1956).

[2] W. Shockley and W. T. Read, Jr., Phys. Rev. **87**, 835 (1952) [see collection Полупроводниковые электронные приборы (Semiconducting Electronic Devices), edited by A. B. Rzhanov, IIL, 1953, p. 121].

[3] E. I. Adirovich, Некоторые вопросы теории люминесценции кристаллов (Some Problems of the Theory of Luminescent Crystals), GITTL, 1951, p. 151.

[4] Adirovich, Goureau, Kuleshov, and Chuenkov, Trudy (Trans.) Phys. Inst. Acad. Sci. U.S.S.R. **8**, 126 (1956).

Translated by W. H. Furry
23

---

* The critical temperature T_{cr} is determined from the equality $\tau_{p0} + \tau_{n0} = \tau_0$, when the decay law throughout its course is the exponential $n' = \Delta n e^{-t/\tau}$.

We have

$$N_0 = 2\,(2\pi mkT_0/h^2)^{3/2} = 2.5 \times 10^{19}\ \mathrm{cm}^{-3}.$$

SOVIET PHYSICS JETP VOLUME 6, NUMBER 1 JANUARY, 1958

CORRELATION THEORY OF THERMAL FLUCTUATIONS IN AN ISOTROPIC MEDIUM

S. M. RYTOV

P. N. Lebedev Physical Institute, Academy of Sciences, U.S.S.R.

Submitted to JETP editor December 29, 1956

J. Exptl. Theoret. Phys. (U.S.S.R.) **33**, 166-178 (July, 1957)

The so-called "fluctuation-dissipation" theorem of Callen and his coworkers is used to develop a spectral theory of thermal fluctuations in an isotropic visco-elastic continuous medium. The mechanical and thermal parameters of the medium in this case can possess any frequency dispersion consistent with the dissipation condition. Correlation functions of $\omega\mathbf{k}$-amplitudes (amplitudes in Fourier time-space expansions), have been found for stress, deformation, velocity, temperature, and entropy fluctuations. With the help of these functions, the spectral intensities (giving the spatial correlation at a frequency ω) and also the spatial correlation functions of quantities which are not decomposed spectrally have been calculated. The results are of interest in the spectral theory of Rayleigh light scattering.

1. INTRODUCTION

THE problem of the spectral description of thermal fluctuations of quantities which characterize dissipative systems, has undergone an important development in recent years. The introduction of certain fluctuating "external" forces, connected with the quantities under consideration in the same energy sense as in the connection between generalized coordinates and forces, has proved to be an extraordinarily effective means for the solution of this problem. The action of a "thermostat" on this system is replaced by the action of these random "external" forces, whose statistical properties are such that they produce just those fluctuations which are actually observed in the real system. In this case, inasmuch as the basic problem is the reproduction of the spectrum of the fluctuations, the necessary statistical characteristics of the "external" forces are reduced to their correlation functions.

The first such problem was solved in 1927 by Nyquist[1] and was applied to the current fluctuations in an electric circuit with lumped constants. Nyquist introduced a random external emf $\mathcal{E}(t)$ which produces thermal current fluctuations $I(t)$ in the circuit — a procedure which also appears in the researches of Langevin[2] and De Haas-Lorentz[3] on the theory of Brownian motion. In contrast to those authors, however, Nyquist transformed to the spectral representation of these random functions and, on the basis of thermodynamics and the equipartition theorem, obtained the spectral intensity of the emf, $\overline{\mathcal{E}^2_\omega}$.

Much later (1951-1952), the Nyquist theorem was greatly generalized by Callen and his coworkers.[4] They extended the whole approach to the case of an arbitrary dissipative system, the state of which is described by some number n of discrete parameters $\xi_j(t)$. Corresponding to this, they introduced n generalized "external" forces $f_j(t)$ and established the form of the correlation matrix $\overline{f_{j\omega} f^*_{k\omega}}$. The derivation of this so-called "fluctuation-dissipation" theorem was given in the papers referred to, both on the basis of classical statistical thermodynamics, and on the basis of quantum theory. By these means it was demonstrated that the correlation functions are proportional to the mean energy of the oscillator $\epsilon(\omega, T)$. Second, what determines the correlation matrix of the "external" forces (this is the impedance matrix of the system under consideration) is the natural extension of the concept of impedance to an arbitrary dissipative system.*

---

*It should be noted that in 1941 Leontovich[5] had come very close to the formulation of this general theorem, but he did not carry his derivation to the explicit expression of the correlation functions in terms of the impedance matrix. In the text of L. D. Landau and E. M. Lifshitz on macroscopic electrodynamics (which will appear shortly), the derivation of the theorem of Callen and his coworkers is given a more complete systematic-spectral form.

Sometimes we are not interested in lumped systems, described by the ordinary differential equations for the set of functions $\xi_j(t)$, but in distributed (in the general case, three dimensional) systems, the fluctuations in which are described by a set of random fields $\xi_j(t, \mathbf{r})$ which satisfy partial differential equations. For example, we may be dealing with the fluctuations of an electromagnetic field (here, we can also include thermal radiation), or with fluctuations of mechanical and thermal parameters which characterize the state of a continuous medium.

The problem of the spectral description of thermal fluctuations, as applicable to the electromagnetic field, was solved in 1952 — first, for a quasi-stationary region (by Leontovich and the author[6]), and then for the general case of a system of Maxwell's equations.[7] The Nyquist theorem served as the starting point of these researches, so that the introduction of "external" electromagnetic fields and the establishment of the form of the correlation function for its spectral amplitudes was carried out on the basis of a series of physical considerations, and not formulated by any regular method. Nonetheless, these basic elements were found to be valid. They allowed one to erect a consistent theory of thermal electric fluctuations[8] which includes as limiting cases the classical theory of thermal radiation (the approximation of geometric optics) and the theory of Nyquist (quasi-stationary region). Subsequently, this general theory was completed and extended in several directions by Levin[9] and Bunkin,[10] and was also applied to a series of more specialized problems,[11] among which was the construction of a macroscopic theory of molecular forces of cohesion (E. M. Lifshitz[12]).

Landau and Lifshitz (in the textbook of macroscopic electrodynamics cited above) have demonstrated that the results of Callen and his collaborators could be applied in a regular fashion to distributed systems. They made use of the division of a continuous system into small volumes and, correspondingly, of the substitution of difference spatial operators for differential ones. Applying this method to the Maxwell equations, they derived those correlation functions for the "external" electromagnetic fields, which were in fact guessed in Refs. 8 and 10.

Starting out from the work of Landau and Lifshitz just cited, I modified the application of the "fluctuation-dissipation" theorem for distributed systems (making use of the expansion of random fields in some complete set of functions) and obtained formulas[13] which are used below for the construction of the spectral theory of thermal fluctuations in a viscoelastic continuous medium.

Application of the "fluctuation-dissipation" theorem to the linearized equations of the theory of elasticity permits us to give a complete spectral description of the thermal fluctuations in the continuous medium for very general assumptions on the frequency dispersion parameters of this medium.* An arbitrary dependence is possible, compatible with the condition that the medium be a dissipative system. The theory developed below, which does not specify the mechanism of the dispersion, is purely phenomenological. Among the problems for which the results flowing therefrom are of interest and of direct application, we can name first of all the spectral theory of Rayleigh light scattering, an account of which I hope to give in a separate paper.

1. INITIAL EQUATIONS

We limit ourselves to the case of an isotropic medium, the mechanical properties of which can be characterized by two elastic moduli, while the thermal properties are characterized by the scalar coefficients of thermal conductivity and thermal expansion (in addition to the heat capacity).

All these parameters of the medium being functions of the frequency ω (or, more precisely, of $z = i\omega$) are, generally speaking, complex.

Thus, for example, the elastic moduli, for which we may take the bulk modulus $\overline{K}$ and the shear modulus $\overline{\mu}$, have the form

$$\overline{K} = K(\omega^2) + i\omega\zeta(\omega^2), \quad \overline{\mu} = \mu(\omega^2) + i\omega\eta(\omega^2), \tag{1.1}$$

where K and μ are the ordinary bulk and shear moduli, and ζ and η are the volume and shear viscosities. The medium can be either a solid (amorphous) body, for which $\mu \neq 0$ at $\omega = 0$, or a liquid $[\mu(0) = 0]$. Since, in the presence of dispersion, the shear modulus cannot be set identically equal to zero, we must even in the case of a liquid start out, not from the hydrodynamic equations, but from the general equations of the theory of elasticity. The presence in liquids at high frequencies of fluctuating deformations of this same type as in solids brings about an added optical anisotropy and therefore is important for the so-called "wing" in the theory of Rayleigh light scattering.[5]

---

*Much earlier, E. M. Lifshitz drew my attention to the analogous theory developed by him and Landau for the case of a viscous liquid in the absence of dispersion (by the method set forth in Ref. 14, Secs. 117-120; see Ref. 20).

Deviations from thermodynamic equation of state of the medium under consideration, along with the random fields of such quantities, as well as the displacement **s** and the velocity **v** of the particles of the medium, the deformation tensor $u_{\alpha\beta}$, the stress tensor $\sigma_{\alpha\beta}$, the temperature T and the specific (per unit mass) entropy S can all be described (under known limitations, see Ref. 14. Secs. 117 and 118) by certain parameters ξ_j, the number of which it is not necessary to limit and which characterize all possible internal processes.

For thermal fluctuations in a medium which is thermostated, the random fields of all these quantities (understood as fluctuating deviations from the corresponding equilibrium values

$$s_0 = 0, \quad v_0 = 0, \quad u_{\alpha\beta 0} = 0, \quad \sigma_{\alpha\beta} = 0, \quad T_0, \quad S_0, \; \xi_{j0} = 0,$$

are statistically stationary in time and homogeneous and isotropic in space. These small deviations satisfy a system of linear differential equations which consists of the linearized equations of the dynamical theory of elasticity, the linearized equation of heat transfer, and the kinetic equations for the parameters ξ_j. We assume that these latter equations are purely temporal; consequently, for the transition to the spectral description ($d/dt \to i\omega$), they are converted into the linear algebraic equations with complex coefficients. With their help, eliminating all the parameters ξ_j, we retain for the description of the behavior of the medium only the mechanical and thermal quantities mentioned above. As a result, we get for the spectral amplitudes of these quantities, the usual equations of elasticity theory and heat transport theory, but with the coefficients depending on $z = i\omega$. Thus the dispersion of these coefficients expresses in terms of the phenomenological theory all the internal kinetics of the medium under consideration.*

For the fields $u_{\alpha\beta}$, $\sigma_{\alpha\beta}$, $\vartheta = T/T_0$, and S, we have, consequently, the linearized equations of motion:†

$$i\omega\rho_0 v_\alpha = \partial\sigma_{\alpha\beta}/\partial x_\beta, \tag{1.2}$$

$$v_\alpha = i\omega s_\alpha, \tag{1.3}$$

$$\sigma_{\alpha\beta} = 2\bar{\mu}\, u'_{\alpha\beta} + \bar{K}(u - C\vartheta)\,\delta_{\alpha\beta}, \tag{1.4}$$

$$u_{\alpha\beta} = {}^1/_2\,(\partial s_\alpha/\partial x_\beta + \partial s_\beta/\partial x_\alpha), \tag{1.5}$$

$$u \equiv u_{\alpha\alpha} = \operatorname{div} s, \quad u'_{\alpha\beta} = u_{\alpha\beta} - \frac{u}{3}\,\delta_{\alpha\beta}, \tag{1.6}$$

and the linearized heat-transfer equation

$$i\omega\rho_0 S = \varkappa\Delta\vartheta. \tag{1.7}$$

In addition to the elastic moduli $\bar{K}$ and $\bar{\mu}$, these equations also contain the (spectral) coefficient of thermal conductivity κ and the coefficient C which determines the dependence of the deformation on the temperature. The deformation tensor $u_{\alpha\beta}$ divides into: (1) the trace $u = u_{\alpha\alpha}$, which is equal, with opposite sign, to the relative compression, and (2) the deformation of pure shear $u'_{\alpha\beta}$, the trace of which vanishes. Such a division is especially convenient in the theory of light scattering.

---

*The considerations set forth are only the continuation of those which were introduced by Leontovich[15] and developed by the researches of him and L. I. Mandel'shtam,[16,17] which touched on the relaxation mechanism of the dispersion and absorption of sound waves in liquids. In Ref. 17, in addition to the linearity of the equation for ξ_j and the condition that $\xi_j \neq$ const. only for deviations from thermodynamic equilibrium, an inertia-free (relaxational) character is assumed for the change of each of the ξ_j. This latter condition, according to which the differential equations for the separated variables ξ_j have a first order, is not generally obligatory. The most general requirement of the dissipativity of the system is sufficient. On the other hand, the assumption that the equation for ξ_j does not contain spatial derivatives of the mechanical and thermal quantities is essential, since only under these conditions can the equations for the spectral amplitudes $u_{\alpha\beta}$, $\sigma_{\alpha\beta}$, T, S be represented in the usual form under the allowance of only frequency dispersion of the parameters of the system.

†In order not to encumber the formulas we shall not use the index ω to indicate that all the equations are written for the spectral amplitudes at the frequency ω (v_ω and so forth).

Since the number of variables in the system just described is greater by one than the number of equations, it is necessary to introduce an additional relation which, naturally, ought to be linear. We write it in the form

$$\rho_0 T_0 S = \frac{C}{3}\sigma + D\vartheta \quad (\sigma \equiv \sigma_{\alpha\alpha}), \tag{1.8}$$

taking here as the coefficient for σ the same C as enters into Eq. (1,4). This is dictated by the condition of symmetry of the spectral kinetic coefficients (see below, Sec. 3).

If dispersion is absent, i.e., if $\overline{K}$, $\overline{\mu}$, C and D do not depend on frequency (and consequently are real), then all the given equations are valid for spectrally non-decomposed quantities and the laws of thermodynamics become applicable, i.e., the state of the system is uniquely defined by six "mechanical" and one "thermal" variables, for example, $\sigma_{\alpha\beta}$ and ϑ. From the group of equations (1.4), and from (1.8), it follows that in this case the coefficients have the following thermodynamic meaning:

$$\frac{1}{K} = 3\left(\frac{\partial u}{\partial \sigma}\right)_\vartheta = \frac{1}{\rho_0}\left(\frac{\partial \rho}{\partial p}\right)_T = \beta_T, \quad C = \left(\frac{\partial u}{\partial \vartheta}\right)_\sigma = -\frac{T_0}{\rho_0}\left(\frac{\partial \rho}{\partial T}\right)_p = \alpha T_0, \quad D = \rho_0 T_0\left(\frac{\partial S}{\partial \vartheta}\right)_\sigma = \rho_0 T_0^2\left(\frac{\partial S}{\partial T}\right)_p = \rho_0 T_0 c_p, \tag{1.9}$$

where β_T is the isothermal compressibility, α is the coefficient of thermal expansion, and c_p is the heat capacity at constant pressure.

Making use of the well known thermodynamic relations

$$\alpha^2 T_0 = \rho_0 c_p (\beta_T - \beta_S), \quad c_p / c_v = \beta_T / \beta_S \equiv \gamma,$$

where β_S is the adiabatic compressibility and c_v is the heat capacity at constant volume, it is easy to obtain the value of one combination of parameters which enters into what follows, namely:

$$D_1 = D - C^2 K = \rho_0 T_0 c_v. \tag{1.10}$$

2. GENERAL FORMULAS FOR THE CORRELATION AND SPECTRAL INTENSITY FUNCTIONS

Let $\xi(t, \mathbf{r})$ be the random field of any of the quantities considered (scalar quantities or components of a vector or tensor) and let $\xi_\omega(\mathbf{r})$ be the corresponding spectral amplitude:

$$\xi(t, \mathbf{r}) = \int_{-\infty}^{+\infty} \xi_\omega(\mathbf{r}) e^{i\omega t}\, d\omega. \tag{2.1}$$

In turn, we can represent (as is frequently convenient) $\xi_\omega(\mathbf{r})$ in the form of a three-dimensional Fourier integral

$$\xi_\omega(\mathbf{r}) = \int_{-\infty}^{+\infty} \xi_{\omega\mathbf{k}} e^{i\mathbf{kr}}\, d\mathbf{k}, \tag{2.2}$$

so that

$$\xi(t, \mathbf{r}) = \iint_{-\infty}^{+\infty} \xi_{\omega\mathbf{k}} e^{i(\omega t + \mathbf{kr})}\, d\omega\, d\mathbf{k}. \tag{2.3}$$

As a consequence of the statistical stationarity of these fields in time and their spatial homogeneity, the correlation functions of the $\omega\mathbf{k}$-amplitudes of any two quantities $\xi(t, \mathbf{r})$ and $\eta(t, \mathbf{r})$ (in particular, $\eta = \xi$) have the form

$$\overline{\xi_{\omega\mathbf{k}} \eta^*_{\omega'\mathbf{k}'}} = \overline{\xi_{\omega\mathbf{k}} \eta^*_{\omega\mathbf{k}}}\, \delta(\omega - \omega')\, \delta(\mathbf{k} - \mathbf{k}'). \tag{2.4}$$

In view of the isotropy of the fluctuations, the spectral ωk-intensity, which we denote by $\overline{\xi_{\omega\mathbf{k}} \eta^*_{\omega\mathbf{k}}}$, in the case of scalar quantities ξ and η, depends (in addition to ω) only on the absolute value of the vector **k**.

It then follows from (2.4) that the correlation functions of the ω-amplitudes that are not spatially decomposed is

$$\overline{\xi_\omega(\mathbf{r} + \rho)\, \eta^*_{\omega'}(\mathbf{r})} = \overline{\xi_\omega(\mathbf{r} + \rho)\, \eta^*_\omega(\mathbf{r})}\, \delta(\omega - \omega'), \tag{2.5}$$

where the ω-intensity which multiplies $\delta(\omega-\omega')$ is equal to

$$\overline{\xi_\omega(\mathbf{r}+\rho)\,\eta_\omega^*(\mathbf{r})}=\int\limits_{-\infty}^{+\infty}\overline{\xi_{\omega\mathbf{k}}\,\eta_{\omega\mathbf{k}}^*}\,e^{i\mathbf{k}\rho}\,d\mathbf{k}. \tag{2.6}$$

For scalar quantities, this intensity depends (in addition to ω) only on the absolute magnitude of the vector ρ, i.e., on the distance between the two points under consideration.

Finally, according to the same general rules, we define the space-time correlation function of the fields $\xi(t,\mathbf{r})$ and $\eta(t,\mathbf{r})$:

$$\Psi_{\xi\eta}(\tau,\rho)\equiv\overline{\xi(t+\tau,\mathbf{r}+\rho)\,\eta(t,\mathbf{r})}=\int\limits_{-\infty}^{+\infty}\overline{\xi_\omega(\mathbf{r}+\rho)\,\eta_\omega^*(\mathbf{r})}\,e^{i\omega\tau}\,d\omega=\iint\limits_{-\infty}^{+\infty}\overline{\xi_{\omega\mathbf{k}}\eta_{\omega\mathbf{k}}^*}\,e^{i(\omega\tau+\mathbf{k}\rho)}\,d\omega\,d\mathbf{k}. \tag{2.7}$$

According to (2.6) and (2.7), one needs to know only the $\omega\mathbf{k}$-intensities for the calculation of any correlation functions. We note that for the theory of Rayleigh scattering, the ω-intensities (2.6) are of immediate interest. These give the spatial correlation at the frequency ω. Let us now set down the formulas giving expressions for the spectral intensities of the "outside" fields[13] which are necessary for what follows.

Let the fluctuations be described by the set of random fields $\xi^{(m)}(t,\mathbf{r})$, $m=1,2,\ldots$, to which correspond the fluctuating "external" forces with volume densities $f^{(m)}(t,\mathbf{r})$ such that the changes in free energy in the volume V associated with their operation take place with velocity

$$\frac{d\overline{E}}{dt}=\sum_m\int\limits_V\overline{f^{(m)}\frac{\partial\xi^{(m)}}{\partial t}}\,dV=-\sum_m\int\limits_V\overline{\xi^{(m)}\frac{\partial f^{(m)}}{\partial t}}\,\Delta V. \tag{2.8}$$

Further, let the spectral amplitudes of the fields $\xi^{(m)}$ and $f^{(m)}$ be connected by the equations

$$f_\omega^{(m)}(\mathbf{r})=\sum_n A_{mn}(\nabla)\,\xi_\omega^{(n)}(\mathbf{r}), \tag{2.9}$$

where the $A_{mn}(\nabla)$ are linear spatial differential operators. Then we have for the matrices of the spatial correlation functions (ω-intensities) of the forces $f^{(m)}$

$$\overline{f_\omega^{(m)}(\mathbf{r}+\rho)\,f_\omega^{(n)*}(\mathbf{r})}=iH(\omega)\,\{A_{nm}^*(-\nabla_\rho)-A_{mn}(\nabla_\rho)\}\,\delta(\rho). \tag{2.10}$$

Here

$$H(\omega)=\frac{\hbar}{4\pi}\coth\frac{\hbar\omega}{2\Theta}, \tag{2.11}$$

$\hbar$ is Planck's constant divided by 2π, $\Theta=kT_0$ is the temperature of the system in energy units. In the classical region ($\hbar\omega\ll\Theta$),

$$H(\omega)=\Theta/2\pi\omega. \tag{2.12}$$

The following expression for the $\omega\mathbf{k}$-intensities of the "external" forces follows from Eq. (2.1):

$$\overline{f_{\omega\mathbf{k}}^{(m)}\,f_{\omega\mathbf{k}}^{(n)*}}=\frac{iH(\omega)}{(2\pi)^3}\,\{A_{nm}^*(-i\mathbf{k})-A_{mn}(i\mathbf{k})\}. \tag{2.13}$$

We now return to the problem of interest — the thermal fluctuations in a visco-elastic isotropic medium.

3. SPECTRAL INTENSITIES OF THE EXTERNAL FORCES

For the description of the fluctuations in a visco-elastic medium, it is appropriate to take as "passive" variables $\xi^{(m)}(t,\mathbf{r})$, the velocity $\mathbf{v}$ of flow of the medium, the stress $\sigma_{\alpha\beta}$ and the reduced temperature $\vartheta=T/T_0$. The generalized forces $f^{(m)}(t,\mathbf{r})$ which should be introduced in correspondence with (2.8), will now be the external momentum with volume density $\mathbf{P}$, the external deformation

$U_{\alpha\beta}$* and the external sources of heat with volume densities Q. Thus the power developed by these forces is

$$\frac{d\overline{E}}{dt} = -\int_V \{\overline{\mathbf{v}\dot{\mathbf{P}}} + \overline{\sigma_{\alpha\beta}\dot{U}_{\alpha\beta}} + \overline{\vartheta\dot{Q}}\}\, dV.$$

The spectral equations (1.2), (1.3), (1.5), and (1.7), if we eliminate the displacement **s** from them, change to the following upon introduction of the external forces:

$$i\omega\rho_0 v_\alpha = \frac{\partial\sigma_{\alpha\beta}}{\partial x_\beta} - i\omega P_\alpha, \quad i\omega u_{\alpha\beta} = \frac{1}{2}\left(\frac{\partial v_\alpha}{\partial x_\beta} + \frac{\partial v_\beta}{\partial x_\alpha}\right) - i\omega U_{\alpha\beta}, \quad i\omega\rho_0 S = \varkappa\Delta\vartheta - i\omega\frac{Q}{T_0}. \tag{3.1}$$

Solving (1.4) for the deformation, we obtain

$$u_{\alpha\beta} = \sigma'_{\alpha\beta}/2\overline{\mu} + (\sigma/9\overline{K})\,\delta_{\alpha\beta} + (C\vartheta/3)\delta_{\alpha\beta}, \tag{3.2}$$

where, in accord with (1.6), we use the notation

$$\sigma \equiv \sigma_{\alpha\alpha}, \quad \sigma'_{\alpha\beta} = \sigma_{\alpha\beta} - \frac{\sigma}{3}\delta_{\alpha\beta}. \tag{3.3}$$

Equations (1.8) and (3.2) permit us to eliminate the deformations $u_{\alpha\beta}$ and the entropy S from (3.1). As a result we obtain ten equations for the variables v_α, $\sigma_{\alpha\beta}$, and ϑ, which we now write in the form (2.9), i.e., solving them for the ω-amplitudes of the external forces. Moreover, making use of the symmetric tensor $\sigma_{\alpha\beta}$, we rewrite the latter in the form $\frac{1}{2}(\sigma_{\alpha\beta} + \sigma_{\beta\alpha})$. Thus,

$$P_\alpha = -\rho_0 v_\alpha + \frac{1}{2i\omega}\nabla_\beta(\sigma_{\alpha\beta} + \sigma_{\beta\alpha}), \qquad U_{\alpha\beta} = \frac{\nabla_\alpha v_\beta + \nabla_\beta v_\alpha}{2i\omega} - \frac{\sigma_{\alpha\beta} + \sigma_{\beta\alpha}}{4\overline{\mu}} + \left(\frac{1}{2\overline{\mu}} - \frac{1}{3\overline{K}}\right)\frac{\sigma}{3}\delta_{\alpha\beta} - \frac{C\vartheta}{3}\delta_{\alpha\beta},$$

$$Q = -\frac{C\sigma}{3} - D\vartheta + \frac{\varkappa T_0}{i\omega}\nabla^2\vartheta. \tag{3.4}$$

In such a description, a comparison of (3.4) with (2.9) easily allows us to establish the form of the matrices of the operators $A_{mn}(\nabla)$, which ought to be symmetric in the given case (absence of fields of the Coriolis type), and which actually satisfies this condition, as already specified in (1.8). Not writing out the elements of this matrix (although 30 of the 55 elements are equal to zero), we at once obtain the ωk-intensities of the external forces, made up from Eq. (2.13). We limit ourselves in this case to the classical frequencies, i.e., we use the expression (2.12) for H(ω). The intensities are then

$$\overline{P_\alpha P^*_\beta} = 0, \quad \overline{P_\alpha U^*_{\beta\gamma}} = 0, \quad \overline{P_\alpha Q^*} = 0, \tag{3.5}$$

$$\overline{U_{\alpha\beta}U^*_{\mu\nu}} = -\frac{\Theta}{(2\pi)^\cdot i\omega}\left\{\frac{1}{4}\left(\frac{1}{\overline{\mu}} - \frac{1}{\overline{\mu}^*}\right)\left(\delta_{\alpha\mu}\delta_{\beta\nu} + \delta_{\beta\mu}\delta_{\alpha\nu} - \frac{2}{3}\delta_{\alpha\beta}\delta_{\mu\nu}\right) + \frac{1}{9}\left(\frac{1}{\overline{K}} - \frac{1}{\overline{K}^*}\right)\delta_{\alpha\beta}\delta_{\mu\nu}\right\}, \tag{3.6}$$

$$\overline{U_{\alpha\beta}Q^*} = -\frac{\Theta}{(2\pi)^\cdot i\omega}(C - C^*)\frac{\delta_{\alpha\beta}}{3}, \tag{3.7}$$

$$\overline{QQ^*} = -\frac{\Theta}{(2\pi)^\cdot i\omega}(d - d^*), \tag{3.8}$$

where the notation

$$d = D + \varkappa T_0 k^2/i\omega. \tag{3.9}$$

has been introduced.

It follows from (3.5) that the external momentum $\mathbf{P} \equiv 0$, i.e., it would have been possible to do without it from the very beginning. One could have foreseen this, since the center of mass of the system should remain at rest in the given arrangement of the problem, and such can be guaranteed only in the absence of the field **P**.

---

*At first glance, it would appear more natural to introduce the external stresses $\Sigma_{\alpha\beta}$ rather than the external deformations $U_{\alpha\beta}$. In essence, both methods are equivalent. As substitution of the second equation of (3.1) in (1.4) shows, the introduction of $U_{\alpha\beta}$ is equivalent to the action of the external stresses $\Sigma_{\alpha\beta} = 2\overline{\mu}U'_{\alpha\beta} + \overline{K}U\delta_{\alpha\beta}$. However, our choice of "passive" variables and generalized forces turns out to be much more convenient from the computational viewpoint.

There is no necessity of our using Eqs. (2.6) and (2.7) to calculate the ω-intensities and space-time correlation functions of the external forces $U_{\alpha\beta}$ and Q. These functions are necessary only to obtain the spectral statistical characteristics of "passive" variables — the velocity **v**, the stress $\sigma_{\alpha\beta}$, and the temperature ϑ, and in addition the others — the deformation $u_{\alpha\beta}$ and the entropy S, which are expressed in terms of $\sigma_{\alpha\beta}$ and ϑ by Eqs. (3.2) and (1.8). We shall now proceed to do so.

4. SPECTRAL ωk-INTENSITIES OF THE STRESS AND TEMPERATURE

In order to express the ω**k**-amplitudes of the quantities v_α, $\sigma_{\alpha\beta}$, and ϑ in terms of the ω**k**-amplitudes of the external forces $U_{\alpha\beta}$ and Q, it is necessary to solve (3.4), rewriting it for ω**k**-amplitudes ($\nabla \rightarrow i\mathbf{k}$) and considering that $\mathbf{P} = 0$:

$$\rho_0\omega v_\alpha - k_\beta\sigma'_{\alpha\beta} - k_\alpha\sigma/3 = 0, \tag{4.1}$$

$$(k_\alpha v_\beta + k_\beta v_\alpha)/2\omega - \sigma'_{\alpha\beta}/2\bar{\mu} - (\sigma/3\bar{K} + C\vartheta)\,\delta_{\alpha\beta}/3 = U_{\alpha\beta}, \tag{4.2}$$

$$C\sigma/3 + d\vartheta = -Q. \tag{4.3}$$

The notation of (3.3) and (3.9) is used here. Using the symbols

$$d_1 = d - C^2\bar{K},\ \Delta = A_1 d - A_3 C^2\bar{K},$$

$$A_1 = \rho_0\omega^2 - (\bar{K} + {}^4/_3\bar{\mu})\,k^2,\ A_2 = \rho_0\omega^2 - 2\bar{\mu}k^2,\ A_3 = \rho_0\omega^2 - {}^4/_3\bar{\mu}k^2,\quad A_4 = \rho_0\omega^2 - \bar{\mu}k^2 \tag{4.4}$$

(the last of these is necessary somewhat later) we obtain the following result:

$$\sigma = -\frac{3\bar{K}}{\Delta}\{2\bar{\mu}dV + A_2 dU - A_3 CQ\}, \tag{4.5}$$

$$\vartheta = \frac{1}{\Delta}\{2\bar{\mu}\bar{K}CV + A_2 C\bar{K}U - A_1 Q\}. \tag{4.6}$$

$$v_\alpha = -\frac{2\omega\bar{\mu}}{A_4}U_{\beta\alpha}k_\beta - \frac{\omega k_\alpha}{\Delta}\left\{\frac{2\bar{\mu}}{3A_4}(3\bar{K}d + \bar{\mu}d_1)V + (\bar{K}d - \frac{2}{3}\bar{\mu}d_1)U - C\bar{K}Q\right\}. \tag{4.7}$$

$$\frac{\sigma'_{\alpha\beta}}{2\bar{\mu}} = -U_{\alpha\beta} - \frac{\bar{\mu}}{A_4}(U_{\gamma\beta}k_\alpha + U_{\gamma\alpha}k_\beta)\,k_\gamma - \frac{k_\alpha k_\beta}{\Delta}\left\{\frac{2\bar{\mu}}{3A_4}(3\bar{K}d + \bar{\mu}d_1)V + \left(\bar{K}d - \frac{2}{3}\bar{\mu}d_1\right)U - C\bar{K}Q\right\}$$
$$+ \frac{\delta_{\alpha\beta}}{3\Delta}\{(2\bar{\mu}V + A_2 U)\,d_1 - C\bar{K}Q\}, \tag{4.8}$$

where $U = U_{\alpha\alpha}$, $V = U_{\alpha\beta}k_\alpha k_\beta$. Expanding the expressions for the ωk-amplitudes of the quantities v_α, $\sigma_{\alpha\beta}$, and ϑ in terms of the ωk-amplitudes of the external forces $U_{\alpha\beta}$ and Q, for which the ωk-intensities are known [Eq. (3.6) – (3.8)], we can now compute the ωk-intensities of these quantities. We omit the rather cumbersome intermediate equations and immediately write down the final results, pertaining to $\sigma'_{\alpha\beta}$, σ, and ϑ. This suffices, since all the intensities which contain v_α, $u_{\alpha\beta}$, and S can then be obtained with the aid of Eqs. (4.1), (3.2), and (1.8), respectively (see Sec. 5).

Making use of the symbols of (4.4), and further introducing

$$\tilde{\delta}_{\alpha\beta} = k_\alpha k_\beta/k^2 - \delta_{\alpha\beta}/3 \qquad (\tilde{\delta}_{\alpha\alpha} = 0), \tag{4.9}$$

we have

$$\overline{\sigma'_{\alpha\beta}\sigma'^{*}_{\mu\nu}} = -\frac{\Theta}{(2\pi)^4 i\omega}\Bigg\{(\bar{\mu}^* - \bar{\mu})\left[\delta_{\alpha\mu}\delta_{\beta\nu} + \delta_{\beta\mu}\delta_{\alpha\nu} - \frac{2}{3}\delta_{\alpha\beta}\delta_{\mu\nu} + 3\tilde{\delta}_{\alpha\beta}\tilde{\delta}_{\mu\nu}\left(\left|\frac{d_1\rho_0\omega^2 - d\bar{K}k^2}{\Delta}\right|^2 - 1\right) - \frac{1}{k^2}\left(\frac{\rho_0^2\omega^4}{|A_4|^2} - 1\right)(\delta_{\alpha\mu}k_\beta k_\nu\right.$$
$$\left. + \delta_{\alpha\nu}k_\beta k_\mu + \delta_{\beta\mu}k_\alpha k_\nu + \delta_{\beta\nu}k_\alpha k_\mu - 4\frac{k_\alpha k_\beta k_\mu k_\nu}{k^2})\right] + 4\tilde{\delta}_{\alpha\beta}\tilde{\delta}_{\mu\nu}\left|\frac{\bar{\mu}k^2}{\Delta}\right|^2(d_1 d^*\bar{K}^* - d_1^* d\bar{K})\Bigg\}, \tag{4.10}$$

$$\overline{\sigma'_{\alpha\beta}\sigma^*} = \frac{6\Theta k^2\tilde{\delta}_{\alpha\beta}}{(2\pi)^4 i\omega}\left(\frac{\bar{\mu}\bar{K}d}{\Delta} - \frac{\bar{\mu}^*\bar{K}^*d^*}{\Delta^*}\right), \tag{4.11}$$

$$\overline{\sigma\sigma^*} = \frac{9\Theta}{(2\pi)^4 i\omega}\left(\frac{A_3\bar{K}d}{\Delta} - \frac{A_3^*\bar{K}^*d^*}{\Delta^*}\right), \tag{4.12}$$

$$\overline{\sigma'_{\alpha\beta}\vartheta^*} = -\frac{2\Theta k^2\tilde{\delta}_{\beta}}{(2\pi)^4\omega}\left(\frac{\bar{\mu}\bar{K}C}{\Delta} - \frac{\bar{\mu}^*\bar{K}^*C^*}{\Delta^*}\right), \tag{4.13}$$

$$\overline{\sigma\vartheta^*} = -\frac{3\Theta}{(2\pi)^4 i\omega}\left\{\frac{A_3C\bar{K}}{\Delta} - \frac{A_3^*C^*\bar{K}^*}{\Delta^*} - (C - C^*)\bar{K}\left(\frac{A_1}{\Delta} - \frac{A_1^*}{\Delta^*}\right)\right\}, \tag{4.14}$$

$$\overline{\vartheta\vartheta^*} = \frac{\Theta}{(2\pi)^1 i\omega}\left(\frac{A_1}{\Delta} - \frac{A_1^*}{\Delta^*}\right). \tag{4.15}$$

5. SPECTRAL ωk-INTENSITIES OF THE VELOCITY AND THE DEFORMATION

As has already been noted, the ωk-intensities of all the remaining quantities can now be found in the form of a linear combination of the intensities (4.10) – (4.15). Thus Eq. (4.1):

$$\rho_0\omega v_\alpha = k_\beta\sigma'_{\alpha\beta} + k_\alpha\frac{\sigma}{3}$$

permits us to obtain any intensities containing the velocity. For example, it follows from this equation that

$$\overline{v_\alpha v_\beta^*} = \frac{1}{\rho_0^2\omega^2}\left\{k_\mu k_\nu\overline{\sigma'_{\alpha\mu}\sigma'^*_{\beta\nu}} + \frac{k_\alpha k_\nu}{3}\overline{\sigma\sigma'^*_{\beta\nu}} + \frac{k_\beta k_\mu}{3}\overline{\sigma'_{\alpha\mu}\sigma^*} + \frac{k_\alpha k_\beta}{9}\overline{\sigma\sigma^*}\right\}$$

– an expression in which it remains to substitute Eqs. (4.10) – (4.12). In this manner, we find

$$\overline{v_\alpha v_\beta^*} = \frac{\Theta}{(2\pi)^4 i\omega\rho_0}\left\{\left(\frac{\bar{\mu}}{A_4} - \frac{\bar{\mu}^*}{A_4^*}\right)(\delta_{\alpha\beta}k^2 - k_\alpha k_\beta) + k_\alpha k_\beta\left[\frac{1}{\Delta}\left(\bar{K}d + \frac{4}{3}\bar{\mu}d_1\right) - \frac{1}{\Delta^*}\left(\bar{K}^*d^* + \frac{4}{3}\bar{\mu}^*d_1^*\right)\right]\right\}, \tag{5.1}$$

$$\overline{v_\alpha\sigma'^*_{\mu\nu}} = \frac{\Theta}{(2\pi)^4 i}\left\{\left(\frac{\bar{\mu}}{A_4} - \frac{\bar{\mu}^*}{A_4^*}\right)\left(\delta_{\alpha\mu}k_\nu + \delta_{\alpha\nu}k_\mu - 2\frac{k_\alpha k_\mu k_\nu}{k^2}\right) + 2k_\alpha\tilde{\delta}_{\mu\nu}\left(\frac{\bar{\mu}d_1}{\Delta} - \frac{\bar{\mu}^*d_1^*}{\Delta^*}\right)\right\}, \tag{5.2}$$

$$\overline{v_\alpha\sigma^*} = \frac{3\Theta k_\alpha}{(2\pi)^4 i}\left(\frac{\bar{K}d}{\Delta} - \frac{\bar{K}^*d^*}{\Delta^*}\right) \tag{5.3}$$

$$\overline{v_\alpha\vartheta^*} = -\frac{\Theta k_\alpha}{(2\pi)^4 i}\left\{\frac{C\bar{K}}{\Delta} - \frac{C^*\bar{K}^*}{\Delta^*} - \frac{(C - C^*)\bar{K}}{\rho_0\omega^2}\left(\frac{A_1}{\Delta} - \frac{A_1^*}{\Delta^*}\right)\right\}. \tag{5.4}$$

Similarly, with the help of Eq. (3.2), from which it follows that

$$u'_{\alpha\beta} = \sigma'_{\alpha\beta}/2\bar{\mu}, \quad u = \sigma/3\bar{K} + C\vartheta,$$

it is not difficult to compute the ωk-intensities of the deformation. We give the corresponding expressions, since they are necessary for the theory of Rayleigh scattering:

$$\begin{aligned}\overline{u'_{\alpha\beta}u'^*_{\mu\nu}} = &-\frac{\Theta}{(2\pi)^4 i\omega}\left\{\frac{1}{4}\left(\frac{1}{\bar{\mu}} - \frac{1}{\bar{\mu}^*}\right)\left[\delta_{\alpha\mu}\delta_{\beta\nu} + \delta_{\beta\mu}\delta_{\alpha\nu} - \frac{2}{3}\delta_{\alpha\beta}\delta_{\mu\nu} + 3\tilde{\delta}_{\alpha\beta}\tilde{\delta}_{\mu\nu}\left(\left|\frac{d_1\rho_0\omega^2 - d\bar{K}k^2}{\Delta}\right|^2 - 1\right)\right.\right.\\ &\left.\left.-\frac{1}{k^2}\left(\frac{\rho_0^2\omega^2}{|A_4|^2} - 1\right)\left(\delta_{\alpha\mu}k_\beta k_\nu + \delta_{\alpha\nu}k_\beta k_\mu + \delta_{\beta\mu}k_\alpha k_\nu + \delta_{\beta\nu}k_\alpha k_\mu - 4\frac{k_\alpha k_\beta k_\mu k_\nu}{k^2}\right)\right] + \tilde{\delta}_{\alpha\beta}\tilde{\delta}_{\mu\nu}\frac{k^4}{|\Delta|^2}(d_1d^*\bar{K}^* - d_1^*d\bar{K})\right\},\end{aligned} \tag{5.5}$$

$$\overline{u'_{\alpha\beta}u^*} = \frac{\Theta k^2\tilde{\delta}_{\alpha\beta}}{(2\pi)^4 i\omega}\left\{\frac{\bar{K}(d - CC^*\bar{K}^*)}{\bar{K}^*\Delta} - \frac{\bar{\mu}^*d_1^*}{\bar{\mu}\Delta^*}\right\}, \tag{5.6}$$

$$\overline{uu^*} = \frac{\Theta}{(2\pi)^4 i\omega}\left\{\frac{A_3d_1}{\bar{K}^*\Delta} - \frac{A_3^*d_1^*}{\bar{K}\Delta^*} - CC^*k^2\left(\frac{\bar{K}}{\Delta} - \frac{\bar{K}^*}{\Delta^*}\right)\right\}, \tag{5.7}$$

$$\overline{u'_{\alpha\beta}\vartheta^*} = -\frac{\Theta k^2\tilde{\delta}_{\alpha\beta}}{(2\pi)^4 i\omega}\left(\frac{C\bar{K}}{\Delta} - \frac{\bar{\mu}^*C^*\bar{K}^*}{\bar{\mu}\Delta^*}\right), \tag{5.8}$$

$$\overline{u\vartheta^*} = -\frac{\Theta}{(2\pi)^4 i\omega}\left(\frac{C\bar{K}k^2}{\Delta} - \frac{C^*\bar{K}^*A_3^* - C\bar{K}A_1^*}{\bar{K}\Delta^*}\right). \tag{5.9}$$

By the same method, we can obtain the mutual intensities of deformation and stress. We set down only one of them – for the scalar quantities u and σ (the relative density and pressure):

$$\overline{u\sigma^*} = \frac{\Theta}{(2\pi)^4 i\omega}\left\{\frac{A_3d_1}{\Delta} - \frac{\bar{K}^*A_3^*(d^* - CC^*\bar{K})}{\bar{K}\Delta^*} - C(C - C^*)\bar{K}^*\left(\frac{A_1}{\Delta} - \frac{A_1^*}{\Delta^*}\right)\right\}. \tag{5.10}$$

So far as the ωk-intensities containing the entropy S are concerned, they are easily computed by means of (1.8). However, we shall not carry out the corresponding derivations since they are not of much interest.

6. SPATIAL CORRELATION

Making use of the ωk-intensities, we can compute, by Eq. (2.6), the corresponding ω-intensities which give the spatial correlation of the quantities under consideration at the frequency ω, while from (2.7) we find the correlation functions of the spectrally-nonexpanded quantities.

For the calculation of the integrals (2.6), it is not difficult to carry out integration in **k** space over the angles, after which there are left single integrals over k, which are taken with residues at the poles which determine the roots k_j of the dispersion equation. It is not difficult to see [from (4.5) to (4.8)] that the dispersion equation divides into two parts:

$$\Delta = 0, \quad A_4 = 0,$$

where the first defines the roots k_1 and k_2, corresponding to the compressional waves and heat waves:

$$k_{1,2}^2 = \frac{i\omega\rho_0}{2\varkappa_1(\bar{K}+\bar{M})}(-P \pm R), \qquad P = i\omega\varkappa_1 + D\bar{K} + D_1\bar{M}, \; R = +\sqrt{P^2 - 4i\omega\varkappa_1 D_1(\bar{K}+\bar{M})}, \tag{6.1}$$

while the second defines the root k_3, corresponding to shear waves:

$$k_3^2 = \rho_0\omega^2/\bar{\mu}. \tag{6.2}$$

In (6.1) the following notation was introduced:

$$\varkappa_1 = \varkappa\rho_0 T_0, \; D_1 = D - C^2\bar{K}, \; \bar{M} = {}^4/_3\bar{\mu}. \tag{6.3}$$

It should be emphasized that the determination of the roots k_j and, it seems, the computation of the ω-intensities also, does not require a concrete form for the dispersion law, i.e., the correlation at a frequency ω can be found for an arbitrary frequency dependence of the parameters of the medium. The root k_3 plays a role only for velocities v_α and tensor quantities $\sigma'_{\alpha\beta}$, $u'_{\alpha\beta}$; the scalar quantities σ, ϑ, u and S naturally are not connected with shear waves.

The spectral correlation lengths are naturally determined by the path length (reduced by a factor e) of waves of different types. As an example, let us introduce the ω-intensity of the temperature ϑ:

$$\overline{\vartheta_\omega(\mathbf{r}+\rho)\vartheta^*_\omega(\mathbf{r})} = \frac{\Theta}{16\pi^2\rho}\left\{\frac{1}{\varkappa}\left[\left(1 - \frac{P - 2i\omega\varkappa_1}{R}\right)e^{-ik_1\rho} + \left(1 + \frac{P - 2i\omega\varkappa_1}{R}\right)e^{-ik_2\rho}\right] + \text{compl. conj.}\right\}$$

If the thermal conductivity $\kappa \to 0$, then, in view of the fact that $k_2 \sim 1/\sqrt{\kappa_1}$, the correlation determined by thermal waves remains (for each ρ) suitable small in comparison with the correlations determined by the compressional waves.

For spectrally non-decomposed quantities, if we limit ourselves to the case $\tau = 0$, we have, in accord with (2.7),

$$\Psi_{\xi\eta}(0, \rho) = \overline{\xi(t, \mathbf{r}+\rho)\eta(t, \mathbf{r})} = \int_{-8}^{+\infty}\!\!\int \overline{\xi_{\omega\mathbf{k}}\eta^*_{\omega\mathbf{k}}}\, e^{i\mathbf{k}\rho}\, d\omega d\mathbf{k}. \tag{6.4}$$

For the calculation of $\Psi_{\xi\eta}$ it turns out to be much more effective to carry out the integration initially over ω. The fact is that the integral

$$I_{\xi\eta}(\mathbf{k}) = \int_{-\infty}^{+\infty} \overline{\xi_{\omega\mathbf{k}}\eta^*_{\omega\mathbf{k}}}\, d\omega \tag{6.5}$$

is evaluated in a number of cases with the help of certain general theorems from the theory of residues, which permit us either to do without a concrete model of the dispersion laws, or to limit ourselves to a precise statement of these laws only for certain ranges of the parameters. We set forth these theorems, omitting their proofs (although they are very simple), and not pursuing the most general form.

Let the path of integration Γ run along the imaginary axis $z = i\omega$ and close up at infinity to include the left half plane (in which all the roots of the dispersion equation of our dissipative system are found for real k). Further, let f(z) be the Hurwitz polynomial of degree N, and g(z) a polynomial of degree ≤ N which does not have common roots with f(z). Finally, let a and α be real positive numbers. Then

$$\frac{1}{2\pi i}\oint_{\Gamma}\left\{\frac{g(z)(z-\alpha)}{f(z)(z-a)}-\frac{g(-z)(z+\alpha)}{f(-z)(z+a)}\right\}\frac{dz}{z}=\frac{g(\infty)}{f(\infty)}-2\frac{g(a)}{f(a)}\left(1-\frac{\alpha}{a}\right)-\frac{g(0)\,\alpha}{f(0)\,a}. \tag{6.6}$$

In particular, for $a = \alpha$,

$$\frac{1}{2\pi i}\oint_{\Gamma}\left\{\frac{g(z)}{f(z)}-\frac{g(-z)}{f(-z)}\right\}\frac{dz}{z}=\frac{g(\infty)}{f(\infty)}-\frac{g(0)}{f(0)}. \tag{6.7}$$

For the same conditions,

$$\frac{1}{2\pi i}\oint_{\Gamma}\left\{\frac{g(z)}{f(z)}-\frac{g(-z)}{f(-z)}\right\}dz=\lim_{z\to\infty}\frac{z}{2}\left\{\frac{g(z)}{f(z)}-\frac{g(-z)}{f(-z)}\right\}. \tag{6.8}$$

It is not difficult to see that most of the ωk-intensities either themselves have the form of the half-integral expressions entering here, or to reduce to such a form for particular assumptions on the character of the dispersion. Thus, for example, the intensities (4.11) – (4.13), (4.15), and (5.1) have the form of the integrand in (6.7), while the intensity (4.14) takes on such a form for real C (absence of dispersion in the coefficient of thermal expansion). The intensities (5.2) and (5.3) [but for real C and (5.4)] have the form of the integrand in (6.8). So far as the integrals (6.5) are concerned, [integrals of the intensities which contain the deformations $u'_{\alpha\beta}$ and u], we must for their computation rely on the laws of dispersion for the compressional modulus $\overline{K}$ and (or) the shear modulus $\overline{\mu}$. Equation (6.6) is obtained for just that case in which use is made of a very simple law with a single relaxation time

$$\overline{K}=\frac{K_{\infty}z+K_0/\tau'}{z+1/\tau'},\qquad \overline{\mu}=\frac{\mu_{\infty}z+\mu_0/\tau}{z+1/\tau}.$$

The expressions for $I_{\xi\eta}(\mathbf{k})$ are so simple that the subsequent calculation of the correlation functions (6.4) presents no difficulties. As a result we obtain formulas in a number of cases which depend materially on the dispersion of the parameters (containing values of the parameters for $z = 0$ and $z = \infty$). Because of lack of space we limit ourselves for illustration only to autocorrelation functions for the relative density u:

$$\Psi_{uu}(0,\rho)=\Theta\left(\frac{1}{K_{\infty}}-\frac{\beta_T^2 M_0}{1+\beta_T M_0}\right)\delta(\rho)+\frac{\Theta(K_{\infty}-K_0)\,\psi(\rho,a)}{2\pi K_0K_{\infty}\varkappa_{1a}(K_a+M_a)}, \tag{6.9}$$

where

$$\psi(\rho,a)=\frac{F(k_{1a}^2)\exp(-|k_{1a}|\rho)-F(k_{2a}^2)\exp(-|k_{2a}|\rho)}{(k_{1a}^2-k_{2a}^2)\,p},\qquad F(k^2)=(\rho_0a^2+M_ak^2)(D_{1a}+\varkappa_{1a}k^2).$$

The index a here denotes parameters at $z = a = K_0/K_{\infty}\tau'$.

In the absence of dispersion in the bulk modulus ($K_{\infty} = K_0 = 1/\beta_T$) the second term of Eq. (6.9) vanishes and the first yields the thermodynamic expression*

$$\Psi_{uu}=\frac{\Theta\beta_T}{1+{}^4\!/_3\,\beta_T\mu_0}\,\delta(\rho).$$

In the case of a liquid ($\mu_0 = 0$), if we consider that $u = -\rho/\rho_0$, where ρ = fluctuations in the density, we then obtain the usual formula

$$\Psi_{\rho\rho}=\Theta\beta_T\rho_0^2\,\delta(\rho).$$

---

[1] H. Nyquist, Phys. Rev. 29, 614 (1927); 32, 110 (1928).

[2] P. Langevin, Compt. rend. 146, 530 (1908).

[3] G. L. de Haas-Lorentz, Die Wissenschaft, 52, 86 (Baunschweig, 1913).

---

*Calculated with account of the correlation of the displacement of the medium at different points (and, consequently, fluctuations of the form also of nonoverlapping volumes), which takes place in a solid, in contrast to a liquid. (See Sec. 3 in Ref. 18, and also Ref. 19, in particular p. 56.)

[4] H. B. Callen and T. A. Welton, Phys. Rev. **83**, 34 (1951); J. L. Jackson, Phys. Rev. **87**, 471 (1952); H. B. Callen and R. F. Greene, Phys. Rev. **86**, 702 (1952); Callen, Barash, and Jackson, Phys. Rev. **88**, 1382 (1952); R. F. Greene and H. B. Callen, Phys. Rev. **88**, 1387 (1952).

[5] M. A. Leontovich, J. Phys. (U.S.S.R.) **4**, 499 (1941).

[6] M. A. Leontovich and S. M. Rytov, J. Exptl. Theoret. Phys. (U.S.S.R.) **23**, 246 (1952).

[7] S. M. Rytov, Dokl. Akad. Nauk SSSR **87**, 535 (1952).

[8] S. M. Rytov, Теория электрических флуктуаций и теплового излучения (Theory of Electrical Fluctuations in Thermal Radiation), Acad. Sci. Press, Moscow, 1953.

[9] M. L. Levin, Dokl. Akad. Nauk SSSR **102**, 53 (1955).

[10] F. V. Bunkin, Dissertation, Moscow, Phys. Inst. Acad. Sci., 1955; J. Exptl. Theoret. Phys. (U.S.S.R.) **32**, 338 and 811 (1957); Soviet Phys. JETP **5**, 277 and 665 (1957).

[11] S. M. Rytov, J. Exptl. Theoret. Phys. (U.S.S.R.) **27**, 571 (1954); S. M. Rytov and M. L. Levin, J. Tech. Phys. (U.S.S.R.) **25**, 323 (1955); M. L. Levin, J. Tech. Phys. (U.S.S.R.) **25**, 2313 (1955).

[12] E. M. Lifshitz, Dokl. Akad. Nauk SSSR **97**, 643 (1954); **100**, 879 (1955); J. Exptl. Theoret. Phys. (U.S.S.R.) **29**, 94 (1955); Soviet Phys. JETP **2**, 73 (1956).

[13] S. M. Rytov, Dokl. Akad. Nauk SSSR **110**, 371 (1956); Soviet Phys. "Doklady" **1**, 555 (1956).

[14] L. D. Landau and E. M. Lifshitz, Статистическая физика (Statistical Physics), Moscow, Leningrad, 1951.

[15] M. A. Leontovich, J. Exptl. Theoret. Phys. (U.S.S.R.) **6**, 561 (1936).

[16] L. I. Mandel'shtam and M. A. Leontovich, Dokl. Akad. Nauk SSSR **3**, 111 (1936); L. I. Mandel'shtam, Collected Works, vol. 2, p. 170, Acad. Sci. Press, Moscow (1947).

[17] L. I. Mandel'shtam and M. A. Leontovich, J. Exptl. Theoret. Phys. (U.S.S.R.) **7**, 438 (1937); L. I. Mandel'shtam, Collected Works, vol. 2, 176.

[18] M. Leontowitsch and S. Mandelstam, Z. Phys. Sowjetunion **1**, 317 (1932).

[19] M. Leontowitsch, Z. Phys. Sowjetunion **3**, 35 (1933).

[20] L. D. Landau and E. M. Lifshitz, J. Exptl. Theoret. Phys. (U.S.S.R.) **32**, 618 (1957); Soviet Phys. JETP **5**, 512 (1957).

Translated by R. T. Beyer
24

SOVIET PHYSICS JETP VOLUME 6, NUMBER 1 JANUARY, 1958

ON INTERPRETATION OF THE LATERAL DISTRIBUTION OF NUCLEAR-ACTIVE PARTICLES IN EXTENSIVE AIR SHOWERS

IU. N. VAVILOV

P. N. Lebedev Physics Institute, Academy of Sciences, U.S.S.R.

Submitted to JETP editor December 30, 1956

J. Exptl. Theoret. Phys. (U.S.S.R.) 33, 179-182 (July, 1957)

Experimental data referring to the shape of the lateral distribution curve of nuclear-active particles near the axis of extensive showers are considered. The data indicate a small value of the averaged minimum angles of emission of nuclear-active particles responsible for generation of the nuclear-active particles directly recorded in the experiments ($< 4 \times 10^{-3}$ radians). It is shown that Landau's theory of multiple particle production can yield such a small value for the emission angle only if it simultaneously predicts a high degree of concentration of energy of the incident particle on a single secondary particle in an elementary act of the nuclear cascade process at energies of $10^{12} - 10^{15}$ ev.

DETAILED measurements of the lateral distribution of nuclear-active particles (NAP) in extensive air showers were recently carried out both at high altitudes and near sea level.[1,2] The characteristic feature of the lateral distribution of NAP obtained from these measurements consists in the sharp increase of the NAP flux density with decreasing distance from the shower axis up to distances $\lesssim 2$ m, the increase being as fast as 1/r at least even for the case of showers with a small total number of all charged particles, $N = 6 \times 10^4$.

It is the aim of the present note to show that it follows from the experimental fact of the sharp increase of the NAP flux up to $r \lesssim 2$ m that the emission angles in nuclear interactions of NAP which generated the particles directly observed in the experiments[1,2] are very small. Furthermore, it will be shown that in the comparison of the obtained estimate of the angles of emission with the value for the angle of emission of the secondary particle possessing the highest energy, derived from the Landau theory, an agreement between the experimental estimate and the theoretical value can be reached only on condition of high average concentration of energy on a single secondary particle in each generation of the nuclear cascade process.

It was shown by Greisen et al.[3] that the steep rise of the lateral distribution function of NAP near the axis, going as 1/r, follows from purely geometrical considerations, on condition that the detected NAP are produced by generating high-energy NAP traveling in a very narrow cone enveloping the shower core.*

The experimental data of Refs. 1 and 2 make it possible to estimate the emission angles of generating NAP. In fact, since the mean free path for nuclear interaction, corresponding to 70 g/cm^2 [4-7] in air† amounts to 800 m for the altitude of observation of Ref. 1 (Pamir station, 3860 m) and to 500 m near sea level, we can estimate the angle of emission of generating particles as follows:

$$\chi \leqslant 2/800 \approx 3 \cdot 10^{-3} \text{ radians} \quad (1)$$

for generating NAP in the core of a shower at the altitude of the Pamir station, and

$$\chi \leqslant 2/500 = 4 \cdot 10^{-3} \text{ radians} \quad (2)$$

---

*In the limit, if the emission angle of generating particles in the core → 0, the 1/r law would hold for arbitrarily small distances from the axis.

†Such is the mean value of the nuclear interaction mean free path according to Refs. 4 — 7 in which the nuclear range was determined in air and graphite for NAP of $\sim 10^9 - 10^{10}$ ev. Since there is no basis for a decrease in the nuclear interaction cross-section for ultra-high energies than the mean free path for nuclear interaction for energies $> 10^{11}$ ev has to be regarded as essentially constant and equal to 70 g/cm^2.

for generating particles in the core of a shower near the sea level.* The minimum angles of emission are expected to be substantially smaller than these estimates.

We shall compare now the estimates for emission angles of generating NAP with the value of the average minimum angle of emission of particles which follows from the theory of Landau[8] for the case of nucleon—nucleus collision. For the estimate of the averaged minimum angle of emission of secondary particles in nucleon—nucleus collisions according to Landau's theory we made use of the model representing the collision as occurring between the nucleon and a column of nucleons of the nucleus forming a cylindrical volume of nuclear matter.[9]

We shall use the expression obtained by Landau for the angle of emission of a secondary particle in the ultra-relativistic case:

$$\chi = e^{-\lambda} / \gamma_c, \quad \gamma_c = 1/\sqrt{1 - v_c^2}. \tag{3}$$

where χ is the emission angle of particle in the laboratory system of coordinates, v_c is the velocity of the center of mass of colliding particles (c-system) with respect to the laboratory system and λ is a parameter of the Landau theory.

We shall generalize relation (3) for the case of a collision between a nucleon and a cylinder of nuclear matter. The averaged (because of the statistical character of the theory) value of the minimum emission angle can be estimated taking for λ its maximum value λ_m. The latter can be found from the condition (cf. Ref. 8)

$$\int_{\lambda_m}^{L} C \exp(\sqrt{L^2 - \lambda^2})\, d\lambda = 1. \tag{4}$$

where $L = -\ln(\Delta/a)$, Δ is the longitudinal dimension of the system nucleon-cylinder of nuclear matter in the c-system at the end of the contraction stage,† a is its lateral dimension, and C is a constant determined from the normalization to the total number of produced particles.

Substituting λ_m found from (4) into (3) we obtain the value of the averaged minimum emission angle in the laboratory system:

$$\bar{\chi}_{\min} \approx {}^1/_2 A^{1/6} ({}^2/_3 A^{1/6} + 1)\, Mc^2 / E. \tag{5}$$

where E is the energy of the incident nucleon, A is the atomic weight of the target nucleus and Mc^2 is the rest energy of the nucleon ($\sim 10^9$ev). For the case of collision between e nucleon and an air atom ($A \approx 14$) we have

$$\bar{\chi}_{\min} \approx 2Mc^2 / E. \tag{6}$$

Expressions (3) and (4) by means of which formula (6) has been obtained, are applicable in the region of the so-called non-trivial solution.[10] Since the non-trivial solution should merge with the solution representable in the form of a traveling wave corresponding to the secondary particle of maximum energy, one should expect that the value of the minimum emission angle (6) will be close to the value of the angle corresponding to the particle of maximum energy described by a traveling wave.

Comparing (6) with the estimates (1) and (2) of the emission angle of generating particles we conclude that the energies of NAP at the altitude of Pamir station and at sea level should equal, respectively,

$$E \gtrsim 10^{12}\ \text{ev} \ \text{and}\ E \gtrsim 5 \cdot 10^{11}\ \text{ev} \tag{7}$$

in order that theoretical values of the angles correspond to experimental estimates.

It can be now easily seen that generating NAP of such high energies can be present in the core of showers at the level of Pamir station and near sea level only on condition of an extremely high concentration of the energy of incident particle on one secondary particle at all stages of the nuclear cascade process producing the recorded extensive showers.*

---

*More accurately, these levels are on the average two nuclear lengths above the shower detection point (Pamir station, Moscow) since the NAP observed directly are produced on the average at the distance of one nuclear mean free path above the detectors and the particles which generate them are in turn produced on the average one free path higher.

†The calculation was made for a cylinder of mean height $\bar{H}$, which was assumed to be equal to the mean chord of the sphere with radius $R = (\hbar/\mu c) A^{1/3}$, where μ is the π-meson mass, i.e., $\bar{H} = 4R/3$.

We shall denote by α the energy fraction of the incident particle, averaged for all stages of the nuclear cascade process, which is transferred to the secondary particle of maximum energy. The value of α necessary for safeguarding the presence of NAP of high energy at the elevation of Pamir station and at sea level can then be found from the relation

$$E = E_0\alpha^n. \tag{8}$$

Here E_0 is the energy of the shower-producing particle, n is the average number of nuclear lengths from the top of the atmosphere to levels two nuclear lengths above observation levels. In the determination of n it should be taken into account that for the case of showers observed in the lower half of the atmosphere by conventional detectors, the mean production level is at about ~100 g/cm² below the top of the atmosphere.[11]

According to Sarycheva[12] the energy of primary NAP initiating extensive air showers with total number of charged particles at sea level $N = 6 \times 10^4$ amounts to $E_0 \approx 10^{15}$ ev and the energy of particles initiating extensive air showers with the same number of particles at the elevation of Pamir station to $E_0 \approx 1.5 \times 10^{14}$ ev. It should be noted that the estimate of E_0 from the number of particles in a shower, given in Ref. 12, differs by less than 1.5 from the estimate using the coefficient of the relation between N and E_0 recently found by Greisen.[13]†

For the case of shower detection at Pamir elevation $n = 7$ and near sea level (Moscow) $n = 12$, under the assumption that the interaction mean free path in air for NAP is 70 g/cm².

Consequently, we find for α [from (8)] the value $\alpha \gtrsim 0.5$ by starting with either (1) or (2) and by assuming the correctness of expression (6) for the averaged minimum emission angle, obtained from Landau's theory.‡ It follows that this theory will yield the value of emission angles of generating NAP required by experimental evidence only in the case when it predicts simultaneously a very high degree of concentration of energy, not less than 50%, on a single secondary particle in elementary processes at the energies of $10^{12} - 10^{15}$ ev.

Gerasimova and Chernavskii calculated the fraction of energy of the incident nucleon carried away by the traveling wave.[10] They found that the average energy concentration on the secondary particle of maximum energy in the energy interval $10^{12} - 10^{15}$ ev amounts to about 35%. The problem of the fraction of energy of the incident particle, carried away by the secondary particle of maximum energy according to the hydrodynamical theory, is extremely difficult and has not been so far worked out in any detail.

It has been pointed out in the work of Vernov et al.[14] that in interactions of the nucleons with nucleons and with light nuclei at ultra-high energies, the total energy of the incident nucleon is in most cases not dissipated within a unique thermodynamical system. The greater part of the energy, on the order of 70%, remains in the nucleon undergoing the collision. The considerations of the present note do not contradict such a view.

In conclusion, I wish to express my deep gratitude to N. A. Dobrotin, G. T. Zatsepin, G. A. Milekhin, and D. S. Chernavskii for discussion of the problems raised in the present note.

---

*The deduction that NAP of high energies ($>10^{11} - 10^{12}$ ev) should be found in the cores of extensive showers at lower atmospheric depths (sea level) was arrived at earlier by Zatsepin. It was not, however, fully substantiated since the relation $\chi_{\min} = Mc^2/E$ was assumed arbitrarily.

†The coefficient in the relation between N and E_0 was obtained in Ref. 13 by means of very general considerations computing the total energy spent on ionization by all charged particles in the total atmospheric depth using experimental data on the longitudinal development of showers.

‡It should be noted that in spite of the fact that formula (6) was derived from the Landau solution which is approximate at the boundary with the traveling wave, this formula nevertheless yields for a given value of the energy of generating particle a value of $\overline{\chi}_{\min}$ only twice as large as that obtained from a more accurate solution of the hydrodynamical equations (G. A. Milekhin — private communication). Since α is almost independent of the energy of the generating particle of maximum energy, estimated from the emission angle at a given level [cf. Eq. (8)], the increase in the estimated value of α due to the use of a slightly inaccurate formula (6) is not very considerable.

[1]Nikol'skii, Vavilov and Batov, Dokl. Akad. Nauk SSSR **111**, 71 (1956); Soviet Phys. "Doklady" **1**, 625 (1956).

[2]Abrosimov, Zatsepin, Solov'eva, Khristiansen and Chikin, Izv. Akad. Nauk SSSR, Ser. Fiz. **19**, 677 (1955).

[3]Greisen, Walker and Walker, Phys. Rev. **80**, 535 (1950).

[4]A. L. Liubimov, Dissertation, Phys. Inst. Acad. Sci., 1954.

[5]R. R. Brown, Phys. Rev. **87**, 999 (1952).

[6]Vernov, Kulikov, and Charakhchian, Izv. Akad. Nauk SSSR, Ser. Fiz. **17**, 13 (1953).

[7]K. I. Alekseeva and N. L. Grigorov, Report at Tbilisi Conference on Cosmic Ray Physics, October, 1956.

[8]L. D. Landau, Izv. Akad. Nauk SSSR, Ser. Fiz. **17**, 51 (1953).

[9]S. Z. Belen'kii and L. D. Landau, Usp. Fiz. Nauk **56**, 309 (1955).

[10]N. M. Gerasimova and D. S. Chernavskii, J. Exptl. Theoret. Phys. (U.S.S.R.) **29**, 372 (1955); Soviet Phys. JETP **2**, 344 (1956).

[11]G. T. Zatsepin and L. I. Sarycheva, Dokl. Akad. Nauk SSSR **99**, 951 (1954).

[12]L. I. Sarycheva, Dissertation, Phys. Inst. Acad. Sci., 1953.

[13]K. Greisen, Progress in Cosmic Ray Physics, vol. III, 1956.

[14]Vernov, Grigorov, Zatsepin and Chudakov, Izv. Akad. Nauk SSSR, Ser. Fiz. **19**, 493 (1955).

Translated by H. Kasha
25

SOVIET PHYSICS JETP VOLUME 6, NUMBER 1 JANUARY, 1958

SOME CHARACTERISTICS OF M1-CONVERSION NUCLEAR TRANSITIONS

D. P. GRECHUKHIN

Submitted to JETP editor January 4, 1957

J. Exptl. Theoret. Phys. (U.S.S.R.) 33, 183-189 (July, 1957)

M1-conversion nuclear transitions are investigated within the framework of the single-particle model with LS coupling.

WITHIN the framework of the strictly single-particle model of the nucleus M1-conversion on nucleonic transitions of the types $n_1 s_{1/2} - n_2 s_{1/2}$ and $n_1 d_{1/2} - n_2 s_{3/2}$ are "forbidden". The contribution from the field of the external electronic current of the transition disappears in the case of a $n_1 s_{1/2} - n_2 s_{1/2}$ transition because of the orthogonality of the nucleonic radial functions and in the case of a $n_1 s_{1/2} - n_2 d_{3/2}$ transition because of the orthogonality of the nucleonic of the nucleonic angular functions. In these transitions the conversion probability is determined only by the contribution of the "internal" electronic transition current. However the spin-orbit interaction of the nucleons and the correlation of nucleonic motion which results from their interaction lead to the inclusion of an interaction with the external electronic current. The conversion probability in these cases is determined by entirely different matrix elements than for the usual "allowed" M1 nuclear transitions (such as $p_{1/2} - p_{3/2}$). The results of calculations of K-electron conversion probabilities for various M1 nuclear transitions are given below. It is assumed that the momentum of the final electronic state $p \gg Ze^2$; the K-electron transition to the state $j = 3/2, \lambda = +1/2, \ell = 2$ is neglected because the probability of this transition is smaller by the factor $\sim (Ze^2)^2/2$ than the transition probability to the state $j = 1/2, \lambda = -1/2, \ell = 0$. The relativistic units $\hbar = m_e = c = 1$ are used throughout.

In the model under consideration the nucleonic wave function is separated into radial and angular parts:

$$\Psi(\mathbf{x}) = R_{I\Lambda}(x)\,\Omega_{IM}(\theta\varphi); \quad x = \xi / R_0,$$

where $R_0 \doteq 1.2 \times 10^{-13} A^{1/3}$ cm and ξ is the coordinate of the transition nucleon. The wave functions of the electron are designated by $\psi_{j\mu\lambda}(\mathbf{r})$. The subscripts 1 and 2 denote the initial and final states, respectively. The electronic functions are normalized to $\delta_{jj'}\delta_{\lambda\lambda'}\delta_{\mu\mu'}\delta(\epsilon-\epsilon')$.

1. THE VECTOR POTENTIAL OF THE M1 TRANSITION

When a K-electron (1, $j = 1/2$, $\lambda = -1/2$, $\ell = 0$) undergoes a transition to a continuum state (2, $p\epsilon$, $j = 1/2$, $\lambda = -1/2$, $\ell = 0$) a transition vector potential **A** is induced in the nucleus. The magnetic-dipole term $\mathbf{A}_1^0$ is

$$\mathbf{A}_1^0 = \sum_M B_{1M}^0(\xi)\,\mathbf{Y}_{1M}^0(\boldsymbol{\xi}).$$

$$B_{1M}^0(\xi) = e\int \left(\langle \psi^*_{j\lambda\mu_2}(2)\,|\,\boldsymbol{\alpha}\,|\,\psi_{j\lambda\mu_1}(1)\rangle\,\mathbf{Y}_{1M}^{0*}(\boldsymbol{\xi})\right)\frac{dr\,d\omega_\xi}{|\mathbf{r}-\boldsymbol{\xi}|}; \quad \boldsymbol{\alpha} = \begin{Bmatrix} 0 & \boldsymbol{\sigma} \\ \boldsymbol{\sigma} & 0 \end{Bmatrix},$$

where $\boldsymbol{\sigma}$ denotes the Pauli matrices

$$\sigma_0 \Rightarrow \sigma_z = \begin{Bmatrix} 1 & 0 \\ 0 & -1 \end{Bmatrix}.$$

We divide B_{1M}^0 into parts corresponding to the contributions of the external and the internal electronic transition currents, for $r \geq R_0$ and $r \leq R_0$:

$$B_{1M}^0 = B_{1M>}^0 + B_{1M<}^0.$$

$B_{1M<}^0$ is calculated with electronic wave functions in the field of a uniformly charged sphere of radius R_0. In the calculation of $B_{1M>}^0$ it is necessary to take account of the distortion of the electronic wave functions which results from finite nuclear size, as was done by Sliv.[1] However, in order to compare the relative contributions of different terms in the interaction of the nucleon with the electromagnetic field of the external current $B_{1M>}^0$ can be obtained with electronic functions in the field of a point nucleus. Neglect of the finite nuclear size does not introduce an essential error; allowance for this effect changes $B_{1M>}^0$ by not more than ~20%. By neglecting the finite size of the nucleus we obtain

$$\mathbf{A}_{1>}^0 = i\frac{\sqrt{2}}{3}\,eC_jN_jJR_0x\sum_M\sqrt{4\pi}\,C_{1Mj\mu_2}^{j\mu_1}\,\mathbf{Y}_{1M}^0(\mathbf{x});$$

$$\mathbf{A}_{1<}^0 = i\frac{\sqrt{2}}{18}\,eC_jN_jS\Sigma R_0^{2\gamma}(3Ze^2 + \Delta R_0)\,K(x)\sum_M\sqrt{4\pi}\,C_{1Mj\mu_2}^{j\mu_1}\,\mathbf{Y}_{1M}^0(\mathbf{x}).$$

Here

$$C_j = (2p)^\gamma \exp(\pi Ze^2\varepsilon/2p)\,|\,\Gamma(\gamma + iZe^2\varepsilon/p)\,|\,/\sqrt{\pi p}\,\Gamma(2\gamma+1). \qquad N_j \doteq 2^\gamma(Ze^2)^{\gamma+1/2}/\sqrt{\Gamma(2\gamma+1)}; \quad \gamma = +\sqrt{1-(Ze^2)^2};$$

$$\varepsilon_1 = 1-(Ze^2)^2/2, \qquad S = -\frac{2(1-\varepsilon_1^2)^{1/2}}{(1-\varepsilon_1)^{1/2}(\gamma+1)(1-\omega_1^2/6)-(1+\varepsilon_1)^{1/2}(\omega_1/3)(1-\gamma)};$$

$$\Sigma = \frac{(\varepsilon^2-1)^{1/2}[\operatorname{Im}Q(-\gamma)\operatorname{Re}Q(+\gamma)-\operatorname{Re}Q(-\gamma)\operatorname{Im}Q(+\gamma)]}{(\varepsilon-1)^{1/2}(1-\omega_2^2/6)\operatorname{Im}Q(-\gamma)-(1+\varepsilon)^{1/2}(\omega_2/3)\operatorname{Re}Q(-\gamma)}; \quad J \approx {}^1/_2\{[(\varepsilon+1)(1-\varepsilon_1)]^{1/2}(I+I^*)-i(I-I^*)[(\varepsilon-1)(1+\varepsilon_1)]^{1/2}\};$$

$$I \approx \frac{e^{i\eta}(\gamma+iZe^2\varepsilon/p)}{(Ze^2+ip)^{2\gamma-1}}\left\{\Gamma(2\gamma-1)\,{}_2F_1\left(\gamma+1+iZe^2\varepsilon/p;\,2\gamma-1;\,2\gamma+1;\,\frac{2p}{p-iZe^2}\right)-\frac{[(Ze^2+ip)R_0]^{2\gamma-1}}{(2\gamma-1)}\exp(-Ze^2R_0)\,{}_1F_1(\gamma+1\right.$$

$$\left.+iZe^2\varepsilon/p;\,2\gamma+1;\,2ipR_0)\right\}; \quad K(x) = \{[1-{}^3/_8(Ze^2)^2-{}^1/_4\Delta R_0]\,x-0{,}6\,x^3\};$$

$$Q(\hat{\gamma}) = e^{i\hat{\eta}}(\hat{\gamma}+iZe^2\varepsilon/p)\,{}_1F_1(\hat{\gamma}+1+iZe^2\varepsilon/p;\,2\hat{\gamma}+1;\,2ipR_0);$$

$$\hat{\gamma} = \pm\gamma; \quad e^{2i\hat{\eta}} = \frac{1+iZe^2/p}{\hat{\gamma}+iZe^2\varepsilon/p}; \quad \omega_1 = 3Ze^2/2; \quad \omega_2 = 3Ze^2/2+\Delta R_0;$$

Δ is the nuclear transition energy.

2. M1 NEUTRON TRANSITIONS

The transition probability W_{M1} is determined by the matrix element of the interaction operator: $\mathscr{H} = (\mu_n e/2M)(\sigma \mathbf{H})$, where μ_n is the magnetic moment in nuclear Bohr magnetons: $\mu_n = -1.97$.

It is easily seen that the potential $\mathbf{A}^0_{1>}$ makes no contribution. Indeed,

$$\mathbf{A}^0_{1>} \sim \xi \mathbf{Y}^0_{1M}(\xi); \ \mathrm{curl}\, \mathbf{A}^0_{1>} \sim \mathbf{Y}^{-1}_{1M}(\xi)$$

and does not contain the radial variable ξ. It can thus be seen that in an $M1(s_{1/2} - s_{1/2})$ transition the matrix element of the operator $\mathscr{H}$ vanishes as a result of the orthogonality of the radial functions and in a $d_{3/2} - s_{1/2}$ transition because of the orthogonality of the angular nucleonic functions. A nonvanishing contribution is made only by the term $\mathbf{A}^0_{1<}$ this is proportional to x^3.

We obtain

$$\mathscr{H}_{<} = 0.1\frac{\sqrt{2}}{3} eC_j N_j S \Sigma R_0^{2\gamma}(3Ze^2 + \Delta R_0)\left\{5\sqrt{\frac{2}{3}}\left(\sum_M \sqrt{4\pi} C^{j\mu_1}_{1Mj\mu_2} \mathbf{Y}^{-1}_{1M}(\mathbf{x})\right)x^2 + \frac{2}{\sqrt{3}}\left(\sum_M \sqrt{4\pi}\, C^{j\mu_1}_{1Mj\mu_2} \mathbf{Y}^{+1}_{1M}\right)x^2\right\}.$$

The first term makes a nonvanishing contribution in an $s_{1/2} - s_{1/2}$ transition and the second term in an $s_{1/2} - d_{3/2}$ transition:

$$W^e_{M1s-s} = \frac{2^{4\gamma}}{54}\frac{(Ze^2)^{2\gamma+1}}{[\Gamma(2\gamma+1)]^3}\left(\frac{e^2R_0}{M}\right)^2 \mu_n^2 (3Ze^2 + \Delta R_0)^2 R_0^{4\gamma-4}\ p^{2\gamma-1} S^2 \Sigma^2 \exp(\pi Ze^2\varepsilon/p)\,|\Gamma(\gamma + iZe^2\varepsilon/p)|^2\,|\langle R^*_{I_2\Lambda_2}|x^2|R_{I_1\Lambda_1}\rangle|^2 P_{ss};$$

$$P_{ss} = \frac{1}{(2j+1)(2I_1+1)}\sum_{\substack{\mu_1\mu_2\\ M_1M_2}}\left|\sum_M \sqrt{4\pi}\, C^{j\mu_1}_{1Mj\mu_2}\langle\Omega^*_{I_2M_2}|\sigma\mathbf{Y}^{-1}_{1M}|\Omega_{I_1M_1}\rangle\right|^2, \quad W^e_{M1s-d} = \frac{2^{4\gamma}}{9\cdot 75}\frac{(Ze^2)^{2\gamma+1}}{[\Gamma(2\gamma+1)]^3}\left(\frac{e^2R_0}{M}\right)^2 \mu_n^2\,(3Ze^2$$

$$+ \Delta R_0)^2\ R_0^{4\gamma-4}\ p^{2\gamma-1} S^2 \Sigma^2 \exp(\pi Ze^2\varepsilon/p)\,|\Gamma(\gamma + iZe^2\varepsilon/p)|^2\,|\langle R^*_{I_2\Lambda_2}|x^2|R_{I_1\Lambda_1}\rangle|^2 P_{sd},$$

$$P_{sd} = \frac{1}{(2\gamma+1)(2I_1+1)}\sum_{\substack{\mu_1\mu_2\\ M_1M_2}}\left|\sum_M \sqrt{4\pi}\, C^{j\mu_1}_{1Mj\mu_2}\langle\Omega^*_{I_2M_2}|\sigma\mathbf{Y}^{+1}_{1M}|\Omega_{I_1M_1}\rangle\right|^2.$$

It is assumed that the nucleon is in the field of the nuclear core with angular momentum J so that

$$\Omega_{IM} = \sum_{m\nu} C^{IM}_{JmF\nu} U_{Jm} V_{F\nu}(\xi).$$

For P_{ss} we obtain

$$P_{ss} = 2(2I_2+1)\,w^2(I_1 J 1\,{}^1\!/_2;\ {}^1\!/_2 I_2).$$

For P_{sd} in the special case $J = 0$

$$P_{sd} = (2I_2+1)/4,$$

and in the general case $J \neq 0$

$P_{sd} = 2(2I_2+1)\,w^2(I_1 J 1\,{}^3\!/_2;\ {}^1\!/_2 I_2)$ for an $s_{1/2} \to d_{3/2}$ transition;

$P_{sd} = 2(2I_2+1)\,w^2(I_1 J 1\,{}^1\!/_2;\ {}^3\!/_2 I_2)$ for a $d_{3/2} \to s_{1/2}$ transition,

where w(abcd; ef) are Racah coefficients.

The probability of γ radiation is obtained in these cases by employing the potential of magnetic dipole radiation (a light quantum with polarization vector ϵ_λ and wave vector Δ)

$$\mathbf{A}_{10} = i4\pi\sqrt{2\pi/\Delta}\sum_M (\varepsilon_\lambda \mathbf{Y}^0_{1M}(\Delta))\, f_1(\Delta\xi)\, \mathbf{Y}^0_{1M}(\xi),$$

where f_1 is a spherical Bessel function. We obtain

$$W^\gamma_{M1s-s} = \frac{1}{108}\frac{R_0^4 e^2}{M^2}\mu_n^2\Delta^7|\langle R^*_{I_2\Lambda_2}|x^2|R_{I_1\Lambda_1}\rangle|^2 L_{ss};\quad L_{ss} = \frac{1}{(2I_1+1)}\sum_{M_1M_2\lambda}\left|4\pi\sum_M(\varepsilon_\lambda \mathbf{Y}^{0*}_{1M}(\Delta))\langle\Omega^*_{I_2M_2}|\sigma\mathbf{Y}^{-1}_{1M}|\Omega_{I_1M_1}\rangle\right|^2;$$

$$W^\gamma_{M1sd} = \frac{1}{1350}\frac{R_0^4 e^2}{M^2}\mu_n^2\Delta^7|\langle R^*_{I_2\Lambda_2}|x^2|R_{I_1\Lambda_1}\rangle|^2 L_{sd};\quad L_{sd} = \frac{1}{(2I_1+1)}\sum_{M_1M_2\lambda}\left|4\pi\sum_M(\varepsilon_\lambda \mathbf{Y}^{0*}_{1M}\Delta())\langle\Omega^*_{I_2M_2}|\sigma\mathbf{Y}^{+1}_{1M}|\Omega_{I_1M_1}\rangle\right|^2.$$

In the same special cases as for P_{ss} and P_{sd} we obtain

$$L_{ss} = 6\,(2I_2+1)\,w^2\,(I_1 J 1 {}^1\!/_2;\ {}^1\!/_2 I_2);\quad L_{sd} = 3\,(2I_2+1)/4 \text{ for } J=0,$$

and for $J \neq 0$:

$$L_{sd} = 6\,(2I_2+1)\,w^2\,(I_1 J 1 {}^3\!/_2;\ {}^1\!/_2 I_2), \text{ for an } s_{1/2} \to d_{3/2} \text{ transition;}$$
$$L_{sd} = 6\,(2I_2+1)\,w^2\,(I_1 J 1 {}^1\!/_2;\ {}^3\!/_2 I_2), \text{ for a } d_{3/2} \to s_{1/2} \text{ transition.}$$

3. M1 PROTON TRANSITIONS. EFFECT OF THE LS INTERACTION

LS proton coupling leads to an additional proton-electron interaction term; the interaction operator for proton transitions is [2,3]

$$\mathcal{H} = (\mu_p e/2M)\,(\boldsymbol{\sigma}\mathbf{H}_<) + eD(x)\,(\boldsymbol{\sigma}[\boldsymbol{\xi}\mathbf{A}_<]).$$

We neglect the contribution of $\mathbf{A}_<$, which is one order smaller than that of the first term $\sim (\boldsymbol{\sigma}\mathbf{H}_<)$.

For the probability of M1 proton transitions with K-electron conversion we obtain:

In an s − s transition

$$W^e_{M1ss} = \frac{2^{4\gamma+3}}{27}(eR_0)^4 \frac{(Ze^2)^{2\gamma+1}}{[\Gamma(2\gamma+1)]^3}\, p^{2\gamma-1} \exp(\pi Z e^2 \varepsilon/p)\,|\Gamma(\gamma + iZe^2\varepsilon/p)|^2 J^2 \times$$
$$\times \left| \langle R^*_{I_2\Lambda_2} | x^2 D(x) | R_{I_1\Lambda_1} \rangle - 0{,}25 \frac{\mu_p}{MR_0} \frac{S\Sigma}{J} R_0^{2\gamma-2}(3Ze^2 + \Delta R_0) \langle R^*_{I_2\Lambda_2} | x^2 | R_{I_1\Lambda_1} \rangle \right|^2 P_{ss};$$

In an s − d proton transition

$$W^e_{M1sd} = \frac{2^{4\gamma+2}}{27}(eR_0)^4 \frac{(Ze^2)^{2\gamma+1}}{[\Gamma(2\gamma+1)]^3}\, p^{2\gamma-1} \exp(\pi Z e^2 \varepsilon/p)\,|\Gamma(\gamma + iZe^2\varepsilon/p)|^2 J^2 \left| \langle R^*_{I_2\Lambda_2} | x^2 D(x) | R_{I_1\Lambda_1} \rangle \right.$$
$$\left. - 0{,}1 \frac{\mu_p}{MR_0} \frac{S\Sigma}{J} R_0^{2\gamma-2}(3Ze^2 + \Delta R_0) \langle R^*_{I_2\Lambda_2} | x^2 | R_{I_1\Lambda_1} \rangle \right|^2 P_{sd}.$$

Here M is the nucleon mass ≈ 2 × 10^3.

The value of J should be calculated with the correct electronic wave functions outside the nucleus, as was done by Sliv,[1] but for comparison of the relative contributions of the two matrix elements we use the approximate value of J with $p \gg Ze^2$:

$$\approx (2p)^{-1}(\varepsilon-1)^{1/2}(1+\varepsilon_1)^{1/2}\gamma\cos\eta_l,\quad S \approx (1+\varepsilon_1)^{1/2},\quad \varepsilon \approx (1+\varepsilon)^{1/2}.$$

Then for the ratio δ of the matrix element $\sim \langle 2|x^2|1\rangle$ to the matrix element $\sim \langle 2|D(x)x^2|1\rangle$, using the rough estimate (see Ref. 3)

$$\langle 2|D(x)x^2|1\rangle \approx \langle D(x)\rangle_{\text{cp}} \langle 2|x^2|1\rangle,\quad \langle D(x)\rangle_{\text{cp}} \approx -9{,}6A^{-1/3},$$

we obtain for s − s transitions

$$\delta_{ss} = \frac{0{,}5}{9{,}6} A^{1/3} R_0^{2\gamma-2} \Delta\,(3Ze^2 + \Delta R_0) \frac{\mu_p}{MR_0} \frac{1}{\gamma\cos\eta_l};$$

and for s − d transitions

$$\delta_{sd} = 0{,}4\,\delta_{ss}.$$

We present a brief table of estimated values of δ_{ss} for $\Delta \approx 1$ as a function of Z:

$Z =$	10	20	30	40	50	60	70	80	90
$\delta_{ss} =$	0.015	0.037	0.067	0.096	0.14	0.195	0.24	0.31	0.39

Unlike the conversion transition, M 1 γ radiation is completely determined in both s − s and s − d transition by the spin-orbit term. For an s − s transition

$$W^{\gamma}_{M1ss} = {}^4\!/_{27} e^2 R_0^4 \Delta^3 |\langle R^*_{I_2\Lambda_2} | x^2 D(x) | R_{I_1\Lambda_1} \rangle|^2 L_{ss};$$

and for an s − d transition

$$W^{\gamma}_{M1sd} = {}^2\!/_{27} e^2 R_0^4 \Delta^3 |\langle R^*_{I_2\Lambda_2} | x^2 D(x) | R_{I_1\Lambda_1} \rangle|^2 L_{sd}.$$

Since we cannot neglect the interaction between the magnetic moment of the nucleon and the field in $W^e_{M1\,ss}$ and $W^e_{M1\,sd}$, in these M1 proton transitions the conversion coefficient depends on the nuclear matrix elements.

4. EFFECT OF NUCLEONIC INTERACTIONS

Thus far we have been considering the ideal case of a strictly single-particle model with **LS** interaction; this does not exist in reality and one can only speak of a certain degree of approximation. The interactions between core nucleons and the nucleon undergoing the transition result in a departure from the model, since the single-nucleon functions become nonorthogonal. They also result in the inclusion of the interaction between the nucleon and the external electronic transition current, thus strongly increasing the probability of a conversion transition. This interaction also sharply increases the probability of a radiative nuclear transition. We shall roughly estimate the effect of nucleonic interactions for a neutron interaction ($\nu s_{1/2} - \mu s_{1/2}$) when a single $ns_{1/2}$ proton is situated outside of the closed shells. It is assumed that the independent-particle model is a good zero-order approximation and that the interaction between nucleons can be taken in the form of the δ function potential

$$\hat{V}(|\xi_n - \xi_p|) = \hat{C}\delta(\xi_n - \xi_p),$$

where $\hat{C}$ is the spin operator with average value of the order 10^{-36} Mev-cm^3. The nucleonic interaction also affects other cases in which the proton is in an $s_{1/2}$ state. But the calculation then requires a specific potential and a finite range of nuclear forces as well as the inclusion of tensor forces, thus making it much more difficult to obtain even a rough estimate.

The zero-order neutron functions will be denoted by $\varphi_\nu(x)$, $\varphi_\mu(x)$, $\int|\varphi|^2 dx = 1$, and the proton functions by $f_n(y)$, $0 \le x \le 1$ and $0 \le y \le 1$ ($x = \xi_n/R_0$, $y = \xi_p/R_0$). The two-particle wave functions will be obtained by perturbation theory:

$$\psi_{\nu n}(x, y) = \chi_{IM}(\varphi_\nu(x) f_n(y) + \varphi'_{\nu n}(x, y))$$

with conservation of the spin of the system; χ_{IM} is the spin wave function of the system.

Assuming that contributions are obtained only from terms with identical radial wave functions we obtain for the probability of K-electron conversion

$$W^e_{M1ss} = \frac{2^{4\gamma+1}}{3}\frac{e^4}{M^2}\frac{(Ze^2)^{2\gamma+1}}{[\Gamma(2\gamma+1)]^3} p^{2\gamma-1} \exp(\pi Ze^2\varepsilon/p)\,|\Gamma(\gamma + iZe^2\varepsilon/p)|^2 \mathfrak{J}^2\alpha^2 A_{ss},$$

where

$$\mathfrak{J}^2 = \left|\frac{\langle\chi^*_{I_1M_1}|\hat{C}|\chi_{I_1M_1}\rangle - \langle\chi^*_{I_2M_2}|\hat{C}|\chi_{I_2M_2}\rangle}{R_0^3\varepsilon_0}\right|^2 \left|\frac{\int f_n^2(x)\,\varphi_\nu(x)\,\varphi_\mu(y)\,dx}{\pi^2(\nu^2-\mu^2)}\right|^2;$$

$$A_{ss} = \frac{1}{(2j+1)(2I_1+1)} \sum_{\substack{\mu_1\mu_2\\ M_2M_2}} \left|\sum_M \sqrt{4\pi}\, C^{j\mu_1}_{1Mj\mu_2} \langle\chi^*_{I_2M_2}|(\mu_p\sigma_p + \mu_n\sigma_n)\,\mathbf{Y}^{-1}_{1M}|\chi_{I_1M_1}\rangle\right|^2;$$

or

$$A_{ss} = (\mu_p - \mu_n)^2\cdot 2(2I_2+1)\,w^2(I_1{}^1/_2 1{}^1/_2;\ {}^1/_2 I_2);$$

and for the probability of gamma radiation

$$W^\gamma_{M1ss} = (e^2/3M^2)\,\Delta^3\alpha^2 B_{ss},$$

where

$$B_{ss} = \frac{1}{(2I_1+1)} \sum_{M_1M_2\lambda} \left|4\pi \sum_M (\varepsilon_\lambda \mathbf{Y}^0_{1M}(\Delta))\,\langle\chi^*_{I_2M_2}|(\sigma_p\mu_p + \sigma_n\mu_n)\,\mathbf{Y}^{-1}_{1M}|\chi_{I_1M_1}\rangle\right|^2$$

or

$$B_{ss} = (\mu_p - \mu_n)^2\cdot 6(2I_2+1)\,w^2(I_1{}^1/_2 1{}^1/_2;\ {}^1/_2 I_2).$$

Here $\epsilon_0 \approx \hbar^2/2MR_0^2$ in ordinary units; ν, μ, n are the principal (radial) quantum numbers of the nucleonic states. The integral $\int f_n^2 \varphi_\nu \varphi_\mu\, dx$ can be calculated with single-particle nucleonic wave functions and a simple potential field.

We have neglected interaction terms which do not vanish in a strict single-particle model.

The ratio of conversion probabilities for a proton transition is

$$\frac{(W)_{LS}}{(W)_{np}}=\frac{4}{9}\,\frac{M^2R_0^4}{(\mu_p-\mu_n)^2}\,\alpha^{-2}\,|\langle 2\,|\,x^2D\,(x)\,|\,1\rangle\,|^2;$$

Here $(\mu_p - \mu_n)^2 = (4.7)^2$ and the subscripts LS and np refer to the LS and n − p interactions. We again make use of the rough estimate

$$|\langle 2\,|\,x^2D\,(x)\,|\,1\rangle\sim 9{,}6\,A^{-2/3}\langle 2\,|\,x^2\,|\,1\rangle$$

and obtain with $A \approx 100\,R_0 \approx 1.4 \times 10^{-4}\,\alpha^{-2}$

$$(W^e_{M1})_{LS}\,/\,(W^e_{M1})_{np}\approx 4\cdot 10^{-4}\alpha^{-2},$$

and for the ratio of the matrix elements

$$((W^e_{M1})_{LS}/(W^e_{M1})_{np})^{1/2}\approx 0{,}02\,/\,\alpha.$$

Since the independent-particle model does not describe reality, the participation of other configurations in a real nuclear state must be of the order $\alpha \sim 0.02$. Therefore even for proton transitions we may neglect all terms except that representing a two-nucleon interaction. The conversion coefficient then is independent of the nuclear structure and agrees with the usual value for "allowed" transitions.[1] The conversion coefficient may be expected to differ from its usual value only for nuclei where the nucleon undergoing transition is in the field of closed shells or where there are other nucleons identical with it outside of the closed shells.

The proton-neutron interaction in M1 transitions considerably alters the probability of γ radiation. Data obtained by Groshev and Demidov* from a study of γ rays emitted in the capture of thermal neutrons by nuclei, in the range $11 \leq Z \leq 20$, show that transitions occur mainly in a $p_{3/2}$ neutron state by emission of an E1 quantum. When the target nucleus is of the $N \cdot He_2^4$ type, the $(s_{1/2}, s_{1/2})$ M1 transition is relatively weak. For target nuclei with an additional odd proton the intensity of M1 transitions increases by a factor of ~ 30, evidently as the result of the neutron-proton interaction.

---

[1] L. A. Sliv, J. Exptl. Theoret. Phys. (U.S.S.R.) 21, 770 (1951).

[2] J. H. D. Jensen and M. Goeppert-Mayer, Phys. Rev. 85, 1040 (1952).

[3] D. H. Grechukhin, J. Exptl. Theoret. Phys. (U.S.S.R.) 31, 513 (1956); Soviet Phys. JETP 4, 448 (1957).

Translated by I. Emin
26

---

* Private communication from L. V. Groshev.

ANALYSIS OF THE PROPERTIES OF THE ELECTRON-PHOTON COMPONENT OF EXTENSIVE AIR SHOWERS IN THE LOWER THIRD OF THE ATMOSPHERE

V. I. ZATSEPIN

P. N. Lebedev Physics Institute, Academy of Sciences, U.S.S.R.

Submitted to JETP editor January 9, 1957

J. Exptl. Theoret. Phys. (U.S.S.R.) 33, 190-196 (July, 1957)

It is concluded from an analysis of the experimental data that in the absence of large fluctuations in the longitudinal development of extensive air showers the energy spectrum in the region $E \lesssim 10^9$ ev and in the lower third of the atmosphere satisfies the condition $1.3 \geq s \geq 1.2$ (if electrons in equilibrium with μ-mesons are subtracted), s being the parameter of the electromagnetic cascade theory, which characterizes the electron energy spectrum. For a spectrum of the indicated type the lateral distribution of electrons at distances from 1.5 to 250 m from the shower axis can be explained completely by multiple Coulomb scattering.

THE lateral distribution of electrons in electronic showers was calculated by Nishimura and Kamata[1] for several values of the parameter s (0.6, 1.0, 1.4, and 2.0) in the approximation B of the cascade theory.[2] Greisen[3] proposed a simple interpolation formula which describes the curves of Nishimura and Kamata with an accuracy to a few percent. One can hope that this formula describes correctly the lateral distribution of electrons for intermediate values of s as well. This would permit a detailed comparison of the experimental data on the lateral distribution of electrons in extensive air showers (abbreviated as EAS in the following) with predictions of the cascade theory, which may yield some information on the singularities of the development of EAS. Such a comparison was already carried out by Greisen[3] who made use of the experimental data of Refs. 4-6 and by Khristiansen[7] who used data obtained in the Soviet Union and partially published in Refs. 8 and 9. It was shown that the lateral distribution of electrons in EAS coincides with the lateral distribution of electrons in electronic cascades with the parameter $s \approx 1.2-1.3$, in the distance interval 1.5 — 250 m at least. This conclusion follows more definitively from Ref. 7 and less so from Ref. 3, since less accurate experimental data have been used in the latter.

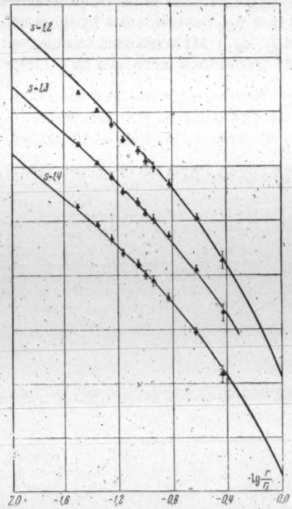

FIG. 3. Experimental dependence of the electron flux density on the distance from shower axis at sea level, shown together with the lateral distribution of electron flux density in electronic showers for s equal to 1.2, 1.3, and 1.4. $r_1 = 80$ m.

We have undertaken an additional analysis of the results* on the lateral distribution of electrons in the distance interval 1.5 — 30 m from the shower axis for two groups of showers, with the mean number of particles equal to 3.6×10^4 and 3.6×10^5 respectively. The lateral distribution of electrons was found to be identical† for both groups and we constructed therefore an average of the two distributions. This distribution is shown in Fig. 1 together with curves drawn according to the interpolation formula of Greisen.[3] The units of the logarithmic ordinate axis of Fig. 1 are proportional to electron flux density. The coefficients are arbitrary, for the sake of convenience different for various values of s. The abscissa represents logarithms (common) of the distance from the axis. The distances are measured in units of $r_1 = E_s t_0/\beta$, where $E_s \approx 21$ Mev, β is the critical energy of electrons in air equal to 72 Mev, and t_0 is the radiation length in air in meters at the level of observation (t_0 = 274 m at sea level).

---

*These results were obtained by us in 1953 at sea level. They were partially analyzed before and published (Ref. 8).

†If the obtained distributions are approximated by the power law $f(r) \sim r^{-n}$, then for $\overline{N} = 3.6 \times 10^4$ we have $n = 0.99 \pm 0.06$ and for $\overline{N} = 3.6 \times 10^5$ $n = 1.02 \pm 0.04$ for the distances between 2.5 and 12 m from the shower axis.

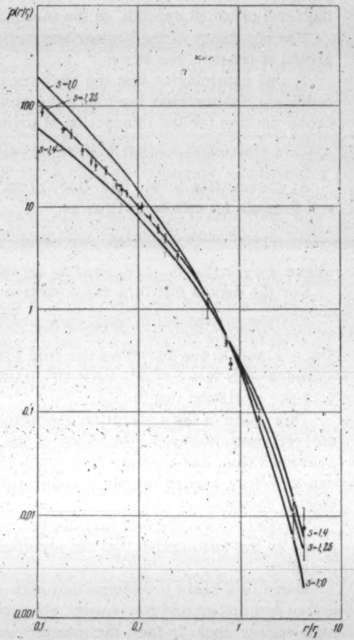

FIG. 2. Dependence of the electron flux density distribution in EAS (without the electrons in equilibrium with μ-mesons) on the distance from shower axis. Solid curves correspond to calculations of Nishimura and Kamata for s equal to 1.0, 1.25 and 1.4. Measurements: x — Moscow, • — Pamir.

It can be seen from Fig. 1 that the experimental distribution for the distances 1.5–30 meters from the axis is in a better agreement with the theoretical curve for s = 1.3. This curve, as it can be seen from Fig. 2 taken from Ref. 7, evidently fits better the experimental data and over a wider distance interval as well. It also does not contradict the experimental data used by Greisen.[3]

The lateral distribution of electrons in electronic showers is basically due to multiple Coulomb scattering and depends on the energy spectrum of shower electrons near the observation level. In EAS, besides multiple scattering, a certain role can be played by the emission angles of π^0-mesons produced in nuclear interactions (nuclear scattering) and which transfer the energy from the nuclear-active into the soft component of the shower, and also by the angles of emission of photons originating in the decay of π^0-mesons. The distribution of electrons in EAS should therefore, for the same energy spectrum of electrons near the observation level, be not less extensive than in purely electronic cascades. Consequently, the agreement between the experimental data on the lateral distribution of electrons in EAS and the electron distribution calculated for electronic cascades with s = 1.3 signifies that the energy spectrum of electrons in EAS at energies $E \lesssim 10^9$ ev* should satisfy the condition $s \leq 1.3$.

Additional information about the energy spectrum of electrons can be obtained from the analysis of their longitudinal development in a single shower. There are no direct data of this kind. Some information can be obtained, however, from the altitude dependence of shower intensity. Numerous experimental data† show that the decreasing intensity $\Phi(>N)$ of showers with number of particles >N in the lower third of the atmosphere can be satisfactorily approximated by an exponential law with the absorption coefficient $\mu = -\partial \ln \Phi(>N)\,\partial t$ which is independent of N and equal to 0.25 per unit radiation length (absorption mean free path equal to 135 g/cm²). This is true both for the total number of showers with number of particles >N at the observation level and for vertical showers.[3] If we assume now that the longitudinal development of showers is not accompanied by large fluctuations, i.e., if the number of particles in showers of identical initial energy and traversed path does not vary greatly from one shower to another, then the change of the intensity of vertical showers with the depth can be expressed in the following way:[10]

$$\Phi_{\text{vert}}(>N,t) \sim \int_0^t \frac{1}{k(t-t_0,E_0)} \exp\left\{\frac{\gamma}{k(t-t_0,E_0)}\left[\ln\frac{N}{A(t-t_0,E_0)}\right]\right\} \exp\left\{\frac{\gamma\lambda(t-t_0)t}{k(t-t_0,E_0)} - \left[\frac{\gamma\lambda(t-t_0)}{k(t-t_0,E_0)} + \mu_0\right]t_0\right\} dt_0. \tag{1}$$

---

*If the lateral distribution of electrons is determined by the multiple scattering, then the bulk of electrons with energies of the order of a few Bev is found within the distance of 1.5 m from the shower axis and, in consequence, it is impossible to draw any conclusions about such electrons from the lateral distribution for distances > 1.5 m.

†For bibliography see Ref. 3.

where t_0 is the depth of the shower initiation level, t is the depth of the observation level, μ_0 is the interaction coefficient of primary cosmic particles in air, γ is the exponent of the energy spectrum of primary particles, $\lambda = \partial \ln N(t-t_0)/\partial t$ is the absorption coefficient of particles in a shower, $k(t-t_0, E_0)$ is a parameter of value close to that of the age parameter s, A is a slowly varying function of E_0 and $t-t_0$, the form of which depends on the mechanism of shower development.

The constancy of the shower absorption coefficient in the lower third of the atmosphere can be interpreted at least in two ways:

1. One can imagine that the showers observed in the lower third of the atmosphere are the tails of cascades originating near the top of the atmosphere. This can take place if μ_0 corresponds to the geometrical cross-section for the interaction of primary particles with nuclei of air atoms, and

$$-\gamma\lambda(t-t_0)/k(t-t_0, E_0) < \mu_0.$$

At observation levels 650—1000 g/cm^2 deep the values of $\gamma\lambda/k$, ln (N/A) and λ will vary slowly with t_0 and formula (1) can be written as

$$\Phi_{\text{vert}}(>N, t) \sim N^{-\varkappa} \frac{\exp[\varkappa\lambda t] - \exp[-\mu_0 t]}{\varkappa\lambda + \mu_0}, \tag{1a}$$

where $\kappa = \gamma/k(t - t_{0\,\text{eff}}, E_0)$ and $t_{0\,\text{eff}}$ is the effective depth of shower initiation.

For the depths fulfilling the condition $\exp[-(\kappa\lambda + \mu_0)t] \ll 1$, we have

$$\Phi_{\text{vert}}(>N, t) \sim e^{\varkappa\lambda t}, \text{ i.e., } \mu = -\partial \ln \Phi_{\text{vert}}(>N, t)/\partial t = -\varkappa\lambda.$$

Since μ and κ are known we can find $\lambda(t-t_{0\,\text{eff}})$. According to numerous experimental data[3] $\kappa \approx 1.5$ for showers with $N \sim 5 \times 10^4 - 5 \times 10^5$ in the lower third of the atmosphere. Consequently, $-\lambda(t-t_{0\,\text{eff}}) = 0.17$ per radiation length.

This value of the absorption coefficient is of course an average for all recorded showers. In the considered case, however, deviations of the particle absorption coefficient in a particular shower from this average value, due to variations in the initiation level, should not be large. In the first approximation we can therefore regard the mean absorption coefficient as corresponding in the mean to each particular recorded shower.

We can explain the fact that the value $-\lambda(t-t_{0\,\text{eff}})$ remains constant in the lower third of the atmosphere by the assumption that the electrons of the shower are in equilibrium with the nuclear-active component.*

There is a basis to assume that high-energy electrons ($E \gg \beta$) are in equilibrium with the nuclear-active component and low-energy electrons are produced as the result of cascade multiplication of the high-energy ones. In fact, the measurements of Nikol'skii and his collaborators[11] have shown that, in showers with the initial energy $E_0 \gg 5 \times 10^{14}$ ev detected in mountains, there are more than 100 electrons per nuclear-active particle, accounting already for the fact that electrons observed at a given level are produced by nuclear-active particles at a higher altitude, where the number of the latter is larger than at the observation level. We can conclude that the mean energy of photons originating in the π^0-meson decay and initiating the electronic cascades in EAS should be $\gtrsim 5 \times 10^9$ ev.† In reality the mean energy of these photons can be still higher, since not all the nuclear-active particles generate the soft component of EAS with the same efficiency.

It is known from the theory of electronic cascades that the coefficient of absorption of the shower particles is determined by the energy spectrum of particles in the high-energy region ($E \gg \beta$). In this theory the energy spectrum for $E \gg \beta$ is

---

*If the constancy of the electron absorption coefficient in the lower third of the atmosphere were caused by a purely electromagnetic mechanism of shower development, then the value of the coefficient would be equal to the minimum value of the photon absorption coefficient which equals 0.585 for air, while the observed value of the coefficient is 0.17.

†In fact, such photons produce about 10 electrons near the cascade maximum. In order to have 100 and more electrons for one generating particle it is necessary to assume that not less than 10 photons are produced in the mean in every interaction. The effective energy of generating particles which may yield such a multiplicity should be equal to several hundred Bev.[12] The effective multiplicity of meson production is in general less than the mean.[14] The effective energy of primary photons should, therefore, be larger than the mean energy.

$$f(E)\,dE \sim dE\,/\,E^{1+s}, \qquad (2)$$

s increasing slowly with increasing energy for showers of finite initial energy. The effective part of the spectrum which contributes to the absorption coefficient is characterized by the value of s determined from the equation

$$\lambda_1(s) = \lambda, \qquad (3)$$

where $\lambda_1(s)$ is a tabulated function evolved in the theory, and $(-\lambda)$ is the absorption coefficient.

These considerations make it possible to find the shape of the energy spectrum of the primary photons of EAS in the region determining the electron absorption coefficient. Since $-\lambda = 0.17$, it follows from Eq. (3) that $s = 1.2$. The energy spectrum of electrons produced by these photons should not be flatter, i.e., the condition $s \geq 1.2$ should be satisfied.

The fact that the electron absorption coefficient of EAS in the lower third of the atmosphere is constant signifies that the shape of the energy spectrum of primary photons (and, consequently, electrons) remains constant (or almost constant) in the region which determines the properties of the soft component of EAS.* The energy spectrum of electrons in the region of lower energies ($E \lesssim \beta$) should then, however, be similar to the one of high-energy electrons, i.e., in the low-energy region we should have $s \geq 1.2$ as well.

It follows therefore from the variation of shower intensity with altitude in the lower third of the atmosphere that the energy spectrum of electrons in EAS is characterized by the condition $s \geq 1.2$ both in the high ($E \gg \beta$) and low ($E \lesssim \beta$) energy region. On the other hand, from the analysis of the lateral distribution of electrons it follows that $s \leq 1.3$ for $E \leq 10^9$ ev. Consequently, in the energy region $E \lesssim 10^9$ ev the energy spectrum of electrons in EAS, in the absence of large fluctuations in the longitudinal development of showers, should satisfy the condition $1.3 \geq s \geq 1.2$.

For this energy spectrum the lateral distribution of electrons (at least at the distances between 1.5 and 250 m from the shower axis) is fully explained by multiple scattering and, in consequence, the contribution of nuclear scattering to the lateral distribution of electrons in EAS in the considered case should be small. An analogous conclusion was already reached by Khristiansen.[7]

2. We considered the case which should occur if the shower tails were absorbed more slowly than the primary radiation. The constancy of the shower absorption coefficient in the lower third of the atmosphere (as well as a number of other properties of showers) can be understood also under the assumption that the tails of showers are absorbed faster than the primary radiation, i.e., when $(-\kappa\lambda_{\text{lim}}) > \mu_0$. In that case the longitudinal development of showers under large thicknesses of matter will be determined by the absorption of the primary radiation, i.e., $\mu_0 = 1/135$ g/cm^2.

Although it is known that in light elements the mean free path for the interaction of protons and neutrons of $\sim 10^9 - 10^{10}$ ev is not larger than 80 g/cm^2 (see Ref. 15) and there are no indications of its increase with the energy, such possibility, nevertheless, is not ruled out for ultra-high energies.

Among the showers registered at any level in the lower layers of the atmosphere there should be some which did not attain their maximum, as well as others far beyond the maximum of their development. It follows from formula (1) that showers for which $-\kappa\lambda = \mu_0$ will be recorded with the greatest probability. The same equation should, in the first approximation, determine the mean age of showers as well. The energy spectrum of electrons in showers of the mean age should, in consequence, fulfill the condition $s \geq 1.2$.

The experimentally determined lateral distribution of electrons should also characterize in the mean all showers, since it is necessary to average over a large number of showers in order to obtain an accurate form of the distribution function. Since it follows from the lateral distribution that $s \leq 1.3$, then the conclusion that the main contribution to the lateral spread of the electrons is due to multiple Coulomb scattering remains valid. However, in contrast to the former case when we were able to draw certain conclusions the details of development of a particular shower, in the present case it is possible to state with respect to a given shower only that the upper limit of the particle absorption length should be smaller than 200 g/cm^2.

---

*This of course cannot be said for the spectrum of primary photons in general, since these photons are in equilibrium with the absorbed component. It is evidently necessary to assume that the above region is gradually shifted towards lower energies.

In conclusion, I consider as my pleasant duty to express my gratitude to S. N. Vernov, G. T. Zatsepin, and I. P. Ivanenko for their participation in the discussion of the presented material.

---

[1] J. Nishimura and K. Kamata, Progr. Theor. Phys. 6, 628 (1951); J. Nishimura and K. Kamata, Inter. Conf. Theor. Phys., Japan, 1953.

[2] B. Rossi and K. Greisen, Revs. Mod. Phys. 13, 240 (1941).

[3] K. Greisen, Progress in Cosmic Ray Physics vol. III, 1956.

[4] Cocconi, Tongiorgi and Greisen, Phys. Rev. 76, 1020 (1949).

[5] S. R. Haddara and D. Jakeman, Proc. Phys. Soc. A66, 549 (1953).

[6] G. Fujioka, J. Phys. Soc. Japan 10, 245 (1955); G. Fujioka, Internat. Conf. Theor. Phys. Japan, 1953.

[7] G. B. Khristiansen, Conference on Extensive Air Showers, Oxford, 1956.

[8] Abrosimov, Bedniakov, Zatsepin et al., J. Exptl. Theoret. Phys. (U.S.S.R.) 29, 693 (1955), Soviet Phys. JETP 2, 357 (1956); Abrosimov, Zatsepin, Solov'eva, Khristiansen, and Chikin, Izv. Akad. Nauk SSSR, Ser. Fiz. 19, 677 (1955).

[9] Vavilov, Nikol'skii, and Tukish, Dokl. Akad. Nauk SSSR 93, 233 (1953); Dobrovol'skii, Nikol'skii, Tukish, and Iakovlev, J. Exptl. Theoret. Phys. (U.S.S.R.) 31, 939 (1956), Soviet Phys. JETP 4, 799 (1956); S. I. Nikol'skii and V. M. Sleznev, J. Exptl. Theoret. Phys. (U.S.S.R.) 32, 1250 (1957), Soviet Phys. JETP 5, 1019 (1957).

[10] G. T. Zatsepin and L. I. Sarycheva, Dokl. Akad. Nauk SSSR 99, 951 (1954).

[11] Nikol'skii, Vavilov, and Batov, Dokl. Akad. Nauk SSSR 111, 71 (1956); Soviet Phys. "Doklady" 1, 625 (1956).

[12] I. A. Ivanovskaia and D. S. Chernavskii, Nuclear Physics, (in press).

[13] N. L. Grigorov, Usp. Fiz. Nauk 58, 599 (1956).

[14] Guzhavina, Guzhavin, and Zatsepin, J. Exptl. Theoret. Phys. (U.S.S.R.) 31, 819 (1956); Soviet Phys. JETP 4, 690 (1957).

[15] A. L. Liubimov, Dissertation, Phys. Inst. Acad. Sci. 1954; Vernov, Kulikov, and Charakhchian, Izv. Akad. Nauk SSSR, Ser. Fiz. 17, 13 (1953).

Translated by H. Kasha
27

SOVIET PHYSICS JETP VOLUME 6, NUMBER 1 JANUARY, 1958

HYDRODYNAMICAL INTERPRETATION OF ONE CHARACTERISTIC OF LARGE SHOWERS RECORDED IN PHOTOGRAPHIC EMULSIONS

G. A. MILEKHIN and I. L. ROZENTAL'

P. N. Lebedev Physics Institute, Academy of Sciences, U.S.S.R.

Submitted to JETP editor January 11, 1957

J. Exptl. Theoret. Phys. (U.S.S.R.) 33, 197-199 (July, 1957)

The experimental distribution of the transverse momentum components of secondary particles is compared with the predictions of the hydrodynamical theory of multiple particle production. It is found that the predictions of the one-dimensional theory for a final temperature of $T_{\text{fin}} = mc^2/k$ (where m is the π-meson mass) agree satisfactorily with the experimental data. This permits us to draw some conclusions concerning the nature of $\pi - \pi$ interaction.

THE comparison of predictions of the various phenomenological theories of multiple particle production with experimental results has a decisive value for the confirmation of their validity. Such a comparison made at first for energies of $\gtrsim 10^{12}$ ev (see Ref. 1) indicated that the hydrodynamical theory proposed by Landau describes qualitatively all the known properties of multiple production processes. In the comparison of the theory with experimental data in Ref. 1, however, additional assumptions were made which, without regard to their nature, caused a certain undecisiveness of the conclusion. It was for instance assumed that in the collisions between nucleons and heavy nuclei there exists a system of coordinates in which the disintegration of the matter is symmetric; for the description of the collision a model was used according to which the particle interacts with a cylindrical volume of nuclear matter; the analysis of extensive showers was carried out under the assumption of the independence of the nuclear interaction cross-section from energy, etc.

Taking all the above into account, it is necessary, for a direct confirmation of the theory, to consider such characteristics of the collisions which do not require any complementary assumptions, the correctness of which would be difficult to ascertain. One of such characteristics is the distribution of the transverse momentum components $p_\perp$ of the secondary particles (i.e., components perpendicular to the shower axis). Distribution of the values of $p_\perp$ can be, strictly speaking, found only from the solution of three-dimensional equations, which is a difficult and so far not investigated problem. Special estimates indicate, however, that a hydrodynamical disintegration of particles is, in its main features, determined by a one-dimensional stage[3] and it can be therefore assumed that the distribution of the values of $p_\perp$ is determined solely by thermal motion. This means that we neglect transverse momentum components due to hydrodynamical motion.

In such approximation we shall find the distribution of transverse momenta using the well-known expression for particle density dN in the momentum interval $dp_x dp_y dp_z$

$$dN = g\,(2\pi\hbar c)^{-3}\,[e^{(\epsilon-\mu)/kT} \pm 1]^{-1}\,dp_x dp_y dp_z, \tag{1}$$

where g is the number of internal degrees of freedom of a particle, ϵ is its energy, and μ is the chemical potential which, according to the thermodynamical conception, we shall set equal to zero. The minus sign corresponds to bosons, and the plus sign to fermions. After integration over p_z we obtain the distribution of transverse components:

$$dN_1 = \frac{g}{(2\pi\hbar c)^3}\,mc\,dp_y dp_z \int_0^\infty \frac{dx}{\exp\left(z\sqrt{x^2+\rho^2+1}\right) \pm 1}, \tag{2}$$

where $x = p/mc$; $z = mc^2/kT$; $\rho^2 = (p_y^2 + p_z^2)/mc^2$.

By means of the relation

$$\int_0^\infty \frac{dx}{\exp\left(z\sqrt{x^2+\rho^2+1}\right) \pm 1} = \sqrt{\rho^2+1}\sum_{n=1}^{\infty} (\mp)^{n-1} K_1\left(nz\sqrt{\rho^2+1}\right) \tag{3}$$

(where K_1 is the Bessel function of imaginary variable) and by integrating over the angle in cylindrical coordinates, we finally obtain

$$dN_\perp = \frac{q}{2\pi^2}\left(\frac{mc}{\hbar}\right)^3 \sum_{n=1}^{\infty} (\mp)^{n-1} K_1\left(n\,\frac{mc^2}{kT}\sqrt{\left(\frac{p_\perp}{mc}\right)^2 + 1}\right)\frac{p_\perp dp_\perp}{(mc)^2}. \tag{4}$$

Theoretical distributions of the transverse components, calculated for bosons for various values of T according to Eq. (4), are shown by the solid curves in the figure. The dotted histogram represents the experimental distributions of $p_\perp$ obtained from the analysis of a single shower recorded in emulsion.[4] Thanks to the unusual path length of secondary particles in the emulsion (16.8 cm) the authors of Ref. 4 were able to determine from scattering measurements the total momentum of the majority of particles (35 out of 39). This permitted us to calculate $p_\perp$ by a simple computation.

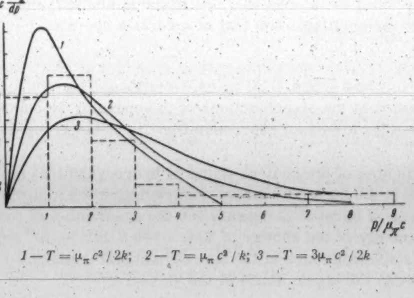

$1 - T = \mu_\pi c^2/2k$; $2 - T = \mu_\pi c^2/k$; $3 - T = 3\mu_\pi c^2/2k$

A very similar distribution of the transverse components was obtained also from the measurement of the total momentum of secondary π^0-mesons by means of the pairs associated with them.[5] Distribution of transverse momenta in that case was, too, characterized by a maximum in the region $1 - 2\mu_\pi c^2$ (where μ_π is the π-meson mass).

Several important conclusions may be drawn from the comparison of the experimental and theoretical curves:

1. The one-dimensional theory describes satisfactorily the character of the distribution of transverse momentum components.[*]

2. Best agreement of both distributions is obtained[†] for $T = \mu_\pi c^2/k$. The values $T = \mu_\pi c^2/2k$ and $T = 3\mu_\pi c^2/2k$ are already difficult to reconcile with experimental data, although the scarcity of the latter does not permit to rule these values out. The value $T = \mu_\pi c^2/k$ is in agreement with previous indications, based on the analysis of other experimental results (for composition of showers see Refs. 6 and 7 and for energy spectrum see Ref. 3).

3. Since the value of temperature is connected with the value of the interaction cross-section of secondary particles[6] (evidently π-mesons) we can conclude that in the order of magnitude the latter equals the geometrical cross-section of the nucleon $(\hbar/\mu_\pi c)^2$.

---

[1] I. L. Rozental' and D. S. Chernavskii, Usp. Fiz. Nauk 52, 185 (1954).
[2] L. D. Landau, Izv. Akad. Nauk SSSR, Ser. Fiz. 17, 51 (1953).
[3] I. L. Rozental', J. Exptl. Theoret. Phys. (U.S.S.R.) 31, 278 (1956); Soviet Phys. JETP 4, 217 (1957).
[4] Debenedetti, Garelli, Talone and Vigone, Nuovo cimento 4, 1142 (1956).
[5] Gramenitskii, Zhdanov, Zamchalova and Shcherbakova, J. Exptl. Theoret. Phys. (U.S.S.R.) 32, 936 (1957 Soviet Phys. JETP 5, 763 (1957).
[6] S. Z. Belen'kii, Dokl. Akad. Nauk SSSR 99, 523 (1954).
[7] Z. Koba, Progr. Theor. Phys. 15, 461 (1956).

Translated by H. Kasha
28

SOVIET PHYSICS JETP VOLUME 6, NUMBER 1 JANUARY, 1958

ON THE RELATION BETWEEN "ACCIDENTAL" DEGENERACY AND "HIDDEN" SYMMETRY OF A SYSTEM

S. P. ALLILUEV

Moscow Physico-Technical Institute

Submitted to JETP editor January 16, 1957

J. Exptl. Theoret. Phys. (U.S.S.R.) 33, 200-203 (July, 1957)

An example is discussed which confirms the connection between "accidental" degeneracy and "hidden" symmetry of a system. The symmetry of a two-dimensional oscillator is studied, and the relation is found between the quantization of the oscillator and that of a certain operator of the type of an angular momentum.

SUPPOSE the operator H is invariant with respect to some group G of transformations. Then the application of these transformations results in the expression of the eigenfunctions of the operator H belonging to an eigenvalue E_n in terms of each other, and thus gives a certain representation D_n of the group G.[1] As a rule this transformation is irreducible. In the opposite case (D_n reducible) one speaks of an "accidental" degeneracy. The study of several systems with "accidental" degeneracy, as carried out by Fock[2] (hydrogen atom), Demkov[3] (three-dimensional oscillator), and Baker[4] (n-dimensional oscillator), has shown that these systems possess in addition to the obvious symmetry group G also a higher "hidden" symmetry group G*. On the application of the transformations of the group G* the eigenfunctions belonging to the eigenvalue E_n give an irreducible representation D_n^* of the group G*.

---

[*] The cited calculations have shown that the introduction of the conical stage[2] of hydrodynamical motion predicts that the mean value of $p_\perp$ is $\gtrsim Mc$ (where M is the nucleonic mass), contradicting the histogram shown in the figure. It is possible that the conical stage of burst is necessary for the description of particle interaction at considerably higher energies than the energy of the shower of Ref. 4 ($\sim 5 \times 10^{12} - 10^{13}$ ev).

[†] It should be noted that since we neglected the possible influence of the hydrodynamical transverse components the given values of T are, strictly speaking, the upper limits of the values.

In the present paper we consider a further example confirming the connection between "accidental" degeneracy and "hidden" symmetry of a system. In addition, the symmetry group of the two-dimensional oscillator is studied and a relation is found between the quantization of the two-dimensional oscillator and the quantization of a certain operator of the type of an angular momentum.

1. Let us consider a system with its Hamiltonian of the form

$$H = -\Delta - 2/r, \tag{1}$$

where

$$\Delta = \sum_{i=1}^{f} \partial^2/\partial x_i^2, \quad r = \left(\sum_{i=1}^{f} x_i^2\right)^{1/2}. \tag{2}$$

The obvious symmetry group of the operator (1) is the group d_f of orthogonal transformations of the f-dimensional space. Separating variables in hyperspherical coordinates, one can readily verify that the eigenfunctions and eigenvalues of the operator (1) are given by

$$\begin{gathered}\psi_{n,k} = Ar^k \exp(-p_0 r)\, F(-n+k,\ 2k+f-1,\ p_0 r/2)\, Y_k^{(f)},\ E_n = -1\Big/\left(n+\frac{f-1}{2}\right)^2,\ p_0 = 1\Big/\left(n+\frac{f-1}{2}\right),\\ k = 0,\ 1,\ 2, \ldots n;\ n = 0,\ 1,\ 2, \ldots,\end{gathered} \tag{3}$$

where F is the confluent hypergeometric function and $Y_k^{(f)}$ denotes the set of f-dimensional hyperspherical functions belonging to the characteristic value $-k(k+f-2)$ of the angular part of the Laplacian operator.

Noting that the functions $Y_k^{(f)}$ for fixed k give an irreducible representation $D_k^{(f)}$ of the group d_f and that E_n does not depend on k, one easily sees that the representation D_n corresponding to E_n is reducible and decomposes into a sum of irreducible representations:

$$D_n = \sum_{k=0}^{n} D_k^{(f)}. \tag{4}$$

Thus we have to do with an "accidental" degeneracy.

To find the "hidden" symmetry group of our system, following Fock[2] we write the equation for the eigenvalues of the operator (1) in the p representation:

$$(\mathbf{p}^2 + p_0^2)\, \Phi(\mathbf{p}) = \pi^{-(f+1)/2}\, \Gamma\left(\frac{f-1}{2}\right) \int \frac{\Phi(\mathbf{p}')\,(d\mathbf{p}')}{|\mathbf{p}-\mathbf{p}'|^{f-1}}, \quad p_0^2 = -E. \tag{5}$$

Regarding the components of the vector $\mathbf{p}/p_0$ as the stereographic projection of a point of an (f + 1)-dimensional unit hypersphere, and introducing the new function

$$Y = B\,(\mathbf{p}^2 + p_0^2)^{(f+1)/2}\, \Phi(\mathbf{p}), \tag{6}$$

we get the equation

$$Y(M) = \frac{\Gamma\left(\frac{f-1}{2}\right)}{2\pi^{(f+1)/2} p_0} \int \frac{Y(M')\, d\Omega'}{\{2(1-\cos\gamma)\}^{(f-1)/2}}, \tag{7}$$

where $d\Omega'$ is the surface element of the (f + 1)-dimensional unit hypersphere and γ is the "angle" between the points M and M′ of the hypersphere.

The invariance of Eq. (7) with respect to the group of orthogonal transformations $d_{(f+1)}$ of the (f + 1)-dimensional space is obvious. Thus the "hidden" symmetry group of the operator (1) is the group $d_{(f+1)}$.

The solutions of Eq. (7) are the (f + 1)-dimensional hyperspherical functions $Y^{(f+1)}$ and the eigenvalues are as given in Eq. (3):

$$p_0 = 1\Big/\left(n+\frac{f-1}{2}\right). \tag{8}$$

For given n the functions $Y_n^{(f+1)}$ give the irreducible representation $D_n^{(f+1)}$ of the group d_{f+1}.

Since the system in question is the f-dimensional analogue of the hydrogen atom, our results are the same as those of Fock[2] for $f = 3$.

2. In Ref. 4 it is shown that the symmetry group of an n-dimensional oscillator is the group of n-dimensional unitary transformations. There is a well known connection between two-dimensional unitary transformations and the three-dimensional rotation group,[1] so that it seems not without interest to examine the symmetry of the two-dimensional oscillator, the more so because there turns up by the way a connection between the quantization of the oscillator and that of a certain operator of the type of an angular momentum.

According to Ref. 4, the Hamiltonian of the two-dimensional oscillator, written in the form

$$H = {}^1\!/_2\,(\dot{a}_1 a_1 + \dot{a}_2 a_2) + 1, \tag{9}$$

where

$$a_1 = x + \frac{\partial}{\partial x}, \quad \dot{a}_1 = x - \frac{\partial}{\partial x}, \quad a_2 = y + \frac{\partial}{\partial y}, \quad \dot{a}_2 = y - \frac{\partial}{\partial y}, \tag{10}$$

is invariant with respect to transformations of the form

$$a'_k = \sum_{l=1}^{2} U_{kl} a_l, \quad k = 1,2, \tag{11}$$

where U_{kl} is a unitary matrix.

We note that under rotations $\Omega(\alpha)$ in the x, y plane and under Fourier transformation Φ of the function $\varphi(x, y)$ with respect to the coordinate x,

$$\Phi\varphi(x, y) = (2\pi)^{-1/2} \int_{-\infty}^{\infty} e^{-ix\xi}\varphi(\xi, y)\,d\xi, \tag{12}$$

the operators a_k are transformed according to Eq. (11) with the matrices

$$\Omega(\alpha) = \begin{pmatrix} \cos\alpha & \sin\alpha \\ -\sin\alpha & \cos\alpha \end{pmatrix}, \quad \Phi = \begin{pmatrix} -i & 0 \\ 0 & 1 \end{pmatrix}. \tag{13}$$

Let us confine ourselves to transformations (11) that are close to the identity and have determinant unity. They can be written in the form

$$U = E + \frac{i}{2} \sum_{l=1}^{3} \alpha_l \sigma_l, \tag{14}$$

where E is the unit matrix and σ_l are the Pauli matrices.

The group of transformations (14) is isomorphic to the three-dimensional rotation group,[1] and the corresponding infinitesimal operators are

$$I_k \equiv iJ_k = \frac{i}{2}\sigma_k, \quad k = 1, 2, 3. \tag{15}$$

Using the following relations (valid for small α_k):

$$E + \frac{i}{2}\alpha_1\sigma_1 = \Phi^{-1}\Omega\left(\frac{\alpha_1}{2}\right)\Phi, \quad E + \frac{i}{2}\alpha_2\sigma_2 = \Omega\left(\frac{\alpha_2}{2}\right), \; E + \frac{i}{2}\alpha_2\sigma_3 = \Omega\left(\frac{\pi}{4}\right)\Phi^{-1}\Omega\left(\frac{\alpha_3}{2}\right)\Phi\Omega\left(-\frac{\pi}{4}\right), \tag{16}$$

and also using the definitions of the operators Ω and Φ (Eq. 12), we can express the operators J_k of Eq. (15) in terms of x and y (cf. Ref. 3):

$$J_1 = {}^1\!/_2\,(xy - \partial^2/\partial x\,\partial y), \quad J_2 = (1/2i)\,(x\partial/\partial y - y\partial/\partial x), \quad J_3 = {}^1\!/_4\,(x^2 - y^2 - \partial^2/\partial x^2 + \partial^2/\partial y^2). \tag{17}$$

The operators (17) commute with the Hamiltonian (9) and satisfy the commutation relations of the angular momentum operators.

The eigenfunctions of the Hamiltonian (9) belonging to the eigenvalue $E_n = n + 1$ are given by

$$\psi_{n_1 n_2}(x, y) = (\pi 2^{n_1+n_2} n_1! n_2!)^{-1/2} \exp\left(-\frac{x^2+y^2}{2}\right) H_{n_1}(x) H_{n_2}(y), \quad n_2 = n - n_1, \quad n_1 = 0, 1, 2, \ldots, n, \quad n = 0, 1, 2, \ldots, \tag{18}$$

where the H_n are Hermite polynomials. Introducing the notations

$$j = (n_1 + n_2)/2 = n/2, \quad m = (n_1 - n_2)/2, \quad m = -j, -j+1, \ldots, j; \quad j = 0, {}^1\!/_2, 1, {}^3\!/_2, \ldots, \tag{19}$$

and using the properties of Hermite polynomials, one can easily verify that the functions

$$Y_{jm}(x, y) = \psi_{n_1 n_2}(x, y) = \{\pi 2^{2j}(j+m)!\,(j-m)!\}^{-1/2} \exp\left(-\frac{x^2+y^2}{2}\right) H_{j+m}(x)\, H_{j-m}(y) \tag{20}$$

satisfy the relations

$$\mathbf{J}^2 Y_{jm} \equiv (J_1^2 + J_2^2 + J_3^2)\, Y_{jm} = j(j+1)\, Y_{jm}, \quad J_3 Y_{jm} = mY_{jm}, \quad (J_1 \pm iJ_2)\, Y_{jm} = \sqrt{(j \mp m)(j \pm m + 1)}\, Y_{jm\pm 1}, \tag{21}$$

which establishes the connection between the quantizations of the operators (9) and (17).

It must be pointed out that the definition of an "angular momentum" operator by Eq. (17) combines the integral and half-integral values of the quantum number j. We also note the appearance in this case of an operator K:

$$K = {}^1\!/_2 H = {}^1\!/_4\left(x^2 + y^2 - \frac{\partial^2}{\partial x^2} - \frac{\partial^2}{\partial y^2}\right), \quad K^2 - {}^1\!/_4 = \mathbf{J}^2, \quad KY_{jm} = (j + {}^1\!/_2)\, Y_{jm}, \tag{22}$$

analogous to the Dirac operator[5]

$$K = (\mathbf{L}\sigma + 1)\,\beta. \tag{23}$$

It follows from Eq. (21)[1] that under the transformations (14) the eigenfunctions (20) of the two-dimensional oscillator that belong to the eigenvalue $E_n = n + 1 = 2j + 1$ transform according to the irreducible representation D_j of the three-dimensional rotation group. Thus the group of transformations (14), isomorphic to the three-dimensional rotation group, suffices to explain the degeneracy of the eigenvalues of the operator (9) and can be regarded as the symmetry group of the two-dimensional oscillator.

In the n-dimensional case one can also restrict the discussion to the unitary transformations that are close to the identity and have determinant unity, but this does not lead to any interesting consequences.

---

[1] B. L. Van der Waerden, Die Gruppentheoretische Methode in der Quantenmechanik, 1938.

[2] V. Fock, Z. Physik. 98, 145 (1935).

[3] Iu. N. Demkov, (J. Leningrad State Univ.) 11, 127 (1953).

[4] G. A. Baker, Jr., Phys. Rev. 103, 1119 (1956).

[5] P. A. M. Dirac, The Principles of Quantum Mechanics, 1947.

Translated by W. H. Furry
29

SOVIET PHYSICS JETP VOLUME 6, NUMBER 1 JANUARY, 1958

TIME REVERSAL AND POLARIZATION PHENOMENA IN $N + N \rightleftarrows d + \pi$ REACTION

L. I. LAPIDUS

Joint Institute for Nuclear Research

Submitted to JETP editor January 17, 1957

J. Exptl. Theoret. Phys. (U.S.S.R.) 33, pp. 204-212 (July, 1957)

By an analysis of the polarization phenomena in the reactions $N + N \rightleftarrows d + \pi$ it is shown how the condition of invariance under time reversal leads to relations between the polarization phenomena in the direct and inverse reactions. A generalization of Wolfenstein's theorem to this binary reaction is obtained. Expressions for the various observable quantities in the reactions $N + N \rightleftarrows d + \pi$ are given both when the treatment is confined to s, p, and d waves with $J \leq 2$, and also in the general case.

INTRODUCTION

As is well known, the requirement of invariance under change of the sign of the time leads[1-3] to the condition of symmetry of the S matrix (notation of Blatt and Bidenharn[2] with an emendation from Ref. 3)

$$S^J_{\alpha's'l';\, \alpha sl} = S^J_{\alpha sl;\, \alpha's'l'}. \tag{1}$$

For the interaction of spinless particles this condition leads to the equality of the differential cross-sections of direct and inverse reactions (apart from a factor of the ratio of the squares of the relative momenta in the direct and inverse reactions). For particles with spin, for which there appears a difference between the time-reversed and inverse processes, this same condition leads to the equality of the averages over spins of the cross-sections of the direct and inverse reactions. But in the case of interaction of particles with spin not equal to zero, one can express in terms of the elements of the S matrix not only the reaction cross-section of unpolarized particles, but also the average values of the spin operators in the direct and inverse processes. Because of the existence of the condition (1) it is of interest to consider its consequences for the polarization phenomena in direct and inverse processes and to try to find relationships analogous to the connections between the cross-sections for the reactions between unpolarized beams and unpolarized targets. Such a connection has been discussed in the literature in a consideration of polarization phenomena in elastic scattering. Dalitz[4] and Wolfenstein and Ashkin[5] have shown that in the case of elastic scattering of particles with spin 1/2 from a target with arbitrary spin, for which the principle of detailed balancing reduces to an identity, the requirement of invariance under change of sign of the time has as a consequence a connection between the polarization $\langle \hat{\sigma}_1 \rangle_f$ of particles appearing from the interaction of unpolarized particles and the azimuthal asymmetry I_p in the scattering cross-section of polarized particles from an unpolarized target. This connection is of the form

$$I_p = \langle \hat{\sigma}_1 \rangle_f \mathbf{N} I_0(\theta), \tag{2}$$

where $I_0(\theta)$ is the scattering cross-section of unpolarized particles and $\mathbf{N}$ is the direction of the polarization of the beam.

As has been shown by Lakin,[6] a similar relation holds also for the elastic scattering of particles with spin 1.

In the present paper a phenomenological analysis of the polarization phenomena is carried out for the reactions

$$p + p \rightarrow d + \pi^+ \ (A), \quad n + p \rightarrow d + \pi^0 \ (C),$$
$$\pi^+ + d \rightarrow p + p \ (B), \quad \pi^0 + d \rightarrow n + p \ (D)$$

in order to find out from this example what consequences arise in virtue of the condition (1) for the more general case of binary reactions (nuclear reactions with two particles in the initial and in the final states).

The main result of this work is a generalization of the Wolfenstein theorem (2) to the case of the reactions here considered. Incidentally we obtain general expressions for the various observable quantities in reactions (A) and (B) in terms of the interaction amplitude, which may prove useful in determining it from experimental data.

THE S MATRIX

We denote the relative angular momenta in the initial and final states of reaction (B) by ℓ' and ℓ, and chose as the z axis the direction of the incident π mesons. Denoting, further, the Clebsch-Gordan coefficients by $C^{j_1 j_2}_{m_1 m_2}$, the four spin functions of the N − N system by ψ_M (M = + 1, 0, − 1 for the triplet, M = c for the singlet) and the spin functions of the deuteron by φ_m, we write the S matrix for the reaction (B) in the form

$$S_B = \sum_{m,\,M} \psi_M \left\{ \sum_{Jll'} (2l'+1)^{1/2} (l \,|\, S_J^B \,|\, l')\, C^{lsJ}_{m-M,\,M} C^{l'1J}_{0m}\, Y_l^{m-M}(\theta,\varphi) \right\} \varphi_m^+ \tag{3}$$

(s is the spin of the system of nucleons). Then the S matrix for reaction (A) takes the form

$$S_A = \sum_{m,\,M} \varphi_m \left\{ \sum_{Jll'} (2l+1)^{1/2} (l' \,|\, S_J^A \,|\, l)\, C^{l'1J}_{M-m,\,m} C^{lsJ}_{0M}\, Y_{l'}^{M-m}(\theta,\varphi) \right\} \psi_M^+ . \tag{4}$$

The condition (1) requires that $(\ell|S_J^B|\ell') = (\ell'|S_J^A|\ell) = (\ell'|S_J|\ell)$. (Here it is essential that the elements of the S matrix be defined to correspond with Ref. 3.)

If we confine ourselves to including the interactions with mesons in only s, p, and d states, then the laws of conservation of total angular momentum and of parity permit transitions ${}^3P_0 \to {}^1S_0$ (amplitude $(0|S_0|1) \equiv a_0$), ${}^3S_1 \to {}^3P_1$ (amplitude a_1), ${}^3P_2 \to {}^1D_2$ (a_2), ${}^3D_1 \to {}^3P_1$ (a_3), ${}^3D_2 \to {}^3P_2$ (a_4), ${}^3D_2 \to {}^3F_2$ (a_5), ${}^3D_3 \to {}^3F_3$ (a_6). In the further analysis we drop the transition ${}^3D_3 \to {}^3F_3$ with J = 3, keeping the transitions with J ≤ 2.* Then the S matrices of reactions (A) and (B) can be put in the form

$$\begin{aligned}4\sqrt{4\pi}\, S_B = {} & \psi_c \{-\sqrt{2}a_0 (\mathbf{k}_0\boldsymbol{\varphi}^+) + \sqrt{10}a_2 [3t(\mathbf{k}\boldsymbol{\varphi}^+) - (\mathbf{k}_0\boldsymbol{\varphi}^+)]\} + i\sqrt{6}a_1 (\mathbf{k}[\boldsymbol{\psi}\boldsymbol{\varphi}^+]) \\ & + i\sqrt{3}a_3 \{3t(\mathbf{k}_0[\boldsymbol{\psi}\boldsymbol{\varphi}^+]) - (\mathbf{k}[\boldsymbol{\psi}\boldsymbol{\varphi}^+]) - 2[(\boldsymbol{\psi}\mathbf{n})(\mathbf{k}_0\boldsymbol{\varphi}^+) + (\boldsymbol{\psi}\mathbf{k})(\mathbf{n}\boldsymbol{\varphi}^+)]\} + i\sqrt{5}a_4 \{3t(\mathbf{k}_0[\boldsymbol{\psi}\boldsymbol{\varphi}^+]) - (\mathbf{k}[\boldsymbol{\psi}\boldsymbol{\varphi}^+]) + [(\boldsymbol{\psi}\mathbf{n})(\mathbf{k}_0\boldsymbol{\varphi}^+) \\ & + (\boldsymbol{\psi}\mathbf{k}_0)(\mathbf{n}\boldsymbol{\varphi}^+)]\} + i\sqrt{10}a_5 \{(5t^2-1)(\mathbf{k}[\boldsymbol{\psi}\boldsymbol{\varphi}^+]) - 2t(\mathbf{k}_0[\boldsymbol{\psi}\boldsymbol{\varphi}^+]) + [(\boldsymbol{\psi}\mathbf{n})(\mathbf{k}_0\boldsymbol{\varphi}^+) + (\boldsymbol{\psi}\mathbf{k}_0)(\mathbf{n}\boldsymbol{\varphi}^+)] - 5t[(\boldsymbol{\psi}\mathbf{n})(\mathbf{k}\boldsymbol{\varphi}^+) + (\boldsymbol{\psi}\mathbf{k})(\mathbf{n}\boldsymbol{\varphi}^+)]\};\end{aligned} \tag{3'}$$

$$\begin{aligned}4\sqrt{4\pi}\, S_A = {} & \{-\sqrt{2}a_0 (\mathbf{k}\boldsymbol{\varphi}) + \sqrt{10}a_2 [3t(\mathbf{k}_0\boldsymbol{\varphi}) - (\mathbf{k}\boldsymbol{\varphi})]\}\psi_c^+ + i\sqrt{6}a_1 (\mathbf{k}_0[\boldsymbol{\varphi}\boldsymbol{\psi}^+]) + i\sqrt{3}a_3 \{3t(\mathbf{k}[\boldsymbol{\varphi}\boldsymbol{\psi}^+]) - (\mathbf{k}_0[\boldsymbol{\varphi}\boldsymbol{\psi}^+]) \\ & - 2[(\boldsymbol{\varphi}\mathbf{n})(\mathbf{k}\boldsymbol{\psi}^+) + (\boldsymbol{\varphi}\mathbf{k})(\mathbf{n}\boldsymbol{\psi}^+)]\} + i\sqrt{5}a_4 \{3t(\mathbf{k}[\boldsymbol{\varphi}\boldsymbol{\psi}^+]) - (\mathbf{k}_0[\boldsymbol{\varphi}\boldsymbol{\psi}^+]) + [(\boldsymbol{\varphi}\mathbf{n})(\mathbf{k}\boldsymbol{\psi}^+) + (\boldsymbol{\varphi}\mathbf{k})(\mathbf{n}\boldsymbol{\psi}^+)]\} \\ & + i\sqrt{10}a_5 \{(5t^2-1)(\mathbf{k}_0[\boldsymbol{\varphi}\boldsymbol{\psi}^+]) - 2t(\mathbf{k}[\boldsymbol{\varphi}\boldsymbol{\psi}^+]) + [(\mathbf{k}\boldsymbol{\varphi})(\mathbf{n}\boldsymbol{\varphi}^+) + (\mathbf{n}\boldsymbol{\varphi})(\mathbf{k}\boldsymbol{\psi}^+)] - 5t[(\mathbf{k}_0\boldsymbol{\varphi})(\mathbf{n}\boldsymbol{\psi}^+) + (\mathbf{n}\boldsymbol{\varphi})(\mathbf{k}_0\boldsymbol{\psi}^+)]\},\end{aligned} \tag{4'}$$

where $\mathbf{k}_0$ and $\mathbf{k}$ are unit vectors giving the directions of the relative momenta in the initial and final states, $t = (\mathbf{k}_0\mathbf{k}) = \cos\theta$, $\mathbf{n} = [\mathbf{k}_0\mathbf{k}]$, and the vectors $\boldsymbol{\psi}$ and $\boldsymbol{\varphi}$ are constructed from the ψ_m and φ_m respectively ($M \neq c$). The quantities $a_0, a_1, a_2, \ldots$ in Eqs. (3) and (4) differ from the corresponding quantities in Ref. 8 by the factor $(2\ell + 1)^{1/2}$.

In the general case the S matrix for the reaction (A) can be put in the form

$$\begin{aligned}\sqrt{4\pi}\, S_A = {} & [A(\mathbf{k}\boldsymbol{\varphi}) + B(\mathbf{k}_0\boldsymbol{\varphi})]\psi_c^+ + i\{C[(\boldsymbol{\varphi}\mathbf{n})(\mathbf{k}\boldsymbol{\psi}^+) + (\boldsymbol{\varphi}\mathbf{k})(\mathbf{n}\boldsymbol{\psi}^+)] \\ & + D[(\boldsymbol{\varphi}\mathbf{n})(\mathbf{k}_0\boldsymbol{\psi}^+) + (\boldsymbol{\varphi}\mathbf{k}_0)(\mathbf{n}\boldsymbol{\psi}^+)] + E(\mathbf{k}[\boldsymbol{\varphi}\boldsymbol{\psi}^+]) + F(\mathbf{k}_0[\boldsymbol{\varphi}\boldsymbol{\psi}^+])\}\end{aligned} \tag{5}$$

(The $\sqrt{4\pi}$ and the factor i are retained for closer correspondence with Eq. (4)). In virtue of the condition (1) we get analogously for reaction (B)

$$\begin{aligned}\sqrt{4\pi}\, S_B = {} & \psi_c[A(\mathbf{k}_0\boldsymbol{\varphi}^+) + B(\mathbf{k}\boldsymbol{\varphi}^+)] + i\{C[(\mathbf{k}_0\boldsymbol{\psi})(\mathbf{n}\boldsymbol{\varphi}^+) + (\mathbf{n}\boldsymbol{\psi})(\mathbf{k}_0\boldsymbol{\psi}^+)] \\ & + D[(\mathbf{k}\boldsymbol{\psi})(\mathbf{n}\boldsymbol{\varphi}^+) + (\mathbf{n}\boldsymbol{\psi})(\mathbf{k}\boldsymbol{\varphi}^+)] + E(\mathbf{k}_0[\boldsymbol{\psi}\boldsymbol{\varphi}^+]) + F(\mathbf{k}[\boldsymbol{\psi}\boldsymbol{\varphi}^+])\}.\end{aligned} \tag{6}$$

---

*Expansion in terms of the conserved quantity J seems more reasonable than expansion in terms of ℓ. The use of the latter can only lead to misunderstanding. For example, in the paper of Clementel and Villi,[7] where expansion in terms of ℓ is used for the analysis of the p − p scattering, it was erroneously found that the mixing coefficients occur in the expression for the integrated cross-section, which cannot be correct (cf. Ref. 2), and which happened because of the incomplete consideration of the states with different values of ℓ for a given J.

With the limitation to s, p, and d waves with J ≤ 2:

$$2A = -(2a_0 + \sqrt{10}a_2);\ 2B = 3\sqrt{10}a_2 t;\ 4C = -2\sqrt{3}a_3 + \sqrt{5}a_4 + \sqrt{10}a_5;$$
$$4D = -5\sqrt{10}a_5 t;\ 4E = (3\sqrt{3}a_3 + 3\sqrt{5}a_4 - 2\sqrt{10}a_5)t;\ 4F = \sqrt{6}a_1 - \sqrt{3}a_3 - \sqrt{5}a_4 + \sqrt{10}a_5(5t^2 - 1). \tag{7}$$

In the general case

$$A(-t) = A(t);\ B(-t) = -B(t);\ C(-t) = C(t);\ D(-t) = -D(t);\ E(-t) = -E(t);\ F(-t) = F(t). \tag{7'}$$

REACTION CROSS-SECTION OF UNPOLARIZED PARTICLES

The equality of the reaction cross-sections for unpolarized particles

$$4I^{(A)}(\theta) = 3I_0^{(B)}(\theta),$$

follows directly from Eqs. (5) and (6), and (with the ratio of the squares of the relative momenta omitted)

$$16\pi I_0^{(A)}(\theta) = 12\pi I_0^{(B)}(\theta) = |A|^2 + |B|^2 + 2\,\mathrm{Re}\,[(A^+B) + 2(E^+F)]\cos\theta$$
$$+ 2|E|^2 + 2|F|^2 + 2\sin^2\theta\,[|C|^2 + |D|^2 + \cos\theta\cdot 2\mathrm{Re}\,(C^+D)]. \tag{8}$$

With the limitation to s, p, and d waves with J ≤ 2 we get from Eqs. (7) and (8)

$$64\pi I_0^{(A)}(\theta) = 48\pi I_0^{(A)}(\theta) = 4\rho_0^2 + 12\rho_1^2 + 10\rho_2^2(1 + 3\cos^2\theta) + [6(\sqrt{2}\omega_{13} + \sqrt{10}\omega_{14} + \sqrt{5}\omega_{34}) - 4\sqrt{10}\omega_{02} + 4\sqrt{15}\omega_{15}$$
$$+ 2\sqrt{30}\omega_{35}](3\cos^2\theta - 1) + 3[\rho_3^2(5 - 3\cos^2\theta) + 5\rho_4^2(1 + \cos^2\theta)] + 10\rho_5^2(1 + 6\cos^2\theta - 5\cos^4\theta) \tag{8'}$$
$$+ 10\sqrt{6}\omega_{45}(10\cos^4\theta - 9\cos^2\theta + 1), \quad a_m = \rho_m e^{i\alpha m}; \quad \omega_{mn} = \rho_m\rho_n\cos(\alpha_m - \alpha_n),$$

which, apart from differences of notation, agrees with results previously obtained.[8,9]

Before going on to the comparison of the polarization phenomena in reactions (A), we note that the study of reaction (B) at total meson energy E_π provides a possibility of obtaining information about the reaction (A) at a (kinetic) energy W of the protons given by

$$W = \frac{M_d}{M}E_\pi + \frac{\mu}{M}\mu c^2 - \varepsilon\left(\frac{M_d}{M} + 1\right) \approx 2E_\pi \tag{9}$$

(M_1, M, μ are the masses of the deuteron, nucleon, and π meson, and ϵ is the binding energy of the deuteron).

From Eq. (9) it follows, for example, that by the use of a π^+ meson beam with energy E_π = 320 + 140 = 460 Mev (from the 680 Mev accelerator at the Joint Institute for Nuclear Research) the study of reaction (B) gives a possibility of getting information about the formation of mesons in reaction (A) at proton energies about 920 Mev, which considerably exceeds the energy of the particles in the accelerator. Such a "gain of energy" is due to the fact that in reaction (A) a considerable part of the whole energy is expanded in motion of the center of mass of the system, whereas in the inverse reaction the energy in the center-of-mass system does not differ by much from the value of the energy in the laboratory system of coordinates.

POLARIZATION PHENOMENA IN THE DIRECT AND INVERSE REACTIONS

1. We now examine the information obtainable from a study of the polarization phenomena. Because of isotopic invariance we can consider all at once the general process N + N ⇄ d + π, where N is a nucleon and π is a π^+ or π^0 meson. The cross-section for meson production by polarized protons in reaction (A) can be put in the form

$$I^{(A)}(\theta, \varphi) = I_0^{(A)}(\theta) + p\cos\varphi P(\theta) = I^{(A)}(\theta) + pI_p \tag{10}$$

(p is the polarization of the nucleon beam, with the direction of polarization taken along the y axis).

Using the formula

$$(\hat{\sigma}_1\mathbf{p})S = S_c(\boldsymbol{\psi}\mathbf{p}) + (\mathbf{S}\mathbf{p})\psi_c + i([\mathbf{p}\boldsymbol{\psi}]\mathbf{S});\quad S = S_c\psi_c + (\mathbf{S}\boldsymbol{\psi});$$

we get

$$16\pi I_{p_1}(\theta)\cos\varphi = 4\pi\,\mathrm{Sp}\,S_A(\hat{\sigma}_1\mathbf{p})S_A^+ = (\mathbf{np})P_1(\theta);$$
$$P_1(\theta) = 2\,\mathrm{Im}\,\{[C^+(A + B\cos\theta) + D^+(A\cos\theta + B) + (B^+E) + (AF^+)]$$
$$+ [\sin^2\theta\,(CD^+) + (F^+E) + C(E + F\cos\theta)^+ + D(E\cos\theta + F)^+]\}. \tag{10'}$$

In the expression for $P_1(\theta)$ the first four terms, which give the contribution of singlet-triplet transitions in reaction (A), do not change sign with the replacement $\theta \rightarrow \pi - \theta$, i.e., they are symmetric with respect to 90°; the remaining terms, which give the contribution of triplet-triplet transitions, change sign with the replacement $\theta \rightarrow \pi - \theta$, i.e., they vanish at $\theta = 90°$.

From a comparison of the formula

$$(\hat{\sigma}_2 \mathbf{p}) S = -[S_c(\hat{\psi}\mathbf{p}) + (\mathbf{S}\mathbf{p})\psi_c] + i([\mathbf{p}\psi]\mathbf{S})$$

with the one we had before for $(\hat{\sigma}_1 \mathbf{p})\mathbf{S}$, it can be seen that the expression for the azimuthal asymmetry, when the target is polarized, differs from (10′) by the sign of the first four terms

$$\begin{aligned} 16\pi I_{p_1}(\theta)\cos\varphi &= 4\pi \operatorname{Sp} S_A(\hat{\sigma}_2\mathbf{p}) S_A^+ = (\mathbf{np}) P_1'(\theta); \\ P_1'(\theta) &= 2\operatorname{Im}\{-[C^+(A + B\cos\theta) + D^+(A\cos\theta + B) + (B^+E) + (AF^+)] \\ &\quad + [\sin^2\theta(CD^+) + (F^+E) + C(E + F\cos\theta)^+ + D(E\cos\theta + F)^+]\}. \end{aligned} \tag{10''}$$

On the other hand, for the polarization of the nucleons in reaction (B), when the deuteron target is unpolarized, we get from Eq. (6)

$$12\pi I_0^{(B)}(\theta)\langle\hat{\sigma}_1\rangle_f = 4\pi \operatorname{Sp} S_B^+ \hat{\sigma}_1 S_B = \mathbf{n} P_1(\theta); \tag{11}$$

$P_1(\theta)$ is given by Eq. (10′). For the polarization of the other nucleon we get

$$12\pi I_0^{(B)}(\theta)\langle\hat{\sigma}_2\rangle_f = \mathbf{n} P_1'(\theta), \tag{11'}$$

$P_1'(\theta)$ is given by Eq. (10″). From Eqs. (7′), (10′), (10″), (11′) and (8):

$$\langle\hat{\sigma}_1(\theta, \varphi)\rangle = \langle\hat{\sigma}_2(\pi - \theta, \pi + \varphi)\rangle;$$

and from Eqs. (10) and (11) there follows the validity of the equation:

$$4 I_p^{(A)} = 3 I_0^{(B)}(\theta)\langle\hat{\sigma}\rangle_f N \tag{12}$$

(the ratio of the momenta is omitted).

Thus a knowledge of the polarization of the nucleons in reaction (B) gives just the same information as the cross-section for the production of mesons by polarized nucleons in reaction (A).

Additional information can be obtained by studying the polarization of the deuterons produced in reaction (A). If in dealing with the interaction of unpolarized particles we limit ourselves to just the polarization vector, then for it we get by means of Eq. (4′) and the formula $\hat{\mathbf{S}}(S_m\varphi_m) = i[\mathbf{S}\boldsymbol{\varphi}]$ the result

$$16\pi I_0^{(A)}(\theta)\langle\hat{S}\rangle_f = \mathbf{n} P_2(\theta); \quad P_2(\theta) = 2\operatorname{Im}\{(AB^+) + \sin^2\theta(D^+C) + (C + F)^+E + (D^+E) + (C^+F + D^+E)\cos\theta\}. \tag{13}$$

With the limitation to waves with $J \leq 2$ the angular dependence takes the form

$$2\sin\theta P_2(\theta) = \sin\theta\cos\theta\{6\sqrt{10}\,\varepsilon_{02} + 9\sqrt{2}\,\varepsilon_{13} + 3\sqrt{10}\,\varepsilon_{14} + 2\sqrt{15}\,\varepsilon_{15} - 6\sqrt{5}\,\varepsilon_{34} - 2\sqrt{30}\,\varepsilon_{35}\},$$

where $\epsilon_{mn} = \rho_m\rho_n \sin(\alpha_m - \alpha_n)$. And in the general case, as can be seen from Eq. (7′), there remains a proportionality to the product of $\sin 2\theta$ by an even function of $\cos\theta$.

Let us now consider the expression for the cross-section of reaction (B) on a polarized target. On the assumption that the target is polarized in such a way that only the average value of the spin vector of the deuteron is different from zero, the cross-section can be put in the form (10). For $\langle\mathbf{S}\rangle \neq 0$ the averages $\langle D_{ik}\rangle$ are also different from zero, but we consider only the contribution of the term proportional to $\langle\mathbf{S}\rangle$.) Then from Eq. (6) we have

$$3 I_p^{(B)} = 12\pi \operatorname{Sp} S_B(\hat{S}\mathbf{p}) S_B^+ = (\mathbf{np}) P_2(\theta). \tag{14}$$

From a comparison of Eqs. (13) and (14) we get still another consequence of invariance under time reversal

$$3 I_p^{(B)} = 4 I_0^{(A)}\langle\hat{S}\rangle_f \mathbf{N}. \tag{15}$$

The equations (12) and (15) are a generalization of the relation (2) to the case of the binary reaction under consideration.

2. As is well known,[4,6] the state of polarization of a deuteron is characterized not only by the average value of the spin vector $\hat{\mathbf{S}}$ of the deuteron but also by a tensor of the second rank which can be constructed from the spin vector. In the literature one finds the tensor

$$\hat{D}_{ik} = \frac{1}{2}(\hat{S}_i\hat{S}_k + \hat{S}_k\hat{S}_i) - \frac{2}{3}\delta_{ik} = \hat{T}_{ik} - \frac{2}{3}\delta_{ik},$$

introduced by Dalitz, and also the tensor $T_{2,m}$ with the components

$$2T_{2,\pm 2} = \sqrt{3}\{(\hat{S}_x^2 - \hat{S}_y^2) \pm i(\hat{S}_x\hat{S}_y + \hat{S}_y\hat{S}_x)\},\quad 2T_{2,\pm 1} = \mp\sqrt{3}\{(\hat{S}_x\hat{S}_z + \hat{S}_z\hat{S}_x) \pm i(\hat{S}_z\hat{S}_y + \hat{S}_y\hat{S}_z)\},$$
$$\sqrt{2}\,T_{2,0} = 3\hat{S}_z^2 - 2. \tag{16}$$

For the elastic scattering of particles with spin 1, as follows from the results of Cheishvili[10] and as has been shown by Lakin,[6] relations of the type (2) hold not only between the average value of the polarization vector and the corresponding term in the cross-section, but also for the tensor terms. The correspondence of the vector terms for reactions (A) and (B) has been established above. Let us now make the comparison, for our binary reaction, between the expression for the polarization tensor of the deuteron in reaction (A), for the interaction of unpolarized protons, and the cross-section of reaction (B) for an arbitrary polarized deuterium target.

From a calculation using the formula

$$[\hat{S}_i\hat{S}_k + \hat{S}_k\hat{S}_i](S_m\varphi_m) = 2\delta_{ik}(S_m\varphi_m) - [S_i\varphi_k + S_k\varphi_i]$$

we have for the average values of the tensor $\hat{D}_{ik}$

$$16\pi I_0^{(A)}(\theta)\{{}^1/_3\,\delta_{ik} - \langle\hat{D}_{ik}\rangle\} = \delta_{ik}\{|E|^2 + |F|^2 + \cos\theta\cdot 2\,\mathrm{Re}\,(E^+F)\} + k_ik_k\{|A|^2 + \sin^2\theta\cdot|C|^2 - |E|^2$$
$$+ 2\,\mathrm{Re}\,[C^+(E\cos\theta + F)]\} + k_{0i}k_{0k}\{|B|^2 + |D|^2\sin^2\theta - |F|^2 - 2\,\mathrm{Re}\,[D^+(E + F\cos\theta)]\} + n_in_k\{|C|^2$$
$$+ |D|^2 + 2\,\mathrm{Re}\,[C^+(D\cos\theta - F) + D^+E]\} + (k_{0i}k_k + k_ik_{0k})\,\mathrm{Re}\,\{(AB^+) + (C^+D)\sin^2\theta - (EF^+) - [C^+(E + F\cos\theta)]$$
$$+ [D^+(E\cos\theta + F)]\} = D_1(\theta)\delta_{ik} + D_2(\theta)k_ik_k + D_3(\theta)k_{0i}k_{0k} + D_4(\theta)n_in_k + D_5(\theta)(k_{0i}k_k + k_{0k}k_i). \tag{17}$$

From eqs. (17) and (7′) there follow for D_1, D_2, ... as functions of $t = \cos\theta$ the symmetry properties

$$D_1(-t) = D_1(t);\quad D_2(-t) = D_2(t);\quad D_3(-t) = D_3(t);\quad D_4(-t) = D_4(t);\quad D_5(-t) = -D_5(t). \tag{17′}$$

It can be verified without difficulty that the condition (1) has as a consequence that the expression for the corresponding term in the cross-section differs from (17) by the replacement $D_2 \rightleftarrows D_3$. Consequently, a study of all the components of the polarization tensor in reaction (A) gives the same information as the study of the cross-section of reaction (B) for a polarized deuterium target.

As can be seen from Eq. (17), for certain contractions of the polarization tenson, for example for $\langle\hat{D}_{ik}\rangle n_in_k$, a relation of the type of Eqs. (12) and (15) follows from the requirement of symmetry with respect to change of the sign of the time.

The expressions for $\langle T_{2,m}\rangle$ are found from Eq. (17), if we use the relations following from Eq. (16),

$$2T_{2,\pm 2} = \sqrt{3}\{(\hat{T}_{xx} - \hat{T}_{yy}) \pm 2i\hat{T}_{xy}\} = \sqrt{3}\{(\hat{D}_{xx} - \hat{D}_{yy}) \pm 2i\hat{D}_{xy}\},\quad T_{2,\pm 1} = \mp\sqrt{3}(\hat{T}_{xy} \pm i\hat{T}_{yz}) = \mp\sqrt{3}(\hat{D}_{xy} \pm i\hat{D}_{yz}),$$
$$\sqrt{2}\,T_{2,0} = 3\hat{T}_{zz} - 2 = \hat{D}_{zz}. \tag{16′}$$

The availability of polarized proton beams makes it possible to study the polarization of the deuterons in reaction (A) under the action of polarized protons. We have

$$\langle\hat{D}_{ik}\rangle = {}^1/_4\,\mathrm{Sp}\,[S_A(1 + \mathbf{p}\hat{\sigma}_1)S_A^+\hat{D}_{ik}]/{}^1/_4\,\mathrm{Sp}\,[S_A(1 + \mathbf{p}\hat{\sigma}_1)S_A^+], \tag{18}$$

where the denominator contains the expression for the cross-section of reaction (A), $I^{(A)}(\theta, \varphi)$, as given in Eqs. (8) and (10). The polarization of the incident protons is denoted by **p**; the expression for the interaction of unpolarized particles is obtained from Eq. (18) for $p = 0$. Thus for polarized protons one needs only to consider the changes arising on account of the second term in the numerator, and to replace $I_0(\theta)$ by $I(\theta, \varphi)$ in the expressions given previously.

For the added term in the polarization vector of the deuteron we get:

$$4\pi\,\mathrm{Sp}\,(\hat{\sigma}_1\mathbf{p})S_A^+\hat{S}S_A = \mathbf{n}(\mathbf{np})\,2\,\mathrm{Re}\,[(BC^+) - (AD^+)] + [\mathbf{np}]\,2\,\mathrm{Re}\,\{C^+(E + F\cos\theta) + D^+(F + E\cos\theta)\}$$
$$+ \mathbf{p}\cdot 2\,\mathrm{Re}\,\{A^+(E + F\cos\theta) + B^+(E\cos\theta + F)\} - \mathbf{k}\cdot 2\,\mathrm{Re}\,\{[(\mathbf{pk})(A + E) + (\mathbf{pk}_0)(B + F)]E^+\}$$
$$- \mathbf{k}_0\cdot 2\,\mathrm{Re}\,\{[(\mathbf{pk})(A + E) + (\mathbf{pk}_0)(B + F)]F^+\} + \mathbf{l}\cdot 2\,\mathrm{Re}\,\{(\mathbf{pk})(BC^+) + (\mathbf{pk}_0)(BD^+) + (\mathbf{pl})|D|^2$$
$$+ (\mathbf{pm})(C^+D)\} + \mathbf{m}\cdot 2\mathrm{Re}\{(\mathbf{pk})(AC^+) + (\mathbf{pk}_0)(AD^+) + (\mathbf{pm})|C|^2 + (\mathbf{pl})(C^+D)\}, \tag{19}$$

where $\mathbf{m} = [\mathbf{kn}]$; $\boldsymbol{l} = [\mathbf{k}_0\mathbf{n}]$.

Analogously we have for the polarization of the protons in reaction (B) with a polarized deuterium target (only $\langle\hat{\mathbf{S}}\rangle \neq 0$)

$$\begin{gathered}4\pi\,\mathrm{Sp}\,\hat{S}S_B^+(\hat{\boldsymbol{\sigma}}_1\mathbf{p})\,S_B=\mathbf{n}\,(\mathbf{np})\,2\,\mathrm{Re}\,[(B^+C)-(A^+D)]+\mathbf{p}\,2\,\mathrm{Re}\,\{[A^+(E+F\cos\theta)]+[B^+(F+E\cos\theta)]\}\\-[\mathbf{np}]\,2\,\mathrm{Re}\,\{[C^+(E+F\cos\theta)]+[D^+(F+E\cos\theta)]\}+\mathbf{l}\,2\,\mathrm{Re}\,\{(\mathbf{pm})(C^+D)+|C|^2(\mathbf{pl})-(A^+D)(\mathbf{pk})-(\mathbf{pk}_0)(A^+C)\}\\+\mathbf{m}2\,\mathrm{Re}\,\{(\mathbf{pl})(C^+D)+|D|^2(\mathbf{pm})-(B^+C)(\mathbf{pk}_0)-(B^+D)(\mathbf{pk})\}-\mathbf{k}2\,\mathrm{Re}\,\{F^+[(\mathbf{pk}_0)(A+E)+(\mathbf{pk})(B+F)]\}\\-\mathbf{k}_0 2\,\mathrm{Re}\,\{E^+[(\mathbf{pk}_0)(A+E)+(\mathbf{pk})(B+F)]\},\end{gathered}\tag{20}$$

from which the correspondence with Eq. (19) can be seen. The analogous correspondence also remains valid for the tensor terms. Therefore we shall present only the expressions for the additions to the polarization of the deuterons in reaction (A). From Eqs. (5) and (18) we have

$$\begin{gathered}4\pi\,\{{}^1/_3\,\delta_{ik}\,\hat{S}\mathrm{p}\,(\hat{\boldsymbol{\sigma}}_1\mathbf{p})\,S_A^+S_A-\mathrm{Sp}\,(\hat{\boldsymbol{\sigma}}_1\mathbf{p})\,S_A^+\hat{D}_{ik}S_A\}=(\mathbf{np})\,\mathrm{Im}\,\{2\,[n_in_k(CD^+)+k_ik_k(AC^+)+k_{0i}k_{0k}(BD^+)]+(k_{0i}k_k+k_{0k}k_i)\,[(AD^+)\\+(BC^+)]\}+(n_ik_k+n_kk_i)\,\mathrm{Im}\,\{(\mathbf{pk})\,[C^+(A+2E)]+(\mathbf{pk}_0)\,[(AD^+)+2\,(C^+F)]+(\mathbf{pl})\,(C^+D)\}+(n_ik_{0k}+n_kk_{0i})\,\mathrm{Im}\,\{(\mathbf{pk})\,[(BC^+)\\+2\,(D^+E)]+(\mathbf{pk}_0)\,[D^+(B+2F)]+(\mathbf{pm})\,(C^+D)\}+(p_in_k+n_ip_k)\,\mathrm{Im}\,\{[C\,(E+F\cos\theta)^+]+D\,(E\cos\theta+F)^++(EF^+)\}\\+\mathrm{Im}\,(AE^+)\,(q_ik_k+q_kk_i)+\mathrm{Im}\,(AF^+)\,(q_{0i}k_k+k_iq_{0k})+\mathrm{Im}\,(BE^+)\,(q_ik_{0k}+k_{0i}q_k)+\mathrm{Im}\,(BF^+)\,(q_{0i}k_{0k}+q_{0k}k_{0i}),\end{gathered}\tag{21}$$

where

$$\mathbf{q}_0=[\mathbf{pk}_0],\quad \mathbf{q}=[\mathbf{pk}].$$

The expression for the term proportional to δ_{ik} is the same as Eq. (10′).

3. As a final example we shall compare the expressions for the correlation of the polarizations of the protons (nucleons) in reaction (B), when the target is polarized, and for the changes in the cross-section for production of mesons by reaction (A) when both the beam and the target are polarized. By means of the formula

$$(\hat{\boldsymbol{\sigma}}_2\mathbf{b})\,\psi_c=-(\mathbf{b}\boldsymbol{\psi});\quad (\hat{\boldsymbol{\sigma}}_2\mathbf{b})\,(\boldsymbol{\psi}\mathbf{p})=-(\mathbf{pb})\,\psi_c+i\,(\boldsymbol{\psi}\,[\mathbf{pb}])$$

it is not hard to get for the correlation of the polarizations

$$\begin{gathered}12\pi\,I_0^{(B)}(\theta)\,\langle(\hat{\boldsymbol{\sigma}}_2\mathbf{b})\,(\hat{\boldsymbol{\sigma}}_1\mathbf{p})\rangle=4\pi\,\mathrm{Sp}\,S_B^+(\hat{\boldsymbol{\sigma}}_2\mathbf{b})\,(\hat{\boldsymbol{\sigma}}_1\mathbf{p})\,S_B=(\mathbf{bp})\,\{12\pi\,I_0^{(B)}(\theta)-2\,[|A|^2+|B|^2+2\,\mathrm{Re}\,(A^+B)\cos\theta+|E|^2+|F|^2\\-2\,\mathrm{Re}\,(EF^+)\cos\theta]\}+(\mathbf{n}\,[\mathbf{pb}])\,2\,\mathrm{Re}\,\{[A^+(C+F+D\cos\theta)]+[B^+(C\cos\theta+D-E)]\}-(\mathbf{np})\,(\mathbf{nb})\,\{|C|^2+|D|^2\\+4\,\mathrm{Re}\,[C^+(D+F)-(D^+E)]\}-2\,(\mathbf{k}_0\mathbf{b})\,(\mathbf{k}_0\mathbf{p})\,\{|C|^2\sin^2\theta-|E|^2\}-2\,(\mathbf{kb})\,(\mathbf{kp})\,\{|D|^2\sin^2\theta-|F|^2\}+[(\mathbf{kb})\,(\mathbf{k}_0\mathbf{p})\\+(\mathbf{kp})\,(\mathbf{k}_0\mathbf{b})]\,2\,\mathrm{Re}\,[(E^+F)-(C^+D)\sin^2\theta]+[(\mathbf{pk}_0)\,(\mathbf{bl})+(\mathbf{bk}_0)\,(\mathbf{pl})]\,2\,\mathrm{Re}\,(C^+E)+[(\mathbf{pk}_0)\,(\mathbf{bm})+(\mathbf{bk}_0)\,(\mathbf{pm})]\,2\mathrm{Re}\,(C^+F)\\+[(\mathbf{pk})\,(\mathbf{bl})+(\mathbf{bk})\,(\mathbf{pl})]\,2\,\mathrm{Re}\,(D^+E)+[(\mathbf{pk})\,(\mathbf{bm})+(\mathbf{bk})\,(\mathbf{pm})]\,2\,\mathrm{Re}\,(D^+F),\end{gathered}\tag{22}$$

where

$$S_B=S_c\psi_c+(\mathbf{S}\boldsymbol{\psi}).$$

The expression for $I_{pp}(\theta,\varphi)$ is obtained from Eq. (22) by the interchange $\mathbf{k}\rightleftarrows\mathbf{k}_0$. Thus, just as for the other tensor quantities, it follows from the condition (1) that the study of all the components of the two quantities gives identical information, and for certain contractions, for example for $\langle(\hat{\boldsymbol{\sigma}}_2\,\mathbf{n})\,(\hat{\boldsymbol{\sigma}}_1\,\mathbf{n})\rangle$, a relation of the type of Eq. (12) holds.

From a comparison of Eq. (22) with Eq. (17) it follows that the study of the correlation of the polarizations of the protons in reaction (B) gives even more extensive information that the study of the polarization of the deuterons in reaction (A).

All results so far obtained for reactions (A) and (B) transfer directly to the reactions

$$n+p\rightleftarrows d+\pi^0.\tag{C – D}$$

Furthermore, isotopic invariance provides the possibility of setting up a connection between properties of the cross-sections of reactions (A – B) and (C – D), since, as is well known,

$$I\,(p+p\rightleftarrows d+\pi^+)=2I\,(n+p\rightleftarrows d+\pi^0).\tag{23}$$

This relation is valid for the reaction cross-sections of both unpolarized[11] and polarized[10] particles. For the case of interaction of polarized particles one can prove additional relations. The primary relation of this sort is of the form

$$\langle\hat{\boldsymbol{\sigma}}\rangle_f I_0^{(A)}(\theta)=2\,\langle\hat{\boldsymbol{\sigma}}\rangle_f I_0^{(D)}(\theta),\tag{24}$$

the existence of which follows from Eqs. (23), (10), and (1). From Eq. (24), in virtue of the validity of Eq. (23) for the interaction of unpolarized particles, there follows the equality of the polarizations of the corresponding nucleons in the reactions $d+\pi^0\to n+p$ and $d+\pi^+\to p+p$. Similar equalities hold for the polarization of the deuterons and the correlation of the polarizations of the nucleons.

DISCUSSION

The existence of the condition (1) makes it evident from the very beginning that the total information obtainable from the study of the direct reaction coincides with the total information obtainable from the study of the inverse reaction. The results of the present paper show that for the binary reaction considered there appear, in virtue of the condition (1), relations of the types of Eqs. (12) and (15) between the azimuthal asymmetry and the polarization, similar to the relation between the unpolarized cross-sections. On consideration of the tensor terms it turns out that for some contractions, for ecample $\langle \hat{D}_{ik} \rangle n_i n_k$, relations of the type of Eq. (12) remain valid. Taken as a whole, the study of all the components of the tensor quantities in reactions (A) and (B) gives identical sets of information.

If in the expressions (5) and (6) one sets C = D = E = F = 0, leaving only the quantities A and B different from zero, the resulting formulas will relate to a process in which the interaction of two spinless particles results in the formation of a spinless particle of the opposite parity and a particle with spin 1. As can be seen from Eq. (13), a relation of the type (15) remains valid in this case also. The expression for the tensor $\langle \hat{D}_{ik} \rangle$ takes the form

$$4\pi \{{}^1/_3\delta_{ik} - \langle \hat{D}_{ik} \rangle\} I_0(\theta) = |A|^2 k_i k_k + |B|^2 k_{0i} k_{0k} + \mathrm{Re}(AB^+)(k_{0i}k_k + k_{0k}k_i).$$

The opposite case with A = B = 0 and C, D, E, and F different from zero corresponds to the conversion of a scalar particle into a pseudoscalar particle in a reaction with a particle of spin 1. The symmetry properties (7′) do not hold in these cases.

The present case of a binary reaction with the spins of the particles different in the initial and final states is a rather general one. The generalization of Wolfenstein's theorem to the case of binary reactions in which the spins of the particles do not change (and the intrinsic parities of the particles are unchanged) is carried through without difficulty. For the simplest case, in which the values of the spins in the initial and final states are 0 and 1/2, the result follows at once from the fact that the transition amplitude can be put in the form

$$M = a(\theta) + b(\theta)(\hat{\sigma}\mathbf{n}),$$

if the intrinsic parities of the spinless particles in the initial and final states are the same, and

$$M = b_1(\theta)(\hat{\sigma}\mathbf{k}_1) + b_2(\theta)(\hat{\sigma}\mathbf{k}_2)$$

($\mathbf{k}_1$ and $\mathbf{k}_2$ are relative momenta) when, for example, in interacting with a nucleon a scalar particle turns into a pseudoscalar particle.

For the case in which the spins of the particles are $s_1 = s_2 = 1/2$, for example for the reaction

$$p + \mathrm{T} \rightleftarrows n + \mathrm{He}_2^3, \tag{E}$$

the validity of the consequences of invariance under time reversal that have been established for the elastic scattering of nucleons by nucleons will be obvious if we show that in this case also the expression for the amplitude M does not differ from the case of elastic scattering. This last assertion can be proved either by requiring, instead of the invariance of M, the invariance of the matrix MM^+, or by considerations like those of Wright[13] on the possible transitions in the reaction (E). Either of these procedures makes it possible to transfer the consequences of the time reversal from the elastic scattering to the case of binary reactions in which there is no change of the spins (and parities) of the particles. For binary reactions different from elastic scattering, in which the particles in the initial state are different from those in the final state, there is a peculiar "doubling" of the relations of the type of Eq. (2).

The writer is grateful to Ia. A. Smorodinskii, S. M. Bilen'kii, and R. M. Ryndin for helpful discussions.

Note added in proof (June 29, 1957). While this paper was in press the writer learned that Baz' [(J. Exptl. Theoret. Phys. **32**, 628 (1957), Soviet Phys. JETP **5**, 521 (1957)] has generalized Wolfenstein's theorem to the case of a reaction of the type of (E) by another method.

---

[1] E. P. Wigner and L. Eisenbud, Phys. Rev. **72**, 29 (1947); F. Coester, Phys. Rev. **89**, 619 (1953); **84**, 1259 (1951).

[2] J. M. Blatt and L. C. Biedenharn, Revs. Mod. Phys. **24**, 258 (1952).

[3] R. Huby, Proc. Phys. Soc. **A65**, 1103 (1952).

[4] R. H. Dalitz. Proc. Phys. Soc. **A65**, 175 (1952).

[5] L. Wolfenstein and J. Ashkin, Phys. Rev. **85**, 947 (1952).

[6] W. Lakin, Phys. Rev. **98**, 139 (1955).

[7] E. Clementel and C. Villi, Nuovo cimento **2**, 1165 (1955).

[8] F. Mandl and T. Regge, Phys. Rev. **99**, 1478 (1955).

[9] S. M. Bilen'kii and L. I. Lapidus, Report of Institute of Nuclear Research of the Academy of Sciences of the U.S.S.R., 1955.

[10] O. D. Cheishvili, J. Exptl. Theoret. Phys. (U.S.S.R.) **30**, 1147 (1956), Soviet Phys. JETP **3**, 974 (1957).

[11] R. L. Garwin, Phys. Rev. **85**, 1045 (1952).

[12] V. B. Berestetskii, Dokl. Akad. Nauk SSSR **94**, 421 (1954).

[13] S. C. Wright, Phys. Rev. **99**, 996 (1956).

Translated by W. H. Furry
30

SOVIET PHYSICS JETP VOLUME 6, NUMBER 1 JANUARY, 1958

ELECTRON DENSITY FLUCTUATIONS AND THE SCATTERING OF RADIO WAVES IN THE IONOSPHERE

IA. L. AL'PERT

Institute for the Study of Terrestrial Magnetism, the Inosphere, and Radio Wave Propagation

Submitted to JETP editor January 19, 1957

J. Exptl. Theoret. Phys. (U.S.S.R.) **33**, 213-224 (July, 1957)

A description is given of results from a determination of electron density fluctuations obtained by measuring the "turbidity coefficient" of the ionosphere and the energy scattered at very high frequencies. The linear dimensions ξ of inhomogeneities at ~ 80 km, which are effective in uhf scattering, were also determined. The formulas employed were based on an expression for the scattering cross section σ which was obtained with the auto correlation coefficient $\rho(r) \sim \exp\{-(r/\xi)^2\}$. The author concludes that when the ionosphere is sounded at frequencies below the critical frequency, the received signal comprises in addition to the "specularly" reflected wave also waves which are principally scattered forward and latter reflected at higher ionospheric levels. In oblique distant uhf transmission through the ionosphere scattering from inhomogeneities of optimum size makes the largest contribution.

1. INTRODUCTION

It is known that one of the principal characteristics of the "calm" unperturbed ionosphere is its "statistical inhomogeneity," the mechanisms of which are still unknown.[1,2] It has been argued that turbulence and in some instances plasma oscillations and waves participate in these processes. However, all such discussions are of a very tentative nature since the theory of the phenomena is still relatively undeveloped. There is also very little reliable experimental information available to serve as a basis for any theoretical model.

Up to the present time the following parameters have been determined experimentally:

1. The ranges of linear dimensions ξ_s of the inhomogeneities, principally at altitudes $z \approx 100 - 120$ km and $\approx 250 - 350$ km. From experiments with vertical sounding of the ionosphere the most frequently encountered values are $\xi_0 \sim 200 - 300$ m.

2. The ranges of random velocities v_s of the inhomogeneities; the values $v_0 \sim 1 - 3$ m/sec have been obtained.

3. The horizontal drift velocities u; at z ~ 80 — 120 km u_0 ~ 70 m/sec, and at z ~ 250 — 350 km u_0 ~ 100 m/sec,* with

$$(du_0/dz)_{100-130\text{ km}} \sim 3.4\text{ m/sec/km}$$

and

$$(du_0/dz)_{250-500\text{ km}} \sim 1\text{ m/sec/km}.$$

4. The ranges of the angles θ of scattered waves, for which the values $\theta_0 \sim 2-5°$ were obtained

5. The degree of turbulence of the ionosphere $\beta_0^2 = a_0^2/\Sigma a_s^2$, which is the ratio between the energy of a specularly reflected wave and the total energy of scattered waves; the values $\beta_0 \sim 2-4$ were obtained.

However, there has thus far been an absence of data on the fluctuations of electron density in the inhomogeneities, which are represented by the quantity $\overline{(\Delta N/N)^2} = (\delta N)^2$. It is quite evident that without knowledge of δN it is impossible to obtain a complete physical picture of the effects under discussion. In particular, it is not possible to make calculations for uhf transmission to great distances, which has attracted much attention in recent years.

Some methods are described below for determining δN and in some instances ξ, and the experimental values are given.

It is shown that the previously accepted picture of scattering in the ionosphere must be changed in some instances. Thus the random oscillations detected in vertical sounding of the ionosphere below the critical frequency do not result from backward scattering (with $\theta \sim 0$), as has hitherto been supposed, but principally from forward scattered waves ($\theta \sim 0$) which are subsequently reflected at higher ionospheric levels. This produces, in particular, the narrow angular spread of the waves which is observed experimentally. In oblique distant uhf transmission inhomogeneities of optimum size are the most important factor in the scattering rather than the angle function $\sin^{-n}(\theta/2)$ which is usually analyzed in the literature. Calculations and measurements are brought into agreement when this fact is taken into account.

The discrepancy found in the literature between the experimental results and the calculations is also apparently a result of improper utilization of the various ionospheric parameters.

When the entire set of the above-mentioned parameters is examined it is a striking fact that they change very little from the beginning of the ionosphere to the region of maximum ionization, despite the fact that the density of neutral particles and accordingly the mean free path changes by a factor of approximately $10^5 - 10^6$, the electron concentration by $10^3 - 10^4$ and the temperature by 5 — 7. It is therefore very important that further experiments should include a detailed investigation of the altitude dependence of these parameters. At the end of this paper certain "dimensional" formulas of the theory of turbulence are used to estimate the quantities under investigation. In a number of instances the estimates agree with the measurements, but for a number of reasons this is insufficient for the drawing of any conclusions.

2. DEDUCTION AND ANALYSIS OF THEORETICAL FORMULAS

(a) Effective Scattering Cross Section

We assume that the inhomogeneous medium V is characterized by any irregular function $\Delta\epsilon$ representing the departure of the dielectric constant from its average value ϵ, and that the linear dimensions of V are large compared with the scale ξ of an inhomogeneity.† Then the complex energy density of the secondary field of volume dipoles excited by the incident wave $E_0 \exp\{i(\omega t - kR_0)\}$ is at the point of observation

$$\frac{c}{4\pi}(EH^*) = \frac{c\sqrt{\varepsilon}}{4\pi}\frac{k^4}{(4\pi)^2}\iint(\Delta\varepsilon)(\Delta\varepsilon')^*\cdot\frac{E_0E_0'\sin\psi\cdot\sin\psi'}{RR'}\exp\{-ik[(R-R')+(R_0-R_0')]\}\,dV\,dV', \qquad (1)$$

where the notation can be understood from Fig. 1, k = 2π/λ, primes denote the values of quantities at the point P′ located a distance r from the point P, and asterisks denote complex conjugates.

Equation (1) is usually calculated as follows. We separate in the double integral

$$\int_V(\Delta\varepsilon)(\Delta\varepsilon')^*dV = \overline{(\Delta\varepsilon)(\Delta\varepsilon')^*}, \qquad (2)$$

---

*The largest inhomogeneities with velocities u_0 ~ 200 — 300 m/sec are evidently to be observed when the ionosphere is in a perturbed state.

†Of course, ϵ can itself be a function of position in the medium.

which is the autocorrelation function of $\Delta\epsilon$. Since for the ionosphere a good approximation of the correlation coefficient, especially according to experimental data on short waves,[1,5] is given by $\rho(r) \sim \exp(-r^2/\xi^2)$, Eq. (2) can be written as

$$\int_V (\Delta\varepsilon)(\Delta\varepsilon')^* dV = V\,\overline{\Delta\varepsilon^2}\,e^{-r^2/\xi^2}, \qquad \overline{\Delta\varepsilon^2} = \frac{1}{V}\int (\Delta\varepsilon)^2 dV. \tag{3}$$

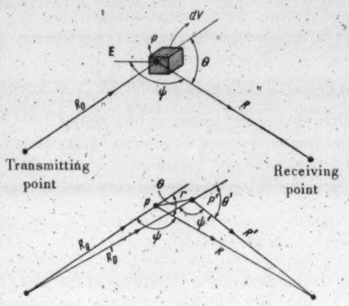

FIG. 1. The geometry underlying the calculation of the scattering cross section.

When (3) is substituted in (1) we find that the integrand in (1) decreases rapidly, so that the integral is effectively contained within distances r amounting to a few lengths ξ. Therefore, since R and R_0 are usually considerably greater than ξ, it can be assumed that the factor

$$E_0 E_0' \sin\psi \sin\psi' / RR' \approx E_0^2 \sin^2\psi / R^2$$

in the integrand is almost unchanged within a radius of a few ξ, so that it can be removed from under the integral sign, after which the limits of integration can be extended to infinity. The calculation of the effective part of the energy P_r [the real part of (1)] at the receiving point gives after a few transformations

$$P_r = \frac{c\sqrt{\varepsilon}}{4\pi R^2}\left(\frac{E_0^2\, k_0^4 \sin^2\psi}{4\pi}\right)^2 \frac{V\overline{\Delta\varepsilon^2}}{2k_0 \sin(\theta/2)} \int_0^\infty e^{-r^2/\xi^2} r \sin\left(2k \sin\frac{\theta}{2}\right) r\, dr. \tag{4}$$

If we now introduce the scattering cross section of the medium, defined as the ratio of the energy P_s scattered by unit volume into unit solid angle to the energy p_0 of the incident wave, i.e., assuming

$$P_s / p_0 = \sigma, \tag{5}$$

with

$$p_0 = c\sqrt{\varepsilon}\, E_0^2/4\pi, \quad P_r = R^{-2}\int P_s dV,$$

using for the ionosphere the formula

$$\varepsilon = 1 - 4\pi N e^2 / m\omega^2 = 1 - \omega_N^2,$$

and assuming $\overline{(\Delta N/N)^2} = (\delta N)^2$, we obtain from (4)*

$$\sigma = (\delta N)^2 \left(\frac{\omega_N}{\omega}\right)^4 \frac{\sqrt{\pi}}{8\lambda}\left(\frac{2\pi\xi}{\lambda}\right)^3 \sin^2\psi \exp\left\{-\left(\frac{2\pi\xi}{\lambda}\sin\frac{\theta}{2}\right)^2\right\}. \tag{6}$$

We must point out here that the deduction of (6) is evidently based on the assumption that all of the physical characteristics of the problem are contained in σ. Therefore, when the autocorrelation function is known from experiment and a rigorous solution based on the actual mechanism has not been obtained, the accuracy of the calculation of the scattered energy depends on the accuracy of the approximation for the autocorrelation coefficient.

An examination of (6) shows that when $\xi/\lambda \gtrsim 1$ energy is scattered predominantly at the angle given by

$$\sin(\theta/2) \sim \lambda/2\pi\xi. \tag{7}$$

Thus when forward-scattered waves, for which $\theta \sim 0$, can reach the receiving point the field energy at the point of reception is determined mainly by scattering from the largest inhomogeneities in the medium, in which case the smallest possible value of the angular range is obtained. In lateral scattering, when waves can be received only in a definite given direction θ the optimum size of the inhomogeneities, scattering from which provides the largest part of the received energy, is determined by the equation $d\sigma/d\xi = 0$, which gives

---

Equation (6) differs from the corresponding formula derived by Pekeris,[3] which was subsequently used by Booker and Gordon[4] because in these two references $\rho(r) \sim e^{-r/\xi}$ (see also footnote marked on page 174).

$$\xi_m = (\sqrt{3}/2\sqrt{2}\,\pi)\,\lambda/\sin(\theta/2). \tag{7a}$$

Furthermore, if we remember that the fluctuations of electron density ΔN must increase with N so that δN^2 does not vary much as N changes, we obtain $\sigma \sim \omega_N^4 \sim N^2$. Therefore if the range of sizes of inhomogeneities is identical in different ionospheric regions the scattered energy increases in proportion to N^2.

We shall now for two kinds of experiments consider what possibilities exist for determining the parameters of the ionosphere from measurements of the energy in scattered waves.

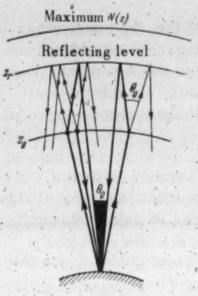

FIG. 2. The geometry for the calculation of the energy scattered during vertical sounding of the ionosphere.

(b) Vertical Sounding of The Ionosphere

We shall assume as a basic fact that in vertical sounding of a "calm ionosphere"[1] the angular spread of the received waves is narrow. The calculations are considerably simplified as a result. Indeed, an element of the scattering volume can be taken to be $dV \approx \pi(z\theta_0/2)^2dz$ so that the received energy at the observation point is

$$P_r = \int_V p_0\sigma dV = \frac{\pi\theta_0^2}{4}\int_{z_0}^{z_r} p_0\sigma z^2dz \approx \sum a_s^2; \tag{8}$$

where z_0 and z_r are, respectively, the heights of the beginning of the layer and the point of wave reflection with $\epsilon = 0$ ($\omega_N^2 = 1$) (Fig. 2). If the dependence of the electron concentration is given by a parabolic curve, which is often in good agreement with experiment especially for a "quiet ionosphere," we have

$$N(z) \sim \frac{\omega_N^2}{\omega^2} = \frac{\omega_c^2}{\omega^2}\left[1 - \left(\frac{z_m + z_0 - z}{z_m}\right)^2\right], \tag{9}$$

$$z_r = z_0[1 + \alpha(1 - m_0)], \quad \alpha = z_m/z_0, \quad m_0 = \sqrt{1 - (\omega/\omega_c)^2} = \sqrt{1 - (\lambda_c/\lambda)^2},$$

where z_m is the half-thickness of the parabolic layer and ω_c is its critical frequency.

We now assume on the basis of the foregoing considerations that $\theta_0 \sim \lambda/2\pi\xi$ [see (7)], that is, we shall take into account only a forward beam, since $\xi_0 \gg \lambda$. If θ_0 is almost constant over the entire path of the wave the exponential term in (6)* is everywhere of the order e^{-1}. Furthermore, since damping is neglected here, $p_0 = P_t/4\pi z^2$ (P_t is the radiating power of the source) and the energy of a specularly reflected wave is given by $a_0^2 = P_t/16\pi z_r^2$. We have finally

$$\frac{\Sigma a_s^2}{a_0^2} = (\beta_0^2)^{-1} = \frac{\pi\sqrt{\pi}}{4e}\,\frac{\lambda^2\xi_0}{\lambda_c^4}(\alpha + 1 - m_0)^2 \int_{z_0}^{z_0[1+\alpha(1-m_0)]} (\delta N)^2\left[1 - \left(\frac{z_m + z_0 - z}{z_m}\right)^2\right]^2 \frac{dz}{z^2} \tag{10}$$

or after calculations in which $(\delta N)^2$ is taken outside of the integral sign we obtain

$$(\delta N)^2 = \frac{4e}{\pi\sqrt{\pi}}\,\frac{\lambda_c^4}{\xi_0 z_m \lambda^2(\alpha + 1 - m_0)^2\,\beta_0^2 M(\alpha, m_0)}, \tag{11}$$

where†

$$M = \frac{1 - m_0}{\alpha + 1 - m_0}\Big\{4\alpha(\alpha + 1)(\alpha + 2) + 2(1 - m_0)(\alpha + 1)(\alpha + 2)$$
$$- \frac{2}{3}(1 - m_0)^2(\alpha + 3) + \frac{(1 - m_0)^3}{3}\Big\} - 4\alpha(\alpha + 1)(\alpha + 2)\ln\left(1 + \frac{1 - m_0}{\alpha}\right). \tag{12}$$

Thus when the values of the parameters in (11) are known it is possible to determine experimentally the fluctuations of electron density in the reflecting region of the ionosphere. Since (10) depends principally on the upper limit of z_r, δN frequently characterizes a region of relatively small thickness Δz adjacent to the point z_r.

It must be kept in mind that here as throughout this paper the dependence of wavelength on height is not taken into account. This will be done in a separate paper.

---

*For waves scattered backward we obtain under actual conditions $\sim e^{-40} - e^{-50}$, that is, negligibly small values of P_r.

†We note that for real ionospheric parameters (12) is the difference between two approximately equal quantities, so that the numerical work must be very accurate.

(c) Oblique Propagation

When scattered waves are received at the angle θ to the incident wave at frequencies for which the ionosphere is transparent, and especially at very high frequencies, the energy P_r at the observation point is calculated as follows. In such experiments directional antennas are usually employed. When the receiving and transmitting antennas have identical directional characteristics $f(\alpha, \gamma)$ (where α and γ are angles measured in the vertical and horizontal planes, respectively) and their maxima are in the direction of the midpoint of the scattering region (Fig. 3), the received energy P_r scattered by an elementary volume dV is

$$\Delta P_r = \sigma p_0 \Delta\Omega_r dV = \sigma \left\{ \frac{P_t g_0 |f(\alpha, \gamma)|^2}{4\pi R_0^2} \right\} \frac{A_0'}{R^2}\, dV, \tag{13}$$

where $\Delta\Omega_r\ A_0'/R^2$ is the solid angle of reception of the antenna, $A_0 = \lambda^2 g_0/4\pi$ is the cross section, $g_0 = 4\pi/\int |f|(\alpha, \gamma)|^2 d\Omega$ is its maximum gain and

$$p_0 = P_t g_0 |f(\alpha,\gamma)|^2 / 4\pi R_0^2.$$

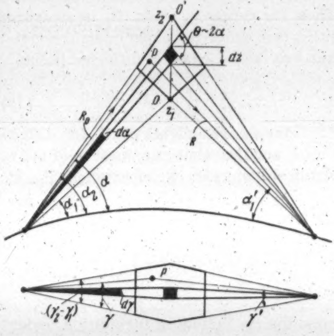

FIG. 3. The geometry for the calculation of the energy scattered in oblique propagation.

Integrating over the entire volume (over the angles α and γ of the transmitting point and the angles α' and γ' of the receiving point) we obtain

$$\frac{P_r}{P_t} = \frac{g_0^2 \lambda^2}{(4\pi)^2} \iiint\limits_{\alpha\ \gamma\ R} \frac{\sigma |f(\alpha, \gamma)|^2 |f(\alpha', \gamma')|^2}{R_0^2 R^2}\, dV. \tag{14}$$

It can easily be seen that (14) is a generalization of the so-called radar formula. Equation (14) can be integrated only under certain simplifications which in practice, however, satisfy the accuracy requirements of such experiments.

It is customary in such calculations to move the antenna directivity functions outside of the integral sign and, depending on their location with respect to the scattering region g_0, to replace them with the effective antenna gain $g = 4\pi A/\lambda^2$ (or effective area A) which is calculated for a given antenna. Also, when the angles of radiation of the antennas are small the integrand is determined principally by the dependence of all quantities on z, so that in the integrand we can write the values of θ, R_0 and R along the line 00′, which is the axis of symmetry of the scattering volume, we can assume that

$$dV = \frac{R_0 d\alpha}{\sin(\theta_0/2)} R_0 \cos\alpha\, d\gamma\, \frac{dz}{2}, \quad R_0 \sim R = \frac{z}{\sin(\theta/2)}$$

and take $\theta_0/2 \sim \alpha$ (neglecting the spherical shape of the earth). As a result, instead of (14) we obtain

$$\frac{P_r}{P_t} = \frac{g^2\lambda^2}{(4\pi)^2} \int_{\gamma_1}^{\gamma_2}\int_{\alpha_1}^{\alpha_2}\int_{z_1}^{z_2} \frac{\sigma(z, \alpha)}{z^2} \sin\alpha \cos\alpha\, d\alpha\, d\gamma\, dz \tag{15}$$

or

$$\frac{P_r}{P_t} = \frac{g^2\lambda^2}{2(4\pi)^2} (\gamma_2 - \gamma_1) \int_{\alpha_1}^{\alpha_2} \exp\left\{-\left(\frac{2\pi\xi}{\lambda}\right)^2 \sin^2\alpha\right\} d\sin^2\alpha \int_{z_1}^{z_2} \frac{\sigma(z)}{z^2}\, dz, \tag{16}$$

where γ_1, γ_2, α_1, α_2 characterize the angular direction of the effective radiation patterns of antennas that radiate into the scattering region and

$$\sigma(z) = (\delta N)^2 (\omega_N/\omega)^4 (\sqrt{\pi}/8\lambda)(2\pi\xi/\lambda)^3.$$

It is easily seen that the integral over z in (16) can be expressed through the integral in (10) which was calculated above. Therefore, assuming that $z_1 \leq z_0$ and $z_2 \geq z_0 + 2z_m$, we have

$$\frac{P_r}{P_t} = \frac{g^2}{2^7\sqrt{\pi}} \left(\frac{\omega_c^4}{\omega}\right) \frac{\xi(\gamma_2 - \gamma_1)}{z_m} (\delta N)^2 M(\alpha, m_0) \left\{\exp\left\{-\left(\frac{2\pi\xi \sin\alpha_1}{\lambda}\right)^2\right\} - \exp\left\{-\left(\frac{2\pi\xi \sin\alpha_2}{\lambda}\right)^2\right\}\right\}. \tag{17}$$

We note that in the calculation of (16) it was assumed that ξ/λ is independent of z.

The derivation of (17) is based on the inherent assumption that the region which is irradiated by the antennas is quite extensive in height and that the waves scattered by the region as a whole make a considerable contribution to the field at the receiving point. Such conditions regarding the magnitude of $z_2 - z_1$ are realized, for example, in connection with short waves. But is not known whether the entire ionosphere then participates in the scattering. For a number of reasons it can be assumed that this is not the case, and the energy can be calculated more simply by taking the effective scattering region to be very thin. Such conditions are undoubtedly realized in the case of very short waves. The solid angles of radiation of the antennas used in these experiments are indeed very small, as are the dimensions of V, so that we can take $\sigma \sim$ const, $R_0 \sim R$ and then write (see Fig. 4)

$$V = \frac{R_0^2 \Delta\Omega}{\sin(\theta/2)} \Delta z = \frac{R^2 \lambda^2 \Delta z}{A \sin(\theta/2)},$$

which by utilizing (14) gives

$$\frac{P_r}{P_t} = (\delta N)^2 \frac{\sqrt{\pi}}{8\lambda} \left(\frac{\omega_N}{\omega}\right)^4 \left(\frac{2\pi\xi}{\lambda}\right)^3 \frac{A \Delta z}{R_0^2 \sin(\theta/2)} \exp\left\{-\left(\frac{2\pi\xi}{\lambda} \sin\frac{\theta}{2}\right)^2\right\}. \tag{18}$$

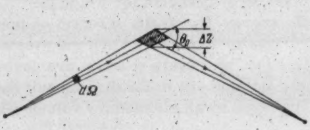

FIG. 4. The geometry underlying energy calculations at ultra high frequencies.

It is easily seen that (18) enables us to determine δN and ξ. Thus, for example, when P_r is measured at different distances and fixed frequencies subject to the assumption that under the experimental conditions $(\delta N)^2$, (ω_N/ω) and ξ remain unchanged, we obtain for the ratio of the energies at different points

$$\frac{(P_r)_2}{(P_r)_1} = \frac{R_1^2}{R_2^2} \frac{\sin(\theta_1/2)}{\sin(\theta_2/2)} \exp\left\{-k^2\xi^2\left(\sin^2\frac{\theta_2}{2} - \sin^2\frac{\theta_1}{2}\right)\right\}, \tag{19}$$

in which only ξ is unknown. It is similarly possible to determine ξ from measurements of P for different frequencies at a single point. Furthermore, from a knowledge of ξ and the other parameters of the ionosphere which characterize the experiments $(\delta N)^2$ can be determined from (18) by measuring P_r at different distances and frequencies.

A corresponding analysis of the experimental results is given below.

3. ANALYSIS OF THE EXPERIMENTAL RESULTS. VALUES OF δN AND ξ

(a) Vertical Sounding of the Ionosphere

The method described in Refs. 1 and 6 has been used to determine the coefficient of turbidity β under various conditions. A complete analysis of the data would proceed as follows. For each value of β_s, δN_s must be calculated from (11), using in each instance the individual values of z_0, z_m, ω, ω_c and ξ_s. It is thus possible to obtain distribution curves and the dependence of δN on height and to investigate their variation under different conditions. Such a detailed treatment of the experimental results will be the subject of a special paper. Here we are primarily interested in determining δN from the measurements of β. For this purpose we shall make use of the theoretical curves of $\{\beta_0^2 (\delta N)^2\}$ (Figs. 5, 6) which were calculated according to (11) and (12) for a number of characteristic parameters of the different ionospheric regions, and we shall also use all of the measurements of β (Fig. 7).

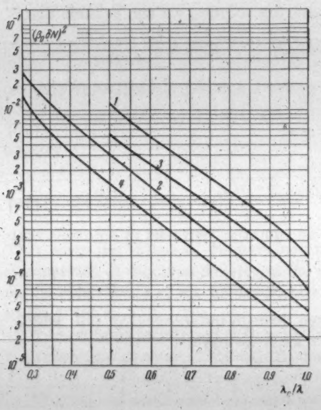

FIG. 5. Theoretical dependence of $(\beta_0 \delta N)^2$ on λ_c/λ for the F layer of the ionosphere with $\xi_0 = 200$ m and $z_0 = 250$ km. Curves 1 and 2 correspond to $z_m = 100$ km and $\lambda_c = 50$ m and 25 m; curves 3 and 4 correspond to $z_m = 200$ km and the same values of λ_c.

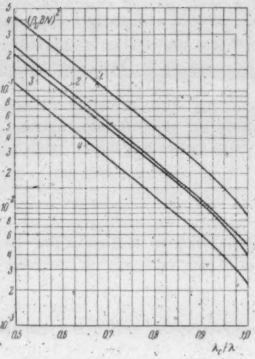

FIG. 6. Theoretical dependence of $(\beta_0\,\delta N)^2$ on λ_c/λ for the E layer of the ionosphere with $\xi_0 = 200$ m and $z_0 = 110$ km. Curves 1 and 2 correspond to $z_m = 10$ km and $\lambda_c = 100$ m and 75 m; curves 3 and 4 correspond to $z_m = 20$ km and the same values of λ_c.

The distribution curve of β in Fig. 7 was plotted from extensive diurnal and seasonal measurements for the F_2 region of the ionosphere ($z \sim 250 - 400$ km). These data correspond mainly to conditions under which ω was $(0.8 - 0.9)\ \omega_c$ and doublets of magnetically split signals were observed, so that the experimental results were of the required clarity. Fig. 7 shows that most frequency $\beta_0 \sim 2 - 4$ so that, taking $\xi \approx 300$ m, we obtain from the curves of Fig. 5

$$\delta N \sim (0.3 - 1)\cdot 10^{-2} \tag{20}$$

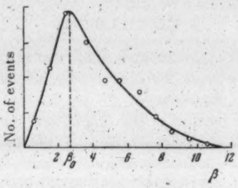

FIG. 7. Distribution of values of the turbidity coefficient β.

and similarly for the E region ($z \sim 100 - 130$ km)

$$\delta N \sim (1 \div 4)\cdot 10^{-2}. \tag{20'}$$

(b) Measurements at Very High Frequencies

The experimental results at very high frequencies are collected in Table 1. The measurements were made at noon when the "ionospheric" field component due to scattering clearly exceeds the "meteoric" component.

From the tabulated data we obtain by means of (19)

$$\xi = 6.2 \text{ m};\ \ 6.9 \text{ m};\ \ 8.0 \text{ m};\ \ 4.8 \text{ m};\ \ 5.6 \text{ m}. \tag{21}$$

The theoretical optimum values of ξ_m are [see (7a)]

$$\xi_m = 10 \text{ m};\ \ 5.8 \text{ m};\ \ 2.7 \text{ m}. \tag{22}$$

Thus from experiment and calculation we obtain as an average

$$\xi \approx 6 \text{ m}. \tag{23}$$

TABLE I. Measurements at various frequencies f and distances d.

	$f = 49.8$ Mc (Fig. 16 of Ref. 7)	
$d_1 = 491$ km	$\theta_{1/2} = 19°$	$(P_r)_3 : (P_r)_1 = 4.8$ and 7.6
$d_2 = 592$ "	$\theta_{2/2} = 16.4°$	$(P_r)_3 : (P_r)_2 = 5.3$
$d_3 = 811$ "	$\theta_{3/2} = 13°$	
	$d = 1243$ km (Fig. 19 of Ref. 7)	
$f_1 = 27.775$ Mc	$\lambda_1 = 10.8$ m	$(P_r)_1 : (P_r)_2 = 69.(50)$
$f_2 - 49.8$ "	$\lambda_2 = 6$ m	$(P_r)_2 : (P_r)_3 = 1580.(2240)$
$f_3 = 107.8$ "	$\lambda_3 = 2.78$ m	
	$d = 1243$ km (Figs. 8, 9 of Ref. 7)	
$f_1 = 27.775$ Mc	$E = 28$ db (34.5 db)	$(P_r)_1 = 2.7 \times 10^{-13}$ w
$f_2 = 49.8$ "	$E = 17$ " (16 ")	$(P_r)_2 = 2.1 \times 10^{-14}$ "
$f_3 = 107.8$ "	$E - 7$ " (-12.15 ")	$(P_r)_3 = 2.1 \times 10^{-16}$ "

(In db above 1 μV; 1 μV corresponds to 4.2×10^{-16} w).

Since the scattering of very short waves during the day takes place at $z \approx 80$ km,[8] our results suggest the presence at this level of inhomogeneous blobs of electrons a few meters in extent, which are able to scatter such wavelengths. If it is assumed, furthermore, on the basis of various experimental findings, that at this altitude $N \approx 5 \times 10^2$ and we select $\Delta z \approx 10$ km, it follows directly from Table 1 [see (18)] that

$$\delta N \sim (0.1 \div 1.3)\cdot 10^{-2}, \tag{24}$$

which is close to the values calculated above for the highest altitudes.

These results are evidently in agreement with the foregoing hypothesis that the principal factor which affects scattering is the size of the inhomogeneities and that a wave "selects" a region containing the optimum size. This may furnish an explanation of the fact that in the experiments with very short waves scattering occurred in a lower part of the ionosphere rather than at $100 - 110$ km, to which height most of the energy was radiated.

If this explanation is not accepted and, as in Ref. 9, we take $\xi \approx 200$ m, we must still account for the fact mentioned above and also explain why very short waves are not scattered mainly at still higher altitudes where the inhomogeneity size is $\xi \sim 200-300$ m with the electron concentration increasing by a factor of about 10^3, so that the scattered energy should increase by 10^6.*

For the purpose of clearing up these questions it would be particularly interesting to perform similar investigations with short waves, accompanied by measurements of the scattering altitude and by altitude sounding of the ionosphere in a range including low frequencies and providing the needed information concerning N(z). Such complete experiments could, in particular, furnish very important information concerning the relation between inhomogeneity size and altitude.

4. CONCLUSIONS

It is well to take note of a number of relationships observed in the present work as well as of previously known facts which can be of importance for theoretical investigations of the mechanisms involved in the statistical inhomogeneities of the ionosphere.

First, it is well known that from the bottom of the ionosphere ($z \sim 80$ km) to the height of maximum ionization ($z \sim 350-400$ km) the electron concentration N changes by a factor of 10^3-10^4, and that the density of neutral particles and the corresponding mean free path changes by 10^5-10^6, while the temperature changes by a factor of 7 to 8. Also, according to the data obtained here the fluctuations of the electron density δN as well as the known values of inhomogeneity size ξ_0 and random velocity v_0 evidently change very little with height.† This is a striking fact which at first glance seems incomprehensible.

Secondly, in vertical sounding of the ionosphere, when the transmitting and receiving points coincide, most of the received field must result from scattering by the largest inhomogeneities. Therefore the most frequent experimental values $\xi \sim 200-300$ m for heights of $100-300$ km and higher must be characteristic of the largest inhomogeneities. In addition, estimates of the sizes of small-scale eddies, plasma wavelengths, and the mean free path lead to the conclusion that inhomogeneity sizes of $200-300$ m would be "forbidden" above $200-250$ km, which is also unexpected and difficult to understand.

Further, the velocity u_0 of horizontal drift in the ionosphere between $z \sim 80-130$ km and $z \sim 300$ km evidently changes from $u_0 \sim 70$ m/sec to ~ 100 m/sec. The velocity gradients du_0/dz at these altitudes are, respectively, about + 3.4 m/sec per km and + 1 m/sec per km, and if their values were of the same order of magnitude over the entire range of heights, then at $z \sim 300$ km u_0 would be $400-500$ m/sec or greater, which does not correspond to reality. It is thus suggested that the velocity gradient has the indicated values only in limited altitude ranges, i.e., there are very narrow local regions with active wind development and large gradients together with extensive relatively windless regions, or that the sign of du_0/dz changes with altitude. If such conditions exist in the ionosphere the retardation at the "walls" of these regions could under certain circumstances result in turbulent streams of particles.

If thus appears that at the present time the picture of these effects is complicated and obscure. We still have no theoretical basis for a profound analysis using definite mechanisms. Since, however, there exists a certain tendency, just as in the case of other similar phenomena, to ascribe these effects to turbulence, we shall briefly summarize estimates based on formulas derived in the theory of turbulence from similarity considerations.[12]

It must first of all be understood that the utilization of formulas from the theory of turbulence for the purpose of calculating the properties of inhomogeneous blobs of electrons is in itself not legitimate. These formulas were derived for media consisting of neutral particles so that without a special analysis they can certainly not be applied, especially to calculations for a highly rarefied plasma. This problem can only be solved by a study of electron motion in a turbulent flow; thus far this has not been done.

---

*We note here that in Refs. 9 and 10, in addition to the unjustified choice $\xi \sim 200$ m, values of $N \sim 2-5 \times 10^4$ are used, which correspond to the electron concentration of the E or sporadic E layer, although the experiments themselves yield values of Z below the heights of E and E_{sporadic}. It is also appropriate to point out that when ξ is determined from the experimental data by the method described in this section and the Booker-Gordon formula[4], imaginary values of ξ are obtained. We recall also that the formula for the autocorrelation coefficient $\rho(r) \sim e^{-r/\xi}$ which is the basis for the deduction of σ in Refs. 3 and 4 is known to lead to fundamental contradictions because of the finite value of the derivative $d\rho/dr$ at $r = 0$, with a corresponding discontinuity of the dielectric constant at this point.

†It must be remembered that in all of the papers in which ξ_0, v_0, and β_0 were determined the altitude dependence of wavelength in the ionosphere was not taken into account. A proper review of these values would require some modification of the familiar methods of determining these quantities. It is not known what changes would result. The auther is now investigating these questions.

It is known that the microscale L_s and velocity change Δu_s of eddies are given by

$$L_s \approx L_0/\mathrm{Re}^{-3/4}, \quad \Delta u_s \approx \Delta u_0/\mathrm{Re}^{-1/4}, \tag{25}$$

where $\mathrm{Re} = \Delta u_0 L_0/\nu$ is the Reynolds number, L_0 is the thickness and Δu_0 is the change in laminar velocity of the turbulent flow, and ν is the kinematic viscosity.

We can also add the formula

$$\overline{(\delta N_s)^2} \approx \Delta u_s^4 / \overline{v_m^2}^2, \tag{26}$$

which is obtained for homogeneous isotropic turbulent flow based on

$$\Delta p_s \approx \rho (\Delta u_s)^2, \tag{27}$$

where Δp_s represents the pressure fluctuation of the inhomogeneities, ρ is the density of the medium and v_m^2 is the root mean square particle velocity; it is assumed that $\Delta p_s/p \sim \Delta\rho_s/\rho \sim \Delta N_s/N = \delta N_s$.

We now assume that L_0 is commensurate with the thicknesses of the layers and that Δu_0 has two possible values: the first of these values corresponds to the velocity u_0 of horizontal drift, and the second to the assumed change in u_0 given by $\Delta u_0 = (du_0/dz)\Delta z$. Then from (25) and (26) there are obtained the values of L_s, Δu_s and δN_s listed in Table 2.

Table 2 shows, first, that the Reynolds number is generally quite large; this is usually a criterion of turbulence. But it is not known whether this criterion is valid for the ionosphere and what is "large" in this instance. It is therefore hardly possible to draw any conclusions from these values.

Secondly, up to the height $z \approx 200$ km the values of L_s and Δu_s corresponding to the minimum (!) size of small-scale inhomogeneities are close to the experimental values of ξ_0 and v_0, but at greater heights there is strong divergence.

TABLE II

$z_{км}$	$\sqrt{\overline{u_m^2}}$, m/sec	L_0, км	Δu_0, m/sec	Re	Δu_s, m/sec	L_s, m	$\delta N_s \cdot 10^4$
80	400	5	70	$4 \cdot 10^5$	3.5	4	6
	400	5	18	$2 \cdot 10^3$	2.6	15	0.8
100	400	5	70	$2 \cdot 10^4$	7	5	3
	400	5	18	10^2	5	140	4
200	1000	30	100	50—400	60	160—1600	3
	1000	30	30	15	15	$4 \cdot 10^3$	2
300	1300	100	200	10—80	70—100	$(4\text{—}18) \cdot 10^3$	40
	1300	100	100	5	70	$30 \cdot 10^3$	90

And, finally, the electron density fluctuations $(\delta N_s)^2$ are everywhere approximately $10^3 - 10^4$ times smaller than the experimental values obtained above. If, however, it is assumed that the change of electron density $|\Delta N_s| \sim |dN/dz| L_s$, thus resulting from the altitude gradient of the electron density, there is obtained for all heights

$$(\delta N)_s \equiv |\Delta N_s| / N \sim (1 \div 3)\, 10^{-3},$$

which is in close agreement with the results obtained above.

It must again be emphasized that although estimates of the ionospheric parameters based on turbulence concepts are in some instances consistent with other data, any conclusions based on this fact would be premature.

---

[1] Ia. L. Al'pert, Usp. fiz. nauk **49**, 49 (1953).

[2] I. A. Ratcliffe, Reports on Progress in Physics **19**, 188 (1956).

[3] C. L. Pekeris, Phys. Rev. **71**, 268 (1947).

[4] H. G. Booker and W. E. Gordon, Proc, Inst. Radio Engrs. **38**, 401 (1950).

[5] Booker, Ratcliffe, and Shinn, Trans. Roy. Soc. (London) **242**, 579 (1950).

[6] Ia. L. Al'pert and A. A. Ainberg, J. Exptl. Theoret. Phys. (U.S.S.R.) **21**, 389 (1951).

[7] Bailey, Bateman, and Kirby, Proc. Inst. Radio Engrs **43**, 1181 (1955).

[8] V. C. Pineo, J. Geophys. Res. **61**, 165 (1956).

[9] D. K. Bailey et al., Phys. Rev. **86**, 141 (1952).

[10] F. Villars and V. F. Weisskopf, Phys. Rev. **94**, 232 (1954); Proc. Inst. Radio Engrs **43**, 1232 (1955).

[11] Ia. L. Al'pert, Проблемы современной физики, (Problems of Mod. Phys.) **7**, 5 (1955).

[12] L. D. Landau and E. M. Lifshitz, Механика сплошных сред, (Mechanics of Continous Media) (GTTI, 1954).

Translated by I. Emin

SOVIET PHYSICS JETP VOLUME 6, NUMBER 1 JANUARY, 1958

FINE STRUCTURE IN THE ALPHA DECAY OF ODD NUCLEI

V. G. NOSOV

Submitted to JETP editor January 23, 1957

J. Exptl. Theoret. Phys. (U.S.S.R.) 33, 226-231 (July, 1957)

The excitation of rotational levels in the α-decay of non-spherical odd nuclei is considered.

As is well known, every odd nucleus is characterized by an angular momentum number K that is different from zero. For this reason the system formed upon α-decay of a nucleus — the daughter nucleus plus an α-particle — is characterized not only by the total energy of decay, E, but also by the total angular momentum, **K**, and its projection on a fixed axis, K_z. On the other hand, the spectrum of emitted particles cannot depend on the orientation of the total system in space. For this reason, without loss of generality, we can set $K_z = K$. Thus we obtain for the wave function of the daughter nucleus plus α-particle system the following equations:

$$\nabla^2\Psi - \frac{m}{I}[\mathbf{j}^2 - \Lambda(\Lambda+1)]\Psi + \frac{2m}{\hbar^2}(E-U)\Psi = 0, \quad \mathbf{K}^2\Psi = K(K+1)\Psi; \quad K_z\Psi = K\Psi. \tag{1}$$

Here $\mathbf{j}$ is the operator for the angular momentum of the daughter nucleus, Λ is the projection of the angular momentum of the daughter nucleus on its axis of symmetry, I is the moment of inertia of the nucleus, m is the reduced mass, and U is the potential energy of the electrostatic interaction of the α-particle with the nucleus. The angular momentum of the daughter nucleus can be expressed in terms of the total angular momentum **K** and the orbital angular momentum of the α-particle, **l**, through the equation:

$$\mathbf{j}^2 = (\mathbf{K} - \mathbf{l})^2 = \mathbf{K}^2 - 2\mathbf{lK} + \mathbf{l}^2.$$

It is convenient to solve Eq. (1) in a system of coordinates rotating with the nucleus. Introducing into this system the spherical coordinates of the α-particle, namely r, $\mu = \cos\vartheta$, and φ, and likewise the Euler angles $\nu = \cos\theta$, and ϕ, which determine the orientation of the rotating axes relative to the stationary ones, we obtain the following expressions for the momentum operators that interest us:[1]

$$\begin{gathered}\mathbf{K}^2 = -\frac{\partial}{\partial\nu}\left[(1-\nu^2)\frac{\partial}{\partial\nu}\right] - \frac{1}{1-\nu^2}\frac{\partial^2}{\partial\phi^2} + \frac{2i\nu}{1-\nu^2}\left(\Lambda - i\frac{\partial}{\partial\varphi}\right)\frac{\partial}{\partial\phi} + \frac{1}{1-\nu^2}\left(\Lambda - i\frac{\partial}{\partial\varphi}\right)^2; \\ \mathbf{lK} = \sqrt{1-\nu^2}\,\frac{\partial}{\partial\nu}\left(\sqrt{1-\mu^2}\sin\varphi\cdot\frac{\partial}{\partial\mu} - \frac{\mu}{\sqrt{1-\mu^2}}\cos\varphi\cdot\frac{\partial}{\partial\varphi}\right) + \frac{1}{\sqrt{1-\nu^2}}\frac{\partial}{\partial\phi}\left(\sqrt{1-\mu^2}\cos\varphi\cdot\frac{\partial}{\partial\mu} + \frac{\mu}{\sqrt{1-\mu^2}}\sin\varphi\cdot\frac{\partial}{\partial\varphi}\right) \\ - \frac{i\nu}{\sqrt{1-\nu^2}}\left(\sqrt{1-\mu^2}\cos\varphi\cdot\frac{\partial}{\partial\mu} + \frac{\mu}{\sqrt{1-\mu^2}}\sin\varphi\cdot\frac{\partial}{\partial\varphi}\right)\left(\Lambda - i\frac{\partial}{\partial\varphi}\right) - i\frac{\partial}{\partial\varphi}\left(\Lambda - i\frac{\partial}{\partial\varphi}\right); \\ \mathbf{l}^2 = -\frac{\partial}{\partial\mu}\left[(1-\mu^2)\frac{\partial}{\partial\mu}\right] - \frac{1}{1-\mu^2}\frac{\partial^2}{\partial\varphi_2}; \quad K_z = -i\frac{\partial}{\partial\phi}.\end{gathered} \tag{2}$$

We will look for a particular solution to (1) which, at large distances, describes an α-particle with momentum $\boldsymbol{\ell}$, leaving the nucleus, and a daughter nucleus in an angular momentum state j. This has the form

$$\Psi_{jl}(r, \mu, \varphi, \nu, \phi) = N_{jl}^{-1/2} e^{iK\phi} Y_{jl}(\nu, \mu, \varphi) e^{\sigma(r, \mu, \varphi, \nu)}. \tag{3}$$

The factor $e^{iK\phi}Y_{j\ell}$ represents the angular part of the wave function and, therefore, satisfies the equations

$$\mathbf{K}^2 e^{iK\phi}Y_{jl} = K(K+1)e^{ik\phi}Y_{jl}, \quad \mathbf{l}^2 Y_{jl} = l(l+1)Y_{jl}, \quad \mathbf{lK}e^{iK\phi}Y_{jl} = \frac{1}{2}[K(K+1) - j(j+1) + l(l+1)]e^{iK\phi}Y_{jl} \tag{4}$$

The solutions of equation (4) have the form

$$\begin{gathered}Y_{jl}(\nu, \mu, \varphi) = \sum_m A_m^{jl}(1+\nu)^{(K+\Lambda+m)/2}(1-\nu)^{(K-\Lambda-m)/2} p_l^m(\mu)e^{im\varphi}, \quad p_l^m(\mu) = \sqrt{\frac{(l-m)!}{(l+m)!}}P_l^m(\mu); \\ P_l^m(\mu) = \frac{(1-\mu^2)^{m/2}}{2^l l!}\frac{d^{l+m}(\mu^2-1)^l}{d\mu^{l+m}}.\end{gathered} \tag{5}$$

The constants $A_m^{j\ell}$ are determined from the recursion relations

$$\begin{gathered}i(K-\Lambda-m+1)\sqrt{(l+m)(l-m+1)}A_{m-1}^{jl} - [K(K+1) - j(j+1) + l(l+1) - 2m(\Lambda+m)]A_m^{jl} \\ - i(K+\Lambda+m+1)\sqrt{(l-m)(l+m+1)}A_{m+1}^{jl} = 0.\end{gathered} \tag{6}$$

The normalization for the angular functions

$$N_{jl} = \int |Y_{jl}(\nu, \mu, \varphi)|^2 d\nu \, d\mu \, d\varphi = \frac{2^{2K+1}}{(2K+1)!} \frac{4\pi}{2l+1} \sum_m (K+\Lambda+m)!\,(K-\Lambda-m)!\; |A_m^{jl}|^2 \tag{7}$$

is introduced into Eq. (3) for convenience.

It is reasonable that σ should not depend on the angular variables μ, φ, ν at large r. Substituting (3) in the first of the equations (1), and taking into consideration (2) and (4), we get

$$\begin{aligned} & Y_{jl}\left[\left(\frac{\partial\sigma}{\partial r}\right)^2 + \frac{\partial^2\sigma}{\partial r^2} + \frac{2}{r}\frac{\partial\sigma}{\partial r}\right] + \left(\frac{m}{I} + \frac{1}{r^2}\right)\Big\{(1-\mu^2)\Big|\Big\{Y_{jl}\left[\left(\frac{\partial\sigma}{\partial\mu}\right)^2 + \frac{\partial^2\sigma}{\partial\mu^2}\right] + 2\frac{\partial Y_{jl}}{\partial\mu}\frac{\partial\sigma}{\partial\mu}\Big\} - 2\mu Y_{jl}\frac{\partial\sigma}{\partial\mu} \\ & + \frac{1}{1-\mu^2}\Big\{Y_{jl}\left[\left(\frac{\partial\sigma}{\partial\varphi}\right)^2 + \frac{\partial^2\sigma}{\partial\varphi^2}\right] + 2\frac{\partial Y_{jl}}{\partial\varphi}\frac{\partial\sigma}{\partial\varphi}\Big\}\Big\} + 2\frac{m}{I}\Big[\sqrt{1-\nu^2}\Big\{\sqrt{1-\mu^2}\sin\varphi\cdot\Big[Y_{jl}\left(\frac{\partial\sigma}{\partial\mu}\frac{\partial\sigma}{\partial\nu} + \frac{\partial^2\sigma}{\partial\mu\,\partial\nu}\right) + \frac{\partial Y_{jl}}{\partial\mu}\frac{\partial\sigma}{\partial\nu} + \frac{\partial Y_{jl}}{\partial\nu}\frac{\partial\sigma}{\partial\mu}\Big] \\ & - \frac{\mu}{\sqrt{1-\mu^2}}\cos\varphi\cdot\Big[Y_{jl}\left(\frac{\partial\sigma}{\partial\varphi}\frac{\partial\sigma}{\partial\nu} + \frac{\partial^2\sigma}{\partial\varphi\,\partial\nu}\right) + \frac{\partial Y_{jl}}{\partial\varphi}\frac{\partial\sigma}{\partial\nu} + \frac{\partial Y_{jl}}{\partial\nu}\frac{\partial\sigma}{\partial\varphi}\Big]\Big\} + \frac{iK}{\sqrt{1-\nu^2}}\Big[\sqrt{1-\mu^2}\cos\varphi\cdot Y_{jl}\frac{\partial\sigma}{\partial\mu} \\ & + \frac{\mu}{\sqrt{1-\mu^2}}\sin\varphi\cdot Y_{jl}\frac{\partial\sigma}{\partial\varphi}\Big] - \frac{\nu}{\sqrt{1-\nu^2}}\Big\{\sqrt{1-\mu^2}\cos\varphi\cdot\Big\{Y_{jl}\left[\frac{\partial\sigma}{\partial\varphi}\frac{\partial\sigma}{\partial\mu} + \frac{\partial^2\sigma}{\partial\varphi\partial\mu}\right] + \left(\frac{\partial Y_{jl}}{\partial\varphi} + i\Lambda Y_{jl}\right)\frac{\partial\sigma}{\partial\mu} + \frac{\partial Y_{jl}}{\partial\mu}\frac{\partial\sigma}{\partial\varphi}\Big\} \\ & + \frac{\mu}{\sqrt{1-\mu^2}}\sin\varphi\cdot\Big\{Y_{jl}\left[\left(\frac{\partial\sigma}{\partial\varphi}\right)^2 + \frac{\partial^2\sigma}{\partial\varphi^2}\right] + \left(2\frac{\partial Y_{jl}}{\partial\varphi} + i\Lambda Y_{jl}\right)\frac{\partial\sigma}{\partial\varphi}\Big\}\Big\} - \Big\{Y_{jl}\left[\left(\frac{\partial\sigma}{\partial\varphi}\right)^2 + \frac{\partial^2\sigma}{\partial\varphi^2}\right] + \left(2\frac{\partial Y_{jl}}{\partial\varphi} + i\Lambda Y_{jl}\right)\frac{\partial\sigma}{\partial\varphi}\Big\}\Big] \\ & + \left\{\frac{2m}{\hbar^2}(E-U) - \frac{l(l+1)}{r^2} - \frac{m}{I}[j(j+1) - \Lambda(\Lambda+1)]\right\} Y_{jl} = 0. \end{aligned} \tag{8}$$

We will express the quasi classical expansion for $\sigma(r, \mu, \varphi, \nu)$ in the form $\sigma = \sigma_{-1} + \sigma_0 + \sigma_1 + \ldots$; we then get an infinite set of equations for the successive approximations $\sigma_{-1}, \sigma_0, \sigma_1, \ldots$ The solution of these equations is made easier in the case of a slightly non-spherical daughter nucleus. In this case the equation of the surface of the nucleus is represented conveniently in the form

$$R(\mu) = R_0 + \xi(\mu) = R_0\left\{1 + \sum_n \alpha_n P_n(\mu)\right\}. \tag{9}$$

The quantities σ_{-1}, σ_0 and $\sigma_1 \ldots$ are expanded in series in powers of ξ:

$$\sigma_{-1} = \sigma_{-1}^{(0)} + \sigma_{-1}^{(1)} + \ldots; \quad \sigma_0 = \sigma_0^{(0)} + \sigma_0^{(1)} + \ldots; \quad \sigma_1 = \sigma_1^{(0)} + \sigma_1^{(1)} + \ldots$$

etc. The electrostatic potential produced by the daughter nucleus is easily calculated in terms of an analogous series. As a result we get

$$\sigma_{-1}^{(0)} = i\int_{a_{jl}}^{r} k_{jl}\,dr; \quad \sigma_0^{(0)} = -\ln(\sqrt{-ik_{jl}r}); \quad \sigma_{-1}^{(1)} = \frac{3}{2} i\varkappa_b^2 \sum_n \frac{\alpha_n}{2n+1} P_n(\mu)\int_r^{\infty}\left(\frac{R_0}{r}\right)^{n+1}\frac{dr}{k_{jl}}. \tag{10}$$

Here

$$k_{jl} = \sqrt{k_\varepsilon^2 - \varkappa_b^2 R_0/r - l(l+1)/r^2}, \quad \varkappa_b^2 = 4mZe^2/\hbar^2 R_0; \quad k_\varepsilon^2 = 2m\varepsilon/\hbar^2; \quad \varepsilon \equiv \varepsilon_j = E - (\hbar^2/2I)[j(j+1) - \Lambda(\Lambda+1)].$$

The turning point of a_{jl} is determined by the equation

$$k_{jl}^2(a_{jl}) = k_\varepsilon^2 - \varkappa_b^2 R_0/a_{jl} - l(l+1)/a_{jl}^2 = 0.$$

The formulae (10) are valid also at $r < a_{jl}$ if it is kept in mind that in this region

$$k_{jl} = i\varkappa_{jl} = i\sqrt{l(l+1)/r^2 + \varkappa_b^2 R_0/r - k_\varepsilon^2}.$$

Further terms of the double series for the function $\sigma(r, \mu, \varphi, \nu)$ are sufficiently small to be neglected.

Introducing (10) into (32) and examining the behavior as $r \to \infty$ it is seen that the corresponding flux through the closed sphere does not depend on j and l. Therefore, if we express the wave function in the form $\Psi = \sum_{jl} c_{jl}\Psi_{jl}$, then the relative probability of exciting a rotational level with angular momentum j, accompanying the emission of the α-particle with angular momentum l, is expressible as $w_{jl} = |c_{jl}|^2$, and the total probability of exciting a level with angular momentum j will be $w_{jl} = \sum_l w_{jl}$.

The coefficients c_{jl} can be expressed in terms of the values of the wave function at the surface of the nucleus $\Psi_S(\mu, \varphi, \nu, \phi)$. Thus we get, in the required approximation,

$$\begin{aligned} \sigma_{-1}^{(0)}(S) &= \sigma_{-1}^{(0)}(R_0)\big|_{j=\Lambda,\, l=0} - \varkappa_{\Lambda 0}(R_0)\,\xi + \frac{\gamma_j}{2}[j(j+1) - \Lambda(\Lambda+1)] + \frac{\gamma_l}{2} l(l+1); \\ \sigma_{-1}^{(1)}(S) &= \sigma_{-1}^{(1)}(R_0)\big|_{j=\Lambda,\, l=0}; \quad \sigma_0^{(0)}(S) = \sigma_0^{(0)}(R_0)\big|_{j=\Lambda,\, l=0}. \end{aligned} \tag{11}$$

In these equations

$$\gamma_j = 2\frac{\partial\sigma_{-1}^{(0)}}{\partial j(j+1)}(R_0)\bigg|_{j=\Lambda,\, l=0} = \frac{m}{Ik^2}\left(\frac{\varkappa_b^2 R_0}{k}\operatorname{arc\,tg}\frac{\varkappa}{k} + \varkappa R_0\right); \quad \gamma_l = 2\frac{\partial\sigma_{-1}^{(0)}}{\partial l(l+1)}(R_0)\bigg|_{j=\Lambda,\, l=0} = \frac{2\varkappa}{\varkappa_b^2 R_0},$$

$$k \equiv k_e = \sqrt{\frac{2mE}{\hbar^2}}, \qquad \varkappa \equiv \varkappa_{\Lambda 0}(R_0) = \sqrt{\varkappa_b^2 - k^2}. \tag{12}$$

Substituting (11) into (3) and keeping in mind Eq. (10) we get

$$\sqrt{\varkappa}\, R_0 \exp\{-\sigma_{-1}^{(0)}| + \varkappa\xi - \sigma_{-1}^{(1)}|\}\,\Psi_S(\mu, \varphi, \nu, \phi)$$

$$= \sum_{j,l} c_{jl} \exp\left\{\frac{\gamma_j}{2}[j(j+1) - \Lambda(\Lambda+1)] + \frac{\gamma_l}{2} l(l+1)\right\} N_{jl}^{-1/2} e^{iK\phi} Y_{jl}(\nu, \mu, \varphi). \tag{13}$$

The vertical lines to the right of quantities in the equation have the meaning that they should be taken at r = R_0, j = Λ, and ℓ = 0. As is seen, Eqs. (10), (9), (4), and (2), show that the function Ψ_S is not completely arbitrary, but satisfies the equations

$$\mathbf{K}^2\Psi_S = K(K+1)\Psi_S, \quad K_z\Psi_S = K\Psi \tag{14}$$

and therefore has the form

$$\Psi_S(\mu, \varphi, \nu, \phi) = e^{iK\phi}\psi_S(\nu, \mu, \varphi), \quad \psi_S(\nu, \mu, \varphi) = \sum_{m'} \chi_{m'}(\mu)(1+\nu)^{(K+\Lambda+m')/2}(1-\nu)^{(K-\Lambda-m')/2} e^{im'\varphi}. \tag{15}$$

This result does not depend on the approximations made, but follows strictly from Eqs. (9), (2), and the two last equations of (1). Using the orthogonality of the functions $Y_{j\ell}$, and likewise (7) and (5), and normalizing the probability by the condition $w_\Lambda = 1$, we finally obtain

$$w_j = e^{-\gamma_j[j(j+1)-\Lambda(\Lambda+1)]} \frac{\sum\limits_{l=|j-K|}^{j+K} \frac{2l+1}{S_{jl}} e^{-\gamma_l l(l+1)} \left|\int \psi_S e^{\varkappa\xi - \sigma_{-1}^{(1)}|} Y_{jl}^* \,d\nu\, d\mu\, d\varphi\right|^2}{\sum\limits_{l=|\Lambda-K|}^{\Lambda+K} \frac{2l+1}{S_{\Lambda l}} e^{-\gamma_l l(l+1)} \left|\int \psi_S e^{\varkappa\xi - \sigma_{-1}^{(1)}|} Y_{\Lambda l}^* \,d\nu\, d\mu\, d\varphi\right|^2} = e^{-\gamma_j[j(j+1)-\Lambda(\Lambda+1)]}$$

$$\times \frac{\sum\limits_{l=|j-K|}^{j+K} \frac{2l+1}{S_{jl}} e^{-\gamma_l l(l+1)} \left|\sum\limits_m A_m^{jl*}(K+\Lambda+m)!\,(K-\Lambda-m)! \int\limits_{-1}^{1} \chi_m(\mu) e^{\varkappa\xi-\sigma_{-1}^{(1)}|} P_l^m(\mu)\, d\mu\right|^2}{\sum\limits_{l=|\Lambda-}^{\Lambda+K} \frac{2l+1}{S_{\Lambda l}} e^{-\gamma_l l(l+1)} \left|\sum\limits_m A_m^{\Lambda l*}(K+\Lambda+m)!\,(K-\Lambda-m)! \int\limits_{-1}^{1} \chi_m(\mu) e^{\varkappa\xi-\sigma_{-1}^{(1)}|} P_l^m(\mu)\, d\mu\right|^2}, \tag{16}$$

where

$$S_{jl} = \sum_m (K+\Lambda+m)!\,(K-\Lambda-m)!\,|A_m^{jl}|^2.$$

Further simplifications can be made if it is assumed that, immediately after the emission of the α-particle, the direction of the axis of the daughter nucleus is the same as the direction of the axis of the mother nucleus just before the decay. The rotational wave function of the mother nucleus has the form

$$e^{iK\varphi}(1+\nu)^{(K+\Lambda_0)/2}(1-\nu)^{(K-\Lambda_0)/2},$$

where Λ_0 is the projection of the angular momentum of the mother nucleus on the axis of symmetry of the nucleus. In the absence of dispersion of the direction of the axis of the daughter nucleus relative to the original direction of the axis of the mother nucleus, only the term $m' = \Lambda_0 - \Lambda$ in the sum appearing in Eq. (15) will be different from zero.* Introducing, in analogy to the case of even even nuclei,[2] the notation $\chi_{\Lambda_0-\Lambda}(\mu) = \Psi(S)$ and substituting into (16), we get

$$w_j = e^{-\gamma_j[j(j+1)-\Lambda(\Lambda+1)]} \frac{\sum\limits_{l=|j-K|}^{j+K} (2l+1) \frac{|A_{\Lambda_0-\Lambda}^{jl}|^2}{S_{jl}} e^{-\gamma_l l(l+1)} \left|\int\limits_{-1}^{1} \Psi(S) e^{\varkappa\xi-\sigma_{-1}^{(1)}|} P_l^{\Lambda_0-\Lambda}(\mu)\, d\mu\right|^2}{\sum\limits_{l=|\Lambda-K|}^{\Lambda+K} (2l+1) \frac{|A_{\Lambda_0-\Lambda}^{\Lambda l}|^2}{S_{\Lambda l}} e^{-\gamma_l l(l+1)} \left|\int\limits_{-1}^{1} \Psi(S) e^{\varkappa\xi-\sigma_{-1}^{(1)}|} P_l^{\Lambda_0-\Lambda}(\mu)\, d\mu\right|^2}. \tag{17}$$

Especially intense are the so-called favored transitions,[3] i.e., transitions with $\Lambda = \Lambda_0 = K$. For such transitions it is natural, analogously to the case in even even nuclei,[2] to assume $\Psi(S)$ = const. It is easy to see that in favored transitions the sums in Eqs. (5) and (7) do not have terms with positive m. Substituting

---

*The assumption that has beem made has no analogue in the case of even even nuclei.[2] In that case, owing to the complete spherical symmetry of the state with zero angular momentum, the wave function does not depend on the Eulerian angles, and the question of the influence of possible dispersion of the direction of the axis has no meaning. The validity of this assumption is examined below.

$A^{jl}_{-|m|} = a^{jl}_{|m|}$, changing signs, and keeping in mind that in heavy nuclei the most important is the quadrupole deformation $\xi = R_0 \alpha_2 P_2(\mu)$, we get

$$w_j = e^{-\gamma_j [j(j+1) - K(K+1)]} \frac{\sum\limits_{l=|j-K|}^{j+K}{}' \frac{2l+1}{S_{jl}} e^{-\gamma_l l(l+1)} \left| \int\limits_0^1 e^{\beta P_2(\mu)} P_l(\mu)\, d\mu \right|^2}{\sum\limits_{l=0}^{2K}{}' \frac{2l+1}{S_{Kl}} e^{-\gamma_l l(l+1)} \left| \int\limits_0^1 e^{\beta P_2(\mu)} P_l(\mu)\, d\mu \right|^2}, \tag{18}$$

in which

$$S_{jl} = \sum_{m=0}^{\min\left\{ {2K \atop l} \right\}} m!\,(2K-m)!\,|a_m^{jl}|^2; \quad i\,(m+1)\sqrt{(l-m)(l+m+1)}\, a_{m+1}^{jl} - [K(K+1) - j(j+1) + l(l+1)$$

$$+ 2m(K-m)]\, a_m^{jl} - i\,(2K-m+1)\sqrt{(l+m)(l-m+1)}\, a_{m-1}^{jl} = 0; \quad a_0^{jl} = 1. \tag{19}$$

The primed summation sign in Eq. (18) means that the summation should be carried out only over the values of the orbital angular momentum l. Just as in the previous work,[2] we have

$$\beta = \left[\frac{4}{5} \varkappa R_0 \left(1 - \frac{k^2}{2\varkappa_b^2} \right) - i\,\frac{2}{5}\,\frac{k^3 R_0}{\varkappa_b^2} \right] \alpha_2.$$

The deformation α_2 was calculated from the experimental values of w_{K+1} for three odd nuclei with $K = 5/2$. The deformations calculated according to (18) are presented in Table I along with the quadrupole moments, $Q_0 = 6/5\ ZR_0^2 \alpha_2 10^{24}$. The results in the table differ but little from the corresponding values in neighboring even even nuclei.[2]

The assumption made above concerning the absence of "rocking" of the axis of the nucleus at the instant of α emission can apparently be checked experimentally. In fact, from formula (17) it is easy to see that

$$w_{jl} / w_{j'l} = (S_{j'l} / S_{jl}) \exp\{-\gamma_l [j(j+1) - j'(j'+1)]\}, \tag{20}$$

where, for favored transitions, the sums S_{jl} are normalized according to Eq. (19). In the case of $K = 5/2$, formula (20) gives, in particular*

$$w_{9/2,2} / w_{7/2,2} = (7/20)\, e^{-9\gamma_l}. \tag{21}$$

In the case of the three nuclei mentioned above, this quantity practically coincides with $w_{9/2}/w_{7/2}$, since, according to (18), the calculated contribution of α-particles with momentum equal to 4 does not exceed 15%. In Table II the experimental values of the ratio $w_{9/2}/w_{7/2}$ are compared with those calculated from formula (21). As is seen from the table all the calculated values deviate somewhat from the experimental ones. The contribution α-particles with $l = 4$ cannot be important and could only increase the discrepancy. It is possible that this disagreement could be explained by actually assuming some dispersion of the direction of the axis of the nucleus to take place upon α decay.

I would like to express my gratitude to D. P. Grechukhin for discussion of this work.

TABLE I

	α_2		Q_0	
$10^{13} A^{-1/3} R_0 =$	1.0	1.4	1.0	1.4
Th^{229}	0.25	0.21	10	17
Np^{237}	0.20	0.16	9	13
Np^{239}	0.18	0.15	8	13

TABLE II

Nucleus	$w_{9/2,2}/w_{7/2,2}$ theor.	$(w_{9/2}/w_{7/2})$ exptl.
Th^{229}	0.14	0.11
Np^{237}	0.16	0.10
Np^{239}	0.16	0.10

---

[1] L. Landau, E. Lifshitz, Квантовая механика (Quantum Mechanics) Chap. I., Gostehizdat (1948).

[2] V. G. Nosov, Dokl. Akad. Nauk SSSR 112, 414 (1957); Soviet Phys. "Doklady" 1, 48 (1957).

[3] A. Bohr, P. Froman, B. Mottelson, Danske Mat. Fys. Medd. 29, 10 (1955).

Translated by A. Turkevich

---

*In the derivation of (20) and (21) it was not assumed that the quadrupole deformation and the behavior of the wave function at the surface of the nucleus were not affected. It has only been assumed that there is no dispersion of the direction of the axis of the nucleus at the instant of α emission.

SOVIET PHYSICS JETP VOLUME 6, NUMBER 1 JANUARY, 1958

ON ANNIHILATION OF ANTINUCLEONS

V. M. MAKSIMENKO

P. N. Lebedev Physics Institute, Academy of Sciences, U.S.S.R.

Submitted to JETP editor January 25, 1957

J. Exptl. Theoret. Phys. (U.S.S.R.) **33**, 232-237 (July, 1957)

The distribution of secondary particles in stars produced in annihilation of nucleon-antinucleon pairs is calculated, using the statistical theory of multiple production of particles. Exact expressions for the statistical weights, taking into account conservation of energy, momentum and isotopic spin, were used in the calculations. The calculations were carried out for several magnitudes of the effective volume in which the energy is distributed, and for several types of particles created in the annihilation. The mean multiplicity (3 — 5) of π-mesons obtained theoretically agrees with the available experimental data, whereas the number of K-mesons predicted by the theory is substantially higher than experimentally observed. The momentum distribution of secondary π-mesons in the center-of-mass system is also computed.

IT has been recently established that antiprotons which are greatly slowed down or stopped in photo emulsions produce stars, caused by the annihilation of nucleon-antinucleon pairs.[1-3] In view of the doubtfulness of perturbation theory calculations, it is of interest to use the statistical theory of Fermi[4] in this case

I. According to the statistical theory, the probability of production of n particles is given by the formula

$$S_n(E_0) = (V/8\pi^3\hbar^3)^{n-1} g_n(T)\, dQ_n(E_0)/dE_0, \tag{1}$$

where V is an effective volume in which the energy E_0 of the annihilating particles is distributed, $g_n(T)$ is a factor which takes into account the conservation of isotopic spin[5] T and the identity of the particles produced in the annihilation,[6] and $Q_n(E_0)$ is the volume in momentum space corresponding to energy E_0. For the calculation of $dQ_0(E_0)/dE_0$ a method propsed by Rozental' and the author[7] was used, which made it possible to obtain exact values of this quantity, taking into account conservation of energy and momentum.

In the present article, calculations are given under various assumptions about the effective volume V and types of particles produced in the annihilation.

A. In the annihilation only π-mesons are produced:

$$\tilde{N} + N \rightarrow n\pi.$$

The following three variants were considered:

(1) The volume V was defined as

$$V = 4\pi r_0^3/3, \text{ where } r_0 = \hbar/\mu c = 1.4 \times 10^{-13} \text{ cm}. \tag{2}$$

The calculation of such a variant was carried out earlier by Belen'kii and Rozental';[8] however, they assumed that all π-mesons produced were ultra-relativistic particles.

(2) With the same V the final-state interaction of the π-mesons was taken into account according to the ideas of Pomeranchuk,[9] which led to an increase of the volume by a factor of $(n-1)$ and to an additional factor $(n-1)^{n-1}$ in Eq. (1).

(3) The interaction of the π-mesons was also taken into account in accordance with Ref. 9, but r_0 was taken equal to 1.0×10^{-13} cm.

The calculated distributions of numbers n of π-mesons in annihilation stars are given in Table 1 (with probabilities of different n given in per cent) for these variants.

Starting from the law of conservation of isotopic spin and its projection, it is possible to obtain the distribution of numbers of charged particles in annihilation stars. The results of the work of Nikishov[10] were used here. These distributions are given in Table 2 (the probabilities are expressed in per cent). The mean number of all particles and the mean number of charged particles from a star were calculated on the basis of Tables I and II and are given in Table III.

TABLE I

Variant	Number of particles in the star	2	3	4	5	6	7
$A(1)$	$\tilde{p}-p$ or $\tilde{n}-n$	10.9	47.4	35.0	6.4	0.3	—
	$\tilde{p}-n$ or $\tilde{n}-p$	7.9	51.3	33.8	6.7	0.3	—
$A(2)$	$\tilde{p}-p$ or $\tilde{n}-n$	0.3	4.5	31.2	39.6	24.3	0.1
	$\tilde{p}-n$ or $\tilde{n}-p$	0.2	5.4	23.7	44.8	25.8	0.1
$A(3)$	$\tilde{p}-p$ or $\tilde{n}-n$	3.5	22,5	41,8	26,2	5,9	—
	$\tilde{p}-n$ or $\tilde{n}-p$	2.6	24,4	40,3	27,0	5,7	—

TABLE II

Variant	Number of charged particles in the star	0	1	2	3	4	5	6	7
$A(1)$	$\tilde{p}-p$ or $\tilde{n}-n$	10.0		71.9		18.0		0.1	
	$p-n$ or $\tilde{n}-p$		30.6		67.5		1.9		
$A(2)$	$\tilde{p}-p$ or $\tilde{n}-n$	2.4		36.8		56.6		4.1	
	$\tilde{p}-n$ or $\tilde{n}-p$		12.4		64,6		22.9		~0.05
$A(3)$	$\tilde{p}-p$ or $\tilde{n}-n$	5.4		55.9		37.8		0.9	
	$\tilde{p}-n$ or $\tilde{n}-p$		20.6		69,0		10.4		

B. In the annihilation, in addition to the process $\tilde{N} + N \rightarrow n\pi$, processes involving the production of K-meson pairs are possible

$$\tilde{N} + N \rightarrow 2K + n\pi.$$

Two variants for the choice of V were considered:

1) The effective radius, as previously, is $r_0 = 1.4 \times 10^{-13}$ cm.

2) The effective radius is $r_0 = 1.0 \times 10^{-13}$ cm and the correction of Pomeranchuk was taken into account, assuming K-mesons to interact just as π-mesons.

TABLE III

Вариант		$A(1)$	$A(2)$	$A(3)$
Mean number of all particles in a star	$\tilde{p}-p$ or $\tilde{n}-n$	3.38	4.86	4.08
	$\tilde{p}-n$ or $\tilde{n}-p$	3.41	4.97	4.14
Mean number of charged particles in a star	$p-p$ or $\tilde{n}-n$	2.17	3.25	2.68
	$\tilde{p}-n$ or $\tilde{n}-p$	2.43	3.20	2.80

TABLE IV

Variant	Final State	2π	3π	4π	5π	6π	$2K$	$2K+\pi$	$2K+2\pi$	$2K+3\pi$
B (1)	$\tilde{p}-p$ or $\tilde{n}-n$	3,8	16,7	12,3	2,2	0,1	6.6	26.4	27.7	4.2
	$\tilde{p}-n$ or $\tilde{n}-p$	2,9	18,8	12,3	2,5	0,1	4.9	26.3	27.7	4.5
B (2)	$\tilde{p}-p$ or $\tilde{n}-n$	1.2	7.9	14.6	9.1	2.4	2.2	13.0	32.7	16.9
	$\tilde{p}-n$ or $\tilde{n}-p$	0.9	8.7	14.3	9.7	2.4	1.6	12.2	32.3	17.9

The distributions of various possible final states in annihilation stars are given in Table 4; the mean number of all particles, the mean number of π-mesons, and the mean number of K-mesons in a star are in Table V.

Recently Sudarshan[11] considered analogous questions for case B, using approximate formulae for the calculation of $dQ_n(E_0)/dE_0$. Several details of the calculation in his work are unclear. Thus, for example, if one goes to a system of units in which $\hbar = M = c = 1$, Eq. (1) can be written

$$S_n(E_0) = (5{,}21V/V_0)^{n-1} g_n(T)\, dQ_n(E_0)/dE_0$$

(where V_0 is defined by Eq. (2), whereas in Ref. 11 the expression

$$S_n(E_0) = (0{,}945V/V_0)^{n-1} g_n(T)\, dQ_n(E_0)/dE_0.$$

is used.

The above results can be compared with the experimental data obtained by Segrè and collaborators.[3] They found in photographic emulsions about 30 annihilation stars caused by antiprotons. The mean number of charged π-mesons in a star was about 2.5, and the mean number of all π-mesons (taking into account neutral ones), about 5 ± 1. A substantial number of K-mesons were not observed among the particles produced as a result of annihilation. It is also well-known, that in the collision of particles of energy $10^9 - 10^{10}$ ev, the number of K-mesons among the secondary particles constitutes not more than $1 - 2\%$ of the number of π-mesons. From this one can conclude that, apparently, variants A corresponds more closely to reality than variants B (and, consequently, also the work of Ref. 11), in which it was found that K-mesons should be formed in $60 - 65\%$ of the cases of annihilation and should constitute $25 - 30\%$ of the secondary particles. It is possible that, within the framework of the statistical theory, K-mesons should be taken into account in a different way than π-mesons. Thus, for example, if it is postulated that the effective volume for formation of a K-meson differs from the effective volume for formation of π-mesons, and an effective radius $r = \hbar/M_K c = 0.4 \times 10^{-13}$ cm (M_K is the mass of the K-meson) is defined, then the number of K-mesons, according to the statistical theory, becomes negligible compared with the number of π-mesons. However, there are no sufficiently convincing arguments for the introduction in this fashion of two effective volumes.

As can be seen from Tables I – III, all variants A agree satisfactorily with existing experiments and it is not possible to choose between them.

The data given relate to the case of annihilation at rest. Calculations have shown that the energy-dependence of the mean number of all particles ($\bar{n}$), coming from a star is very accurately given by the formula

$$\bar{n} = 2.87\,(E/Mc^2)^{1/4},$$

where E is the total energy of the nucleon–antinucleon pair in the laboratory system.

II. The momentum distribution of π-mesons produced as a result of annihilation was also calculated (only for case A).

The probability that a given particle created in the process of multiple production with energy E_0 in the center-of-mass system, has in this coordinate system,* a momentum in the interval from p to p + dp, is[12]

$$\omega_n(E_0, p)\,dp = 4\pi p^2 S_{n-1}(E_0 - \sqrt{p^2+\mu^2},\ p)\,dp. \tag{3}$$

Generalizing the formulae of Ref. 7 to the case $P_0 \neq 0$ and neglecting factors independent of p, we obtain the following formula†

$$\omega_n(E_0, p)\,dp = p^2\left(E_0 - \sqrt{p^2+\mu^2}\right)^{3n-7}\Big\{D_{n-1}^{(0)} + C_{n-1}^1 D_{n-1}^{(1)}\nu^2 \tag{4}$$
$$+ C_{n-1}^1 D_{n-1}^{(2)}\nu^4 \ln\frac{1}{\nu} + \left[\left(\frac{3}{4}C_{n-1}^1 + C_{n-1}^2\right)D_{n-1}^{(2)} + \frac{1}{2}C_{n-1}^1 F_{n-1}^{(2)}\right]\nu^4 + \cdots\Big\}.$$

TABLE V

Variant		B (1)	B (2)
Mean number of π-mesons in a star	$\tilde{p}-p$ or $\tilde{n}-n$ $\tilde{p}-n$ or $\tilde{n}-p$	2,11 2,16	2,73 2,78
Mean number of K-mesons in a star	$\tilde{p}-p$ or $\tilde{n}-n$ $\tilde{p}-n$ or $\tilde{n}-p$	1,29 1,27	1,28 1,27
Mean number of all particles in a star	$\tilde{p}-p$ or $\tilde{n}-n$ $\tilde{p}-n$ or $\tilde{n}-n$	3,40 3,43	4,01 4,05

Here

$$D_N^{(A)} = \frac{(1-k^2)^{N-2}}{2k}(-1)^A\sum_{r=0}^{N} C_N^r\left\{\frac{(1+k)^{N-r+1}(1-k)^r}{(2N-r-(A+1))!\,(N+r-(A+2))!} - \frac{(1+k)^{N-r}(1-k)^{r+1}}{(2N-r-(A+2))!\,(N+r-(A+1))!}\right\},$$

$$F_N^{(A)} = \frac{(1-k^2)^{N-2}}{2k}(-1)^A\sum_{r=0}^{N} C_N^r\left\{(1+k)^{N-r}(1-k)^{r+1}\left[\frac{\alpha(N+r-A)}{(2N-r-(A+2))!} + \frac{\alpha(2N-r-(A+1))}{(N+r-(A+1))!}\right] - (1+k)^{N-r+1}(1-k)^r\right.$$
$$\left.\times\left[\frac{\alpha(N+r-(A+1))}{(2N-r-(A+1))!} + \frac{\alpha(2N-r-A)}{(N+r-(A+2))!}\right]\right\},\quad k = p/(E_0 - \sqrt{p^2+\mu^2}),\quad \nu = \mu\left[(E_0-\sqrt{p^2+\mu^2})^2 - p^2\right]^{-1/2};$$

$$\alpha(z) = \begin{cases} (-1)^{z-1}|z|! & \text{for } z = 0, -1, -2, -3\ldots \\ 0 & \text{for } z = 1 \\ \dfrac{1}{(z-1)!}\displaystyle\sum_{r=1}^{z-1}\frac{1}{r} & \text{for } z = 2, 3, 4, \ldots \end{cases}$$

For the special case n = 3, Eq. (4) can be written in the simpler form

$$\omega_3(E_0, p)\,dp = p^2\left(E_0 - \sqrt{p^2+\mu^2}\right)^2 \times \left[1 - {}^1/_3 k^2(1-4\nu^2)\right]\sqrt{1-4\nu^2})\,dp. \tag{4'}$$

The momentum distributions of π-mesons (case A) obtained according to Eqs. (4) and (4′), are given in Fig. 1.

In conclusion I should to thank I. L. Rozental' for continuing interest in this work and for discussion of the problems involved in it. I should also like to thank Z. S. Maksimov for carrying out numerical calculations.

---

[1] O. Chamberlain et al. Phys. Rev. **101**, 909 (1956).

[2] Hill, Johansson, and Gardner, Phys. Rev. **101**, 907 (1956).

---

*In our case of annihilation at rest, the center-of-mass system coincides with the laboratory system.

†See Ref. 7 for the remaining terms of the series in the braces where Eqs. (5) and (6) should be taken for $D_N^{(A)}$ and $F_N^{(A)}$. The first term of the series, corresponding to the case of ultra-relativistic particles, was obtained earlier by Rozental'.[12]

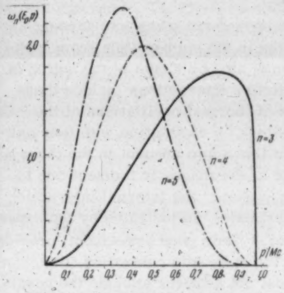

FIG. 1. Momentum distribution $\omega_n(E_0, p)$ of π-mesons for the process $N + N \rightarrow n\pi$ ($n = 3, 4, 5$). Here p is in units $Mc = 0.93$ Bev/c. The curves are normalized such that $\int \omega_n(E_0, p)\,dp = 1$.

[3] E. Segrè, Report at the All Soviet Conference on High Energy Physics, Moscow (1956); Vestnik Akad. Nauk SSSR 10, 26 (1956).

[4] E. Fermi, Progr. Theoret. Phys. 5, 570 (1950); Phys. Rev. 81, 683 (1951).

[5] J. Jeivin and A. deShalit, Nuovo cimento 1, 1147 (1955).

[6] E. Fermi, Phys. Rev. 93, 1434 (1954).

[7] V. M. Maksimenko and I. L. Rozental', J. Exptl. Theoret. Phys. (U.S.S.R.) 32, 658 (1957); Soviet Phys. JETP 5, 546 (1957).

[8] S. Z. Belen'kii and I. L. Rozental', J. Exptl. Theoret. Phys. (U.S.S.R.) 30, 595 (1956); Soviet Phys. JETP 3, 786 (1956).

[9] I. Ia. Pomeranchuk, Dokl. Akad. Nauk SSSR 78, 889 (1951).

[10] A. I. Nikishov, J. Exptl. Theoret. Phys. (U.S.S.R.) 30, 1149 (1956); Soviet Phys. JETP 3, 976 (1957).

[11] G. Sudarshan, Phys. Rev. 103, 777 (1956).

[12] I. L. Rozental', J. Exptl. Theoret. Phys. (U.S.S.R.) 28, 118 (1955); Soviet Phys. JETP 1, 166 (1955).

Translated by G. E. Brown
33

SOVIET PHYSICS JETP VOLUME 6, NUMBER 1 JANUARY, 1958

CONTRIBUTION TO THE PHENOMENOLOGICAL THEORY OF PARAMAGNETIC RELAXATION IN PARALLEL FIELDS

N. K. BELOUSOVA and I. G. SHAPOSHNIKOV

Molotov University

Submitted to JETP editor January 25, 1957

J. Exptl. Theoret. Phys. (U.S.S.R.) 33, 238-242 (July, 1957)

The role of spin-lattice interaction in the phenomenological theory of complex paramagnetic susceptibility is taken into account in the case of parallel fields to a greater extent than was previously done in Ref. 3.

I. In the first work on the phenomenological theory of paramagnetic relaxation in parallel fields (Casimir and Du Pre[1] and others,(see Ref. 2) considered only the spin-lattice relaxation (see Ref. 2 for terminology). Later Shaposhnikov[3] (whose work will be designated hereafter by I) presented a phenomenological theory of complex paramagnetic susceptibility for the case of parallel fields, taking both spin-lattice and spin-spin relaxation into account, while Khutsishvili[4] has made a general phenomenological analysis of paramagnetic relaxation in a constant field using the Onsager principle, and has shown in particular under what assumptions the corresponding results of the theory given in I are obtained. Recently Yokota[5] repeated independently the examination of paramagnetic relaxation, previously carried out in I, generalizing somewhat the statement of the problem, and arriving at a final result (coinciding with the results of I) in only one particular case. In the present communication the theory of I is generalized with account of the work of Khutsishvili and Yokota. Here, as in I, we have in mind isotropic non-conducting paramagnetic materials in condensed state (for example, polycrystalline powders of paramagnetic salts, which are frequently used in experiments).

2. The theory of I is not general enough in the following two respects.

First, the expression given in I for the rate of change of the magnetic moment takes into account only the portion of this change that is effected by the interaction resulting in the spin-system from lack of internal equilibrium. In fact, however, the magnetic moment can change also by virtue of the action of the lattice on the spin system, provided only the various types of spin-lattice interactions include those involving the magnetic moment (for example, interaction by modulation of thermal oscillations of the spin-spin magnetic couplings or interaction through the spin-orbit couplings by modulation with thermal oscillations of the electric field of the lattice). This circumstance is not taken into account in the theory of I, making the latter suitable only for substances in which the change of the magnetic moment due to the spin-lattice interaction is sufficiently small compared with the change due to the internal interaction in the spin system. At room temperatures this is indeed so in many substances, as indicated by the experiments of Garif'ianov,[6] Sitnikov,[7] and Kurushin,[8] with which the theory of I is in good agreement, provided one takes into account the quantity τ_s, contained in I and called there the spin-spin relaxation time, which is independent of the value of the constant magnetic field. One must not however exclude the possibility of existence of substances in which one can no longer neglect the change in the magnetic moment due to the spin-lattice interaction. Calculations of the spin-lattice interaction made by Al'tshuler[9] for hydrated salts of rare-earth elements under the assumption that the basic mechanism of this interaction is the coupling between the spin, orbit, electric field, and thermal oscillations have shown that at room temperatures the spin-lattice relaxation time, defined as the reciprocal of the corresponding transition probability, is two orders shorter than the relaxation time of the magnetic moment due to the non-equilibrium state of the spin system and caused by the internal interaction in the spin system. With such a strong spin-lattice coupling one can expect that the portion of the change in the magnetic moment, due to the spin-lattice interaction, will also be substantial. Yokota[5] took this component of the change in magnetic moment into account, but it appears to us in a somewhat inconclusive manner.

Second, in the theory of I, as in all earlier phenomenological works on paramagnetic relaxation, the heat received by the spin system from the lattice was taken into account only by a term proportional to the difference in temperature between the spin system and the lattice. In the general case, however, the expression for the heat received by the spin system from the lattice should also contain a term due to the change in the magnetic moment under the influence of the spin-lattice interaction, as first pointed out by Khutsishvili.[4] In fact, the heat received by the spin system from the lattice is part of the change in the spin-system energy due to the action of the lattice on the spin system. But this action leads, generally speaking, to a change in both the spin-system temperature and the magnetic moment (see the remarks made above concerning spin-lattice interactions involving the magnetic moment), while the energy of the spin system depends in general on both these quantities. In particular cases the above-mentioned new term in the expression for the heat may be insignificant; this will occur if the spin-lattice interactions involving the magnetic moment are insignificant or if the energy of the spin system depends weakly on the magnetic moment.

The theory of I will be generalized below in the above two respects. This generalization consists, thus, of a more complete accounting for the role of the spin-lattice interaction.

3. As in I, we shall assume that the states (generally speaking not in equilibrium) of the spin system of a paramagnetic located in an external magnetic field of constant direction and magnitude

$$H = H_0 + \eta_0 e^{i\omega t}, \tag{1}$$

are fully determined by the temperature of the spin system T, by the magnetization M along the field (assume that the magnetization has no other components), and the intensity field H. In the presence of internal equilibrium in the spin system we would have

$$M = f(H, T), \tag{2}$$

but generally speaking there is no such relation. The lattice temperature will be assumed constant and equal to T_0.

Let us introduce the symbols

$$H - H_0 \equiv \eta, \quad T - T_0 \equiv \vartheta, \quad M - M_0 \equiv \xi, \tag{3}$$

where $M_0 = f(H_0, T_0)$ is the magnetization at full equilibrium of the paramagnetic in a constant field H_0 at a temperature T_0. The quantities η, ϑ, and ξ characterize the deviation of the paramagnetic from the state of complete equilibrium at H_0 and T_0; we shall assume the quantities small and linearize the equations of our problem relative to these quantities.

In the steady-state mode

$$\vartheta = \vartheta_0 e^{i\omega t}, \quad \xi = \xi_0 e^{i\omega t} \tag{4}$$

with complex amplitudes ϑ_0 and ξ_0. We have to find the complex magnetic susceptibility of the paramagnetic

$$\chi = \xi_0 / \eta_0. \tag{5}$$

For this purpose we use, as in I, the following two relations: an expression for the rate of change of the magnetization

$$\dot{M} = \dot{M}(H, T, M) \tag{6}$$

and the first law of thermodynamics for the spin system

$$dE = \delta Q + HdM, \tag{7}$$

where δ_Q is the heat received by the spin system from the lattice, and E is the energy of the spin system.

4. For the right half of (6) we use an expression given by Yokota

$$M = -\frac{1}{\tau_1}[M - f(H, T)] - \frac{1}{\tau_2}[\dot{M} - f(H, T_0)], \tag{8}$$

where τ_1 and τ_2 are certain functions of H and T or of H and T_0 respectively. The form of these functions remains unknown within the framework of the phenomenological analysis. The first term characterizes here the change in the magnetic moment, occurring under the influence of the interaction in the spin system by virtue of the absence of internal equilibrium in the system, while the second term characterizes the change in the magnetic moment, occurring under the influence of the action of the lattice on the spin system. After linearization with respect to η, ϑ, and ξ Eq. (8) assumes the form

$$\dot{\xi} = -\frac{1}{\tau_1}\left(\xi - \frac{\partial f}{\partial T}\vartheta - \frac{\partial f}{\partial H}\eta\right) - \frac{1}{\tau_2}\left(\xi - \frac{\partial f}{\partial H}\eta\right), \tag{9}$$

where the quantities τ_1, τ_2 and the derivatives of f are taken at $H = H_0$ and $T = T_0$. The derivatives of f contained in (9) can be expressed in terms of the second derivatives of the thermodynamic potential $\Phi(H, T, N)$ of the spin system, taken at $H = H_0$, $T = T_0$, and $M = M_0$:

$$\partial f / \partial H = -\Phi_{MH} / \Phi_{MM}, \quad \partial f / \partial T = -\Phi_{MT} / \Phi_{MM}. \tag{10}$$

Furthermore, since $\partial f / \partial H$ is the isothermal equilibrium susceptibility χ_0, and $\Phi_{MH} = -1$ (because $\partial\Phi/\partial H = -M$), we get

$$\Phi_{MM} = \chi_0^{-1}, \tag{11}$$

and (10) can be rewritten

$$\partial f / \partial H = \chi_0, \quad \partial f / \partial T = -\chi_0 \Phi_{MT}. \tag{12}$$

Inserting (12) into (9) we obtain one of the equations needed for the determination of the quantity ξ_0, which is contained in formula (5) for the complex magnetic susceptibility

$$\tau_1\dot{\xi} + (\tau_1/\tau)\xi + \chi_0\Phi_{MT}\vartheta = \chi_0(\tau_1/\tau)\eta, \tag{13}$$

where

$$\tau \equiv \tau_1\tau_2 / (\tau_1 + \tau_2). \tag{14}$$

Since it follows from (13) that it at $\eta = 0$ and $\vartheta = 0$

$$\tau\dot{\xi} + \xi = 0, \tag{15}$$

the quantity τ characterizes the rate at which equilibrium magnetization is established in a constant field at a constant temperature of the spin system, equal to the lattice temperature (for actual realization of such isothermal conditions for the spin system it is necessary that its coupling to the lattice be sufficiently strong). We shall call this quantity the time of isothermal relaxation of the magnetization (cf. Ref. 10). If the second term of the right half of Eq. (8) is assumed negligible, i.e., if $\tau_1/\tau_2 \ll 1$, we obtain by virtue of (14) in practice $\tau = \tau_1$, so that τ_1 is the time of isothermal relaxation of magnetization for that case, when the rate of change of the magnetic moment is determined primarily by the internal interaction in the spin system. Then (13) becomes, as it should, the corresponding equation of the theory of I, with τ_1 taking the role of the quantity τ_s, introduced in I and called there the spin-spin relaxation time. Thus, τ_1 coincides with the τ_s of I.

5. For δ_Q, which enters in (7), we assume the following expression

$$\delta Q = -\alpha\vartheta\, dt + \beta\,[M - f(H, T_0)]\, dt, \tag{16}$$

where α and β are functions of H_0 and T_0, which remain unknown in the phenomenological treatment, while dt is the time element; here the form of the second term, connected with the change of the magnetic moment under the influence of the spin-lattice interaction (see Sec. 2 above) is taken to conform with the form of the second term of the right half of (8).

Using the thermodynamic relations, it is possible to transform expression (7), after insertion of (16) and linearization with respect to η, ϑ, and ξ, and after making allowances for (11) and (12), to the following form

$$\rho_1\dot{\vartheta} + \gamma^{-1}\vartheta + \Phi_{TT}^{-1}\Phi_{MT}\,\rho_1\xi - \chi_0^{-1}\gamma^{-1}\Phi_{MT}^{-1}[(\rho_1/\rho) - 1]\,\xi = -\gamma^{-1}\Phi_{MT}^{-1}[(\rho_1/\rho) - 1]\,\eta, \tag{17}$$

where

$$\gamma \equiv (1 - \chi_0\Phi_{TT}^{-1}\Phi_{MT}^2)^{-1}, \tag{18}$$

$$\rho = T_0\,(\chi_0\Phi_{MT}^2 - \Phi_{TT})\,(\alpha + \beta\chi_0\Phi_{MT})^{-1}, \tag{19}$$

$$\rho_1 = T_0\,(\chi_0\Phi_{MT}^2 - \Phi_{TT})\,\alpha^{-1}. \tag{20}$$

Equation (17) is the other equation needed to determine ξ_0.

Let the interaction in the spin system be so strong, that it causes internal equilibrium in the system to become established practically instantaneously ($\tau_1 = 0$), and let the external magnetic field remain constant ($\eta = 0$). We then obtain from (17) and (13), taking (14) into account,

$$\rho\dot{\vartheta} + \vartheta = 0, \tag{21}$$

so that the quantity ρ characterizes the rate at which the spin system and lattice temperatures become equalized in a constant field under that condition, that the spin system passes through a state of internal equilibrium. This quantity has been called spin-lattice relaxation time (see Refs. 1–3). If $\beta = 0$, i.e., if the energy exchange between the spin system and the lattice depends only on the difference in their temperatures, then, as can be seen from (19) and (20), the spin-lattice relaxation time is the quantity ρ_1, which coincides with the time of the spin-lattice relaxation employed in I, while Eq. (17) becomes in this case the corresponding equation in I, as should be.

6. To determine the complex susceptibility χ given by (5) it is necessary to insert (1) and (4) into Eqs. (13) and (17) and determine ξ_0 from these equations. We thus obtain

$$\frac{\chi}{\chi_0} = \frac{-1 + \rho_1/\rho + \tau_1/\tau + i\gamma\rho_1(\tau_1/\tau)\,\omega}{-1 + \rho_1/\rho + \tau_1/\tau - \gamma\rho_1\tau_1\omega^2 + i\,\{\rho_1 + \tau_1 + \gamma\rho_1[\tau_1/\tau - 1]\}\,\omega}. \tag{22}$$

If only the first terms are significant in (8) and (16), then $\tau_1/\tau \sim 1$ and $\rho_1/\rho \sim 1$, and (22) goes over into the formula for χ given in I with relaxation times ρ_1 and τ_1.

So far we have been unable to use the results of this general analysis to solve any particular problems in paramagnetic relaxation. It is possible, however, that these results will turn out to be useful in the evaluation of the recent experiments by Gorter and his associates[11] on paramagnetic absorption in parallel fields at high frequencies and at a temperature on the order of 20° K, in which maxima were observed in the curves for the absorption vs. the constant field at a given alternating field frequency, as contrasted with the monotonic decrease in this curve always observed in the previous experiments[6-8] at high and microwave frequencies at room temperatures.

[1] H. B. G. Casimir and F. K. Du Pre, Physica **5**, 507 (1938).

[2] C. J. Gorter, Парамагнитная релаксация (Paramagnetic Relaxation) (Russ. Transl.) IIL, Moscow, 1949.

[3] I. G. Shaposhnikov, Dissertation, Molotov State University, 1949; J. Exptl. Theoret. Phys. (U.S.S.R) **18**, 533 (1948).

[4] G. R. Khutsishvili, J. Exptl. Theoret. Phys. (U.S.S.R.) **29**, 329 (1955); Soviet Phys. JETP **2**, 187 (1956).

[5] M. Yokota (Jokota), J. Phys. Soc. Japan **10**, 762 (1955).

[6] N. S. Garif'ianov, J. Exptl. Theoret. Phys. (U.S.S.R.) **25**, 359 (1953).

[7] K. P. Sitnikov, Dissertation, Kazan' State University, 1954.

[8] A. I. Kurushin, Izv. Akad. Nauk SSSR, Ser. Fiz. **20** 1232 (1956).

[9] S. A. Al'tshuler, J. Exptl. Theoret. Phys. (U.S.S.R.) **24**, 681 (1953).

[10] I. G. Shaposhnikov, Izv. Akad. Nauk SSSR, Ser. Fiz. **20**, 1255 (1956).

[11] Smits, Derkesen, Verstelle, and Gorter, Physica **22**, 773 (1956).

Translated by J. G. Adashko
34

SOVIET PHYSICS JETP VOLUME 6, NUMBER 1 JANUARY, 1958

*ELASTIC COLLISION CROSS SECTION FOR HYDROGEN ATOMS**

V. S. KUDRIAVTSEV

Submitted to JETP editor January 26, 1957

J. Exptl. Theoret. Phys. (U.S.S.R.) **33**, 243-250 (July, 1957)

The method of perturbed stationary states is used to calculate the cross sections for elastic scattering of unexcited hydrogen atoms with each other. These cross sections are encountered in the kinetic theory of gases. A graph is given for the dependence of the cross sections on the energy of relative motion in the energy interval from 0.05 to 3 kev.

1. INTRODUCTION

THE system consisting of two hydrogen atoms moving past each other at a certain distance is examined. If the relative velocity of the atoms is small compared to the velocity of the electrons inside the atoms, then both atoms are in an almost adiabatic condition, and the wave function can be first approximated by the wave function of the stationary states of the hydrogen molecule for given positions of the nuclei. In the next approximation the kinetic energy of the nucleus appears as a small perturbation causing transition.[1] Atomic units are used henceforth.

The Schrödinger equation for the system under consideration has the form (the center of mass is at rest):

$$\left\{-\frac{1}{M}\Delta_{\mathbf{r}}+\hat{H}(\mathbf{r},\mathbf{r}_1,\mathbf{r}_2)\right\}\Psi(\mathbf{r},\mathbf{r}_1,\mathbf{r}_2)=E\Psi(\mathbf{r},\mathbf{r}_1,\mathbf{r}_2), \tag{1}$$

where H is the Hamiltonian of the system for stationary nuclei, i.e.,

$$\hat{H}(\mathbf{r},\mathbf{r}_1,\mathbf{r}_2)=-\frac{1}{2}\Delta_{\mathbf{r}_1}-\frac{1}{2}\Delta_{\mathbf{r}_2}-\frac{1}{r_1}-\frac{1}{r_2}-\frac{1}{|\mathbf{r}+\mathbf{r}_1|}-\frac{1}{|\mathbf{r}-\mathbf{r}_2|}+\frac{1}{|\mathbf{r}+\mathbf{r}_1-\mathbf{r}_2|}+\frac{1}{r}. \tag{2}$$

In equations (1) and (2) $\mathbf{r}$ is the radius vector of the nucleus of the first atom relative to the nucleus of the second; $\mathbf{r}_1$ and $\mathbf{r}_2$ are the radius vectors of the electrons in the first and second atoms relative to the respective nuclei. The mass of the electron is unity and the mass of the nucleus is M. Since $M \gg 1$, the center of mass of each atom may be considered as coincident with that of the nucleus. Then the center of mass of the atoms bisects the line joining the nuclei. The reduced mass of the atom in relation to the motion, equal to $(M+1)/2$, is replaced by $M/2$ in Eq. (1), and in Eq. (2) the reduced mass of the electron and nucleus, equal to $M/M+1$, is replaced by unity. The eigenfunctions $\varphi_n(\mathbf{r},\mathbf{r}_1,\mathbf{r}_2)$ of the Hamiltonian (2) and the eigenvalues of the energy $\epsilon_n(r)$ prove to be electron functions and electron terms of the hydrogen molecule for a given position of the nuclei, determined by the radius vector r

$$\hat{H}(\mathbf{r},\mathbf{r}_1,\mathbf{r}_2)\varphi_n(\mathbf{r},\mathbf{r}_1,\mathbf{r}_2)=\varepsilon_n(r)\varphi_n(\mathbf{r},\mathbf{r}_1,\mathbf{r}_2). \tag{3}$$

The functions φ_n represent an orthonormalized system (for any $\mathbf{r}$):

$$\iint\varphi_m^*\varphi_n\,d\mathbf{r}_1 d\mathbf{r}_2=\delta_{mn}. \tag{4}$$

We expand the wave function of the system $\Psi(\mathbf{r},\mathbf{r}_1,\mathbf{r}_2)$ in terms of the eigenfunctions $\varphi_n(\mathbf{r},\mathbf{r}_1,\mathbf{r}_2)$, where the coefficients of expansion χ_n are functions of $\mathbf{r}$

$$\Psi(\mathbf{r},\mathbf{r}_1,\mathbf{r}_2)=\sum_n\chi_n(\mathbf{r})\varphi_n(\mathbf{r},\mathbf{r}_1,\mathbf{r}_2). \tag{5}$$

Substituting the expansion (5) in (1), multiplying both sides by φ_m^*, and integrating over $\mathbf{r}_1$ and $\mathbf{r}_2$ using (3) and (4), we obtain

$$(1/M)\Delta_{\mathbf{r}}\chi_m(\mathbf{r})+[E-\varepsilon_m(r)]\chi_m(\mathbf{r})=-\frac{1}{M}\left\{\sum_{n\neq m}{}'\nabla_{\mathbf{r}}\chi_n\iint\varphi_m^*\nabla_{\mathbf{r}}\varphi_n\,d\mathbf{r}_1 d\mathbf{r}_2+\sum_n\chi_n\iint\varphi_m^*\Delta_{\mathbf{r}}\varphi_n\,d\mathbf{r}_1 d\mathbf{r}_2\right\}, \tag{6}$$

---

*This work was performed in 1953.

which is exact. On the right side of Eq. (6) the integrand contains derivatives of the electron function φ_n with respect to the nuclear coordinate **r**. When the relative velocity of the atom is small compared to the electron velocities in the atom, this derivative is small compared to the derivative of the nuclear function with respect to the nuclear coordinates, and since on the right side of Eq. (6) there is still a small factor 1/M, the terms on the right side may, in general, be disregarded and we obtain the equation

$$(1/M)\,\Delta_{\mathbf{r}}\chi_m(\mathbf{r}) + [E - \varepsilon_m(r)]\,\chi_m(\mathbf{r}) = 0, \tag{7}$$

which describes the motion of one particle with mass M/2 in a field with potential energy $\epsilon_m(r)$. Thus the problem of the elastic scattering of atoms on each other leads to the problem of the scattering of a particle in a field $\epsilon_m(r)$. The solution of Eq. (7) should have an aysmptotic form

$$\chi(\mathbf{r}) \sim e^{ikz} + f(\theta)\,e^{ikr}/r, \tag{8}$$

which corresponds to elastic scattering. The wave function of the system for $r \to \infty$ corresponds to two unexcited hydrogen atoms moving with respect to one another, and consists of the product $\chi(\mathbf{r})\,\psi(\mathbf{r}_1)\,\psi(\mathbf{r}_2)$ [$\psi(\mathbf{r}_1) = \pi^{-1/2}e^{-r_1}$ is the wave function of the unexcited hydrogen atom], which is symmetric or anti-symmetric with respect to the electron coordinates depending on whether the total electron spin of the system is zero or one. (The spins of the nuclei are not essential for the given problem since they have a small influence on the electron motion which determines the atomic interaction.) For a finite r, the electronic parts of the wave function are determined by the eigenfunctions $\varphi_n(\mathbf{r}, \mathbf{r}_1, \mathbf{r}_2)$ of Eq. (3), which for $r \to \infty$ have the required asymptotic form, while the corresponding $\epsilon_n(r)$ determine with Eq. (7) the nuclear parts of the wave functions $\chi_n(r)$. The function $\varphi_1(\mathbf{r}, \mathbf{r}_1, \mathbf{r}_2)$, which goes for $r \to \infty$ into the wave function

$$[\psi(\mathbf{r}_1)\psi(\mathbf{r}_2) + \psi(|\mathbf{r} + \mathbf{r}_1|)\psi(|\mathbf{r} - \mathbf{r}_2|)]/\sqrt{2},$$

is a function of the ${}^1\Sigma_g^+$ state of the hydrogen molecule, while the function $\varphi_2(\mathbf{r}, \mathbf{r}_1, \mathbf{r}_2)$ which changes for $r \to \infty$ into the wave function

$$[\psi(\mathbf{r}_1)\psi(\mathbf{r}_2) - \psi(|\mathbf{r} + \mathbf{r}_1|)\psi(|\mathbf{r} - \mathbf{r}_2|)]/\sqrt{2},$$

is a function of the ${}^3\Sigma_u^+$ state of the hydrogen molecule. The state of the entire systems is a mixture of the singlet state with wave function $\chi_g(\mathbf{r})\varphi_g(\mathbf{r}, \mathbf{r}_1, \mathbf{r}_2)$ and the triplet state with wave function $\chi_u(\mathbf{r})\varphi_u(\mathbf{r}, \mathbf{r}_1, \mathbf{r}_2)$, with probabilities 1/4 and 3/4 respectively.* The cross section for elastic scattering in such a systems consists of two parts: scattering in the singlet state and scattering in the triplet state, with

$$d\sigma = {}^1/_4\, d\sigma_g + {}^3/_4\, d\sigma_u. \tag{9}$$

2. MOLECULAR TERMS

In order to solve the problem it is necessary to know the energy of the terms ${}^1\Sigma_g^+$ and ${}^3\Sigma_u^+$ of molecular hydrogen as a function of the distance r between nuclei. The term ${}^1\Sigma_g^+$ corresponds to the basic bound state of the hydrogen molecule. Rydberg[2] calculated the energy of the term ${}^1\Sigma_g^+$ in the interval 0.78 $< r <$ 3.75 from analysis of the vibration spectra of the basic electronic state. The energy of the term outside this interval, and also the energy of the term ${}^3\Sigma_u^+$ are given in the work of Hirschfelder and Linnett[3] where they also give the most probable energy of the term, taking into account calculations by previous authors.

For dilution of the atoms, i.e., for $r \to \infty$, the above molecular term changes to a state of unexcited atoms: the term ${}^3\Sigma_u^+$ to a state with parallel spin, and the term ${}^1\Sigma_g^+$ to a state with antiparallel spin. The energy of interaction of the unexcited atoms at a large distance $r \gtrsim 9$ is determined by the van der Waals force, whereupon for the hydrogen atom[4]

$$U(r) = -6.47/r^6. \tag{10}$$

For increased density of atoms, i.e., for $r \to 0$, the term ${}^1\Sigma_g^+$, after subtraction of the energy of electrostatic repulsion of the nucleus, goes into the ground state ${}^1S_0$ of the helium atom with energy equal to − 1.89 atomic units. Hence, we obtain for the energy of the term ${}^1\Sigma_g^+$ for small distances

---

*Subscripts g and u will designate quantities corresponding respectively to states ${}^1\Sigma_g^+$ and ${}^3\Sigma_u^+$.

$$\varepsilon_g = 1/r - 1.89. \tag{11}$$

Term $^3\Sigma_u^+$ for $r \to 0$, after subtracting the energy of electrostatic repulsion of the nucleus, changes to the excited state $^3P_0$ of the helium atom having an energy -1.12 atomic units. Therefore, for small distances

$$\varepsilon_u = \frac{1}{r} - 1.12. \tag{12}$$

A table of energies for the terms $^1\Sigma_g^+$ and $^3\Sigma_u^+$ up to $r = 9$ is given in the Appendix.

3. QUANTUM EFFECTS

Besides the total cross section $\sigma = \int d\sigma$ for elastic collision, which determines the departure of the particles from the parallel beam, in kinetic theory of gases there also occur the cross sections σ^* and σ^{**} which determine the coefficients of diffusion, viscosity, and thermal conductivity. These cross sections are determined by the formulae[5]

$$\sigma^* = \int (1 - \cos\theta)\, d\sigma, \tag{13}$$

$$\sigma^{**} = \int (1 - \cos^2\theta)\, d\sigma, \tag{14}$$

where θ is the angle of variation of the relative velocity with respect to the direction of collision. In the present work we calculate the cross sections σ^* and σ^{**} for elastic collision of unexcited hydrogen atoms.

The solution of Eq. (7) with condition (8) can be considered in a quasi-classical approximation. Disregarding for a while small-angle scattering, which is determined by diffraction effects, it is possible to say that approach, at atomic energies on the order of or less than molecular energies, a condition for the validity of the quasi-classical approach is the smallness of the de Broglie wavelength of the atom in relative motion as compared with the radius of the atom, which in atomic units equals unity, i.e.,

$$\lambda = 1/\sqrt{2ME} \ll 1, \tag{15}$$

where E is the kinetic energy of relative motion of the atom. In the usual units for atomic hydrogen this means that

$$E \gg 0.01 \text{ ev}. \tag{16}$$

For atoms with energies of relative motion large compared with the molecular energies the interaction of the atoms is determined principally by the Coulomb repulsion between the nuclei. The condition for the applicability of the quasi-classical approximation in this case has the following form[6]

$$1/v \gg 1, \tag{17'}$$

where v is the relative velocities of the atoms. This introduces a restriction for large energies.

Applicability of the obtained formulae at large energies is further restricted by the condition that the relative velocities of the atoms should be small compared with the electron velocities inside the atom.

$$v = \sqrt{2E/M} \ll 1. \tag{17''}$$

It turns out that the condition of "adiabaticity" (17″) coincides in this case with the condition of applicability of the quasi-classical approximation for large energies (17′). In the usual units (17′) and (17″) give for hydrogen atoms

$$E \ll 25 \text{ kev}. \tag{18}$$

As to the quantum effect, associated with the identity of the atoms, going over to the quasi-classical case we obtain for the differential cross section for elastic scattering at angles not too close to zero or 180° the classical expressions, and diffraction effects appear for small-angle scattering both forward and backward. These effects make a finite contribution to the total cross section $\sigma = \int d\sigma$. However, we consider not the total cross section σ, but the cross sections σ^* and σ^{**} for which the contribution of the small forward angles is not significant, owing to of the factors $1 - \cos\theta$ and $1 - \cos^2\theta$, respectively, which vanish for $\theta = 0$. For the cross section σ^{**} small backward angles are also not important since the factor $1 - \cos^2\theta$ goes to zero also for $\theta = 180°$. The factor $1 - \cos\theta$ in the cross section σ^* does not go to zero for $\theta = 180°$ and even has a maximum value, so that the quantum effects should remain as we go over to the quasi-classical case. The point, however, is that the cross section σ^* determines the coefficient of diffusion, and for identical particles diffusion concept has no meaning. Thus, the quantum phenomena associated with small-angle scattering forward and backward, are insignificant in our case, and for the calculation of the cross sections σ^* and σ^{**} it is possible to make use of formulae of classical mechanics.

4. CALCULATION OF CROSS SECTION

We thus proceed to the calculation of the cross sections σ^* and σ^{**} according to classical mechanics. Cross sections σ^* and σ^{**} according to (9), have the form

$$\sigma^* = {}^1/_4\, \sigma_g^* + {}^3/_4\, \sigma_u^*, \tag{19}$$

$$\sigma^{**} = {}^1/_4\, \sigma_g^{**} + {}^3/_4\, \sigma_u^{**}, \tag{20}$$

where the subscripts g and u correspond to scattering on potentials $\epsilon_g(r)$ and $\epsilon_u(r)$ respectively. The angle of deflection θ for scattering is connected with impact parameter ρ by the relation[7]

$$\theta = \pi - 2\int_{r_0}^{\infty} \frac{\rho\, dr}{r^2 \sqrt{1 - U(r)/E - (\rho/r)^2}}, \tag{21}$$

where U(r) is potential energy, i.e., $\epsilon_g(r)$ and $\epsilon_u(r)$; r_0 is root of the denominator in the integrand with the maximum absolute values. Cross sections $\sigma^*_{g,u}$ and $\sigma^{**}_{g,u}$ are therefore obtained from the formula

$$\sigma^*_{g,u} = 2\pi \int_0^{\infty} (1 - \cos\theta(\rho))\, \rho\, d\rho, \tag{22}$$

$$\sigma^{**}_{g,u} = 2\pi \int_0^{\infty} (1 - \cos^2\theta(\rho))\, \rho\, d\rho. \tag{23}$$

Formula (21), and also (22) and (23), contain only the energy of relative motion of the atoms — energy of the atoms in a system of coordinates where the center of mass is at rest. The mass does not enter into these equations.

E	σ_g^*	σ_u^*	σ_g^{**}	σ_u^{**}	σ^*	σ^{**}
0.00184	138	81	87	68	95	73
0.0115	110	48	66	44	63	49
0.0460	76	26	46	26	39	31
0, 184	13.7	11.1	21.6	14.6	11.7	16.3

The values of the cross sections are determined from (21) — (23) by numerical integration* for four values of energy (E = 0.00184, 0.0115, 0.0460, 0.184 atomic units) small compared with the molecular energy (the energy of dissociation of molecular hydrogen from the ground state is 0.174 atomic units = 4.46 ev). These four values of atomic hydrogen correspond to relative velocities v = 1/500, 1/200, 1/100 and 1/50 atomic units. For each value of energy we calculate the cross sections $\sigma^*_{g,u}$ and $\sigma^{**}_{g,u}$, each for both types of U(r): $\epsilon_g(r)$ and $\epsilon_u(r)$. We obtain the final values of σ^* and σ^{**} from these cross sections by using (19) and (20). The results of the numerical calculation are given in the table (in atomic units), and are marked in the figure by dots.

For atoms with energies of relative motion large compared with the molecular energy (for velocities, as before, small compared with atomic) it is possible to proceed in the following manner. As the energy of relative motion increases, the atoms upon collision gradually come closer to each other. Therefore, the atomic interaction at the ever diminishing distances result in angles that are continuously more significant for the cross sections. At small distances the energy of interaction is given by (11) and (12), and at large distances it tends to zero. At medium distances its order of magnitude is equal to the molecular energy, which in the given case is small compared with the energy of relative motion. Therefore, for large energies it is possible to approximate the energy of interaction by

$$U_{g,u}(r) = 1/r - U_0, \quad r < 1/U_0 = r_0, \quad U_{g,u}(r) = 0, \qquad r > 1/U_0 = r_0, \tag{24}$$

upon which we get from (11) and (12) $U_0 = 1.89$ and 1.12 for the terms ${}^1\Sigma_g^+$ and ${}^3\Sigma_u^+$, respectively, and the differences $\epsilon_g(r) - U_g(r)$ or $\epsilon_u(r) - U_u(r)$ are considered as corrections. Thus, r_0 proves to be a certain effective radius of interaction.

---

*The numerical integration was done by D. F. Davidenko.

The problem of scattering in the field U(r) defined by Eq. (24) is solved rigorously. Carrying out the integration in (21) we obtain

$$\sin\frac{\theta}{2} = [(1-\xi^2)/(1+a\xi^2)]^{1/2}, \quad \rho < r_0, \qquad \theta = 0, \quad \rho > r_0, \tag{25}$$

where

$$\xi = \rho / r_0, \quad a = (4E/U_0)(1+E/U_0).$$

Integrating (22) and (23) we get

$$\dot{\sigma}_{g,u} = \frac{2\pi r_0^2}{a}\left[\frac{1+a}{a}\ln(1+a) - 1\right], \tag{26}$$

$$\ddot{\sigma}_{g,u} = 8\pi r_0^2 \frac{1+a}{a^2}\left[\frac{2+a}{2a}\ln(1+a) - 1\right]. \tag{27}$$

The values of r_0 and a are different for the terms ${}^1\Sigma_g^+$ and ${}^3\Sigma_u^+$. It is now necessary to calculate the correction that results from replacing the interaction energy according to (24). Let

$$V_{g,u}(r) = \varepsilon_{g,u}(r) - U_{g,u}(r). \tag{28}$$

It is possible to calculate the correction to cross sections (26) and (27), necessitated by superimposing a linear potential V(r) on the main field U(r), but this leads to very cumbersome expressions. The equations become simpler if this correction is expanded in powers of 1/E and the first non-vanishing term calculated. It turns out that the first term is $1/E^2$ and, therefore, V(r) enters in this term in a non-linear manner. Actually, let us designate the quantity $\theta(\rho)$, given by (25) and obtained by substituting expression (24) for U(r) into (21), by $\theta_0(\rho)$, and designate correspondingly, the cross section in (26) by σ_0^*, i.e.,

$$\dot{\sigma}_0 = 2\pi\int_0^\infty (1-\cos\theta_0(\rho))\rho d\rho. \tag{22'}$$

By $\theta(\rho)$ we now designate the quantity obtained from (21) by replacing U(r) with the exact energy of interaction $\epsilon(r) = U(r) + V(r)$ (tabulated in the Appendix).

$$\sigma^* = 2\pi\int_0^\infty (1-\cos\theta(\rho))\rho\, d\rho. \tag{22''}$$

The expansion in powers of 1/E of $\theta_0(\rho)$ and $\theta(\rho)$, contained in (22′) and (22″), has the form

$$\theta_0(\rho) = -\frac{\rho}{E}\int_\rho^\infty \frac{U'(r)\,dr}{\sqrt{r^2-\rho^2}} + O\left(\frac{1}{E^2}\right), \tag{29}$$

$$\theta(\rho) = -\frac{\rho}{E}\int_\rho^\infty \frac{U'(r)+V'(r)}{\sqrt{r^2-\rho^2}}\,dr + O\left(\frac{1}{E^2}\right). \tag{30}$$

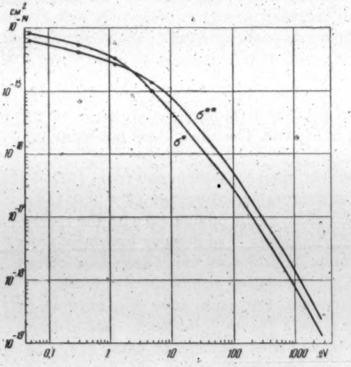

Energy dependence of the elastic collision cross section of hydrogen atoms.

Substituting (29) and (30) in (22′) and (22″) we find

$$\dot{\sigma} - \dot{\sigma}_0 = 2\pi\int_0^\infty \rho d\rho\,\frac{\rho^2}{E^2}\int_\rho^\infty\int_\rho^\infty \frac{U'(r_1)V'(r_2)+U'(r_2)V'(r_1)+V'(r_1)V'(r_2)}{\sqrt{(r_1^2-\rho^2)(r_2^2-\rho^2)}}\,dr_1 dr_2 + O\left(\frac{1}{E^3}\right). \tag{31}$$

Analogous calculations give

$$\ddot{\sigma} - \ddot{\sigma}_0 = 2(\dot{\sigma} - \dot{\sigma}_0), \tag{32}$$

It is possible to carry out the integration with respect to ρ in formula (31) by substituting expression (24) for U(r). We introduce in the double integral the variables r_1 and $k = r_2/r_1$, which makes for easier calculation, and obtain

$$\overset{*}{\sigma} - \overset{*}{\sigma}_0 = \frac{2\pi}{E^2}\int_0^\infty V(r)\,dr + \frac{\pi}{2E^2}\int_0^1 dk\left(\frac{1+k^2}{2}\ln\frac{1+k}{1-k} - k\right)\int_0^\infty dr_1 r_1^3 V'(r_1)\,V'(kr_1). \tag{33}$$

The correction to σ^{**} is obtained from (32). The value of the additional potential V(r) is determined from (24) and (28) and from the table in the Appendix.

Numerical calculation of the first integral in (33) gives 0.19 and 0.53; the double integral in (33) equals 0.23 and 0.22 for the terms ${}^1\Sigma_g^+$ and ${}^3\Sigma_u^+$, respectively. Substituting these values in (33) and using (32) we obtain the corrections $\sigma^* - \sigma_0^*$ and $\sigma^{**} - \sigma_0^{**}$.

The cross sections (26) and (27), with the corrections from (33) and (32) added, are determined by

$$\overset{*}{\sigma}_g = \frac{2\pi r_{0g}^2}{a_g}\left[\frac{1+a_g}{a_g}\ln(1+a_g) - 1\right] - \frac{0{,}83}{E^2}, \quad \overset{*}{\sigma}_u = \frac{2\pi r_{0u}^2}{a_u}\left[\frac{1+a_u}{a_u}\ln(1+a_u) - 1\right] + \frac{3{,}68}{E^2}; \tag{34}$$

$$\overset{**}{\sigma}_g = 8\pi r_{0g}^2\,\frac{1+a_g}{a_g^2}\left[\frac{2+a_g}{2a_g}\ln(1+a_g) - 1\right] - \frac{1{,}66}{E^2}, \quad \overset{**}{\sigma}_u = 8\pi r_{0u}^2\,\frac{1+a_u}{a_u^2}\left[\frac{2+a_u}{2a_u}\ln(1+a_u) - 1\right] + \frac{7{,}36}{E^2}; \tag{35}$$

with $r_{0g} = 0.529$; $r_{0u} = 0.894$; $a_g = 2.116\,E(1 + 0.529\,E)$; and $a_u = 3.776\,E(1 + 0.894\,E)$.

The correction to the cross sections for large energy is of the order of 1/ln E. The figure shows the cross sections σ^* and σ^{**} obtained from (19) and (20). In the region of intermediate energies the cross sections are obtained by graphical joining.

I wish to thank A. B. Migdal for suggesting the problem and for attention to the work.

APPENDIX

Energy of interaction for terms ${}^1\Sigma_g^+$ and ${}^3\Sigma_u^+$ of the hydrogen molecule

r	$\varepsilon_g(r)$	$\varepsilon_u(r)$	r	$\varepsilon_g(r)$	$\varepsilon_u(r)$	r	$\varepsilon_g(r)$	$\varepsilon_u(r)$
0.1	8.135	8,910	2.6	—0,0855	0.0505	5.1	—0.00270	0.00122
0.2.	3.195	3,965	2.7	—0,0775	0.0440	5.2	—0.00230	0.00103
0.3	1.600	2.360	2.8	—0,0695	0.0380	5.3	—0.00195	0.000870
0.4	0,855	1.590	2,9	—0,0625	0.0330	5.4	—0.00165	0,000740
0.5	0.450	1.150	3.0	—0,0565	0.0285	5,5	—0.00142	0.000620
0.6	0.207	0,850	3.1	—0,0510	0.0255	5.6	—0.00120	0.000520
0.7	0.0590	0,685	3.2	—0,0460	0.0220	5.7	—0.00102	0.000435
0,8	—0.0355	0.555	3.3	—0,0415	0.0192	5.8	—0.000860	0,000360
0.9	—0,0885	0.460	3.4	—0,0365	0.0168	5.9	—0.000750	0.000305
1.0	—0.1240	0,390	3.5	—0,0315	0.0140	6.0	—0.000640	0.000250
1.1	—0.1475	0.332	3.6	—0.0275	0.0123	6.2	—0.000480	0.000165
1.2	—0.1610	0.288	3.7	—0,0240	0,01075	6,4	—0,000360	0.000107
1.3	—0,1700	0,247	3.8	—0.0210	0.00920	6.6	—0,000265	0.0000680
1.4	—0,1740	0.216	3.9	—0.0185	0.00810	6.8	—0.000195	0.0000400
1.5	—0.1735	0,190	4.0	—0.0160	0.00700	7.0	—0.000147	0.0000222
1.6	—0.1695	0.168	4.1	—0.0138	0,00620	7 2	—0.000110	0,0000110
1.7	—0,1630	0.150	4.2	—0.0120	0,00540	7.4	—0.0000830	0.0000027
1.8	—0,1565	0.134	4.3	—0,0100	0,00460	7.6	—0.0000640	—0.0000027
1.9	—0.1490	0.120	4.4	—0.00800	0.00385	7.8	—0.0000510	—0.0000060
2.0	—0.1410	0.1084	4.5	—0.00660	0.00330	8.0	—0.0000400	—0.0000094
2.1	—0.1325	0,0965	4.6	—0.00570	0.00280	8.2	—0,0000310	—0.0000114
2.2	—0.1230	0.0855	4.7	—0.00490	0.00240	8.4	—0.0000250	—0.0000119
2.3	—0.1130	0.0755	4.8	—0,00420	0.00205	8.6	—0.0000200	—0.0000118
2.4	—0.1035	0.0665	4.9	—0.00365	0.00170	8.8	—0.0000165	—0.0000113
2.5	—0,0940	0.0580	5.0	—0.00320	0,00145	9.0	—0.0000140	—0,0000100

Translated by L. B. Leder

---

[1] N. F. Mott and H. S. W. Massey, Theory of Atomic Collisions, I.I.L. (Russ. Transl.) (1951), Chapt. VIII, p. 7

[2] R. Rydberg, Z. Physik **73**, 376 (1931).

[3] J. O. Hirschfelder and J. W. Linnett, J. Chem. Phys. **18**, 130 (1950).

[4] R. Eisenschitz and F. London, Z. Physik **60**, 491 (1930).

[5] S. Chapman and T. G. Cowling, The Mathematical Theory of Uniform Gases, Ch. 9.

[6] L. D. Landau and E. M. Lifshitz, Квантовая механика (Quantum Mechanics) GITTL (1948), p. 49.

[7] L. D. Landau L. Piatigorskii, Механика (Mechanics) GITTL (1940), p. 21.

SOVIET PHYSICS JETP VOLUME 6, NUMBER 1 JANUARY, 1958

ON THE KINETIC THEORY OF AN ELECTRON GAS IN THE PRESENCE OF BOUNDARIES

L. E. PARGAMANIK

Kar'kov State University

Submitted to JETP editor January 29, 1957

J. Exptl. Theoret. Phys. (U.S.S.R.) **33**, 251-255 (July, 1957)

The kinetic equations of an electron gas in a plane diode are used to show how one can construct a distribution function satisfying given conditions of emission and reflection at the electrodes for the one-dimensional case, neglecting the collision integral. Corrections to Langmuir's result, important for small anode potentials, are obtained.

PHYSICAL processes occurring in vacuum tubes are determined by the interactions of charged particles and physical conditions on the boundaries (for instance, on electrodes).

Particles of different energies satisfy different physical boundary conditions and we must thus use kinetic onsiderations in our calculations. We give below a method of integrating the kinetic equation for charged particles, suitable for one-dimensional problems. As an example we shall consider the flow of a direct electron current through a plane diode. The collective interactions of the electrons will be taken into account by using a self-consistent field; the individual interactions between electrons — collisions — will not be taken into account.

With these assumptions the distribution function $f(x, v)$ of the electron gas satisfies the kinetic equation

$$v\frac{\partial f}{\partial x} - \frac{u'(x)}{m}\frac{\partial f}{\partial v} = 0. \tag{1}$$

The potential energy $u(x)$ of an electron in a self-consistent field must be determined from Poisson's equation

$$d^2u/dx^2 = -4\pi e^2 n(x), \quad n(x) = \int_{-\infty}^{\infty} f(x,v)\,dv. \tag{2}$$

We formulate the boundary conditions for the distribution function for the most typical case, namely, a region bounded by two surfaces (in the case of a diode, the anode and the cathode).

The solution of the kinetic equation in the presence of two boundaries involves well-known mathematical difficulties. If the boundary values of the distribution function at both boundaries are arbitrary, the problem is incompatible. Actually, the kinetic equation together with data on one of the boundaries corresponds to the usual Cauchy problem, and determines uniquely the solution in the whole region, and in particular on the second boundary.

This problem was solved by Vainshtein[1] for a particular case (corresponding to no reflection of particles from the electrodes), where one can limit oneself to giving the distribution function on part of the boundary, for instance, on the cathode for positive velocities and on the anode for negative velocities. That distribution function was formulated by introducing discontinuous functions.

In the general case, the difficulties just mentioned result from incorrectly specifying the boundary conditions. The physical processes on the boundaries, viz. emission, reflection, and absorption of the particles, are mathematically formulated in the form of functional equations for its boundary values, but not in terms of the boundary values themselves. Below it is shown that for such boundary conditions one can find a solution of the kinetic equation.

The boundary conditions in the case of a diode must describe the emission of electrons from the cathode [with a distribution function $f_e(mv^2/2)$] and the elastic reflection of the electrons, characterized by a reflection coefficient $R(mv^2/2)$ that depends on the electron energy.

Such reflection, indeed, exists and is a quantum effect, connected with the passage of charged particles through a potential jump on the metal-vacuum boundary. Below we shall construct the solution for any function $R(mv^2/2)$.*

The presence of emission and reflection on the cathode ($x = 0$) leads to the boundary condition

$$f(0, v>0) = f_e(mv^2/2) + R_c(mv^2/2)\, f(0, v<0); \tag{3}$$

Reflection at the anode ($x = a$) leads to the condition

$$f(a, v<0) = R_a(mv^2/2)\, f(a, v>0). \tag{4}$$

The boundary conditions for the Poisson equation are determined by giving the potentials of the cathode and the anode,

$$u(0) = 0, \quad u(a) = u_a. \tag{5}$$

For a given density of the electron gas (that is, for a given distribution function) Eq. (2) together with the boundary conditions (5) determines the distribution of the potential inside the diode; therefore, additional data of the field on one of the electrodes is not only unnecessary, but even, in general, incompatible with equation (5).

Our problem reduces thus to solving the differential-functional equations (1) and (2) with the boundary conditions (4) and (5).

The solution of Eq. (1) is a function of the electron energy.

$$f(x, v) = f(\varepsilon), \quad \varepsilon = mv^2/2 + u(x). \tag{6}$$

It would appear at first glance that $f(\epsilon)$ is an even function of the velocity and thus leads to zero current and is useless for our problem. To prove the opposite, let us consider the lines of constant energy in the (x, v) plane, along which $f(\epsilon)$ stays constant (see figure). The form of the function $u(x)$ corresponds to a large emission current which leads to a potential barrier of height u_m near the cathode.

The lines ϵ = constant go for $\epsilon \leq u_m$ continuously from regions of positive to regions of negative velocities. Since the function $f(x, v) = f(\epsilon)$ stays constant along these lines, it is indeed an even function of the velocity. However, for $\epsilon > u_m$ each line comprises two unconnected parts, one of which lies in the region of positive, and the other in the region of negative velocities. On each part $f(\epsilon)$ stays constant, but the values are not the same, meaning that $f(\epsilon)$ is, generally speaking, not an even function of the velocity for $\epsilon > u_m$.

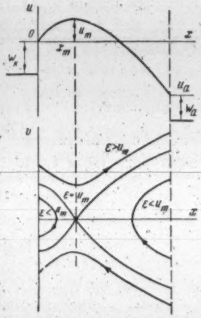

The distribution function can thus be written in the following form,

$$f(x, v) = \begin{cases} f_1(\varepsilon), & x \leqslant x_m \\ f_2(\varepsilon), & x \geqslant x_m \end{cases} \varepsilon \leqslant u_m,\ v \gtrless 0; \quad f(x, v) = \begin{cases} f_+(\varepsilon), & v > 0 \\ f_-(\varepsilon), & v < 0 \end{cases} \varepsilon \geqslant u_m. \tag{7}$$

These functions are simply determined by the boundary conditions. Substitution of f_1 into (3) and of f_2 into (4) gives

$$\left.\begin{aligned} f_1(\varepsilon) &= \frac{f_e(\varepsilon)}{1 - R_c(\varepsilon)}, & x \leqslant x_m \\ f_2(\varepsilon) &= 0 & x \geqslant x_m. \end{aligned}\right\} v \gtrless 0,\ \varepsilon \leqslant u_m. \tag{8}$$

Substituting f_+ and f_- into (3) and (4) yields a set of linear equations with a solution of the form

$$\left.\begin{aligned} f_+(\varepsilon) &= \frac{f_e(\varepsilon)}{1 - R_c(\varepsilon) R_a(\varepsilon - u_a)}, & v > 0 \\ f_-(\varepsilon) &= \frac{f_e(\varepsilon) R_a(\varepsilon - u_a)}{1 - R_c(\varepsilon) R_a(\varepsilon - u_a)}, & v < 0 \end{aligned}\right\} \varepsilon \geqslant u_m. \tag{9}$$

Equations (8) and (9) give us the complete solution of the problem of finding the distribution function of an electron gas, moving in a given field $u(x)$ with boundary conditions (3) and (4). We emphasize that the distribution functions (8) and (9) which we have found show a discontinuity on the line $\epsilon = u_m$. If we neglect reflection, Eqs. (8) and (9) go over into the solution given by Vainshtein[1] for the case when there is no emission from the anode.*

---

*To get an estimate we use the formula $R(\epsilon) = [\sqrt{1 + \epsilon/W} - \sqrt{\epsilon/W}]^4$ (see Ref. 2), which does not take into account the influence of the field at the surface of the metal on the reflection; W is here the total work needed to get the electron out of the metal.

We can construct the function f_e for the electrons emitted by the cathode by assuming for the electrons inside the metal a Fermi distribution and by taking into account their reflection from the metal-vacuum boundary with the same coefficient R_K

$$f_e\left(\frac{mv^2}{2}\right) = \begin{cases} Ae^{-mv^2/2\Theta}[1 - R_c(mv^2/2)], & v>0, \\ 0, & v<0, \end{cases} \qquad A = (m^2\Theta / 2\pi^2\hbar^3)\, e^{-\varphi/\Theta}. \tag{10}$$

From Eqs. (8) to (10) we obtain the following expression for the current density in the diode,†

$$j = \frac{eA}{m}\int_{u_m}^{\infty} e^{-\varepsilon/\Theta} D_1(\varepsilon)\,d\varepsilon \simeq \frac{eA\Theta}{m} e^{-\frac{u_m}{\Theta}}[D_1(u_m) + \Theta D_1'(u_m) + \cdots],$$
$$D_1(\varepsilon) = [1 - R_c(\varepsilon)][1 - R_a(\varepsilon - u_a)] / [1 - R_c(\varepsilon)\, R_a(\varepsilon - u_a)]. \tag{11}$$

Here and henceforth we expand the integrals in a power series of the parameter $y_m^{-1} \equiv \Theta/m$; the terms written out are sufficient for the case $y_m \gg 1$.

The distribution functions (7) to (9) are expressed in terms of the potential energy u(x) which must be found from Eq. (2). An evaluation of the density of the electron gas from Eqs. (2) and (9) to (11) gives

$$n(x) = A\sqrt{2\pi\Theta/m}\, e^{\eta - y_m}\,\Phi(\eta^{1/2}) + n_2(\eta), \quad x \leqslant x_m; \quad (\eta\ n(x) \doteq n_2(\eta)$$
$$\equiv A\sqrt{\frac{\Theta}{2m}}\, e^{-u/\Theta}\int_{\eta}^{\infty} e^{-\xi} D_2[u_m + \Theta(\xi - \eta)]\,\xi^{-1/2}\,d\xi \simeq \frac{1}{2}\sqrt{\frac{2\pi\Theta}{m}}\, D_2(u_m)\, e^{\eta - y_m}\left\{1 - \Phi(\eta^{1/2}) + \Theta\frac{D_2'(u_m)}{D_2(u_m)}\right.$$
$$\left.\times\left[\sqrt{\frac{\eta}{\pi}}\, e^{-\eta} + \left(\frac{1}{2} - \eta\right)(1 - \Phi(\eta^{1/2}))\right]\right\}, \quad x \geqslant x_m; \quad \eta(x) = \frac{u_m - u(x)}{\Theta}; \quad D_2(\varepsilon) = \frac{[1 - R_K(\varepsilon)][1 - R_a(\varepsilon - u_a)]}{1 - R_K(\varepsilon)\, R_a(\varepsilon - u_a)}. \tag{12}$$

where Φ is the probability integral.

Substituting this expression for the density into Eq. (2) and integrating we find the dependence $x(\eta, y_m)$ of the coordinate on the potential. This dependence differs from Langmuir's results[4] through correction terms, connected with reflection. We calculate also the distance a between the electrodes from $y_a \equiv -u_a/\Theta$ and y_m (instead of y_m we can introduce as parameter the field on one of the electrodes). In this way we obtain a relation between y_a and y_m from which we can find their interdependence $y_m(y_a)$. Substituting this into Eqs. (7) to (9), (11), and (12) we can express $f(x, v)$, n(x), u(x) and j in terms of two parameters, u_a and Θ, i.e., we have obtained a complete solution of the diode problem.

The dependence of y_m on y_a is approximately of the form

$$y_m = \ln\alpha - \frac{\varphi}{\Theta} - \ln\frac{(y_a + \ln\alpha - \varphi/\Theta)^{3/2}}{D_2(\Theta\ln\alpha - \varphi)}, \qquad \alpha = (9/2^{1/2}\pi)\, e^2 m^{3/2}\Theta^{1/2} a^2\hbar^{-3} = 6{,}93\cdot 10^{15}\,\Theta^{1/2}(\mathrm{eV})\, a^2(\mathrm{cm}). \tag{13}$$

This formula enables us to calculate the barrier height at the cathode for given cathode temperature and anode potential; for instance, for a tungsten cathode, $\Theta = 2320°$ K, a = 1 cm, u_m decreases from 1.8 to 0.5 ev if the anode potential increases from 1 to 160 v.

The diode characteristic is obtained by substituting expression (13) into (11),

$$j = \frac{1 - R_a(u_m - u_a)}{1 + R_a(u_m - u_a)}\,\frac{\sqrt{2}\,\Theta^{3/2}}{9\pi m^{1/2} a^2}(y_a + y_m)^{3/2}\left[1 + \frac{3\sqrt{\pi}}{2}(y_a + y_m)^{-1/2}\right]; \tag{14}$$

The expression within the square brackets on the right hand side is the series expansion of the function D_1 and D_2 up to terms of the order $(y_a + y_m)^{-1}$.

Equation (14) takes the reflection of the electrons from the anode into account only through the factor $(1 - R_a)/(1 + R_a)$, and thus differs from the "3/2-law."[4] For $u_m - u_a < W_a$ this factor is nearly equal to unity which means that reflection is unimportant. However, for $u_m - u_a > W_a$ reflection appreciably decreases the current; this in the above example of an anode potential of 1 v the current is less than the value for the "3/2-law" by 20%.

---

*However, the value given in Ref. 1 for the distribution function on the line of discontinuity is wrong.

†If $\varepsilon - u_a > W_a$, the functions $D_1(\epsilon)$ and $D_2(\epsilon)$ will be the transmission coefficients of the cathode.

Equations (13) and (14) enable us to calculate the diode characteristic directly, and not in parametric form as is usually done.[5]

As we have shown above, the present method of integrating the kinetic equation for charged particles makes it possible to construct a distribution function satisfying boundary conditions of emission and reflection on two boundaries and to find the self-consistent field.

The author expresses his thanks to G. Ia. Liubarskii and Ia. B. Fainberg for a discussion of the results of the present paper.

---

[1] L. Vainshtein, Collection of scientific papers, Soviet Radio Press, **10** (1948).

[2] A. Sommerfeld and H. Bethe, Electron Theory of Metals, Handb. Phys. **24**, part 2, 1933, p. 333 (Russ. Transl).

[3] L. D. Landau and E. M. Lifshitz, Квантовая механика (Quantum Mechanics) OGIZ, 1948, Sec. 23.

[4] I. Langmuir, Phys. Rev. **21**, 419 (1923).

[5] N. A. Kaptsov, Электроника (Electronics) GITTL, 1953, Sec. 39.

Translated by D. ter Haar
36

SOVIET PHYSICS JETP VOLUME 6, NUMBER 1 JANUARY, 1958

CORRELATION OF POLARIZED QUANTA IN THE CASE OF NONCONSERVATION OF PARITY

IU. V. GAPONOV and V. S. POPOV

Moscow State University

Submitted to JETP editor April 4, 1957

J. Exptl. Theoret. Phys. (U.S.S.R.) **33**, 256-259 (July, 1957)

The angular correlation between the electron and the circularly polarized γ-quantum emitted in a cascade β-transition is considered in the case when parity is not conserved. The effect of the nuclear coulomb field is neglected.

As it has been shown by Lee and Yang[1] (see also the review by Shapiro[2]), parity nonconservation in β-decay implies an angular correlation between the circularly polarized γ-quantum and the electron. We calculated of this effect for allowed transitions, without taking into account the influence of the nuclear Coulomb field. If the β-decay is followed by a γ-transition, the probability for the γ-quantum to be emitted at an angle θ with respect to the direction of emission of the electron is equal to:

$$w(\theta) = 1 - (\mu\alpha v/c)\cos\theta, \tag{1}$$

where $\mu = \pm 1$ corresponds to right-hand or left-hand polarization of the γ-quantum, v is the election velocity, and α a coefficient depending on the interaction constants, on the momenta of the nuclei, and on the multipole order of the γ-quantum:

$$\alpha = \frac{2B\sqrt{j_2(j_2+1)}\,\delta_{j_3 j_1} + D[2 + j_2(j_2+1) - j_1(j_1+1)]}{2\sqrt{j_2(j_2+1)}\,(A\,\delta_{j_3 j_1} + C)}\;\frac{j_2(j_2+1) + L_1(L_1+1) - j_3(j_3+1)}{2L_1(L_1+1)\sqrt{j_2(j_2+1)}}. \tag{2}$$

Here j_1, j_2 and j_3 are the total angular momenta of the initial nucleus and of the excited and of the ground-state of the final nucleus, while L_1 is the multipole order of the γ-quantum. The coefficient α does not depend on the type of radiation (electric or magnetic), but only on its multipole order. The constants involved in Eq. (2) are

$$A = \{|c_s|^2 + |c_s'|^2 + |c_v|^2 + |c_v'|^2 + (2mc^2/E)\,\mathrm{Re}\,(c_s^* c_v + c_s'^* c_v')\}\,|a|^2, \quad B = 2\,\mathrm{Re}\,\{(c_s^* c_t' + c_s'^* c_t - c_v^* c_a' - c_v'^* c_a)\,a^* b\},$$
$$C = \left\{|c_t|^2 + |c_t'|^2 + |c_a|^2 + |c_a'|^2 + \frac{2mc^2}{E}\,\mathrm{Re}\,(c_t^* c_a + c_t'^* c_a')\right\}|b|^2, \quad D = 2\mathrm{Re}\,\{c_t^* c_t' - c_a^* c_a'\}\,|b|^2. \tag{3}$$

The quantities $c_s c_s'$ etc. are constants involved in the β-decay Hamiltonian, in which parity non-conservation is taken into account (see, for instance, Ref. 1). The primed constants correspond to the terms arising because of parity nonconservation in β-decay (if parity is conserved all the c' are 0), m and E are the mass and energy of the electron, while a and b are the nuclear matrix elements and do not depend on the magnetic quantum numbers:

$$a = \langle j_1 \| 1 \| j_1 \rangle\, \delta_{j_2 j_1} \quad b = \langle j_2 m_1 | \sigma_z | j_1 m_1 \rangle\, \varepsilon_{j_1 j_2}^{m_1}, \qquad \varepsilon_{j_1 j_2}^{m_1} = \begin{cases} \left[\dfrac{(2j_1+1)(j_1+1)}{(j_1-m_1+1)(j_1+m_1+1)}\right]^{1/2}, & j_2 = j_1+1, \\ \dfrac{\sqrt{j_1(j_1+1)}}{m_1}, & j_2 = j_1, \\ -\left[\dfrac{j_1(2j_1+1)}{(j_1+m_1)(j_1-m_1)}\right]^{1/2}, & j_2 = j_1 - 1. \end{cases} \tag{4}$$

A and B enter Eq. (2) when $j_2 = j_1$. As seen from Eqs. (3) and (2), the angular distribution is anisotropic only if parity is not conserved.

The experiments of Wu and Lederman (see Ref. 2) confirm the hypothesis of a longitudinal neutrino, made independently by Landau[3] and Lee and Yang.[4] In this case, the equations in (3) take a simpler form because $c = \pm c'$. It follows from Wu's experiment that $c = -c'$.

Then:

$$A = 2\{|c_s|^2 + |c_v|^2 + (2mc^2/E)\,\mathrm{Re}\,c_s^* c_v\}\,|a|^2, \quad B = -4\,\mathrm{Re}\,[(c_s^* c_t - c_v^* c_a)\,a^* b],$$
$$C = 2(|c_t|^2 + |c_a|^2 + (2mc^2/E)\,\mathrm{Re}\,c_t^* c_a)\,|b|^2, \quad D = -2(|c_t|^2 - |c_a|^2)\,|b|^2. \tag{5}$$

Equation (1) can be generalized to the case when the β-decay is followed by several consecutive γ-transitions. The probability of emission of the n-th ($n > 1$) γ-quantum at an angle θ with respect to the direction of emission of the electron is determined by the same formula (1) where

$$\alpha = \frac{2B\sqrt{j_2(j_2+1)}\,\delta_{j_2 j_1} + D\,[2 + j_2(j_2+1) - j_1(j_1+1)]}{2\sqrt{j_2(j_2+1)}\,(A\delta_{j_2 j_1} + C)} \quad \frac{j_{n+1}(j_{n+1}+1) + L_n(L_n+1) - j_{n+2}(j_{n+2}+1)}{2L_n(L_n+1)\sqrt{j_{n+1}(j_{n+1}+1)}}$$
$$\times \prod_{i=1}^{n-1} \frac{j_{i+1}(j_{i+1}+1) + j_{i+2}(j_{i+2}+1) - L_i(L_i+1)}{2\sqrt{j_{i+1}(j_{i+1}+1)\,j_{i+2}(j_{i+2}+1)}}. \tag{6}$$

Here j_1 is the total angular momentum of the initial nucleus, which makes a γ-transition to an excited state of the final nucleus with a total angular momentum j_2, emitting consecutive γ-quanta with multipole orders $L_1, L_2, \ldots L_n$, and making transitions to states $j_3, \ldots j_{n+2}$; A, B, C, and D are determined, as before by Eq. (3) or, for a longitudinal neutrino, by Eq. (5).

The experimental data indicate that $c_V = c_a = 0$ (see Ref. 6), and this yields a considerable simplification of Eq. (4). The values of α have been computed in this assumption for a series of nuclei, and the results are shown in Tables 1 and 2. Let us note that in the case of transitions with $j_2 = j_1 \pm 1$ the nuclear matrix elements a and b are not involved in the expression for α. In the case $j_2 = j_1$, α does obviously depend on the values of a and b which, at the present time, are known well enough only for light and mirror nuclei.[7]

In Tables 1 and 2, A, B, C and D have been computed using Eq. (5) with $c_V = c_a = 0$. The nuclear decay schemes used in Tables 1 and 2 are taken from Ref. 8.

In conclusion let us note that, although the measurement of the γ-quantum polarization involves difficulties (see Ref. 2), an experimental investigation of the effect considered here would be interesting, especially for the case $j_2 = j_1$, for the following reasons: the value of α depends on the relative phase of the constants c_s and c_t which can, generally speaking, be complex (let us note that the nuclear matrix elements a and b, which are involved in α in this case, are real). However, if Landau's hypothesis[3] on the conservation of the combined parity is true, c_s and c_t have to be either both real or both pure imaginary. In this fashion the investigation of the effect considered here can give information on the properties of the Hamiltonian for β-decay, which is very interesting from the point of view of the question on the nature of parity nonconservation.

TABLE I

Initial nucleus	j_1	j_2	γ-transition	α	E_γ (kev)
K_{19}^{43}	$^3/_2{}^+$	$^5/_2{}^+$	$^5/_2{}^+ (E1)\ ^3/_2{}^-$	−0.700	373
			$^3/_2{}^- (M1)\ ^5/_2{}^-$	0.420	258
			$^5/_2{}^- (M1)\ ^7/_2{}^-$	0.420	369
			$^3/_2{}^- (E2)\ ^7/_2{}^-$	0.280	627
Co_{27}^{60}	5+	4+	$4^+ (E2)\ 2^+$	0.333	1172
			$2^+ (E2)\ 0^+$	0.333	1332
J_{57}^{131}	$^7/_2{}^+$	$^5/_2{}^+$	$^5/_2{}^+ (E2)\ ^1/_2{}^+$	0.333	284
			$^1/_2{}^+ (M1)\ ^3/_2{}^+$	−0.167	80
			$^5/_2{}^+ (M1)\ ^3/_2{}^+$	0.500	364
			$^5/_2{}^+ (E2)\ ^3/_2{}^+$	0.262	364
W_{74}^{187}	$^3/_2{}^-$	$^5/_2{}^-$	$^5/_2{}^- (E1)\ ^3/_2{}^+$	−0.200	686
			$^5/_2{}^- (E1)\ ^7/_2{}^+$	0.500	552
			$^7/_2{}^+ (M1)\ ^5/_2{}^+$	−0.643	134*
			$^5/_2{}^- (E2)\ ^9/_2{}^-$	0.333	480
			$^9/_2{}^- (M2)\ ^5/_2{}^+$	−0.407	206
			$^9/_2{}^- (E3)\ ^5/_2{}^+$	−0.259	206
			$^9/_2{}^- (E1)\ ^7/_2{}^+$	−0.611	72
			$^7/_2{}^+ (M1)\ ^5/_2{}^+$	−0.611	134**

*2nd γ-quantum in the cascade $^3/_2{}^-\ (\beta^-)\ ^5/_2{}^-\ (E1)\ ^7/_2{}^+\ (M1)\ ^5/_2{}^+$.

**3rd γ-quantum in the cascade $^3/_2{}^-\ (\beta^-)\ ^5/_2{}^-\ (E2)\ ^9/_2{}^-\ (E1)\ ^7/_2{}^+\ (M1)\ ^5/_2{}^+$.

TABLE II

Initial nucleus	j_1	j_2	γ-transition	$(A + C)\alpha$	E_γ (kev)
Na_{11}^{24}	4+	4+	$4^+ (E2)\ 2^+$	$0.373\ B + 0.083\ D$	2750
			$2^+ (E2)\ 0^+$	$0.373\ B + 0.083\ D$	1370
Sc_{21}^{46}	4+	4+	$4^+ (E2)\ 2^+$	$0.373\ B + 0.083\ D$	890
			$2^+ (E2)\ 0^+$	$0.373\ B + 0.083\ D$	1120
Sc_{21}^{48}	6+	6+	$6^+ (E2)\ 4^+$	$0.360\ B + 0.056\ D$	1050
			$4^+ (E2)\ 2^+$	$0.360\ B + 0.056\ D$	1325
			$2^+ (E2)\ 0^+$	$0.360\ B + 0.056\ D$	990

The authors express their gratitude to I. S. Shapiro, Doctor of Physico-Mathematical Sciences, for suggesting the problem, for valuable advices and for constant interest.

Note added in proof (June 25, 1957). One of the authors (Iu. G.) calculated the effect of the nuclear Coulomb field on the coefficient α (1) for allowed β-transitions. It has been shown that the coefficient α does not change if $c_V = c_{V'} = c_a = c'_a = 0$.

---

[1] T. D. Lee and C. N. Yang, Phys. Rev. **104**, 254 (1956).

[2] I. C. Shapiro, Usp. Fiz. Nauk **61**, 313 (1957).

[3] L. D. Landau, J. Exptl. Theoret. Phys. (U.S.S.R.) **32**, 407 (1957); Soviet Phys. JETP **5**, 337 (1957).

[4] T. D. Lee and C. N. Yang, Phys. Rev. **105**, 1671 (1957).

[5] C. S. Wu et al. Phys. Rev. (in press).

[6] Ia. B. Zel'dovich, Usp. Fiz. Nauk **56**, 165 (1955).

[7] Ia. A. Smorodinskii, Usp. Fiz Nauk **56**, 201 (1955).

[8] B. C. Dzhelepov and L. K. Peker, Схемы распада радиоактивных изотопов (Decay Schemes of Radioactive Isotopes), Academy of Sciences Press, 1957.

Translated by E. S. Troubetzkoy
37

LETTERS TO THE EDITOR

*THE PROBLEM OF NUCLEON STRUCTURE**

B. S. NEGANOV

Joint Institute for Nuclear Research

Submitted to JETP editor November 3, 1956

J. Exptl. Theoret. Phys. (U.S.S.R.) 33, 260-262 (July, 1957)

If it is assumed that the nucleon is not an elementary particle but a system composed of particles which are tightly bound by the π-meson field, the resonance interaction between π-mesons and nucleons can be interpreted in terms of an excited nucleon state while the associated production of hyperons and K-mesons can be interpreted as dissociation of the nucleon into constituent particles. Hence, we propose that the fundamental particles are the K-meson and the cascade hyperon (Ξ) and postulate that there exists between the K^{0+} and Ξ^{0-} particles and the corresponding anti-particles $\tilde{K}^{0-}$ and Ξ^{0+} a strong attractive force which results in the formation of a bound state with a very large mass defect. This attraction does not exist between the K^{0+}, $\tilde{\Xi}^{0+}$ and $\tilde{K}^{0-}$ Ξ^{0-} particles respectively. The K^{0+} and Ξ^{0-} particles can then form the following four bound states (isotopic spin T = 0 and T = 1) which can be identified with charged and neutral hyperons:

$$\begin{array}{l|l} \Psi_{1,1} = \Xi^0 K^+ & \Sigma^+ \\ \Psi_{1,-1} = \Xi^- K^0 & \Sigma^- \\ \Psi_{1,0} = (\Xi^0 K^0 + \Xi^- K^+)/\sqrt{2} & \Sigma^0 \\ \Psi_{0,0} = (\Xi^0 K^0 - \Xi^- K^+)/\sqrt{2} & \Lambda^0 \end{array} \qquad (1)$$

If the Coulomb interaction is not taken into account the $\Psi_{1,1}$, $\Psi_{1,-1}$ and $\Psi_{1,0}$ states are energetically degenerate if the Ξ^0 and Ξ^- and K^0 and K^+ masses are equal respectively. Because of the Coulomb interaction the mass of the Σ^0 should be smaller than the mean mass of $\Sigma^\pm$-particles by an amount which depends only on the distance between the Ξ- and K-particles.

If we consider a system consisting of a Ξ-particle and two K-mesons we obtain two groups of states with T = 1/2 and one with T = 3/2:

$$\begin{aligned} &\eta_{1/2,\,1/2} = \Psi_{0,0}\,\varphi_{1/2,\,1/2}, \quad \chi_{3/2,\,1/2} = 3^{-1/2}\Psi_{1,1}\,\varphi_{1/2,\,-1/2} + \sqrt{2/3}\,\Psi_{1,0}\,\varphi_{1/2,\,1/2};\\ &\eta_{1/2,\,-1/2} = \Psi_{0,0}\,\varphi_{1/2,\,-1/2}, \quad \chi_{3/2,\,-1/2} = 3^{-1/2}\Psi_{1,-1}\,\varphi_{1/2,\,+1/2} + \sqrt{2/3}\,\Psi_{1,0}\,\varphi_{1/2,\,-1/2};\\ &\chi_{3/2,\,3/2} = \Psi_{1,1}\,\varphi_{1/2,\,1/2}, \quad \chi_{1/2,\,1/2} = \sqrt{2/3}\,\Psi_{1,1}\,\varphi_{1/2,\,-1/2} - 3^{-1/2}\Psi_{1,0}\,\varphi_{1/2,\,+1/2};\\ &\chi_{3/2,\,-3/2} = \Psi_{1,-1}\,\varphi_{1/2,\,-1/2}, \quad \chi_{1/2,\,-1/2} = 3^{-1/2}\Psi_{1,0}\,\varphi_{1/2,\,-1/2} - \sqrt{2/3}\,\Psi_{1,-1}\,\varphi_{1/2,\,1/2}. \end{aligned} \qquad (2)$$

Here $\varphi_{1/2,1/2}$ and $\varphi_{1/2,-1/2}$ denote the wave functions for K^+ and K^0-mesons.

The states $\eta_{1/2,1/2}$ and $\eta_{1/2,-1/2}$ are to be identified with the proton and neutron in the ground state. Then $\chi_{3/2}$ and $\chi_{1/2}$ are excited nucleon states which appear in the interaction of π-mesons with nucleons.

Thus the structure of the nucleon is as follows:

$$p = K^+ + \Xi^- + K^+ \rightleftarrows K^+ + (\Xi^0 + K^0), \qquad (3)$$

$$n = K^0 + \Xi^0 + K^0 \rightleftarrows K^0 + (\Xi^- + K^+). \qquad (4)$$

The degeneracy of states (3) and (4), which holds when the masses of the K^+ and K^0-meson are equal, is removed by the Coulomb interaction in (3) between the K^+ and Ξ^--particles; this interaction can not be compensated for by the repulsion of the K^+-mesons if the mean distance between these particles is larger than the distance between the K^+ and Ξ^-.

---

*Reported at the All-Union Conference on the Physics of High-Energy Particles, May 22, 1956.

It is easy to see that the new "strangeness" quantum number introduced be Gell-Mann can now be interpreted as the meson charge of the K and Ξ particles which is responsible for the interaction between these particles. In contrast with electric charge, the quanta of the meson-charge field are π-mesons and this change is not conserved in weak interactions occuring 10^{12} times slower than nuclear interactions. As slower than nuclear interactions. As a consequence we have the spontaneous transformation of hyperons into nucleons according to the following scheme:

$$Y \underset{\text{(fast)}}{\rightleftarrows} (Y+\pi+\pi+\ldots) \underset{\text{(slow)}}{\rightleftarrows} (Y+K) \underset{\text{(fast)}}{\longrightarrow} N+\pi.$$

We now consider nucleon disintegration on the basis of the structural schemes in (3) and (4). The disintegration can occur as a result of the absorption of the incident π-meson by a K-meson or Ξ-particle. In the first case the K-meson angular distribution [which we denote by $f_1(\theta)$] should be highly peaked in the forward direction. In the case in which the π-meson is absorbed by the Ξ-particle, the K-meson angular distribution [which we designate by $f_2(\theta)$] should be approximately isotropic with some predominance of the K-mesons emitted in the backward direction.[1] The table lists various nucleon disintegration reactions produced by the absorption of a π-meson. To find the relative weights to be assigned to the ratio of the cross sections for the various reactions we have assumed that the absorption of the π-meson is equally probable in K and Ξ particles.

Reaction	Particle which absorbs the π-meson	Weight for the reaction	Angular distribution
$\pi^- + p \to K^0 + \Lambda^0;\ \Sigma^0$ $K^+ + \Sigma^-$	K^+ or Ξ^0 Ξ^0	$3 + {}^1/_2 = {}^7/_2$ ${}^1/_2$	$6f_1 + f_2$ f_2
$\pi^+ + n \to K^+ + \Lambda^0;\ \Sigma^0$ $K^0 + \Sigma^+$	K^0 or Ξ^- Ξ^-	$3 + {}^1/_2 = {}^7/_2$ ${}^1/_2$	$6f_1 + f_2$ f_2
$\pi^- + n \to K^0 + \Sigma^-$	K^+ or Ξ^0	$1+1=2$	$f_1 + f_2$
$\pi^+ + p \to K^+ + \Sigma^+$	K^0 or Ξ^-	$1+1=2$	$f_1 + f_2$

In work with a beam of 1.3-Bev negative pions it has actually been observed that the K^0-particles produced in the reaction ($\pi^- + p \to K^0 + \Lambda^0;\ \Sigma^0$) exhibit a highly pronounced asymmetry in the forward direction in the center-of-mass system while the angular distribution of the K^+-particles produced in the reaction $\pi^- + p \to K^+ + \Sigma^-$ is relatively isotropic with some predominance in the backward direction.[2]

The system which we have formulated is absolutely stable against decay into light particles if the Ξ-particle is absolutely stable against the analogous process. It is known that the nucleon lifetime is greater than 10^{22} years.[3] From this estimate we can conclude that the lifetime of the Ξ-particle can not be less than 10^8 years since nucleon decay can occur only if the Ξ-particle decay coincides with the decay of one of the K-mesons. The probability of this event is approximately 10^{14} times smaller than the probability of decay of a Ξ-particle. If the Ξ-particle is not the bare core of the nucleon but is itself a system consisting of a heavy hyperon, in whose π-meson field we find n K-mesons, this hyperon can undergo in the free state comparatively rapid decay into light particles. Thus we arrive at the conclusion that the law of conservation of the number of baryons, formulated in the form of a conservation law for nuclear charge, may be completely invalid. In this case there is a possibility of liberating in individual collisions the total energy corresponding to the nucleon mass.

---

[1] J. Schwinger, Phys. Rev. **104**, 1164 (1956).

[2] J. Steinberger, Proceedings of Sixth Rochester Conference on High-Energy Physics, 1956.

[3] Reines, Cowan, and Goldhaber, Phys. Rev. **96**, 1157 (1957).

Translated by H. Lashinsky
38

POLAR THEORY OF METALS

I. Z. FISHER

Belorussian State University

Submitted to JETP editor November 27, 1956

J. Exptl. Theoret. Phys. (U.S.S.R.) 33, 262-264 (July, 1957)

IN the polar model of metals proposed by Vonsovskii one introduces a new parameter of the metal — the degree of polarization s, which can be defined as the ratio of the mean number of "pairs" or "holes" to the total number of valence electrons. In the final analysis the degree of polarization determines all the physical properties of the metal; as yet, however, the theory cannot give the magnitude of this quantity. We give below an estimate of the degree of polarization s, relating this quantity to fluctuations of the electron density in the metal.

We divide the entire metal into equal elementary polyhedra with centers at the interstices of the crystal lattice; let z be the valence of the metal atoms. Interpreting the degree of polarization as the probability of finding a given atom in the "hole" or "pair" state, the mean number and the mean square of the number of electrons in one polyhedron is given by

$$\overline{N} = s(z+1) + s(z-1) + (1-2s)z = z,$$
$$\overline{N^2} = s(z+1)^2 + s(z-1)^2 + (1-2s)z^2 = z^2 + 2s. \tag{1}$$

Whence, for the square of the fluctuation we obtain a value 2s, so that

$$s = {}^1\!/_2\,\overline{(\Delta N)^2}. \tag{2}$$

The degree of polarization of the metal is thus related in a simple way to fluctuations in the density of valence electrons in an elementary polyhedron.

The problem of finding $\overline{(\Delta N)^2}$ is in itself no easier than the problem of determining s directly; however, in the alkali metals we can estimate $\overline{(\Delta N)^2}$ by starting from the free-electron model, since this model is qualitatively valid in these metals. Thus we have[1]

$$\overline{(\Delta N)^2} = 1 + n\iint \nu(|\mathbf{r}_1 - \mathbf{r}_2|)\, dV_1\, dV_2, \tag{3}$$

where $\nu(r)$ is the electron correlation function, n is the mean electron density, and the integration is carried out twice over an elementary polyhedron. The calculations can be simplified by replacing the polyhedron by a sphere of radius $R = (3/4\pi n)^{1/3}$. The unity term in (3) is obtained by substituting $N=1$.

The correlation function for a completely degenerate ideal Fermi gas can be used for $\nu(r)$.[1]

$$\nu(r) = -\frac{1}{4\pi^4 n r^6}\left\{\sin\frac{p_0}{\hbar}r - \frac{p_0}{\hbar}r\cos\frac{p_0}{\hbar}r\right\}^2, \tag{4}$$

where $p_0 = \hbar(3\pi^2 n)^{1/3}$ is the limiting momentum of the Fermi distribution or, using the correlation function for a Fermi gas with allowance for the Coulomb interaction between electrons according to the Debye–Hükkel method,[1]

$$\nu(r) = -(\varkappa^2/4\pi)e^{-\varkappa r}/r, \quad \varkappa^2 = (4me^2/\hbar^2)(3n/\pi)^{1/3}. \tag{5}$$

It is assumed that the positive charge of the metal ions is uniformly distributed over the entire lattice.

In (4) it is apparent that the quantity n can be completely determined by calculation and by direct integration we find $s = 0.4145$. In (5), in the same way, we find[2]

$$s = \frac{1}{4}\left\{1 + \frac{3(x^2-1)}{2x^3} + \frac{3(x+1)^2}{2x^3}e^{-2x}\right\}, \tag{6}$$

where $x = (e/\hbar)(6m/\pi)^{1/2} n^{-1/6} = 2 \times 10^4 n^{-1/6}$. In the alkali metals $x \sim 4$, so that Eq. (6) can be simplified considerably and

$$s = {}^1\!/_4 + 1{,}875\cdot 10^{-5}\cdot n^{1/6}. \tag{7}$$

With $n = 4 \times 10^{22}$ we find $s = 0.361$. Thus, taking into account the electronic Coulomb interaction tends to reduce s.

Although both estimates are somewhat lower than the value $s = 0.5$ proposed by Vonsovskii for alkali metals,[3] they are both still too high. Taking account of the Coulomb interaction between the electrons and ions could reduce the magnitude of s still further; however, a calculation of this effect is impossible within the framework of the Debye–Hükkel approximation. (The calculation itself is not difficult but if one assumes point ions the effect becomes so large that $s < 0$.)

If we assume that the electron gas is not completely degenerate, we must introduce a temperature correction for s in the estimate given above. For example, in (5) we must replace the quantity κ everywhere by $\kappa\{1-(\pi^2/48)(kT/\mu)^2\}$ where μ is the limiting Fermi energy. A simple calculation leads to the expression

$$s(T) = s_0 + 2{,}63\cdot 10^{15}\cdot n^{-7/6}\, T^2. \tag{8}$$

where s_0 is the value of s given before in (7). With $n \sim 10^{22}$ the temperature effect is insignificant although, in principle, the degree of polarization should increase with increasing temperature.

---

[1] L. Landau and E. Lifshitz. Статистическая физика, (Statistical Physics) Gostekhizdat 1951.
[2] I. Z. Fisher, J. Exptl. Theoret. Phys. (U.S.S.R.) **22**, 520 (1952).
[3] S. V. Vonsovskii, Usp. Fiz. Nauk **48**, 239 (1952).

Translated by H. Lashinsky
39

PROBABILITY FOR CHARGE EXCHANGE IN NUCLEONS WITH ENERGIES OF $3\times10^9-10^{10}$ ev IN INTERACTIONS WITH AIR NUCLEI

V. A. VOROBIEV

Institute for Applied Geology, Academy of Sciences, U.S.S.R.

Submitted to JETP editor October 5, 1956; resubmitted April 2, 1957

J. Exptl. Theoret. Phys. (U.S.S.R.) 33, 264-265 (July, 1957)

IN the last several years a number of papers have been published in which the authors, investigating nuclear-cascade showers in cosmic rays, have reached the conclusion that in the interaction of high-energy nucleons (several Bev and higher) with air nuclei, the main part of the energy (about 70 percent) in the stars which are produced is carried off by one of the emitted nucleons, which in turn also produces stars.[1,2] It is of interest to examine the dependence of the charge of this nucleon on the charge of the incoming nucleon.

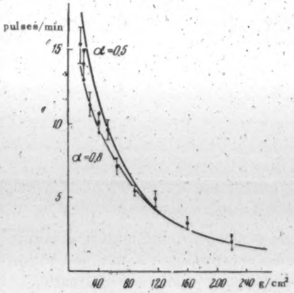

We shall assume that protons and neutrons with the energies in question ($3\times10^9-10^{10}$ ev) interact with air nuclei in the same way. We shall denote the probability of charge exchange for a high-energy nucleon in collision with an air nucleus by the quantity $1-\alpha$, i.e., α is the probability that the main energy of the star produced by the proton (neutron) is carried away by a nuclear-active proton (neutron). We neglect deviations from the direction of the primary nucleon. Then the cascade equations which describe the nucleon history can be solved rather simply if it is assumed that the nucleon energy spectra are independent of depth. The latter assumption is in satisfactory agreement with the experimental data obtained in investigations of high-energy cosmic rays.

Depth	$\alpha=0.5$	$\alpha=0.8$	Experiment
0.9	0.6	0.4	0.35 ± 0.1[4] 0.45 ± 0.2[6]
11	0.99	0.91	0.83 ± 0.1[5] 0.72 ± 0.15[6]

We denote the flux of primary particles incident on the boundaries of the atmosphere by $i_0(E)$. Then the dependence of the global proton flux P(E, x) and neutron flux N(E, x) on the depth x assumes the following form

$$P(E,x)={}^1/_2\, i_0(E)\,[\mathscr{E}_1(\mu x)+\mathscr{E}_1(\eta x)],\quad N(E,x)={}^1/_2\, i_0(E)\,[\mathscr{E}_1(\mu x)-\mathscr{E}_1(\eta x)]$$

(x is expressed in units of free path $\approx 60\ \mathrm{g/cm^2}$) where $\eta=1-(2\alpha-1)(1-\mu)$ and $\mathscr{E}_1$ is the Gol'dovskii integral. The absorption coefficient μ, found from numerous experiments, is approximately $60\ \mathrm{g}\times\mathrm{cm}^{-2}/120\ \mathrm{g}\times\mathrm{cm}^{-2}=0{,}5$. The presence of multiply-charged nuclei in primary cosmic radiation (chiefly He) tends to increase the number of protons and neutrons by an amount which is independent of α and equal to

$$\xi a i_0(E)\,[\mathscr{E}_1(\mu x)-\mathscr{E}_1(\xi x)]/(\xi-\mu),$$

where $a \approx 0.2-0.3$ and $\xi \approx 60/45$.

The quantity α can be determined from the results of two independent series of experiments. The first is the direct investigation of the absorption of high-energy protons or neutrons as a function of depth at great heigths; the second is the change in the ratio of the number of stars produced by neutrons and protons as a function of height.

In the figure we compare the calculated flux of charged high-energy particles with $\alpha = 0.5$ and $\alpha = 0.8$ and the experimental data[3] taking account of the geometry in approximate fashion. However, the experimental accuracy is not sufficient for a reliable determination of α. More definite results can be obtained from photoemulsion experiments. The Table lists the results of experiments[4-6] and our calculations for the ratio of the number of stars produced by neutrons and multiply-charged particles to the number of stars produced by protons. It is apparent from the table that α is 0.7—0.8 rather than the usually assumed value of 0.5. More exact measurements will be required, however, before definite conclusions can be reached.

---

[1] N. L. Grigorov and V. Murzin, Izv. Akad Nauk SSSR Ser. Fiz **17**, 21 (1953).
[2] G. T. Zatsepin, J. Exptl. Theoret. Phys. (U.S.S.R) **19**, 1104 (1949).
[3] S. N. Vernov and T. N. Charakhch'ian, Dokl. Akad. Nauk SSSR **69**, 629 (1949).
[4] U. Camerini et al., Phil. Mag. **42**, 1241 (1952).
[5] G. D. Rochester, Rep. Prog. Phys. **14**, 227 (1951).
[6] K. F. Powell and V. Camerini, Usp. Fiz. Nauk **40**, 76 (1950).

Translated by H. Lashinsky
40

REMARKS ON THE MULTIPLICATIVE RENORMALIZATION GROUP IN THE QUANTUM THEORY OF FIELDS

V. Z. BLANK,* V. L. BONCH-BRUEVICH, and D. V. SHIRKOV

Moscow State University

Submitted to JETP editor January 11, 1957

J. Exptl. Theoret. Phys. (U.S.S.R.) **33**, 265-266 (July, 1957)

In papers by Bogoliubov and one of us[1-3] an examination had been made of the renormalization group in quantum electrodynamics and meson dynamics. In these papers the group relations were obtained within the framework of perturbation theory. Having in view the practical usefullness of the renormalization method, it is of interest to obtain the group relations without the use of a series expansion → directly from the Schwinger equation for the Green's function. This approach is all the more important because it makes possible a true picture of the origin of the renormalization group. We shall see that the latter is not necessarily connected with the existence of a divergence and can occur in "finite" theories, for example, in the theory of the electron-photon field in a solid body.

We consider a quantum field in which the interaction Lagrangian (in the interaction representation) is of the form ($\hbar = 1$)

$$L(x) = \{g\bar{\psi}(x)\Gamma_0\psi(x) + J(x)\}A(x). \tag{1}$$

Here g is the coupling constant, $\bar{\Psi}$, Ψ and A are Fermi and Bose operators, Γ is the "elementary" vertex part, $x = \{\mathbf{x}, x_0\}$, and J is the "external current." The tensor dimensionality of Γ_0, J and A are not specified; we may note only that A may contain coordinate derivatives of the elementary Bose-field operators. The contractions of the free fields, the total Green's function, and the vertex part are determined by the relations*

---

*Deceased

$$G_0(x, y) = i\langle T\{\psi(x)\bar{\psi}(y)\}\rangle_0, \quad D_0(x, y) = i\langle T\{A(x)A(y)\}\rangle_0 \tag{2}$$

$$G(x, y) = i\langle T\{\psi(x)\bar{\psi}(y)S\}\rangle_0 / \langle S\rangle_0, \tag{3}$$

$$D(x, y) = \delta a(x)/\delta J(y); \quad \Gamma(x, y, z) = \delta G^{-1}(x, y)/\delta[ga(z)], \quad a(x) = -i\delta \ln\langle S\rangle_0/\delta J(x). \tag{4}$$

In this case the Green's function equations become (they are easily derived, for example, by the method developed by Polivanov[4]):

$$G = G_0 + ig^2 G_0\Gamma_0 G\Gamma DG + gG_0G\Gamma_0 a, \tag{5}$$

$$D = D_0 - ig^2 D_0\Gamma_0 G\Gamma GD. \tag{6}$$

It is immediately obvious that Eqs. (5) and (6) are invariant under the following multiplicative transformation of the quantities which appear in them:

$$G \to z_2 G, \quad D \to z_3 D, \quad \Gamma \to z_1^{-1}\Gamma; \quad g \to z_2^{-1} z_3^{-1/2} z_1 g. \tag{7}$$

Here z_1, z_2 and z_3 are continuous finite parameters; it should be kept in mind that we are transforming not only the total functions G, D and Γ but also the elementary functions G_0, D_0 and Γ_0. The relations given in Eq. (7) determine in general form the renormalization group in the quantum theory of fields with an interaction Lagrangian of the form in (1).

It should be kept in mind, however, that if the theory includes additional conditions (such as gradient invariance in quantum electrodynamics), some of the constants which appear in Eq. (7) may be interrelated. Thus, for example, in a gradient transformation of the electromagnetic field potentials the fermion Green's functions transforms according to[5]

$$G(x, y) \to G(x, y)\exp(ig^2\{F(x-y) - F(0)\}), \quad F(x) = (2\pi)^{-4}\int e^{ikx} d_l^{(0)}(k)\frac{dk}{(k^2)^2}, \tag{8}$$

where the function $d_l^{(0)}(k)$ determines the longitudinal matching; it is apparent that F transforms in the same way as D. The invariance condition for this relation with respect to a transformation of a type given in (7) yields

$$z_1 = z_2. \tag{9}$$

The relation given in (8) is nothing else than Ward's identity. In this case the relations given in (7) become the well-known renormalization group of quantum electrodynamics.

Thus, the renormalization group actually expresses only the "self-similarity" property of the Schwinger equations. In conclusion we may note that similar analysis can be carried out in theories with an interaction Lagrangian different from that given in (1).

---

[1] N. N. Bogoliubov and D. V. Shirkov, Dokl. Akad. Nauk SSSR **103**, 203, 391 (1955).

[2] D. V. Shirkov, Dokl. Akad. Nauk SSSR **105**, 972 (1955).

[3] N. N. Bogoliubov and D. V. Shirkov, Nuovo cimento **3**, 845 (1956).

[4] M. K. Polivanov, Dokl. Akad. Nauk SSSR **100**, 1061 (1955).

[5] A. V. Svidzinskii, Dissertation, L'vov University (1955).

Translated by H. Lashinsky
41

---

*As is customary, the Green's functions and vertex part considered here do not contain divergences. They are either finite at the outset (in the case of a solid) or the divergences are removed by an appropriate subtraction procedure.

RADIO-FREQUENCY METHOD FOR MEASURING THE MASS OF RELATIVISTIC ELECTRONS

V. N. LAZUKIN

Moscow State University

Submitted to JETP editor January 31, 1957

J. Exptl. Theoret. Phys. (U.S.S.R.) 33, 267-269 (July, 1957)

THE Einstein-Lorentz formula

$$m = m_0 (1 - \beta^2)^{-1/2}, \tag{1}$$

which describes the velocity dependence of the mass of a moving body has been tested experimentally many times.[1-6] It is usually maintained that Eq. (1) has been verified, with a high degree of accuracy, both by these direct experiments and by certain indirect conclusions based on analyses of accelerator operation. Although there is no reason, at the present time, to doubt relativity theory and its consequences, it cannot be said that the validity of the formula given above has been established absolutely.

Without exception, all efforts at the direct verification of Eq. (1) have met with serious difficulties. An analysis of the most accurate measurements indicates that Eq. (1) has not been rigorously verified; indeed, it is impossible, on the basis of these data, to make a choice between Eq. (1) and, say, the Abraham formula.[7] A similar critical analysis of these experiments has recently been carried out by Farago and Janossy[8] in work as yet unpublished to the best of our knowledge. These authors conclude that measurements of electron mass carried out up to this time can not be used to verify Eq. (1) since even the most accurate experiment has inherent errors which are comparable to the difference in mass which results from the use of Eq. (1) and the Abraham formula. Without dwelling on the remarks of these authors concerning possible deviations from Eq. (1) and the effect of these deviations in certain theoretical problems, we wish to emphasize the desirability of further attempts to verify Eq. (1) by present-day methods. In this connection it is interesting to discuss the possibilities offered by electron-physics techniques. The high sensitivity and accuracy of radio-frequency techniques indicate that it should be possible to measure the mass of electrons over a wide region of velocities with an accuracy exceeding the accuracy of the well-known methods. This type of experiment can be carried out using a scheme very similar to that employed in radio-frequency mass-spectrometers based on the application of the cyclotron resonance or the diamagnetic resonance of charged particles.

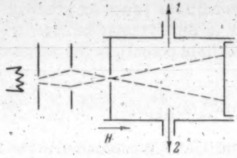

FIG. 1. Diagram of an experiment for measuring relativistic masses in the range $0 \leq \beta < 0.7$. (1) to UHF generator, (2) to detection system.

Suppose that a diverging electron beam (Fig. 1) with a given energy enters a cylindrical resonator in which transverse electric oscillations are excited (for example TE_{01} or TE_{11} mode). Because of the fixed magnetic field H, parallel to the axis of the resonator, the electrons in the resonator move in an helical trajectory, the radius and pitch of which are respectively:

$$\rho = mv_{\perp} c/eH; \; l = v_{\parallel} T, \tag{2}$$

where $v_{\perp}$ and $v_{\parallel}$ are respectively the velocity components perpendicular and parallel to the H field while T is the period of the high-frequency field in the resonator. When the field frequency coincides with the cyclotron frequency resonance absorption of the high-frequency power occurs; this effect can be observed by ordinary radio-frequency spectroscopy methods. Using the values of ν and H at which strong absorption is observed, it is possible to calculate the mass with an accuracy which is limited only by the accuracy with which these two quantities can be measured.

In principle the above scheme can be used to measure the mass of electrons with any energy; in practice, however, this scheme is usless for values of β greater than 0.6—0.7. It follows from Eq. (2) that fixed value of H the diameter and length of the resonator must be increased in proportion to $\beta \sqrt{1-\beta^2}$ and β respectively; an increase in these dimensions requires a larger homogeneous field and leads to greater losses in the walls of the resonator. Hence this arrangement becomes exceedingly cumbersome and less sensitive at high electron velocities ($\beta > 0.7$).

It would appear that there are greater potentialities in a system based on the so-called inverse cyclotron; this scheme is somewhat more difficult but still realizable in practice (Fig. 2).

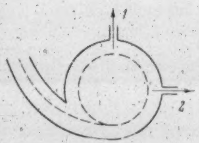

FIG. 2. Diagram of an experiment for measuring relativistic masses in the range $0 < \beta \leq 1.0$; the magnetic field is perpendicular to the plane of the diagram. (1) to UHF generator, (2) to detection system.

A half-wave cylindrical (or coaxial) resonator, in which H is paralled to the axis, is placed in a homogeneous field between the pole pieces of an electromagnet. An electron beam, accelerated to any desired value of β (up to $\beta \approx 1$), is introduced into the resonator through a narrow slit in the cylindrical wall. Inside the resonator the electrons move along a spiral, which asymptotically approaches the periphery as the field gradient falls off.

The merit of both schemes is approximately the same; specifically, both can be used to measure the mass of the electron at practically zero values of β. Assuming that an accuracy of 10^{-4}–10^{-5} is easily attainable in the measurements of ν and H, the electron mass should be determined with an error of less than 0.01 percent. This accuracy makes it possible to detect a relativistic change in mass corresponding to an energy variation of the order of a hundred electron volts. It is apparent that good results can be obtained only by achieving narrow resonance lines. In this sense the second scheme is preferable to the first.

Equations (1) can be verified using the above scheme without measurements of the absolute values of the frequency or accelerating potential; if Eq. (1) holds, the relation $\Delta T = (2\pi/cH)\Delta U$, which expresses the change in frequency as a function of the corresponding potential change, also holds true. To verify the above relation we require only the appropriate stability of the field H and accurate measurements of ΔU. These requirements are easily satisfied.

The intensity of the resonance line, a quantity which is extremely important from the point of view of realizing the best signal to noise ratio, is determined basically by two factors: the charge density of the beam and the ratio of the electron time-of-flight in the resonator to the period of the high-frequency field; if either of these quantities increases the intensity also increases. It is undesirable to increase the current strength of the beam because of possible effects on the width of the resonance line and undesirable secondary effects, namely x-ray radiation and resonator heating. Hence, it is more expedient to increase the number of orbits traversed by an electron in the resonator before it is no longer affected by the effect in question.

There are two effects which might complicate the experiment being discussed: (a) radiation from fast electrons in the magnetic field, which can broaden the resonance line and lead to (in the case in which the electrons move in a volume bounded by conducting walls) the appearance of spurious lines and (b) the effect of the electric field in the resonator on the cyclotron resonance absorption frequency. It has been shown experimentally and theoretically that the intensity of the indicated radiation is inconsequential up to energies of several megavolts and that its effect on the resonance line can be neglected. However, the effect of the electric field on frequency must be taken into account; this correction can be evaluated by measurements at two neighboring frequencies at two values of the magnetic field with the same accelerating potential.

The author is indebted to Ia. P. Terletskii for calling his attention to Ref. 8 and for many valuable discussions.

---

[1] W. Kaufmann, Ann. Physik **19**, 487 (1906).

[2] A. Bucherer, Ann. Physik **28**, 585 (1909); **30**, 974 (1909); Physik. Z. **9**, 755 (1908); Ber. deut. physik Ges. **6**, 688 (1908).

[3] Guye, Ratnowsky, and Lavanchy, Mem. Soc. Phys. Genev. **39**, 6, 273 (1921).

[4] R. A. R. Tricker, Proc. Roy. Soc. (London) **A109**, 384 (1925).

[5] C. T. Zahn and A. H. Spees, Phys. Rev. **53**, 357 (1938).

[6] E. J. Williams. Phys. Rev. **58**, 292 (1940).

[7] M. Abraham. Ann. Physik **10**, 105 (1905); Physik. Z. **5**, 576 (1904).

[8] P. Farago, Janossy. Review of the Experimental Evidence for the Law of Variation of Electron Mass with Velocity. Budapest, 1956.

Translated by H. Lashinsky
42

GENERALIZATION OF GAUGE INVARIANCE AND COMBINED INVERSION

V. L. POKROVSKII

West-Siberian Branch, Academy of Sciences, U.S.S.R.

Submitted to JETP editor February 15, 1957

J. Exptl. Theoret. Phys. (U.S.S.R.) 33, 269-271 (July, 1957)

At the present time it is generally believed that certain particles (π-mesons, K-particles, hyperons, etc.) can exist in different charge states. The appropriate wave functions may be written in the form

$$\psi = \sum_Q c_Q \psi_Q, \tag{1}$$

where ψ_Q is the wave function associated with the state with charge Q and the summation is taken over all possible values of the charge (including zero). A description of particles of this type requires an extension of the notion of gauge invariance. In particles which exist in only one charge state a gauge transformation leads to the multiplication of the wave functions by a trivial phase factor $e^{i\alpha Q}$. In the general case (1) the gauge transformation is obviously given by the formula

$$\psi' = \sum_Q c_Q e^{i\alpha Q} \psi_Q. \tag{2}$$

We may note that the function ψ' depends parametrically on α.

The invariance requirement for infinitely small gauge transformations (2) leads to the law of conservation of charge; this relation is written in the form of the continuity equation for electric current:

$$j_\mu = \sum_Q Q c_Q c_Q^* (\psi_Q^* \Gamma_\mu \psi_Q - \psi_Q \Gamma_\mu \psi_Q^*). \tag{3}$$

Here, we have used the orthogonality of the different charge states ψ_Q and the usual Lagrangian, which gives a first order equation for the wave functions ψ. We may note that the current j_μ is independent of the parameter α, as is to be expected.

Charge conjugation

$$\psi'_Q = \psi_{-Q} \tag{4}$$

in the theory of particles which have only one charge state is defined so as to make the current and charge change sign. In the theory of bosons, with several charge states, the following transformation must be carried out for a change of sign of the current and charge.

$$\psi'_Q = \psi_{-Q}; \quad c'_Q = c_{-Q}, \tag{5}$$

for the case of a single charge state this expression leads to Eq. (4). We may note that charge conjugation (5) is equivalent to the transformation $\alpha' = -\alpha$.

As is well known, the wave functions of particles which exist in only one charge state can be subjected to a gauge transformation in which α is an arbitrary function of the coordinates. In the extension of this transformation to the general case (1) the parameter α is replaced by the quantity α' which is an arbitrary function of coordinates and, in general, the parameter α:

$$\alpha' = f(x, \alpha). \tag{6}$$

In a theory of particles which are free to assume different charge states we must require invariance under generalized gauge transformations (6) and the Lorentz group

$$x' = Lx. \tag{7}$$

In this connection the problem arises of assigning the transformation laws for quantities which are transformed by (6) and (7), which we will call the general group.

Let $f(x, \alpha)$ be an arbitrary numerical function of coordinates x and the parameter α. Then, under transformations of the general group, the quantity $\partial f/\partial\alpha'$ is a linear function of the quantities $\partial f/\partial\alpha$ and $\partial f/\partial x_k$. Hence, we will define a tensor of the general group as a quantity that transforms like products of $\partial f/\partial x_k$ and $\partial f/\partial\alpha$. The quantity $\partial f/\partial\alpha$ appears in the theory since $-i\partial/\partial\alpha$ is essentially the charge operator.

Any tensor of the general group transforms as:

$$T_{\underbrace{0\ldots 0}_{s}\, i\ldots k} \sim (\partial f/\partial\alpha)^s (\partial f/\partial x_i) \ldots (\partial f/\partial x_k). \tag{8}$$

In particular, in tensor analysis of the general group there is a totally anti-symmetric "tensor," one component of which we designate by ϵ. It is well known that in the transformations of the general group it is multiplied by Jacobian J of the transformation. Furthermore, from a tensor of the second rank T we can form $\det T$ which under transformations of the general group is multiplied by the square of the Jacobian J^2. Hence, a quantity of the type

$$P = \epsilon/\sqrt{\det T}$$

is multiplied by the sign of the Jacobian under transformation of the general group and plays the rôle of a pseudoscalar of the general group.

In the theory of particles which exist in only one charge state we require invariance under the Lorentz group with positive Jacobian and under infinitely small gauge transformations; from this requirement follows conservation of charge. In the theory considered here this requirement is extended in a unique manner: it becomes a requirement for invariance under transformations of the general group with positive Jacobian.

If we require from the theory invariance under transformations of the general group with any sign of the Jacobian, the Lagrangian must be a scalar with respect to the general group. However, experiments on K-meson decay indicate that in decays of this type the theory need not be invariant under space inversion, i.e., under the transformation $x' = -x$, $\alpha' = \alpha$. Whence it follows that in a theory which describes K-mesons we cannot require invariance under the transformations of the general group with negative Jacobian. In this theory the Lagrangian must be the sum of two terms: a gauge scalar and a gauge pseudoscalar $L = S + P$. Thus the Lagrangian will not be invariant under the transformation $\alpha' = -\alpha$, i.e., under charge conjugation the sign of P is changed.

Thus, we may formulate the following general statement. A theory which is not invariant under a change of the orientation of space directions will not be invariant under a change of the sign of the charge. However, such a theory is invariant with respect to the Landau combined inversion, i.e., under the simultaneous transformations $\mathbf{x}' = -\mathbf{x}$ and $\alpha' = -\alpha$.

We now see that the combined inversion hypothesis, suggested by Landau, is equivalent to the requirement that the theory be invariant with respect to the group of generalized gauge transformations with positive Jacobian.

Translated by H. Lashinsky
43

DIFFERENTIAL CROSS SECTION FOR PHOTOPRODUCTION OF π-MESONS ON NUCLEONS TAKING ACCOUNT OF d-STATES

N. F. NELIPA

P. N. Levedev Physics Institute, Academy of Sciences U.S.S.R.

Submitted to JETP editor February 16, 1957

J. Exptl. Theoret. Phys. (U.S.S.R) 33, 271-273 (July, 1957)

1. A wealth of experimental data has been obtained recently on the angular distribution of mesons* produced by photons on nucleons (cf. for example Refs. 1 and 2). To interpret the experimental data it is necessary to have a theoretical expression for the differential cross section $\sigma_p(\vartheta)$ for photoproduction of mesons on nucleons. Since there is, at the present time, no consistent analysis by which this problem can be examined, special interest attaches to those methods which are based on general considerations. Using two such relations – conservation of momentum and conservation of parity – expressions for $\sigma_p(\vartheta)$ have been obtained by various methods in several papers.[3-5]

In the present note we wish to call attention to a more refined expression for the meson-photoproduction differential cross section in nucleons[6] (details are given in Ref. 2). Using this expression we have calculated $\sigma_p(\vartheta)$ for cases in which mesons are produced in s-, p- and d-states. This formula contains as particular cases all the expressions for $\sigma_p(\vartheta)$ (without d-states) which have been obtained earlier.[4,5] Using this expression for $\sigma_p(\vartheta)$ it is possible to compute the relative yield due to the d-state in meson production at various photon energies and to establish the γ-ray energies for which this process must be taken into account. The interest in this analysis is explained by the fact that the experimental data[1,2] indicate the necessity for taking account of meson production in the d-state even at energies $E_\gamma \leq 300$ Mev.

Transition	L	j'	l'
E_{11}	1	$^1/_2-$	0
E_{13}	1	$^3/_2-$	2
M_{11}	1	$^1/_2+$	1
M_{13}	1	$^3/_2+$	1
E_{23}	2	$^3/_2+$	1
M_{23}	2	$^3/_2-$	2
M_{25}	2	$^5/_2-$	2
E_{35}	3	$^5/_2-$	2

2. We now consider the photoproduction of mesons in s-, p- and d-states. All the possible transitions associated with this process are given in the table. The symbols in the first column denote the matrix elements of the corresponding transitions; E denotes an electric transition while M denotes a magnetic transition.

If one takes account of all the transitions which have been enumerated and the interference between them, the photomeson angular distribution in the center-of-mass system is written as follows:†

$$\begin{aligned}
\frac{1}{2N}\sigma_p(\vartheta) &= P_0(\cos\vartheta)\,[\,|E_{11}|^2 + 2|E_{13}|^2 + |M_{11}|^2 + 2|M_{13}|^2 + 2|E_{23}|^2 + 2|M_{23}|^2 + 3|M_{25}|^2 + 3|E_{35}|^2] \\
&+ P_1(\cos\vartheta)\,\mathrm{Re}\Big[-2E_{11}^*M_{11} + 2E_{11}^*M_{13} + 2\sqrt{3}\,E_{11}^*E_{23} - 2E_{13}^*M_{11} + 2E_{13}^*M_{13} - 0.692\,E_{13}^*E_{23} + 2\sqrt{3}\,M_{11}^*M_{23} \\
&+ 0.692\,M_{13}^*M_{23} + \frac{18\sqrt{3}}{5}M_{13}^*M_{25} - 1.2\,E_{23}^*M_{23} + 6.77\,E_{23}^*E_{35} + 1.2\,E_{23}^*M_{25}\Big] + P_2(\cos\vartheta)\Big\{-|E_{13}|^2 - |M_{13}|^2 + |E_{23}|^2 \\
&+ |M_{23}|^2 + 1.711\,|M_{25}|^2 + \frac{18}{7}|E_{35}|^2 + \mathrm{Re}\Big[2E_{11}^*E_{13} - 2\sqrt{3}\,E_{11}^*M_{23} + 3.462\,E_{11}^*M_{25} + 4.884\,E_{11}^*E_{35} - 2\sqrt{3}\,E_{13}^*M_{23} \\
&+ 3.46\,E_{13}^*M_{25} - 1.399\,E_{13}^*E_{35} - 2M_{11}^*M_{13} - 2\sqrt{3}\,M_{11}^*E_{23} - 2M_{11}^*M_{13} + 2\sqrt{3}\,E_{23}M_{13} + \frac{6}{7}M_{23}^*M_{25} - 2.423\,M_{23}^*E_{35} \\
&+ 2.424\,M_{25}^*E_{35}\Big]\Big\} + P_3(\cos\vartheta)\,\mathrm{Re}\Big[4.148\,E_{13}^*E_{23} - 3.453\,M_{11}^*M_{25} - 4.894\,M_{11}^*E_{35} - \frac{12\sqrt{3}}{5}M_{13}^*M_{23} - 2.772\,M_{13}^*M_{25} \\
&+ 4.87\,M_{13}^*E_{35} - \frac{24}{5}E_{23}^*M_{23} + \frac{24}{5}E_{23}^*M_{25} + 1.692\,E_{23}^*E_{35}\Big] + P_4(\cos\vartheta)\,\{-1.707\,|M_{25}|^2 + 0.426\,|E_{35}|^2 \\
&+ \mathrm{Re}\,[6.301\,E_{13}^*E_{35} - 6.835\,M_{23}^*M_{25} - 6.056\,M_{23}^*E_{35} + 6.013\,M_{25}^*E_{35}]\},
\end{aligned} \tag{1}$$

where $P_n(\cos\vartheta)$ is the Legendre polynomial; $N = 1/16k^2$ and k is the photon wave number. It can easily be shown that if all transitions associated with the production of mesons in the d-state are neglected (that is, if we set $E_{13} = M_{23} = M_{25} = E_{35} = 0$ the expression in (1) goes over to the expression for $\sigma_p(\vartheta)$

---

*In what follows the term meson will always mean π-meson.

†The calculations are simplified considerably if use is made of the tables of numerical values for the Racah coefficients[8] and the Z coefficients.[9] These coefficients are considered in greater detail in Ref. 7.

obtained earlier* [cf. Ref. 10, Eq. (27)]. Similarly, we can obtain the particular forms for $\sigma_p(\vartheta)$ found by Feld.[4]

3. An analysis of the experimental data on the angular distribution of mesons produced by photons on nucleons in the energy region $E_\gamma \leq 400$ Mev has been carried out in a paper by Watson et al. (this work is considered in greater detail in Ref. 2). This analysis has shown that in the indicated energy region it is impossible to obtain good agreement between the theory and the experimental data if meson production in only s- and p-states is taken into account. In this connection it would be of interest to analyze the indicated experimental data using the method used in Ref. 1 but taking account of meson production in d-states using the expression given in (1).

In conclusion the author wishes to express his gratitude to M. A. Markov for discussion of this material.

[1] Watson, Keck, Tollestrup and Walker, Phys. Rev. **101**, 1159 (1956).

[2] N. F. Nelipa, Usp. Fiz. Nauk (in preparation).

[3] K. A. Ter-Martirosian, J. Exptl. Theoret. Phys. (U.S.S.R.) **21**, 895 (1951).

[4] B. T. Feld, Phys. Rev. **89**, 330 (1953).

[5] K. M. Watson, Phys. Rev. **95**, 228 (1954).

[6] Morita, Sugie and Yoshida, Prog. Theor. Phys. **12**, 713 (1954).

[7] Biedenharn, Blatt and Rose, Rev. Mod. Phys. **24**, 249 (1954).

[8] Simon, Vander Sluis and Biedenharn, Oak Ridge National Laboratory, ORNL-1679 (1955).

[9] L. C. Biedenharn, Oak Ridge National Laboratory, ORNL-1501 (1953).

[10] M. Gell-Mann and K. Watson, Usp. Fiz. Nauk **59**, 399 (1956); [Annual Review of Nuclear Sciences **4**, 219 (1954)].

Translated by H. Lashinsky
44

---

*It is necessary to make the following substitutions for the unknown matrix elements $E_{11} \to E_{11}$, $M_{11} \to -M_{11}$, $M_{13} \to -M_{13}$, $E_{23} \to E_{23}/2\sqrt{3}$.

PHASE OF A SCATTERED WAVE

F. S. LOS'

Submitted to JETP editor February 16, 1957

J. Exptl. Theoret. Phys. (U.S.S.R.) **33**, 273-274 (July, 1957)

WE consider here the application of one form of the method of variation of constants for determining the phase of the scattered wave in a spherically-symmetric one-particle problem in quantum mechanics. We have the equation

$$d^2G/d\rho^2 + [1 - l(l+1)/\rho^2 - U(\rho)]\,G = 0, \tag{1}$$

where $l = 0, 1, 2\ldots$, while $U(\rho)$ satisfies the condition $\int^{\infty} U(\rho)\,d\rho < C$ and may be given as $U(\rho) = \gamma(\rho)/\rho$, where $\gamma(\rho) = \gamma_0 + \gamma_1\rho + \ldots$.

We seek a solution of Eq. (1) which may be represented in the following form when $\rho \to 0$

$$G = A_0\rho^{l+1} \tag{2}$$

and which takes on the following asymptotic form at large values of ρ

$$G = \text{const}\cdot\sin\left(\rho - \frac{\pi l}{2} + \delta_l\right); \quad \delta_l = \text{const}. \tag{3}$$

If we try a solution of Eq. (1) in the form

$$G = A(\rho)\sin(\rho + \delta(\rho)) \tag{4}$$

imposing the additional condition

$$dG/d\rho = A(\rho)\cos(\rho + \delta(\rho)), \tag{5}$$

on the functions $A(\rho)$ and $\delta(\rho)$, we obtain from Eq. (1), in view of Eqs. (4) and (5), the following expressions for $A(\rho)$ and $\delta(\rho)$:

$$dA/d\rho = A[l(l+1)\rho^{-2} + U(\rho)]\sin(\rho+\delta)\cos(\rho+\delta), \tag{6}$$

$$d\delta/d\rho = -[l(l+1)\rho^{-2} + U(\rho)]\sin^2(\rho+\delta). \tag{7}$$

We may note that since $d\ln G/d\rho = \cot[\rho + \delta(\rho)]$, in view of Eq. (2), when $\rho \to 0$

$$\sin(\rho + \delta(\rho)) = \rho/(l+1). \tag{8}$$

Using the last expression and Eq. (7) we find

$$\delta(\rho) = -\frac{l}{l+1}\rho - \frac{1}{(l+1)^2}\int_0^\rho \rho\gamma(\rho)\,d\rho.$$

Using Eq. (8) we find the following expression from Eq. (6):

$$A(\rho) = A_0\rho^l(1 + \gamma_0\rho/(l+1) + \ldots),$$

which applies for values of ρ close to zero.

If the limitations imposed on the function $U(\rho)$ are satisfied it is obvious that

$$\delta(\rho) \to -\pi l/2 + \delta_l \quad \text{for} \quad \rho \to \infty.$$

It should be noted that in the case $\gamma(\rho) = \gamma_0$, in view of the fact that $\sin^2(\rho + \delta)$ is bounded, it follows from Eq. (7) that at large values of ρ

$$\delta(\rho) = -\pi l/2 + \delta_l - \alpha\ln\rho,$$

where α is a constant.

Because of the monotonic variation of $\delta(\rho)$ at large values of ρ it is possible to integrate Eqs. (6) and (7) numerically with high accuracy and to determine the quantity δ_l – the phase of the scattered wave. It is obvious that this form of the method of variation of arbitrary constants can be easily extended to the case in which the function $U(\rho)$ is complex.

Translated by H. Lashinsky
45

NUCLEAR SUBSHELLS AND DEFORMATION IN THE REGION PAST LEAD

N. N. KOLESNIKOV and A. P. KRYLOVA

Moscow State University

Submitted to JETP editor March 11, 1957

J. Exptl. Theoret. Phys. (U.S.S.R.) 33, 274-277 (July, 1957)

NUCLEAR deformation causes a change in the shape of the nuclear potential well. As a result the usual sequence for filling levels, described by Mayer,[1] becomes inaccurate and the scheme proposed by Nilsson must be employed.[2] An interesting feature is the fact that nuclear deformation is not a gradual effect; rather, it is found that the onset of deformation occurs suddenly at certain critical nucleon numbers. There is a sharp increase in deformation in the region of the lanthanides after $N = 88$. There is evidence that the collective properties of the nuclei become important at $Z = 64$.[3] The reverse trend, that from highly-deformed nuclei to spherically-symmetric nuclei, is not so sharp (this change probably takes place at $N = 112$ and $Z = 74$[3]). The sudden depression of the lowest levels, which are of rotational character, after $Z = 86$ indicates that the abrupt increase in deformation in the region of the heavy nuclei sets in after $Z = 86$.[4]

At the present time the scheme by which the levels are filled in the heavy-nucleus region has not been determined. The energy classification of α-decay indicates the presence of irregularities at $N = 152$[5] and, to a lesser extent, at $Z = 96$ but it is still not clear whether or not these numbers are to be associated with a nuclear deformation effect. We have set ourselves the problem of determining: a) with which N and Z numbers nuclear deformation effects are to be associated, b) whether or not any of the subshells are filled in the heavy-nucleus region, c) the energy associated with filling of the subshells and the effect of deformation.

We consider this problem from the point of view of energetics, assuming at the outset, that any irregularity effects are to be associated only with an even number of protons or neutrons. For this purpose we compare the energy increments required to add neutrons and protons. We are interested not in the absolute values of the energy increments for adding neutrons but in their difference. Provisionally we assume that no energy is required for adding neutrons in the nuclei Pu^{238} and Pu^{239} and assume that the difference is 0.2 Mev in Pu^{240} and Pu^{241}. Using the energetics of $\alpha - n$ and $\beta - n$ chains[6] we have calculated the energy involved in adding neutrons to almost all the known heavy nuclei.[7] As has already been indicated by one of us,[8] the energy $E_n(A^*, N)$ required for adding a neutron to a fictitious nucleus (A^*, N), lying on the β-stability curve Z^*, is in general different from the energy $E_n(A, N)$ required to add a neutron to another nucleus with the same number of neutrons N (but naturally with a different number of protons Z and which does not lie on the Z^* curve) by an amount which is proportional to $Z - Z^*(A)$:

$$E_n(A^*, N) = E_n(A, Z) - \alpha\{Z - Z^*(A)\}, \qquad (1)$$

where $\alpha = 0.425$ Mev and $Z^*(A)$ is the value of the fictitious isobar which can have the smallest mass for a given A. In the region of heavy nuclei, which is being considered here, the dependence of Z^* on A is given approximately by the empirical formula[8]

$$Z^* = 0.356\,A + 9.1, \qquad (2)$$

not taking account of the small fluctuations that odd-even effects and periodic effects produce in the empirical curve $Z^*(A)$.

According to Eqs. (1) and (2), the quantities $E_n(A^*, N)$ computed from the empirical values of $E_n(A, Z)$ for different nuclei with the same parity and with the same N should be approximately the same. Actually, as is apparent from the figure (in which we have plotted $E_n(A^*, N)$ vs. N), points pertaining to the same N are almost coincident. In order to show with greatest clarity the discontinuity points in the curve $E_n(A^*, N) = f(N)$, this curve is drawn through the mean (for each N) value. It is apparent from the figure that the curve of "reduced" incremental neutron energies goes through a number of discontinuities (which are found in the same places for nuclei with all four types of parity) which indicate singularities in the energies at $N = 130$, 136, 144, and 152.

A similar investigation of the energies required for adding protons leads to singularities at $Z = 86$, 92 and 96.

To evaluate the significance of these numbers we have examined the positions of the lowest rotational levels; it has been found that a sharp drop occurs at $N = 130$, particularly after $Z = 86$; this effect extends, in a less pronounced manner, to $N = 136$ and $Z = 92$, after which the levels become stabilized. It may be assumed in any case that the numbers $Z = 86$ and $N = 130$ are to be associated with a sharp change in deformation. The forbidenness factor in α-decay in even-even nuclei in which the ground state of the initial nucleus is the ground state for the final nucleus, in particular, in transitions to the second level of the final nucleus, is reduced sharply after $Z = 86$ and $N = 130$ and then increases following $Z = 92$;[9] subsequently it is reduced somewhat after $Z = 96$. In nuclei with an odd number of neutrons there is a sharp increase in the forbiddenness factor for α-decay with neutron number following the numbers $N = 136$, 144 and 152; $Z = 92$ and 96. Comparing these results with data on the position of the levels we may conclude that the numbers $Z = 86$ and $N = 130$ are to be associated with a sharp increase in deformation. The decrease in the forbiddenness factor for α-decay following $N = 130$ and $Z = 86$ is due to the

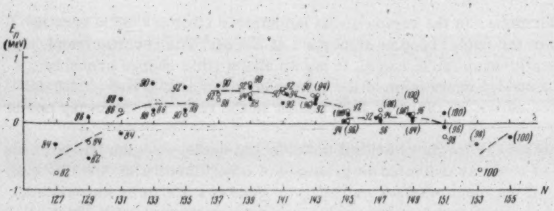

The "reduced" energies for adding neutrons E_n^* as a function of the number of neutrons N for nuclei with Z-even, N-odd; ●—for nuclei with, A = 4n + 3; ○—for nuclei with A = 4n + 1. The numbers around the points indicate the number of protons Z; the values of Z are enclosed in brackets when interpolated values of E_α have been used for calculating E_n^*.

reduction of the potential barrier in the direction of nuclear elongation. The particular numbers N = 144 and N = 156, Z = 96 are, however, not connected exclusively with deformation. To what has been said it should be added that: (a) the probability of spontaneous fission increases sharply following the number N = 152[10] and the numbers Z = 92 and Z = 96 are somewhat fissionable, (b) the total cross sections for slow-neutron capture increase sharply after N = 152[11] and become weaker after N = 144, and (c) if one of the nuclei between the ground states of which β-decay occurs has N = 145, N = 137, or Z = 95, it is found that log $f\tau$ is larger than in other neighboring nuclei.

It is interesting to note that all the sub-magic numbers which have been found N = 136, 144, 152 and Z = 92 and 96 are included in the usual Mayer scheme if the order of neutron levels is taken as (Ref. 5):

$$\ldots \vert i_{13/2}\,\vert\,126\; 2g_{9/2}\,\vdots\,(136)\; 3d_{5/2}\,\vdots\,(142)\; 4s_{1/2}\,\vdots\,(144)\; g_{7/2}\,\vdots\,(152) \ldots,$$

and the proton order is taken as:

$$\ldots h_{11/2}\,\vert\,82\; h_{9/2}\,\vdots\,92\; p_{3/2}\,\vert\,96 \ldots .$$

In reality, however, both situations are much more complicated; for example, in some cases the known spins of the heavy nuclei are not even remotely in agreement with the described schemes.

The total effect of nuclear deformation, as it is apparent from the figure, is about 0.7 Mev for neutrons and for protons. The subshell effect is only about 0.2 Mev except for N = 152 in which the effect is of the order of 0.4 Mev.

The authors wish to express their gratitude to Professor D. Ivanenko for his continued interest in this work.

---

[1] Mayer and Jensen, Elementary Theory of Nuclear Shell Structure, New York (1955).

[2] S. G. Nilsson, Kgl. Danske Videnskab. Selskab, Mat-fys. Medd. **29**, 16 (1955); R. B. Motelson and S. G. Nilsson, Phys. Rev. **99**, 1615 (1955); K. Gootfried, Phys. Rev. **103**, 1017 (1956).

[3] L. A. Sliv and L. K. Peker. Report to the Conference on Nuclear Spectroscopy, Leningrad (1957).

[4] G. Scharff-Goldhaber, Phys. Rev. **103**, 837 (1956).

[5] Giorso, Thomson, Seaborg et al., Phys. Rev. **95**, 293, (1954); S. I. Larin and N. N. Kolesnikov, J. Exptl. Theoret. Phys. (U.S.S.R.) **28**, 243 (1955); Soviet Phys. JETP **1**, 178 (1955).

[6] J. R. Huizenga, Physica **21**, 410 (1955); V. A. Kravtsov, Izv. Akad. Nauk SSSR, Ser. Fiz. **18**, 5 (1954).

[7] R. W. King, Rev. Mod. Phys. **26**, 326 (1954); F. Asaro and I. Perlman. Rev. Mod. Phys. **26**, 456 (1954). B. S. Dzhelepov and L. K. Peker, Схемы распада радиоактивных изотопов, (Decay Schemes for Radioactive Isotopes), Acad. of Sciences Press, 1956, Nuclear Science Abstr., **10**, 14 (1956); F. Asaro and I. Perlman. Phys. Rev. **104**, 91 (1956); D. C. Hoffman, J. Inorg. and Nuclear Chem. **2**, 209 (1956).

[8] N. N. Kolesnikov. J. Exptl. Theoret. Phys. (U.S.S.R.) **30**, 889 (1956); Soviet Phys. JETP **3**, 844 (1957).

[9] J. O. Rasmussen and B. Segal, Phys. Rev. **103**, 1298 (1956).

[10] R. E. Lingenfelter, Phys. Rev. **101**, 1615 (1956).

[11] B. G. Harvey, Phys. Rev. **99**, 333 (1955).

Translated by H. Lashinsky

CONSERVATION OF PARITY IN THE THEORY OF ELEMENTARY PARTICLES

V. L. POKROVSKII and IU. B. RUMER

West-Siberian Branch, Academy of Sciences, U.S.S.R.

Submitted to JETP editor March 14, 1957

J. Exptl. Theoret. Phys. (U.S.S.R.) 33, 277-279 (July, 1957)

THERE have been a number of recent experiments which indicate that parity is not conserved in the decay of elementary particles. In view of the fact that the requirement for invariance of physical effects under spatial reflections does not now seem to be self-evident it is natural to wonder why parity is conserved in one class of effects (strong and electromagnetic interactions), while in another (weak interactions, following the Gell-Mann designation) there is the possibility of parity non-conservation.

We wish to call attention to the fact that the system of five-dimensional optics[1] proposed by one of the present authors gives a natural method for classifying effects in which parity is conserved and is not conserved.

Five-optics starts from the recently discovered deep-lying symmetry of the equations of classical and quantum mechanics in space, time, and action. In 5-optics the coordinates, time, and action are combined in a five-dimensional metric space which is topologically bounded in the action coordinate with a period equal to the Planck constant h. Correspondingly, the momentum energy, and charge are combined in a five-dimensional vector for which a single conservation law is formulated. In five-dimensional optics the action, like a coordinate, is an algebraic quantity. A change in the sign of the action is equivalent to ordinary charge conjugation.

The interaction Lagrangian in five-dimensional optics, as in four-dimensional optics, must be formed from wave functions of the interacting particles. We consider all possible products of the components of the spinors $\bar{\xi}_\alpha \xi_\beta$ and $\xi_\alpha \eta_\beta$. All these can be broken down into irreducible groups.[2]

(1) Scalars: $\bar{\xi}\xi$ and $\xi\Omega\gamma_5\eta$.

(2) 4-Vectors: $\bar{\xi}\gamma_k\xi$ and $\xi\Omega\gamma_5\gamma_k\eta$.

(3) Anti-symmetric tensors of the second rank $\bar{\xi}\gamma_i\gamma_k\xi$, $\xi\Omega\gamma_i\gamma_k\eta$ (6 components).

(4) 4-pseudovectors: $\bar{\xi}\gamma_5\gamma_k\xi$ and $\xi\Omega\gamma_k\eta$.

(5) Pseudoscalars $\bar{\xi}\gamma_5\xi$ and $\xi\Omega\eta$, where the matrix Ω is defined by the relation:[3] $\gamma_k^T = \Omega\gamma_k\Omega^{-1}$.

In five-dimensional space a spinor is also a four-component quantity and the products $\bar{\xi}_\alpha \xi_\beta$ and $\xi_\alpha \eta_\beta$ can be broken down into the following irreducible groups:

(1) Pseudoscalar $\bar{\xi}\gamma_5\xi$; scalar $\xi\Omega\gamma_5\eta$.

(2) 5-vector $(\bar{\xi}\gamma_k\xi, \bar{\xi}\xi)$, 5-pseudovector $(\xi\Omega\gamma_k\eta, \xi\Omega\eta)$.

(3) Anti-symmetric pseudotensor of the second rank $(\bar{\xi}\gamma_i\gamma_k\xi, \xi\gamma_5\gamma_k\xi)$, anti-symmetric tensor of the second rank $(\xi\Omega\gamma_i\gamma_k\xi, \xi\Omega\gamma_5\gamma_k\xi)$ (10 components).

In particular, we wish to emphasize that in five-dimensional space it is impossible to form a bilinear conbination having the properties of a scalar and pseudovector from $\bar{\xi}$ and ξ and that it is impossible to form a pseudoscalar and a vector from ξ and η.

Following Pauli[3] we designate the following wave functions for bosons: Φ scalar, φ pseudoscalar, Φ_k vector, φ_k pseudovector.

We now consider two types of effects.

A. Emission of a boson by a fermion (pair production). The interaction Lagrangians for pseudoscalar and vector bosons are respectively:

$$L = \varphi\,(\bar{\xi}\gamma_5\xi),\ L = \Phi_k\,(\bar{\xi}\gamma_k\xi) + \Phi_5\,(\bar{\xi}\,\xi)$$

(we do not consider interaction Lagrangians which contain derivatives). We see that parity is conserved in the emission of a pseudoscalar or vector boson in the five-dimensional theory. This fact is of particular interest in connection with the emission of a π-meson by a nucleon and a photon by an electron. The interaction Lagrangians can be pseudoscalar only for scalar and pseudovector mesons. Hence, if scalar and pseudovector mesons exist, parity cannot be conserved in emission processes.

B. Decay of a boson into two fermions. The interaction Lagrangian for a pseudoscalar boson is $L = \varphi^*(\xi\Omega\gamma_5\eta)$ while for a vector boson it is $L = \Phi_k^*(\xi\Omega\gamma_k\eta)$. We see that parity cannot be conserved in the decay of a pseudoscalar or vector boson into two fermions. In particular, parity is not conserved in the reaction $\pi^\pm \rightarrow \mu^\pm + \nu$. If there are scalar and pseudovector mesons which can decay into two fermions, parity cannot be conserved in this decay.

Since the action coordinate is on equal footing with the other spatial coordinates in five-dimensional theory, simultaneous spatial reflection and change of sign of the action leave the Lagrangian invariant in all product combinations.

Consequently, even a theory which is not invariant under spatial reflection becomes invariant with respect to the combined inversion proposed by Landau,[4] i.e., simultaneous spatial reflection and charge conjugation.

---

[1] Iu. B. Rumer, Исследования по 5-оптике, (Investigation of 5-Optics), GTTI 1956; Usp. Mat. Nauk 8, 6 (1953).

[2] E. Cartan, Theory of Spinors (Russ. Transl.), GIIL 1948.

[3] W. Pauli, Exclusion Principle, Lorentz Group and Reflection of Space-Time and Charge. (In the collection "Niels Bohr and the Development of Physics," London, Pergamon Press, 1955).

[4] L. Landau, J. Exptl. Theoret. Phys. (U.S.S.R.) 32, 405 (1957); Soviet Phys. JETP 5, 336 (1957); T. D. Lee and C. N. Yang, Phys. Rev. 105, 1671 (1957).

Translated by H. Lashinsky
47

POLARIZATION IN DOUBLE SCATTERING OF ELECTRONS

IU. V. ANISHCHENKO and A. A. RULCHADZE

P. N. Lebedev Institute of Physics, Academy of Sciences, U.S.S.R.

Submitted to JETP editor March 19, 1957

J. Exptl. Theoret. Phys. (U.S.S.R.) 33, 279-280 (July, 1957)

As is well known, β-decay electrons are polarized longitudinally. This effect can be observed in double scattering of β-electrons. The differential cross section for double scattering of a longitudinally polarized beam of electrons is given as follows:[1]

$$I^{(2)} = (|f_1|^2 + |g_1|^2)(|f_2|^2 + |g_2|^2)(1 + \delta_1 \cos\varphi + \delta_2 \sin\varphi), \tag{1}$$

where

$$\delta_1 = (f_1 g_1^* - f_1^* g_1)(f_2^* g_2 - f_2 g_2^*) / (|f_1|^2 + |g_1|^2)(|f_2|^2 + |g_2|^2), \tag{2}$$

$$\frac{\delta_2}{\delta_1} = i\eta \frac{\sin\vartheta_1 (|g_1|^2 - |f_1|^2) + \cos\vartheta_1 (f_1^* g_1 + f_1 g_1^*)}{f_1^* g_1 - g_1^* f_1}, \tag{3}$$

where $f_1 \equiv f(\vartheta_1)$, $f_2 \equiv f(\vartheta_2)$ etc. and the angles ϑ_1 and ϑ_2 are the angles associated with the first and second scattering respectively, φ is the azimuthal angle measured from the plane of the first scattering, and η is the degree of longitudinal electron polarization. In the Born approximation Eqs. (2) and (3) assume the following form:

$$\delta_1 = -\frac{Z_1 Z_2 e^4}{(\hbar c)^2} 4 \frac{v^2}{c^2}\left(1 - \frac{v^2}{c^2}\right) \frac{\sin^4(\vartheta_1/2)\sin^4(\vartheta_2/2)}{\sin\vartheta_1 \cdot \sin\vartheta_2} \frac{\ln\operatorname{cosec}^2(\vartheta_1/2) \cdot \ln\operatorname{cosec}^2(\vartheta_2/2)}{[1-(v/c)^2\sin^2(\vartheta_1/2)][1-(v/c)^2\sin^2(\vartheta_2/2)]}; \tag{4}$$

$$\delta_2/\delta_1 = 2\eta \frac{\hbar c}{Z_1 e^2} \frac{c}{v} \frac{\cot^2(\vartheta_1/2)}{\ln\operatorname{cosec}^2(\vartheta_1/2)}. \tag{5}$$

It is apparent from Eq. (5) that $\delta_2 \gg \delta_1$, so that the effect of azimuthal asymmetry is much greater in double scattering of a polarized electron beam than scattering of a non-polarized beam.[1,2]

If we neglect recoil of the nucleus for a two-component neutrino the β-electron longitudinal polarizations is $\eta = v/c$.

Experiments on double scattering of a polarized beam are difficult because of the relatively low activity of β-active samples. However, experiments of this type are of great interest both for verifying the calculation given above as well as for understanding the phenomenology of β-decay. At the present time attempts are being made to verigy this effect experimentally.

On the other hand, neglect of the azimuthal symmetry in double scattering of decay electrons may lead to its own experimental error. The first scattering is over small angles ($5 - 15°$) and is likely to be lost in the cover which protects the sample. It should be noted that the factor in the expression for δ_2 which depends on ϑ_1 is changed by only a factor of three as the angle varies from $10 - 90°$ so that even for a first scattering at small angles, δ_2 in Eq. (1) remains large.

It is of interest, in this regard, to point out a possible connection between double scattering and the so-called "anomalous" electron scattering which has been observed by a number of authors.[3,4] These observations refer to a discrepancy between the experimental and theoretical electron distribution over the angle ϑ. It is of interest to note that the "anomalous" scattering has been observed in investigations of β-radiation of radioactive materials while, on the other hand, there has been good agreement with theory in investigations using accelerator beams.[2,5]

We wish to express our gratitude to Academician I. E. Tamm for valuable discussions in connection with this paper.

---

[1] H. Mott and Massey, Theory of Atomic Collisions, (Russ. Transl.) IIL 1951.

[2] H. A. Tolhoek, Revs. Mod. Phys. **28**, 277 (1956).

[3] F. C. Champion and A. Barber, Phys. Rev. **55**, 111 (1939).

[4] W. Bosshard and P. Scherrer, Helv. Phys. Acta **14**, 85 (1941).

[5] Van de Graaff, Buechner, and Feshbach, Phys. Rev. **69**, 452 (1946).

Translated by H. Lashinsky
48

THEORY OF THE PRODUCTION OF ELECTRON-POSITRON PAIRS IN COLLISIONS OF SLOW μ^--MESONS WITH NUCLEI

L. M. AFRIKIAN

Institute of Physics, Academy of Sciences, Armenian S.S.R.

Received by JETP editor March 30, 1957

J. Exptl. Theoret. Phys. **33**, 280-281 (July, 1957)

In Refs. 1–5 several approximate formulas have been obtained for the cross sections for the production of electron-positron pairs in collisions of non-relativistic heavy charged particles. The most complete analysis of the problem has been given by Okun'[5] who has derived expressions for the pair-production cross sections in Born approximation as well as the quasi-classical approximation. Thus, almost the entire non-relativistic region of heavy-particle energies has been investigated; the only exception is the small region near threshold.

In the present report we present the results of calculations which have been carried out for the threshold region for the production of electron-positron pairs in the collision of negative μ^--mesons with nuclei. The calculations have been carried out in the framework of quantum electrodynamics; two cases have been considered: the first corresponds to the condition:

$$T_0 - 2m < 2m, \tag{1}$$

where T_0 is the initial energy of the μ^--meson and m is the mass of the electron.

In the second case it is assumed that the following condition is satisfied:*

$$2\pi Z/137 \gg \beta_1, \beta, \beta_+, \beta_-; 2\pi/137 \ll \beta_\pm, \tag{2}$$

where β_0, β, β_+ and β_- are correspondingly the velocities of the μ-mesons and the pair particles with respect to the nucleus, $\beta_\pm$ is the relative velocity of the particles of the pair.

In this approximation the total cross section for the production of electron-positron pairs by μ^--mesons on nuclei is:

$$\sigma = 8\pi^3\left(\frac{Z}{137}\right)^6\left(\frac{e^2}{m}\right)^2\frac{m}{T_0}\left(\frac{T_0-2m}{2m}\right)^2 \left\{\eta^4\left(\frac{1}{4!}-\frac{1}{2\eta^2}\right)\mathrm{Ei}\,(-\eta)+I\,(\eta)\exp\,(-\eta)\right\}\exp\left\{-\frac{\pi Z}{137}\left(\frac{2\mu}{T_0}\right)^{1/2}\right\}. \tag{3}$$

Here: μ is the mass of the μ-meson,

$$I\,(\eta) = \sum_{k=0}^{1}\frac{(-1)^k\,\eta^k}{2\ldots(2-k)} - \sum_{k=0}^{3}\frac{(-1)^k\,\eta^k}{4\ldots(4-k)}; \quad \eta = \frac{\pi Z}{137}\left(\frac{T_0-2m}{2m}\right)^{-1/2}.$$

The function $\mathrm{Ei}(-\eta)$ is the exponential integral, the values of which are tabulated in Ref. 6.

The second case corresponds to the Born approximation for the pair particles:

$$2\pi Z/137 \ll \beta_+, \beta_-, \beta_\pm;\ 2\pi Z/137 \gg \beta_0, \beta. \tag{4}$$

In this approximation the total effective cross section for pair production is

$$\sigma = \frac{\pi^2}{6}\left(\frac{Z}{137}\right)^4\left(\frac{e^2}{m}\right)^2\frac{m}{T_0}\left(\frac{T_0-2m}{2m}\right)^3\cdot\exp\left\{-\frac{\pi Z}{137}\left(\frac{2\mu}{T_0}\right)^{1/2}\right\}. \tag{5}$$

The formulas in (3) and (5) do not go over directly to Eq. (11) of Ref. 5 which pertains to a region of considerably higher energies. We may note, however, that the exponential factor in Eq. (11) of Ref. 5 becomes approximately the same as the exponential factor in Eqs. (3) and (5) when $T_0 \rightarrow 2m$.

---

[1] W. Heitler and L. Nordheim, J. phys. et radium **5**, 449 (1934).
[2] J. R. Oppenheimer, Phys. Rev. **47**, 146 (1935).
[3] E. M. Lifshitz, Physik. Z. Sowjetunion **7**, 385 (1935).
[4] A. B. Migdal, J. Exptl. Theoret. Phys. (U.S.S.R.) **15**, 401 (1945).
[5] L. B. Okun. Dokl. Akad. Nauk SSSR, **89**, 833 (1953).
[6] Janhke and Emde, Tables of Functions, OGIZ, 1948, p. 97.

Translated by H. Lashinsky
49

---

*Here and in the following we will not specifically state the condition

$$2\pi/137 \ll \beta_{e-\mu}$$

[where $\beta_{e-\mu}$ is the relative velocity of the scattered μ-meson and electron (positron)] since it is easily satisfied.

SOFT COMPONENT IN AN ELECTRON-NUCLEAR SHOWER AT ENERGIES OF 10^{14} EV

I. M. GRAMENITSKII, G. B. ZHDANOV, M. I. TREM'IAKOVA and M. N. SHCHERBAKOVA

P. N. Lebedev Physics Institute, Academy of Sciences, U.S.S.R.

Submitted to JETP editor April 2, 1957

J. Exptl. Theoret. Phys. (U.S.S.R.) 33, 282-283 (July, 1957)

IN an earlier note[1] we presented a short report concerning an investigation in an emulsion of the angle-energy characteristics of the rare case of a nuclear interaction between an α-particle with an energy of $(8^{+3}_{-4}) \times 10^{13}$ ev and a nucleon. The observation conditions were such that it was also possible to develop the electron-photon component in the emulsion over a region of two cascade lengths.

TABLE I

Space-Energy distribution of electron pairs.

$h\nu$, Bev	$\vartheta_x < 0.6\cdot 10^{-3}$		$0.6\cdot 10^{-3} < \vartheta_x < 5\cdot 10^{-3}$		
	>500	70–500	>500	70–500	9–70
$t \leqslant 0.6$	1	3	0	0	3
$0.6 < t \leqslant 1.1$	2	3	0	0	1
$1.1 < t \leqslant 1.6$	1	1	0	0	0
$1.6 < t \leqslant 2.1$	0	0	0	0	0

TABLE II

Space distribution of electrons.

$\vartheta\cdot 10^{3}$ (at $t=2$)	n_e	$t(\vartheta < 5\times 10^{-3})$	n_e
<0.2	8	0.5	14
0.2 —0.4	15	1.0	43
0.4 —0.6	11	1.5	90
0.6 —1.25	29	2.0	149
1.25—2.5	32		
2.5 —5	34		

The results of the study of the soft component can be given in the form of a space-energy distribution of the non-bremsstrahlung electron-positron pairs (Table I) and an electron space distribution (Table II and figure). In this analysis the quantities which characterize the spatial distribution have been chosen as the distance t along the axis of the cascade (expressed in cascade units) and the deflection angles of the pairs and the particles with respect to the same axis in space ϑ or in projection on the plane of the emulsion ϑ_x. The photon energies $h\nu$ were determined from the opening angle of the components of the pair α in accordance with the formula given in Ref. 1 in which use was made of the relations between the energy $h\nu$ and the mean-square value of the angle α.

The distribution of electrons along the axis of the cascade (Table II, right half) makes it possible, using the usual cascade curves, to verify the energy estimates given in Table I.

As is apparent from the figure, the spatial distribution of particles of the soft component in the direction perpendicular to the axis of the shower at a depth $t = 2$, can be approximated by the power function $f(r) \sim r^{-\gamma}$ where $\gamma = 1.62 \pm 0.05$, $r = t\vartheta$ (solid line in the figure).

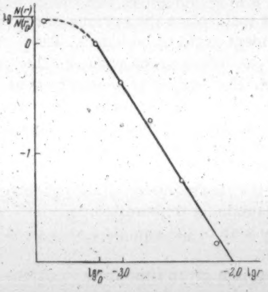

Electron spatial distribution at a depth $t = 2$($r = t\vartheta$, r_0 is an arbitrary point).

An analysis of the data given in Tables I and II and in the figure leads to the following conclusions: (1) the total number of photons is approximately equal to the number of penetrating particles emitted within the forward cone (in the c.m. system) within the limits of the statistical errors; (2) the energy flux carried by the photons is approximately 0.1 (with an error of approximately 0.05) of the energy of one nucleon of the primary particle; twice the mean energy carried by one photon is approximately equal to the mean energy of one penetrating particle if it is assumed (cf. Ref. 1) that the mean energy associated with the transverse momentum component of the mesons is 1.5 μc; (3) the concentration of photons and associated energy flux close to the axis of the shower is considerably higher than that which would be expected on the basis of the angular distribution measurements and the transverse momentum of the penetrating particles of the shower.

It is extremely probable that the last feature of the soft component of the shower is related, at least to some degree, to fluctuations, in view of the fact that the major part of the energy flux is carried by a small number (1 — 2) of π^0-mesons. It is also possible that part of the effect is due to differences in the efficiency for pair detection at different distances from the axis of the shower and the "addition" of a small number of pairs of bremsstrahlung origin.

There is still one other possible origin of this effect; this is the presence of an additional proton source in the form of bremsstrahlung produced (cf. for example, Ref. 2) as a consequence of the rapid deceleration of the quickly-moving electric charge of the primary particle.

The authors are indebted to Professor S. N. Vernov and Professor N. A. Dobrotin for illuminating discussions of the results of this work and to technicians R. M. Gryzunov and M. I. Pachkov for assistance in processing the experimental data.

---

[1] Gramenitskii, Zhdanov, Zamchalova, and Scherbakov, J. Exptl. Theoret. Phys. (U.S.S.R.) **32**, 936 (1957); Soviet Phys. JETP **5**, 763 (1957).

[2] E. L. Feinberg, J. Exptl. Theoret. Phys. (U.S.S.R.) **19**, 1098 (1949).

Translated by H. Lashinsky
50

CALORIMETRIC METHOD OF DETERMINING THE OPTICAL CONSTANTS OF METALS IN THE INFRARED REGION AT LOW TEMPERATURES

N. E. ALEKSEEVSKII and E. V. POTAPOV

Institute for Physical Problems, Academy of Sciences U.S.S.R.

Submitted to JETP editor, April 3, 1957

J. Exptl.Theoret. Phys. (U.S.S.R.) 33, 283-284 (July, 1957)

MEASUREMENTS of the optical constants of metals, as has already been noted,[1] are extremely important since these measurements, under certain conditions, afford the possibility of determining conduction-electron density.*

In the low temperature region it is convenient to determine the optical constants by calorimetric methods because these methods are simple and because the small heat capacities of metals make it possible to achieve high sensitivity. The calorimetric method has already been used by a number of authors;[2,3] in these experiments, however, only the absorption was measured i.e., A = 1—r, where r is the reflection coefficient for normal incidence on the surface of the sample.

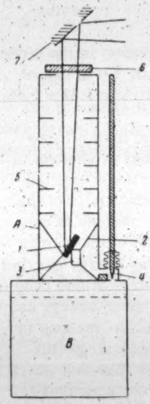

FIG. 1. (A) vacuum calorimeter, (B) carbon "pump," (1) sample, (2) caprone rods, (3) bronze thermometer, (4) valve for carbon "pump," (5) diaphragms, (6) window of KRS—5, (7) mirror.

Measurements of this kind cannot be used to calculate both optical constants of a metal. Two independent measurements are required. For this reason we have used an instrument with which both quantities can be measured. A schematic diagram of the apparatus is shown in Fig. 1.

A plane-polarized beam of infrared radiation is incident on the surface of the sample 1 at an angle φ close to the principle incident angle of incidence. The sample is located inside a vacuum calorimeter A on thin caprone rods 2. The calorimeter is suspended in a liquid-helium Dewar. The sample is cooled by heat exchange with helium with which the calorimeter is filled. During the measuremets the helium coolant is removed by the carbon pump B (Ref. 4) located in a separate chamber under the calorimeter and the sample is slowly heated by the absorbed radiation.

The temperature of the sample is measured by the thermometer 3 of phosphor bronze which is in good thermal contact with the sample. A thin-walled copper coil, which acts as a black body, is soldered to one side of the sample and is used to determine the intensity of the incident radiation.

By carrying out measurements of simple heating in a given time for two orientations of the polarized radiation (in the plane of incidence and perpendicular to the plane of incidence) it is possible fo find $A_{par} = 1-r_{par}$ and $A_{perp} = 1-r_{perp}$. Then, the quantities η and κ can be computed graphically using Eqs. (5) and (1) of Ref. 1.

This method was used to determine the optical constants of bismuth for wavelengths from 1 to 7μ at an angle of incidence $\varphi = 70°$. In this case, at 7μ the values of η and κ were found to be respectively 2 and 2.5, whence $|\epsilon| = 2.2$. An estimate based on the assumption that in this region $|\epsilon| \sim 1/\omega^2$ gives for bismuth $N \approx 3 \times 10^{20}$. This assumption can be verified at longer wavelengths; however, because of the low intensity it is extremely difficult to make the measurements. The intensity of the radiation incident on the sample can be increased by using a wider beam and by introducing the radiation into the calorimeter through an optical window in the side wall of the Dewar. It is convenient to use a metal Dewar with one side window for this purpose and to place the samples in the general vac-

---

*As has been pointed out by Ginzburg and Motulevich, if the dielectric constant of a metal $\epsilon = \eta^2 - \kappa^2 \sim 1/\omega^2$, then

$$N = (n^2 - \varkappa^2)\, m\omega^2/4\pi e^2,$$

where N is the number of conduction electrons per unit volume, n is the index of the refraction, κ is the absorption index, m is the mass of the free electron, e is the charge of the electron, and ω is the frequency of the incident radiation.

uum space of the Dewar on a fixed heat conductor. A detailed report on work being carried out will be published in the near future.

---

[1] V. L. Ginzburg and G. P. Motulevich, Usp. Fiz. Nauk **55**, 469 (1955).
[2] K. G. Ramanathan, Proc. Phys. Soc. **A65**, 532 (1952).
[3] M. A. Biondi, Phys. Rev. **96**, 534 (1954); **102**, 964 (1956).
[4] P. G. Strelkov, J. Exptl. Theoret. Phys. (U.S.S.R) **24**, 248 (1953).

Translated by H. Lashinsky
51

CONVERGENCE OF THE PERTURBATION-THEORY SERIES FOR A NON-RELATIVISTIC NUCLEON

A. G. GALANIN and IU. N. LOKHOV

Submitted to JETP editor April 4, 1957

J. Exptl. Theoret. Phys. (U.S.S.R.) 33, 285-286 (July, 1957)

IN the quantum theory of interacting fields the perturbation-theory series is an asymptotic series.[1] On the other hand, the problem of a non-relativistic nucleon interacting with a neutral scalar-meson field (n.s. theory) has an exact solution.[2] In this case the exact Green's function of the nucleon is an analytic function of the coupling constant with an infinite radius of convergence (in the coordinate representation; in the momentum representation the radius of convergence is finite[3]).

The problem of a non-relativistic nucleon which interacts with a symmetric pseudoscalar meson field (s.p.s. theory) does not as yet have an exact analytical solution. In spite of this fact an analysis of the convergence of the perturbation-theory series can be carried out.

For the interaction

$$(g_0/2\mu)\,\psi^*[(\sigma\nabla)(\tau_i\varphi_i)]\,\psi \tag{1}$$

there is a definite rule for writing the Feynman diagrams. The rule can be completely stated if we write only one matrix element, corresponding to the self-energy diagram in the first approximation

$$M(E) = -i\left(\frac{g_0}{2\mu}\right)^2\frac{1}{8\pi^2}\int\frac{(\sigma\mathbf{k})\,\tau_j\,(\sigma\mathbf{k})\,\tau_j\,d^3k\,dk_4}{(E-k_4-i\eta)(k_4^2-\mathbf{k}^2-\mu^2+i\varepsilon)}, \tag{2}$$

where E is the nucleon energy (we neglect the kinetic energy of the nucleon), and the integration extends to some upper limit. We go around the poles in the complex plane K_4 by infinitesimal increments $\epsilon > 0$ and $\eta > 0$. The symbol η corresponds to the appropriate Green's function in the non-relativistic case.[4] In the upper half plane of k_4 there is only one pole $k_4 = -\sqrt{\mathbf{k}^2+\mu^2}$. Closing the integration path in the k_4 plane in an upward direction, it is easy to calculate the integral over k_4 in (2). After integrating over the angles we have

$$M(E) = \frac{1}{6}\left(\frac{g_0}{2\mu}\right)^2\sigma_i\tau_j\sigma_i\tau_j\int_0^\Lambda k^4dk/(E+\sqrt{k^2+\mu^2})\sqrt{k^2+\mu^2}, \tag{3}$$

where Λ is the cut-off momentum. In what follows we neglect the meson mass; going over to dimensionless variables of integration we have

$$M(z) = \frac{1}{6}\left(\frac{g_0\Lambda}{2\mu}\right)^2\Lambda\sigma_i\tau_j\sigma_i\tau_j\int_0^1\frac{x^3dx}{z+x}, \tag{4}$$

$(z = E/\Lambda)$. The rules for forming more complicated diagrams can be obtained easily by generalizing this example.

Similarly, in n.s. theory with the interaction $g_1\psi\varphi\psi$, we obtain in place of (4)

$$\frac{1}{2} g_1^2 \Lambda \int_0^1 \frac{x\,dx}{z+x}. \tag{5}$$

In this case the theory can be renormalized and the cut-off momentum Λ can approach infinity after renormalization. However, since the expressions under the integrals are positive (for a given diagram), by introducing a finite cut-off momentum we reduce the magnitude of the integral and improve the convergence of the power series in g_1^2. We now compare (4) and (5) and the more complicated diagrams. We denote an arbitrary diagram of order n s.p.s. theory by $I_n^{(p)}$ and the same diagram in n.s. theory by $I_n^{(s)}$. Inasmuch as all the variables of integration in (4) and in the more complicated diagrams are less than unity, we have $I_n^{(p)} < I_n^{(s)} A_n$ if $g_1^2 = {}^1/_3 (g_0\Lambda/2\mu)^2$ and A_n denotes a combination of the matrices σ and τ. Since the matrices σ and τ have the same properties,

$$A_n = (\sigma_{i_1} \sigma_{i_2} \ldots \sigma_{i_{2n}})^2, \tag{6}$$

in which the indices contain n identical pairs for which we carry out a summation from 1 to 3. Hence the expression in the parentheses in (6) consists of 3^n terms. We consider one of these terms. Let the first matrix be σ_x while the next successive matrix after σ_x stands in the k'th position. Having made k−2 substitutions we change sign k−2 times and, further, since $\sigma_x^2 = 1$, we have reduced the number of matrices by 2. Carrying out this operation n times, we calculate one of the terms in $\sigma_{i_1} \ldots \sigma_{i_{2n}}$. The quantity A_n increases only if we drop the factor $(-1)^{k-2}$ which arises from the fact that the σ matrices do not commute. Since the number of terms is 3^n, $A_n < 3^{2n}$ and

$$I_n^{(p)} < I_n^{(s)}, \tag{7}$$

if now $g_1^2 = 3(g_0\Lambda/2\mu)^2$.

Thus, the power series in g_1^2 in n.s. theory is the majorant for s.p.s. theory.

In n.s. theory the Green's function has, in the p-representation, a finite radius of convergence (cf. Ref. 3) if the cut-off momentum $\Lambda \to \infty$. If Λ remains finite, however, (the inequality in Eq. (7) is obtained specifically in this case), the radius of convergence in n.s. theory also becomes infinite for a Green's function written in the p-representation. Hence, from Eq. (7) it follows that the perturbation-theory series in s.p.s. theory has an infinite radius of convergence.

The convergence of the perturbation series in non-relativistic theories is due to the fact that the integral which corresponds to a diagram of n'th order, has a denominator of the following form:

$$(E + k_1)(E + k_1 + k_2) \ldots (E + k_1 + \ldots + k_n),$$

where k_i is the energy of the i'th virtual meson ($k_i > 0$).

This denominator leads to a very rapid, factorial reduction of each diagram of n'th order with increasing n. This means that the n'th term of the power series in g_0^2 falls off with increasing n in spite of the fact that the number of diagrams of n'th order increases as n!

Thus, in non-relativistic theories it is assumed that the energy of a nucleon in virtual states increases with an increase in the number n. It is obvious that relativistic theories, in which pair production is possible, will differ in a fundamental way from non-relativistic theories at this point. Hence, in the example of a relativistic theory chosen by Thirring each matrix element of n'th order does not fall off factorially with increasing n and the perturbation theory series becomes asymptotic.

The authors wish to express their gratitude to B. L. Ioffe for some illuminating discussions.

---

[1] W. Thirring, Helv. Phys. Acta **26**, 33 (1953).

[2] S. F. Edwards and R. E. Peierls, Proc. Roy Soc. (London) **224**, 24 (1954).

[3] Проблемы современной физики, (Problems of Contemporary Physics) IIL 3 (1955) p. 119.

[4] R. F. Feynman, Phys. Rev. **76**, 749 (1946).

Translated by H. Lashinsky
52

THE INFLUENCE OF PRESSURE ON THE MAGNETIC PROPERTIES OF ZINC SINGLE CRYSTALS AT LOW TEMPERATURES

I. M. DMITRENKO, B. I. VERKIN, and B. G. LAZAREV

Physico-Technical Institute, Academy of Sciences, Ukranian S.S.R.

Submitted to JETP editor April 5, 1957

J. Exptl. Theoret. Phys. (U.S.S.R.) 33, 287-289 (July, 1957)

An investigation of the magnetic properties of metals at low temperatures and under pressure if of interest in connection with the possible effect of the pressure on the structure of the electron energy spectrum in the metal. For metals in which the de Haas-van Alphen effect is observed, such an investigation is of particular interest in connection with the presence of different types of binding forces between the atoms of the lattice. It is possible that this may explain one of the fundamental magnetic properties of this group of metals, namely the presence of anomalously small groups of electrons.[1]

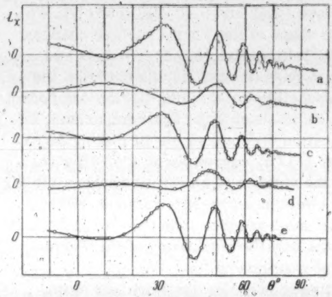

FIG. 1. The torque acting on a zinc crystal in a homogeneous magnetic field as a function of the angle θ between the field vector and the hexagonal crystal axis; $T = 4.2°$ K, $H = 8400$ oersteds. (a) $P = 0$ kg/cm^2; (b) $P \sim 1500$ kg/cm^2; (c) pressure removed; (d) pressure $P \sim 1500$ kg/cm^2 reapplied; (e) reapplied pressure removed.

The influence of pressure on the magnetic properties of Bi at low temperatures has already been communicated.[2] It is of interest to perform a more detailed investigation of this effect on zinc, a metal whose magnetic properties at low temperatures have been investigated in detail by several authors.[3-5]

Monocrystals of Zn were prepared in glass by the Obreimov-Shubnikov method, using "Hilger spectroscopic" metal. The method for creating a pressure of about 1500 kg/cm^2 and measuring the differences in the principal specific susceptibilities of a monocrystal were the same as those used previously.[2,6] The crystal was oriented in the field so that the suspension axis was perpendicular to the binary crystal axis. The principal axis of the crystal makes an angle θ with the magnetic field vector **H** in the horizontal plane. The curves shown in Fig. 1 were then obtained for the angular dependence of the torque L_x acting on the crystal at $T = 4.2°$ K and $H = 8400$ oersteds, and those of Fig. 2 were obtained for the function $\chi(1/H)$ at two values of θ (20° and 80°).

As is seen from Fig. 1, the application of pressure causes a significant decrease of the amplitude and increases the period of the oscillations; the amplitude decreases most in the region of high θ, while the period changes most at small values of θ.

When the pressure is removed, the initial curve is re-established with some amplitude hysteresis. Repetition of the application and removal of pressure reproduces the first cycle, except that the amplitude hysteresis is much less after the second application of pressure.

Figure 2 verifies the data obtained from the rotation diagrams. The period is increased both for $\theta = 80°$ and for $\theta = 20°$, with the increase being 52% in the latter case and 43% in the former. The amplitude decreases in both cases, the decrease being greater for 80°. At this value of θ the amplitude hysteresis is also larger, being about 60%, while at 20° it is only 6 — 8%. Removal of the pressure leads to complete re-establishment of the periodicity within the limits of experimental error. The slant of the median line in the $\chi(1/H)$ curves, together with the noncoincidence of the zeroes in the rotation diagrams, is explained by a torque component due to the weak magnet anisotropy of the cylinder.

The pressure effect in zinc is thus found to be quite large. It has the following interesting property. Although pressure makes the zinc lattice more isotropic, causing it to approach dense hexagonal packing, the anisotropy of the angular dependence of the periods (or the anisotropy of the Fermi electron surface, which causes this effect) increases.

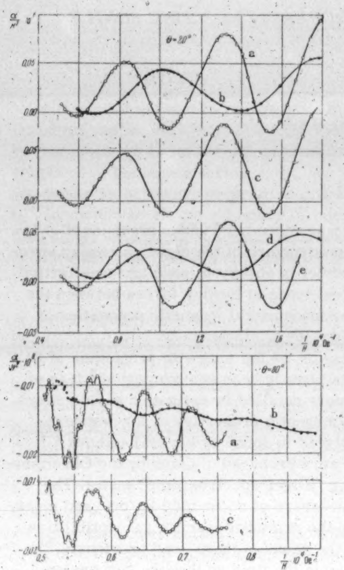

FIG. 2. The differences of the principal specific susceptibilities of a zinc crystal as a function of the applied magnetic field strength at T = 4.2° K. At $\theta = 20°$; (a) P = 0 kg/cm^2; (b) P ~ 1500 kg/cm^2; (c) pressure removed; (d) pressure P ~ 1500 kg/cm^2 reapplied; (e) reapplied pressure removed. At $\theta = 80°$: (a) P = 0 kg/cm^2; (b) P ~ 1500 kg/cm^2; (c) pressure removed.

Using the data obtained, one can estimate the number of electrons in the group responsible for the investigated longest-period component of the de Haas-van Alphen effect in Zn. If n is the number of electrons in the given group, and Ω is the volume bounded by the corresponding Fermi surface in momentum space, then $n = \Omega V/h^3$, where V is the volume of the metal and h is Planck's constant. The equation $\Omega = \alpha S^{3/2}$ gives the relation between the volume Ω and the extremal cross sectional area of the Fermi surface, and $S = A/\Delta$ [where Δ is the period of the $\chi(1/H)$ curve]. Here α is a form factor that depends in general on the orientation of the field vector relative to the crystal axis. From these formulas we obtain

$$\delta n/n = \delta V/V - {}^3/_2\,(\delta\Delta/\Delta) + \delta\alpha/\alpha.$$

In our case, in spite of the significant anisotropy of the compressibility of Zn, the fractional changes of the periods for $\theta = 20°$ and $\theta = 80°$ are close (0.52 and 0.43 respectively). We can thus assume that the shape of the Fermi surface changes but little, and set $\delta\alpha = 0$. Taking next $(\delta\Delta/\Delta)_{\text{av}} = 0.47$ and $(\delta V/V) \approx 3.10^{-3}$, we obtain $\delta n/n \approx -0.7$. In other words, the number of electrons responsible for the long-period component in the $\chi(1/H)$ curve for Zn is about 70%. For comparison, we note that a similar evaluation undertaken for Bi [taking $\delta\Delta/\Delta = 0.13$, obtained from the $\chi(1/H)$ curves for $\theta = -70°$] gives only a 10% decrease of the number of electrons responsible for the de Haas-van Alphen effect at a pressure of about 1500 kg/cm^2. This estimate is much rougher than the one performed here for zinc, owing to the way the anisotropy of the Fermi surface of Bi changes under pressure.[2]

Finally, it is interesting to note that the work per atom done by the external forces in compressing the crystal is 2×10^{-6} ev. To some extent this value characterizes the magnitude of the change of the binding forces in the Zn lattice under a pressure of about 1500 kg/cm^2. It is interesting that such a small change in the binding forces leads to so large a change in the parameters of the de Haas-van Alphen effect, owing to the anomalously small group of electrons in zinc with the Fermi energy $E_0 \sim 10^{-2}$ ev.

In conclusion the authors consider it their pleasant duty to thank I. M. Lifshitz for discussing the results of the work.

---

[1] B. I. Verkin, Doctoral Dissertation, Kharkov State University, 1956.

[2] Verkin, Dmitrenko, and Lazarev, J. Exptl. Theoret. Phys. **31**, 538 (1956); Soviet Phys. JETP **4**, 432 (1957).

[3] B. I. Verkin, Dokl. Akad. Nauk SSSR **81**, 529 (1951); B. I. Verkin and I. F. Mikhailov, J. Exptl. Theoret. Phys. (U.S.S.R.) **24**, 342 (1953).

[4] S. Sidoriak and D. Robinson, Phys. Rev. **75**, 118 (1949); J. Marcus, Phys. Rev. **84**, 787 (1951); F. Donahoe and F. Nix, Phys. Rev. **95**, 1395 (1954); T. Berlincourt and M. Steele, Phys. Rev. **95**, 1421 (1954).

[5] B. I. Verkin and I. M. Dmitrenko, Izv. Akad. Nauk SSSR, ser. fiz. **19**, 409 (1955).

[6] B. I. Verkin, I. F. Mikhailov, J. Exptl. Theoret. Phys. (U.S.S.R.) **25**, 471 (1953).

Translated by E. J. Saletan
53

USE OF THE HARTREE-FOCK EQUATIONS FOR A SYSTEM OF QUASI-PARTICLES

V. M. ELEONSKII and P. S. ZYRIANOV

Ural' Polytechnic Institute

Submitted to JETP editor April 6, 1957

J. Exptl. Theoret. Phys. (U.S.S.R.) 33, 289-291 (July, 1957)

THE state of a system of many strongly interacting particles in states close to some ground state can be described in terms of a set of quasi-particles. In a weakly "nonideal" system, the number of quasi-particles in states close to the ground state may be considered insignificant, and their interaction can be ignored. In strongly "nonideal" systems, the number of quasi-particles may be quite large and their interaction can no longer be ignored. We present an attempt to account for the interaction between quasi-particles by means of a self-consistent field.

The time-dependent Hartree equations for a system having on the average N quasi-particles per unit volume can be written

$$i\hbar\dot{\psi}_j = -\frac{\hbar^2}{2m}\Delta\psi_j + \int G(|\mathbf{r}-\mathbf{r}'|)\sum_i |\psi_i(\mathbf{r}')|^2 d\mathbf{r}'\,\psi_j, \tag{1}$$

where $G(|\mathbf{r}-\mathbf{r}'|)$ is the interaction kernel for quasiparticles. Writing $\psi_j = \rho_j^{1/2}\exp\{iS_j/h\}$, these equations can be written in the hydrodynamic form

$$\dot{S}_j + \frac{1}{2m}(\nabla S_j)^2 + \int G(|\mathbf{r}-\mathbf{r}'|)\sum_i \rho_i(\mathbf{r}')\,d\mathbf{r}' - \frac{\hbar^2}{4m}\frac{\Delta\sqrt{\rho_j}}{\rho_j} = 0, \quad \dot{\rho}_j + \operatorname{div}(\rho_j\nabla S_j) = 0. \tag{2}$$

This system has an exact solution with $\rho_j^0 = \text{const} = 1/V$ (where V is the volume of the system, assumed equal to unity) and

$$S_j^0 = m(\nabla_p\varepsilon_j^0)\mathbf{r} - \varepsilon_j^0 t + \text{const}, \tag{3}$$

where ϵ_j^0 is the energy and $\mathbf{p}$ is the momentum of a quasi-particle in a state of constant density. For a weakly "nonideal" system, $\nabla_p\epsilon_j^0$ can be set equal to the velocity $\mathbf{v}_j^0$. The energy spectrum of a system in a state close to the constant-density state may be found by linearizing Eqs. (2). Calculations similar to those performed previously[1] lead to the dispersion equation

$$1 = \frac{1}{m}G(k)k^2\sum_j\left[(\omega - \mathbf{k}\nabla_p\varepsilon_j^0)^2 - \frac{\hbar^2k^4}{4m^2}\right]^{-1}, \tag{4}$$

where G(k) is the Fourier component of the interaction kernel, and k is the wave number. For small k this equation has the solution

$$\omega^2 = \frac{N}{m}G(k)k^2 + \overline{(\mathbf{k}\cdot\nabla_p\varepsilon)^2}. \tag{5}$$

Suitable choice of the dependence of ϵ_j on $\mathbf{p}_j$ makes it possible to account for nonlocal interactions.

If exchange interactions are accounted for within the framework of the Hartree-Fock equation, we obtain instead of (4)

$$1 - \frac{k^2}{m}G(k)\sum_i F(\omega, \mathbf{kp}_i) + \left(\sum_i\rho_i\right)^{-1}\sum_{j,i}G\left(\frac{1}{\hbar}|\mathbf{p}_j + \mathbf{p}_i|\right)F(\omega, \mathbf{kp}_i)\rho_i = 0, \quad F(\omega, \mathbf{kp}_i) = \left[\left(\frac{\omega - \mathbf{kp}_i}{m}\right)^2 - \frac{\hbar^2k^4}{4m^2}\right]^{-1}. \tag{6}$$

When $\omega \gg \langle \mathbf{kp}/m\rangle_{av}$, the function $G(|\mathbf{p}_i + \mathbf{p}_j|)$ can be taken outside of the summation over j and evaluated at some intermediate point $\mathbf{p}'$ between zero and the maximum value of the Fermi momentum. The last term in (6) then becomes

$$-(k^2/m)\sum_i G(|\mathbf{p}_i + \mathbf{p}'|/\hbar).$$

The maximum and minimum values of the correction for the exchange interaction differ from each other by a factor of two. For small k the maximum value of this exchange correction leads to

$$\omega^2 = \omega_0^2 + (\overline{p^2}/m^2)k^2 - 3\omega_0^2(\hbar k/p_{\max})^2.$$

This equation was first obtained by Silin[2] with a somewhat different numerical coefficient on the last term.

The method here described is generalized by indicating a general way of finding the quantity $\overline{(\nabla_p \epsilon)^2}$, which enters into the dispersion equation (5). Since this quantity is given in terms of quantities characterizing the ground state, it is sufficient to write the energy $\epsilon = (1/2)m(\nabla_p \epsilon)^2$ of a single particle for this state as a function of the momentum, accounting for all possible interactions by single-particle wave functions (which are plane waves in the constant-density state).

We take this opportunity to thank V. P. Silin for correcting a serious error in the first version of this communication.

---

[1] P. S. Zyrianov and V. M. Eleonskii, J. Exptl. Theoret. Phys. (U.S.S.R.) 30, 592 (1956); Soviet Phys. JETP 3, 620 (1956).

[2] V. P. Silin, Физика металлов и металловедение, (Physics of Metals and Metal Reseach) 3, 193 (1956).

Translated by E. J. Saletan
54

NEW FORM OF ISOMERISM IN EU^{152}

L. K. PEKER

Library of the Academy of Sciences, U.S.S.R.

Submitted to JETP editor April 7, 1957

J. Exptl. Theoret. Phys. (U.S.S.R.) 33, 291-293 (July, 1957)

EXPERIMENTAL data on the β-decay of Eu^{152} indicates that the β and γ spectra of its ground state (T = 13 years) and isomeric state (T = 9.2 hr) are very complex.[1-4] Certain details of the decay schemes, however, are quite well established and can be used to determine the spin of the isomer. These are shown in Fig. 1. The log τf value of 7.6 for the 9.2 hr β^- transition of Eu^{152} to the ground state 0+ of Gd^{152} is characteristic for singly forbidden β^- transitions and indicates that the spin of the Eu^{152} isomer is 1—. The value 0— is excluded, since K-capture is observed to the 1537 kev 2— level of Sm^{152}. The value 2— is less likely, since in this case the β^- transition would be "unique" and one would expect to have log $\tau f \geq 7.6$.

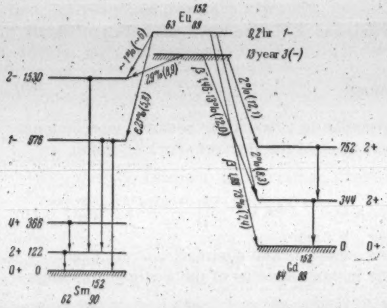

FIG. 1

The spin of 13-year Eu^{152} was directly measured by the paramagnetic resonance method,[5] and was found to be 3. These experimental values of 3 (—) and 1— for the spins of the ground state and isomeric state of Eu^{152} lead to several serious difficulties:

1. The spin difference of these two states is 2. Therefore the γ-transition between the isomeric and ground states of Eu^{152} must be* E2. Nevertheless, this transition is never observed. If it does exist, it is retarded by a factor of more than 10^{12} compared to the usual E2 transitions. One is not able[6,8] to explain this in terms of the selection rules for any of the known quantum numbers (for deformed nuclei) I, K, N, n_z, Λ, or Σ. The isomerism of Eu^{152}

---

*From a more detailed analysis of the decay scheme it follows that the parity of 13-year Eu^{152} would seem to be the same as that of 9.2-hour Eu^{152}. It is, however, impossible to eliminate completely the possibility that 13-year Eu^{152} has positive parity.

must thus be of a new type which cannot be explained in terms of the previously known ones (which are easily explainable in terms of selection rules for the above quantum numbers).

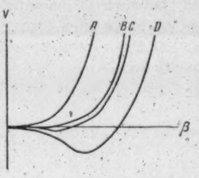

FIG. 2. Dependence of the nuclear potential energy V on the deformation β. Curve A represents nuclei with almost filled shells and with a spherical equilibrium shape ($\beta = 0$). Curve D represents nuclei with ellipsoidal equilibrium shapes ($\beta \neq 0$). Curves B and C represent nuclei close to the transition point between spherical and ellipsoidal equilibrium shapes. Curve B refers to the spherically symmetric 9.2-hr isomer of Eu^{152}, and C refers to the 13-year ground state (ellipsoidal equilibrium shape).

2. The singly forbidden β^- decay of 13-year Eu^{152} to the first and second 2+ levels of Gd^{152} has a log τf value of 12, which means that it is slower than ordinary transitions by a factor of about 10^5. K-transitions to the Sm^{152} level are about equally slowed down (log $\tau f \approx 10$). No K-capture is observed[2,3] to the 123 kev (2+) and 366 kev (4+) levels, which belong to a rotational band of the ground state.

3. Comparison of the probabilities for β^- and K-transitions of the same type, as well as the values for the total ratios K/β^- for the ground state plus isomeric state of Eu^{152} show that 9.2-hr Eu^{152} decays primarily to Gd^{152} levels, and that 13-year Eu^{152} decays to Sm^{152} levels.

In order to understand the properties of Eu^{152} decay, let us consider the question of the equilibrium shape of the nucleus. It is known that all nuclei with 88 neutrons are spherical, whereas those with 90 neutrons have an ellipsoidal equilibrium shape. It is natural to assume that nuclei with $N = 89$ are in "neutral" equilibrium and can be either spherical or ellipsoidal depending on the number of protons. Analysis shows that nuclei with $N = 89$ and $Z = 60$ or 62 are spherical, whereas that with $Z = 64$ is ellipsoidal.[6]

Thus the nucleus with $N = 89$ and $Z = 63$ is in "neutral" equilibrium with respect both to the neutrons and protons. Such a nucleus should have unique properties. The potential vs. deformation plot in Fig. 2 shows that for this nucleus (curves B and C) the states with $\beta = 0$ and $\beta \neq 0$ are almost equally stable, and transitions between them may be caused even by weak excitation of the nucleus.

The nucleus with $Z = 63$ and $N = 89$ is Eu^{152}. In agreement with the above, let us assume that its ground state ($T = 13$ years) has an ellipsoidal equilibrium shape, and that the isomer is spherical in equilibrium. In this case the isomeric transition in Eu^{152} is related to the change of the equilibrium shape, and therefore to a realignment of the nuclear levels. Such a realignment can explain the factor $F > 10^{12}$ in slowing down the γ transitions. It is natural to assume that the equilibrium deformation parameter β for Eu^{152} is minimal and therefore[9] equal to about 0.2. In ${}_{64}G^{152}_{88}$ the deformation parameter $\beta = 0$, and in ${}_{62}Sm^{152}_{90}$ it has the value $\beta = 0.3$. The β-transitions to the Gd^{152} levels and the K-transitions to the Sm^{152} levels are accompanied by a large change in the deformation parameter (the β^--decay causes a change in the equilibrium shape). The significant realignment of nuclear levels which takes place in these transitions may strongly decrease the decay probability, thus explaining the fact that $F \approx 10^3 - 10^5$.

In these processes, the β^--decay is accompanied by a larger change in the deformation parameter ($\Delta\beta = 0.2$) than the K-capture ($\Delta\beta = 0.1$). Thus in the 13-year Eu^{152} we have $K/\beta^- > 1$, and log $\tau f_K <$ log τf_{β^-}. The possibility of K-transitions to the 122 kev and 366 kev rotational levels of Sm^{152} is reduced not only by the change in the deformation parameter, but also by forbiddenness with respect to the quantum number K, which decreases the probability[6] by a factor of 10^4 when $\Delta\nu = \Delta K - L = 2$. Such K transitions should be practically unobserved.

These conclusions, as we have seen, are in agreement with the experimental data. No change in the equilibrium shape takes place in the β^--decay of the spherical nucleus Eu^{152} ($T = 9.2$ hr), since Gd^{152} is also a spherical nucleus. In complete agreement with this, log τf_{β^-} has the usual value for singly forbidden β-transitions, as already mentioned above.

The probability for K-capture should be much lower, since it is accompanied by a change of the equilibrium shape. This is in agreement with the general features of the experimental data, since $K/\beta^- < 1$ in 9.2-hr Eu^{152}. The observed probability for β^+ and K-transitions, however, is more than could be expected. It should be noted that the existing experimental data on the intensity of β^+-transitions is contradictory,[3,10] so that further study of these transitions is necessary.

It is interesting to note that the hypothesis that the equilibrium shape of Eu^{152} ($T = 13$ years) is ellipsoidal is supported by data on its spin and magnetic moment. They agree exactly with the data for the

Eu^{154} nucleus ($I = 3$, $\mu = 2.0$ nuclear magnetons), which is known to be ellipsoidal.[5,11] The spin of the Eu^{152} isomer, namely 1−, is in agreement with the hypothesis that the nucleus is spherical.

Thus Eu^{152} is a rare (if not the only) example of a nucleus located intermediately between states with known spherical and ellipsoidal equilibrium shapes, and must thus have several unique properties (other than those considered above). Therefore further experimental study of this nucleus and the establishment of its complete decay scheme is very important for the development of concepts on its structure.

I offer my deep gratitude to L. A. Sliv for detailed discussion of the work.

---

[1] B. V. Bobykin, Тезисы 7 совещания по ядерной спектроскопии, (Theses of the 7th Conference on Nuclear Spectroscopy), L., Acad. of Sciences Press, 1957.

[2] O. Nathan and M. A. Waggoner, Nuclear Phys. 2, 548 (1957).

[3] L. Grodsins and H. Kendall, Bull. Am. Phys. Soc. 1, 163 (1956); Nuclear Sc. Abstr. 10, No. 12, B. (1956).

[4] Dzhelepov, Zhukovskii, Kondakov, Nedovesov, and Shuikin, Тезисы 7 совещания по ядерной спектроскопии, 1957.

[5] Manenkov, Prokhorov, Trukhliaev, and Iakovlev, Тезисы 7 совещания по ядерной спектроскопии, 1957.

[6] L. K. Peker, Тезисы 7 совещания по ядерной спектроскопии, 1957.

[7] Alaga, Alder, Bohr, and Mottelson, Проблемы соврем. физики, (Problems of Modern Physics) No. 1 (1956); [Probably a translation of Kgl. Danske Videnskab, Selskab, Mat.-Fys. Medd. 29, No. 9 (1955).]

[8] Alaga, Alder, Bohr, and Mottelson, Kgl. Danske Videnskab, Selskab, Mat.-Fys. Medd. 29, No. 16 (1956).

[9] A. Bohr and B. Mottelson, Проблемы соврем. физики, 1, (1956).

[10] Hollander, Perlman, and Seaborg, Table of Isotopes, ILL, 1956. [Translation of Revs. Mod. Phys. 25, 469 (1953).]

[11] Kedzie, Abraham, and Jeffries, Bull. Amer. Phys. Soc. 1, 390 (1956).

Translated by E. J. Saletan
55

SMALL-ANGLE SCATTERING OF FAST NEUTRONS BY HEAVY NUCLEI

IU. A. ALEKSANDROV

Atomic Energy Institute

Submitted to JETP editor April 10, 1957

J. Exptl. Theoret. Phys. (U.S.S.R.) 33, 294-296 (July, 1957)

WE have studied the angular distribution of fast neutrons elastically scattered from Pu, U, Pb, Bi, Sn, and Cu nuclei in the interval of angles* from 4 to 25°. This work may be considered an attempt at the experimental investigation of the possible "polarizability" of the neutron in the strong Coulomb field of the nucleus, which is of interest from the point of view of studying the internal structure of the neutron. As has previously been noted,[1,2] the "polarizability" of the neutron would be observed in the anomalous behavior of the differential elastic scattering cross section at small angles.

A fast neutron beam is extracted from the reactor with the aid of a collimator previously described.[1] The detector was a cylindrical chamber filled with He^4 to a pressure of 15 atmos. In order to improve the characteristics of the chamber, as well as to determine the energy scale, 5% of N_2 was added to the chamber. The chamber diameter was 4 cm, and the operating length was approximately 45 cm. The counting efficiency was several percent for neutrons of energy on the order of 1.3 Mev.

---

*The angular distribution of fast neutrons in the interval of angles from 0.7 to 5° will be published later.

The operation of the chamber was tested by the N^{14} (n, p) C^{14} reaction with thermal neutrons, which gives 600 kev protons. The differential pulse amplitude distribution is shown in Fig. 1.

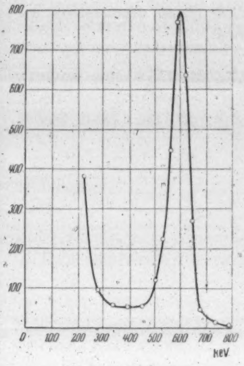

FIG. 1

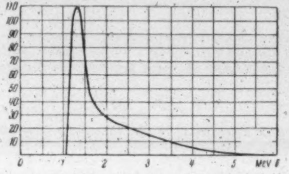

FIG. 2

In measuring the angular distribution, the analyzer separated the band from 680 to 890 kev. The energy spectrum of neutrons counted by the chamber was found by calculation, and is shown in Fig. 2. The spectrum was calculated using the data of Adair[3] and Seagrave.[4]

The scatterers were 1 cm thick plates of the substance being investigated. The absolute magnitudes of the cross sections were found by comparison with the paraffin cross section, as well as by the method previously described.[1] The mean effective energy, as found from the paraffin cross section, was about 2 Mev.

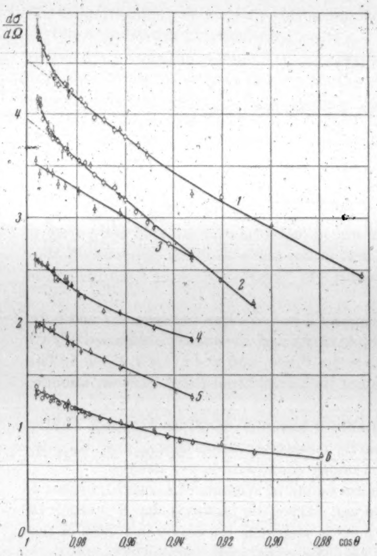

FIG. 3. Experimental results. All experimental points are corrected for the Schwinger scattering cross section. Curves 1, 2, 3, 4, 5, and 6 refer to Pu, U, Sn, Pb, Bi, and Cu, respectively. The vertical scales for curves 4 and 5 are decreased by factors of 1.5 and 2.

The experimental results are shown in Fig. 3. The ordinate gives $d\sigma/d\Omega$ in barn/sterad. The points indicated by circles were obtained from the angular distribution in the vicinity of 0.5°. To obtain these points, an additional paraffin collimator with an opening 0.5 cm by 2 cm was placed between the chamber and the scatterer. The length of this collimator was 1.5 m. The other points were obtained without this additional collimator. The angular resolution was then about 2.5°.

In obtaining the experimental points of Fig. 3, we have subtracted the quantity $\gamma^2 \cot^2(\theta/2)$, which is the Schwinger scattering cross section [Eq. (10) of Ref. 5]. Nevertheless, Pu (with $Z = 94$) and U (with $Z = 92$) have sharp rises in the cross section for angles less than 11° (or for $\cos\theta > 0.982$). In the other elements, the increase of the cross section is within the limits of experimental error.

The increase of the cross section mentioned above may be due to the "polarizability" of the neutron. Calculations performed on the assumption that the nucleus can be approximated as a solid sphere for the scattering problem give a coefficient of polarizability $\alpha = (8.0 \pm 3.5) \times 10^{-41}$ cm^3. In this calculation the amplitude of pure nuclear scattering was found by extrapolating the curves from the high-angle regions (dotted curves of Fig. 3). It is also possible that the increase in the cross section at angles less than 11° for Pu and U is due to some other reasons. In any case, no final conclusion as to the "polarizability" of the neutron can be made until a careful theoretical analysis has been performed on the experimental data. It is also desirable to perform investigations with monoenergetic neutrons.

The author expresses his deep gratitude to A. I. Leipunskii, Active Member of the Academy of Sciences, Ukranian S.S.R., and O. D. Kazachkovskii for their interest in the work, to I. I. Bondarenko for much advice and many remarks, to V. S. Barashenkov, L. N. Usachev, and I. P. Stakhanov for helpful discussions, as well as to the reactor maintenance personnel for aid in setting up the experiment.

---

[1] Iu. A. Aleksandrov and I. I. Bondarenko, J. Exptl. Theoret. Phys. (U.S.S.R.) **31**, 726 (1956); Soviet Phys. JETP 4, 612 (1957).

[2] Barashenkov, Stakhanov, and Aleksandrov, J. Exptl. Theoret. Phys. (U.S.S.R.) **32**, 154 (1957); Soviet Phys. JETP 5, 144 (1957).

[3] R. K. Adair, Phys. Rev. **86**, 155 (1952).

[4] I. D. Seagrave, Phys. Rev. **92**, 1222 (1953).

[5] J. Schwinger, Phys. Rev. **73**, 407 (1948).

Translated by E. J. Saletan
56

DECAY PROBABILITIES OF THE Σ-HYPERON WITH PARITY NONCONSERVATION

I. IU. KOBZAREV and L. B. OKUN'

Submitted to JETP editor April 11, 1957

J. Exptl. Theoret. Phys. (U.S.S.R.) **33**, 296-297 (July, 1957)

SEVERAL works[1-3] have investigated the relation between the Σ-hyperons

$$\Sigma^+ \to p + \pi^0 \ (w^0), \quad \Sigma^+ \to n + \pi^+ \ (w^+), \quad \Sigma^- \to n + \pi^- \ (w^-)$$

and it was shown that the quantities

$$X = w^0 / w^+ \text{ and } Y = w^- / (w^+ + w^0) = \tau^+ / \tau^-$$

(where $\tau^\pm$ is the lifetime of the $\Sigma^\pm$-hyperon) should lie on a curve depending on the spin and parity of the Σ-hyperon. This conclusion is based on the assumptions that in the decay of the Σ-hyperon (1) the selection rule ΔT = 1/2 (where T is the isotopic spin) is valid, (2) invariance under time inversion is maintained, and (3) parity is conserved.

It has been shown[1] that data of the Sixth Rochester Conference (X = 1, Y lies between 0.1 and 0.2) are in agreement with the theoretical curves. Later, however, Alvarez and co-workers obtained $w^0/w^+ = 1.0 \pm 0.2$, $\tau^- = (1.86 \pm 0.26) \times 10^{-10}$ sec, $\tau^+ = (0.86 \pm 0.17) \times 10^{-10}$ sec, and $\tau^-/\tau^+ = 2.2 \pm 0.5$. The corresponding X, Y point (X = 1 ± 0.2, Y = 0.45 ± 0.10) does not lie on the theoretical curves, whence Alvarez[4] concludes that assumption (1) is not valid.

We should like to indicate that this conclusion is not inevitable if assumption (3) is dropped. Parity nonconservation in the case of hyperon decay follows from parity nonconservation in K_{π_2} and K_{π_3} decays, since the hyperon decay can always go through a virtual decay chain with $K \to \pi$ decays.

We shall assume as before that assumption (2) is valid in the sense of Wigner;[5] i.e., with respect to the combined inversion CI.[6] This assumption, from which one can derive the fact that the S matrix is symmetric, makes it possible[1] to express the phases of the matrix elements for decay in terms of the scattering phases in the final state,

$$a_+ = i\,{}^1/_3\,(\rho_3 e^{i\alpha_3} + \sigma_3 e^{i\alpha'_3}) + i\,{}^2/_3\,(\rho_1 e^{i\alpha_1} + \sigma_1 e^{i\alpha'_1}), \quad a_0 = i\,(\sqrt{2}/3)\,(\rho_3 e^{i\alpha_3} + \sigma_3 e^{i\alpha'_3}) - i\,(\sqrt{2}/3)\,(\rho_1 e^{i\alpha_1} + \sigma_1 e^{i\alpha'_1}),$$

$$a_- = i\,(\rho_3 e^{i\alpha_3} + \sigma_3 e^{i\alpha'_3})$$

(ρ_3 and ρ_1 here correspond to $\sqrt{3}\rho_3$ and $\sqrt{3/2}\rho'_1$ of the previous work referred to[1]). Here the parameters ρ and σ are real, and α and α′ are the phases of π-meson—nucleon scattering. For a Σ-hyperon spin of 1/2, the values of (ρ, α) and (σ, α′) correspond to transitions in the π-meson—nucleon system to the $S_{1/2}$ and $P_{1/2}$ states, and for Σ spin of 3/2, they correspond to the $P_{3/2}$ and $D_{3/2}$ states, respectively. The indices 3 and 1 refer to isotopic spin states with T = 3/2 and T = 1/2. The scattering phases α and α′ are known and such that $\alpha' \approx 0$.

To calculate the ratios of the probabilities, we make use of the fact that the total probabilities for transitions to states with different parities do not interfere, since their wave functions correspond to orthogonal Legendre polynomials. We then obtain

$$X = \frac{2(\rho_3^2+\sigma_3^2)+2(\rho_1^2+\sigma_1^2)-4(\rho_3\rho_1\cos(\alpha_3-\alpha_1)+\sigma_3\sigma_1)}{(\rho_3^2+\sigma_3^2)+4(\rho_1^2+\sigma_1^2)+4(\rho_3\rho_1\cos(\alpha_3-\alpha_1)+\sigma_3\sigma_1)}, \quad Y = 3(\rho_3^2+\sigma_3^2)/[(\rho_3^2+\sigma_3^2)+2(\rho_1^2+\sigma_1^2)].$$

Introducing the notation

$$z = \sqrt{(\rho_1^2+\sigma_1^2)/(\rho_3^2+\sigma_3^2)}, \qquad \varkappa = \frac{\rho_3}{\sqrt{\rho_3^2+\sigma_3^2}}, \qquad \mu = \frac{\rho_1}{\sqrt{\rho_1^2+\sigma_1^2}},$$

we obtain

$$X = \frac{2+2z^2-4z\,[\varkappa\mu\cos(\alpha_3-\alpha_1)\pm\sqrt{(1-\mu^2)(1-\varkappa^2)}]}{1+4z^2+4z\,[\varkappa\mu\cos(\alpha_3-\alpha_1)\pm\sqrt{(1-\varkappa^2)(1-\mu^2)}]}, \quad Y = \frac{3}{1+2z^2}.$$

This expression differs from the previous one[1] in that cos $(\alpha_3-\alpha_1)$ is replaced by

$$Q = \varkappa\mu\cos(\alpha_3-a_1)\pm\sqrt{(1-\varkappa^2)(1-\mu^2)},$$

which can take on arbitrary values with $|Q| \leq 1$. It follows from this that the X, Y point lies in a region bounded by the curve

$$X = (2+2z^2\mp 4z)/(1+4z^2\pm 4z), \quad Y = 3/(1+2z^2),$$

which corresponds to curve (1) of the previous work.[1] This region is the same as that obtained by Gatto[7] in investigating the restrictions following only from the selection rule $\Delta T = 1/2$ without accounting for invariance under time inversion.

It is easily seen that the data of Alvarez lies in the allowed region, and thus does not contradict the assumption of the validity of the selection rule $\Delta T = 1/2$.

---

[1] L. B. Okun', J. Exptl. Theoret. Phys. (U.S.S.R.) **31**, 333 (1956); Soviet Phys. JETP **4**, 284 (1957).
[2] J. Prentki and B. d'Espagnat, Nuovo cimento **3**, 1045 (1956).
[3] M. Kawaguchi and K. Nishigima, Progr. Theoret. Phys. **15**, 182 (1956).
[4] L. Alvarez et al., Phys. Rev. **105**, 1127 (1957).
[5] E. Wigner, Nachr. Akad. Wiss Göttingen, Mat.-physik. Kl., 546 (1932).
[6] L. D. Landau, J. Exptl. Theoret. Phys. **32**, 405 (1957); Soviet Phys. JETP **5**, 336 (1957).
[7] R. Gatto, Nuovo cimento **3**, 318 (1956).

Translated by E. J. Saletan
57

A "SYMMETRIC" CIRCULAR SYNCHROCYCLOTRON WITH OPPOSITELY DIRECTED BEAMS

A. A. KOLOMENSKII

P. N. Lebedev Physics Institute, Academy of Sciences, U.S.S.R.

Submitted to JETP editor April 15, 1957

J. Exptl. Theoret. Phys. (U.S.S.R.) 33, 298-299 (July, 1957)

THE possibilities of using the collision of intense beams of particles accelerated to relativistic energies have recently been considered.[1] The energy used directly for a physical experiment (for instance for particle production) is then greater than that available when a beam hits a stationary target by a factor of about $2E/m_0c^2$, where E is the energy of each beam. The suggestions so far made in this regard involve the use of two adjacent or concentric annular accelerators having a common section or sections in which the collision is to occur.[1]

The present note suggests a means for achieving the collision of beams travelling in opposite direction in a single accelerator, a "symmetric" circular synchrocyclotron. This instrument is a variation on that suggested by the author together with Petukhov and Rabinovich,[2] a strong-focusing accelerator with a magnetic field constant in time and composed of sectors with oppositely directed fields (see also Refs. 3 – 6).

Let θ_1, θ_{01}, θ_2, and θ_{02} be the azimuth angles of sectors with fields $H_1 > 0$, $H_{01} = 0$, $H_2 < 0$, and $H_{02} = 0$, which taken together add up to an element of periodicity θ_{per}. The suggested "symmetric" circular synchrocyclotron should be made of sectors θ_1 and θ_2 having a common point at the center O of the apparatus and having the same geometric and magnetic characteristics (except for the sign of the field), i.e., $\theta_1 = \theta_2$, $H_2(r) = -H_1(r)$, $H \sim r^{-n}$, and $n_0 = \mathrm{const}$. The mean field along a circle of radius r about the point O will obviously be zero. However the closed orbits about which betatron oscillations take place are not circular, being wave-like curves which pass through the sectors with $H_1 > 0$ at higher absolute values of the field than through the sectors with $H_2 < 0$, or vice versa (see figure). Therefore the mean field along the orbit is either positive or negative, depending on the initial direction of motion. It is clear that in a "symmetric" circular synchrocyclotron the two directions of motion (clockwise and counterclockwise) are equally possible for a particle. Therefore with such an accelerator one can simultaneously accelerate particles of the same kind (for instance electrons or protons) in opposite directions. The closed orbits of these two oppositely directed beams are of the same geometric shape, but are rotated with respect to each other by an angle of $\theta_{\mathrm{per}}/2$.

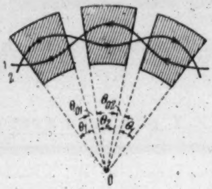

Part of a "symmetric" circular synchrocyclotron. 1 and 2 are the orbits of the oppositely directed beams (schematically drawn).

Our calculations,[6] which account for edge effects, show that with appropriate choice of the parameters (in particular when N lies between 6 and 7 times $\sqrt{|n_0|}$, where N is the number of elements of periodicity) one can satisfy the simultaneous conditions for stability of radial and vertical betatron oscillations in the "symmetric" instrument. A disadvantage of this accelerator, which is a general characteristic of circular synchrocyclotrons,[4] is the increase of the radius of the instrument compared with the radius of curvature of the orbit in the sectors (by a factor between about 5 and 6).

For acceleration in resonant (synchrotron) operation, both of the beams will obtain energy from the same rf accelerating system. The equilibrium phases of these beams, obviously, will be out of phase by an angle π, and it follows from the general theory of resonant self-phasing accelerators that such a simultaneous acceleration of oppositely directed beams will be essentially the same as that of a single beam in an ordinary synchrotron or synchrocyclotron. When the particles attain the necessary relativistic energy, the accelerating voltage is turned off, and the free beams continue to rotate in opposite directions undergoing head-on collisions for a time determined by scattering on whatever gas remains in the chamber of the accelerator, and by similar phenomena. The accelerating cycle can then be repeated.

We note that the use of resonant operation makes it possible, in principle, to collect particles in beams of the required orbit during several accelerating cycles. This makes it possible to increase the efficiency of the method of colliding beams.

The case of induction (betatron) acceleration as applied to "symmetric" equipment differs from the resonance method. In each half period of fluctuation of the betatron magnetic flux, the beam moving in one direction accelerates, and that moving in the other direction decelerates. One can, true, obtain in this case head-on collisions of the beams, one of which is accelerated and the other decelerated in a given cycle, the latter having been accelerated in the previous one, but the efficiency would then seem to be much less than in the case of resonance acceleration. Nevertheless, betatron operation in a "symmetric" circular synchrocyclotron may also, in principal, be of definite interest.

---

[1] Kerst, Cole, et al., Phys. Rev. 102, 590 (1956); D. W. Kerst, CERN 1, 36 (Geneva, 1956).

[2] Kolomenskii, Petukhov, and Rabinovich, Phys. Inst. Acad. Sci. Report RF-54, 1953; Symposium: Some Problems in the Theory of Cyclic Accelerators, Acad. of Sciences Press M. 1955, p. 7; Приборы и техника эксперимента, (Instr. and Exptl. Techn.) 2, 26 (1956).

[3] K. R. Symon, Phys. Rev. 98, 1152 (1955).

[4] A. K. Burtsev and A. A. Kolomenskii, Приборы и техника эксперимента, 2, 11 (1957).

[5] Symon, Kerst, et al., Phys. Rev. 103, 1837 (1956).

[6] A. A. Kolomenskii, Dissertation, Phys. Inst. Acad. Sci., M. 1957.

Translated by E. J. Saletan
58

SECOND ORDER PHASE TRANSITION IN SODIUM NITRATE

I. E. DZIALOSHINSKII and E. M. LIFSHITZ

Institute of Physical Problems, Academy of Sciences, U.S.S.R.

Submitted to JETP editor April 16, 1957

J. Exptl. Theoret. Phys. (U.S.S.R.) 33, 299-301 (July, 1957)

IN the theory of phase transitions[1] a body is usually considered isotropic with respect to its elastic properties, and is characterized by a single modulus of compressibility. But the behavior of the elastic constants of a monocrystal may exhibit various properties in a second order phase transition which are strongly related to specific types of structural changes of the crystal lattice at the transition point. It would hardly be reasonable to investigate this problem in general, in view of the very large number of possibilities that may arise.

We here consider a second order phase transition in sodium nitrate. Kornfel'd and Chudinov[2] have recently measured the temperature dependence of the elastic constants of this substance in the neighborhood of the transition point.

The $NaNO_3$ crystal is rhombohedral. Below the transition point its elementary cell contains two molecules, and the NO_3 groups have two different crystallographic orientations (symmetry group D_{3d}^6; see Wyckoff's[3] description). Above the transition point there is no difference between the NO_3 groups, each of which can have one of two possible orientations with equal probability.[4] This reduces the elementary cell by a factor of two (symmetry group D_{3d}^5). Thus the transition is related to ordering the NO_3 groups.

In the present case the density function $\rho(x, y, z)$, which enters into the general theory of second order phase transitions, can be thought of as the density distribution of oxygen atoms. Using the general methods[1,5] one can show that the change $\delta\rho(x, y, z)$ of the density function corresponding to the given transition has the same symmetry as the function $\sin \pi(x + y + z)$, where x, y, and z are the coordinates relative to the axes of the rhombohedral cell. Therefore the transition being considered in sodium nitrate is described by a single parameter η which transforms as the functions $\sin \pi(x + y + z)$ under all transformations of the symmetry group D_{3d}^5 of the high-temperature phase (including translations).*

From this it follows immediately that in the series expansion for the thermodynamic potential there will be no term proportional to η^3, so that the transition may indeed take place as a second order transition.

To determine the change of the elastic constants at the transition point, we write the thermodynamic potential in the neighborhood of this point in the form

$$\Phi = \Phi_0(T) + A(T - T_c)\eta^2 + \tfrac{1}{2}B\eta^4 + a\eta^2(\sigma_{xx} + \sigma_{yy}) + b\eta^2\sigma_{zz} - \alpha_1(T - T_c)(\sigma_{xx} + \sigma_{yy}) - \alpha_3(T - T_c)\sigma_{zz}$$
$$- \tfrac{1}{2}s_{11}(\sigma_{xx}^2 + \sigma_{yy}^2 + 2\sigma_{xy}^2) - \tfrac{1}{2}s_{33}\sigma_{zz} - \tfrac{1}{2}s_{44}(\sigma_{xz}^2 + \sigma_{yz}^2) - s_{12}(\sigma_{xx}\sigma_{yy} - \sigma_{xy}^2) - s_{13}(\sigma_{xx} + \sigma_{yy})\sigma_{zz}$$
$$- s_{14}[(\sigma_{xx} - \sigma_{yy})\sigma_{zz} - 2\sigma_{zx}\sigma_{xy}],$$

where σ_{ik} is the elastic strain tensor, and T_c is the transition temperature in the absence of strain; we have here accounted for the rhombohedral symmetry of the elastic properties of the crystal, and the specific symmetry of the parameter η. The phase transition occurs at the point at which the coefficient of η^2 vanishes, i.e., at the temperature

$$T_c' = T_c - (a/A)(\sigma_{xx} + \sigma_{yy}) - b\sigma_{zz}/A.$$

---

*The parameter η may be defined as $(w_1 - w_2)/(w_1 + w_2)$, where w_1 and w_2 are the probabilities for the two orientations of the NO_3 group at some lattice site.

Determining η^2 from the condition that the thermodynamic potential be a minimum when $T < T_C'$, and inserting this into the expression for Φ, we obtain the potential of the low-temperature phase, namely

$$\Phi = \Phi_0(T) - (A^2/2B)(T - T_c)^2 - (\alpha_1 + aA/B)(T - T_c)(\sigma_{xx} + \sigma_{yy}) + (\alpha_3 + bA/B)(T - T_c)\sigma_{zz} -$$

$$- {}^1/_2(s_{11} + a^2/B)(\sigma_{xx}^2 + \sigma_{yy}^2 + 2\sigma_{xy}^2) - {}^1/_2(s_{33} + b^2/B)\sigma_{zz}^2 - {}^1/_2 s_{44}(\sigma_{xz}^2 + \sigma_{yz}^2) - (s_{12} + a^2/B)(\sigma_{xx}\sigma_{yy} - \sigma_{xy}^2) -$$

$$- (s_{13} + ab/B)(\sigma_{xx} + \sigma_{yy})\sigma_{zz} - s_{14}[(\sigma_{xx} - \sigma_{yy})\sigma_{zz} - 2\sigma_{zx}\sigma_{xy}],$$

from which we can immediately determine the discontinuities in the elastic coefficients at the transition point,

$$\Delta s_{11} = \Delta s_{12} = a^2/B, \quad \Delta s_{33} = b^2/B; \quad \Delta s_{13} = ab/B, \quad \Delta s_{14} = \Delta s_{44} = 0,$$

and the discontinuities in the coefficients of thermal expansion

$$\Delta\alpha_1 = aA/B, \quad \Delta\alpha_3 = bA/B.$$

Although the coefficients s_{14} and s_{44} have no discontinuities at the transition point, they have a break at this point when considered as functions of the temperature. The magnitude of this break can be found if we include terms proportional to the product of η^2 and quadratic combinations of the strain tensor components in the series expansion of the thermodynamic potential.

According to the measurements of Austin and Pierce,[6] in the temperature region we are here concerned with $\alpha_1 \sim 0.1\alpha_3$. It is reasonable to assume that the discontinuities $\Delta\alpha_1$ and $\Delta\alpha_3$ are in at least the same ratio, so that $a \lesssim 0.1b$. Then for the discontinuities in the elastic coefficients, we obtain

$$\Delta s_{11} = \Delta s_{12} \leqslant 0{,}01\,\Delta s_{33}, \quad \Delta s_{13} \leqslant 0{,}1\,\Delta s_{33},$$

which would seem to be in agreement with the results of Kornfel'd and Chudinov.

---

[1] L. Landau and E. Lifshitz, Статистическая физика, (Statistical Physics), 3rd ed., M., 1951.

[2] M. O. Kornfel'd and A. A. Chudinov, J. Exptl. Theoret. Phys (U.S.S.R.) this issue, p. 33, Soviet Phys. JETP, this issue, p.

[3] R. W. G. Wyckoff, The Structure of Crystals (New York, 1931).

[4] Kracek, Posnjak, and Hendriks, J. Am. Chem. Soc. 53, 1183, 2609, 3399 (1931).

[5] E. M. Lifshitz, J. Exptl. Theoret. Phys. (U.S.S.R) 11, 255 (1941).

[6] J. B. Austin and R. H. Pierce, J. Am. Chem. Soc. 55, 661 (1933).

Translated by E. J. Saletan
59

A MEASUREMENT OF THE DEPTH OF PENETRATION OF A MAGNETIC FIELD INTO MERCURY FILMS

I. S. KHUKHAREVA

Moscow State University

Submitted to JETP editor April 17, 1957

J. Exptl. Theoret. Phys. (U.S.S.R.) 33, 301-303 (July, 1957)

MEASUREMENTS of the critical temperature and critical magnetic field were performed for mercury films whose thickness varied from 3.7×10^{-6} to 95×10^{-6} cm so as to determine the depth of penetration.

The first attempts to measure this depth of penetration were those of Appleyard, Brostow, H. London, and Misener[1] in films, Shoenberg[2] in colloidal samples, Desirant and Shoenberg[3] in thin wires, and Laurmann and Shoenberg[4] in a bulk sample. Recently the depth of penetration was measured by Whitehead[5] in colloidal mercury, and Prozorova* in thin films at a frequency of 9400 Mc.

Method and author	$10^6\,\delta_0$ (cm)
Thin films[1,8]	6.15*
Thin wires[3]	7.6
Bulk sample[4]	3.8**
	4.5***
Thin films (present work)	5.3 ± 0.4
Thin films (Prozorova[1])	5.5 ± 0.5

*According to Ginzburg $\delta_T = 6.6 \times 10^{-6}$ cm at 2.5° K.

**Magnetic field parallel to the crystal axis.

***Magnetic field perpendicular to the crystal axis.

The relatively high vapor tension of mercury made it possible to obtain films up to a micron thick at temperatures of liquid helium, without using a heater of more than 0.4 w.

The films were obtained by the Shal'nikov-Zavaritskii method[6] of condensation on the plane polished surface of a container with platinum leads soldered through it. To obtain a more homogeneous film, the sides of the container were covered by a screen. An evaporated drop of mercury was placed in a thin-walled glass tube about 10 mm long with an opening about 1.5 mm, on which was wound a platinum wire half embedded in the glass for better thermal contact.

Before the start of condensation, the apparatus was evacuated with a diffusion pump, and its upper part was treated in an oven at a temperature of about 300° C for three hours. The lower part of the apparatus containing the vaporizer and mercury was placed in liquid nitrogen. The unsoldered apparatus was then mounted within a helium-filled Dewar flask. Condensation of the film continued from 15 min to 1 hr. and its thickness was calculated from the weight of the evaporated mercury. The inhomogeneity of the film thickness from the side of the container to the center was no greater than 0.3%.

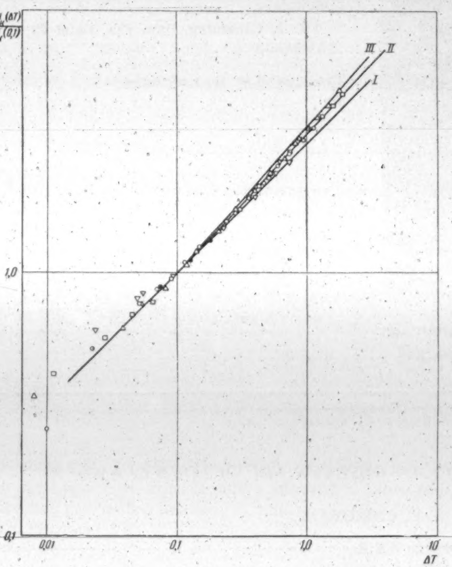

The film thicknesses for the various points (in 10^{-6} cm) are ○ — 3.7, △ — 4.5, □ — 8.3, ▽ — 21, ● — 31. The solid line is calculated from the formula $\delta = \delta_0 [1 - T/T_k)^n]^{-1/2}$, with the following values of n. (I) n = 3, (II) n = 4, (III) n = 5.

The resistance of the film was measured by an ordinary potentiometer circuit, and in the case of the thickest films it was measured directly in terms of galvanometer deflection. First the temperature dependence of the film resistance was measured, and then at several temperatures the transition curves from the superconducting to the normal state was measured as the external magnetic field strength, parallel to the plane of the film, was increased. The properties of the films were measured both immediately after condensation and after annealing to the temperature of liquid nitrogen.

On the basis of the R(H) curves obtained, we found the critical magnetic field strength H_k of the film (at which $R = R_N/2$) as a function of $T = T_k - T$. The films satisfied the law $H_k \sim (\Delta T)^{1/2}$ in a completely satisfactory way, with the thickest films indicating a characteristic break in these curves, on one side of which the above law remains valid.

Using the Ginzburg-Landau formula[7] $H_k/H_{km} = 2\sqrt{6}\,\delta/d$, one can obtain the depth of penetration $\delta(T)$ from the experimental results.

It is seen from the figure that the temperature dependence of δ is not in contradiction to

$$\delta(T) = \delta_0 [1 - (1 - T/T_k)^4]^{-1/2}.$$

The table gives values of δ_0 as obtained by various authors.

In conclusion I express my sincere gratitude to Professor A. I. Shal'nikov for directing the work and constant attention, and to N. V. Zavaritskii for participating in discussions of the results.

---

*Reported at All-Union Conference on Low-Temperature Physics, Leningrad, 1956.

[1] Appleyard, Bristow, London, and Misener, Proc. Roy. Soc (London) 172A, 540 (1939).

[2] D. Shoenberg, Proc. Roy. Soc. (London) 175A, 49 (1940).

[3] M. Desirant and D. Shoenberg, Proc. Phys. Soc. (London) 60, 413 (1948).

[4] E. Laurmann and D. Shoenberg, Proc. Roy. Soc. (London) 198A, 560 (1949).

[5] C. S. Whitehead, Proc. Roy. Soc. (London) 238, 175 (1956).

[6] N. V. Zavaritskii, Dokl. Akad. Nauk SSSR 78, 665 (1951).

[7] V. L. Ginzburg and L. D. Landau, J. Exptl. Theoret. Phys. (U.S.S.R.) 20, 1064 (1950).

[8] V. L. Ginzburg, Usp. Fiz. Nauk 42, 169 (1950).

Translated by E. J. Saletan
60

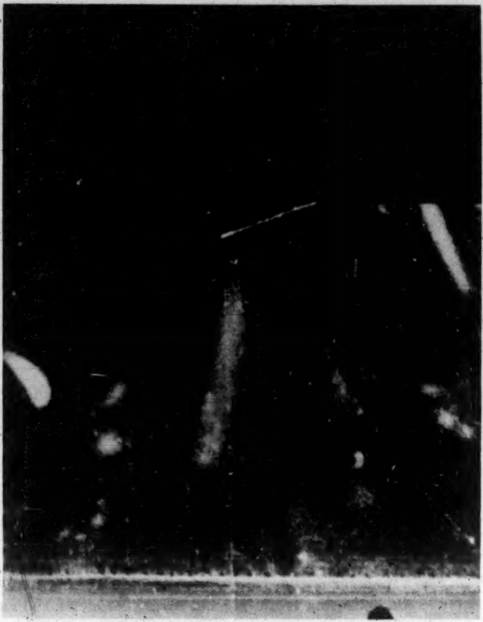

For the article by Mandzhavidze, N. N. Roinishivili and G. E. Chikovani entitled "Anomalous Decay of a Charged Particle Observed in a Cloud Chamber."

ANOMALOUS DECAY OF A CHARGED PARTICLE OBSERVED IN A CLOUD CHAMBER

Z. SH. MANDZHAVIDZE, N. N. ROINISHVILI, and G. E. CHIKOVANI

Physics Institute, Academy of Sciences, Georgian S.S.R.

Submitted to JETP editor April 19, 1957

J. Exptl. Theoret. Phys. (U.S.S.R) 33, 303 (July, 1957)

THE unusual event whose photograph is shown in the figure was recorded among the decays of charged hyperons and K-particles observed in a cloud chamber at the El'brus Laboratory.

A slow particle with an ionization multiplicity factor greater than twenty enters the chamber through the front window and decays emitting at an angle of 95° a positive particle with momentum 352^{+94}_{-61} Mev/c and close to minimum ionization. The transverse component of the secondary particle momentum is 351 Mev/c, which is much larger than the maximum momentum of the decay products in the rest system for all known decay schemes of hyperons and K-mesons.

The anomalously large momentum of the secondary particle is hard to explain in terms of experimental error. It is true that the track passes close to a small vapor cloud, but this does not interfere with the measurement of the curvature and does not distort the track. On the other hand, kinematic analysis excludes the possibility of interpreting the given event as the decay of a Λ^0, θ^0, or V_3^0-particle.

All this gives reason to suppose that we have observed the decay of a particle heavier than a K-meson. A detailed analysis of this case will be published later.

The authors consider it their duty to express their gratitude to Professor E. L. Andronikashvili for directing the work, as well as to their colleagues at the Tibilisi State University, L. D. Gedevanishvili and E. I. Tsagareli and those at the Institute of Physics of the Academy of Sciences, Georgian S.S.R., R. I. Dzidziguri, A. I. Tsintsabadze, and V. D. Tsintsadze for aid in the work.

Translated by E. J. Saletan
61

APPLICATION OF THE EINSTEIN-FOKKER EQUATION TO FINDING PARTICLE LOSSES DUE TO GAS SCATTERING IN ACCELERATORS

B. M. BOLOTOVSKII and A. P. FATEEV

P. N. Lebedev Physics Institute, Academy of Sciences, U.S.S.R.

Submitted to JETP editor April 22, 1957

J. Exptl. Theoret. Phys. (U.S.S.R.) 33, 304-306 (July, 1957)

THE influence of multiple scattering on betatron oscillations of particles was first investigated by Blachman and Courant,[1] who used the Einstein-Fokker equation to describe the scattering process. Somewhat later, in 1951, one of the present authors[2] used the Einstein-Fokker equation in studying the influence of inelastic scattering of electrons on synchrotron oscillations. This method has also been used by other authors.[3,4]*

Let P (y, t) be the probability that the betraton or synchrotron oscillation amplitude of a particle is y at time t. Without accounting for damping of the oscillations, the Einstein-Fokker equation for P(y, t) is

$$\frac{\partial P(y,t)}{\partial t} = -\frac{\partial}{\partial y}(\overline{\Delta y}P) + \frac{1}{2}\frac{\partial^2}{\partial y^2}(\overline{\Delta y^2}P), \tag{1}$$

where

$$\overline{\Delta y^n} = \lim_{\Delta t \to 0} \frac{1}{\Delta t} \int_{-\infty}^{+\infty} Q(y, \Delta y, \Delta t)(\Delta y)^n \, d(\Delta y),$$

in which Q(y, Δy, Δt) is the probability that the amplitude y changes by an amount Δy in a time Δt → 0. In our case Q is found from the interaction cross section between the accelerated particles and the remaining gas in the chamber. Furthermore, $Q(y, \Delta y, \Delta t) \doteqdot Q(y, \Delta y)\Delta t$. As was shown by Kolmogorov,[5] Eq. (1) is valid if

$$\overline{(\Delta y)^3} \ll \overline{(\Delta y)^2}, \overline{\Delta y}. \tag{2}$$

Equation (2) means that for large Δy, the probability Q(y, Δy) should rapidly approach zero.

Let us investigate whether this condition is fulfilled by the process of exciting betraton oscillations by elastic scattering. In this case Δy is the increase of the amplitude of free vibrations due to scattering through an angle Θ, and Q is the cross section (up to a proportionality factor) for Rutherford scattering through an angle Θ. Since this cross section is proportional to Θ^{-4}, it is clear that (2) is satisfied and the results of Blachman and Courant[1] are valid

The situation is different if Q(y, Δy) has no sharp maximum at small Δy. As an example, let us consider the excitation of synchrotron oscillations due to inelastic collisions between accelerated particles and the gas in the chamber. For high-energy electrons, the fundamental process leading to excitation of synchrotron oscillations is bremsstrahlung,* while for heavy particles this process is ionization loss. The change Δy of the synchrotron oscillation amplitude y is linearly related to the energy loss of a particle. In this case, Q is the cross section for collision with energy loss (to within a factor). For inelastic collisions, a particle may lose a significant fraction of its energy with measurable probability, which corresponds to large values of Δy. The maximum value of Δy which is consistent with stable acceleration is given by the equation (see, for example, Bolotovskii[2] or Rabinovich[6])

---

*Note made in proof. See also D. G. Koshkareva, Приборы и техника эксперимента, (Instr. and Exptl. Tech.) 2, 15 (1957).

$$(\Delta y)_{\max} = \omega_0 (2 eV_0 \sin\varphi_0 K/\pi E)^{1/2}, \quad K = 1 + n/\beta^2 (1-n), \tag{3}$$

where $eV_0 \cos\varphi_0$ is the increase in energy per revolution, E is the particle energy, ω_0 is the frequency of rotation, n is the magnetic field index, and $\beta = v/c$. A change of y by an amount $(\Delta y)_{\max}$ corresponds to an energy loss of

$$(\Delta E)_{\max} = (2 eV_0 \sin\varphi_0 E/\pi K)^{1/2}. \tag{4}$$

If the energy loss of a particle on collision is greater than this amount, the particle immediatedly stops being accelerated. The probability for such a single loss due to inelastic collision is significantly large. For instance, in the case of bremsstrahlung the energy loss is of the same order of magnitude as the energy of the particle, whereas $(\Delta E)_{\max}$ is several orders of magnitude lower.

If we are interested in the excitation of oscillations, we need account only for small losses no greater than those given by (4). Then in calculating $\overline{\Delta y}$ and $\overline{(\Delta y)^2}$ the integration should be in the interval $0 \leq \Delta y < (\Delta y)_{\max}$. Only in this case will Eq. (1) describe excitation of oscillations due to small multiple losses. Large single losses must be treated separately. Separation of losses into classes according to ΔE (such that $\Delta E < (\Delta E)_{\max}$ corresponds to multiple losses, and $\Delta E > (\Delta E)_{\max}$ corresponds to single losses) is only approximate, since strictly speaking losses for which $\Delta E \ll (\Delta E)_{\max}$ are multiple. However, the separation we are using would seem to give the correct order of magnitude for multiple and single losses.

On the basis of the above concepts, we have calculated the losses due to multiple inelastic interactions for a 250 Mev synchrotron and for a 10 Bev proton synchrotron.

Let the solution of Eq. (1) satisfy the conditions

$$P(y, 0) = P_0 = \text{const}\,(0 \leqslant y < y_{\max}); \quad P(y_{\max}, t) = 0. \tag{5}$$

The first of conditions (5) means that at the initial instant of time the amplitude distribution of particles is uniform on the phase plane, and the second that a particle whose amplitude of vibrations is greater than $y_{\max}$ stops being accelerated. Then†

$$P(y, \tau) = 2P_0 \sum_s \frac{J_0(\lambda_s y/y_{\max})}{\lambda_s J_1(\lambda_s)} \exp\left\{-\frac{\lambda_s^2}{2y_{\max}}\tau\right\}, \quad \tau = \int_0^t \overline{(\Delta y)^2}\,dt. \tag{6}$$

Here J_0 and J_1 are Bessel functions, and λ_s is the s'th root of $J_0(x)$. The quantity $\overline{(\Delta y)^2}$ is related to the mean square energy loss of a particle per unit time by the expression

$$\overline{(\Delta y)^2} = (\pi K/eV_0 \sin\varphi_0)\,\overline{(\Delta E)^2}/E; \quad \overline{(\Delta E)^2} = \int E^2 w(E)\,dE, \tag{7}$$

where $w(E)$ is the probability that the energy loss will be E per unit time. The limits of integration with respect to E are 0 and $(\Delta E)_{\max}$, the latter being given by Eq. (4). If the integral is not cut off at this upper limit, $\overline{(\Delta E)^2}$ will contain losses which lead to cases in which the particle stops being accelerated only momentarily. Therefore the final result would be incorrect.

Knowing τ, Eq. (6) can be used to find the fraction of particles lost. For instance, in a 250 Mev synchrotron (taking $y_{\max} \simeq \pi/2$, $eV_0 \cos\varphi_0 \sim 10^3$ ev, and $K \simeq 3$), $\tau_{\max}$ lies between 10^{-3} and 10^{-4} at a chamber pressure between 10^{-5} and 10^{-6} mm Hg, so that losses are negligibly small.

In the case of ionization losses in a 10 Bev proton synchrotron ($eV_0 \cos\varphi_0 \sim 10^4$ ev, $K \simeq 3$) $\tau_{\max}$ is about 10^{-2} at a pressure of about 10^{-6} mm Hg, which corresponds to particle losses of several percent.

---

*The necessity for accounting for bremsstrahlung in electron accelerators was pointed out by V. I. Veksler.

†It can be shown[2] that for synchrotron oscillations $\overline{(\Delta y)^2} = 2y\overline{\Delta y}$, which simplifies Eq. (1).

We express our gratitude to V. I. Veksler, M. S. Rabinovich, and A. A. Kolomenskii for aid and interest in the work.

---

[1] N. M. Blachman and E. D. Courant, Phys. Rev. **74**, 140 (1948).

[2] B. M. Bolotovskii, Particle Losses in a Synchrotron Due to Radioactive Damping by Gas Scattering, Phys. Inst. Acad. Sci. Report RF-37, 1951.

[3] J. M. Greenberg and T. H. Berlin, Rev. Sci. Instr. **22**, 293 (1951).

[4] A. A. Kolomenskii and A. N. Lebedev, On the Effect of Radiation on Electron Motion in Cyclic Accelerators, Phys. Inst. Acad. Sci. Report RF-372, 1952.

[5] A. N. Kolmogorov, Usp. Mat. Nauk **5**, 30 (1938).

[6] M. S. Rabinovich, Dissertation, Phys. Inst. Acad. Sci., 1948.

Translated by E. J. Saletan
62

CHARGE-EXCHANGE CROSS SECTION OF NITROGEN IONS IN GASES

V. S. NIKOLAEV, L. N. FATEEVA, I. S. DMITRIEV, and IA. A. TEPLOVA

Moscow State University

Submitted to JETP editor April 23, 1957

J. Exptl. Theoret. Phys. (U.S.S.R.) **33**, 306-307 (July, 1957)

WE have determined the cross sections for capture and loss of electrons by N^{+2}, N^{+3}, and N^{+4} ions in nitrogen, argon, and hydrogen. The ions were accelerated in the 72-centimeter cyclotron to energies between 1.3 and 9.7 Mev. The extracted and focused beam of ions with charge i passed through a 0.1 cm by 1 cm channel 3 cm long and entered into a cylindrical chamber about 40 cm long. The exit channel of the chamber had a cross section 0.3 cm by 1 cm and a length of 3 cm. After passing through the chamber the beam was analyzed in a magnetic field and recorded with proportional counters. The pressure was measured by an ionization manometer, which was calibrated for the different gases with an oil compression manometer. When the gas was admitted into the chamber, the pressure was increased from between 1 and 2×10^{-5} mm Hg (pressure remaining after evacuation) to between 4 and 10×10^{-4} mm Hg. When this was done, the relative numbers n_{i+1} and n_{i-1} of particles with charges $i \pm 1$ formed as a result of loss and capture of a single electron were increased from 3 – 5% to 8 – 15%, respectively. In calculating the cross sections $\sigma_{i,\, i\pm1}$ for loss and capture of an electron, we accounted both for interactions with the gas remaining after evacuation and for the small deviation from linearity in the relation between $n_{i\pm1}$ and the gas pressure. The error in the value of $\sigma_{i,\, i\pm1}$ was between 10 and 20%. We also evaluated the cross section for loss and capture of two electrons ($\sigma_{i,\, i\pm2}$). This cross section was found to be one order of magnitude smaller than the corresponding value of $\sigma_{i,\, i\pm1}$. From the values obtained for $\sigma_{i,\, i\pm1}$ and the experimental data on the equilibrium distribution of nitrogen ions in gases[1] we calculated the cross sections $\sigma_{i\pm1,\, i}$.

The results of the determination of the electron capture and loss cross sections for nitrogen ions in nitrogen are shown in the figures. These same figures give the values obtained previously.[2,3] The value of $\sigma_{i,\, i-1}$ (Fig. 1a for doubly, triply, and quadruply ionized ions varies as $v^{-k} i^m$, where v is the velocity of the ion. It is seen from the figure that the exponent k is close to 5, and that $m \sim 2.5$. When ions pass through argon and hydrogen, the charge dependence is the same as in nitrogen ($m \approx 2.5$), though k is somwhat larger (about 6) only in hydrogen. The absolute magnitude of $\sigma_{i,\, i-1}$ with $v \sim 6 \times 10^8$ cm/sec in argon is about 2 times greater, and in hydrogen is about 4 times less than in nitrogen. The values obtained for the capture cross section of an electron by nitrogen ions in nitrogen and in argon can be written approximately in the form

$$\sigma_{i,\, i-1} = 2\pi a_0^2 (v_0 / v)^5 i^{5/2} Z^{1/3},$$

where a_0 and v_0 are the radius of the first Bohr orbit and the velocity of the electron in the hydrogen atom, and Z is the atomic number of the medium. (The values calculated according to the formula are shown in Fig. 1a by the solid lines.)

A theoretical calculation of the electron capture cross section performed by Nikolaev[2,4] gives a dependence of $\sigma_{i,\,i-1}$ on v, i and Z which is close to the experimental one. The electron capture cross sections in argon, as calculated by Gluckstern,[5] differs significantly from the experimental values. According to these calculations, the cross sections are proportional to $v^{-3.5}$, and are 1.5 times greater than the experimental values for $v \sim 7 \times 10^8$ cm/sec.

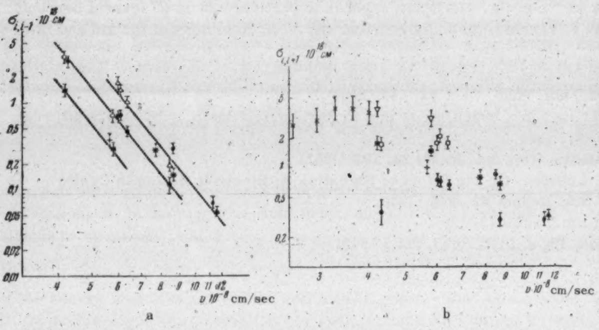

FIG. 1. Cross sections for (a) electron capture and (b) electron loss by nitrogen ions in nitrogen. The blacked-in symbols indicate directly measured values, and the symbols not blacked in indicate those calculated from the data on the equilibrium charge distribution. ∇ — i = 1, ■ — i = 2, ● — i = 3, ▲ — i = 4; +, *, ◆ — results of Nikolaev[2]; × — the values of σ_{12} obtained by Korsunskii et al.[3]

The cross sections $\sigma_{i,\,i+1}$ for electron loss (Fig. 1b) in the velocity region investigated hardly depend on v. This is in agreement with the assumption that $\sigma_{i,\,i+1}$ have maxima close to these velocities, since at high velocities the cross sections for loss should decrease,[2,6] and at velocities less than those of the removal electrons, they should also be small due to the adiabatic character of the collisions. The value of $\sigma_{i,\,i+1}$ in argon is between 2 and 2.5 times greater than, and in hydrogen is between 6 and 10 times less than, the cross section for loss in nitrogen.

---

[1] Teplova, Dmitriev, Nikolaev, and Fateeva, J. Exptl. Theoret. Phys. (U.S.S.R.) **32**, 974 (1957); Soviet Phys. JETP **5**, 979 (1957).

[2] V. S. Nikolaev, Dissertation, 2nd Sci. Res. Phys. Inst., Moscow State University (1954).

[3] Korsunskii, Pivovar, Markus, and Leviant, Dokl. Akad. Nauk SSSR **103**, 399 (1955).

[4] V. S. Nikolaev, J. Exptl. Theoret. Phys. (U.S.S.R.) **33**, 534 (1957); Soviet Phys. JETP **6**, (in press).

[5] R. L. Gluckstern, Phys. Rev. **98**, 1817 (1955).

[6] N. Bohr, Passage of Atomic Particles Through Matter (Russ. Transl.) IIL, 1950.

Translated by E. J. Saletan
63

CAPTURE OF POLARIZED μ^--MESONS BY NUCLEI

B. L. IOFFE

Submitted to JETP editor April 25, 1957

J. Exptl. Theoret. Phys. (U.S.S.R.) **33**, 308-309 (July, 1957)

As has been shown by Lederman's[1] experiments, μ^--mesons coming from the decay of π^--mesons are polarized to a large degree, and this polarization is maintained to a measurable extent even after the μ^--meson is captured into a Bohr orbit. A theoretical examination of the capture of polarized μ^--mesons by nuclei is of definite interest, since a comparison of the experimental and theoretical results would then make it possible to arrive at certain conclusions on the character of the weak interaction between

μ^--mesons and nucleons.

Let us consider the capture of a completely polarized μ^--meson by a nucleus. The interaction Hamiltonian can be written as the sum of all five types of interactions, namely

$$H = {}^1/_2 \sum_i{}' g_i (\bar{\psi}_n O_i \psi_p)(\bar{\psi}_\nu (1-\gamma_5) O_i \psi_\mu) + \text{Hermitian conjugate} \tag{1}$$

(i = S, V, T, A, P). We shall consider the neutrino a two-component particle.[2-4]* When a μ^--meson is captured, the nucleons in the nucleus gain an energy no greater than a few Mev, so that for the S, V, T, and A interactions we may go over to the nonrelativistic approximation for the nucleons. The pseudoscalar interaction, which vanishes in the nonrelativistic approximation, then gives a contribution only if the coupling constant g_p is much greater than the coupling constants for the other interactions.

The matrix element calculated from (1) is

$$\begin{gathered} M = {}^1/_2 \bar{u}_\nu (1-\gamma_5)\{g_S I + g_V I\beta + g_T \mathbf{S}\boldsymbol{\sigma} + g_A \mathbf{S}\boldsymbol{\sigma}\beta + g_P P\} u_\mu, \\ I = \int \Psi_f^* \Psi_i e^{-i\mathbf{qr}} d\tau; \quad \mathbf{S} = \int \Psi_f^* \boldsymbol{\sigma} \Psi_i e^{-i\mathbf{qr}} d\tau; \quad P = \int \Psi_f^* \gamma_5 \Psi_i e^{-i\mathbf{qr}} d\tau, \end{gathered} \tag{2}$$

where Ψ_f and Ψ_i are the final and initial wave functions of the heavy particles, and $\mathbf{q}$ is the neutrino momentum. Let us denote the mean value of the μ-meson spin by $\boldsymbol{\sigma}_0$. We now calculate the square of the matrix element of Eq. (2), obtaining (setting $\boldsymbol{\nu} = \mathbf{q}/q$):

$$\begin{aligned} 2|M|^2 = {} & |(g_S + g_V) I + g_P P|^2 (1 + \boldsymbol{\sigma}_0 \boldsymbol{\nu}) + |g_T + g_A|^2 \{|\mathbf{S}|^2 (1 - \boldsymbol{\sigma}_0 \boldsymbol{\nu}) + S_i S_k^* (\nu_k \sigma_{0i} + \nu_i \sigma_{0k}) + i[\mathbf{SS}^*](\boldsymbol{\nu} - \boldsymbol{\sigma}_0)\} \\ & + 2\operatorname{Re}\{(g_T + g_A)[(g_S + g_V)^* I^* + g_P^* P^*](\mathbf{S}\boldsymbol{\sigma}_0 + \mathbf{S}\boldsymbol{\nu} - i\mathbf{S}[\boldsymbol{\nu}\boldsymbol{\sigma}_0])\}. \end{aligned} \tag{3}$$

Let us consider the most common case, when capture of the μ^--meson leads to a neutron and a recoil nucleus. Quadratic combinations of the matrix elements I, **S**, and P, after they are averaged over projections of the nuclear spin, can depend only on two vectors. These are the unit vector **n** directed along the neutron momentum $\mathbf{p} = \mathbf{n}p$, and the unit vector $\boldsymbol{\nu}$. Further, we shall select only those cases in which $\mathbf{n} = -\boldsymbol{\nu}$, which can be done by selecting neutrons whose energy lies close to the upper bound of the neutron energy spectrum. The products of matrix elements that enter into Eq. (3) can then depend only on $\boldsymbol{\nu}$. It follows from this that after averaging over projections of the nuclear spin, $\overline{IP^*}$, $\overline{[\mathbf{SS}^*]}$, and $\overline{I^*\mathbf{S}}$ must vanish. Indeed, $\overline{IP^*}$ is a pseudoscalar,† and $\overline{[\mathbf{SS}^*]}$ and $\overline{I\mathbf{S}^*}$ are pseudovectors and can therefore not be constructed with the aid of a single vector $\boldsymbol{\nu}$. Let us write

$$\overline{|I|^2} = |C_I|^2, \qquad \overline{|P|^2} = |C_P|^2, \qquad \overline{|\mathbf{S}|^2} = |C_S|^2.$$

The most general forms for $\overline{S_i S_k^*}$ and $\overline{P^*\mathbf{S}}$ are

$$\overline{S_i S_k^*} = |C_S|^2 \frac{1}{1+\alpha}\left(\frac{1}{3}\delta_{ik} + \alpha \nu_i \nu_k\right), \quad \overline{P^*\mathbf{S}} = C_P^* C_S \gamma \boldsymbol{\nu}, \tag{4}$$

where $\alpha > -1/3$. Inserting (4) into (3), we obtain

$$\begin{aligned} 2|M|^2 = {} & \{|g_S + g_V|^2 |C_I|^2 + |g_P|^2 |C_P|^2 + 2\operatorname{Re} g_P^* (g_T + g_A) C_P^* C_S \gamma\} \\ & \times (1 + \boldsymbol{\sigma}_0 \boldsymbol{\nu}) + |g_T + g_A|^2 |C_S|^2 \left(1 - \frac{1}{3}\frac{1-3\alpha}{1+\alpha}\boldsymbol{\sigma}_0 \boldsymbol{\nu}\right). \end{aligned} \tag{5}$$

From Eq. (5) one can conclude that when the capture process gives rise to neutrons whose momentum is in the direction opposite to that of the neutrino, these neutrons are directed primarily along (or against) the μ-meson spin, and their angular distribution is given by the expression $dW/d\Omega = 1 - \beta \cos\theta$, where θ is the angle between the direction of motion of the neutron and the μ-meson spin. For the scalar, vector, and pseudoscalar interactions (and their cross products) $\beta = 1$. For the tensor and axial vector interactions (and their cross products) β cannot in general be calculated from (5). (It follows from (5) that $\beta = -(1-3\alpha)/3(1+\alpha)$, where $-1/3 < \alpha < \infty$, so that $-1 < \beta < 1$.) For μ^--meson capture by protons, $\alpha = 0$ and $\beta = -1/3$. Since nonzero values of α are due to trapping of the neutron in the nucleus, one may expect that in lighter nuclei α is almost zero, so that for these, β is close to $-1/3$.

If we select neutrons whose energy lies in the upper part of their energy spectrum, where the intensity begins to decrease (the neutron energy is greater than, or of the order of E_0, the binding energy of the neutron in the nucleus), their angular distribution will be confined to a relatively narrow cone about a direction opposite to that of the neutrino momentum. The width of this angular distribution is of the order of $\Delta \cos \vartheta \sim mE_0/pq \sim 0.4$.

---

*The factor $1 - \gamma_5$ in Eq. (1) corresponds to the creation of a neutrino whose spin is directed along its momentum; $\gamma_5 = \begin{pmatrix} 0 & 1 \\ 1 & 0 \end{pmatrix}$.

†The bar indicates averaging over spin projections of the initial nucleus and summing over those of the final.

Thus an experimental measurement of the angular distribution of the high-energy neutrons arising from the capture of polarized μ^--mesons by light nuclei may make it possible to distinguish between two classes of interaction between μ^--mesons and nucleons. One class comprises the scalar, vector, and pseudoscalar ($\beta = 1$) interactions, the other the tensor and axial-vector ($\beta \approx -1/3$) interactions.

---

[1] Garwin, Lederman, and Weinrich, Phys. Rev. **105**, 1415 (1957).

[2] L. D. Landau, J. Exptl. Theoret. Phys. (U.S.S.R.) **32**, 407 (1957); Soviet Phys. JETP **5**, 337 (1957).

[3] T. D. Lee and C. N. Yang, Phys. Rev. **105**, 1671 (1957).

[4] A. Salam, Nuovo cimento **5**, 299 (1957).

Translated by E. J. Saletan
64

ON THE POSSIBLE EFFICIENCY OF THE CATALYSIS OF NUCLEAR REACTIONS BY MESONS

IA. B. ZEL'DOVICH

P. N. Lebedev Physical Institute, Academy of Sciences, U.S.S.R.

Submitted to JETP editor April 29, 1957

J. Exptl. Theoret. Phys. (U.S.S.R.) **33**, 310-311 (July, 1957)

THERE exists at present experimental evidence[1] of the ability of negative mesons to catalyze a nuclear reaction between two singly charged ions (p, d, t) by bringing the reacting nuclei closer together (see Zel'dovich and Sakharov,[2] where additional references are given). The meson is not lost in the nuclear reaction.

For μ^--mesons in a liquid mixture of p and d, the reaction probability is no greater than several hundredths per meson entering the mixture. This small probability is determined by the ratio between the mean time for creating a mesomolecule ($pd\mu$, $dd\mu$) and the lifetime of the μ meson, which is 2×10^{-6} sec. One is naturally led to enquire whether there exist in nature some long-lived mesons, and whether such mesons may not in practice make possible a self-maintaining nuclear reaction of hyperon isotopes.

The second of these questions can definitely be answered in the negative. For all imaginable reactions there exists the probability that the meson will be bound to the helium nucleus produced in the nuclear reaction. Owing to the positive charge of the $He\mu$ system, other nuclei, including those of hydrogen, cannot come very close, so that the bound meson leaves the reaction and can no longer perform its catalyzing action.

The probability of binding was calculated by a method developed by Migdal[3] in treating the probability that an atom is ionized during β-decay. At the time the nuclear reaction is taking place, the two nuclei involved are close together and the wave function of the meson in the adiabatic approximation is that of the mesohelium ion $\psi_1(r)$, where r is the distance between the meson and the point at which the two nuclei meet.

The helium nucleus produced in the reaction has a definite energy E_0 (which is 0.8 Mev for $d + d \rightarrow He^3 + n$, and 3.5 Mev for $d + t \rightarrow He^4 + n$) and a corresponding velocity. To account for this, the meson wave function should be multiplied by $e^{ipz/\hbar}$, where the z axis is along the direction of motion of the nucleus, and the momentum p is the product of the nuclear velocity by the reduced mass $m = M\mu/(M + \mu)$, where μ is the meson mass and M is the mass of the helium nucleus. Expanding $\psi_1(r)e^{ipz/\hbar}$ in meson eigenfunctions in the field of the helium nucleus, we obtain the probability for one or the other final meson states after the nuclear reaction.

In particular,

$$K = \left| \int \psi_i^2 (r) e^{ipz/\hbar} dv \right|^2$$

gives the probability that the meson remains bound to the helium in the ground state inserting $\psi_i \sim e^{-br}$, we obtain

$$K = (1 + p^2/4\hbar^2 b^2)^{-4}.$$

Writing p^2 in terms of E_0,

$$p^2 = m^2 v^2 = 2m^2 E_0/M; \qquad b = mZe^2/\hbar^2, \qquad \text{where } Z = 2.$$

We note that $p^2/\hbar^2 b^2$ does not depend on the meson mass, and is equal to the ratio of the recoil nucleus energy E_0 to $\epsilon = MZ^2e^4/2\hbar^2 = \text{Ry}\,Z^2M^2/m_e$. For He^3, $\epsilon = 0.3$ Mev, $E_0 = 0.8$ Mev, and $K = 0.13$; for He^4, $\epsilon = 0.4$ Mev, $E_0 = 3.5$ Mev, and $K = 0.01$. Thus a nondecaying meson could give on the average 8 neutrons from the d + d reaction, or 100 neutrons from the d + t reaction. In d + t mixtures, however, in addition to $d + t \rightarrow \text{He}^4 + n$, there would also be the reactions $d + d \rightarrow \text{He}^3 + n$, and $t + t \rightarrow \text{He}^4 + 2n$, which would decrease the neutron yield.

The binding of a meson to helium can easily be observed in a hydrogen bubble chamber, since singly charged $(\text{He}\mu)^+$ should give a longer track with lower ionization and smaller curvature (in a magnetic field) at a given energy than does He^{++}.

It is easy to see that μ mesons (or heavier mesons) will not be stripped from the helium nucleus by electron collisions.

The probability that a meson enters an excited state (with a wave function ψ_f) near the helium nucleus is small compared with the probability that it remains in the ground state.

Since the integral $\int \psi_f^* \psi_i e^{ipz/\hbar} dv$ contains the rapidly oscillating function $e^{ipz/\hbar}$, its magnitude is determined by the singularity of $\psi_f^* \psi_i$. The Coulomb functions ψ_f and ψ_i have a singularity at the origin. The formation of excited mesohelium in a state with $\ell \neq 0$, for which $\psi_f(0) = 0$, has a probability which is inversely proportional to a higher power of the momentum p than the probability for states with $\ell = 0$. States with $\ell = 0$, $n > \ell$ have probability proportional to $|\psi_f(0)|^2 \sim 1/n^3$, and therefore contribute less than 20% to the probability of forming the ground state with $n = 1$.

Finally, in the $pd\mu$ case, Alvarez[1] observed a process in which the total energy of the reaction was given to the meson. Calculation,[2] however, leads to the result that emission of this energy in the form of a photon is equally probable. In this case the energy of the recoil nucleus is only 5 kev, and the meson must remain with the He^3 nucleus. It would seem that the tracks of such nuclei could not be observed in bubble chambers.

---

[1] L. W. Alvarez et al., Phys. Rev. **105**, 1127 (1957).

[2] Ia. B. Zel'dovich and A.D. Sakharov, J. Exptl. Theoret. Phys. (U.S.S.R.) **32**, 947 (1957); Soviet Phys. JETP **5**, 775 (1957).

[3] A. B. Migdal, J. Exptl. Theoret. Phys. (U.S.S.R.) **9**, 1163 (1939).

Translated by E. J. Saletan
65

BREAKUP OF H_2^+, HD^+, AND D_2^+ IONS BY SINGLE COLLISIONS WITH HYDROGEN, DEUTERIUM, AND AIR MOLECULES

S. E. KUPRIIANOV, V. K. POTAPOV

L. Ia. Karpov Physico-Chemical Institute

Submitted to JETP editor April 30, 1957

J. Exptl. Theoret. Phys. (U.S.S.R.) 33, 311-312 (July, 1957)

When a beam of accelerated molecular ions passes through a gas at low pressure, the ions are found to break up without a measurable change of the initial velocity.[1,2] The study of such processes[3-6] has shown that breaking up is caused by single collisions of the ions with gas molecules along their path.

When H_2^+, HD^+, and D_2^+ ions are scattered, they may break up in the following ways:*

$$1)\ H_2^+ \to p + H, \qquad 2)\ D_2^+ \to d + D,$$
$$3)\ HD^+ \to p + D, \qquad 4)\ HD^+ \to d + H.$$

We have determined the relative probabilities q for these processes when H_2^+, HD^+, and D_2^+ ions accelerated to 3000 ev are passed through hydrogen, deuterium, and air at pressures of about 5×10^{-4} mm Hg.

The measurements were performed on a modernized MS-1 mass spectrograph. The ions were obtained by using 70 ev electrons to ionize hydrogen enriched to 82% D.

The results are presented in the table. The probability for process (2) is in all cases taken as 1.0. The experimental error is ± 15%.

Molecules used for scattering	q_1	q_2	q_3	q_4
Hydrogen	0.9	1.0	0.4	0.9
Deuterium (82% D)	1.3	1.0	0.4	1.0
Air	1.1	1.0	0.4	1.0

The table gives the ratios between the ion currents of the molecules that have been broken up and the ion currents of the original molecular ions. These ion currents were in all cases measured at the maxima of the respective peaks. This accounts only for those ions which are practically unscattered by the collision processes.

It is seen from the table that the general character of the breakup is independent of the scattering molecule within the experimental limits. The probabilities for processes (1) and (2) are the same, a fact which had been found previously,[5] and the total probability for process (3) plus (4) is somewhat larger. It should be noted that the probability for process (4) is, as may have been expected, much greater than that for process (3).

We express our gratitude to Professor N. N. Tunitskii for discussing the results of this work.

---

[1] J. Mattauch, H. Lichtblau, Physik Z. **40**, 16 (1939).
[2] A. Henglein, Z. Naturforsch. **7A**, 165 (1952).
[3] Kolotyrkin, Tikhomirov, and Tunitskii, Dokl. Akad. Nauk SSSR **92**, 1193 (1953).
[4] N. V. Fedorenko, J. Tech. Phys. (U.S.S.R.) **24**, 669 (1953).
[5] Tunitskii, Smirnova, and Tikhomirov, Dokl. Akad. Nauk SSSR **101**, 1083 (1955).
[6] Kupriianov, Tikhomirov, Potapov, and Karpova, J. Exptl. Theoret. Phys. (U.S.S.R.) **30**, 569 (1956); Soviet Phys. JETP **3**, 459 (1957).

Translated by E. J. Saletan
66

---

*For the conditions of our experiment it is less likely that breaking up will occur with the simultaneous formation of two ions.

CONTENTS—continued

Russian Reference

On Annihilation of Antinucleons . . . . . . V. M. Maksimenko 180 33, 232

Contribution to the Phenomenological Theory of Paramagnetic Relaxation in Parallel Fields . . . . . . N. K. Belousova and I. G. Shaposhnikov 183 33, 238

Elastic Collision Cross Section for Hydrogen Atoms . . . . . . V. S. Kudriavtsev 188 33, 243

On the Kinetic Theory of an Electron Gas in the Presence of Boundaries . . . . . . L. E. Pargamanik 194 33, 251

Correlation of Polarized Quanta in the Case of Nonconservation of Parity . . . . . . Iu. V. Gaponov and V. S. Popov 197 33, 256

LETTERS TO THE EDITOR

The Problem of Nucleon Structure . . . . . . B. S. Neganov 200 33, 260

Polar Theory of Metals . . . . . . I. Z. Fisher 201 33, 262

Probability for Charge Exchange in Nucleons with Energies of $3 \times 10^9 - 10^{10}$ ev in Interactions with Air Nuclei . . . . . . V. A. Vorob'ev 203 33, 264

Remarks on the Multiplicative Renormalization Group in the Quantum Theory of Fields . . . . . . V. Z. Blank, V. L. Bonch-Bruevich, and D. V. Shirkov 204 33, 265

Radio-Frequency Method for Measuring the Mass of Relativistic Electrons . . . . . . V. N. Lazukin 206 33, 267

Generalization of Gauge Invariance and Combined Inversion . . . . . . V. L. Pokrovskii 208 33, 269

Differential Cross Section for Photoproduction of π-Mesons on Nucleons Taking Account of d-States . . . . . . N. F. Nelipa 210 33, 271

Phase of a Scattered Wave . . . . . . F. S. Los' 211 33, 273

Nuclear Subshells and Deformation in the Region Past Lead . . . . . . N. N. Kolesnikov and A. P. Krylova 212 33, 274

Conservation of Parity in the Theory of Elementary Particles . . . . . . V. L. Pokrovskii and Iu. B. Rumer 215 33, 277

Polarization in Double Scattering of Electrons . . . . . . Iu. V. Anishchenko and A. A. Rulchadze 216 33, 279

Theory of the Production of Electron-Positron Pairs in Collisions of Slow μ^--Mesons with Nuclei . . . . . . L. M. Afrikian 217 33, 280

Soft Component in an Electron-Nuclear Shower at Energies of 10^{14} ev . . . . . . I. M. Gramenitskii, G. B. Zhdanov, M. I. Trem'iakova, and M. N. Shcherbakova 218 33, 282

Calorimetric Method of Determining the Optical Constants of Metals in the Infrared Region at Low Temperatures . . . . . . N. E. Alekseevskii and E. V. Potapov 220 33, 283

Convergence of the Perturbation-Theory Series for a Non-Relativistic Nucleon . . . . . . A. G. Galanin and Iu. N. Lokhov 221 33, 285

The Influence of Pressure on the Magnetic Properties of Zinc Single Crystals at Low Temperatures . . . . . . I. M. Dmitrenko, B. I. Verkin, and B. G. Lazarev 223 33, 287

Use of the Hartree-Fock Equations for a System of Quasi-particles . . . . . . V. M. Eleonskii and P. S. Zyrianov 225 33, 289

New Form of Isomerism in Eu^{152} . . . . . . L. K. Peker 226 33, 291

Small-Angle Scattering of Fast Neutrons by Heavy Nuclei . . . . . . Iu. A. Aleksandrov 228 33, 294

Decay Probabilities of the Σ-Hyperon with Parity Nonconservation . . . . . . I. Iu. Kobzarev and L. B. Okun' 230 33, 296

A "Symmetric" Circular Synchrocyclotron with Oppositely Directed Beams . . . . . . A. A. Kolomenskii 231 33, 298

Second Order Phase Transition in Sodium Nitrate . . . . . . I. E. Dzialoshinskii and E. M. Lifshitz 233 33, 299

A Measurement of the Depth of Penetration of a Magnetic Field into Mercury Films . . . . . . I. S. Khukhareva 234 33, 301

Anomalous Decay of a Charged Particle Observed in a Cloud Chamber . . . . . . Z. Sh. Mandzhavidze, N. N. Roinishvili, and G. E. Chikovani 236 33, 303

Application of the Einstein-Fokker Equation to Finding Particle Losses Due to Gas Scattering in Accelerators . . . . . . B. M. Bolotovskii and A. P. Fateev 237 33, 304

Charge-Exchange Cross Section of Nitrogen Ions in Gases . . . . . . V. S. Nikolaev, L. N. Fateeva, I. S. Dmitriev, and Ia. A. Teplova 239 33, 306

Capture of Polarized μ^--Mesons by Nuclei . . . . . . B. L. Ioffe 240 33, 308

On the Possible Efficiency of the Catalysis of Nuclear Reactions by Mesons . . . . . . Ia. B. Zel'dovich 242 33, 310

Breakup of H_2^+, HD^+, and D_2^+ Ions by Single Collisions with Hydrogen, Deuterium, and Air Molecules . . . . . . S. E. Kupriianov and V. K. Potapov 244 33, 311

SOVIET PHYSICS JETP VOLUME 6, NUMBER 1 JANUARY, 1958

CONTENTS

Russian Reference

Electrodynamic Acceleration of Plasma Bunches . . . . . . L. A. Artsimovich, S. Iu. Luk'ianov, I. M. Podgornyi, and S. A. Chuvatin 1 33, 3
Measurements with a Slowing-Down-Time Neutron Spectrometer Employing Lead. Excited Level of the He^4 Nucleus . . . . . . A. A. Bergman, A. I. Isakov, Iu. P. Popov, and F. L. Shapiro 6 33, 9
On the Production of the Electron-Photon Component in the Interaction of Cosmic-Ray Particles of Energies Greater than 10^{11} ev with Beryllium Nuclei . . . . . . L. T. Baradzei, V. I. Rubtsov, Iu. A. Smorodin, M. V. Solov'ev, B. V. Tolkachev, and Z. I. Tulinova 12 33, 17
Photodisintegration of Helium, I. . . . . . . A. N. Gorbunov and V. M. Spiridonov 16 33, 21
Change in the Elasticity Constants of Sodium Nitrate During a Phase Transition of the Second Kind . . . . . . M. I. Kornfel'd and A. A. Chubinov 26 33, 33
Polarization in (p—p) Scattering at 635 Mev . . . . . . M. G. Mescheriakov, S. B. Nurushev, and G. D. Stoletov 28 33, 37
Coupling Between Intermolecular and Intramolecular Vibrations in a Crystal . . . . . . N. N. Porfir'eva 35 33, 47
Angular Distributions of Photofission Fragments from Uranium . . . . . . B. P. Bannik, N. M. Kulikova, L. E. Lazareva, and V. A. Iakovlev 39 33, 53
Inconsistency Between the Theoretical and Experimental Delta-Shower Frequencies at High Energies . . . . . . P. S. Chikin 41 33, 56
Nonlinear Meson Field Equations . . . . . . A. A. Borgardt 43 33, 60
Interaction Between Gravitational-Capillary and Magnetohydrodynamic Waves . . . . . . M. F. Shirokov 50 33, 67
On the Dynamics of a Bounded Plasma in an External Field . . . . . . L. M. Kovrizhnykh 54 33, 72
Magnetoresistive Phenomena in n-Ge Type Semiconductors in Strong Magnetic Fields . . . . . . M. I. Klinger and P. I. Voroniuk 59 33, 77
On the Theory of the Shubnikov-De Haas Effect . . . . . . I. M. Lifshitz and L. M. Kosevich 67 33, 88
On the Brightness of Strong Shock Waves in Air . . . . . . Iu. P. Raizer 77 33, 101
Dispersion of Sound in a Fermi Liquid . . . . . . I. M. Khalatnikov and A. A. Abrikosov 84 33, 110
Flow Instability of a Superfluid Film . . . . . . R. G. Arkhipov 90 33, 116
Many-Phonon Processes in Crystals . . . . . . V. F. Turchin 96 33, 124
Quantum Kinetic Equation for Plasma with Account of Correlation . . . . . . Iu. L. Klimontovich and S. V. Temko 102 33, 132
Energy Spectrum of Cascade Electrons in Light Materials . . . . . . I. P. Ivanenko 105 33, 135
Contribution to the Theory of Scattering of Light near Points of Second-Order Phase Transitions . . . . . . M. A. Krivoglaz and S. A. Rybak 107 33, 139
On the Effective Field in a Plasma . . . . . . B. B. Kadomtsev 117 33, 151
Decay Law for the Concentration of Non-Equilibrium Charge Carriers in Semiconductors . . . . . . G. M. Goureau 123 33, 158
Correlation Theory of Thermal Fluctuations in an Isotropic Medium . . . . . . S. M. Rytov 130 33, 166
On Interpretation of the Lateral Distribution of Nuclear-Active Particles in Extensive Air Showers. . . . . . . Iu. N. Vavilov 141 33, 179
Some Characteristics of M1-Conversion Nuclear Transitions . . . . . . D. P. Grechukhin 144 33, 183
Analysis of the Properties of the Electron-Photon Component of Extensive Air Showers in the Lower Third of the Atmosphere . . . . . . V. I. Zatsepin 150 33, 190
Hydrodynamical Interpretation of One Characteristic of Large Showers Recorded in Photographic Emulsions . . . . . . G. A. Milekhin and I. L. Rozental' 154 33, 197
On the Relation Between "Accidental" Degeneracy and "Hidden" Symmetry of a System . . . . . . S. P. Alliluev 156 33, 200
Time Reversal and Polarization Phenomena in $N + N \rightleftarrows d + \pi$ Reactions . . . . . . L. I. Lapidus 160 33, 204
Electron Density Fluctuations and the Scattering of Radio Waves in the Ionosphere . . . . . . Ia. L. Al'pert 167 33, 213
Fine Structure in the Alpha-Decay of Odd Nuclei . . . . . . V. G. Nosov 176 33, 226

(Contents continued on inside back cover)